Characterisation of Neuroserpin Protein Expression Throughout Development and Investigation of Putative Neuroprotective Properties in Rodent Models of Neonatal Hypoxia Ischaemia



Lancelot Jamie Millar
University College

A thesis submitted for the degree of
Doctor of Philosophy

Trinity Term 2018

Abstract

Characterisation of Neuroserpin Protein Expression Throughout Development and Investigation of Putative Neuroprotective Properties in Rodent Models of Neonatal Hypoxia Ischaemia

Lancelot Jamie Millar

University College

Thesis submitted for the degree of *Doctor of Philosophy*

Trinity Term 2018

Neonatal hypoxia ischaemia remains the most common cause of infant mortality globally, accounting for persistent motor and cognitive disorders in a substantial proportion of survivors. Currently, there is only one licensed treatment which aims to reduce brain damage and improve cognitive function: hypothermia. Increased understanding of the infant brain's response to hypoxic ischaemic injury and novel treatment design are of utmost importance. This thesis characterises expression of neuronally-secreted serine protease inhibitor neuroserpin, previously established as a protective factor in rodent models of adult stroke, throughout development and in rodent models of mild-to-moderate neonatal hypoxic ischaemic injury.

The expression profile of neuroserpin protein was examined in the developing mouse and human brain using immunohistochemistry. Results closely corresponded with published mRNA expression patterns, demonstrating an enrichment of neuroserpin-immunoreactive neurons in Layer V and the transitory deep layer known as subplate in murine cerebral cortex. Within the subplate, neuroserpin-immunoreactive neurons formed an early-born subpopulation, partially overlapping conserved subplate molecular markers. Expression peaked at the murine brain development stage equivalent to birth in human, suggesting a potential developmental function for neuroserpin. Investigations in human foetal brain tissue confirmed neuroserpin-immunoreactivity within the deep layers of the cortical plate.

Neuroserpin expression patterns were also quantified in rodent models of neonatal hypoxia ischaemia, adapted from the Rice-Vannucci method. In a preterm rat model and a neonatal mouse model, the number of neuroserpin-immunoreactive neurons within the subplate underwent a statistically significant increase in the hypoxic-ischaemic hemisphere compared to the control hemisphere and sham-operated brains, with no significant change in any other cortical layer. However, semi-quantitative Western blot detected no significant difference in total cortical neuroserpin protein between hypoxic-ischaemic and control hemispheres in neonatal mouse brains. It is possible that neuroserpin contributes to a highly anatomically-localised or time-point specific endogenous response to neonatal hypoxia ischaemia.

The proposed neuroprotective properties of neuroserpin were investigated in two models of neonatal hypoxia ischaemia, yielding inconclusive results. Oxygen glucose deprivation experiments in cultured Neuro-2-A neuroblastoma cells and primary cortical neurons *in vitro* demonstrated a modest but statistically significant increase in staining for metabolic viability marker 3-(4,5-dimethylthiazol-2-yl)-2,5-diphenyltetrazolium bromide (MTT) when treated with exogenous neuroserpin. The functional significance of this effect remains to be evaluated.

The *Serpini1* knock-out mouse, which does not manufacture functional neuroserpin protein, was used to assess the vulnerability of neurons to hypoxic-ischaemic brain damage in the absence of neuroserpin *in vivo*. *Serpini1* knock-out mouse pups and wild-type littermates underwent adapted Rice-Vannucci neonatal hypoxia ischaemia, before being perfused with metabolic activity marker 2,3,5-triphenyltetrazolium chloride (TTC) 48 hours after injury. No significant difference in staining intensity was detected between genotypes, although methodological refinement is required. Immunohistochemistry for glial inflammatory markers also found mixed results, with only one of three markers investigated demonstrating a significant difference in immunoreactivity between genotypes.

This thesis examines putative neuroprotective protein neuroserpin expression and reports a neuron-specific expression enrichment around term. Any endogenous upregulation of neuroserpin expression following rodent neonatal hypoxia ischaemia is modest, and evidence for substantial variability in injury severity in the absence of neuroserpin from these initial investigations is weak.

Acknowledgements

I would like to thank Professor Zoltán Molnár for welcoming me into his laboratory and giving me the opportunity to pursue this fascinating project. I greatly admire the supportive atmosphere, spirit of collaboration, and above all the science that this group pursues. Thank you for my small part in that.

Over the last four years I have received technical, theoretical, and personal support from many talented people. I would particularly like to thank Dr. Anna Hoerder-Suabedissen who has trained me in many of the experimental techniques used in this thesis, and more importantly broadened my mind with her unique way of thinking with great precision. I would also like to thank Dr. Kristina Parley for all her technical help and cheerfulness, Professor Lei Shi for taking me on a whirlwind tour of *in vitro* experiments, Dr. Eleanor Grant for taking me under her wing when I first joined the lab, and Dr. Wei-Zhi Wang, Dr. Fernando García-Moreno, Kim Korrell, and Melissa Bailey for brightening my time in Oxford with brilliant science and kind words.

I am greatly indebted to the team at King's College London, including Professor David Edwards, Professor Pierre Gressens, Dr. Claire Thornton, and Dr. Ana Baburamani, for all their expert advice on the neonatal hypoxia ischaemia animal model. Their support has been invaluable. The team at the Biomedical Services facility, particularly Angela Curran, Denise Jelfs, and Laura Thomas, have given me and my experimental animals tremendous support throughout. I would also like to thank my visiting students over the years; Christiana Trandafir for her passionate commitment to science, Tom Van Acker for all his help setting up Western blot, and Suzu Chida, my exceptionally bright and personable student from Tokyo with a dazzling future ahead of her. I wouldn't have been able to throw myself into my work without the dedicated support of the University College welfare team led by Dr. Andrew Gregory, and the help I received from the University of Oxford Disability Advisory Service, especially from Dr. Yujin Chen, Marion Frostick, and Dr. Jonathan Pointer. I can't imagine where I would be now without any of these people.

Finally, I would like to thank my partner Adam for all the joy you brought to me and your enthusiasm and support through every day of my DPhil, and all the calm, gentle swans and cygnets who have helped keep me sane and see the good in the world.

Statement of Authorship

The work presented in this thesis is my own with the following exceptions:

Chapter 1
The introduction is largely based on a previously published review article, which I have reproduced here with the kind permission of the other authors and the journal Frontiers in Cellular Neuroscience. The full reference is:
Millar L. J., Shi L., Hoerder-Suabedissen A. and Molnár Z. (2017). "Neonatal Hypoxia Ischaemia: Mechanisms, Models, and Therapeutic Challenges." *Frontiers in Cellular Neuroscience*. 11:78. doi: 10.3389/fncel.2017.00078

Chapter 3
Dr. Anna Hoerder-Suabedissen made a substantial contribution to mouse colony management for experimental animals used in all chapters.
Section 3.3.1.1 – Many of the brains used in the NIHS mouse developmental time series were perfused by Dr. Anna Hoerder-Suabedissen or Dr. Eleanor Grant. All staining, imaging, and analysis is my own. Immunohistochemistry and imaging for the C57/BL6 mouse developmental time series was carried out in collaboration with visiting MSc student Tom van Acker of the University of Louvain, Belgium.
Section 3.3.1.3 – Immunohistochemistry and quantification of neuroserpin co-localisation with subplate molecular markers in NIHS mouse was carried out by Yucheng Pan, formerly of Harvard University, USA. All staining, imaging, and analysis in the C57/BL6 mouse is my own.
Section 3.3.1.4 – Bromodeoxyuridine (BrdU) injection at E11.5 and E12.5, and subsequent perfusion at P8, were carried out by Dr. Anna Hoerder-Suabedissen for a previous investigation (Hoerder-Suabedissen and Molnár, 2013). All staining, imaging, and analysis is my own.
Section 3.3.2.1 – Immunohistochemistry and imaging of neuroserpin co-localisation with endoplasmic reticulum (ER) molecular markers was carried out in collaboration with Tom van Acker.
Section 3.3.2.2 – Immunohistochemistry, imaging and quantification of neuroserpin co-localisation with heat shock proteins (HSP) was carried out in collaboration with visiting student Christiana Trandafir of the University of Cluj-Napoca, Romania.
Section 3.3.3 – Monocular enucleation at P1, and subsequent perfusion at P6, were carried out by Dr. Eleanor Grant for a previous investigation (Grant et al., 2016). All staining, imaging, and analysis are my own.
Section 3.3.4 – Immunohistochemistry in 15 post-conceptional week (PCW) human brain tissue was carried out by Professor Kjeld Møllgård of the University of Copenhagen, Denmark. Immunohistochemistry in 40 PCW term human brain tissue was carried out by Dr. István Adorján of the University of Oxford, UK, and the University of Budapest, Hungary. Experimental design and protocol are my own.
Section 3.3.5 – Non-quantitative Western Blot methods for antibody validation were optimised in collaboration with Tom van Acker and visiting student Suzu Chida of Tokyo Medical and Dental University, Japan. Membrane imaging was carried out in collaboration with Suzu Chida and Dr. Kristina Parley. Immunohistochemistry for antibody validation was carried out in collaboration with Suzu Chida.

Chapter 4
Dr. Anna Hoerder-Suabedissen continued to contribute to mouse colony management.
Section 4.3.1 – Preterm hypoxia ischaemia at P2, and subsequent perfusion at P6, was carried by collaborators Dr. Vanessa Ginet and Dr. Anita C. Truttmann of the University of Lausanne, Switzerland, for a previous investigation (Okusa et al., 2014). All staining, imaging, and analysis are my own.
Section 4.3.2 – The adapted Rice-Vannucci hypoxia ischaemia procedure was developed with substantial advice from Dr. Ana Baburamani, King's College London, UK (Baburamani et al.., 2017; Thornton et al., 2017; Kichev et al., 2018). Non-aseptic surgical support was provided for several litters by Dr. Kristina Parley.
Section 4.3.3 – Several of the brains used in the initial validation and optimisation of the adapted Rice-Vannucci neonatal hypoxia ischaemia mouse model were sectioned, stained, or imaged by either Dr. Kristina Parley or Dr. Anna Hoerder-Suabedissen. All surgical procedures and analysis are my own.
Section 4.3.6 – Semi-quantitative Western Blot methods were optimised in collaboration with Dr. Kristina Parley, Tom van Acker, and Suzu Chida. Semi-quantitative Western Blot experiments comparing total neuroserpin expression between hemispheres in neonatal hypoxia ischaemia brains were carried out by Dr. Kristina Parley. All surgical procedures and analysis are my own.

Chapter 5
Dr. Anna Hoerder-Suabedissen continued to contribute to mouse colony management. A substantial number of animals used in this chapter were genotyped by Dr. Kristina Parley. All cell culture experiments were designed in collaboration with Professor Lei Shi of Jinan University, China.
Section 5.3.1.1 – Neuro-2-A neuroblastoma cells were maintained, and oxygen glucose deprivation optimisation procedures were carried out, in collaboration with Professor Lei Shi.
Section 5.3.1.2 – Primary cortical neurons from C57BL/6 and *Serpini1* knock-out mouse were extracted and maintained in collaboration with Professor Lei Shi. Oxygen glucose deprivation experiments summarised in Figure 5.7 and Table 5.11, were carried out in collaboration with Professor Lei Shi. Oxygen glucose deprivation experiments in primary cortical neurons summarised in Figure 5.8 were carried out by Dr. Qinghua Zhang, Dr. Qiaoyun Shi, and Professor Lei Shi at Jinan University, China. Figure 5.8 is adapted from a figure generated by these authors.
Section 5.3.2.1 – Imaging and pixel intensity analysis of neonatal hypoxia ischaemia mouse brains stained with 2,3,5-Triphenyltetrazolium chloride (TTC) was performed by Dr. Anna Hoerder-Suabedissen. Figure 5.9 is adapted from a figure generated by Dr. Anna Hoerder-Suabedissen. Some of the brains depicted in Figure 5.10 were sectioned by Dr. Anna Hoerder-Suabedissen.

Chapter 6
The discussion is based on a book chapter, which I have reproduced here with the kind permission of the editor, Professor Kusal Das of BLDE University, India, and the publishers, InTechOpen, London, UK. The full reference is:
Millar L. J. (2018). "Perinatal and Neonatal Hypoxia Ischaemia; The Unique Challenges of Treating the Infant Brain." In: Kusal Das (ed.), *Hypoxia and Anoxia*, London, InTechOpen, (in press).

Contents

1 Introduction 1
- **1.1 Neurodevelopmental Disorders** 2
  - **1.1.1** Outline of Brain Development 3
- **1.2 The Subplate`** 6
  - **1.2.1** Role of Subplate in Establishing Thalamocortical Connectivity 8
  - **1.2.2** Subplate and Neurodevelopmental Disorders 15
  - **1.2.3** Microarray Investigating Subplate-Enriched Genes 17
- **1.3 Neonatal Hypoxia Ischaemia** 18
  - **1.3.1** Prevalence and Prognosis in Human Neonatal Hypoxia Ischaemia Patients 20
  - **1.3.2** Molecular Pathogenesis of Neonatal Hypoxia Ischaemia 23
  - **1.3.3** Animal Models of Neonatal Hypoxia Ischaemia 36
  - **1.3.4** Subplate in Neonatal Hypoxia Ischaemia 47
  - **1.3.5** Novel Treatment Development 51
- **1.4 Neuroserpin** 54
  - **1.4.1** Molecular Characteristics and Functions of Neuroserpin 54
  - **1.4.2** Neuroprotective Role of Neuroserpin in Adult Hypoxic Ischaemic Stroke and Oxygen-Glucose Deprived Culture 59
  - **1.4.3** Role of Neuroserpin in Neonatal Hypoxia Ischaemia 62
- **1.5 Aims of the Thesis** 64
  - **1.5.1** Aims of Chapter 3: Characterisation of Neuroserpin Protein Expression Throughout Development in Mouse and Human 65
  - **1.5.2** Aims of Chapter 4: Characterisation of Neuroserpin Protein Expression in Rodent Models of Neonatal Hypoxia Ischaemia 66
  - **1.5.3** Aims of Chapter 5: Preliminary Investigations into Vulnerability to Neonatal Hypoxia Ischaemia in the Absence of Neuroserpin Protein, using the *Serpini1* Knock-Out Mouse 67

2 General Methods 68
- **2.1 Experimental Animals** 68
- **2.2 Genotyping** 70
- **2.3 Tissue Collection** 73
- **2.4 Image acquisition** 74
- **2.5 Statistics** 75
- **2.6 Frequently Used Solutions** 76
- **2.7 Non-Quantitative Western Blot** 78
- **2.8 Validation of Primary Antibodies Against Neuroserpin** 83
  - **2.8.1** Validation of Primary Antibodies Against Neuroserpin Protein by Non-Quantitative Western Blot 84
  - **2.8.2** Validation of Primary Antibodies Against Neuroserpin Protein by Fluorescent Immunohistochemistry 92

3 Characterisation of Neuroserpin Protein Expression Throughout Development in Mouse and Human 94
- **3.1 Introduction** 94
  - **3.1.1** Aims of Chapter 3 96

3.2 Methods 98
3.2.1 Immunohistochemistry 98
3.2.2 Quantification of Cell Numbers with Immunohistochemistry 103
3.2.3 Quantification of Cortical Area with Immunohistochemistry 105
3.3 Results 109
3.3.1 Quantification of Cortical Neuroserpin Protein Expression Throughout Development in Mouse 109
3.3.2 Subcellular Localisation of Neuroserpin Protein with Molecular Markers of Endoplasmic Reticulum (ER) and Metabolic Stress 133
3.3.3 Quantification of Cortical Neuroserpin Protein in a Model of Neonatal Neuronal Plasticity, Monocular Enucleation at P1 143
3.3.4 Neuroserpin Protein Expression in Preterm and Neonatal Human Brain Tissue 146
3.4 Discussion 149
3.4.1 Satisfaction of Chapter Aims 149
3.4.2 Developmental Neuroserpin Protein Expression Peak in Subplate Coincides with the End of Natural Neuronal Death in Mouse 151
3.4.3 Conclusions 156

4 Characterisation of Neuroserpin Protein Expression in Rodent Models of Neonatal Hypoxia Ischaemia 157
4.1 Introduction 157
4.1.1 Aims of Chapter 4 159
4.2 Methods 161
4.2.1 Neonatal Hypoxia Ischaemia in Mouse 161
4.2.2 Immunohistochemistry 166
4.2.3 Semi-Quantitative Western Blot 167
4.2.4 Semi-Quantitative Western Blot Analysis 172
4.3 Results 175
4.3.1 Quantification of Neuroserpin Protein Expression Following Neonatal Hypoxia Ischaemia in Rat by Cortical Layer 175
4.3.2 Development of Mouse Model of Neonatal Hypoxia Ischaemia 183
4.3.3 Verification of Cortical Damage Following Neonatal Hypoxia Ischaemia by Adapted Rice-Vannucci Method in Mouse 187
4.3.4 Optimisation of Neonatal Hypoxia Ischaemia Protocol in Mouse 197
4.3.5 Quantification of Neuroserpin Protein Expression Following Neonatal Hypoxia Ischaemia in Mouse by Cortical Layer 206
4.3.6 Semi-Quantitative Analysis of Total Cortical Neuroserpin Protein Following Neonatal Hypoxia Ischaemia in Mouse 214
4.4 Discussion 218
4.4.1 Satisfaction of Chapter Aims 219
4.4.2 Neuroserpin Expression Following Neonatal Hypoxia Ischaemia 220
4.4.3 Evaluation of Methodology 224
4.4.4 Conclusions 228

5 Preliminary Investigations into Vulnerability to Neonatal Hypoxia Ischaemia in the Absence of Neuroserpin Protein, using the *Serpini1* Knock-Out Mouse 229
5.1 Introduction 229
5.1.1 Aims of Chapter 5 231

5.2 Methods 232
5.2.1 Dissociated Neuro-2-A Neuroblastoma Cell Line and Primary Cortical Neuron Culture 233
5.2.2 Oxygen Glucose Deprivation in Dissociated Neurons 239
5.2.3 Adapted Rice-Vannucci Neonatal Hypoxia Ischaemia in the *Serpini1* Knock-Out Mouse 243 241
5.2.4 2,3,5-Triphenyltetrazolium chloride (TTC) Perfusion 247
5.2.5 Analysis of TTC Staining in Whole Brains 249
5.2.6 Immunohistochemistry 252
5.3 Results 253
5.3.1 Neuroprotective Properties of Exogenous Neuroserpin Protein *In Vitro* in Neuro-2-A Neuroblastoma Cells and Primary Cortical Neurons Following Oxygen Glucose Deprivation 253
5.3.2 Brain Damage in *Serpini1* Knock-Out Brains Following Neonatal Hypoxia Ischaemia *In Vivo* 263
5.4 Discussion 276
5.4.1 Satisfaction of Chapter Aims 276
5.4.2 Evaluation of Vulnerability to Neonatal Hypoxia Ischaemia in the *Serpini1* Knock-Out Mouse 277
5.4.3 Evaluation of Methodology 283
5.4.4 Conclusions 287

6 Discussion 289
6.1 Summary of Key Findings 290
6.1.1 Cortical Neuroserpin Protein Expression Peaks in Subplate during Neonatal Development in Mouse and Human 290
6.1.2 Neuroserpin Protein Expression May be Regulated in Subplate Following Neonatal Hypoxia Ischaemia in Rodents 291
6.1.3 Inconclusive Evidence Consistent with Modest Neuroprotective Properties of Neuroserpin Protein in Models of Neonatal Hypoxia Ischaemia 293
6.2 General Discussion 294
6.2.1 Role of Neuroserpin in Brain Development and Neonatal Hypoxia Ischaemia 294
6.2.2 Development of New Therapeutics for Neonatal Hypoxia Ischaemia 305
6.3 Conclusions 314

7 References 317

8 Appendices 445
8.1 Appendix 1 – Summary of Hypoxia-Only Literature 445

Alphabetical List of Abbreviations

α2AP	α 2 antiplasmin
ADD	attention deficit disorder
AMPA	alpha-amino-3-hydroxy-5-methyl-4-isoxazole propionic acid
ASD	autism spectrum disorder
Apsm	abnormal spindle microtubule assembly
Atg7	autophagy related 7
BBB	blood brain barrier
Bcl11b	BAF chromatin remodeling complex subunit
BiP	binding immunoglobulin protein
BrdU	bromodeoxyuridine
C57BL/6	C57 black 6 mouse
CCA	common carotid artery
Cdk5r1	cyclin dependent kinase 5 regulatory subunit 1
CHOP	C/EBP-homologous protein
CPR	cardiopulmonary resuscitation
CNS	central nervous system
CSF	cortico-spinal fluid
CSPG	chondroitin sulphate proteoglycan
CTGF	connective tissue growth factor
DAPI	4′,6-diamidino-2-phenylindole
DMEM	Dulbecco's modified Eagle medium
DMSO	dimethyl sulphoxide
DNA	deoxyribonucleic acid
E(18)	embryonic day (18)
ECM	extracellular matrix
Edg2	endothelial differentiation gene 2
EDTA	ethylenediaminetetraacetic acid
EEG	electroencephalography
(e)GFP	(enhanced) green fluorescent protein
EM	electron microscopy
Epo	erythropoietin
ER	endoplasmic reticulum
FAS	foetal alcohol syndrome
GABA	γ-amino butyric acid
GAPDH	glyceraldehyde 3-phosphate dehydrogenase
GFAP	glial fibrillary acid protein
Gli3	glioma-associated oncogene family zinc finger protein 3
HBS	Hank's balanced salt solution
HI	hypoxia-ischaemia
HIE	hypoxic ischaemic encephalopathy
HIF-1	hypoxia inducible factor 1
HRP	horseradish peroxidase
HSP	heat shock protein
Iba1	ionised calcium binding adaptor molecule 1
Ibfbp5	insulin-like growth factor binding protein 5
IL-1ß	interleukin-1ß
IL-6	interleukin-6

IL-9	interleukin-9
IZ	intermediate zone
KDEL	lysine-glutamic acid-aspartic acid-leucine amino acid sequence
KO	knock-out mouse (refers to strain B6.129-Serpini1^{tm1Dpw}/J)
LCC	left common carotid artery
Lpar1	lysophosphatidic acid receptor 1
LPS	lipopolysaccharide
Map1b	microtubule-associated protein 1 B
MAP-2	microtubule-associated protein 2
MBP	myelin basic protein
MEM	Eagle's minimum essential medium
MRI	magnetic resonance imaging
mRNA	messenger ribonucleic acid
MRS	magnetic resonance spectroscopy
MTT	3-(4,5-dimethylthiazol-2-yl)-2,5-diphenyltetrazolium bromide
MZ	marginal zone
N2A	Neuro-2-A neuroblastoma cell line
NE	Neonatal encephalopathy
NeuN	Neuronal Nuclei
NIHS	National Institute of Health, Swiss
NMDA	*N*-methyl-D-aspartate
Nptx1	neuronal pentaxin 1
Nurr1	nuclear receptor related 1 protein
Olig2	oligodendrocyte transcription factor 2
OGD	oxygen glucose deprivation
P(8)	postnatal day (8)
PAI1	plasminogen activator inhibitor 1
PBS(-A)	phosphate buffer solution (plus sodium aside)
PCR	polymerase chain reaction
PCW	post-conceptional weeks
PKG-NEO	neomycin resistance gene under phosphoglycerate kinase 1 promotor
PFA	paraformaldehyde
Plat	plasminogen activator, tissue type (gene)
poly(I:C)	polyinosinic-polycytidylic acid
PTFE	polytetrafluoroethylene
PVDF	polyvinylidene fluoride or polyvinylidene difluoride
PWM	periventricular white matter
RCC	right common carotid artery
Rbfox3	RNA-binding Fox1 homologue 3
Reln	reelin
rER	rough endoplasmic reticulum
RG	radial glia
RT	room temperature
S1	primary somatosensory cortex
Satb2	special AT-rich sequence-binding protein homeobox 2
Serpini1	serine protease inhibitor, Clade I, member 1 (neuroserpin gene)
Sox5	sex-determining region Y related homeobox 5
SVZ	subventricular zone
Tbr1	T-box, brain 1
TNFα	tumour-necrosis factor-α

tPA	tissue plasminogen activator
TTC	2,3,5-triphenyl tetrazolium chloride
TUNEL	terminal deoxynucleotidyl transferase dUTP nick-end labeling
uPA	urokinase plasminogen activator
V1	primary visual cortex
VEGF	vascular endothelial growth factor
Vol. I, II	volume I or II of this thesis, volume II contains Appendix 8.2
VZ	ventricular zone
WT	wild-type mouse (non-transgenic, refers to C57BL/6 or NIHS)

1 Introduction

Almost every aspect of human experience is mediated by the brain. Perception, movement, social interaction, and "higher cognition" which allows humans to master language and abstract thought, are all dependent on healthy brain cells (reviewed in Frackowiak, 2004; Bear et al., 2007; Kandel, 2013; Squire et al., 2012). To accommodate these diverse functions, the human brain is one of the most complex processors in the natural world (Tononi et al., 1994; Sporns, 2002; reviewed in Bullmore and Sporns, 2009; 2012). Building a brain from sheets of undifferentiated stem cells therefore requires precisely regulated genetic and environmental signals to correctly orchestrate construction (reviewed in Price et al., 2011; Sadler, 2011; Schoenwolf et al., 2014).

When one or more of these pathways are disrupted, redundant signals may support the brain to normal maturation (Glassman, 1987; Wegner and Stolt, 2005). However, disrupted brain development can result in permanently abnormal connectivity. This broad group of clinical presentations associated by the developmental window of first presentation but with diverse aetiology are described as "neurodevelopmental disorders" (Tager-Flusberg, 1999; Hansen and Rogers, 2012). Recognised neurodevelopmental disorders include; foetal alcohol syndrome (FAS), cerebral palsy, neonatal hypoxia-ischaemia (HI), schizophrenia, autism spectrum disorder (ASD), attention deficit disorder (ADD), and many others, all associated with lasting morbidity (American Psychiatric Association, 1994; 2013). These often present during childhood or adolescence, suggesting the pathophysiological origin occurred

before the brain was fully developed (reviewed in Weinberger, 1995; Stolp and Dziegielewska, 2009; Brandon and Sawa, 2011).

There are clear motivations for investigating the elusive neurodevelopmental origins of these conditions: a better understanding of patient cognition, earlier diagnosis, and development of potential treatments. A comprehensive analysis across all neurodevelopmental disorders will require many decades of intensive research. Yet there are important questions a single research project can address. This thesis focuses on the role of the transitory neocortical neurons within the subplate, and subplate-enriched putative neuroprotective protein neuroserpin, in animal models of neonatal hypoxia ischaemia (HI). This introduction outlines current scientific understanding of the disorder and reasons for investigating subplate and the protein neuroserpin.

1.1 Neurodevelopmental Disorders

Neurodevelopmental disorders are defined by sensory, motor and/or cognitive dysfunction which initially present during childhood or adolescence (reviewed in Bale et al., 2010; American Psychiatric Association, 1994; 2013). The most common functional limitations concern mobility (18%), communication (22%), and learning and cognition (24%) (Department of Work and Pensions, 2012; 2013). The cost to the National Health Service (NHS) in the UK of just one of these disorders, ASD, is over £4 million annually (Knapp et al., 2007; 2009; Buescher et al., 2014), and yet many people diagnosed with neurodevelopmental disorders have low socioeconomic status and impaired opportunities (Department of Work and Pensions, 2013; Jones et al.,

2012). Understanding these disorders and offering more effective therapies is of high priority for improving quality of life.

1.1.1 Outline of Brain Development

Embryonic development of the central nervous system (CNS) from ectoderm begins early in embryogenesis (reviewed in Price et al., 2011; Sadler, 2011; Schoenwolf et al., 2014). Although there are significant differences between species, many aspects of the gross anatomy of brain development is greatly conserved between mammalian species (Clancy et al., 2007; Pressler and Auvin, 2013; Semple et al., 2013; Miller et al., 2014). Development of the CNS has been divided into stages (reviewed in Epstein, 1986; Hudspeth and Pribram, 1990; Temple, 2001; O'Rahilly and Müller, 2006). Each stage has its own complex set of regulators, all of which are open to vulnerability (reviewed in Dobbing, 1974; Shore, 1997; Andersen, 2003; Atkinson and Braddick, 2010; Semple et al., 2013), each meriting close study.

1.1.1.1 Cortical Development

The six-layered neocortex, the most phylogenetically recently evolved portion of the cerebral cortex, is formed from the developing forebrain. Cerebral cortex forms a sheet superficial to the rest of the brain (reviewed in Price et al., 2011; Sadler, 2011; Schoenwolf et al., 2014). In the adult brain, the cortex is organised in six distinct layers (Brodmann, 1909; von Economo and Koskinas, 1925; reviewed in Shipp, 2007; Rockland and DeFelipe, 2018) which can be identified by characteristic cell morphology, density, and specific molecular markers (Molyneaux et al., 2007).

Neurons within each layer demonstrate specific connectivity (Gilbert and Kelly, 1975; Gilbert, 1983), which contributes to the function of columnar cortical units (reviewed in Thomson and Bannister, 2003; Douglas and Martin, 2004; Lubke and Feldmeyer, 2007; Thomson and Lamy, 2007; Gao et al., 2013). The major input to the cortex in the adult brain originates from the thalamus projecting to Layer IV, whereas Layer V and VI of cortex mediate cortical output (Caviness and Frost, 1980; reviewed in Sherman and Guillery, 2013). A summary of adult cortical structure is shown in Figure 1.1.

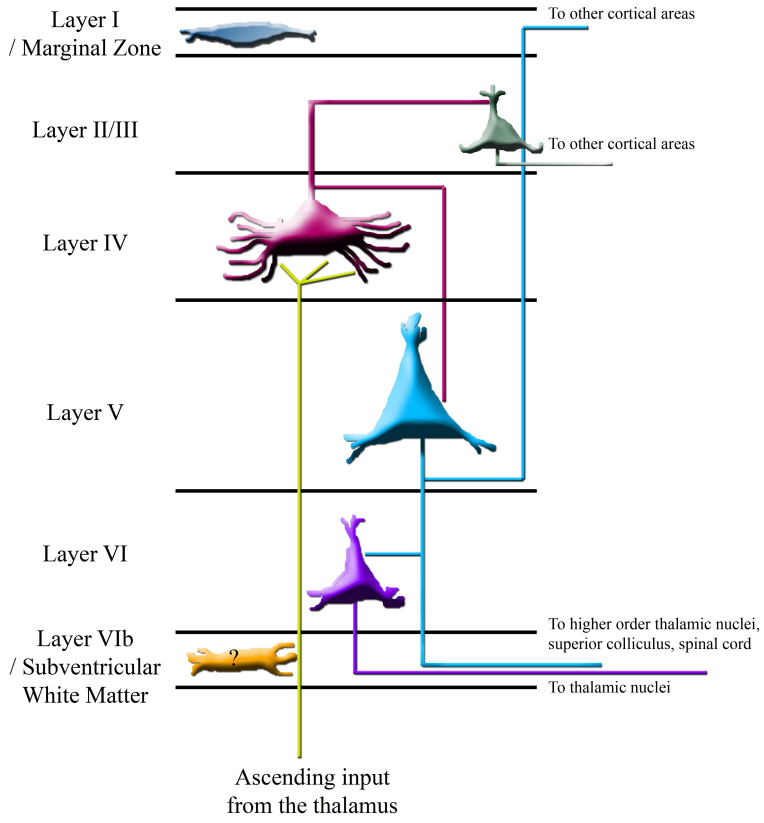


Figure 1.1 – Schematic Diagram of Cortical Structure and Classical Connection in the Adult Mammalian Brain. The primary type of glutamatergic neuron in each of the six established cortical layers are shown alongside the destination of the major projections from these neurons. The major input to the cerebral cortex is from the thalamus onto Layer IV, and the output Layers V and VI project to many structures throughout the brain. Neurons have been marked in the interstitial white matter, although the connectivity and any functional role for these neurons in adult animals in not currently known. Adapted from Sherman and Guillery, *Exploring the Thalamus*, 2nd Edition, 2009.

Neuronal circuitry within the neocortex is widely believed to contribute to a range of higher cognitive processes including language, sensory processing, and abstract thought (reviewed in Fuster, 2003; Elston, 2003; Rugg, 2013; Güntürkün and Bugnyar, 2016).

Cortical glutamatergic and GABAergic neurons are generated in different proliferative zones and follow different migration paths to cortex (reviewed in Kriegstein and Noctor, 2004; Molyneaux et al., 2007). The first glutamatergic cortical neurons are generated in the ventricular zone (VZ), a layer of stem cells in the telencephalon lining the lateral ventricles (Angevine and Sidman, 1961; Noctor et al., 2004). Within the ventricular zone, pluripotent stem cells known as radial glia (RG) undergo asymmetric mitosis to produce a second radial glia and a cortical neuron (Malatesta et al., 2003; Miyata et al., 2001; Noctor et al., 2001; 2002; 2004; Anthony et al., 2004). The newly generated cortical neurons then migrate along the process of the radial glia towards the pial surface (Mission et al., 1991; Hatanaka and Murakami, 2002; reviewed in Rakić, 1990; Kreigstein and Noctor, 2004). Glutamatergic and GABA-ergic cortical neurons are also generated in the subventricular zone (SVZ) (Letinic et al., 2002; Haubensak et al., 2004; Miyata et al., 2004; Noctor et al., 2004; Wu et al., 2005) superficial to the VZ, while the majority of GABA-ergic cortical interneurons originate in the subcortical ganglionic eminences and migrate into the cortex (de Car los et al., 1996; Lavdas et al., 1999; Xu et al., 2003).

Deep cortical layers are born first, with the superficial layers migrating through the deep layers to reach the pial surface, generating the cortex in an “inside out” arrangement (Angevine and Sidman, 1961; Berry and Rogers, 1965; Luskin and Shatz, 1985; Mission et al., 1991; Hatanaka and Murakami, 2002; reviewed in Rakić,

1990; Kreigstein and Noctor, 2004; Tan and Shi, 2013). The earliest born cortical neurons migrate through the ventricular zone to form the preplate, which then splits into the superficial marginal zone and the deep subplate, with later generated neurons settling between these two layers (Marin-Padilla, 1971; Luskin and Shatz, 1985; reviewed in Del Rio et al., 2000).

1.2 The Subplate

The subplate is an early-born transitory neuronal layer of neocortex (reviewed in Kostović and Judaš, 2010; Kanold and Luhmann, 2010; Hoerder-Suabedissen and Molnár, 2015). Subplate can be identified in a range of mammals by expression of conserved molecular markers (Hoerder-Suabedissen et al., 2009; Oeschger et al., 2012; Hoerder-Suabedissen and Molnár, 2013). Functional roles for subplate in the formation of mature thalamocortical (reviewed in Allendoerfer and Shatz, 1994; Kanold and Luhmann, 2010) and corticothalamic (Grant et al., 2012; 2016) connectivity during development have been described in rodent.

Early anatomical studies do not identify subplate as a functionally-distinct cortical population, although these transitory neurons in white matter have been documented historically (reviewed in Judaš et al., 2010). Discovery of subplate was prompted by findings that cortical neurons in embryonic sheep respond to nasal sensory stimulation (Molliver, 1967). Electron microscopy identifies synapses above the intermediate zone (IZ) in human foetal cortex (Kostović and Molliver, 1974), a population which has become known as the subplate. Extensively described in macaque and human by Nissl-staining (Kostović and Rakić, 1980), subplate is present during the third

trimester of pregnancy, then largely disappears from these preparations after infancy (Kostović and Rakić, 1990). The subplate zone is recognised as a "waiting compartment" for developing cortical afferents (Kostović and Krmpotic, 1976; Krmpotic-Nemanic et al., 1983; Kostović and Goldman-Rakić, 1983; Kostović and Rakić, 1984; 1990; Kostović, 1986) and a site of early functional synapses (Friauf et al., 1990; Friauf and Shatz, 1991). A general schematic of subplate development is shown in Figure 1.2.

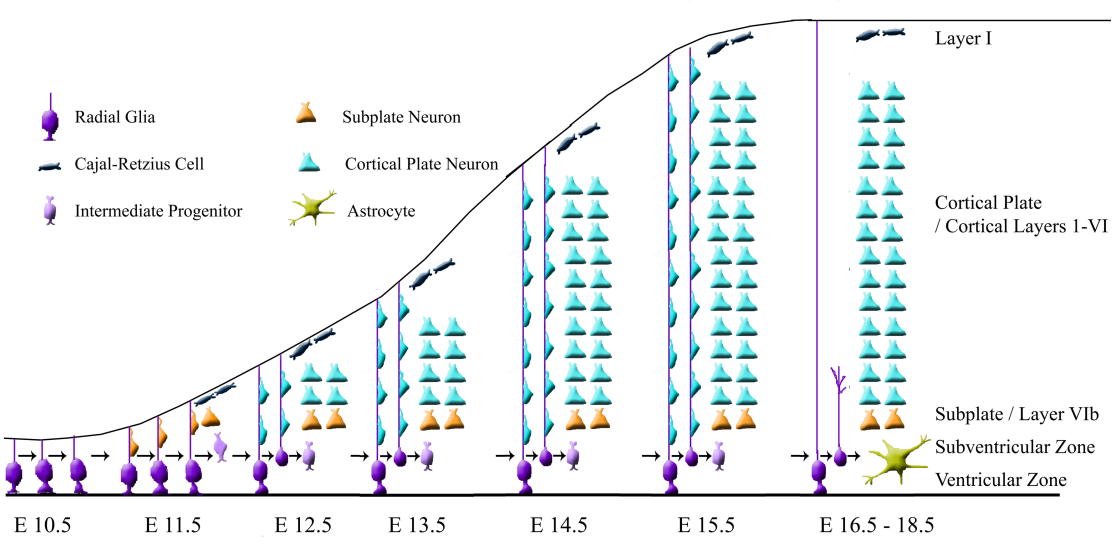


Figure 1.2 – Schematic of Neurogenesis and Neuronal Organization in Developing Mouse Cerebral Cortex. Radial glia (RG) in the ventricular zone (VZ) begin to undergo asymmetric cell division to give rise to projection neurons around E10.5. Simultaneously, radial glia generate intermediate progenitors and outer radial glia, which establish the subventricular zone (SVZ). The SVZ also contributes to neurogenesis. After neurogenesis is complete, neural progenitors transition to a gliogenic phase, producing astrocytes and oligodendrocytes. Subplate neurons (orange) are amongst the earliest born population of cortical neurons, generated between E10.5 and E13.5. These migrate to form a relative mature lamina directly above the zones of neurogenesis. Cajal–Retzius cells primarily migrate into Layer I from non-cortical locations, whereas other projection neurons are born in the neocortical VZ or SVZ and migrate along radial glial processes to reach their laminar destinations. Adapted from Greig et al., 2013.

It is accepted that the majority of subplate neurons undergo natural cell death during early infancy. The density of neurons labelled with neuronal nuclei (NeuN) marker

within human white matter decreased sharply throughout the first year of life, but remained stable thereafter (Connor et al., 2009). A similar loss of early-born NeuN-labelled subplate neurons has been reported in mouse (Price et al., 1997; Hoerder-Suabedissen and Molnár, 2013), and golden hamster (Woo et al., 1991), with a smaller proportion of subplate neurons lost in rat (Valverde et al., 1995; Robertson et al., 2000). Examination with neuronal markers (Chun et al., 1987; Hamre et al., 1989) demonstrate that subplate cells are among the first neocortical neurons to express molecular markers associated with maturity. Analysis with markers of cell death (Al-Ghoul and Miller, 1989; Hamre et al., 1989), confirm that subplate disappearance is due to apoptosis. The molecular mechanisms behind this programmed cell-death remain largely unknown (reviewed in McQuillen and Ferriero, 2005; Hoerder-Suabedissen and Molnár, 2015).

The subplate is essential for normal cortical development in mammals, with important roles in thalamocortical circuit formation (reviewed in Allendoerfer and Shatz, 1994; Kanold and Luhmann, 2010). This transitory lamina is also beginning to be associated with neurodevelopmental disorders (reviewed in Suarez-Sola et al., 2009; Kostović, et al., 2011; Hoerder-Suabedissen and Molnár, 2015), particularly as a site of potential sensitivity to damage in neonatal hypoxia ischaemia (reviewed in Millar et al., 2017).

1.2.1 Role of Subplate in Establishing Thalamocortical Connectivity

Subplate was implicated in the development of thalamocortical circuitry shortly after its discovery. Early anatomical studies observe that thalamocortical axons associate with and grow alongside subplate neurons (Herrmann et al., 1994; Molnár et al., 1998a), and synapses form between these neurons (Herrmann et al., 1994; Kostović

and Judaš, 2006). These histological results have since been confirmed by electrophysiology (Hanganu et al., 2002; Molnár et al., 2003a; Zhao C. et al., 2009; reviewed in Kanold and Luhmann, 2010).

Selective ablation of subplate neurons demonstrates that these synapses are essential for establishment of normal thalamocortical circuitry (reviewed in Hoerder-Suabedissen and Molnár, 2015). Loss of subplate at various developmental time-points disrupts thalamocortical connectivity. Prior to the critical period, when direct thalamocortical inputs onto Layer IV are being established (reviewed in Kanold, 2009; Kanold and Luhmann, 2010), ablation of subplate in mouse prevents thalamic afferents from entering the telencephalon (Ghosh et al., 1990; Magnani et al., 2013). Selective subplate lesioning by excitotoxic injections (Ghosh et al., 1990; Lein et al., 1999; Ghosh and Shatz, 1992a; Kanold and Shatz, 2006) or a p75-immunotoxin injection (Kanold et al. 2003; Kanold and Shatz, 2006) results in a lack of organised synaptic input from the thalamus on to Layer IV. Following ablation concurrent with monocular deprivation, thalamocortical projections representing the deprived eye are retained, whereas those representing the open eye are removed (Kanold et al., 2003; Kanold and Shatz, 2006; Zhao C. et al., 2009). In the absence of subplate, the "handshake" between subplate and thalamocortical axons (Molnár and Blakemore, 1995; Kostović and Jovanov-Milošic, 2006; reviewed in Lopez-Bendito and Molnár, 2003) cannot occur, and thalamic axons fail to cross the pallial–subpallial boundary.

Later in development, during or after the critical period, excitotoxic or immunotoxic ablation of subplate prevents: strengthening of thalamocortical synapses onto Layer IV neurons, precluding formation of ocular dominance columns (Kanold, et al., 2003; Kanold and Shatz, 2006); barrel field formation (Tolner et al., 2012); normal

synchronous cortical oscillatory activity (Dupont et al., 2006); and maturation of Layer IV inhibition (Kanold et al., 2003). Few researchers have investigated the effect on cortical and thalamic inputs to the subplate outside primary somatosensory (S1) or visual (V1) cortex (Viswanathan et al., 2012; Meng et al., 2014; reviewed in Hoerder-Suabedissen and Molnár, 2015).

Altered development or migration of subplate also disrupts thalamocortical connectivity. For example, the *Reln* mutant mouse, which does not produce functional reelin protein, exhibits development of cortical laminae below the preplate, thalamic afferents grow obliquely through the cortical plate to target the marginal zone (MZ) before invading Layer IV (Caviness and Sidman, 1973; Molnár et al., 1998b; reviewed in Tissir and Goffinet, 2003). Other models of subplate disruption include a mouse with a mutation in the gene *Cdk5r1*, encoding cyclin dependent kinase 5 regulatory subunit 1, in which late-born cortical neurons fail to migrate through subplate (Kwon and Tsai, 1998; Rakić et al., 2006). In the naturally occurring Gli3Xt/Xt mouse, expressing a mutation in the gene encoding glioma-associated oncogene family zinc finger protein 3, subplate neurons fail to be generated (Magnani et al., 2013; Chen et al., 2012). Both models demonstrate misguidance of thalamic afferents into the marginal zone (Kwon and Tsai, 1998; Rakić et al., 2006; Chen et al., 2012). However, in the *Sox5* (sex-determining region Y related homeobox gene 5) knockout mice, in which connective tissue growth factor (*Ctgf*) mRNA-expressing subplate neurons are located throughout cortex, corticothalamic projections form relatively normally (Lai et al., 2008).

Physiological experiments confirm the importance of subplate in the development of thalamocortical circuitry (McConnel et al., 1989; 1994; reviewed in Allendoerfer and

Shatz, 1994; Friedlander and Torres-Reveron, 2009; Kanold and Luhmann, 2010). In neonatal rat (Hanganu et al., 2001; 2002), foetal cat (Friauf et al., 1990), and foetal human tissue (Mrzljak et al., 1988; 1992), subplate neurons show extensive axonal and dendritic arborisation within subplate. Subplate neurons project to the cortical plate (Friauf et al., 1990; Finney et al., 1998; Clancy and Cauller 1999), and send long-range axons to thalamus (McConnell et al., 1989; Kim et al., 1991; De Carlos and O'Leary, 1992). Subplate neurons have mature passive and active membrane properties compared to other neurons in neonatal cortex in whole-cell patch-clamp recordings (Friauf et al., 1990; Luhmann et al., 2000; Hanganu et al., 2001; 2002; Hirsch and Luhmann 2008; Moore et al., 2009; 2011). In neonatal rats, one subplate neuron is electrically coupled by gap junctions to an average of nine other neurons (Dupont et al., 2006), forming a columnar cortical network.

Subplate neurons receive synaptic inputs and generate action potentials throughout embryonic development (Hanganu et al., 2001; Kanold et al., 2003; Luhmann et al., 2009). Thalamic axons arrive in the subplate around the time Layer IV cells are born, and wait in subplate before growing into Layer IV (Kageyama and Robertson, 1993; Ghosh and Shatz 1993; Molnár et al., 2003). These thalamic-subplate glutamatergic synapses are functional (Friauf et al., 1990; Hanganu et al., 2002; Higashi et al., 2002; Molnár et al., 2003; Hirsch and Luhmann, 2008; Zhao C. et al., 2009). This input is then relayed by transitory circuitry to Layer IV of cortex. Electrical white matter stimulation in neonatal cat primary visual cortex results in short latency responses in subplate and long latency responses in Layer IV, indicating that subplate neurons strongly excite Layer IV neurons (Friauf and Shatz, 1991). At later developmental stages, short latency responses to white matter stimulation start to emerge in Layer IV (Higashi et al., 2002; Molnár et al., 2003; Zhao C. et al., 2009), demonstrating the loss

of subplate relay circuitry and the emergence of direct synapses between thalamic projection neurons and Layer IV neurons. Layer IV temporarily receives innervation from both subplate and thalamus (Kanold et al., 2003; Kanold, 2004), followed by removal of subplate inputs through a competitive process (Friauf et al., 1990; Kanold et al., 2003). A schematic of these developing synapses can be seen in Figure 1.3.

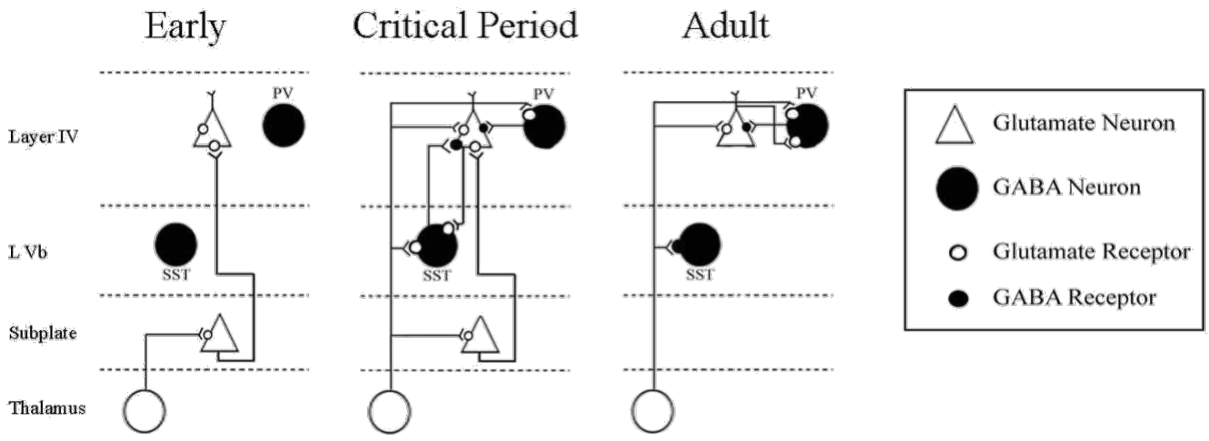


Figure 1.3 – Classical Schematic of Subplate Architecture Throughout Development. In the earliest phase of thalamocortical circuit establishment subplate neurons (white) receive inputs from thalamus, and project axons to Layer IV. At the onset of critical period, both subplate and thalamic neurons project to Layer IV directly. In the adult, subplate neurons have been eliminated by programmed cell death and Layer IV neurons receive inputs only directly from thalamus. The classical view has been augmented by the inclusion of GABA-ergic (black) Layer Vb interneurons which have been demonstrated to contribute to the development of thalamocortical circuitry in murine primary somatosensory cortex (S1) (Marques-Smith et al., 2016; Anastasiades et al., 2016). Adapted from Kanold, 2009.

Beyond this classical role, understanding of subplate function continues to evolve. GABA-ergic subplate neurons have been observed by immunohistochemistry studies in rat (van Eden et al., 1989) and primate (Meinecke and Rakić, 1992), where comparison of these two studies suggest a greater proportion of GABA-ergic neurons in the subplate of the rhesus macaque. Although these GABA-ergic neurons remain understudied, electrophysiological experiments have identified a minimum of two

subtypes based on connectivity pattern and birth dating in rats (Voigt et al., 2001) and several subpopulations of GABA-ergic subplate neurons have been identified based on expression of molecular markers in ferret (Antonini and Shatz, 1990). More results from dissociated cortical culture suggest both glutamatergic (Sun and Luhmann, 2007; Yang et al., 2009) and GABAergic subplate neurons (Voigt et al., 2001) may contribute to synchronous oscillatory network activity. Another potentially interesting development is the discovery of transitory thalamic projections to a population of Layer V interneurons which in turn project to Layer IV (Marques-Smith et al., 2016; Anastasiades et al., 2016), suggesting that subplate plays an interactive role with other neurons in establishing thalamocortical architecture.

Additionally, persistent subplate neurons in periventricular white matter may retain synaptic input to other cortical layers (Torres-Reveron and Friedlander, 2007; reviewed in Friedlander and Torres-Reveron, 2009). Although the connectivity map of neurons in the subplate zone of adult rodents or humans has not been determined (reviewed in Friedlander and Torres-Reveron, 2009), extensive dendritic branching has been characterised (Torres-Reveron and Friedlander, 2007), and results of birth-dating (Chun and Shatz, 1989) and electrophysiology studies (Torres-Reveron and Friedlander, 2007) have found subplate characteristics in adult interstitial white matter neurons. Therefore, the physiological role of subplate in the developing cortex is far from fully understood.

1.2.1.2 Comparative Anatomy and Development of Subplate

Evolutionary data suggests that human subplate may demonstrate unique anatomical complexity (Kostović and Rakić, 1980; 1990; Wang et al., 2010) and increased

variation in subplate cell types (Mrzljak et al., 1988; 1990; 1992). This enlarged subplate may play a qualitatively different role in humans compared to other mammals (reviewed in Judaš et al., 2013).

Subplate thickness, relative to the rest of developing cortex, is substantially greater in human compared to other mammals, human subplate is estimated to be twice the thickness ratio seen in macaque (Kostović and Rakić, 1990). Four stages of subplate development are demonstrable in humans (Kostović and Rakić, 1990; Kostović et al., 2002; Judaš et al., 2005; Bayatti et al., 2008; Corbett-Detig et al., 2011). However, these stages are less clear in rodents, with early subplate difficult to distinguish from intermediate zone (Kostović and Molliver, 1974; Bayatti et al., 2008; reviewed in Hoerder-Suabedissen and Molnár, 2015). Loss of the majority of subplate neurons occurs six months after birth in human (Kostović and Rakić, 1980; 1990; Perkins et al., 2008), compared to a persistent presence in rodent (Price et al., 1997; Robertson et al., 2000; Hoerder-Suabedissen and Molnár, 2013). In addition, the number of interneurons reported in subplate varies between mouse (Del Rio et al., 1992), rat (Luth et al., 1994) ferret (Antonini and Shatz, 1990), cat (Mizukawa et al., 1989; Chun and Shatz, 1989; Wahle et al., 1994) and human (Yan et al., 1992; Zecevic and Milocevic, 1997; Garcia-Marin et al., 2010; reviewed in Kostović et al., 2014), although this may reflect different methodologies (Estrada and De Felipe, 1998; Moore et al., 2009).

Golgi staining in the prefrontal cortex of human foetal and neonatal tissue identifies several distinct morphological subtypes of subplate neuron, including fusiform, inverted pyramidal, and multipolar non-pyramidal neuronal morphology (Mrzljak et al., 1988; 1992). These studies noted a particular abundance of “polymorphic”

neurons in neonatal human subplate (Mrzljak et al., 1988), defined as having cell bodies of multiple different shapes and patterns of dendritic arborisation. These polymorphic neurons could represent a number of physiologically distinct subtypes. This diversity in cell types may be unique to the developing brain, and large scale *in situ hybridisation* studies in adult human only propose two subtypes of subplate neuron, the mostly glutamatergic subplate neurons in Layer VIb, and the mostly GABA-ergic persistent interstitial white matter neurons (Zeng et al., 2012).

Yet many characteristics are conserved between species. Certain molecular markers specific to subplate neurons are expressed across species, including mouse and human (Wang et al., 2010; Miller et al., 2014). This shared genetic profile supports the rationale for studying rodent subplate to better understand how this short-lived structure contributes to brain function in human.

1.2.2 Subplate and Neurodevelopmental Disorders

Evidence continues to emerge that damage to subplate may occur in some neurodevelopmental disorders (reviewed in Gressens, 2005; Suarez-Sola et al., 2009; Kostović et al., 2011; Hoerder-Suabedissen and Molnár, 2015). In humans, the peak of subplate development coincides with the gestational age of highest vulnerability to preterm periventricular white matter injury, estimated to occur between 24-32 post-conceptional weeks (Bunney et al., 1997; Back et al., 2001; reviewed in McQuillen and Ferriero, 2005).

In post-mortem human tissue, adult schizophrenia patients demonstrate increased populations of surviving subplate neurons in the periventricular white matter (PWM)

(Akbarian et al., 1993a; 1993b; 1996; Eastwood and Harrison, 2003; 2005; reviewed in Kostović et al., 2011). However, these abnormalities are found in only 35% of subjects (Akbarian et al., 1996), with other studies failing to document any difference (Beasley et al., 2002). In adolescent and adult schizophrenic subjects, imaging studies show increased thickness of periventricular white matter (reviewed in Bunney and Bunney, 2000; Kubicki et al., 2007; Kyriakopoulos et al., 2008). Similar post-mortem investigations in autism spectrum disorder (ASD) subjects also identify increased density of persistent subplate neurons in the temporal lobe of a minority of individuals (Hutsler et al., 2007; Avino and Hutsler, 2010). Although this supports a role for subplate in developmental brain disorders, work in adult humans will always be limited as the majority of subplate cells have undergone apoptosis (Kostović and Rakić, 1990; reviewed in Hoerder-Suabedissen and Molnár, 2015).

A plethora of other neurodevelopmental disorders have been proposed to include a subplate phenotype. A human chromosomal disorder 22q11 deletion syndrome subject exhibited an excess of periventricular interstitial white-matter neurons, although this pathology could have been caused by abnormal neuronal migration or persistence of subplate neurons, the subject also had a mixed condition including a heart condition not commonly associated with 22q11 deletion syndrome (Wu et al., 2014). In the trisomy 16 mouse, subplate neurons are generated relatively late at embryonic day 13.5 (E13.5) as demonstrated by bromodeoxyuridine (BrdU) brith-dating (Cheng et al., 2004). A transgenic mouse in which the microcephaly gene abnormal spindle microtubule assembly (*Aspm*) has been knocked-out demonstrates an abnormally high level of transcription factors T-box brain 1 (*Tbr1*) and special AT-rice sequence-binding protein homeobox 2 (*Satb2*) in the subplate (Fujimori et al., 2014). It has been proposed that cortical dysplasia associated with pharmaco-resistant

epilepsy could be related to postnatal retention of subplate (Emery et al., 1997; Thom et al., 2001; Cepeda et al., 2007; reviewed in Friedlander and Torres-Reveron, 2009). However, all these conditions are also associated with diverse alterations to neuronal and glial function throughout the brain, making it difficult to assess the importance of deviations in subplate function to overall pathology.

This eclectic range of results hint towards disabling effects of abnormal subplate, yet also reveal the dearth of investigations into subplate anatomy and function across more common and idiopathic brain disorders. A great deal of work in animals and humans is required before more general theories about subplate contribution to neurodevelopmental disorders can be formulated.

1.2.3 Microarrays Investigating Subplate-Enriched Genes

A concurrent approach to investigating subplate in neurodevelopmental disorders employs transcriptomics. The transcriptome of mouse subplate neurons has been analysed at several developmental stages (Hoerder-Suabedissen et al., 2009; 2013; Osheroff and Hatten, 2009; Belgard et al., 2011; Oeschger et al., 2012), along with transcriptomes of human embryonic, foetal and adult cortex (Johnson et al., 2009; Kang et al., 2011; Miller et al., 2014). Analysis of subplate-specific gene expression for functional annotation highlights the relative maturity of subplate in mouse and human (Hoerder-Suabedissen et al., 2013; Miller et al., 2014).

Functions associated with subplate-enriched gene expression in mouse include: axon extension and pathfinding (Oeschger et al., 2012; Hoerder-Suabedissen et al., 2009; 2013; Osheroff and Hatten, 2009); synaptic maturation (Oeschger et al., 2012;

Hoerder-Suabedissen et al., 2013; Osheroff and Hatten, 2009); myelination (Hoerder-Suabedissen et al., 2013); cell death and apoptosis (Hoerder-Suabedissen et al., 2013; Oeschger et al., 2012; Osheroff and Hatten, 2009); regulation of cell division (Belgard et al., 2011; Oeschger et al., 2012; Hoerder-Suabedissen et al., 2013); cellular secretion (Hoerder-Suabedissen et al., 2013; Kondo et al., 2015); and oestrogen-regulated signalling (Osheroff and Hatten, 2009).

In addition to functional correlations, one study screened genes enriched in mouse subplate at P8, the developmental time-point associated with birth in human (Clancy et al., 2007), against databases of known autism, schizophrenia and Alzheimer's risk genes (Hoerder-Suabedissen et al., 2013). Significantly more risk genes are subplate-enriched or subplate-specific than would have been expected by chance, including 11 autism risk-associated genes and 10 schizophrenia risk-associated genes (Sun et al., 2009; Pinto et al., 2010; Mowry and Gratten, 2013). There is no significant enrichment of Alzheimer's disease risk genes subplate compared to cortical Layer VI. Additionally, of the 1,000 genes which undergo increased expression in subplate during preplate splitting, 88% of identified non-syndromic intellectual disability genes are expressed at this time (Olson, 2014). This provides strong rationale for further investigating subplate specifically in neurodevelopmental disorders.

1.3 Neonatal Hypoxia Ischaemia

One neurodevelopmental disorder in which the role of subplate and other developing cortical layers remains far from understood is neonatal hypoxia ischaemia (HI). The classical clinical definition of neonatal HI injury is "asphyxia of the umbilical blood

supply to the human foetus occurring at 36 gestational weeks or later" (Perlman, 1997; 2006; Volpe, 2001; 2012; Shah et al., 2006). Neonatal HI is synonymous with hypoxic-ischaemic encephalopathy (HIE) occurring in the term infant, where "term" is defined as 36 gestational weeks or later. A more modern definition of neonatal HI, also known as neonatal encephalopathy (NE), is: "a condition occurring in babies born over 35 weeks gestational age in which there is disturbed neurological function. The key feature is the disturbance in the degree or quality of consciousness; other features, such as seizures, cardiorespiratory compromise or abnormal tone and reflexes, may occur alongside it but are not necessary to make the diagnosis" (Task Force on Neonatal Encephalopathy, 2014; Martinello et al., 2017b). This disorder encompasses a wide range of physiological origins and clinical outcomes in human patients (reviewed in Volpe, 1995).

Neonatal hypoxia ischaemia remains a common birth complication throughout the world, associated with high incidence of persistent disability in survivors. Many complex molecular pathways exacerbate brain damage caused by hypoxia ischaemia, several of which also contribute to healthy brain development. Finding new safe treatments which reduce brain damage without compromising normal development, or at the very least increasing scientific understanding of the neonatal brain's response to hypoxia, is essential to care and treatment of these individuals. The current mixed evidence on the effect of neonatal HI on subplate highlights how much remains to be empirically understood.

1.3.1 Prevalence and Prognosis in Human Neonatal Hypoxia Ischaemia Patients

The diagnostic criteria for neonatal hypoxia ischaemia are based on a set of markers demonstrated to correlate with clinical outcome (reviewed in Finer et al., 1981; Perlman, 1997; Richer et al., 2001). These include: 5-min Apgar score of less than 5 (Levene et al., 1986; Finer et al., 1981; Ruth and Raivio, 1988; Laptook et al., 2009); need for delivery room intubation or cardio-pulmonary resuscitation CPR (Salhab et al., 2004a; reviewed in Shalak and Perlman, 2004; Kattwinkel et al., 2010); umbilical cord arterial pH less than 7.00 (Ruth and Raivio, 1988; Perlman and Risser, 1993; Robertson et al., 2002; Salhab et al., 2004b); and abnormal neurological signs, such as hypotonic muscles or lack of sucking reflex (Levene et al., 1986; Robertson et al., 1989; Thomson et al., 1997; Richer et al., 2001). Electroencephalography (EEG) has also proved helpful as a predictor of clinical outcome (reviewed in Walsh et al., 2011; van Laerhoven et al., 2013; Horn et al., 2016; Weeke et al., 2017). This is by no means an exhaustive list of risk factors and signs of clinical concern that can occur during the early postnatal period (reviewed in Shalak and Perlman, 2004; Hagberg et al., 2015).

Neonatal HI is the most common cause of death and disability in human neonates (reviewed in Grow and Barks, 2002; Ferriero, 2004; Shalak and Perlman, 2004), accounting for 23% of infant mortality worldwide, and affecting 0.7–1.2 million infants annually (Lawn et al., 2005). In developed countries, incidence of HI injury has not decreased in the past two decades (Himmelmann et al., 2005; Vincer et al., 2006), remaining a significant cause of fatality and disability. The frequency of motor and cognitive disorders linked to preterm and early postnatal brain injury increased

during the 1990s, and currently remains stable (Vincer et al., 2006; Wilson-Costello et al., 2007). Progress in assisted respiratory and intensive care technology has led to greater than 90% survival of infants born after gestational week 23 (Larroque et al., 2004; Fellman et al., 2010), perhaps accounting for the increased burden of disability within the population as mortality rates decrease.

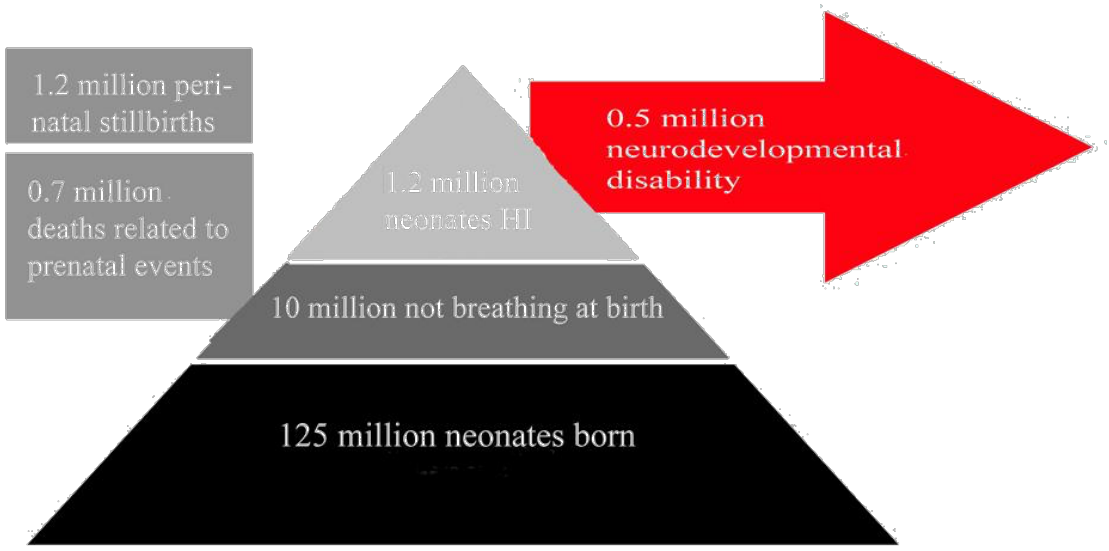


Figure 1.4 – Summary of Clinical Impact of Neonatal Hypoxia Ischaemia (HI). This figure summarises the number of neonates affected by neonatal HI annually across the globe relative to the number of live births per annum. Estimated figures for persistent disability associated with neonatal HI are also included. Estimates are based on data from studies referenced (Hack et al., 1992; Vohr et al., 2000; Dilenge et al., 2001; Volpe, 2001, 2012; Graham et al., 2008; reviewed in Lee et al., 2013).

Among those who survive the initial injury, rates of disability remain high throughout life. 5–10% of infants demonstrate motor deficits, and 20–50% display sensory or cognitive abnormalities that persist to adolescence (Hack et al., 1992; Vohr et al., 2000; Volpe, 2001, 2012; Lee et al., 2013). A meta-analysis of seven studies including 386 infant subjects investigated the average incidence of mortality and morbidity: 5.9% of all patients across died, 16.3% suffered neonatal seizures, and 17.2% experienced neurological deficits, with 14.2% qualifying for a diagnosis of

cerebral palsy (Graham et al., 2008). Long-term outcomes in neonatal asphyxia infants have also been investigated. One meta-analysis found that 1–18% of patients were identified as having severe sensorimotor or learning disorders by the age of 2–5 years, with only 50–60% of patients reported as developmentally normal (Dilenge et al., 2001). This study covers a wide range of injury severities and follow-up ages. Neurodevelopmental disorders reported in survivors (Dilenge et al., 2001) include seizures, hearing and vision loss (Robertson and Finer, 1985), language disorders, microcephaly, and gross motor coordination (Shankaran et al., 1991; 2012). Studies also report more severe neurological signs in subjects who had suffered severe HI (Robertson and Finer, 1985). However, many individuals who show abnormal neurological signs at birth were normal at 2-year follow-up (De Souza and Richards, 1978). Clinical features and outcomes of neonatal HI are summarised in Figure 1.4.

Despite the high disability burden associated with survivors of neonatal HI, there are very few preventative or protective treatments available for infants suspected to have suffered an HI event. The only licensed treatment currently available is hypothermia. This treatment involves subjecting either the infant's whole body or head-only to temperatures of around 33°C (reviewed in Choi et al., 2012; Tagin et al., 2012). Hypothermia was first demonstrated to improve survival in cases of cardiac arrest (Bernard et al., 2002; Nikolov and Cunningham, 2003), and has since been applied as a neuroprotective treatment in acute neonatal HI injury patients (Gunn et al., 1997; Gunn and Gunn, 1998; Shankaran et al., 2002, 2005; Eicher et al., 2005; Gluckman et al., 2005; Jacobs et al., 2005; Azzopardi et al., 2009; reviewed in Gunn et al., 2005; Shah et al., 2007; Shah, 2010; Jacobs et al., 2013). A recent meta-analysis finds that hypothermia carried out in over 1,200 infants reduced the rate of death and neurological handicaps at 18 months follow-up across all severity categories of

neonatal HI injury (Tagin et al., 2012). Including results from six clinical trials, whole body hypothermia increased the rate of subjects surviving with no normal neurological development at 18 month follow-up from to 27-63% of infants, compared to 18-32% in the untreated control group (Tagin et al., 2012). However, hypothermia alone is not sufficient to prevent all brain injury or neurological symptoms, highlighting the need for additional therapies to use in conjunction. Despite the efficacy of hypothermia, death and disability remain a common feature of neonatal HI prognosis. Observations concerning global prevalence and poor long-term outcome reiterate the urgency of finding novel neuroprotective treatments for use during and directly following HI injury.

1.3.2 Molecular Pathogenesis of Neonatal Hypoxia Ischaemia

There is ample evidence that brain damage occurs in human neonatal HI patients with poor clinical outcomes, from imaging and histopathological studies (reviewed in Mortola, 1999; Volpe, 2008, 2012; Northington et al., 2011). Grey and white matter lesions are both described at term after HI (Eken et al., 1994; Marin-Padilla, 1996; 1997; 1999). Localisation and extent of neuropathology has been shown to be associated with neurodevelopmental symptoms, giving insights into the nature of disability the patients may present with.

1.3.2.1 Neuroanatomy: Structural Imaging

Infants who survive the initial HI insult display cerebral damage visible with structural imaging. Magnetic resonance imagining (MRI) studies of term infants with

neurological signs and combinations of foetal distress, cord acidaemia, and depressed Apgar scores have been carried out in over 1,000 infants (reviewed in Volpe, 2012; Chau et al., 2012). These studies report great variation in the anatomical areas involved between individual subjects, yet most samples described either predominant injury to cerebral cortex often including subcortical white matter (Barkovich et al., 1995; Rutherford et al., 2004; Miller et al., 2005; Chau et al., 2008; 2013; Li et al., 2009), or deep structures including the basal ganglia and thalamus (Barkovich et al., 1995; Rutherford et al., 1998; 2004; Cowan et al., 2003; Kaufman et al., 2003; Miller et al., 2005). In many subjects, these two injury patterns partially overlapped (Barkovich et al., 1995; Cowen et al., 2003). These two common patterns of injury are shown in Figure 1.5.

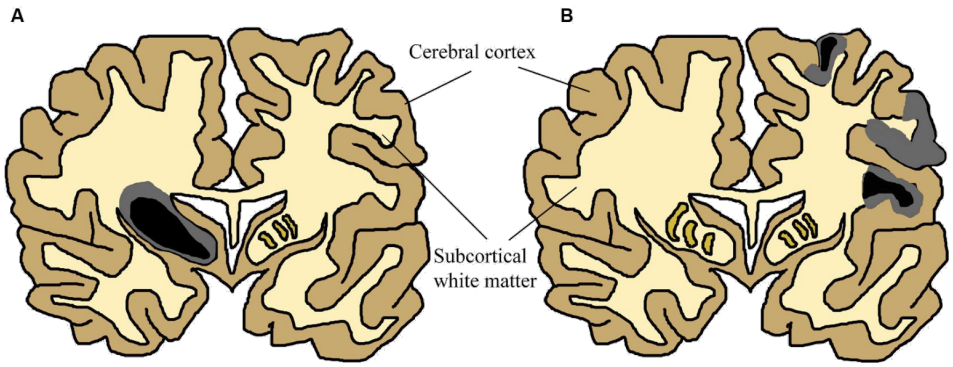


Figure 1.5 – Simplified Schematic of Brain Damage in Neonatal Hypoxia Ischaemia (HI), approximately at the level of primary somatosensory (S1) and motor cortex (M1). The two main patterns of injury, partially overlapping in human subjects, are shown separately. Two colours have been used to show that many neonatal HI injuries consist of a centre of necrosis (black) and a penumbra of less acutely damaged tissue (grey). The exact location of these sites will vary depending on the nature of the injury. Black/grey areas represent the potential site of lesions, those shown in this schematic are severe yet unilateral. (A) Primary basal ganglia and thalamus injury pattern. (B) Primary watershed cortex and underlying white matter injury. Injury can primarily occur either to cortical grey matter or subcortical white matter, depending on the nature of the injury. Severity varies substantially between individuals. These patterns have been documented in many human structural imaging studies (Barkovich et al., 1995; Cowan et al., 2003; Kaufman et al., 2003; Rutherford et al., 2004; Miller et al., 2005; Li et al., 2009). Adapted from Budday et al., 2014.

Although less common, severe selective involvement of subcortical white matter does occur (reviewed in Neil et al., 2002; Vermeulen et al., 2003). Cerebral white matter has been described as selectively sensitive to term HI injury in human (Inder et al., 1999) and in rodent models (Craig et al., 2003). One review describes the literature concerning structural MRI scans in the acute phase (within 2 weeks after birth): approximately 15–30% of scans are normal, lesions in basal ganglia and thalamus are present in 40–80% of cases, with abnormalities of watershed white matter and cortex present in 40–60% of patients (Volpe, 2012). MRI anatomy has been shown to agree well with post-mortem studies (Cowan et al., 2003). Therefore, no single area of the brain is specifically damaged following neonatal HI.

The MRI scan is currently the method of choice for investigation of neonatal anatomy (reviewed in Ment et al., 2002; Li et al., 2009). Diffusion-weighted MRI imaging has greatly improved identification of the time of onset of brain lesions (L'Abee et al., 2005; Chau et al., 2009). Sequential imaging shows that lesions in the basal ganglia may increase in size during the first week after birth (Soul et al., 2001; Barkovich et al., 2006), and asymmetric diffusion within white matter has been correlated with clinical severity of hemiparesis (Glenn et al., 2007). Cranial ultrasound also remains a valuable clinical tool (Daneman et al., 2006).

Another technique promising to add to understanding of neonatal HI is magnetic resonance spectroscopy (MRS), which allows brain metabolism to be imaged in real time (reviewed in Kemp and Radda, 1994; Soares and Law, 2009). Full-term neonates with preterm asphyxia have been studied, indicating that brain metabolism becomes abnormal after 6 to 12 hours only to decrease even further after 24 hours (Wyatt et al., 1989; Moorcraft et al., 1991; Roth et al., 1992). This coincides with clinical

deterioration such as development of seizures. The concept of a delayed metabolic abnormality or "secondary energy failure" has been elaborated in animal models (Lorek et al., 1994; Penrice et al., 1997; Groenendaal et al., 1994). 1H-MRS and 31P-MRS studies have demonstrated metabolic abnormalities following HI insult, which may persist for weeks (Groenendaal et al., 1994; Robertson et al., 1999). The magnetic field strength of current clinical systems allows only large brain areas to be examined, limiting the use of this technique.

Infants who have suffered neonatal HI often exhibit abnormal EEG activity (reviewed in Walsh et al., 2011; van Laerhoven et al., 2013). A range of abnormalities have been described, including: low voltage in isoelectric EEG (Finer et al., 1983; Legido et al., 1991); mild voltage depression (Watanabe et al., 1980; Toet et al., 2002; Murray et al., 2010); and asymmetry of trace (Aso et al., 1989; Zeinstra et al., 2001; reviewed in Murray et al., 2009); although all of these criteria have been differently defined by different experimenters (reviewed in Rennie et al., 2004; Shellhaas et al., 2007).

Lesions occur in many clinical patients, yet the effect on cognitive function is as diverse as the neuroanatomy. The area of cortex and basal ganglia damaged during initial HI injury is directly predictive of language and motor outcome in childhood (Steinman et al., 2009; Martinez-Biarge et al., 2011). Examination of diffusion-tensor imaging of neonates was predictive of survival and motor disability (Hunt et al., 2004; Ward et al., 2006). Children with basal-ganglia-thalamus pattern of injury tend to be severely disabled due to dyskinetic cerebral palsy and epilepsy (Himmelmann et al., 2007). Infants with predominant watershed white matter and cortex lesions had more prominent cognitive than motor deficits (Miller et al., 2005; Gonzalez and Miller, 2006; Steinman et al., 2009). Severe motor impairment is uncommon, and this group

is often considered to have a normal outcome when seen at 12–18 months, although suboptimal head growth (Mercuri et al., 2000), behavioural problems (Steinman et al., 2009), epilepsy (Miller et al., 2002a; Miller et al., 2002b; Oguni et al., 2008), and a delay in language can emerge during late childhood (Sato et al., 2008; Steinman et al., 2009). Therefore, localisation of cortical damage appears to be relevant to functional outcome in surviving neonatal HI patients. This information could be used to predict future susceptibility to disability before it manifests, allowing social and educational supports to be put in place early.

1.3.2.2 Molecular Mechanisms of Cell Death

Anatomical studies describe loss of brain volume following moderate and severe neonatal HI. However, the underlying molecular mechanisms responsible for cell death remain debated (reviewed in McLean and Ferriero, 2004; Fatemi et al., 2009; Northington et al., 2011; Baburamani et al., 2012; Millar et al., 2017). Many pathways have been implicated in HI injury in the term brain, primarily: excitotoxicity, oxidative stress, and inflammation.

1.3.2.2.1 Differences between the neonatal and the adult brain

There are many mechanistic differences between neonatal HI and adult ischaemic stroke. For example, severe HI events in the infant brain can lead to liquefactive disintegration, a form of necrosis which rapidly transforms tissue into a viscous fluid mass not seen after adult stroke (Larroche, 1977; Rorke, 1992). Newly formed blood vessels in the neonatal brain are fragile and prone to rupture (Trommer et al., 1987;

Ment et al., 1991; Jones et al., 2002; reviewed in Volpe et al., 1989), and surrounded by fewer astrocyte end-feet (El-Khoury et al., 2006). Additionally, the common belief that the neonatal blood brain barrier (BBB) is less effective has been challenged (Saunders et al., 1999; reviewed in Saunders et al., 2012; 2014; McLean and Ferriero, 2004; Baburamani et al., 2012; Stolp et al., 2016). Tight junctions, the occlusive element of the BBB, are shown to be present from the earliest time-point that embryonic vessels invade the brain in rodents (Schulze and Firth, 1992; Bauer et al., 1993; Stewart and Hayakawa, 1994; Kniesel et al., 1996), and functional (Ek et al., 2003; 2006; Daneman et al., 2010). Studies in rodents indicate that the BBB may be compromised as a result of neonatal HI (Muramatsu et al., 1997; Svedin et al., 2007; Tu et al., 2011; Yang et al., 2012; reviewed in Ferreri et al., 2010). In a model of hypoxia in new-born piglet, BBB integrity is maintained (Stonestreet et al., 1992), yet others document damage to the BBB following neonatal HI (reviewed in Alvarez-Diaz et al., 2007; Leonardo and Pennypacker, 2009).

Cerebrovascular autoregulation is another factor which must be considered in neonates. Clinically ill term infants (Pryds et al., 1990; Boylan et al., 2000) and animal models of neonatal HI (Hardy et al., 1999) demonstrate impaired autoregulation. The range of blood pressure values over which cerebrovascular autoregulation functions is proposed to expand with maturity (Tuor and Grewal, 1994; Verma et al., 2000). Also, the concentrations and actions of various signalling molecules have been shown to be different in the developing brain compared to the adult. These include: caspase-3 (Cheng et al., 1998), vascular endothelial growth factor (VEGF) (reviewed in Carmeliet and Storkebaum, 2002), and hypoxia inducible factor 1 (HIF-1) (Sheldon et al., 2009).

One surprising difference between neonatal hypoxia ischaemia and adult ischaemic stroke injury is the sexual dimorphism in response to neonatal HI. Male babies are at higher risk of cerebral palsy than females (Jarvis et al., 2005). Cognitive and motor outcomes are worse in male than in female low birth weight infants (reviewed in Marlow et al., 2005; Johnston and Hagberg, 2007). Quantitative imaging shows that male premature infants are more vulnerable to white matter injury, whereas females are more vulnerable to grey matter injury (Reiss et al., 2004). This sex difference has been replicated in rodent *in vitro* models of hypoxic cell death (Zhu et al., 2006; Nijboer et al., 2007; Du et al., 2009). Although many molecular mechanisms are under investigation, including differences in mitochondrial function (reviewed in Blomgren and Hagberg, 2006), and differences in neuronal maturation driven by hormone exposure *in utreo* (reviewed in Weinstock, 2007; Manson, 2008) this sexual dimorphism remains largely unexplained (Chavez-Valdez et al., 2014; Demarest et al., 2016a; 2016b; Waddell et al., 2016; reviewed in Hill and Fitch, 2012).

Neonatal HI injury evolves over time (reviewed in McLean and Ferriero, 2004). Injuries seen with MRI scans within the first few hours after asphyxia are subtle, restricted diffusion typically starting as small lesions in the putamen and thalamus, progressing over the next 3 to 4 days to involve more extensive areas of the brain (reviewed in Takeoka et al., 2002). Within the first few hours, regionally specific fluctuations in blood flow trigger excitotoxicity, free radical generation, and oedema (Wigglesworth and Pape, 1978; Bennet et al., 1998; Jensen et al., 1999; Shalak and Perlman, 2004; Ferrari et al., 2010). A secondary phase of injury occurs during the following hours and days, resulting in neuroinflammation, mitochondrial permeabilisation, and loss of cerebral autoregulation (Scheepesn et al., 2003; reviewed in Inder and Volpe, 2000; Hamrick and Ferriero, 2003; Hagberg et al., 2009;

Leonardo and Pennypacker, 2009). A tertiary phase of brain injury may exacerbate injury through persistent inflammation (Fleiss and Gressens, 2012).

1.3.2.2.2 Apoptosis and Necrosis

The balance between molecular cell-death processes which cause this damage in neonatal HI remains under investigation. Understanding the interaction between the molecular cascades that cause cell death in the neonatal brain is crucial to the development of effective therapies, as each mechanism of cell death have unique time-frames and regulatory molecules, neuronal cell death is far from a uniform process in which any inhibitory treatment will prove neuroprotective in the complex chemical landscape of the neonatal brain.

Early evidence indicates the majority of cell death in neonatal HI was necrotic, however, all regions also undergo increased apoptotic death (Edwards and Mehmet, 1996; Edwards et al., 1997; Northington et al., 2001). Some studies suggest a more prominent role for apoptosis (Hill et al., 1995; Sidhu et al., 1997; Pulera et al., 1998; Hu et al., 2000; reviewed in McLean and Ferriero, 2004). Immature neurons *in vitro* are more susceptible to apoptotic death than mature neurons (McDonald et al., 1997). Others report that necrosis was the major cellular death pathway in humans and animals (Myers, 1975; Towfighi et al., 1995; Northington et al., 2001; 2005; Folkerth, 2005; Carloni et al., 2007; Stridh et al., 2013; reviewed in Adamsons and Myers, 1973; Northington et al., 2011). Yet others recognise that both occur. Some report that necrosis predominates in severe cases, whereas apoptosis occurs in milder injury (Daval and Vert, 2004; reviewed in Fatemi et al., 2009). Neurons often displayed

morphologic features along an apoptosis-necrosis continuum (Portera-Cailliau et al., 1997a; 1997b; Nakajima et al., 2000; Northington et al., 2007, 2011).

In addition to apoptosis and necrosis, some neurons in the neonatal HI brain undergo autophagy (reviewed in Klionsky and Emr, 2000; Northington et al., 2011; Balduini et al., 2012). Neuronal autophagy of non-necrotic cells occurs in rodent neonatal HI models (Lockshin and Zakeri, 2004; Carloni et al., 2008; Ginet et al., 2009). However, there is conflicting evidence as to whether the occurrence of autophagy augments brain damage (Koike et al., 2008; Puyal et al., 2009), or prevents the spread of necrotic cell death (Carloni et al., 2008). Many necrotic cells are recycled by autophagy, and these pathways can be activated in parallel, which makes it difficult to separate these pathways at a conceptual level (reviewed in Nikoletopoulou et al., 2013). Artificially exclusive classifications of cell death may hinder research and therapy development.

To add to this complexity, neonatal HI injury appears to activate several interacting molecular cascades. The predominant pathways behind neonatal HI neuropathology are generally recognised as: excitotoxicity, oxidative stress, and inflammation (reviewed in McLean and Ferriero, 2004; Fatemi et al., 2009; Millar et al., 2017). A simple schematic of the three major cascades is shown in Figure 1.6.

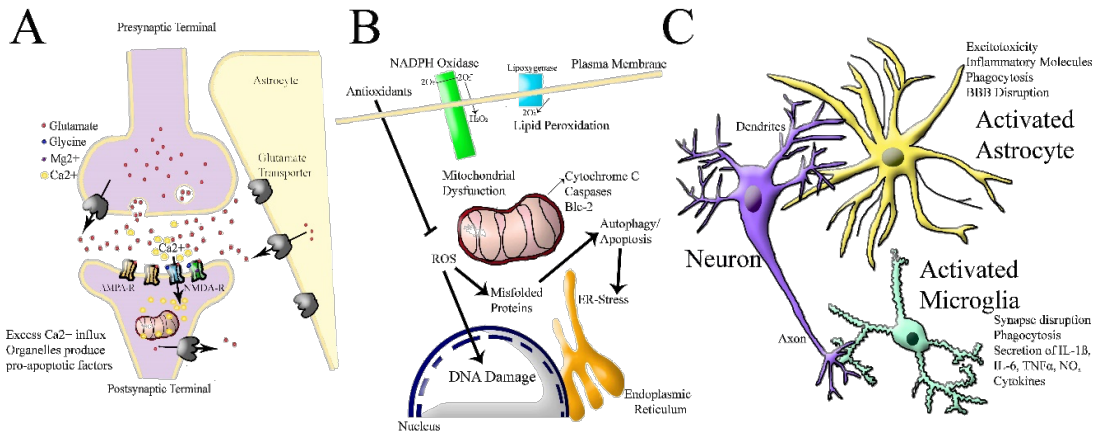


Figure 1.6 – Simplified Schematic of Major Molecular Cascades involved in Neonatal Hypoxia Ischaemia (HI) Neuropathology. A vast number of molecules contribute to neonatal HI injury in the brain and all included here have been investigated in this disorder. Molecular targets can be divided into three cascades. (A) Excitotoxicity. Adapted from Vandenberg and Ryan, 2013. Ca^{2+} = calcium ion, Mg^{2+} = magnesium ion AMPA-R = α-amino-3-hydroxy-5-methyl-4-isoxazole propionic acid receptor, NMDA-R = N-methyl-D-aspartate receptor. (B) Oxidative Stress. Adapted from: http://www.enzolifesciences.com/platforms/cellular-analysis/oxidative-stress/, last accessed: 10/08/2018). For simplicity, only free radicals are shown and physiological substrates have been omitted. NADPH = Nicotinamide Adenine Dinucleotide Phosphate Hydrogen, O_2 = oxygen, O_2^- = negatively-charged oxygen free radical, H_2O_2 = hydrogen peroxide, ROS = reactive oxygen species, Blc = B cell leukaemia protein, ER = endoplasmic reticulum, DNA = deoxyribose nucleic acid. (C) Inflammation. Adapted from Santiago et al., 2014. BBB = blood brain barrier, IL-6 = interleukin 6, IL-1B = interleukin 1 beta, TNFα = tumour necrosis factor alpha, NO = nitric oxide.

1.3.2.2.3 Excitotoxicity

The first cell death pathway recognised to contribute to neonatal hypoxic ischaemic brain damage is excitotoxicity, in which physiological glutamate neurotransmission leads to over-activation of postsynaptic receptors and cell death (reviewed in Hagberg et al., 1987; Choi, 1988, 1992; Hattori and Wasterlain, 1990). The N-methyl-D-aspartate (NMDA) receptor is relatively over-expressed in the developing brain (Represa et al., 1989; Gonzalez et al., 1993; Fox et al., 1996). In P6 rats, the NMDA receptor is expressed at 150–200% of adult levels (Tremblay et al., 1988). The predominating combination of NMDA receptor subunits in the preterm period favoured prolonged calcium influx for a given excitation (Hori and Kanda, 1994;

reviewed in Danysz and Parsons, 1998). The same NMDA receptor that promotes plasticity can lead to massive Na^+ and water influx, cellular swelling, pathologically elevated intracellular calcium, and energy failure (reviewed in Choi, 1988). Oxygen glucose deprivation (OGD) in rat hippocampal neurons leads to a marked reduction in glutamate removal from the synapse (Jabaudon et al., 2000; Tao et al., 2001). Injection of NMDA into neonatal rat brain produces more extensive cell death in the neonate than in the adult (McDonald et al., 1988). Elevated glutamate has also been documented in the cerebrospinal fluid (CSF) of infants who have suffered severe HI injury (Riikonen et al., 1992; Hagberg et al., 1993; Pu et al., 2008).

The neonatal brain is more prone to seizure activity than the mature brain (reviewed in Holmes, 1991; Holmes and Ben-Ari, 2001), suggesting a prominent role for neuronal hyperexcitability and excitotoxicity although the molecular mechanisms explaining this have not been fully elucidated (reviewed in Rakhade and Jensen, 2009). However, seizure activity could also be explained by paradoxical excitatory activity of the neurotransmitter γ-amino butyric acid (GABA) in the developing brain (Staley et al., 1995). The developmental time-point that this switch occurs at remains unresolved, with studies in rat reporting that the switch from depolarising to hyperpolarising GABA activity occurring at P5 (Ben-Ari et al., 1989), P8 (Tyzio et al., 2007), P10 (Tyzio et al., 2007), or P12 (Dzhala and Staley, 2003), therefore the normal developmental time-frame of this switch across the brain is not fully described in rodent or human (reviewed in Khazipov et al., 2015). Drugs that block NMDA receptors are protective against HI injury in neonatal rodent models (McDonald et al., 1989a; 1989b, 1989c; 1990). Activation of α-amino-3-hydroxy-5-methyl-4-isoxazolepropionic acid (AMPA) receptors also contributes to injury (McDonald et al., 1990; McDonald et al., 1992; McDonald and Johnston, 1992; Deng et al., 2003;

Talos et al., 2006). However, AMPA antagonists are not as protective and NMDA antagonists (Ikonomidou et al., 1999; Noh et al., 2006). These findings are yet to be exploited in human clinical trials, as the integral role of glutamate receptors in healthy neuronal plasticity (Ikonomidou et al., 1999; Failor et al., 2010) could be damaged by the use of NMDA and AMPA antagonists at such a sensitive developmental stage.

1.3.2.2.3 Oxidative Stress

An integrally linked cascade is that of oxidative stress. Excitotoxicity causes energy depletion, mitochondrial dysfunction, and cytosolic calcium accumulation, which in turn leads to generation of free radicals (Dawson et al., 1991; Reynolds and Hastings, 1995; Gunasekar et al., 1995; Ferriero et al., 1996; reviewed in Ferriero, 2001; Forder and Tymianski, 2009). Free radicals alter membrane pump function, allowing more glutamate release and NMDA receptor activation, leading to more excitotoxicity (Iadecola et al., 1997; Yu et al., 1999; Robertson J.D. et al., 2002; reviewed in Schanne et al., 1979; Starkov et al., 2004).

Oxidative stress is a general term for the increase in free radical production as a result of oxidative metabolism under pathological conditions (reviewed in Inder and Volpe, 2000; Ferriero, 2001). When oxygen floods the microenvironment of cells damaged by hypoxia, mitochondrial oxidative phosphorylation is overwhelmed and reactive oxygen species accumulate (reviewed in Ferriero, 2001). Foetal life elapses in a low oxygen environment (East et al., 1998). In the first minutes of life, an abrupt increase in O_2 partial pressure occurs, which creates a pro-oxidant condition (Stiller et al., 2002). During birth asphyxia, excess calcium influx and other factors lead to severe oxidative stress (Iadecola et al., 1997; reviewed in Forder and Tymianski, 2009).

Accumulation of hydrogen peroxide (H_2O_2) is detected after HI in neonatal mice but not in adult stroke (Lafemina et al., 2006). Because of its high lipid content, the brain is particularly susceptible to free radical attack (O'Brien and Sampson, 1965; Northington et al., 2001). The polyunsaturated fatty acid content of the brain increases during gestation (Crawford and Sinclair, 1971; Mishra and Delivoria-Papadopoulos, 1989). Lipid peroxidation may be a major factor in the white matter damage (Back et al., 1998; Baud et al., 2004). The developing brain's immature antioxidant defence also contributes to increased sensitivity to oxidative stress (reviewed in Mishra and Delivoria-Papadopoulos, 1999; Li and Jackson, 2002; Felderhoff-Mueser et al., 2002; Vannucci and Hagberg, 2004; Blomgren and Hagberg, 2006; Ikonomidou and Kaindl, 2011; Miller et al., 2012).

1.3.2.2.4 Brain Inflammation

Finally, inflammation is a major component of neonatal HI injury. Low-dose treatment with intrauterine lipopolysaccharide (LPS) substantially increases severity of HI injury in neonatal mice, but protects against HI in adult rodents (Wang et al., 2007b). Intracerebral injection of an NMDA receptor agonist produces a pattern of white matter injury, in which pre-treatment with systemic interleukins IL-1ß, IL-6, IL-9, or tumour necrosis factor alpha (TNF-α) leads to a significant increase in lesion size (Marret et al., 1995; Dommergues et al., 2000).

There is now substantial experimental evidence that intrauterine inflammation can exacerbate neonatal HI (Lehnardt et al., 2003; Eklind et al., 2005), which some have referred to as the "double-hit hypothesis" (reviewed in Agrawal and Hirsch, 2012; Hagberg et al., 2012; Dammann and Leviton, 2014). Microglia, the resident

macrophages of the CNS, are among the first cells to become activated after HI (Fujimoto et al., 1989; Tahraoui et al., 2001; reviewed in Kaur et al., 2007). Activated microglia migrate to damaged regions (Ivacko et al., 1996; Rivera et al., 2002; Deng et al., 2008) and produce inflammatory cytokines, glutamate, nitric oxide, and free radicals (reviewed in Wood, 1995; Kaur and Ling, 2009). Drugs that block microglial activation may protect the neonatal brain (Dommergues et al., 2003). Following HI, compromise of the BBB allows the entry of macrophages (Ivacko et al., 1997; reviewed in Alvarez-Diaz et al., 2007; Leonardo and Pennypacker, 2009). Astrocytes also play a role in inflammation (Wang et al., 2003; Girard et al., 2008; 2009). CSF cytokines are elevated in term infants who later develop cerebral palsy (Savman et al., 1998; reviewed in Dammann and O'Shea, 2008).

The diverse network of interacting mechanisms discussed demonstrates the molecular complexity of neonatal HI injury. Often single molecular injury markers are part of immense biological pathways with many interacting components. The sheer number of these active molecules have restricted scientific study to a small proportion of representative agents. Potential protective treatments should strive to tackle common mediators of these cascades relevant to all three pathways, otherwise full protection will not be achievable.

1.3.3 Animal Models of Neonatal Hypoxia Ischaemia

Neonatal hypoxia ischaemia has been modelled extensively in mice and rats (reviewed in Hagberg et al., 2002; van der Worp et al., 2007; Yager and Ashwal, 2009; Dean et al., 2015; Millar et al., 2017), with a minority of researchers also

studying larger animals such as pigs and sheep (reviewed in Roohey et al., 1997; Dean et al., 2015), or primates (Fahn et al., 1979; reviewed in Volpe, 2012).

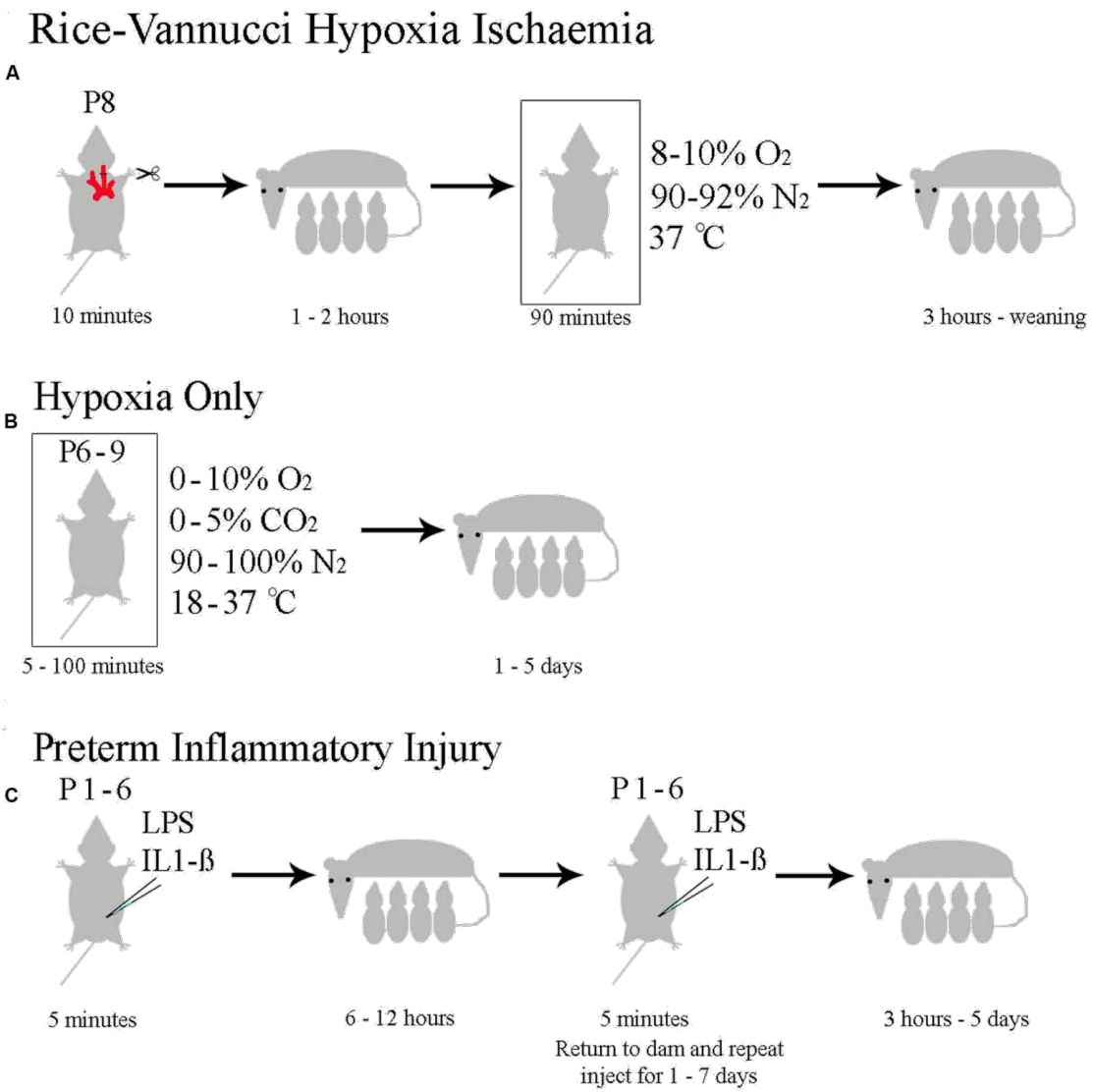


Figure 1.7 – Schematic of Currently Used Rodent Models of Neonatal Hypoxia Ischaemia (HI). (A) The Rice–Vannucci method, first outlined in rats (Rice et al., 1981), but since adapted to replicate multiple injury severities in mouse and rat. (B) A general schematic of Hypoxia-Only methods with specifications taken from the pool of papers summarised in Appendix 8.1 (reviewed in Millar et al., 2017). (C) Example inflammatory models from across the literature (reviewed in Dean et al., 2015). Large animal models are not depicted here but are discussed in Section 1.3.3.4 below.

Models intending to replicate the clinical symptoms of neonatal human HI can be divided into the four general categories: rodent models adapted from the Rice-Vannucci method of hypoxia ischaemia (Rice et al., 1981; reviewed in Hagberg et al., 2002; Yager and Ashwal, 2009; Millar et al., 2017); rodent models exposing animals to hypoxia only in the absence of an ischaemic event (reviewed in Millar et al., 2017); preterm models of intracerebral inflammatory injury (reviewed in Hagberg at el., 2002 Dean et al., 2015); and large animal models (reviewed in Roohey et al., 1997; Volpe 2012; Dean et al., 2015; Millar 2017). A summary of available rodent models is shown in Figure 1.7.

1.3.3.1 Rice–Vannucci Model of Term Hypoxia Ischaemia

Most published studies modelling neonatal HI in animals have employed an adapted model based on the Rice-Vannucci method (Rice et al., 1981). This model comprises unilateral common carotid artery (CCA) ligation, recovery with the dam for approximately 1–2 hours, followed by exposure to 8% oxygen in rat and 10% oxygen in mouse for 1–3 hours at 37°C. Although the model was initially described in rat (Rice et al., 1981), it has been successfully adapted for mouse (Ditelberg et al., 1996; Ferriero et al., 1996; Sheldon et al., 1998).

Rice' and Vannucci's model replicates anatomical damage seen in human neonates. The initial study showed selective grey-matter sensitivity to neuronal necrosis, with injury observed in cortex, hippocampus, thalamus, and basal ganglia (Rice et al., 1981; Andine et al., 1990; Towfighi et al., 1991; 1995; reviewed in Vannucci et al., 1999). Histologically, there is a gradation of injury that correlates with the duration or severity of insult (Towfighi et al., 1991, 1995). White matter lesions have also been

described in this model (de Torres et al.; 1997; Ness et al., 2001; Liu et al., 2002; Drobyshevsky et al., 2005; 2007b), the extent of which correlate with duration of exposure to hypoxia (Liu et al., 2002). However, bilateral common carotid artery ligation appears a stronger model of white matter damage (Jelinski et al., 1999; Uehara et al., 1999; Cai et al., 2001). Metabolic alterations in the Rice–Vannucci model include decreased cerebral blood flow (Sakurada et al., 1978; Vannucci et al., 1988), brain acidosis (Welsh et al., 1982; Yager et al., 1991), and decreased cerebral glucose uptake (Vannucci et al., 1989; Sokoloff et al., 1977). An inflammatory response has also been described (Bona et al., 1998).

Another advantage of the Rice-Vannucci model is its ability to predict the therapeutic effect of hypothermia following neonatal HI (reviewed in Millar et al., 2017). Mice treated with hypothermia showed smaller lesion volumes, in addition to better performance on behavioural tests such as the Morris water maze and circling tests (Yager et al., 1993; Lee et al., 2010; Kida et al., 2013; Lin et al., 2014). Many papers have investigated behavioural outcomes of Rice-Vannucci injury in adult rodents. These include: impaired spatial learning and memory (Balduini et al., 2000; 2001; Ikeda et al., 2001; Wang et al., 2002; Arteni et al., 2003; Pereira et al., 2007; Cai et al., 2009; Greggio et al., 2011; Hill et al., 2012; Zheng and Weiss, 2013; Alexander et al., 2014; Gillani et al., 2015); impaired motor function as assessed by rotarod test, open field, and motor reflexes (Barth and Stanfield, 1990; Jansen and Low, 1996a, 1996b; Jansen et al., 1997; Balduini et al., 2000; 2001; Tomimatsu et al., 2002; Ådén et al., 2003; Lubics et al., 2005; Pazaiti et al., 2009; Im et al., 2010; Nijboer et al., 2010; Karalis et al., 2011; Chen et al., 2012; Ruiz et al., 2012; Sanches et al., 2012; Zheng et al., 2012; Xiong et al., 2013; Alexander et al., 2014; Gillani et al., 2014, 2015; Kim et al., 2014; Zhang et al., 2014; Park D. et al., 2015; Park W.S. et al.,

2015); sensory processing abnormalities (Alexander et al., 2014); and other cognitive phenotypes, such as reduced attention (Buwalda et al., 1995; Martin et al., 1997; Sanches et al., 2013; Perera et al., 2014; Miguel et al., 2015). Despite this broad range of documented behavioural effects, there are some contradictions between individual investigators (reviewed in Lubics et al., 2005), which suggest that different genetic backgrounds, injury severity, or experimenter can significantly affect the outcome of Rice-Vannucci neonatal hypoxia ischaemia.

The Rice-Vannucci model of neonatal hypoxia ischaemia has several advantages. One is its prevalence, allowing direct comparisons with many other publications throughout the literature (reviewed in Vannucci et al., 1993; 1999; 2005; Yager and Ashwal, 2009; Dean et al., 2015). Another is that the contralateral hemisphere, exposed to hypoxia in the absence of ischaemia, provides a control hemisphere within the experimental brain (Yager et al., 1991; 1992; 1996; Vannucci and Yager, 1992). Thorough behavioural characterisation supports the long-term consequences of this model mimicking neonatal HI. One significant drawback is the high variability in size and severity of infarct between littermates (reviewed in Vannucci and Hagberg, 2004; Vannucci and Vannucci, 2005). Additionally, the invasive nature of severing the common carotid artery does not replicate human injury, such severe vascular abnormalities occur rarely in humans, if at all (Ment et al., 1984; Hill, 1991).

1.3.3.2 Hypoxia-Only Models

Some experimenters induce hypoxia in rodents exclusively using an oxygen deprivation chamber, without a preceding ischaemic procedure. These models are not as widely used as the Rice-Vannucci method, but have the potential to describe milder

injuries and avoid the unphysiological occlusion of the common carotid artery. There are currently no published meta-analyses of hypoxia-only investigations, and only one published review (Millar et al., 2017). Appendix 8.1 contains a summary of 122 published papers using hypoxia-only methodology.

Historically, hypoxia-only methods have been used to investigate brain biochemistry. Several studies have documented altered levels of neurotransmitters (Hedner et al., 1980; Kaneko et al., 1985; Yamamoto et al., 1985; Yamamoto and Kato, 1986; Hadjiconstantinou et al., 1990; Seidler and Slotkin, 1990; Dell'Anna et al., 1993; Tanaka et al., 1995; Anju et al., 2010a; 2010b; Anju and Paulose, 2011; 2013). However, there is little consensus over the direction or magnitude of changes across models or experimenters (Decker et al., 2003; 2005). Hypoxia-only models have become an established method for generating seizures in neonatal rats (Jensen et al., 1995; Applegate et al., 1996; Rodríguez-Alvárez et al., 2015; Sampath et al., 2015). In one such model, P6 rat pups are placed in chambers at 9% O_2 partial pressure and 20% CO_2 partial pressure for 60 min. Some pups are immediately restored to room air, whereas others undergo gradual reduction of CO_2 (Helmy et al., 2011; Tolner et al., 2011). Pups which undergo hypoxia with immediate restoration of CO_2 had a greater mortality rate. However, subsequent anatomical analysis of these brains at P8 (Boss et al., 2005; Wang et al., unpublished), failed to show any differences in expression of cell death markers or markers of healthy cortical neurons. Hypoxia-only insults resulting in seizures appear to generate only subtle injury to the brain, far short of that seen in some human patients.

A range of behavioural phenotypes have been reported in hypoxia-only models, including hyperactivity (Shimomura and Ohta, 1988; Dell'Anna et al., 1991; Speiser

et al., 1991; Decker et al., 2005); increased aggression (Mikati et al., 2005; Tang et al., 2006); altered ultrasonic vocalization (Venerosi et al., 2006); and disturbed sleep (Decker et al., 2003). Relatively few investigators have pursued standard tests of spatial memory and locomotor behaviour, and those few publications obtained mixed results, (Dell'Anna et al., 1991; Speiser et al., 1998; Rotstein et al., 2006; Coq et al., 2008; Raveendran and Skaria, 2013; Wang et al., 2015). The majority of hypoxia-only phenotypes are based on custom behavioural tests, making these difficult to interpret. Additionally, some studies report no behavioural deficit following neonatal hypoxia alone (Buwalda et al., 1995; Iuvone et al., 1996; Casolini et al., 2005; Blaise et al., 2009; Mikhailenko et al., 2009; Anju et al., 2010c; Wang et al., 2015).

Although hypoxia-only models offer the potential to replicate the mechanism of hypoxia without major ischaemia, models currently available are not ideal. One significant problem is the lack of methodological unity between different experimenters. There is little consensus on the age of animals, background strain, oxygen partial pressure, time of exposure to hypoxia, or body temperature (see Appendix 8.1, Table 8.1).

1.3.3.3 Inflammatory Models of Preterm Brain Injury

Intrauterine infection is strongly associated with preterm birth and brain injury (Stoll et al., 2004; Mitha et al., 2013; reviewed in Strunk et al., 2014). Several models have been described which introduce inflammation-inducing molecules at different ages (reviewed in Dean et al., 2015), many of which cause and white matter damage.

Administration of live *Escherichia coli* (*E. coli*) bacteria into the uterus of pregnant rats can result in neutrophil infiltration in the foetal brain, increased foetal reabsorption and stillbirth, while surviving pups exhibit increased brain chemokines, cytokines, white matter injury, and behavioural phenotypes (Debillon et al., 2003; Rodts-Palenik et al., 2004; Pang et al., 2005; Yuan et al., 2005; Bergeron et al., 2013). The effects of bacterial mimetics such as the cell wall component lipopolysaccharide (LPS), have also been investigated. Intracervical injection in E15 mice is associated with mild white matter injury but no behavioural deficits (Bell and Hallenbeck, 2002; Poggi et al., 2005; Wang et al., 2007a; Girard et al., 2009), whereas repeated intracervical LPS is associated with delayed neurosensory development (Toso et al., 2005; Rousset et al., 2006; 2013). Other inflammatory models include simulation of viral infection by injection of polyinosinic-polycytidylic acid (poly(I:C)), a synthetic double stranded viral RNA, which causes long-term behavioural deficits (Shi et al., 2009; Richetto et al., 2013).

Postnatal administration of inflammatory agents is widely used in rodents to model postnatal infection. Subcutaneous injection of live *E. coli* in P3 mouse pups is associated with microgliosis, loss of oligodendrocytes, and impaired motor coordination (Lieblein-Boff et al., 2013). Most techniques which employ live bacterial injection have very high mortality rates (Rodewald et al., 1992; Tran and Weisman, 2004; Placencia et al., 2009; Loron et al., 2011). Postnatal intraperitoneal injection of LPS can also cause white matter damage and cerebral cytokine response (Brochu et al., 2011; Brehmer et al., 2012; Nobuta et al., 2012; Smith et al., 2014). Repeated daily injection of LPS in mice resulted in elevated serum IL-6, reduced grey matter volume, decreased oligodendrocyte numbers, and decreased myelin staining (Wang et al., 2009; Malaeb et al., 2014). Similarly, repeated IL-1β injection in P1–P5

mice has been associated with impaired oligodendrocyte progenitor maturation, and severe memory deficits (Favrais et al., 2011).

One of the strengths of the inflammatory models reflects the exposure to infectious or inflammatory agents present outside of the highly sterile individually ventilated cages where many academic institutions keep experimental animals. Most of the inflammatory risk factors for increased severity of HI injury in humans, such as maternal infection (Stoll et al., 2004; Girard et al., 2012; reviewed in Dean et al., 2015), will result in systemic inflammation in addition to CNS-specific recruitment of microglia. However, there is currently debate concerning the relevance of maternal inflammation to foetal brain damage (Leviton et al., 1999; Redline and O'Riordan, 2000; Neufeld et al., 2005).

Although the majority of publications cited above administer pro-inflammatory agents by intracerebral injection, some studies have administered LPS by intravenous injection (reviewed in Wang et al., 2006). In foetal sheep, intravenous LPS causes white-matter specific damage (Garnier et al., 2001; 2006; Duncan et al., 2002; Mallard et al., 2003; Peebles et al., 2003; Svedin et al., 2005), suggesting that systemic inflammation may be sufficient to trigger brain injury. Separating systemic and brain-specific inflammation parameters in future experiments will prove technically demanding.

Data suggest that gene expression in mouse models of inflammation closely corresponds to that seen in human (Takao and Miyakawa, 2015). However, postnatal murine response to inflammation is likely different to that experienced by a human foetus. An important limitation of inflammatory studies is the impact of proto-inflammation or infection on cardiovascular function and the potential for secondary

cerebral HI (Eklind et al., 2001; Favrais et al., 2011). Another is that varying results have been reported. This may be due to differences in LPS purification methods used between experimenters (Westphal, 1965; Lam et al., 2014), or dose (Fujihara et al., 2003). Alternatively, there is increasing evidence that considerable individual variability in response to clinical sepsis between patients is related to host genetics (Christaki and Giamarellos-Bourboulis, 2014). Inflammation is doubtless an important factor in neonatal brain injury, yet the variation between different models makes these methods difficult to evaluate. The precise relationship between preterm and neonatal infection and brain damage has yet to be fully resolved in humans, limiting the validity of rodent models.

1.3.3.4 Alternative Animal Models

In many ways, non-rodent models are more representative of neonatal HI as it affects human patients. Relatively few experimenters have investigated neonatal HI in primates. Classical studies asphyxiated term monkey foetuses by covering their heads with a rubber sac and clamping the umbilical cord (Fahn et al., 1979). Foetuses resuscitated after 20 min had extremely high mortality. However, 12 min of asphyxia were required to produce any neuropathological injury. Foetuses displayed damage predominantly within the brainstem. In a model of partial ischemia (Fahn et al., 1979), pregnant females were rendered hypotensive during the third trimester. When blood oxygen saturation was reduced to 10% for 5 hours, foetuses became profoundly acidaemic. At birth, these displayed opisthotonus, decerebrate posturing, and convulsions. There is one model of white-matter injury based on baboons delivered prematurely by hysterotomy (Inder et al., 2004, 2005a; 2005b). Premature baboons

are treated in an intensive care setting. Approximately half display white-matter injury. Analysis of behaviour has not been undertaken.

More work has been carried out in sheep by umbilical cord occlusion and term asphyxia (Gunn et al., 1992; Williams et al., 1992; Mallard et al., 1993; Richardson et al., 1996; de Haan et al., 1997a; 1997b; 1997c; Richardson and Bocking, 1998; Dalitz et al., 2003). Repeated asphyxia at 5 hour intervals results in injury to the striatum almost exclusively, whereas episodes of asphyxia repeated every 5 minutes cause diffuse and extensive damage to cortex, thalamus, and cerebellum in 40% of animals, and selective neuronal necrosis in the remainder. White matter injury has also been investigated in sheep (Ting et al., 1983), where only those foetuses in which the mean arterial blood pressure fell below 30 mmHg exhibit brain damage, irrespective of hypoxia. Neuropathological injury after arterial occlusion for 30 minutes cause grey and white matter damage (Reddy et al., 1998; Petersson et al., 2002). Several laboratories have developed models in sheep of systemic endotoxemia (Duncan et al., 2002; Mallard et al., 2003). Unfortunately, no behavioural outcomes are currently available. PIG (Richardson B.S. et al., 1996). Although there are fewer publications using neonatal pig, these models could provide valuable complementary information in future (Richardson B.S. et al., 1996; Thoresen et al., 2001; Karlsson et al., 2008; Lafuente et al., 2011).

Other small laboratory animals have also been investigated. Preterm rabbit foetuses exposed to sustained placental insufficiency via intrauterine occlusion of the descending aorta display significant alterations in motor responses to olfactory stimuli, coordination of suck and swallow reflexes, and marked hypertonia, reminiscent of spastic quadriplegia (Yoon et al., 1997; Derrick et al., 2004, 2007;

Saadani-Makki et al., 2008). Diffusion-weighted imaging detected a threshold in white matter loss below which all rabbit kits develop hypertonia, (Drobyshevsky et al., 2005, 2007a). Another promising small animal model is the spiny mouse, *Acomys cahirinus*, a rodent which shows a similar level of brain development to a human neonate at birth (Brunjes, 1985; 1989a; Gozzo et al., 1985; Brunjes et al., 1989; reviewed in Brunjes, 1990; D'Undine and Alleva, 1988). Following neonatal hypoxia ischaemia, the spiny mouse demonstrates reduced survival and motor deficits (Ireland et al., 2008; 2010) and neuroanatomical pathology (Ireland et al., 2009; Hutton et al., 2009; O'Connell et al., 2013).

Large animals can better replicate the conditions of a single human foetus exposed to a non-sterile environment. However, none of these models have access to the same extent of transgenic manipulation or validated behavioural tests that are possible in rodent studies. These models are invaluable for aiding comparison of brain development at birth which occur across species (Clancy et al., 2007), whereas the relative immaturity of mouse and rat brains at birth introduce an unwelcome variable into these experiments. For the foreseeable future, insights from both rodent work and larger animals will remain important.

1.3.4 Subplate Damage in Neonatal Hypoxia Ischaemia

One brain region exemplifies how much remains unknown about the developing brain's response to HI, and the uncertainties involved in interpreting results from animal studies. It is the subplate (see Section 1.2).

The susceptibility of subplate neurons to neonatal HI remains a controversial topic (reviewed in Millar et al., 2017). Early studies claimed subplate is selectively vulnerable. Cultured rat subplate neurons are more vulnerable to oxygen glucose deprivation (OGD) than mixed cortical neuron cultures (Nguyen and McQuillen, 2010). In rats exposed to systemic HI at E18, a significant decrease in nuclear receptor related 1 protein (Nurr1)-expressing subplate neurons is documented by P2 (Jantzie et al., 2014; 2015a; 2015b; 2015c). Similar results are obtained in foetal sheep, although Nurr1-expressing Layer VI neurons were also decreased (Dean et al, 2011). It is also possible that HI induces differential marker expression in subplate neurons, rather than cell death. *In vitro* electrophysiological recordings in cortical slices from neonatal rats have demonstrated a pronounced functional impairment of subplate neurons following OGD (Albrecht et al., 2005).

One study, which claimed selective vulnerability of subplate to hypoxia, used immunohistochemistry to detect cell-death in neurons labelled with bromodeoxyuridine (BrdU) at E10.5 following a modified Rice–Vannucci model in P1 rats (McQuillen et al., 2003; reviewed in McQuillen and Ferriero, 2004; 2005). However, Layer VI neurons born at this date also expressed cell-death markers, suggesting subplate may not be selectively susceptible to HI injury. This group have also reported subplate death in a left common carotid artery coagulation experiment in P2 rats, without confirmation of brain damage follow HI (Mikhailova et al., 2017). Conversely, another investigation which carried out systematic quantification of cell death markers throughout subplate and other deep cortical layers using immuno-histochemistry failed to detect increased subplate vulnerability (Okusa et al., 2014). Three subplate-specific marker immunoreactive populations showed little co-staining with caspase-3 in P6 rat brains with mild to moderate HI lesions generated by adapted

Rice-Vannucci hypoxia ischaemia at P2. In severely damaged brains, caspase-3 staining was found throughout cortex. Layer-specific sensitivity of cortical neurons to HI remains debated. A double birth-dating study, targeting subplate and Layer V or VI combined with HI could resolve this issue.

The human literature supports the proposition that interstitial white matter, the equivalent of subplate in the postnatal human brain (reviewed in Clancy et al., 2009; Suarez-Sola et al., 2009; Garcia-Marin et al., 2010; Hoerder-Suabedissen and Molnár, 2015), shows structural damage as a result of neonatal HI injury. Tissue from preterm human infants with periventricular leukomalacia show a deficit in the number of microtubule-associated protein 2 (MAP-2) expressing neurons throughout interstitial white matter (Kinney et al., 2012). Scarring is observed in interstitial white matter, alongside cell death markers, in brain tissue from human infants (Pogledic et al., 2014). The number of interstitial neurons present in white matter is known to peak at the developmental stage most sensitive to white matter injury (Kostović et al., 2002; reviewed in Kostović and Judaš, 2010). Immunohistochemical analysis of neonatal telencephalon samples obtained post-mortem from infants born at 25–32 weeks gestation showed a significant loss of GABAergic subplate neurons (Robinson et al., 2006). Many reviews have highlighted the interstitial white matter as a site which should be more thoroughly investigated in neonatal brain injury (reviewed in Volpe et al., 1996; Leviton and Gressens, 2007; Volpe, 2009; Kostović et al., 2011). Several of these propose a role for subplate in resultant cognitive deficits (Volpe, 1977; 2009; Kostović et al., 2011), based on the established role of subplate in thalamocortical development. Unfortunately, post-mortem studies are unable to link subplate pathology to clinical outcomes in patients. The response of both human and rodent subplate to neonatal HI remains unclear, despite assertions of interest from the field.

There are several reasons for believing that subplate could be critical in neonatal HI. One the proposed transient secretory function of subplate neurons. Subplate is enriched in Chondroitin sulphate proteoglycans (CSPGs), whereas the adjacent intermediate zone is not (Kostović et al., 2014). CSPGs are generally secreted from cells, and the subplate transcriptome catalogues a plethora of genes involved in production of extracellular matrix (ECM) and proteoglycans (Belgard et al., 2011; Hoerder-Suabedissen et al., 2013). Additional genes with subplate-restricted expression in the cortex which encode secreted proteins include: neuroserpin (*Serpini1*), neuronal pentraxin 1 (*Nptx1*), and insulin-like growth factor binding protein 5 (*Igfbp5*) (Hoerder-Suabedissen et al., 2013), several of which have had their protein expression confirmed in subplate by immunohistochemistry (Kondo et al., 2015). Connective tissue growth factor (CTGF), a secreted extracellular matrix-associated protein involved in cell adhesion, migration, mitogenesis, differentiation and cell survival (Stritt et al., 2009; reviewed in Brigstock, 1999), is detectable in subplate neurons at E18, increasing in intensity at P3 and P8 (Hoerder-Suabedissen et al., 2009; 2013; Wang et al., 2010; Oeschger et al., 2012). It is unknown whether subplate-secreted proteins serve a protective function in the developing brain.

Related to this secretory function, subplate neurons express relatively mature rough endoplasmic reticulum (rER) (Kondo et al., 2015), an organelle essential for production of secreted proteins (reviewed in Novikoff, 1976; Pfeffer and Rothman, 1987; Lodish, 1988; Hurtley and Helenius, 1989; Pelham, 1989). As a result of the cellular pressures of high protein production, cells activate a series of mechanisms referred to as the ER-stress response (reviewed in Schroder and Kaufman, 2005; Wu and Kaufman, 2006; Kondo et al., 2011). Nissl staining demonstrates enriched protein production in mouse subplate at P8, although staining is fainter in adult (Kondo et al.,

2015). Morphology of subplate neurons is similar to that of rER-rich plasma cells under electron microscopy (EM) (Bloom, 1968; Kondo et al., 2015), and immunohistochemistry for ER stress marker binding immunoglobulin protein (BiP) (Okiyoneda et al., 2004; Kondo et al., 2005; 2012) supports the proposition that ER stress occurs in developing subplate (Kondo et al., 2015). BiP protein synthesis is up-regulated throughout the whole brain under stress conditions, such as glucose deprivation, hypoxia, or the presence of toxins (Lee, 1987; 2001; 2005). It is not known exactly which proteins are secreted throughout development by the subplate, but the enhanced metabolic stress during hypoxia and the potential for neuroprotective secretion reinforce the value of further study of subplate in neonatal HI.

1.3.5 Novel Treatment Development

The development of novel treatments to supplement the sole currently licensed therapy, hypothermia (reviewed in Jacobs et al., 2005, 2013; Shah et al., 2007; Tagin et al., 2012), is imperative. Since this discovery, little progress has been made in identifying additive pharmacological therapies. Few potential treatments have translated to human clinical trials.

Resuscitation at room temperature (Vento et al., 2001a; reviewed in Ventro et al., 2001b; Rabi et al., 2007) and xenon gas administration alongside hypothermia (Hobbs et al., 2008; Thoresen et al., 2009) are among the few therapies shown to have any additive effect in humans. However, more recent publications have questioned the efficacy of xenon. Randomized clinical trials demonstrated that although xenon gas is a safe treatment, there is little or no therapeutic effect of combined hypothermia and

xenon gas in moderate and severe cases of neonatal HI at 18 months follow-up (Azzopardi et al., 2013; 2015; Dingley et al., 2014). A similar experiment in rats found that xenon treatment made no difference to lesion size or neuronal cell numbers in cases of severe HI (Sabir et al., 2016). Barbiturate anticonvulsants also have no effect on long-term neurological development when given following neonatal HI (Goldberg et al., 1986; Hall et al., 1998; Singh et al., 2004; Vargas-Origel et al., 2004; reviewed in Evans et al., 2007).

Recent clinical studies suggest that high dose erythropoietin (EPo) treatment in term HI neonates reduced disability (Strunk et al., 2008; Zhu et al., 2009; McPherson and Juul, 2010). However, even proponents of this potential treatment advise caution in interpreting these early results, and the therapeutic effect does not completely prevent disability. Combination therapy of N-acetylcysteine, a free radical scavenger, and systemic hypothermia reduced infarct volume after focal HI injury in neonatal rats (Jatana et al., 2006), now under investigation in human clinical trials and showing some promise (Moss et al., 2018). Another free radical scavenger, allopurinol, reduced cerebral oedema and neuropathological damage in rats (Palmer et al., 1990), also under safety testing in humans (Martinello et al., 2017a). Canabidiol is also under investigation as a treatment in rodents (Pazos et al., 2012). However, most of these treatments have only been trialled in animals, and the field is still awaiting a candidate neuroprotective molecule which is both safe and effective in neonatal humans (reviewed in Lai and Yang, 2011).

Another therapeutic approach under development is stem cell therapy (reviewed in Parolini et al., 2010; Bonifacio et al., 2011; Zhang et al., 2014; Douglas-Escobar and Weiss, 2015; Lawton et al., 2015 Ruiz et al., 2017). These therapies make use of

evidence that transplantation of human bone-marrow derived stem cells into the lesion can assist brain plasticity (Tajiri et al., 2013). Results of this therapy have been promising in animal models (Jendelová et al., 2004; Daadi et al., 2009a; 2009b), however, the technique awaits validation in a clinical setting. Additionally, the use of stem cell therapy for cerebral palsy in human patients has produced mixed results (Li et al., 2012; Liao et al., 2013; Sharma, 2014), which will likely delay the progress of stem cell trials in human HI patients.

New approaches are required to identify potential neuroprotective molecules as treatments for neonatal HI. Drawing on detailed yet incomplete knowledge of the physiology of neonatal HI, several factors must be satisfied in a new potential therapy. All potential treatments should be safe for vulnerable neonates and not interfere with essential developmental milestones. This challenges the NMDA-inhibition strategies (Meldrum, 1990; reviewed in Johnston, 2001; 2005), as the glutamate system is essential for setting up normal synaptic plasticity within the developing brain (reviewed in Aoki and Siekevitz, 1988; Hattori and Wasterlein, 1990; Johnston, 2009; Partanen et al., 2013; Simpson et al., 2014). Treatments should also be specific. The ideal therapy would target molecules common to the excitotoxicity, oxidative stress, and inflammation pathways (reviewed in Chaudhari et al., 2014; Fischer and Maier, 2015; Chamorro et al., 2016; Burd et al., 2016). Targeting these common mediators would allow a single pharmaceutical to be efficacious against multiple mediators of brain damage and neuronal death, instead of eliciting a reshuffle of pathways to favour a different type of cell death. One such potential candidate is neuroserpin.

1.4 Neuroserpin

Neuroserpin is a neuronally secreted serine-protease inhibitor enzyme with roles in cell death, neuronal plasticity, and microglial activation. The protein neuroserpin is encoded in mouse and human by the gene *Serpini1*. mRNA expression is specific to the CNS in mouse (Osterwalder et al., 1996; Krueger et al., 1997) and neuroserpin protein is found in the human brain (Teesalu et al., 2004; Adorján et al., 2019). This specificity of localisation, coupled to the breadth of damage pathways it targets through its substrate tissue plasminogen activator (tPA), highlights neuroserpin as an interesting molecule to study in neonatal HI. Evidence of a neuroprotective function in animal models of adult ischaemic stroke confirms its pedigree.

1.4.1 Molecular Characteristics and Functions of Neuroserpin

Neuroserpin was first identified in the secreted product of cultured neuronal axons (Osterwalder et al., 1996). Protein expression is primarily localized to neurons (Osterwalder et al., 1996; Hastings et al., 1997; Lee et al., 2015b). *In situ* hybridization studies demonstrate expression of *Serpini1* mRNA throughout cerebral cortex, hippocampus, and olfactory bulbs, with scattered expression in cerebellum, pons, and thalamus from birth to adulthood (Krueger et al., 1997). High *Serpini1* mRNAexpression has been identified in subplate relative to Layer VI of cortex in P8 mouse brain by microarray (Hoerder-Suabedissen et al., 2009), confirmed by immunohistochemistry for neuroserpin protein (Kondo et al., 2015). Although neuroserpin protein has been demonstrated in human brain tissue (Teesalu et al., 2004; Adorján et al., 2019), detailed maps of expression are currently missing. This specific localisation suggests that putative neuroserpin-modulatory treatments may

not create dangerous side effects in other vulnerable organs such as the cardiovascular and pulmonary systems.

Neuroserpin is an inhibitory enzyme. Its primary known target is the adult human stroke treatment, tissue plasminogen activator (tPA) (Osterwalder et al., 1998; Barker-Carlson et al., 2002; Ricagno et al., 2009; 2010; reviewed in Yepes and Lawrence, 2004a; Miranda and Lomas, 2006). Neuroserpin has also been shown to exhibit weak inhibition of plasmin and urokinase plasminogen activator (uPA) (Osterwalder et al., 1998). The *Serpini1* gene sequence, brain-enriched expression, and proposed enzymatic function is highly conserved across species including *Drosophila melanogaster* (Hill et al., 2001; Ellisdon et al., 2014), zebrafish (Toro et al., 2009), mouse (Osterwalder et al., 1996; 1998; Barker-Carlson et al., 2002), chicken (Schrimpf et al., 1997), and human (Schrimpf et al., 1997).

Through inhibition of tPA, neuroserpin has the potential to influence many distinct molecular cascades (reviewed in Yepes and Lawrence, 2004b; 2004c; Benarroch, 2007; Yepes, 2015; Millar et al., 2017). tPA, also secreted by neurons (Krystosek and Seeds, 1981a; 1981b; Lochner et al., 2006), interacts with a large number of pathways; activating NMDA receptors (Qian et al., 1993; Nicole et al., 2001), activating microglia (Rogove et al., 1999; Siao and Tsirka, 2002), and recruiting cell death related cascades (Tsirka et al., 1995; Wang et al., 1998; reviewed in Yepes and Lawrence, 2004a; Zhao et al., 2007), in addition to its function in vascular thrombosis (Rijken et al., 1979; 1980). The known components of the neuroserpin/tPA molecular cascade are summarised in Figure 1.8.

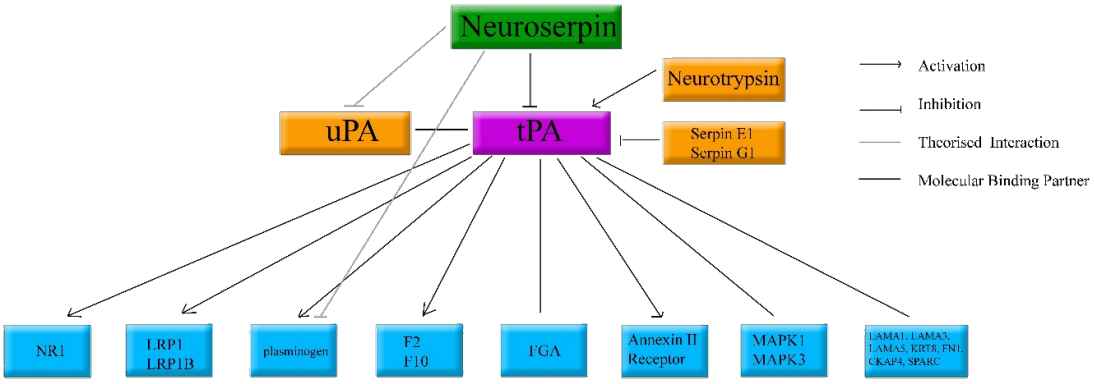


Figure 1.8 – Classical Binding Cascade for Neuroserpin Serine Protease Inhibitor. The main molecular target of neuroserpin is inhibition of the enzyme tissue plasminogen-activator (tPA.) Confirmed molecular binding partners are shown with a black line. Arrows denote confirmed activation. Orthogonal lines denote confirmed inactivation. Lines without caps denote confirmed binding with no documented physiological data. Dotted lines denote theoretical interactions which have not yet been demonstrated physiologically. tPA = tissue plasminogen activator, uPA = urokinase plasminogen activator. All other abbreviations denote standard gene names.

Other, tPA-independent enzymatic pathways for neuroserpin have also been described (reviewed in Ma et al., 2012a; Millar et al., 2017). Cell lines over-expressing neuroserpin demonstrate an increase in N-cadherin protein expression and related cell adhesion, this is maintained when the tPA binding site of neuroserpin is mutated (Lee et al., 2008). Neuroserpin has been shown to prevent excitotoxic neuronal death induced by plasmin and kainic acid in transgenic mice which do not express tPA protein (Wu et al., 2010). In addition, the 20 methionine residues present within neuroserpin have been claimed to convey protection against oxidative stress (Mohsenifar et al., 2007), and exogenous neuroserpin has been shown to possess anti-inflammatory properties outside the central nervous system on arterial plaque growth (Munuswamy-Ramanujam et al., 2010). The molecular cascades behind these tPA-independent functions are not well understood (reviewed in Ma et al., 2012a).

The balance between the classical neuroserpin/tPA pathway and other, currently unidentified, molecular targets of neuroserpin in its physiological action in the brain requires substantial further investigation. Many publications have focused on the known tPA-related interactions, yet this does not necessarily demonstrate that tPA is the primary molecular target of neuroserpin.

1.4.1.1 Neuroserpin and Cell Death

The physiological actions of neuroserpin can be broadly categorised into three major pathways: cell death, neuronal plasticity, and immune cell activation and inflammation. These closely follow the major classes of molecular change proposed by neuropathological theories of neonatal HI (reviewed in McLean and Ferriero, 2004; Fatemi et al., 2009; Volpe, 2012; Millar et al., 2017).

Neuroserpin has been implicated in protection against neuronal death (reviewed in Galliciotti and Sonderegger, 2006; Lee et al., 2017). Exogenous neuroserpin administration *in vitro* decreases apoptosis caused by tPA (Wu et al., 2010; Rodríguez-González et al., 2011a), NMDA (Lebeurrier et al., 2005a; 2005b; Ma et al., 2012b), kainic acid (Wu et al., 2010), oxidative stress produced by hydrogen peroxide administration (Mohsenifar et al., 2007), and OGD (Wu et al., 2010; Rodríguez-González et al., 2011a; Ma et al., 2012b), but not AMPA-induced toxicity (Lebeurrier et al., 2005a). In addition, aberrant initiation of neuroserpin expression in cancer cells preserved the tumour and has been linked with increases treatment-resistance in prostate cancer (Chang et al., 2000; Hasumi et al., 2005; Valiente et al., 2014). Exogenous neuroserpin administration has also been shown to reduce spread of

kainate-induced seizures in mouse, and decreases the expression of cell death markers (Yepes et al., 2002).

1.4.1.2 Neuroserpin and Inflammation

Of the three classes of neuroserpin function, its role in inflammation is the least understood. When applied to vascular plaques *in vitro*, recombinant neuroserpin reduces T-Cell lymphocyte invasion (Munuswamy-Ramanujam et al., 2010). Administration of intracerebral neuroserpin directly following adult HI stroke in mouse, is accompanied by a qualitative decrease in the volume of infarct infiltrated by activated microglia (Yepes et al., 2000), and lower microglial inflammatory marker expression (Gelderblom et al., 2013). In human adult stroke patients, higher levels of neuroserpin in blood samples correlate with lower levels of immune marker proteins (Rodríguez-González et al., 2011c).

There is considerable debate over whether microglial activation is beneficial or detrimental in neonatal HI (reviewed in McRae et al., 1995; Mallard et al., 2013; Kaur et al., 2013), so understanding the role of neuroserpin in balancing this cascade could prove important. The lack of a complete molecular network explaining these anti-inflammatory effects is currently a restriction.

1.4.1.3 Neuroserpin and Neuronal Plasticity

In addition, neuroserpin is likely involved in neuronal plasticity (reviewed in Man and Ma, 2012). This could be problematic if neuroserpin becomes a pharmacological

substrate for the development of neonatal HI treatments for human patients, as the neonatal human brain circuitry is undergoing a great deal of developmental plasticity at this time (reviewed in Aoki and Siekevitz, 1988; Hattori and Wasterlein, 1990; Johnston, 2009; Partanen et al., 2013; Simpson et al., 2014).

The first evidence that neuroserpin may have a role in neuronal plasticity originates from studies of endocrine cell lines, which grow neurite-like processes when neuroserpin is administered to the media (Hastings et al., 1997; Hill et al., 2000; Jacovina et al., 2001) and mouse neurons (Borges et al., 2010). Although a publication claiming a similar dendrite-regulating function for neuroserpin in hippocampal neurons has been retracted (Lee et al., 2012). At the molecular level, neuroserpin secretion from dense core vesicles is enhanced by depolarisation in cultured neurons (Berger et al., 1999; Ishigami et al., 2007). Monocular enucleation at P11 in mouse *in vivo* leads to decreased *Serpini1* mRNA expression in contralateral primary visual cortex (V1) compared to the control hemisphere (Wannier-Morino et al., 2003). The relative importance of these findings for functional developmental plasticity remain unclear.

1.4.2 Neuroprotective Role of Neuroserpin in Adult Hypoxic Ischaemic Stroke and Oxygen-Glucose Deprived Culture

Neuroserpin has been studied extensively in cell culture models of HI stroke. Administration of neuroserpin protects mouse cortical neurons *in vitro* against NMDA-induced excitotoxicity, but not AMPA-induced excitotoxicity (Lebeurrier et al., 2005a; 2005b; Ma et al., 2012b). Further, neuroserpin is protective in an *in vitro* model of HI, oxygen glucose deprivation (OGD) (Wu et al., 2010; Rodríguez-

González et al., 2011a; Ma et al., 2012b). Both neurons and astrocytes cultures undergo less apoptosis following OGD, and do not exhibit damaged neural processes when exogenous neuroserpin is administered directly after OGD (Rodríguez-González et al., 2011a; Ma et al., 2012b). Hippocampal neurons from both wild-type and *Plat* knockout mice, which do not produce functional tPA protein, are protected from OGD, plasmin-mediated cell death and kainic acid by exogenous neuroserpin administration (Wu et al., 2010), demonstrating that the neuroserpin neuroprotective effect is not exclusively dependent on tPA inhibition.

Neuroserpin is also neuroprotective *in vivo*. One major model used to simulate hypoxic-ischaemic stroke in adult rodents is analogous to the Rice–Vannucci model for neonates (Eklöf and Siesjö, 1973; Rice et al., 1981; reviewed in Bederson et al., 1986). Adult rats given intracerebral injections of exogenous neuroserpin protein before left common carotid artery ligation showed a decrease in infarct volume compared to saline-injected controls, in addition to decreased expression of apoptosis markers (Yepes et al., 2000). *Serpini1* knock-out mice exhibited increased lesion volumes following adult HI (Cinelli et al., 2001; Gelderblom et al., 2013), whereas transgenic mice expressing six-times normal neuroserpin protein demonstrated smaller infarct volumes (Cinelli et al., 2001). Exogenous neuroserpin injection is also protective against NMDA-induced excitotoxicity in live adult rat (Lebeurrier et al., 2005a). Currently, the only evidence for this has come from adult models of HI stroke, far from conclusive evidence of neonatal protection due to the differences in neuroanatomy and neurochemistry between the developing and adult brain. However, this work remains of utility, as at the very least investigating the neuroserpin-tPA system in neonatal models will add to understanding of the differences between neonatal and adult response to HI.

Exogenous neuroserpin administration in rats increases the window for effective tPA treatment in a model of adult stroke (Zhang et al., 2002). Increased tPA expression is found in *Serpini1* knock-out mice undergoing adult HI injury compared to controls (Cinelli et al., 2001; Gelderblom et al., 2013). However, exogenous neuroserpin is also neuroprotective in *Plat* knock-out mice (Wu et al., 2010). Ischaemic-reperfusion-induced injury in the retina of *Plat* knock-out mice demonstrate rescued retinal apoptotic marker expression when injected with neuroserpin (Gu et al., 2015). The neuroprotective properties of neuroserpin appear to involve both tPA-dependent and tPA-independent cascades.

A role for neuroserpin in human adult HI stroke has also been described. Correlative studies have shown that high concentrations of neuroserpin in blood serum from human patients are associated with better functional outcome (Rodríguez-González et al., 2011b), and reduced inflammation (Rodríguez-González et al., 2011c). However, attempts to find a relationship between neuroserpin polymorphisms in humans and likelihood of stroke have produced little evidence of protective neuroserpin variants (Cole et al., 2007; Tjärnlund-Wolf et al., 2011). Mutations in the human *Serpini1* gene have been associated with two rare hereditary disorders (reviewed in Galliciotti and Sonderegger, 2006; Miranda and Lomas, 2006; Caccia et al., 2010). Individuals present either with epilepsy (Yepes et al., 2002; Coutelier et al., 2008) or dementia with neuroserpin inclusion bodies (Davis et al., 1999a; 1999b, 2002; Yazaki et al., 2001; Belorgey et al., 2004; Ricagno et al., 2010). It is not currently known whether these disorders are caused by novel functions of the mutated protein or by loss of physiological functions (reviewed in Lee et al., 2015a).

1.4.3 Role of Neuroserpin in Neonatal Hypoxia-Ischaemia

Evidence of a role for neuroserpin in neonatal HI is not entirely absent. A patent application published online claims that neuroserpin injection 4 hours after neonatal HI in rat pups reduced infarct volume but had no effect on LPS-sensitized HI, although it amalgamates neuroserpin and PAI-1 treatment in the figures, making this claim impossible to interpret (Kuan et al., 2010). However, the small number of published rodent microarrays following neonatal HI fail to detect significant changes in *Serpini1* expression in the hypoxic-ischaemic rodent brain (Carmel et al., 2004; Maj et al., 2004a; 2004b; Juul et al., 2009; Nagel et al., 2012; Rognlien et al., 2014). This could be explained by the delay between HI injury and sample collection, 6 hours to 7 days post injury in these studies, which may be too early or too late to expect to see genomic changes in *Serpini1* expression. Additionally, microarray studies cannot reveal whether neonatal HI caused differences in neuroserpin translation or secretion, neither of which have yet been studied in neonatal HI.

Despite the lack of evidence for a direct role in neonatal HI, substantially more has been published documenting effects of the primary molecular target of neuroserpin, tPA, in neonatal HI. tPA is broadly considered to be deleterious to cerebral recovery from neonatal HI (Adhami et al., 2008; Omouendze et al., 2013; reviewed in Millar et al., 2017). In P7 rats which undergo unilateral common carotid artery ligation, tPA treatment impairs blood flow throughout the brain, an effect rescued by injection of the tPA inhibitor α2-antiplasmin (α2AP) (Adhami et al., 2008). Release of tPA by the cerebral microvasculature, as seen following neonatal HI, has also been shown to compromise the glucose content of the extracellular medium in cultured cortical neurons from neonatal mouse (Henry et al., 2013). Administration of tPA inhibitor

plasminogen-activator-inhibitor 1 (PAI1) reduces locomotor disorder and white matter damage in LPS-sensitised neonatal HI rats (Yang et al., 2013a; 2013b; Yang and Kuan, 2015). This pathway is relatively understudied in neonatal HI, despite the potential to target a multitude of injury-relevant molecules.

Neonatal HI remains one of the most common causes of infant death and disability globally. Reducing the burden of morbidity should be a high priority for biomedical research. A dearth of treatments is currently available postnatally for these vulnerable infants, restricted to only hypothermia, a breakthrough treatment which is not fully effective in all cases. There are no currently licensed additive pharmacological treatments. Drawing attention to molecules such as neuroserpin and tPA, potential common moderators of injury pathways, will be essential to the development of new efficacious pharmacological treatments.

1.5 Aims of the Thesis

This introduction details the high prevalence and long-term disability associated with neonatal hypoxia ischaemia, alongside the wealth of scientific methods employed to study this condition in a laboratory setting which have thus far led to few treatments reaching clinical trials in human patients. The molecular complexity of neonatal HI leaves many questions open to research, with each new discovery giving rise to more accessible unknowns. This thesis contends with the unanswered questions related to neuroserpin and its role in neonatal HI injury.

First, the pattern of neuroserpin protein expression was investigated in healthy developing brains of mice and humans. Expression was quantified in the context of proposed neuroserpin functionality, and used to gather evidence of developmental tolerance to neuroserpin. Second, the pattern of neuroserpin expression in cerebral cortex was examined following adapted Rice-Vannucci neonatal HI models in rats and mice. Total protein and neuronal expression pattern were quantified to investigate whether neuroserpin forms part of the endogenous response to HI in the neonatal brain. Finally, preliminary experiments investigating the proposed neuroprotective properties of neuroserpin in the neonatal brain were undertaken, using the *Serpini1* knock-out mouse to study the absence of functional neuroserpin. Both *in vitro* and *in vivo* experiments were designed to test whether neuroserpin plays an analogous role in neonatal HI to the more extensively documented neuroprotective function in adult models.

1.5.1 Aims of Chapter 3: Characterisation of Neuroserpin Protein Expression Throughout Development in Mouse and Human

This chapter undertakes a detailed analysis of the expression of neuroserpin protein in the brain, specifically the subplate layer of cerebral cortex, throughout development in mouse and confirms neuroserpin expression in foetal human tissue.

Fluorescent immunohistochemistry is used across postnatal developmental time points in mouse primary somatosensory cortex (S1), capturing the equivalent period to birth in humans (Clancy et al., 2007), to quantify the nature and proportion of neuroserpin-immunoreactive neurons and glial in each layer of neocortex. The *Serpini1* mRNA and neuroserpin-immunoreactivity enriched subpopulation of subplate (Layer VIb) neurons are further characterised by birth-dating and co-expression of subplate-specific or -enriched molecular markers (Hoerder-Suabedissen et al., 2009; 2013; Kondo et al., 2015). The peak in neuroserpin-immunoreactivity detected over the rodent equivalent of term is applied to detection of neuroserpin in second trimester and term human foetal brain tissue.

Expression patterns are also discussed in relation to proposed neuroserpin functionality. Neuroserpin-immunoreactivity was linked to the proposed neurosecretory function of subplate (Kondo et al., 2015) through co-localisation immunohistochemistry with structural and stress markers of endoplasmic reticulum (ER) and with metabolic stress markers the heat-shock proteins (HSPs). A preliminary investigation into endogenous neuroserpin expression at P6 following monocular deprivation in P1 mouse was also undertaken to investigate the link between neuroserpin protein and plasticity in the developing brain.

1.5.2 Aims of Chapter 4: Characterisation of Neuroserpin Protein Expression in Rodent Models of Neonatal Hypoxia Ischaemia

This chapter expands the development time series through a rat and a mouse model of infant hypoxia ischaemia adapted from the Rice-Vannucci method (Rice et al., 1981). Quantitative fluorescent immunohistochemistry and semi-quantitative Western blot are used to study neuroserpin protein during the endogenous response to HI injury.

Cortical neuroserpin-immunoreactivity is examined per cortical layer in a preterm equivalent rat model of HI extensively validated for injury severity (Okusa et al., 2014). Results suggest a highly subplate-specific up-regulation in number and proportion of neuroserpin-immunoreactive neurons in the injured hemisphere of animals with moderate, but not mild, HI injury.

To investigate this result further, a neonatal mouse model is established and optimised to replicate mild-to-moderate neonatal HI injury, and validated for evidence of brain damage qualitatively using metabolic activity marker 2,3,5-triphenyl tetrazolium chloride (TTC) and quantitatively using immunohistochemistry for cerebral inflammation markers.

Neuroserpin protein is quantified in both the hypoxic-ischaemic and hypoxia-only control hemisphere 48 hours after injury. Immunohistochemistry experiments replicating the methods used in the preterm rat model detect a subtle subplate-specific increase in neuroserpin-immunoreactivity in the injured hemisphere, with no difference detected in any other cortical layer. Western blot comparing total protein in whole cortex between the two hemisphere of neonatal HI brains is carried out to provide a measure of total protein. Semi-quantitative Western blot fail to find a statistically significant difference in cortical neuroserpin between hemispheres.

1.5.3 Aims of Chapter 5: Preliminary Investigations into Vulnerability to Neonatal Hypoxia Ischaemia in the Absence of Neuroserpin Protein, using the *Serpini1* Knock-Out Mouse

This chapter interrogates the proposed neuroprotective properties of neuroserpin using the *Serpini1* knock-out mouse, which does not express neuroserpin (Cinelli et al., 2001; Madani et al., 2003). Vulnerability to neonatal HI is compared between *Serpini1* knock-out animals and wild-type controls through *in vitro* oxygen glucose deprivation (OGD) experiments with cultured cortical neurons and *in vivo* using measures of brain damage following an adapted Rice-Vannucci model of neonatal HI.

Oxygen glucose deprivation protocols are established using Neuro-2-A (N2A) neuroblastoma cells to generate partial loss of cell viability as measured by 3-(4,5-dimethyl-thiazol-2-yl)-2,5-diphenyl-tetrazolium Bromide (MTT), and to test the effect of administration of exogenous purified neuroserpin protein on cell survival. This protocol is then extended to primary cortical neurons from E18 wild-type and *Serpini1* knock-out mice, although data from knock-out neurons is inconclusive. Pre- and post-treatment with exogenous neuroserpin are also investigated.

Sensitivity to neonatal HI brain damage is also investigated in *Serpini1* knock-out mice and wild-type littermates 48 hours after undergoing an adapted Rice-Vannucci model of neonatal HI. Two methods are used to quantify brain damage. The first employs 2,3,5-triphenyl tetrazolium chloride (TTC) to measure metabolic activity in whole brains, the second quantifies immunoreactivity for inflammatory brain damage markers in primary somatosensory cortex (S1) in both hemispheres across genotypes. Both require methodological refinement, but can be used to inform future experiments investigating neuroserpin neuroprotection in the developing brain.

2 General Methods

This chapter describes general experimental methods relevant to all subsequent chapters. Each experimental chapter describes methods unique to that chapter in full in the respective methods section.

2.1 Experimental Animals

All experiments were approved by local ethical review committee and conducted in accordance with personal (PIL) and project licenses (PPL), as mandated by the Animals Scientific Procedures Act, 1986 (ASPA).

C57BL/6 wild-type (WT), B6.129-Serpini1^{tm1Dpw}/J (*Serpini1* knock-out or KO), Golli-τ-eGFP, National Institute of Health Swiss (NIHS), and Lpar1-eGFP mice were maintained on a standard diet and light cycle in accordance with ASPA and were mated in the Biomedical Sciences Building, University of Oxford, UK. Details of the genotype, phenotypic description, breeding partners, and source of experimental mouse strains are given in Table 2.1.

Paraformaldehyde (PFA)-fixed Sprague Dawley rat brains were generated by and received from Dr. Vanessa Ginet and Dr. Anita C. Truttmann of the Department of Neonatology, Department of Paediatrics, University Hospital Centre and University of Lausanne, Switzerland.

Strain Name	Genotype	Description	Mated With	Source
C57BL/6	Wild-Type (WT) (Sigmund, 2000; Seong et al., 2004; Zurita et al., 2011; Fontaine and Davis, 2016).	Wild-Type Inbred black mouse strain (Zurita et al., 2011).	C57BL/6	Charles River http://www.criver.com/products-services/basic-research/find-a-model/c57bl-6n-mouse Last accessed: 10/08/2018
B6.129-Serpini1^{tm1Dpw}/J	Targeted vector containing PGK-NEO cassette inserted into exon 2 of mouse *Serpini1* gene. No gene product detected by Western blot, or immunohistochemistry analysis of brain tissue (Osterwalder et al., 1996; 1998).	Homozygous *Serpini1* -/- demonstrates anxiety-like hypoactivity behaviour, reduced exploration behaviour; heterozygotes exhibit an intermediate phenotype (Madani et al., 2003). Homozygous *Serpini1* -/- show increased sensitivity to adult hypoxic ischaemic stroke (Cinelli et al., 2001; Gelderblom et al., 2013).	Serpini1 -/- Serpini1 +/- C57BL/6	Jackson Laboratories https://www.jax.org/strain/019121 Last accessed: 10/08/2018
Golli-τ-eGFP	Homozygous expression of eGFP under the Golli-τ promotor of myelin basic protein (MBP) promotor complex (Jacobs et al., 2007).	Expression of GFP in cortical neurons in Layers VI and subplate (Layer VIb) (Jacobs et al., 2007; Grant et al., 2012; 2016; Hoerder-Suabedissen et al., 2018).	C57BL/6 Golli-τ-eGFP	Gift from Erin Jacobs, University of California, Los Angeles (UCLA), USA
National Institute of Health, Swiss (NIHS)	Outbred albino mouse strain, females only used in this thesis (Rice and O'Brien, 1980; Chia et al., 2005).	Outbred albino mouse strain (Chia et al., 2005).	Lpar1-eGFP males	Harlan Sprague Dawley, UK http://www.envigo.com/products-services/research-models-services/models/research-models/mice/outbred/nih-swiss-outbred-mice/ Last accessed: 10/08/2018
Lpar1-eGFP (also known as Edg2-eGFP)	Expression of eGFP on the Y chromosome (http://www.gensat.org/imagenavigator.jsp?imageID=32798 Last accessed: 10/08/2018)	Lpar1-eGFP expression in a proportion of subplate (Layer VIb) cells throughout development and in a proportion of Layer V interneurons, (http://www.gensat.org/ Last accessed: 10/08/2018 Grant et al., 2012; Pedraza et al., 2014; Marques-Smith et al., 2016; Hoerder-Suabedissen et al., 2018).	NIHS females	Harlan Sprague Dawley, UK (no longer available from this source)

Table 2.1 – Mouse Strains used Experiments in This Thesis

2.2 Genotyping

Animals which did not undergo Rice-Vannucci hypoxia ischaemia were ear-clipped for genotyping between postnatal day 10 (P10) and weaning (P21). Animals which underwent Rice-Vannucci hypoxia-ischaemia were ear-clipped under anaesthesia during surgery at postnatal day 8 (P8).

2.2.1 *Serpini1* Genotyping

For DNA extraction, ear clips were submerged in 200 µl DNA extraction buffer with 2 µl Proteinase-K (#03115828001, Roche, Welwyn Garden City, UK) at 37℃ overnight, or for a minimum of 4 hours. Subsequently, Proteinase-K was heat-inactivated at 95℃ for 10 minutes. Crude extract was centrifuged at 13 kRPM for 20 seconds. The composition of DNA extraction buffer is shown in Table 2.2.

For polymerase chain reaction (PCR), 1 µl of DNA extract was added to 19 µl OneTaq®Quick-Load® 2x Master Mix with Standard PCR Reaction Buffer (#M0486S, New England Biolabs, Hitchin, UK). 1 µl of each required custom primer (Eurofins, Wolverhampton, UK), with annealing temperatures between 50-56℃, was added to the PCR mix. Full primer sequences are shown in Table 2.3. The complete composition of PCR Mix is shown in Table 2.4. DNA extract was run twice, once with wild-type primers, once with knock-out primers, as the bands revealed by these two sequences are of extremely similar length. Cycling conditions for *Serpini1* PCR are shown in Table 2.5.

PCR product was run on 1.5% agarose gels made with powdered agarose (#A9539, Sigma Aldrich, Gillingham, UK) in electrophoretic buffer solution. DNA was

visualised by staining with SYBR® Safe DNA Stain (#S33102, Thermo Fisher, Hemel Hempstead, UK). Full composition of electrophoresis gels is given in Table 2.6. Gels were run for 50 minutes at 95 Volts. The wild-type DNA revealed a single band of approximately 500 base-pairs (bp) in length, whereas the *Serpini1* null mutant DNA reveals a single band of approximately 600 base-pairs (bp) in length.

DNA Lysis Buffer Solution Component	pH	Supplier
50mM Tris-HCl	8.8	Sigma Aldrich, T3253
1mM EDTA	8.0	Sigma Aldrich, E5134
0.5% Tween-20	7.0	Sigma Aldrich, P9416

Table 2.2 – DNA Extraction Buffer

Primer Name	Base Pair Sequence
Serpini1 WT Forwards Primer	5' TCCTTAATAGGCCTTGGTTTG 3'
Serpini1 WT Reverse Primer	5' TTGAATGGCGGATTTCTTTC 3'
Serpini1 KO Forwards Primer	5' ATGCGATGTTTCGCTTGG 3'
Serpini1 KO Reverse Primer	5' CCTTTCGACCTGCAGCCAAT 3'

Table 2.3 – *Serpini1* Genotyping Primers

PCR Mix Solution Component	Volume	Supplier
OneTaq®Quick-Load® 2x Master Mix with Standard PCR Reaction Buffer	10µl	New England Biolabs, M0486S
$MgCl_2$	0.08µl	Sigma Aldrich, 208337
Serpini1 WT/Serpini1 KO Common Primer	1µl	Eurofins, custom
Serpini1 WT /Serpini1 KO Reverse Primer	1µl	Eurofins, custom
DNA extract	1µl	-
Deionised Nano H_2O	7µl	-

Table 2.4 – Polymerase Chain Reaction (PCR) Mix used for *Serpini1* Genotyping

Wild-type (Serpini1 +)				**Knock-out (Serpini1 -)**			
Step		**Temperature**	**Time (seconds)**	**Step**		**Temperature**	**Time (seconds)**
Initial Denaturation		94	120	Initial Denaturation		94	120
Cycles	1	94	20	Cycles	1 (repeat 40x)	94	15
		65	30			55	30
		68	30			72	55

	2	94	20				
		64.5	30				
		68	30				
	3	94	20				
		64	30				
		68	30				
	4	94	20				
		63.5	30				
		68	30				
	5	94	20				
		63	30				
		68	30				
	6	94	20				
		62.5	30				
		68	30				
	7	94	20				
		62	30				
		68	30				
	8	94	20				
		61.5	30				
		68	30				
	9	94	20				
		61	30				
		68	30				
	10	94	20				
		60.5	30				
		68	30				
	11	94	15				
		60	30				
		72	30				
Final		72	60	Final		72	60
Hold		10	-	Hold		10	-

Table 2.5 – Cycling Conditions for *Serpini1* Genotyping Polymerase Chain Reaction (PCR)

Electrophoresis Gel Buffer Component	**Quantity**	**Supplier**
Trizma® Base	242mg	Sigma Aldrich, 93352
Boric Acid	120mg	Sigma Aldrich, B6768
0.5M EDTA (pH = 8.0)	100µl	Thermo Fisher, 15575020
Deionised Nano H_2O	Up to 50ml	-
Agarose Powder	750mg	Sigma Aldrich, A9539
SYBR® Safe DNA Gel Stain	500ml	Invitrogen, S33102

Table 2.6 – 1.5% Agarose Electrophoresis Gel Composition for *Serpini1* Genotyping

2.3 Tissue Collection

Tissue collection methods varied according experimental purpose. This section outlines all tissue collection methods used throughout this thesis, methods used for individual experiments are specified in the relevant results chapter.

2.3.1 Embryonic fixed tissue collection

Timed-pregnant female mice were killed by cervical dislocation (confirmation of death by cervical dislocation), and embryos were removed by caesarean section with surgical tools. Embryonic brains (E13-E18) were dissected out and post-fixed in 4% paraformaldehyde (PFA) (#441244, Sigma Aldrich, Gillingham, UK) in 0.1M Phosphate Buffered Saline (PBS) at pH 7.4 at 4°C overnight. Brains were stored at 4°C in 0.1M PBS with 0.05% sodium azide (PBS-A) (#S2002, Sigma Aldrich, Gillingham, UK). The composition of 4% PFA, 0.1M PBS, 0.1M PBS-A and other frequently used solutions is shown in Table 2.7.

2.3.2 Postnatal fixed tissue collection

Mice aged P0-P7 were given an intra-peritoneal injection of 150mg/kg pentobarbitone (#XVD 135, Pentoject, Animal Care Ltd, York, UK), then underwent transcardial perfusion with 0.1M PBS (see Table 2.7). Perfusion ceased when further circulation of PBS failed to cause further decrease in haemoglobin pigment of the extremities. Brains were then dissected out and post-fixed in 4% PFA in 0.1M PBS without

sucrose at 4°C overnight. PFA was removed and brains washed with 0.1M PBS without sucrose. Brains were then stored in 0.1M PBS-A without sucrose at 4°C.

Mice aged from P8 to adult were transcardially perfused with 0.1M PBS, followed by perfusion with 4% PFA in 0.1M PBS. Brains were then dissected out and post-fixed in 4% PFA in 0.1M PBS at 4°C overnight. PFA was removed and brains washed with 0.1M PBS. Brains were then stored in 0.1M PBS-A at 4°C.

2.3.3 Fresh tissue collection for Western Blot

Animals aged P0-adult were killed by cervical dislocation (confirmation of death by cervical dislocation), and brains were dissected out on ice in 0.1M PBS chilled to 4°C with autoclave-sterilised dissection tools to prevent sample contamination with any protein transferred to the tools during previous dissection or handling. All dissection tools were autoclaved for a minimum of 30 minutes at a maximum temperature of 120°C. Dissected brain tissue was briefly washed in 0.1M PBS to remove blood, and then transferred to autoclave-sterilised Eppendorf tubes on solid CO_2 (dry ice). Tissue was stored at -80°C.

2.4 Image Acquisition

Fluorescence microscopy images were taken using a Leica DMR fluorescence microscope (#933789, Leica Microsystems, Milton Keynes, UK) with DC500 camera (#12447108, Leica Microsystems, Milton Keynes, UK) and Leica FireCam software

(Leica Microsystems, Milton Keynes, UK) (https://meyerinst.com/digital-cameras/leica/ec3/DFC_FireCam.pdf, last accessed 10/08/2018).

Confocal images were taken using a Zeiss LSM 710 confocal microscope (Carl Zeiss Microimaging, Oberkochen, Germany). Images were compiled and analysed using Adobe Photoshop CS5 (Adobe Systems Inc., California, USA) (https://help.adobe.com/archive/en_US/photoshop/cs3/ photoshop_cs3_help.pdf, last accessed 10/08/2018) and Image J (Image analysis in Java) (https://imagej.nih.gov/ij/, last accessed 10/08/2018; Schneider et al., 2012).

2.5 Statistics

All cell quantification analysis which included more than two groups were tested for statistical significance using analysis of variance (ANOVA) performed in Microsoft Office Excel (Microsoft, Missouri, USA). Most analysis employed a two-way ANOVA to test for significance across experimental condition and cortical layer. All experiments detail statistical test used and groups compared in the relevant results figure and table. When the F value generated by the ANOVA test was less than or equal to the F critical value, no statistical significance existed between groups and no further statistical analysis was performed. When the F value was greater than the F critical value, the null hypothesis was rejected and it was accepted that a statistically significant difference existed between at least two of the groups. T-test was then used to compare pairs of groups.

Semi-quantitative Western blot analysis, and cell quantification analysis which produced an F value greater than F critical with ANOVA analysis, were analysed for

statistical significance using paired t-test in Microsoft Office Excel (Microsoft, Missouri, USA). Graphs were generated using Microsoft Office Excel and R (Liaw and Weiner, 2002; Chessel et al., 2004; R Core Team, 2014; https://www.r-project.org/, last accessed 10/08/2018). Methods for data analysis prior to statistical comparison are detailed in the methods sections of the results chapters.

2.6 Frequently used solutions

Details of common solutions used throughout this thesis are given in Table 2.7. Details of solutions unique to individual experiments, such as antibody concentrations, are given in the methods section of the relevant results chapter.

Solution	pH	Components	Quantity	Supplier
0.5M Phosphate Buffer Saline (PBS)	7.4	$Na_2HPO_4.2H_2O$	72.1g	Sigma Aldrich, 30435
		$NaH_2PO_4.2H_2O$	14.8g	Sigma Aldrich, 71500
		$NaCl_2$	45g	Sigma Aldrich, 57653
		Deionised H_2O	Up to 1L	-
		1M NaOH	Add dropwise until pH = 7.4	Sigma Aldrich, S8045
		2M HCl	Add dropwise until pH = 7.4	Sigma Aldrich, H1756
0.1M Phosphate Buffered Saline	7.4	0.5M PB	200ml	-
		Deionised H_2O	Up to 1L	-
		1M NaOH	Add dropwise until pH = 7.4	Sigma Aldrich, S8045
		2M HCl	Add dropwise until pH = 7.4	Sigma Aldrich, H1756
Phosphate Buffered Saline with 0.005% Sodium Azide (PBS-A)	7.4	0.1M PBS	1L	-
		5% NaN_3 in H_2O (stock solution)	10ml	Sigma Aldrich, S2002
5µg/ml DAPI	-	0.1M PBS	50ml	-
		DAPI	50µl	Sigma Aldrich, D9542
PBS with Tween 20 (PBS-T)	7.4	0.1M PBS	1L	-
		Tween 20	1ml	Sigma Aldrich, P9416
50mM Citrate Buffer	6.0	$NaC_6H_7O_7$	2.94g	Sigma Aldrich, C3434
		Deionised H_20	1L	-
		2M HCl	Add dropwise until pH = 6.0	Sigma Aldrich, H1756

4% paraformaldehyde (PFA)	7.4	Deionised H_2O	50ml	-
		PFA powder	4g	Sigma Aldrich, F8775
		0.1M PBS	50ml	-
		1M NaOH	Add dropwise until pH = 7.4	Sigma Aldrich, A8045
		2M HCl	Add dropwise until pH = 7.4	Sigma Aldrich, H1756
1M Tris-Buffered Saline with Tween 20 (TBS-T)	7.4	Trizma® Base	6.05g	Sigma Aldrich, T1503
		NaCl	8.76g	Sigma Aldrich, 57653
		Deionised H_2O	Up to 1L	-
		2M HCl	Add dropwise until pH = 7.4	Sigma Aldrich, H1756
		Tween 20	100µl	Sigma Aldrich, P9416
10x Transfer Buffer (non-quantitative Western Blot, see Chapter 2, Section 2.7)	8.3	Trizma® Base	24g	Sigma Aldrich, T1503
		Glycine	112g	Sigma Aldrich, G8898
		Deionised H_2O	Up to 1L	-
		1M NaOH	Add dropwise until pH = 8.3	Sigma Aldrich, A8045
		2M HCl	Add dropwise until pH = 8.3	Sigma Aldrich, H1756
1x Transfer Buffer (non-quantitative Western Blot, see Chapter 2, Section 2.7)	8.3	10x Transfer Buffer	100ml	-
		Methanol	200ml	Sigma Aldrich, 32213
		Deionised H_2O	700ml	-
		1M NaOH	Add dropwise until pH = 8.3	Sigma Aldrich, A8045
		1M HCl	Add dropwise until pH = 8.3	Sigma Aldrich, H1756
1x Transfer Buffer (semi-quantitative Western blot, see Chapter 4, Section 4.2.3)	-	TruPAGE™ Transfer Buffer	50ml	Sigma Aldrich, PCG,3011
		Methanol	100ml	Sigma Aldrich, 32213
		Deionised nano H_2O	850ml	-
10x Running Buffer (non-quantitative Western Blot, see Chapter 2, Section 2.7)	8.3	Trizma® Base	30.2g	Sigma Aldrich, T1503
		Glycine	144g	Sigma Aldrich, G8898
		SDS	10g	Sigma Aldrich, L3771
		Deionised H_2O	Up to 1L	-
		1M NaOH	Add dropwise until pH = 8.3	Sigma Aldrich, S8045
		2M HCl	Add dropwise until pH = 8.3	Sigma Aldrich, H1756
1x Running Buffer (non-quantitative Western Blot, see Chapter 2, Section 2.7)	8.3	10x Running Buffer	100ml	-
		Deionised H_2O	900ml	-
		1M NaOH	Add dropwise until pH = 8.3	Sigma Aldrich, S8045
		2M HCl	Add dropwise until pH = 8.3	Sigma Aldrich, H1756
1 x Running Buffer	-	TruPAGE™ TEA-Tricine SDS Running Buffer	50ml	Sigma Aldrich, PCG3001
		Deionised nano H_2O	950ml	-

Table 2.7 – Frequently Used Solutions

2.7 Non-Quantitative Western blot

In order to validate primary antibody specificity, non-quantitative Western blot analysis was undertaken (Towbin et al., 1979) (for semi-quantitative Western blot, See Chapter 4, Section 4.2.3). Details of the number and genotype of tissue used are shown in Table 2.8, antibodies used in Table 2.9. An overview of the methodology is given in Figure 2.1.

Protein for Western blot was extracted from fresh tissue dissected with autoclave-sterilised tools and stored at -80°C (see Section 2.3.3). To extract protein, tissue samples were mechanically homogenised. Tissue was transferred to autoclave-sterilised 2ml screw-cap tubes for homogenisation. Tubes were pre-filled with 0.5g ceramic beads (#11079110z, Thistle Scientific, Glasgow, UK) prior to autoclave-sterilisation. 300µl RIPA lysis buffer (#sc-364162, Santa Cruz Biotechnology, Heidelberg, Germany) was added to each tube. Tissue was homogenised in a Precellys® 24 tissue homogeniser (#432-3750, Peqlab Biotechnologie, Erlangen, Germany), at 5,000 rpm for 2 x 20 second intervals. The supernatant was transferred to new 2ml Eppendorf tubes. 3µl of protein inhibitor cocktail (#sc-364162, Santa Cruz Biotechnology, Heidelberg, Germany) was added to each tube to prevent protein degradation.

Protein concentration was assayed using either a Micro BCA™ Protein Assay Kit (#23235, Thermo Fisher Scientific, Basingstoke, UK) or a QuickStart™ Bradford Protein Assay Kit (#500-0205, Bio-Rad Laboratories, Watford, UK). Total concentration of protein from each sample was measured against a set of standards. Samples were stored at -80°C for up to six months after collection.

Protein samples were prepared for gel electrophoresis when required. A volume of sample containing 25µg of extracted protein was added to a new Eppendorf tube, and the total volume made up to 35µl with sterile deionised water. 7µl of Laemmli buffer (#S3401-1VL, Sigma Aldrich, Gillingham, UK) was added to each labelled tube inside a biological safety cabinet. Each tube was then vortexed to mix thoroughly, and spun down in a microcentrifuge. Tubes were placed on a heat-block for 5 minutes at 95°C then allowed to cool to room temperature.

Samples were transferred to a BioRad Mini-PROTEAN® TGX™ pre-cast gel (#456-1084, Bio-Rad Laboratories, Watford, UK) for electrophoresis. 18µl of sample solution was loaded into each well of a pre-cast electrophoresis gel. 2µl Spectra™ Multicolour Broad Spectrum Protein Ladder (#26634, Thermo Fisher, Basingstoke, UK) was loaded into the first well of each gel. Gels were run in a BioRad Mini Trans-Blot Electrophoretic Transfer Cell blotting apparatus (#170-3930, Bio-Rad Laboratories, Watford, UK) filled with 1x Running Buffer (see Table 2.7). Gels were run at 60V for 20 minutes at room temperature, or until samples were clearly running into the stacking gel, at this point protein ladder separation was also visible. The gel was then run at 160V for approximately one hour at room temperature, on until the ladder separated into clear coloured bands and the Laemmli buffer blue line approached the bottom of the gel.

Protein was then transferred from the gel to a nylon membrane (#RPNSEL/98/01, Amersham Biosciences, Little Chalfont, UK). Hybond™-XL Nylon Membranes were soaked in 1x Transfer Buffer prior to transfer. The gel was removed from the running plate and the membrane placed on top. Air bubbles were removed using a plastic pressing tool (accessory to #170-3930, Bio-Rad Laboratories, Watford, UK). Filter

paper (#1703932, Bio-Rad Laboratories, Watford, UK) and sponges (#1703933, Bio-Rad Laboratories, Watford, UK) were placed on either side of the gel and membrane. These items were then inserted into a transfer cassette. The blotting tank was filled with 1x Transfer Buffer, and a custom ice-pack slotted in place (accessory to #170-3930, Bio-Rad Laboratories, Watford, UK). The transfer was run in a BioRad Mini Trans-Blot Electrophoretic Transfer Cell blotting apparatus (#170-3930, Bio-Rad Laboratories, Watford, UK). Transfer was run at 360 mA for 1 hour at approximately 4°C. Membranes were then placed in 1M TBS-T.

Membranes were blocked in 20ml of 1% skimmed milk (#70166, Fluka® Analytical, Berkshire, UK) in 1M TBS-T for 2 hours at room temperature on a shaker plate. At this point, the membrane was cut. A minimum of two lanes per gel/membrane acted as negative controls, exposed to secondary antibodies but not primary antibodies. Negative control lanes always included one sample of extracted protein from wild-type cortex and one from wild-type liver. The negative control portion of the membrane was incubated in 20ml 1M TBS-T for a minimum of 20 hours at 4°C. The remainder of the membrane was incubated with primary antibody in 1% milk in 20ml 1M TBS-T for a minimum of 20 hours at 4°C on a shaker plate. All primary and secondary antibodies are shown in Table 2.9.

Primary antibody was removed by three 5 minute washes in 20ml 1M TBS-T at room temperature on a shaker plate. Membranes were then incubated with secondary antibody in 1% milk in 20ml 1M TBS-T for 2 hours at room temperature on a shaker plate. Secondary antibody was removed by a further three 5 minute washes in 20ml 1M TBS-T at room temperature on a shaker plate. Finally, membranes were incubated with streptavidin-biotinylated horseradish peroxidase complex (#RPN1051V,

Amersham Biosciences, Little Chalfont, UK) diluted 1:1,000 in 20ml 1M TBS-T for 1 hour at room temperature on a shaker plate. Streptavidin was removed by three 5 minute washes in 20ml 1M TBS-T at room temperature on a shaker plate.

Protein-antibody binding was detected using photographic film. The membrane was loaded into an X-Ray Cassette (#60406, International Electrotechnical Commission, Geneva, Switzerland), and air bubbles pressed out. The remaining steps were carried out in a dark room. A Clarity™ Western Enhanced Chemiluminescence (ECL) Blotting Substrate kit (#1705060, Bio-Rad Laboratories, Watford, UK) was used to visualise the horseradish peroxidase (HRP) coupled antibody staining. The membrane was incubated in ECL solution for 5 minutes. A sheet of transparent plastic was then placed over the membrane. Photographic film (Kodak Scientific Imaging Film, #8952855, Kodak, Hemel Hempstead, UK) was exposed to the membrane for either 30 seconds, 60 seconds, or 5 minutes. Films were then developed using a Xograph Compact X4 development machine (Xograph, Gloucestershire, UK).

Alternatively, following incubation in ECL solution, the membrane was covered in transparent plastic clingfilm and chemiluminescence imaged using the ChemiDoc™ XRS+ imaging station (#1708265, Bio-Rad Laboratories, Watford, UK) at manually-selected exposure times. An additional direct image was acquired using the light imaging setting to capture the protein ladder.

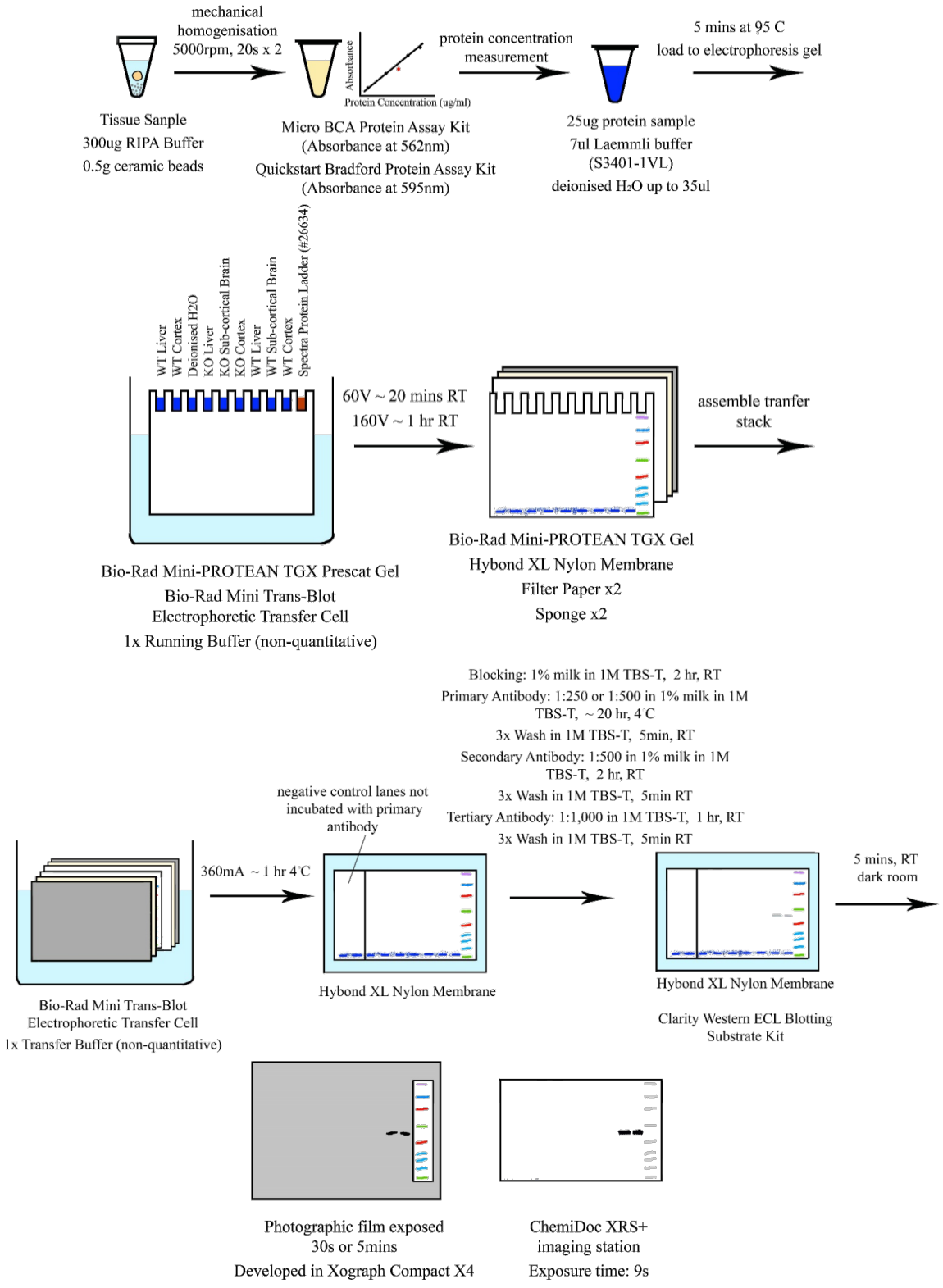


Figure 2.1 – Schematic Summary of Non-Quantitative Western Blot Methodology. Important reagents, stages, and procedures and detailed in this figure. All unique features of the non-quantitative Western blot protocol are marked on this figure. See Table 2.8 for more information about frequently used solutions.

Experiment	Genotype	Developmental Time Point (Postnatal Days)	Brains	Litters	Tissue Collected
Validation of Antibodies					
	C57/BL6J	P8	5	2	cerebral cortex, subcortical brain regions, liver, skeletal muscle
	B6.129-Serpini1^{tm1Dpw}/J	Adult (3 months)	3	2	cerebral cortex, subcortical brain regions, liver, skeletal muscle

Table 2.8 – Breakdown of the Number, Genotype, and Condition of Mouse Brains used across all Non-Quantitative Western blot experiments. Brains categorised by developmental time-point (age of animals) and experimental aims. Experiments were repeated a minimum of twice with tissue from different individual animals of each genotype and tissue type.

Experiment	Primary Antibody	Concentration	Supplier	Secondary Antibody
Validation of Primary Antibodies Against Neuroserpin				
	Goat anti-neuroserpin	1:250	Abcam, Ab32901	Donkey anti-Goat IgG Biotinylated 1:500 (Abcam, Ab6884)
	Rabbit anti-neuroserpin	1:250	Abcam, Ab33077	Donkey anti-Rabbit IgG Biotinylated Preabsorbed 1:500 (Abcam, Ab7082)
	Mouse anti-neuroserpin	1:500	Abcam, Ab55587	Donkey anti-Mouse IgG Biotinylated Preabsorbed 1:500 (Abcam, Ab7060)

Table 2.9 – Primary and Secondary Antibodies used for non-quantitative Western blot. Listed by relevant experimental aims, along with concentrations and sources.

2.8 Validation of Primary Antibodies Against Neuroserpin

Specificity validation of antibodies against neuroserpin protein was essential before drawing conclusions from the immunohistochemistry studies described in this thesis. Successful validation reduced the likelihood of off-target antibody binding, accounted for differences in staining pattern in mouse and human, and informed the choice of the most suitable primary antibody for immunohistochemistry and semi-quantitative Western blot in the neonatal rodent brain.

2.8.1 Validation of Primary Antibodies Against Neuroserpin Protein by Non-Quantitative Western Blot

To ensure specificity of primary antibodies, three negative controls were included in Western blots. The first was protein extracted from the livers of P8 C57BL/6J wild-type (WT) mouse, as previous Northern blot experiments detected no *Serpini1* mRNA in murine (Osterwalder et al., 1996; Krueger et al., 1997) or human (Hastings et al., 1997) liver. The second negative control employed the B6.129-Serpini1^{tm1Dpw}/J (KO) mouse, which expresses no functional *Serpini1* mRNA (Cinelli et al., 2001; Madani et al., 2003). Protein extracted from cerebral cortex, subcortical brain tissue, and liver of *Serpini1* knock-out mice was included to provide a match for each of the C57BL/6J tissue samples. The final negative control used sterile deionised water in place of protein samples. Some C57BL/6J brain and liver protein samples were incubated with secondary antibodies without prior exposure to primary antibody to prevent secondary antibody artefact being interpreted as primary antibody binding.

In addition to verifying antibody specificity, these Western blots also extend the characterisation of neuroserpin protein. Previous studies have only investigated *Serpini1* mRNA (Hastings et al., 1997; Krueger et al., 1997; Cinelli et al., 2001; Madani et al., 2003), allowing the possibility that neuroserpin protein manufactured in the brain, or elsewhere in the body, could be transported to organs that do not express *Serpini1* mRNA. A precedence for this has been set by the protein fetuin (Dziegielewska et al., 2000; Jahnen-Dechent et al., 2011), which is synthesised in the liver of developing mice from where it is transported to neurons in the cerebral cortex. Traces of neuroserpin detected in wild-type liver but not in knock-out could imply transport and metabolism of this protein outside the brain.

Western blot and immunohistochemistry validation were undertaken to determine the specificity of primary antibodies against neuroserpin. At the time of investigation, three such antibodies were commercially available: Ab55587, Ab32901, and Ab33077, each was investigated using analogous methodology.

Mouse anti-neuroserpin Ab55587 (Abcam, Cambridge, UK), is no longer commercially available, although online archived resources documented a single 46 kDa band detected by Western blot with protein from HeLa cell line lysate (http://www.abcam.com/neuroserpin-antibody-ab55587.html, last accessed: 10/08/2018). This antibody has previously been shown to produce strong neuronal staining in permanent immunohistochemistry in brain tissue from human Alzheimer's patients (Barker et al., 2011), although this publication did not validate antibody specificity. Ab55587 has also been used to detect neuroserpin in cultured human T cell lysate by Western blot and fluorescent immunohistochemistry (Lorenz et al., 2015) and ELISA experiments (Barker et al., 2011).

Results of the validation Western blot for Ab55587 are shown in Figure 2.2. At the recommended antibody concentration of 1:500, the only bands visible were approximately 140 kDa in size and appeared in both WT and KO liver. These bands are inconsistent with studies documenting neuroserpin protein as 45-58 kDa in size (Osterwalder et al., 1996; 1998; Krueger et al., 1997; Hastings et al., 1997; Hill et al., 2001). The presence of bands in KO liver tissue, and the absence of bands from WT brain tissue strongly suggested non-specific binding. It is possible that Ab55587 binds to a human-specific subsequence within neuroserpin, accounting for previously published results in human tissue (Barker et al., 2011; Lorenz et al., 2015; Adorján et al., 2019). However, this staining pattern indicated Ab55587 as unsuitable for

detecting neuroserpin in mouse tissue.

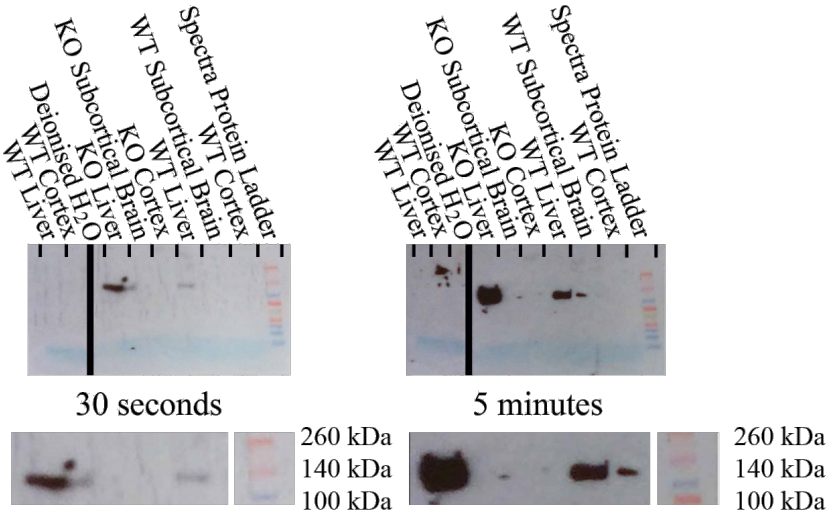


Figure 2.2 – Western Blot Validation of Mouse Anti-Neuroserpin Primary Antibody Ab55587 (Abcam, Cambridge, UK). ECL signal was captured on photographic film after an exposure time of 30 seconds or 5 minutes. Lanes were loaded, from right to left, with: Spectra™ Multicolour Broad Spectrum Protein Ladder (#26634, Thermo Fisher, Basingstoke, UK); P8 WT cerebral cortex; P8 WT subcortical brain regions from the same animal; WT liver; Adult (3 month) KO cerebral cortex; KO subcortical brain regions from the same animal; KO liver; sterile deionised water; WT cortex; and WT liver. Short vertical black lines denote lane boundaries. Long vertical black line marks the point where the membrane was cut to allow the section on the left to be incubated with secondary antibody in the absence of primary antibody. Thick bands are visible in both the WT liver and KO liver, with no bands visible in brain protein. The protein ladder indicates these bands are approximately 140 kDa in size, greatly in excess of the 46-58 kDa molecular size reported for neuroserpin (Osterwalder et al., 1996; 1998; Hastings et al., 1997; Hill et al., 2001). This is strong evidence that mouse anti-neuroserpin antibody Ab55587 is not specific in mouse. WT = C57BL/6J wild-type, KO = B6.129-Serpini1^{tm1Dpw}/J Serpini1 knock-out

Ab55587 was used by a collaborator, in addition to rabbit anti-neuroserpin antibody Ab33077, to stain foetal human tissue for neuroserpin (Adorján et al., 2019). This study found extensive, potentially ubiquitous, neuronal staining in human foetal tissue, in addition to neuroserpin-positive cells with glial morphology, as shown in Figure 2.3. This suggested more expansive expression of neuroserpin in neonatal human, compared to that documented in mouse brain (see Chapter 3, Section 3.3.1). However, Western blot validation with mouse tissue, and the absence of validation

with human tissue, questions the soundness of these interesting novel expression patterns in human.

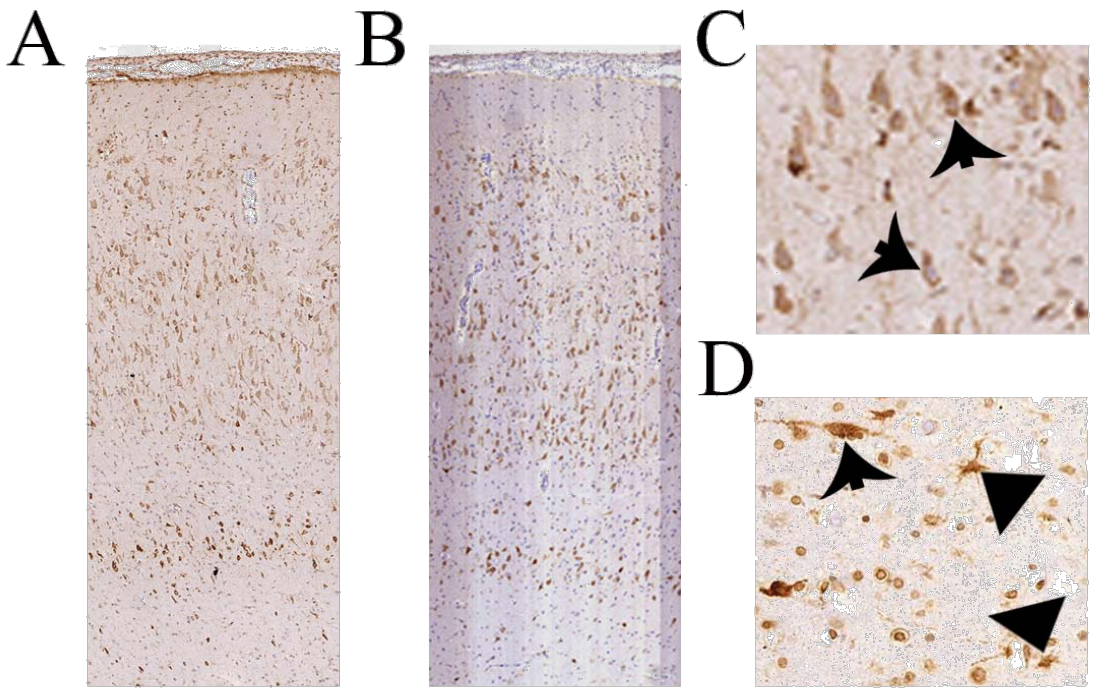


Figure 2.3 – Differential Staining Pattern for Primary Antibodies Ab33077 and Ab55587 in Human Foetal and Adult Cerebral Cortex with Permanent Immunohistochemistry. Images acquired using a light microscope using the 20 x magnification objective. Ab55587 detected a greater number of immunoreactive cells in cortex, capturing both neurons and glia. Ab33077 had a more restricted staining pattern and only labeled cells with neuronal morphology. (A) Human 40 post-conceptional week cortex stained with Ab33077 primary antibody against neuroserpin. (B) Human 40 post-conceptional week cortex stained with Ab55587 primary antibody against neuroserpin. (C) Enlarged image of adult sensory cortex stained with Ab33077. Fluted arrowheads denote immunoreactive cells consistent with neuronal morphology. Triangular arrowheads denote immunoreactive cells consistent with astrocytic glial morphology. Only cells with neuronal morphology are labelled. (D) Enlarged image of adult sensory cortex stained with Ab55587. Cells with both neuronal and astrocytic morphology are immunoreactive. Immunohistochemistry carried out and imaged acquired by Dr. István Adorján, University of Oxford, University of Budapest (Adorján, unpublished). Images are reproduced here with permission.

Polyclonal goat anti-neuroserpin antibody Ab32901 (Abcam, Cambridge, UK) was shown by the suppliers to be effective in fluorescent immunohistochemistry at low concentration of 1:2,000 – 1:4,000, and demonstrated a single band with Western blot

between 50-70 kDa in size in mouse and rat brain tissue (http://www.abcam.com/neuroserpin-antibody-ab32901.html, last accessed: 10/08/2018). In addition, Ab32901 has been used to investigate neuroserpin inclusion bodies in HeLa cells via Western blot and *in situ* hybridisation (Giampietro et al., 2017) and in immunohistochemistry on uterus trophoblast cells (Gormley et al., 2017), where no additional validation methods were employed.

Results of validation Western blot for Ab32901 are shown in Figure 2.4. A single band was detected in WT cortex and WT subcortical brain tissue, whereas no staining was detected in any of the negative control lanes. This band pattern supported neuroserpin specificity in Western blot for the primary antibody Ab32901. As this is a polyclonal antibody, specificity and antibody concentration required may vary between commercial batches. It is also possible that off-target binding occurred in other organs not investigated here. For the purposes of this thesis, Western blot validation was consistent with neuroserpin specificity of Ab32901.

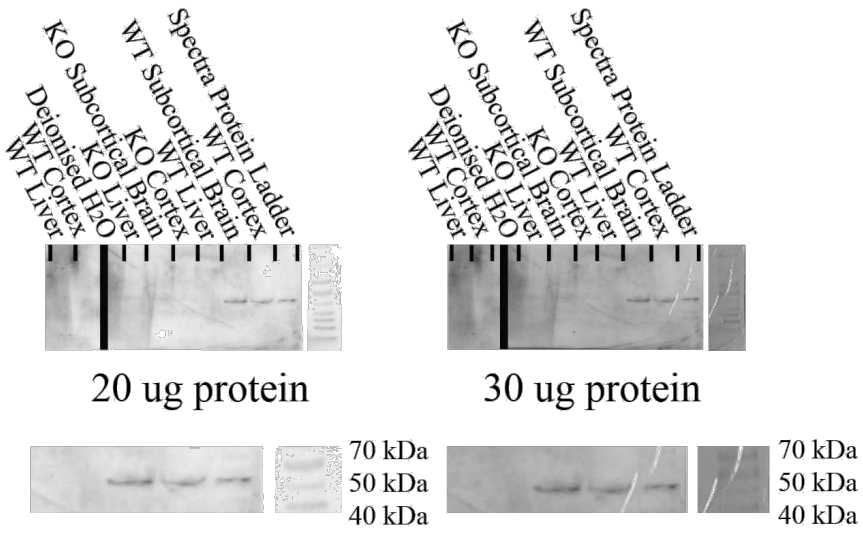


Figure 2.4 – Western Blot Validation of Goat Anti-Neuroserpin Primary Antibody Ab32901 (Abcam, Cambridge, UK). ECL signal was captured on ChemiDoc™ XRS+. Exposure time was 9 seconds across both membranes, the left loaded with 20µg protein per lane, the right with 30µg protein per lane. Lanes were loaded, from right to left, with: Spectra™ Multicolour Broad Spectrum Protein Ladder (#26634, Thermo Fisher, Basingstoke, UK); P8 WT cerebral cortex; P8 WT subcortical brain regions from the same animal; WT liver; Adult (3 month) KO cerebral cortex; KO subcortical brain regions from the same animal; KO liver; sterile deionised water; WT cortex; and WT liver. Short vertical black lines denote lane boundaries. Long vertical black line marks the point where the membrane was cut to allow the section on the left to be incubated with secondary and tertiary antibody in the absence of primary antibody. Bands are visible in both WT cerebral cortex and subcortical brain tissue, with no bands visible in WT liver or KO tissue. The protein ladder indicates the bands are approximately 50 kDa in size, in line with the previously reported 46-58 kDa molecular size of neuroserpin (Osterwalder et al., 1996; 1998; Hastings et al., 1997; Hill et al., 2001). This supports the claim that goat anti-neuroserpin primary antibody Ab32901 is specific to neuroserpin in mouse tissue.
WT = C57BL/6J wild-type, KO = B6.129-Serpini1^{tm1Dpw}/J Serpini1 knock-out

Rabbit anti-neuroserpin Ab33077 (Abcam, Cambridge, UK) was used in this thesis when co-staining with a primary antibody raised in goat, including: neuroserpin-Iba1 co-expression in glia (see Chapter 3, Section 3.3.1.2), neuroserpin co-expression with subplate markers CTGF and Nurr1 (see Chapter 3, Section 3.3.1.3), and subplate neuroserpin-expressing neuron birth-dating (see Chapter 3, Section 3.3.1.4). Ab33077 was also used in permanent immunohistochemistry experiments in human tissue (see Chapter 3, Section 3.3.4) (Adorján, et al., 2019), as Ab32901 was ineffective at staining paraffin-embedded tissue.

Of the commercially available antibodies at the time of writing, this antibody was most extensively documented in previous publications. Ab33077 has been used to label neuroserpin-immunoreactive neurons by fluorescent immunohistochemistry (Kondo et al., 2015), and in Western blot experiments on protein extracted from cultured astrocytes (Yang et al., 2018), although was not validated in either study. Significantly, Ab33077 has been used to demonstrate an increase in neuronal neuroserpin expression by immunohistochemistry in adult mice undergoing ischaemic stroke (Wu et al., 2010; Li et al., 2017) and in cultured hippocampal neurons (Wu et al., 2010). The supplier described a 50-70 kDa band in mouse and rat brain tissue generated by Western blot assay with this antibody (http://www.abcam.com/neuroserpin-antibody-ab33077.html, last accessed 10/08/2018).

Results of validation Western blot for Ab33077 are shown in Figure 2.5. Bands were visible in all tissue samples, across brain and liver in WT and KO mouse, strongly suggesting that non-specific antibody binding occurred. Absence of bands from lanes containing deionised water, or exposed to secondary antibodies in the absence of primary antibodies, show that all bands are generated by primary antibody binding to protein in the tissue. All bands were 40-70 kDa in size, neuroserpin may be included within this product. Western blot data suggested that this antibody should be interpreted with caution in mouse.

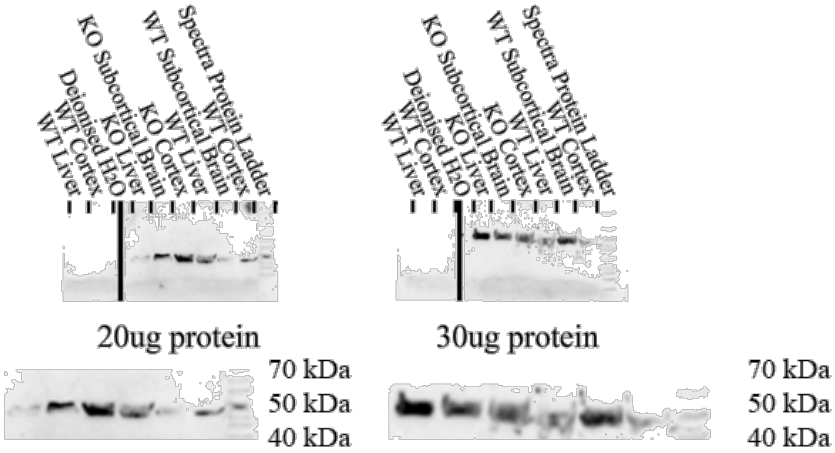


Figure 2.5 – Western Blot Validation of Rabbit Anti-Neuroserpin Primary Antibody Ab33077 (Abcam, Cambridge, UK). ECL signal was captured on ChemiDoc™ XRS+. Exposure time was 24 seconds across both membranes, one loaded with 20µg protein per lane, the other with 30µg protein per lane. Lanes were loaded, from right to left, with: Spectra™ Multicolour Broad Spectrum Protein Ladder (#26634, Thermo Fisher, Basingstoke, UK); P8 WT cerebral cortex; WT subcortical brain regions from the same animal; WT liver; Adult (3 month) KO cerebral cortex; KO subcortical brain regions from the same animal; KO liver; sterile deionised water; WT cortex; and WT liver. Short vertical black lines denote lane boundaries. Long vertical black line marks the point where the membrane was cut to allow the section on the left to be incubated with secondary and tertiary antibody in the absence of primary antibody. Thick bands are visible in the WT cortex, subcortical brain, and liver, and in KO cortex, subcortical brain, and liver. The protein ladder indicates these bands are approximately 40-70 kDa in size, in line with the molecular size reported for neuroserpin (Osterwalder et al., 1996; 1998; Hastings et al., 1997; Hill et al., 2001). However, the strong bands in KO tissue suggest that rabbit anti-neuroserpin primary antibody Ab33077 is not specific to neuroserpin in mouse, although it may bind neuroserpin in addition to other proteins similar in size present in WT and KO mouse.
WT = C57BL/6J wild-type, KO = B6.129-Serpini1^{tm1Dpw}/J Serpini1 knock-out

Overall, goat anti-neuroserpin antibody Ab32901 was most consistent with neuroserpin-specific binding across validation Western blot assays. This supported the preferential use of Ab32901 in immunohistochemistry experiments, and the selection of Ab32901 for use in semi-quantitative Western blot throughout this thesis.

2.8.2 Validation of Primary Antibodies Against Neuroserpin Protein by Fluorescent Immunohistochemistry

Primary antibodies against neuroserpin were used to stain C57BL/6J wild-type (WT) and B6.129-Serpini1tm1Dpw/J *Serpini1* knock-out (KO) mouse cerebral cortex tissue by fluorescent immunohistochemistry.

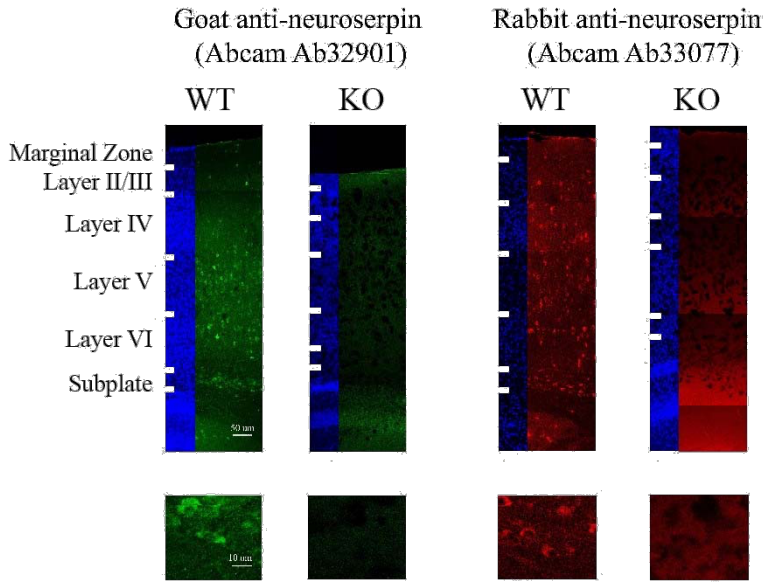


Figure 2.6 – Validation of Primary Antibodies Against Neuroserpin Ab32901 and Ab33077 by Fluorescent Immunohistochemistry in C57BL/6J Wild-Type (WT) and B6.129-Serpini1^{tm1Dpw}/J *Serpini1* Knock-Out (KO) Cerebral Cortex (both supplied by Abcam, Cambridge, UK). Representative confocal images taken with 20 x magnification objective of coronal cortical stacks from primary somatosensory cortex (S1) stained for DAPI in blue, and either Ab32901 in green or Ab33077 in red. Scale bars indicate 50µm width areas. Beneath are expanded inserts of subplate from these confocal images, scale bars indicate 10µm width areas. Goat anti-neuroserpin antibody Ab32901 demonstrated clear intracellular neuronal staining in WT cortex, with little immunoreactivity in KO cortex under identical methodology and imaging settings. Rabbit anti-neuroserpin Ab33077 produced a similar pattern to Ab32901 in WT cortex, with higher background staining in KO cortex, but no discrete intracellular staining pattern in the KO negative control.

Mouse anti-neuroserpin antibody Ab55587 failed to stain formaldehyde-fixed free-floating WT or KO cortex at the recommended concentration of 1:500, or at 1:100. Both goat anti-neuroserpin Ab32901 and rabbit anti-neuroserpin Ab33077 produced neuronal staining patterns in WT, but did not give cellular labelling in KO cortex.

Results are shown in Figure 2.6. These staining patterns are similar to that previously documented for *Serpini1* mRNA in the developing mouse brain (Osterwalder et al., 1996; Krueger et al., 1997; Hastings et al., 1997). Background staining was significantly higher in KO cortex for Ab33077 compared to Ab32901, suggesting potential non-specific binding. However, no cellular labelling was evident in the KO cortex with Ab33077 at antibody concentrations used for quantification.

Validation of antibodies by immunohistochemistry supported data from Western blot experiments. Goat anti-neuroserpin antibody Ab32901 was preferable among the three commercially available antibodies, giving results most consistent with specificity to neuroserpin. Quantitative data from rabbit anti-neuroserpin antibody Ab33077 may be acceptable in fluorescent immunohistochemistry studies, but caution should be exercised in interpreting results generated with this antibody alone in Western blot or other experimental methods. It is possible that Ab33077 binds to a specific tertiary structure preserved by fixative conditions in formaldehyde-fixed free-floating immunohistochemistry but made more ubiquitous by protein homogenisation and heating processes in the samples used for validation Western blot.

3 Characterisation of Neuroserpin Protein Expression Throughout Development in Mouse and Human

3.1 Introduction

Any molecule associated with a neurodevelopmental disorder must be rigorously studied in normal physiology. The endogenous expression profile over development, sub-cellular localisation pattern, and molecular marker co-localisation can provided insights essential for designing experiments focused on the most relevant molecular functions for neuropathology.

It remains to be determined in what way the pattern of neuroserpin protein expression relates to that of its coding *Serpini1* mRNA. Previous publications document *Serpini1* mRNA expression in various species, including *Drosophila* (Hill et al., 2001; Ellisdon et al., 2014), chicken (Schrimpf et al., 1997), mouse (Krueger et al., 1997; Osterwalder et al., 1998) and human (Schrimpf et al., 1997). *In situ* hybridisation experiments describe rich expression of *Serpini1* mRNA in postnatal murine cortical neurons (Krueger et al., 1997), a pattern of neuroserpin protein distribution which the adult human brain replicates (Schrimpf et al., 1997; Teesalu et al., 2004). However, no quantitative anatomical documentation of expression patterns is available for mRNA or protein.

Neuroserpin protein is first described in the secreted product of cultured neurons (Osterwalder et al., 1996), therefore there is no guarantee that neuroserpin remains within the neurons that manufacture it. Knowing the profile of protein expression is

essential to validating neuroserpin as a neuron-specific enzyme (Osterwalder et al., 1996; Hastings et al., 2007; Lee et al., 2015b). Tracking the localisation of secreted neuroserpin gains greater relevance with the knowledge that neocortical subplate cells rich in *Serpini1* mRNA are also hubs of endoplasmic reticulum (ER) protein secretion apparatus (Kondo et al., 2015).

The neuroserpin/tPA molecular cascade is a complex network of molecules, included dozens of individual proteins which span cascades involved in: excitotoxicity (Quian et al., 1993; Yepes et al., 2002; Lebeurrier et al., 2005); oxidative stress (Kim et al., 1999; Mohsenifar et al., 2007); neuronal plasticity (Berger et al., 1999; Wannier-Morino et al., 2003; Borges et al., 2010); and thrombosis (Rijkin et al., 1979; 1980); amongst other functions (reviewed in Yepes and Lawrence, 2004b; 2004c; Millar et al., 2017). Characterisation of the cellular populations and subcellular compartments in which neuroserpin is expressed could focus future research on key pathways associated with high neuroserpin expression.

Another factor which prevents direct application of findings relating to neuroserpin function in the adult brain to neonatal development were the manifold differences in brain organisation and neurochemistry at these ages (reviewed in McLean and Ferriero, 2004; Baburamani et al., 2012; Millar et al., 2017). Basic research into neuroserpin expression and function in the developing brain is paramount as the unique neurochemical landscape of the infant brains can support categorical differences in distribution, molecular interactions, and function of an individual protein (reviewed in Millar et al., 2017).

This chapter thoroughly characterises the anatomical expression pattern of neuroserpin protein in the developing mouse neocortex, and provides confirmation of

neuroserpin protein expression in foetal human tissue. This is essential for informed interpretation of neuroserpin loss of function data presented in Chapter 5.

3.1.1 Aims of Chapter 3

The neuroprotective role of neuroserpin in adult rodent models of ischaemic stroke is a relatively recent discovery. Neuroserpin protein itself has received only modest scientific attention, hence little is known about its physiological role during development. Mapping the endogenous developmental expression profile of neuroserpin using quantitative immunohistochemistry could indicate which brain circuits may be associated with each documented function of neuroserpin.

1) Expression pattern of neuroserpin protein in mouse cerebral cortex was assessed by immunohistochemistry across developmental time-points.

(i) Number and proportion of neuroserpin-expressing neurons were quantified per cortical layer against the pan-neuronal marker neuronal nuclei (NeuN).

(ii) Number and proportion of neuroserpin-expressing glial cells were quantified against: astrocyte marker glial fibrillary acidic protein (GFAP); microglia marker ionised calcium binding adaptor molecule 1 (Iba1); and oligodendrocyte marker oligodendrocyte transcription factor 2 (Olig2).

(iii) Neuroserpin-immunoreactive subplate neurons were co-stained with known murine subplate markers, connective tissue growth factor (CTGF), complexin-3, and nuclear receptor related 1 protein (Nurr1) to

determine if these markers can be used to define a neuroserpin-immunoreactive subplate neuronal subpopulation.

(iv) Birth-dating was carried out for neuroserpin-immunoreactive subplate neurons to determine whether this putative neuronal population can be characterised by date of neurogenesis.

2) Expression pattern of neuroserpin within subplate neurons was co-localised with molecular markers of endoplasmic reticulum and metabolic stress to determine whether neuroserpin expression was enriched specifically in subplate neurons undergoing high metabolic demand.

(i) Neuroserpin-immunoreactive subplate neurons were co-stained with structural and stress-related markers of endoplasmic reticulum (ER) secretory apparatus: conserved lysine-aspartic acid-glutamic acid-leucine amino acid sequence (KDEL); calreticulin; and C/EBP homologous protein (CHOP), to provide evidence supporting neuroserpin secretion in the proposed secretory function for subplate.

(ii) Neuroserpin-immunoreactive cortical neurons were co-stained with metabolic stress markers heat shock protein 60 (HSP60) and HSP90, to investigate metabolic stress load in this neuronal population.

3) The role of neuroserpin in cortical plasticity was briefly investigated in a mouse model primary sensory input deprivation generated by monocular enucleation at P1. The number and distribution of neuroserpin-expressing neurons was compared between the input-deprived and control cortical hemispheres.

4) Paraffin-embedded neonatal human brain tissue was stained using comparable immunohistochemical procedures to detect endogenous

expression of neuroserpin protein in the developing human brain at 15 (preterm) and 40 (term) post-conceptional weeks.

3.2 Methods

Animal husbandry and tissue collection are described in Chapter 2, sections 2.1 and 2.3 respectively.

3.2.1 Immunohistochemistry

Immunohistochemistry was used to characterise the expression profile of neuroserpin protein in cerebral cortex throughout development in mouse and human. Details of the number, genotype, and other relevant experimental conditions relating to tissue used are given in Table 3.1, subdivided by experimental aims. Specifics of primary and secondary antibodies are given in Table 3.2 and Table 3.3, respectively. An overview of fluorescent immunohistochemistry methodology is shown in Figure 3.1.

All immunohistochemistry in mouse tissue was carried out with free-floating sections. Brains were post-fixed overnight, or for 48 hours for more fragile HI brains, in 4% PFA then embedded in 4% agarose (#A9539, Sigma Aldrich, Gillingham, UK) (see Chapter 2, Section 2.3). A vibrating microtome was used to cut 50µm coronal sections which were stored in 0.05% PBS-A at 4°C.

Brain sections for immunohistochemistry against BrdU or CHOP underwent antigen retrieval prior to blocking. Sections were incubated in 1M HCl (#H1756, Sigma Aldrich, Gillingham, UK) in deionised water for 60 minutes on a shaker plate in a

hybridisation oven at 38.5°C. Sections were washed for 5 minutes in 0.1M PBS three times to remove HCl, then blocked as detailed below. Sections not being stained for BrdU or CHOP were transferred directly from storage in 0.1M PBS-A at 4°C into block at room temperature.

Sections were blocked in 0.1% Triton™-X100 (#T8787, Sigma Aldrich, Gillingham, UK) and 5% donkey serum (#D9663, Sigma Aldrich, Gillingham, UK) in 500µl 0.1M PBS (see Chapter 2, Table 2.7). Blocking was carried out for 2 hours at room temperature on a shaker plate. When staining for CTGF, sections were blocked with 1% Triton™-X100 and 5% donkey serum in 500µl 0.1M PBS, duration and temperature remained the same.

Sections were then incubated with primary antibody in 0.1% Triton™-X100 and 2% donkey serum in 500µl 0.1M PBS for a minimum of 20 hours at 4°C on a shaker plate. When staining for CTGF, primary antibodies were made up with 1% Triton™-X100 and 2% donkey serum in 500µl 0.1M PBS. Primary antibodies were removed by three 5 minute washes with 0.1M PBS at room temperature on a shaker plate.

Sections were incubated with secondary antibodies in 0.1% Triton™-X100 and 2% donkey serum in 500µl 0.1M PBS for 2 hours at room temperature on a shaker plate. Secondary antibodies were removed by two 5 minute washes with 0.1M PBS at room temperature on a shaker plate. Sections were counterstained with the DNA stain 0.1% 4',6-diamidino-2-phenylindole (DAPI) (#D9542, Sigma Aldrich, Gillingham, UK) in 0.1M PBS for 5 minutes at room temperature on a shaker plate.

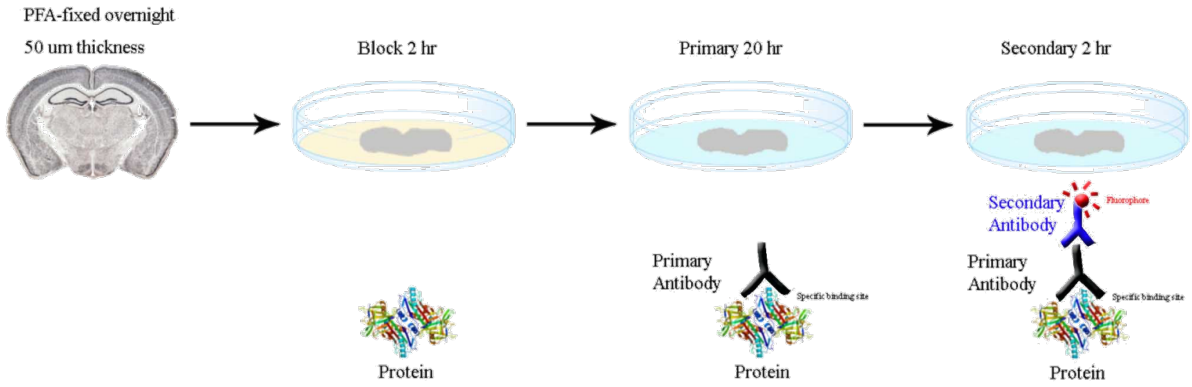


Figure 3.1 – Schematic of Free-Floating Fluorescent Immunohistochemistry Methodology. PFA-fixed coronal brain sections, cut to 50µm thickness, were blocked for 2 hours at room temperature on a shaker plate in 0.1% Triton™-X100 (1% for CTGF) and 5% donkey serum in 0.1M PBS. Sections were then incubated with the primary antibody of choice (in 0.1% Triton™-X100, 2% donkey serum, 0.1M PBS) for a minimum of 20 hours at 4°C on a shaker plate. Following three 5 minutes washes in 0.1M, sections were incubated with the relevant secondary antibody (in 0.1% Triton™-X100, 2% donkey serum, 0.1M PBS) for 2 hours at room temperature on a shaker plate. For fluorescent immunohistochemistry experiments, all secondary antibodies were directly conjugated to a fluorophore. Sections were washed a further two times in 0.1M PBS for 5 minutes per wash prior to mounting. The image of neuroserpin protein was taken with permission from https://en.wikipedia.org/wiki/SERPINI1, last accessed 10/08/2018.

Stained sections were mounted on Superfrost™ Plus glass microscope slides (#9951PLUS, Thermo Fisher, Hemel Hempstead, UK). Sections were liberally immersed in 0.1M PBS on the slides to maintain hydration before being sealed with Menzel™ glass coverslips (#11778691, Thermo Fisher, Hemel Hempstead, UK) or Corning® coverslips (#C9056, Sigma Aldrich, Gillingham, UK) and nail varnish. Slides were stored at 4°C in opaque slide boxes. All imaging of fluorescent stained slides was carried out within one month of staining to avoid decay of fluorescence.

Experiment	Developmental Time Point (Postnatal Days)	Brains	Litters	Slices	Collection Method	Fixation (hours in 4% PFA)	Strain (Condition)
Neuroserpin Developmental Time Series							
	P3	3	1	3	PBS Perfused	24	NIHS
	P5	3	1	3	PBS Perfused	24	NIHS
	P6	3	1	3	PBS Perfused	24	NIHS
	P6	5	1	3	PBS Perfused	24	C57BL/6J

	P7	3	1	3	PBS Perfused	24	NIHS
	P8	8	3	3	PBS Perfused	24	NIHS
	P8	5	1	3	PBS Perfused	24	C57BL/6J
	P9	3	1	3	PBS Perfused	24	NIHS
	P9	5	1	3	PFA Perfused	24	C57BL/6J
	P10	3	1	3	PFA Perfused	24	NIHS
	P11	3	1	3	PFA Perfused	24	NIHS
	P12	3	1	3	PFA Perfused	24	NIHS
	P12	5	1	3	PFA Perfused	24	C57BL/6J
	P21	3	1	3	PFA Perfused	24	NIHS
	Adult (3 months)	3	1	3	PFA Perfused	24	NIHS
	Adult (3 months)	5	2	3	PFA Perfused	24	C57BL/6J
Neuroserpin Expression in Glia							
	P3	3	1	3	PBS Perfused	24	C57BL/6J
	P8	3	1	3	PBS Perfused	24	C57BL/6J
	Adult (3 months)	3	2	3	PFA Perfused	24	C57BL/6J
Neuroserpin Expression in Subplate							
	P8	5	1	3	PBS Perfused	24	NIHS
	P8	5	1	3	PBS Perfused	24	C57BL/6J
Neuroserpin Neuron Birth-Dating with BrdU							
	P8	3	1	3	PBS Perfused	24	NIHS (BrdU injected E11.5)
	P8	3	1	3	PBS Perfused	24	NIHS (BrdU injected E12.5)
	P8	3	1	3	PBS Perfused	24	Lpar1-eGFP
Neuroserpin Expression in ER Stress							
	P3	3	1	3	PBS Perfused	24	C57BL/6J
	P8	3	1	3	PBS Perfused	24	C57BL/6J
	Adult (3 months)	3	2	3	PFA Perfused	24	C57BL/6J
Neuroserpin Expression in Metabolic Stress							
	E18	6	1	3	PBS Perfused	24	NIHS
	P3	6	2	3	PBS Perfused	24	NIHS
	P8	4	3	3	PBS Perfused	24	NIHS
	P9	4	1	3	PFA Perfused	24	B6.129-Serpini1^{tm1Dpw}/J *Serpini1* -/-
	P9	2	1	3	PFA Perfused	24	B6.129-Serpini1^{tm1Dpw}/J *Serpini1* +/-
	P9	2	1	3	PFA Perfused	24	C57BL/6J
	P21	3	3	3	PFA Perfused	24	NIHS
Neuroserpin in Plasticity following Monocular Enucleation							
	P6	3	2	3	PBS Perfused	24	Golli-τ-eGFP (P1 monocular enucleation)
Validation of Neuroserpin Primary Antibodies in Serpini1 Knock-Out Mouse							
	P8	3	1	3	PBS Perfused	24	C57BL/6J
	Adult (3 months)	3	3	3	PFA Perfused	24	B6.129-Serpini1^{tm1Dpw}/J

Table 3.1 – Breakdown of the Number, Genotype, and Condition of Mouse Brains used across all Fluorescent Immunohistochemistry Experiments described in this chapter. Brains categorised by developmental time-point (age of animals) and experimental aims. Results for each individual brain were generated from an average of cell counts across three pial to white matter cortical sections.

Experiment	Primary Antibody	Concentration	Supplier
Neuroserpin Developmental Time Series			
	Goat anti-neuroserpin	1:2,000	Abcam, Ab32901
	Mouse anti-NeuN	1:1,000	Chemicon, MAB377
Neuroserpin Expression in Glia			
	Goat anti-neuroserpin	1:2,000	Abcam, Ab32901
	Rabbit anti-neuroserpin	1:1,000	Abcam, Ab33077
	Rabbit anti-GFAP	1:500	DAKO, Z0334
	Goat anti-Iba1	1:500	Abcam, Ab107159
	Rabbit anti-Olig2	1:500	Abcam, Ab109186
Neuroserpin Expression in Subplate			
	Goat anti-neuroserpin	1:2,000	Abcam, Ab32901
	Rabbit anti-neuroserpin	1:1,000	Abcam, Ab33077
	Goat anti-CTGF	1:1,000	Santa Cruz, sc-14939
	Rabbit anti-complexin-3	1:2,000	Synaptic Systems, 112302
	Goat anti-Nurr1	1:50	R&D, AF2156
Neuroserpin Neuron Birth-Dating with BrdU			
	Rabbit anti-neuroserpin	1:1,000	Abcam, Ab33077
	Mouse anti-BrdU	1:500	Progen, 11200
Neuroserpin Expression in ER Stress			
	Goat anti-neuroserpin	1:2,000	Abcam, Ab32901
	Mouse anti-KDEL	1:200	Abcam, Ab12223
	Rabbit anti-calreticulin	1:500	Thermo Fisher, PA3-900
	Mouse anti-CHOP	1:100	Cell Signalling, 2895
Neuroserpin Expression Metabolic Stress			
	Goat anti-neuroserpin	1:2,000	Abcam, Ab32901
	Mouse anti-HSP60	1:500	StressMarq Biosciences, SCM110A/B
	Mouse anti-HSP90	1:500	StressMarq Biosciences, SCM149A/B
Neuroserpin in Plasticity following Monocular Enucleation			
	Goat anti-neuroserpin	1:2,000	Abcam, Ab32901
	Mouse anti-NeuN	1:1,000	Chemicon, MAB377
Neuroserpin Expression in 15 Post-Conceptional Week Human Tissue			
	Goat anti-neuroserpin	1:2,000	Abcam, Ab32901
Neuroserpin Expression in 40 Post-Conceptional Week Human Tissue			
	Rabbit anti-neuroserpin	1:550	Abcam, Ab33077
	Mouse anti-neuroserpin	1:200	Abcam, Ab55587
	Mouse anti-NeuN	1:100	Millipore, MAB377
Validation of Neuroserpin Primary Antibodies in *Serpini1* Knock-Out Mouse			
	Goat anti-neuroserpin	1:2,000	Abcam, Ab32901
	Rabbit anti-neuroserpin	1:1,000	Abcam, Ab33077

Table 3.2 – Primary Antibodies. Listed by experimental aims, alongside relevant concentrations and sources. Relevant secondary antibodies listed in Table 3.3. Relevant combinations of primary and secondary antibodies detailed in Section 3.3.

Experiment	Secondary Antibody	Concentration	Source
Neuroserpin Developmental Time Series			
	Donkey anti-goat Alx568	1:500	Invitrogen, A11057
	Donkey anti-mouse Alx488	1:500	Invitrogen, A21202
Neuroserpin Expression in Glia			
	Donkey anti-goat Alx568	1:500	Invitrogen, A11057
	Donkey anti-rabbit Alx488	1:500	Invitrogen, A21206
Neuroserpin Expression in Subplate			
	Donkey anti-goat Alx568	1:500	Invitrogen, A11057
	Donkey anti-rabbit Alx488	1:500	Invitrogen, A21206

Neuroserpin Neuron Birth-Dating with BrdU			
	Goat anti-rabbit Alx568	1:500	Molecular Probes, A11011
	Goat anti-mouse Alx488	1:500	Molecular Probes, A11029
Neuroserpin Expression in ER Stress			
	Donkey anti-goat Alx568	1:500	Invitrogen, A11057
	Donkey anti-rabbit Alx488	1:500	Invitrogen, A21206
	Donkey anti-mouse Alx488	1:500	Invitrogen, A21202
Neuroserpin Expression in Metabolic Stress			
	Donkey anti-goat Alx568	1:500	Invitrogen, A11057
	Donkey anti-mouse Alx488	1:500	Invitrogen, A21202
	Donkey anti-mouse Alx568	1:500	Invitrogen, A10037
Neuroserpin in Plasticity following Monocular Enucleation			
	Donkey anti-goat Alx568	1:500	Invitrogen, A11057
	Donkey anti-mouse Alx488	1:500	Invitrogen, A21202
Neuroserpin Expression in 15 Post-Conceptional Week Human Tissue			
	Donkey anti-goat horseradish peroxidase (HRP)	1:500	Invitrogen, A16005
Neuroserpin Expression in 40 Post-Conceptional Week Human Tissue			
	REAL™ EnVision™ horseradish peroxidase (HRP) Rabbit/Mouse	-	DAKO, K5007
Validation of Neuroserpin Primary Antibodies in *Serpini1* Knock-Out Mouse			
	Donkey anti-goat Alx568	1:500	Invitrogen, A11057
	Donkey anti-rabbit Alx488	1:500	Invitrogen, A21206

Table 3.3 – Secondary Antibodies. Listed by experimental aims, alongside relevant concentrations and sources. Relevant primary antibodies listed in Table 3.2. Relevant combinations of primary and secondary antibodies detailed in Section 3.3.

3.2.2 Quantification of Cell Numbers with Immunohistochemistry

In order to characterise the neuroserpin-immunoreactive neuronal population, the number of neurons co-expressing neuroserpin and other molecular markers was quantified within certain anatomically-defined brain cell populations.

Confocal microscope (Zeiss LSM 710, Carl Zeiss Microimaging, Oberkochen, Germany) images were acquired using the 20x objective. Images spanning the cortex were 425 µm in width, and between 850 µm and 2,125 µm in height. All images included the pial surface of cortex and the subcortical white matter. Images were taken within primary somatosensory cortex (S1) unless otherwise stated, identified in P5 to adult brains by the presence of barrels in Layer IV (Woolsey and van der Loos, 1970; 1973; 2016; Rice and van der Loos, 1977) as revealed by DAPI staining. In

P2-P5 brains, where barrel cortex is not readily visible (Agmon et al., 1993; reviewed in Petersen, 2007; Inan and Crair, 2007), online developmental mouse brain atlas Allen Brain Developing Mouse Brain Atlas P4 Nissl Stain Coronal (http://developingmouse.brain-map.org/experiment/ivt?id=100034998&popup=true, last accessed 10/08/2018; reviewed in Jones et al., 2009; Sunkin et al., 2012) was used as a guide to aid identification of S1. A z-stack of three planes was acquired, each 3.8μm apart, with quantification restricted to the middle z-plane.

The images of cortex were divided into horizontal bins of 425 μm width and 50 μm height, as shown in Figure 3.2. Bins were assigned to cortical layers using documented nuclear size and density (Cajal, 1899; Jones and Wise, 1977; Schüz and Palm, 1989), here visible with the DAPI stain (confirmed with NeuN where applicable) (Gittins and Harrison, 2004). When quantifying proteins expressed in the nucleus, only nuclear-labelled cells brightest in the middle z-plane were counted. Those nuclear-labelled cells brighter in either of the external planes were not included in quantification. When quantifying proteins expressed in the cytoplasm, cytoplasmic-labelled cells were also counted in the middle z-plane only, those with the visible presence of an empty nucleus surrounded by stained cytoplasm in the middle z-plane were counted. Cytoplasmic-labelled cells brighter, or with a visible empty nucleus, in either external plane were not counted.

Raw numbers of marker-immunoreactive cells were recorded for each anatomical layer of cortex. Three sections were quantified from each experimental brain, results for each brain averaged across these sections, total number of brains of each developmental stage used for each experiment shown in Table 3.1.

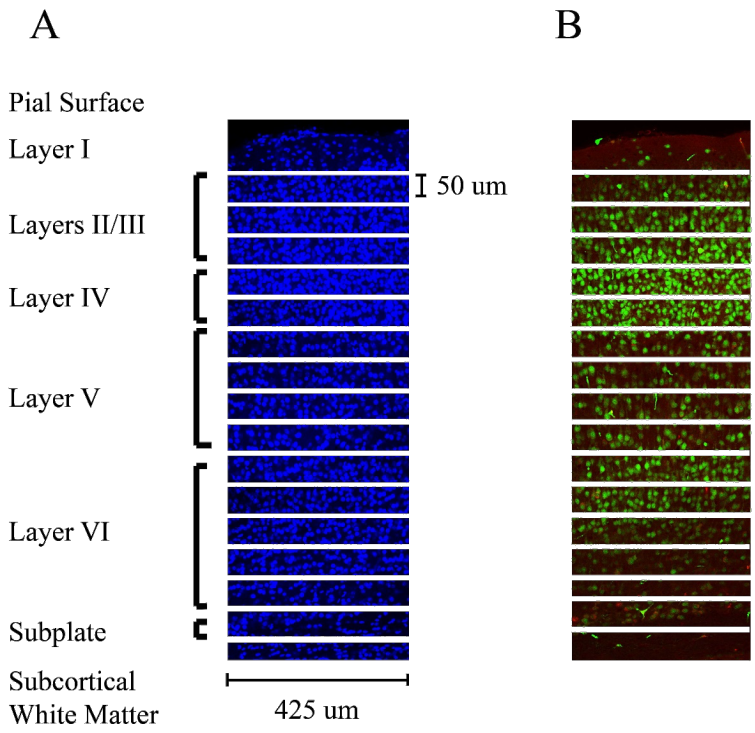


Figure 3.2 – Example of Cell Number Quantification Grids. (A) 50µm thickness coronal cortical section stained with DNA counterstain 4′,6-diamidino-2-phenylindole (DAPI). Cortex is divided into bins of dimension 425µm width by 50µm height. Anatomy is used to assign bins to cortical layers. Layer II/III is identified by the increased density of nuclei below Layer I, ending in the increased density of small-sized nuclei which marks the boundary of layer IV. Layer IV extends to the large-sized low-density nuclei of Layer V, which are replaced themselves by the higher density small-sized nuclei of Layer VI. Subplate is defined as the deepest 50µm of cortex directly above the subcortical white matter. (B) 50µm thickness coronal section from P8 C57BL/6J S1 region of cortex, stained for NeuN in green and neuroserpin in red, with bins super-imposed.

3.2.3 Quantification of the Cortical Area with Immunohistochemistry

In order to capture an alternative measure of glial cell infiltration in addition to cell number, the proportion of total cortical area covered by certain molecular markers was quantified.

The cell counting method described in Section 3.2.2 is significantly limited in that it only includes cells which have their nucleus within the middle z-plane of the image stack as part of the count. This can be a helpful gross measure of cell density, but does

not capture presence of cellular processes which may have invaded the plane in the absence of cell bodies being translocated. Cell counting could detect an increased number of glia or other inflammatory cells associated with brain injury invading the site of injury including astrocytes (Sizonenko et al., 2008), microglia (Ivacko et al., 1996; Rivera et al., 2002; Deng et al., 2008), and mast cells (Jin et al., 2007; 2009). However, several publications detected little or no increase in absolute glial cell numbers, particularly astrocytes, following brain injury (Tsai et al., 2012; Hayahsi et al., 2005; Ferrazzano et al., 2013; Bardehle et al., 2013). Therefore, direct cell counting could capture invasion of microglia and monocytes, but is unlikely to detect changes in astrocytes which contribute to gliosis in the neonatal hypoxic ischaemic brain. Surface area analysis was used to detect changes in overall coverage of the injury site with glial activation associated markers. For example, GFAP production is known to increase following neonatal hypoxic ischaemic injury (Burtrum and Silverstein, 1994; Ennen et al., 2011; reviewed in Hol and Pekny, 2015), therefore GFAP immunoreactivity may increase at the site of injury while the number of astrocytes does not change.

Activated glia have been shown to increase in cytoplasmic volume and protein production (reviewed in Hol and Pekny, 2015), independent of potential increases in number of cells within the lesion area. A single measure was derived here include total cytoplasmic volume of all marker-immunoreactive glial cells, capturing processes in addition to cells bodies and potentially hypertrophic cells. This effect was quantified by analysing the proportion of total cortical volume covered by glial marker-immunoreactive pixels.

Cell counting and surface area analysis were unable to detect the activation of

astrocytes (Norenberg et al., 2005; 2007; Wilhelmsson et al., 2006; reviewed in Hol and Pekny, 2015) and microglia (Fujimoto et al., 1989; Tahraoui et al., 2001; Kaur et al., 2007) resident within the site of injury. An evaluation of this methodology, and a comparison with standard quantification by cell counting, are given in Chapter 4, Section 4.4.3.

Fluorescent image acquisition was carried out as described in Section 3.2.3. Confocal microscope (Zeiss LSM 710, Carl Zeiss Microimaging, Oberkochen, Germany) images were generated using the 20x objective. Images spanning S1 barrel cortex were 425µm in width and 1,700µm in height. Multiple plane z-stack images were not used for area quantification.

Analysis of these images was carried out using ImageJ 1.50i (http://imagej.nih.gov/ij, last accessed 10/08/2018), using techniques previously described for particle detection (Jensen, 2013; https://imagej.nih.gov/ij/docs/menus/analyze.html, last accessed: 10/08/2018), as shown in Figure 3.3. A region of interest (ROI) spanning cortical Layers I-VIb (marginal zone to subplate) was defined using the ROI Manager tool. The upper boundary of the ROI was beneath the pial surface, as preservation of this highly-immunoreactive meningeal layer varied significantly between brains. The lower boundary of the ROI was above the subcortical white matter. ROI boundaries were drawn freehand from DAPI for each image.

The thresholding tool was used to select a range of fluorescence values corresponding to visible immunoreactivity. Identical threshold settings were used across all brains analysed for a single marker. Three glial markers were investigated: glial fibrillary acidic protein (GFAP), ionised calcium-binding adaptor molecule 1 (Iba1), and cluster of differentiation 68 (CD68), all of which were assigned individual

thresholding values. Each thresholded image was then analysed using the Particle Analysis tool. No limitations were set for particle size or shape, allowing any pixels which met the thresholding criteria to be included, ensuring that both cell bodies and processes were included in the intensity map. The Particle Analysis tool automatically generated a metric for the percentage of the ROI covered by detected particles. This number was recorded as the proportion of total cortical area covered by GFAP, Iba1, or CD68 immunoreactivity. At least three brains were quantified for each condition and three sections were quantified from each brain. Details of the total number and condition of brains used are given in Table 4.1 and Table 4.2.

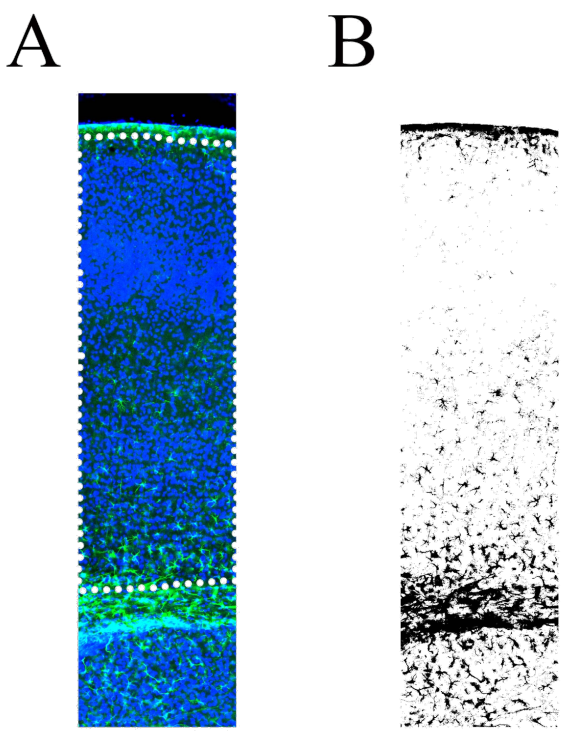


Figure 3.3 – Schematic of Pixel Intensity Cortical Area Analysis Method. (A) Example 50µm thickness cortical slice from P10 mouse S1 cortex, with white dotted line drawn freehand to mark the boundaries of the region of interest (ROI). The ROI includes cortical layers I-VIb, excluding the pial surface directly above and the subcortical white matter directly below. (B) Example thresholded binary image. The threshold chosen is between 0 and 255 arbitrary intensity units in ImageJ, with all pixels below the threshold being excluded from analysis, and all pixels above the threshold being included as immunoreactive signal. Here the threshold chosen was 62. Particle size analysis was then carried out on the thresholded ROI. These methods were used for images of GFAP, Iba1, and CD68 stained cortex (see Chapter 4, Section 4.3.3). The example shown here depicts GFAP in green and DAPI in blue.

3.3 Results

3.3.1 Quantification of Cortical Neuroserpin Protein Expression Throughout Development in Mouse

Previous publications have extensively profiled the expression of *Serpini1* mRNA within the mouse brain (Osterwalder et al., 1996; Krueger et al., 1997). However, little is known concerning neuroserpin protein localisation, with the exception that neuroserpin protein can be secreted by neurons (Osterwalder et al., 1996). In addition, qualitative immunohistochemistry experiments in post-mortem tissue from mature adult human brains demonstrated expression of neuroserpin in some neurons (Teesalu et al., 2004). This is far from a systematic documentation of neuroserpin-expressing cells across development. In this section, results from quantitative fluorescent immunohistochemistry conducted across a range of postnatal developmental time-points in mouse are described. Experiments employed antibodies against neuroserpin, in addition to molecular markers for neurons, glia, neuronal subpopulations, and subcellular structures. Validation of primary antibodies against neuroserpin is described in Chapter 2, Section 2.8.

3.3.1.1 Quantification of Cortical Neuroserpin Protein Expression Throughout Development in Mouse Neurons

Fluorescent immunohistochemistry was used to stain cortical slices from the primary somatosensory (S1) barrel cortex for the presence of neuroserpin protein. Pan-neuronal marker neuronal nuclei (NeuN) was chosen as a reference protein that reliably labels the majority of neurons in the mature brain (Mullen et al., 1992; Wolf

et al., 1996; Kim K.K. et al., 2009; Kim B.J. et al., 2009; reviewed in Gusel'Nikova and Korzhevskiy, 2015).

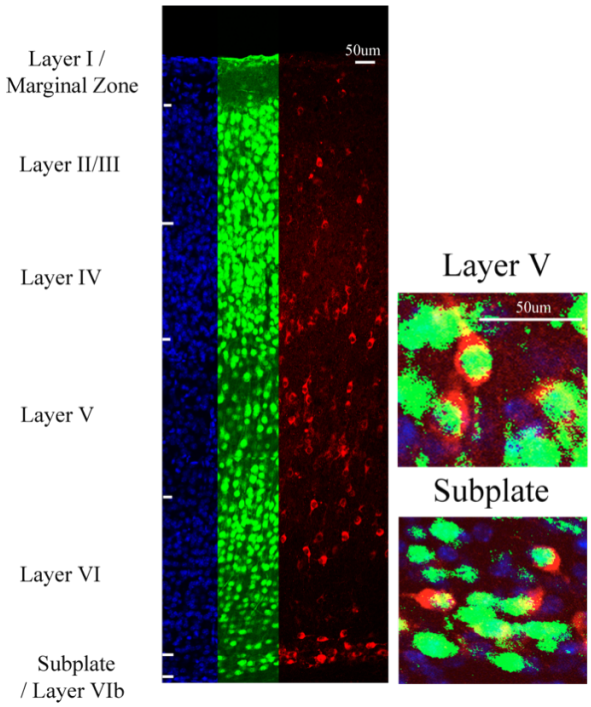


Figure 3.4 – Representative Confocal Microscope Image of P8 Cortical Stack stained for NeuN in Green and Neuroserpin in Red. DNA counterstain, 4′,6-diamidino-2-phenylindole (DAPI), (blue) was used to identify cortical layers. NeuN is a nuclear marker, whereas neuroserpin is a cytoplasmic marker which reveals the soma of neurons at the antibody concentrations used. Neuroserpin-immunoreactive cells are visible in all cortical layers, with highest density within Layer V and subplate (Layer VIb). The magnified insets to the right in Layer V and subplate show co-localisation of neuroserpin-immunoreactive cytoplasm with corresponding NeuN-immuno-reactive neuronal nuclei. The great majority of neuroserpin-immunoreactive cells clearly corresponded to a NeuN-immunoreactive nucleus, this confirmed that most cells within mouse cortex that express neuroserpin protein are neurons. In addition, cytoplasmic morphology of neuroserpin-immunoreactive neurons correspond to that of neurons throughout cortex.

NeuN is not expressed in all immature neurons over development and may underestimate these numbers (Sarnat et al., 1998; Weyer and Schilling, 2003). Some researchers have also reported certain subsets of mature cortical neurons are not labelled by NeuN (Sarnat et al., 1998; Ünal-Çevik et al., 2004), while others observed minor differences in the number of human cortical neurons labelled by Nissl and

NeuN staining methods (Gittins and Harrison, 2004; Balaram et al., 2014). The NeuroExpresso database records low levels of non-neuronal mRNA expression of the NeuN-coding gene Rbfox3 in oligodendrocytes from microarray and RNAseq data (Mancarci et al., 2016; http://neuroexpresso.org/, last accessed 11/04/2019). Despite these caveats, NeuN was chosen as a widely studied and previously validated neuronal marker. A representative confocal image of P8 mouse cortex stained for DNA-counterstain 4′,6-diamidino-2-phenylindole (DAPI) in blue, NeuN in green, and neuroserpin in red is shown in Figure 3.4.

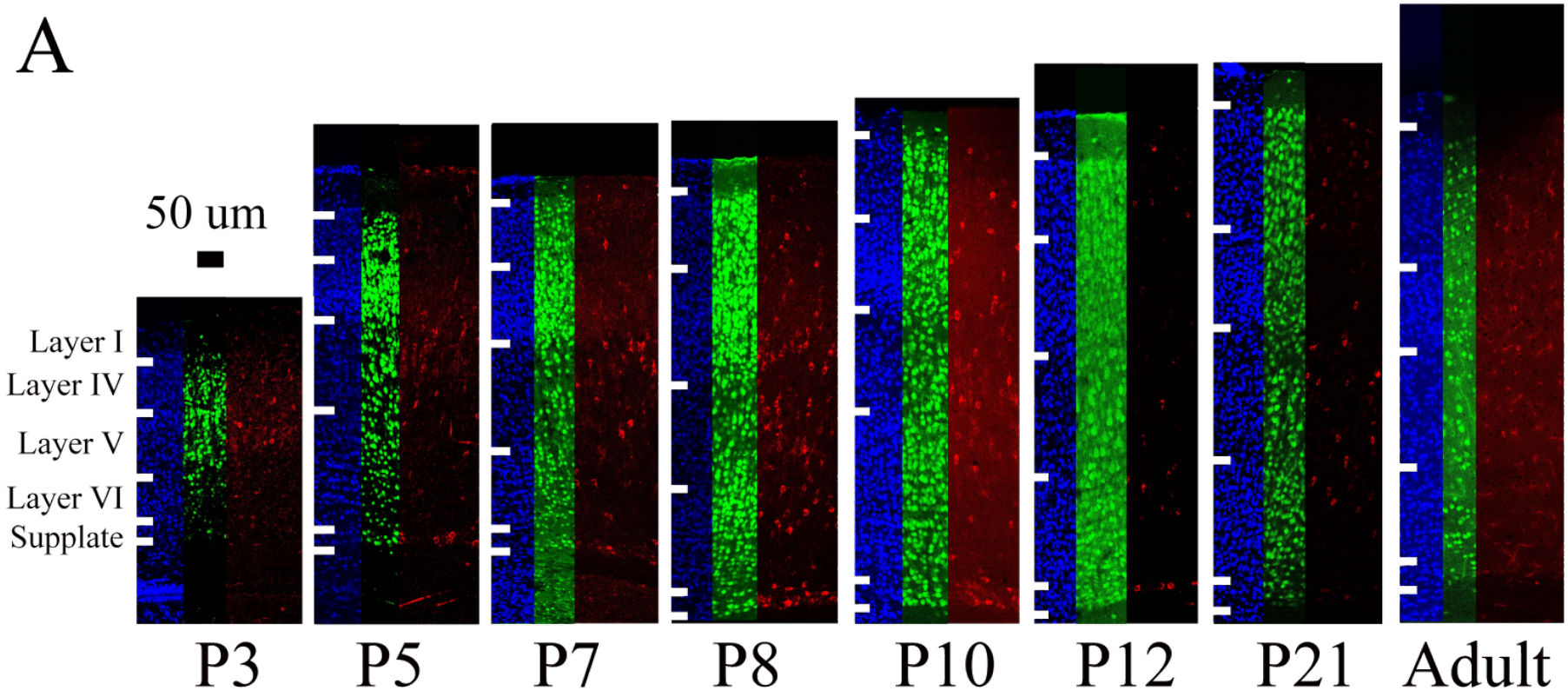
Neuroserpin-immunoreactive neurons were counted against NeuN-immunoreactive neuronal nuclei in the cortex of two wild-type mouse strains: the out-bred National Institute of Health, Swiss (NIHS) mouse (Rice and O'Brien, 1980; Chia et al., 2005) and the C57BL/6J inbred mouse (Crawley et al., 1997; Zurita et al., 2011). Parallel analysis of two mouse strains aided in the elimination of a possible atypical neuroserpin expression profile specific to the highly inbred C57BL/6J strain.

Several developmental time points were selected, immunohistochemistry and analysis was under identical conditions. Time-points chosen included: P3, P5, P6, P7, P8, P9, P10, P12, P21, and 3 months of age (referred to as adult from now on) for the NIHS mouse strain and P6, P8, P9, P12, and 3 months (adult) for the C57BL/6J strain. The series included several times points around P8, as brain development in mouse pups of this age is considered approximately equivalent to brain development at birth in humans (Finlay and Darlington, 1995; Clancy et al., 2000; 2001; 2007), although no single time-point in mouse is directly equivalent for the development of all brain regions and functionalities. Previous work identified enriched *Serpini1* mRNA expression in mouse subplate at P8 (Hoerder-Suabedissen et al., 2009), which

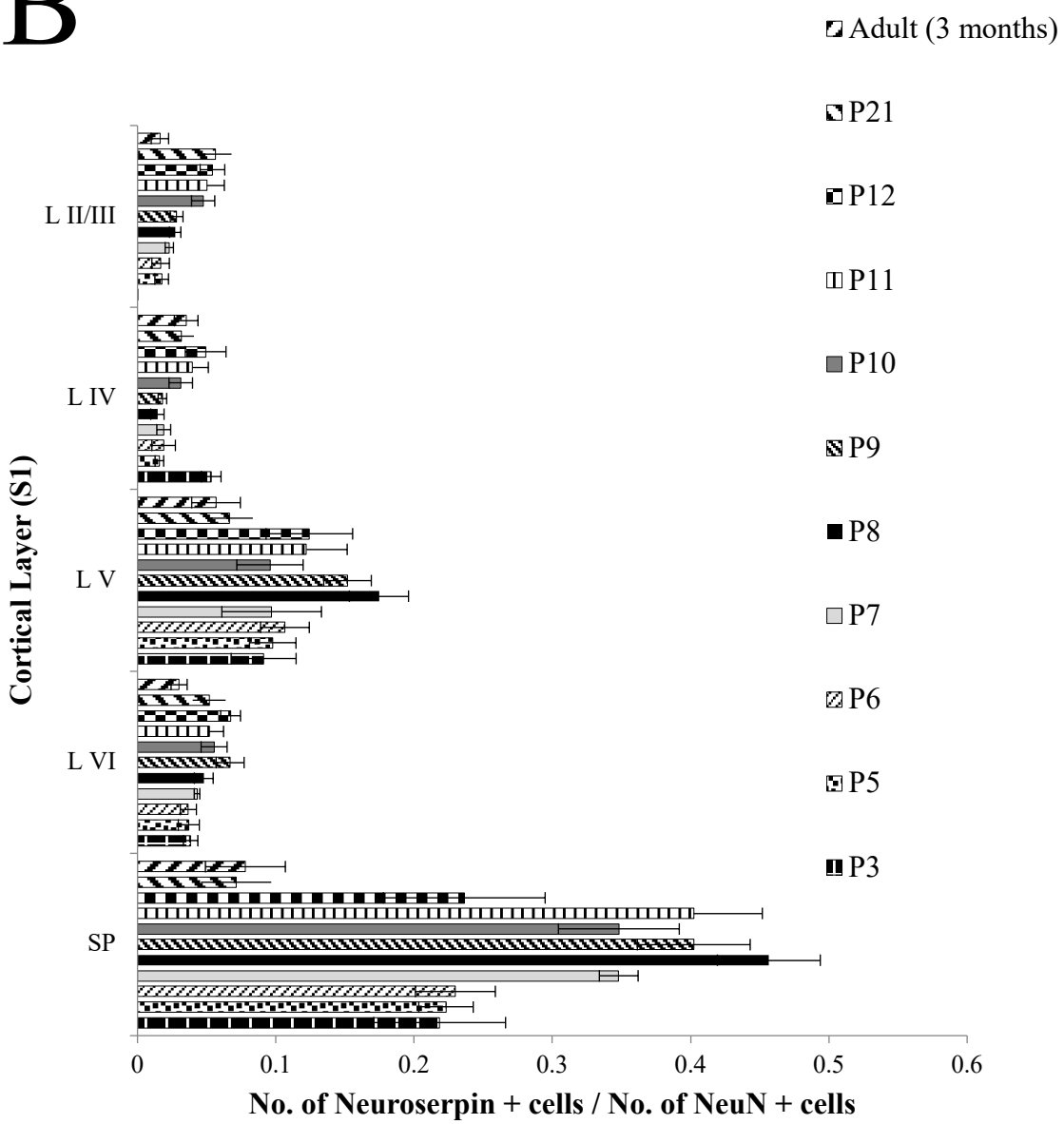
complemented non-quantitative results of *Serpini1* mRNA *in situ* hybridisation studies (Osterwalder et al., 1996; Krueger et al., 1997).

Neuroserpin-expressing neurons were found in all cortical layers throughout the developmental time-points investigated. Two cortical layers exhibited a higher proportion of neuroserpin-immunoreactive neurons relative to the total number of NeuN-immunoreactive neurons in that layers: Layer V and subplate (Layer VIb). Results from the NIHS and C57BL/6J strains are summarised in together in Table 3.4, and separately in Figure 3.5 and Figure 3.6, respectively.

In the NIHS mouse, subplate (Layer VIb in the adult brain) was most strongly enriched for neuroserpin-immunoreactive neurons. The proportion of neuroserpin-immunoreactive subplate neurons remained at approximately 20% of the total number of subplate neurons from P3 to P6 (22% ± 9% at P3, 22% ± 4% at P5, 23% ± 6% at P6), before increasing to a peak of 46% of subplate neurons from P8 to P9 (35% ± 3% at P7, 46% ± 7% at P8, 40% ± 10% at P9). This expression level then gradually dropped to 8% of subplate neurons immunoreactive for neuroserpin in the adult brain (23% ± 11% at P12, 7% ± 10% at P21, 8% ± 6% in adult). Layer V of cortex was also relatively enriched for neuroserpin expression. Around 10% of NeuN-immunoreactive Layer V neurons expressed neuroserpin (9% ± 6% at P3, 10% ± 3% at P5, 10% ± 6% at P6), with a trend towards increased expression at P8 (10% ± 7% at P7, 17% ± 1% at P8, 15% ± 2% at P9). Other cortical layers quantified did not exceed proportional neuroserpin-immunoreactivity of 5% of NeuN-immunoreactive neurons across development, with neuroserpin expression declining in all layers during adulthood.


A
50 um
Layer I
Layer IV
Layer V
Layer VI
Supplate
P3
P5
P7
P8
P10
P12
P21
Adult

B


Adult (3 months)
P21
P12
P11
P10
P9
P8
P7
P6
P5
P3
L II/III
L IV
L V
L VI
SP
Cortical Layer (S1)
0
0.1
0.2
0.3
0.4
0.5
0.6
No. of Neuroserpin + cells / No. of NeuN + cells

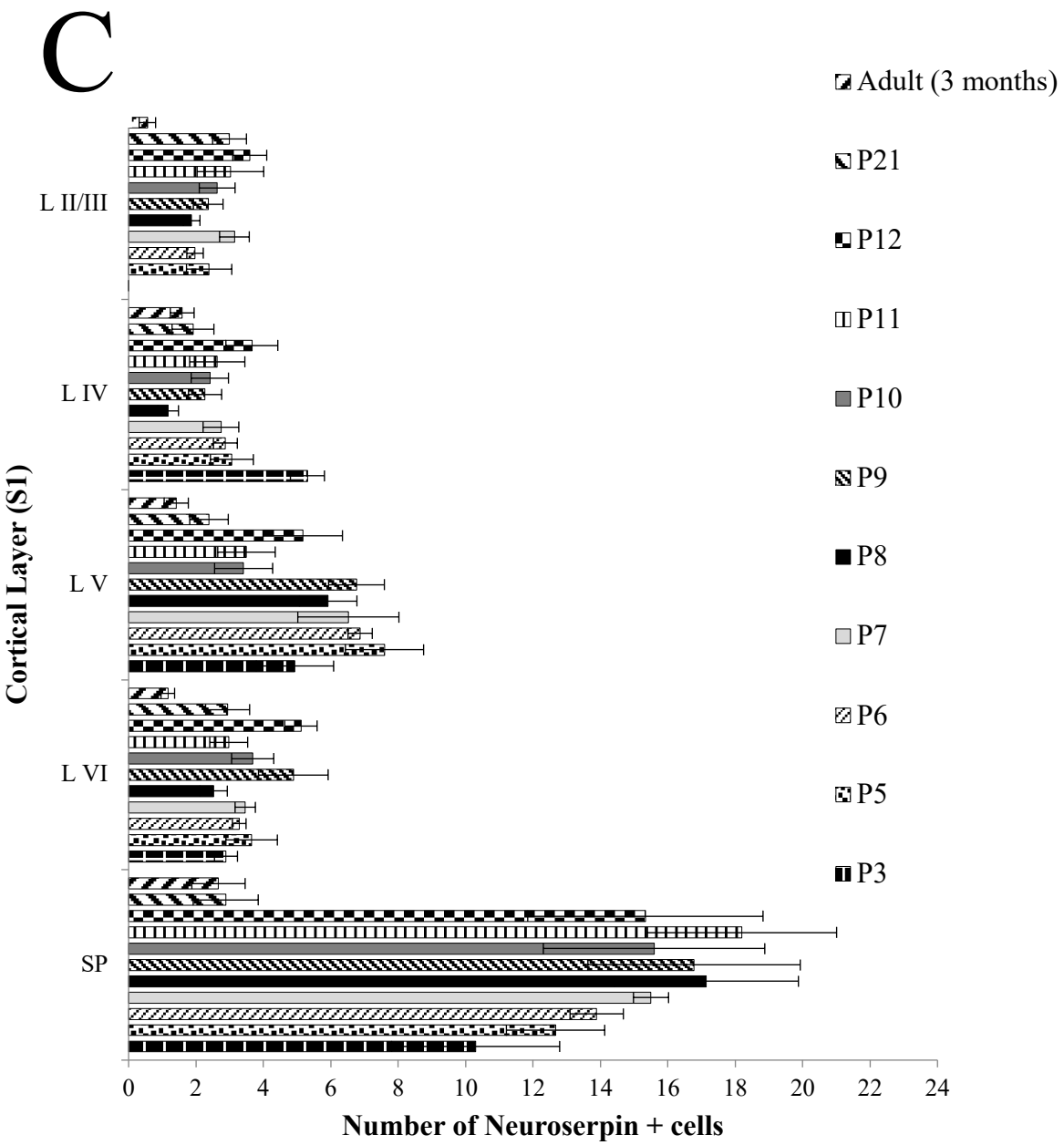
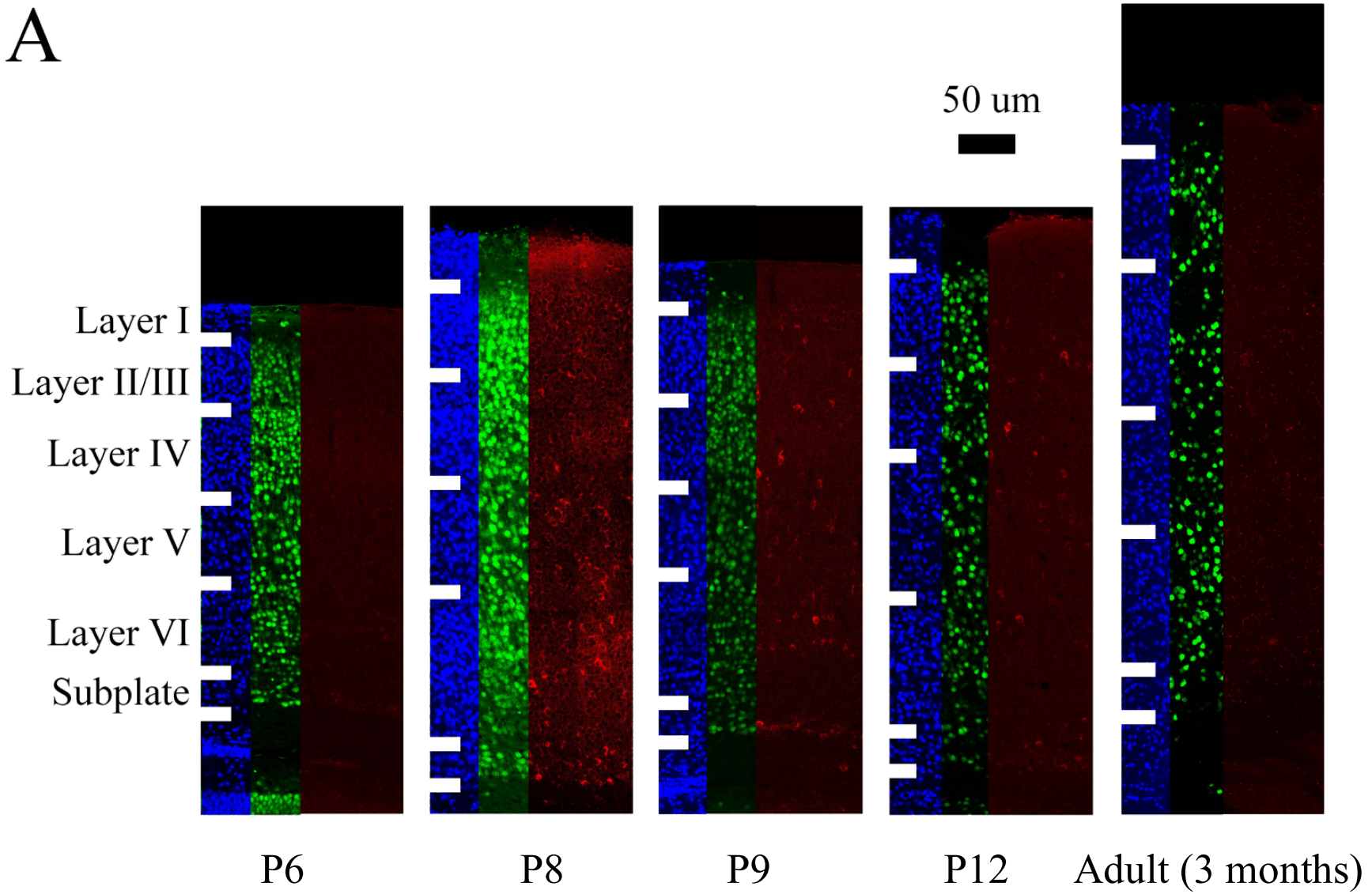
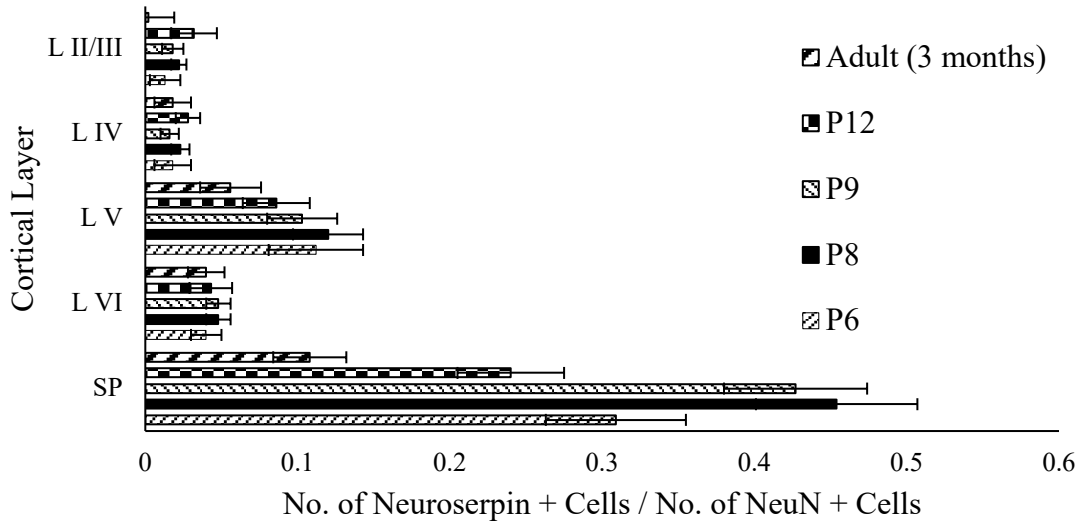


Figure 3.5 – Quantitative Analysis of Neuroserpin Expression Per Cortical Layer over Postnatal Development in the National Institute of Health Swiss (NIHS) Mouse. All panels show evidence of peak subplate (Layer VIb in the adult brain) neuroserpin immunoreactivity in the developmental window around P8, with neuroserpin immunoreactive cells detected throughout all cortical layers. (A) Representative confocal images of cortical stacks stained for NeuN in green, neuroserpin in red, and DAPI in blue. Scale bars indicate 50 μm width areas. Cortical layers are defined to the right of the image using white horizontal lines. (B) Quantitative analysis of the proportion of NeuN-immunoreactive cells co-immunoreactive for neuroserpin per cortical layer across developmental time points. Mean average number of neuroserpin-immunoreactive cells was divided by the mean average number of NeuN-immunoreactive cells per cortical layer per age. Error bars represent mean ± 1 standard deviation (± SD). (C) Quantitative analysis of mean average total number of neuroserpin-immunoreactive cells per cortical layer per age. Error bars represent mean ± 1 standard deviation (± SD). As the aim of this experiment was an exploratory overview of the pattern of neuroserpin protein expression patterns in developing mouse, no comparative statistical testing was applied to this data.

These results were replicated in the C57BL/6J inbred mouse model, as summarised in Table 3.4 and Figure 3.6. Overall numbers of neuroserpin-immunoreactive neurons in C57BL/6J cortex appeared slightly reduced at all ages, although this may be due to a different batch of polyclonal antibody used to stain these brains by necessity. Despite this reduction, a substantial subset of cortical NeuN-immunoreactive neurons were neuroserpin-immunoreactive, and the trend towards increased neuroserpin expression at P8 was conserved.


A
50 um
Layer I
Layer II/III
Layer IV
Layer V
Layer VI
Subplate
P6
P8
P9
P12
Adult (3 months)

B



C

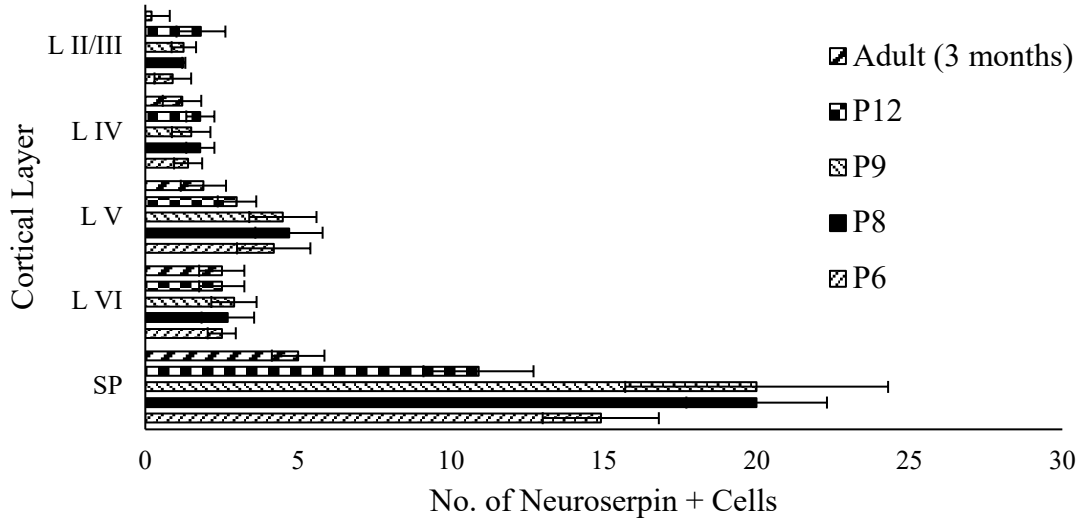


Figure 3.6 – Quantitative Analysis of Neuroserpin Expression Per Cortical Layer over Postnatal Development in the C57BL/6J In-Bred Mouse. (A) Representative confocal images of cortical stacks stained for NeuN in green, neuroserpin in red, and DAPI in blue. Images acquired using the 20 x magnification objective. Scale bars indicate 50 µm width areas. (B) Quantitative analysis of the proportion of NeuN-immunoreactive cells co-immunoreactive for neuroserpin per cortical layer across developmental time points. Mean average number of neuroserpin-immunoreactive cells was divided by the mean average number of NeuN-immunoreactive cells per cortical layer per age. Error bars represent mean ± 1 standard deviation (± SD). (C) Quantitative analysis of mean average total number of neuroserpin-immunoreactive cells per cortical layer per age. Error bars represent mean ± 1 standard deviation (± SD). As the aim of this experiment was an exploratory overview of the pattern of neuroserpin protein expression patterns in developing mouse, no comparative statistical testing was applied to this data.

Strain	Age	N	Raw Number Neuroserpin-Immunoreactive Cells Counted	Raw Number NeuN-Immunoreactive Cells Counted	Proportion of Neuroserpin-Immunoreactive Cells NeuN-Co-Immunoreactive (± SD)
NIHS	P3	3	211	2,389	0.90 (± 0.08)
NIHS	P5	3	264	5,179	0.96 (± 0.03)
NIHS	P6	3	260	1,669	0.95 (± 0.09)
C57BL/6J	P6	5	749	13,880	0.90 (± 0.06)
NIHS	P7	3	468	6,503	0.98 (± 0.09)
NIHS	P8	8	1,031	8,421	0.92 (± 0.10)
C57BL/6J	P8	5	993	15,733	0.93 (± 0.07)
NIHS	P9	3	298	3,271	0.97 (± 0.09)
C57BL/6J	P9	5	957	15,207	0.95 (± 0.09)
NIHS	P10	3	250	2,707	0.96 (± 0.03)
NIHS	P11	3	273	2,295	0.94 (± 0.06)
NIHS	P12	3	296	2,829	0.97 (± 0.10)
C57BL/6J	P12	5	802	15,033	0.97 (± 0.09)
NIHS	P21	3	118	2,215	0.91 (± 0.08)
NIHS	Adult	3	67	1,680	0.96 (± 0.06)
C57BL/6J	Adult	5	465	12,972	0.98 (± 0.09)

Table 3.4 – Raw Numbers of Neuroserpin- and NeuN- Immunoreactive Neurons Counted Across All Cortical Layers Across Developmental Time-Points. The far-right column shows the proportion of neuroserpin-immunoreactive cells which were also immunoreactive for NeuN, revealing that across ages the majority of neuroserpin expressing cells were identified as NeuN-immunoreactive neurons.

Overall, these results complement non-quantitative *in situ* hybridisation investigations of *Serpini1* mRNA expression in developing mouse (Krueger et al., 1997; Osterwalder et al., 1998). Immunohistochemistry revealed a similar distribution of neuroserpin expressing neurons throughout developing cortex, with a substantial enrichment in the subplate compartment, peaking around P8.

This pattern was conserved in both the NIHS and C57BL/6J mouse strains. Table 3.4 documents that the vast majority of neuroserpin-immunoreactive cells also expressed pan-neuronal marker NeuN, identifying these as neurons. The small proportion of neuroserpin-immunoreactive cells which did not express NeuN did not appear to be more prevalent in any one cortical layer, so data is shown for the whole cortex. These neuroserpin-immunoreactive NeuN-negative cells may be explained by misappropriation of neuroserpin-immunoreactive cells to the wrong z-plane during

manual counting, incomplete labelling of cortical neurons with NeuN immunoreactivity (Sarnat et al., 1998; Weyer and Schilling, 2003; Ünal-Çevik et al., 2004), or genuine expression of neuroserpin in glial cells within the brain.

3.3.1.2 Quantification of Cortical Neuroserpin Protein Expression over Development in Mouse in Glia

To determine whether the NeuN-negative neuroserpin-immunoreactive cells identified in Section 3.3.1.1 corresponded to neuroserpin-immunoreactive glia, fluorescent immunohistochemistry was carried out to stain for neuroserpin and known glial markers: glial fibrillary acidic protein (GFAP) for astrocytes (Eng et al., 1970; 1971; reviewed in Eng, 1985; Eng et al., 2000; Sofroniew, 2009; Sofroniew and Vinters, 2010); ionised calcium binding adaptor molecule 1 (Iba1) for microglia (Ito et al., 1998; Ohsawa et al., 2000; 2004; Khozhai and Otellin, 2013; reviewed in, Sukhorukova et al., 2010; Korzhevskii and Kirik, 2016); and oligodendrocyte transcription factor 2 (Olig2) for oligodendrocytes (Lu et al., 2000; Zhou et al., 2000; Takebayashi et al., 2000; Marie et al., 2001; reviewed in Lu et al., 2001).

Preliminary permanent immunohistochemistry studies detected neuroserpin immunoreactivity in human cortical glia (Adorján et al., 2019), although several of the antibodies used in this publication have been shown in this thesis to be non-specific (see Chapter 2, Section 2.8). There is some evidence that *Serpini1* mRNA may be expressed in glial cells from *in situ* hybridisation studies (Hastings et al., 1997; Docagne et al., 1999) and RNAseq studies (Tasic et al., 2016; Zhong et al., 2018; http://casestudies.brain-map.org/celltax#section_explorea, last accessed: 22/04/2019; http://neuroexpresso.org/, last accessed 22/04/2019), and exogenous

neuroserpin protein has been shown to protect cultured astrocytes from oxygen glucose deprivation (OGD) (Rodríguez-González et al., 2011a; Wang et al., 2015), suggesting a potential functional role for this protein in glia.

Recent RNAseq studies have documented *Serpini1* mRNA concentrations in both 15 post-conceptional week and adult human cells documented substantial Serpini1 mRNA expression in subplate neurons co-positive for known subplate markers Complexin-3, Bcl11b, and Map1b (Lake et al., 2016; Adorján et al., 2019). In this study, human astrocytes also expressed significant levels of Serpini1 mRNA, whereas no significant expression was detected in oligodendrocytes or microglia. This is corroborated by another study which documented high levels of *Serpini1* mRNA in adult mouse Layer VIb cortical neurons, with astrocytes, oligodendrocytes, and microglia expressing approximately 5 orders of magnitude lower counts per million of *Serpini1* mRNA (Tasic et al., 2016; Zhong et al., 2018).

Across the three developmental time points selected, few neuroserpin-immunoreactive cells were found to be co-immunoreactive for glial lineage markers. Less than 1% of neuroserpin-immunoreactive cells in cortex co-expressed GFAP at any age (1% ± 1% at P3 and P8, 1% ± 2% in adult). A similar proportion of cells, below 5% of the total number of neuroserpin-immunoreactive cells, co-expressed Iba1 (1% ± 1% at P3 and P8, 2% ± 2% in adult) or Olig2 (1% ± 1% at P3, 3% ± 3% at P8, and 1% ± 1% in adult). Results are summarised in Figure 3.7 and Table 3.5.

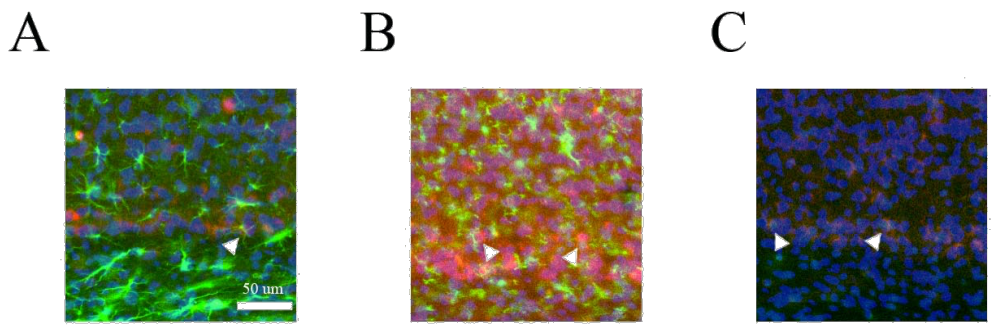


Figure 3.7 – Quantitative Analysis of Neuroserpin Protein Expression in Cortical Glia in P8 Mouse. (A) Representative confocal image of subplate zone within a P8 cortical stack stained for DAPI in blue, astrocyte marker GFAP in green, and neuroserpin in red. Arrowheads indicate examples of neuroserpin-GFAP co-immunoreactive cells. Scale bar indicates 50µm. (B) Representative confocal image of subplate zone within a P8 cortical stack stained for DAPI in blue, microglial marker Iba1 in green, and neuroserpin in red. Arrowheads indicate examples of Neuroserpin-Iba1 co-immunoreactive cells. (C) Representative confocal image of subplate zone within a P8 cortical stack stained for DAPI in blue, oligodendrocyte marker Olig2 in green, and neuroserpin in red. Arrowheads indicate examples of Neuroserpin-Olig2 co-immunoreactive cells.

Morphology of the neuroserpin-immunoreactive cells confirmed that these retained neuronal cytosolic morphology, with none showing the classical morphology of oligodendrocytes, microglia, or the extensive sprawling processes characteristic of activated astrocytes (reviewed in Glees, 1955; Vaughan and Peters, 1974; Chan-Palay and Palay, 1977; Murabe and Sano, 1982a; 1982b; Robillard et al., 2016). The fluorophores used to label marker-immunoreactive cells shared a partially overlapping emission spectrum (reviewed in Lichtman and Conchello, 2005), so it is also possible that cells here identified as faintly co-labelled only appeared so due to bleed through signal from another fluorescent channel.

Strain	Age	N	Raw Number GFAP Immunoreactive Cells Counted	Proportion Neuroserpin-Immunoreactive Cells GFAP Co-Immunoreactive (± SD)
C57BL/6J	P6	3	880	0.009 (± 0.006)
C57BL/6J	P8	3	1,458	0.009 (± 0.008)
C57BL/6J	Adult	3	802	0.009 (± 0.020)
			Raw Number of Iba1 Immunoreactive Cells Counted	**Proportion Neuroserpin-Immunoreactive Cells Iba1 Co-Immunoreactive**
C57BL/6J	P6	3	620	0.009 (± 0.013)
C57BL/6J	P8	3	2,008	0.012 (± 0.013)
C57BL/6J	Adult	3	1,377	0.017 (± 0.025)
			Raw Number Olig2 Immunoreactive Cells Counted	**Proportion Neuroserpin-Immunoreactive Cells Olig2 Co-Immunoreactive**
C57BL/6J	P6	3	2,589	0.009 (± 0.013)
C57BL/6J	P8	3	1,991	0.032 (± 0.030)
C57BL/6J	Adult	3	165	0.005 (± 0.011)
			Raw Number Neuroserpin Immunoreactive Cells Counted	
C57BL/6J	P6	3	2,170	
C57BL/6J	P8	3	1,458	
C57BL/6J	Adult	3	802	

Table 3.5 – Raw Numbers of Neuroserpin and Glial Marker Immunoreactive Cells Counted Across Cortical Sections Across Three Developmental Time-Points. Column 5 shows proportions of neuroserpin-immunoreactive cells which co-expressed glial markers at neuroserpin antibody concentrations that give a strong signal in neurons. Columns 5 shows that although there is co-staining of neuroserpin in cortical astrocytes, microglia, or oligodendrocytes, only a small subpopulation of these cells express neuroserpin.

These counts demonstrate that neuroserpin protein expression in cortical glia is either substantially lower than that observed in neurons, and therefore cannot be detected at these antibody concentrations, or that the majority of cortical glia do not express neuroserpin in mouse at the postnatal time-points investigated. It is possible that the small number of cells identified as co-immunoreactive were astrocytes in close proximity to neurons, rather than neuroserpin-immunoreactive glia. Electron microscopy could resolve this, if increasing evidence emerges linking neuroserpin to glial cells. The *Serpini1* mRNA in glial cells may undergo alternative splicing to that in neurons, rending glial gene products undetected by the primary antibody. Alternative splicing has been reported for the *Serpini1* homologue genes in nematode

worms (Krüger et al., 2002), *Drosophila* (Osterwalder et al., 2004; Brüning et al., 2007; Ellisdon et al., 2014), and human (Fagerberg et al., 2014).

Previous findings demonstrating *Serpini1* mRNA expression in glia (Hastings et al., 1997; Docagne et al., 1999) may not apply to cortical glia in the healthy developing brain, or the *Serpini1* mRNA detected may not be translated into functional protein. These results support the theory that neuroserpin is a neuron-specific protein (Yepes, 2004; Miranda and Lomas, 2006; Galliciotti and Sonderegger, 2013).

3.3.1.3 Quantification of Neuroserpin Protein Expression Relative to Known Subplate Neuronal Molecular Markers

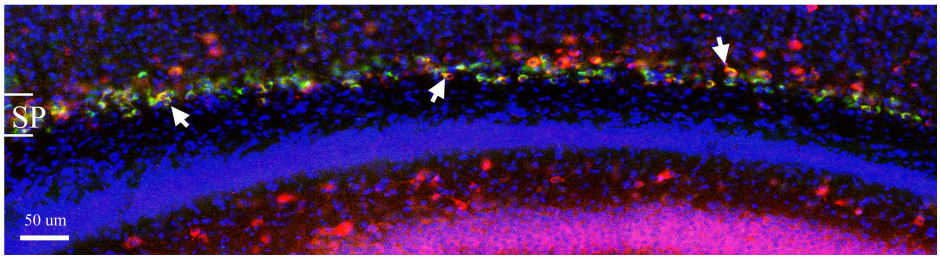
In light of the high proportion of neuroserpin-immunoreactive cells in mouse subplate quantified over early postnatal development (see Section 3.3.1.1), the neuroserpin-immunoreactive subplate neuron subpopulation was further investigated. The relative enrichment of *Serpini1* mRNA in P8 mouse subplate compared to Layer VI detected by microarray (Hoerder-Suabedissen et al., 2009) and previous non-quantitative indications of increased neuroserpin-immunoreactivity in mouse subplate at P8 by immunohistochemistry (Kondo et al., 2015), suggested neuroserpin as a potential subplate-enriched molecular marker, perhaps localised to functionally distinct subpopulation of subplate neurons. Previous studies have identified several subplate-specific or subplate-enriched molecular markers which reliably identified neurons in this layer across species (Bayatti et al., 2007; Watakabe et al., 2007; reviewed in Hoerder-Suabedissen and Molnár, 2015), including mouse (Hoerder-Suabedissen et al., 2009; Wang et al., 2010; 2011; Oeschger et al., 2012), rat (Wang et al., 2011), opossum (Wang et al., 2011), chick (Wang et al., 2011), turtle (Wang et al., 2011) and

human (Wang et al., 2010). Connective tissue growth factor (CTGF) (Heuer et al., 2003; Hoerder-Suabedssen et al., 2009), complexin-3 (Xue et al., 2008; Hoerder-Suabedissen et al., 2009), and nuclear receptor-related protein 1 (Nurr1) (Arimatsu et al., 2003; Navarro et al., 2014) have each be used to stain a partially overlapping subpopulation of subplate neurons in the postnatal mouse cortex. The relevance of these reliable molecular markers to neuronal function is currently unknow (reviewed in Hoerder-Suabedissen and Molnár, 2015).

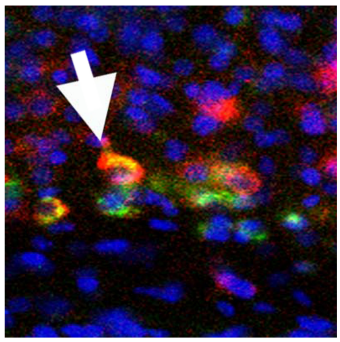
All three mouse subplate-markers showed partial overlap with the neuroserpin-immunoreactive subpopulation in P8 C57BL/6 mouse brain. 59% (± 8%) of neuroserpin-immunoreactive subplate neurons were co-immunoreactive for CTGF, 63% (± 12%) of neuroserpin-immunoreactive subplate neurons were co-immunoreactive for complexin-3, and 36% (± 4%) of neuroserpin-immunoreactive subplate neurons were co-immunoreactive for Nurr1. Figure 3.8 and Table 3.6 demonstrate that neuroserpin expression does not exclusively or completely overlap with any one subplate marker investigated. Neuroserpin protein did not itself define a novel exclusive subplate neuronal subpopulation.

A

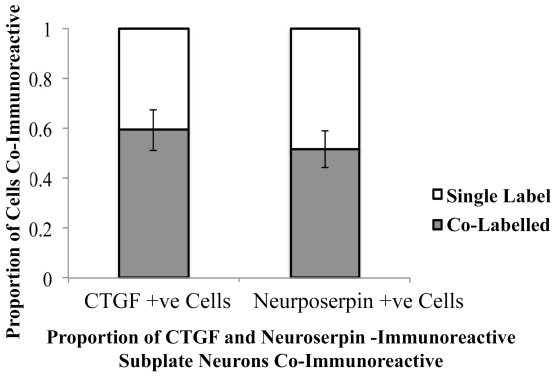
CTGF x Neuroserpin



B

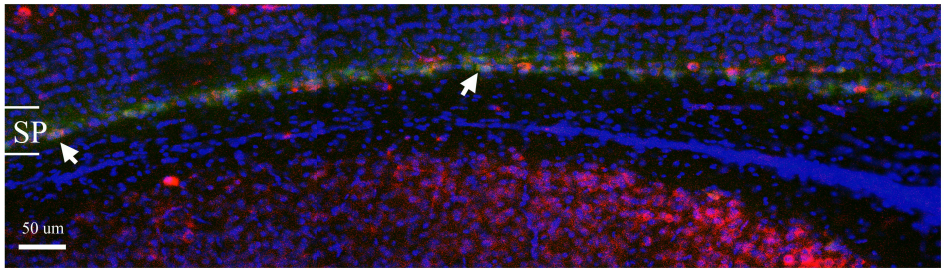


C

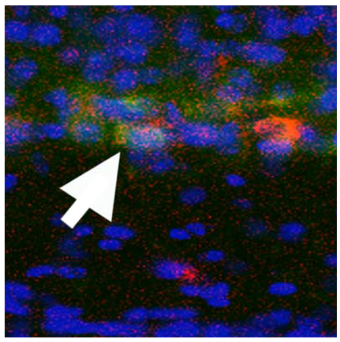


Proportion of CTGF and Neuroserpin -Immunoreactive Subplate Neurons Co-Immunoreactive

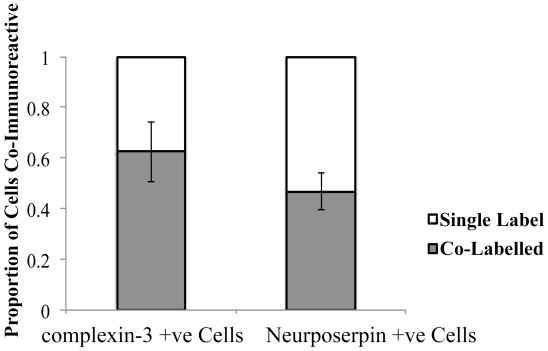
D complexin-3 x Neuroserpin



E



F



Proportion of complexin-3 and Neuroserpin -Immunoreactive Subplate Neurons Co-Immunoreactive

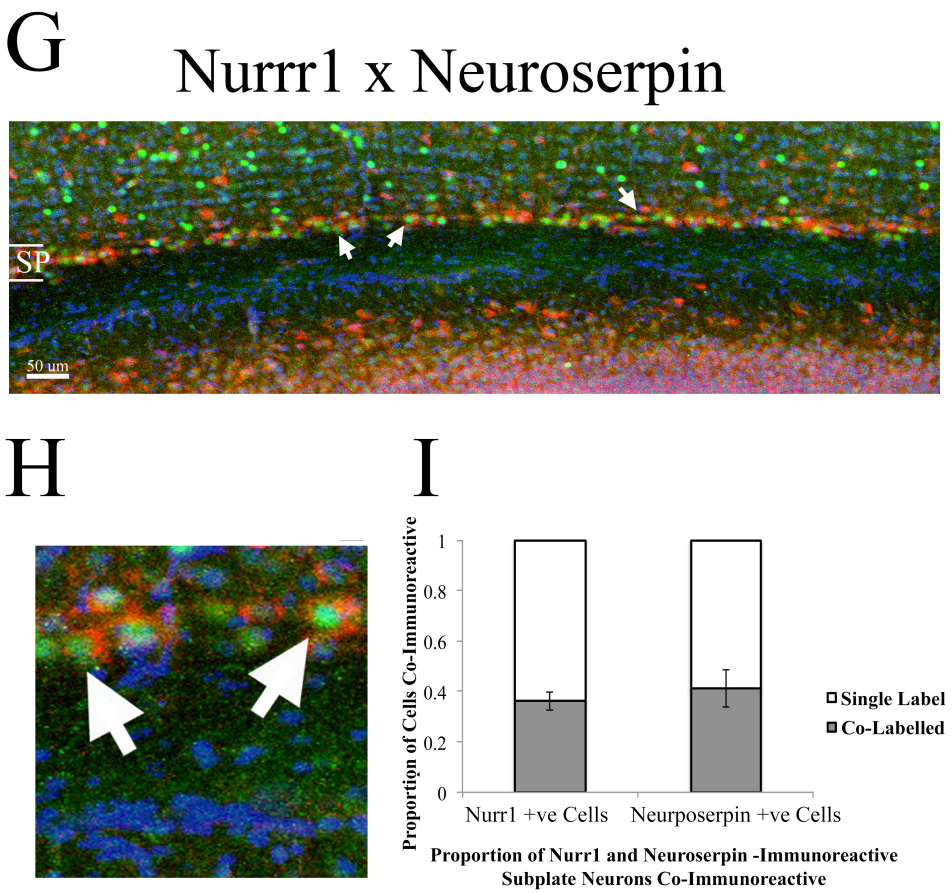


Figure 3.8 – Quantitative Analysis of Neuroserpin Immunoreactivity Overlapping with Known Subplate Molecular Marker Immunoreactive Neuronal Sub-Populations in Primary Somatosensory (S1) Barrel Cortex of P8 C57BL/6 Mouse. The neuroserpin-immunoreactive subpopulation overlaps partially with CTGF, complexin-3, and Nurr1 -immunoreactive subpopulations. Arrowheads indicate neuroserpin and subplate marker co-immunoreactive subplate neurons. Scale bars indicate 50µm width area. (A) Representative confocal image of subplate stained for CTGF in green, neuroserpin in red, and DAPI in blue. (B) Magnified section of Panel A, highlighting double labelled cells in the subplate layer. (C) Quantitative analysis of the proportion of subplate neurons co-immunoreactive for CTGF and neuroserpin. (mean ± SD). (D) Representative confocal image of subplate stained for complexin-3 in green, neuroserpin in red, and DAPI in blue. (E) Magnified section of Panel D, highlighting double labelled cells in the subplate layer. (F) Quantitative analysis of the proportion of subplate neurons co-immunoreactive for complexin-3 and neuroserpin. (mean ± SD). (G) Representative confocal image of subplate stained for Nurr1 in green, neuroserpin in red, and DAPI in blue. (H) Magnified section of Panel G, highlighting double labelled cells in the subplate layer. (I) Quantitative analysis of the proportion of subplate neurons co-immunoreactive for Nurr1 and neuroserpin. (mean ± SD).

Strain	Age	N	Raw Number CTGF-Immunoreactive Cells Counted	Proportion Neuroserpin-Immunoreactive Cells CTGF Co-Immunoreactive (± SD)
NIHS	P8	3	156	0.60 (± 0.13)
C57BL/6J	P8	5	1,781	0.59 (± 0.08)
			Raw Number Complexin-3-Immunoreactive Cells Counted	**Proportion Neuroserpin-Immunoreactive Cells Complexin-3 Co-Immunoreactive (± SD)**
NIHS	P8	3	110	0.59 (± 0.20)
C57BL/6J	P8	5	1,632	0.63 (± 0.12)
			Raw Number Nurr1-Immunoreactive Cells Counted	**Proportion Neuroserpin-Immunoreactive Cells Nurr1 Co-Immunoreactive (± SD)**
NIHS	P8	3	131	0.28 (± 0.07)
C57BL/6J	P8	5	1,657	0.36 (± 0.04)
			Raw Number Neuroserpin-Immunoreactive Cells Counted	
NIHS	P8	3	236	
C57BL/6J	P8	5	4,767	

Table 3.6 – Raw Numbers of Neuroserpin and Subplate Molecular Marker Immunoreactive Cells Counted Across Cortical Sections in P8 Mouse Primary Somatosensory Cortex (S1). Proportions of CTGF, complexin-3, and Nurr1 -immunoreactive subpopulations which were also immunoreactive for neuroserpin are shown in Column 5. Neuroserpin-immunoreactive neurons overlapped partially with each of the subplate sub-populations investigated, no markers showed a mutually exclusive expression pattern with neuroserpin.

These results demonstrate that neuroserpin co-localised with currently known subplate molecular markers, confirming that neuroserpin presence within subplate neurons. However, neuroserpin did not appear to demonstrate an exclusive or complementary relationship with any one of the markers tested in P8 mouse, hence functional properties of the neuroserpin-immunoreactive subpopulation are unlikely to be closely linked to any of the evolutionarily conserved molecular markers tested.

3.3.1.4 Birth-dating of Neuroserpin-Expressing Subplate Neurons using Bromodeoxyuridine (BrdU) and Lpar1-eGFP Mouse

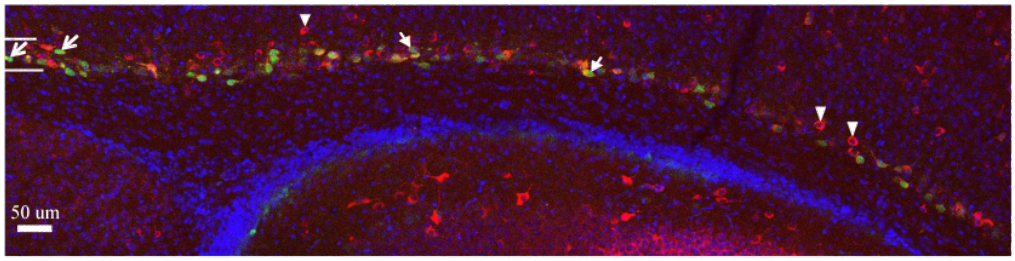
Neuronal subpopulations can also be defined by date of neurogenesis. Subplate

neurons are among the earliest born in the cerebral cortex (Angevine and Sidman, 1961; Price et al., 1997; Smart et al., 2002; Bystron et al., 2008; Hoerder-Suabedissen and Molnár, 2013; reviewed in Hoerder-Suabedissen and Molnár, 2015). The first subplate neurons are generated at E10.5, with the majority born between E11.5 and E12.5, followed by a late contribution at E13.5 (Hoerder-Suabedissen and Molnár, 2013). Birth-dating was undertaken to determine whether subplate neurons which go on to be immunoreactive for neuroserpin at P8 undergo neurogenesis at a conserved developmental time-point.

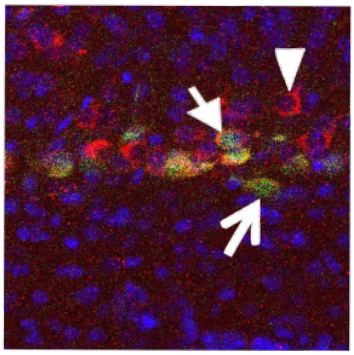
Subplate neurons generated on E11.5 and E12.5 were detected using bromodeoxyuridine (BrdU), a thymidine DNA-base analogue incorporated into cell nuclei during S-phase of cell division (Jose and Soriano, 1989; reviewed in Taupin, 2007; Kuhn and Cooper-Kuhn, 2007). Embryonic mouse brains injected with BrdU were generated by Dr. Anna Hoerder-Suabedissen using methods outlined in Hoerder-Suabedissen and Molnár, 2013. During quantification, only neurons with fully labelled nuclei were documented as born on the day of BrdU injection. Subplate neurons born at E10.5 were detected using co-expression of the molecular marker lysophosphatidic acid receptor 1 (Lpar1), also known as endothelial differentiation gene 2 (Edg2), in male Lpar1-eGFP mice (Grant et al., 2012; Pedraza et al., 2014; Walker et al., 2016; Hoerder-Suabedissen et al., 2018). Lpar1-eGFP labelled subplate neurons were previously characterised as early-born (Hoerder-Suabedissen and Molnár, 2013; Pedraza et al., 2014).

A

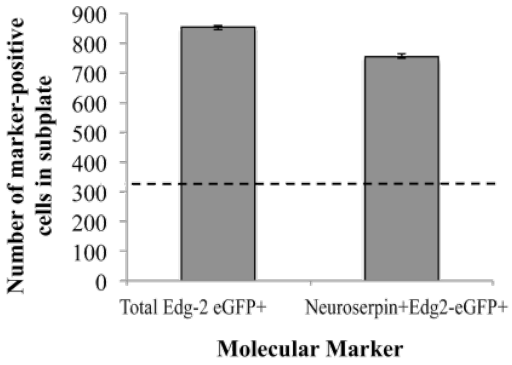
Neuroserpin x Lpar1-eGFP



B

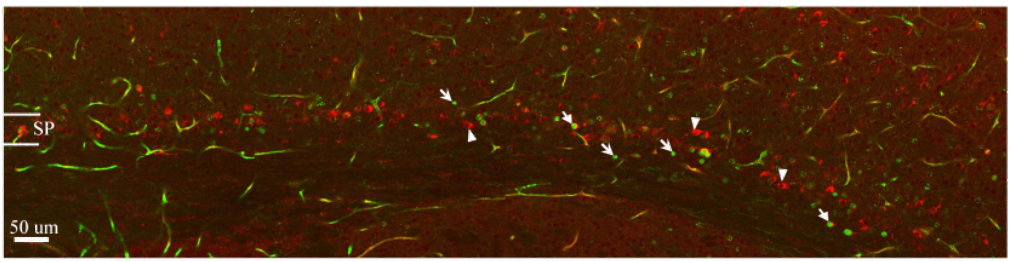


C

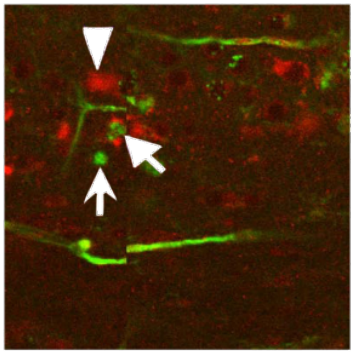


D

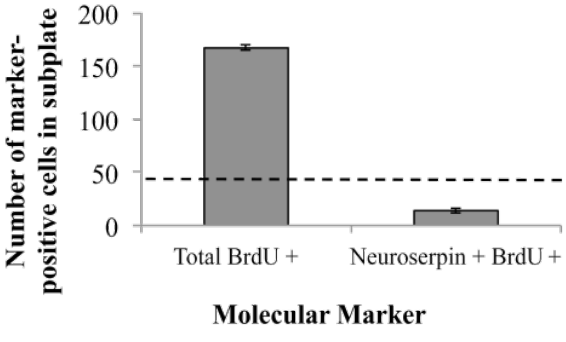
E 11.5 BrdU Injection



E



F



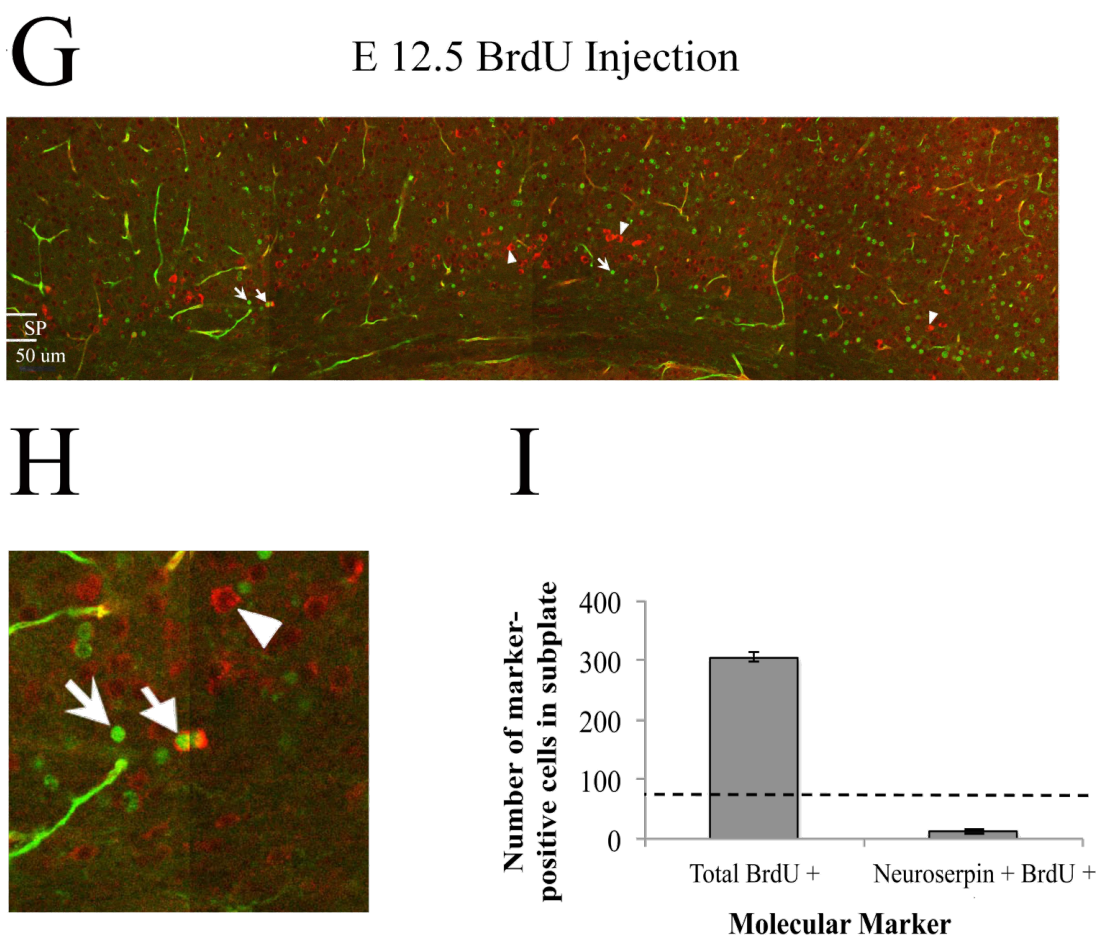


Figure 3.9 – Quantitative Birth-Dating of Neuroserpin-Immunoreactive Neurons in P8 NIHS and Lpar1-eGFP Mouse Subplate. Fluted arrows indicate examples of Lpar1-eGFP cells or BrdU-labelled nuclei. Triangles indicate examples of neuroserpin-immunoreactive cells. Arrowheads indicate examples of Neuroserpin-Lpar1-eGFP-co-labelled cells or Neuroserpin-BrdU-co-labelled cells. (A) Representative confocal image of P8 subplate stained for neuroserpin in red, and DAPI in blue. Lpar1-eGFP-expressing cells are green. Scale bars indicate 50µm width areas. (B) Magnified section of Panel A, highlighting double labelled cells in the subplate layer. (C) Quantitative analysis of the proportion of Lpar1-eGFP-expressing cells immunoreactive for neuroserpin (mean ± SD). The horizontal dotted line signifies the expected level of co-localisation given by chance if neuroserpin-immunoreactive neurons are generated equally across all time points. (D) Representative confocal image of P8 NIHS subplate stained for BrdU in green, and neuroserpin in red. (E) Magnified section of Panel D, highlighting double labelled cells in the subplate. (F) Quantitative analysis of the proportion of E11.5 born cells expressing neuroserpin (mean ± SD). (G) Representative confocal image of P8 NIHS subplate stained for BrdU in green, and neuroserpin in red. (H) Magnified section of Panel A, highlighting double labelled cells in the subplate. (I) Quantitative analysis of the proportion of E12.5 born cells expressing neuroserpin (mean ± SD).

Results indicated that subplate neurons which are immunoreactive for neuroserpin at P8 are relatively early-born for subplate neurons, and among some of the first born

cortical neurons. Relatively few neuroserpin-immunoreactive subplate neurons were generated at E11.5 compared to the total number of BrdU-labelled neurons in P8 mice injected at E11.5 (9% ± 6%). Even fewer neuroserpin-immunoreactive neurons were co-labelled with BrdU at E12.5 compared to the total number of BrdU labelled neurons in P8 mice injected at E12.5 (3% ± 2%). Significantly fewer co-labelled neurons were generated at these time points than expected by chance, as 46% ± 8% of all NIHS mouse subplate neurons express neuroserpin at P8. In contrast, 88% ± 5% of the early-born Lpar1-eGFP neurons were immunoreactive for neuroserpin, suggesting a substantial proportion of neuroserpin-expressing subplate neurons were born at or around E10.5 in NIHS mouse. Results are summarised in Figure 3.9 and Table 3.7.

The primary antibody against BrdU generated significant off-target labelling within the cytoplasm of vascular endothelial cells, as observed in previous studies that employed this antibody (Hoerder-Suabedissen and Molnár, 2013). This staining was also present in negative control sections from brains which had not been injected with BrdU. Therefore, care was taken assess the spherical nature of candidate BrdU-immunoreactive nuclei prior to inclusion in quantitative analysis.

Strain (Condition)	Age	N	Birth-Date	Raw Number of Neuroserpin-Immunoreactive Cells Counted	Raw Number of Birth-Dated Cells Counted	Proportion of Neuroserpin-Immunoreactive Cells Born (± SD)
Lpar1-eGFP (NIHS background)	P8	3	E10.5	1,787	852	0.88 (± 0.05)
NIHS (BrdU injected at E11.5)	P8	3	E11.5	1,069	167	0.09 (± 0.06)
NIHS (BrdU injected at E12.5)	P8	3	E12.5	1,142	305	0.03 (± 0.02)

Table 3.7 – Raw Numbers of Neuroserpin-Immunoreactive Cells Counted Within The Subplate of Lpar1-eGFP Mouse, and NIHS Mice Injected with Bromodeoxyuridine (BrdU) at E11.5 and E12.5. Although some cells that go on to become immunoreactive for neuroserpin by P8 are born at each of the three time-points investigated, fewer are born at E11.5 and E12.5 than would be expected by chance, with the largest subset of neuroserpin-immunoreactive subplate neurons indicated as early born by co-labelling with Lpar1-eGFP on an NIHS background.

These birth-dating studies in P8 mouse suggested that subplate neurons which go on to express neuroserpin protein are some of the earliest born among this cortical layer, with majority generated at around E10.5. It would be interesting to investigate whether this early origin is specific to neuroserpin-immunoreactive neurons in the subplate, or whether neuroserpin-immunoreactive neurons in other layers are also relatively early born for the average cell in each of these respective layers.

3.3.2 Subcellular Localisation of Neuroserpin Protein with Molecular Markers of Endoplasmic Reticulum (ER) and Metabolic Stress

Previous investigators have proposed a role for subplate in secretory functions (Belgard et al., 2011; Hoerder-Suabedissen et al., 2013; Kostović et al., 2014; Kondo et al., 2015). High endoplasmic reticulum-mediated secretory function have also been linked to increased metabolic stress on cells (reviewed in Schroder and Kaufman, 2005; Wu and Kaufman, 2006; Kondo et al., 2011). This function may encompass neuroserpin, a known secreted protein (Osterwalder et al., 1996). To investigate the proposed functional secretory properties of subplate alongside the enriched neuroserpin immunoreactivity in this layer, two anatomical investigations were carried out. The first documented neuroserpin co-immunoreactivity with structural and stress-related markers of the secretory endoplasmic reticulum (ER) (reviewed in Kondo et al., 2015). The second investigated neuroserpin co-immunoreactivity with general metabolic stress markers, the heat shock proteins (Whitley et al., 1999).

3.3.2.1 Neuroserpin Protein Expression within the Endoplasmic Reticulum (ER), Co-Localisation using Structural and ER-Stress Markers

Neuronal secretion products such as chondroitin-sulphate proteoglycans (CSPGs) and growth factors have been shown to be expressed by P8 mouse subplate (Hoerder-Suabedissen et al., 2013), complementing anatomical studies which have demonstrated relatively mature endoplasmic reticulum (ER) structure in subplate compared to developing neurons in other cortical layers (Kondo et al., 2015). It is currently not known which proteins are secreted by subplate neurons, or whether subplate neurons with high secretory load can be characterised by expression of specific molecular markers. The secretory load of neuroserpin-immunoreactive subplate neurons was probed by co-staining with antibodies against structural and stress-induced ER molecular markers.

Markers selected included the KDEL motif, which encodes the sequence of amino acids lysine-glutamic acid-aspartic acid-leucine. This succession of amino acids is found in several proteins, including BiP, calreticulin, and GRP94 (Lewis and Pelham, 1990; 1992; reviewed in Pelham, 1990; Teasdale and Jackson, 1996), and prevents the secretion of these proteins from the ER (Munro and Pelham, 1987; Nilsson et al., 1989; Dean and Pelham, 1990; Jackson et al., 1990; Pichon et al., 1997). Antibodies against the KDEL motif have been associated with ER structure and ER-stress (Han et al., 2013; reviewed in Ellgaard and Helenius, 2003; Kondo et al., 2011). As KDEL is a broad marker targeting many different proteins which share an amino acid sequence, two protein-specific ER markers were also investigated: calreticulin (Ostwald and McLennan, 1974; reviewed in Michalak et al., 1999; Johnson et al., 2001) and C-EBP

homologous protein (CHOP) (Ron and Habener, 1992; Tsukano et al., 2010; reviewed in Oyadomari and Mori, 2004).

Co-staining demonstrated that subplate neurons with high ER-stress labelling also indicated immunoreactivity for neuroserpin using a confocal microscope under the 20 x magnification objective. These results replicated previous Golgi and fluorescent immunohistochemistry experiments which showed a peak in mature ER-marker immunoreactivity in mouse subplate at P8, coinciding with the peak in developmental neuroserpin immunoreactivity (Kondo et al., 2015). When observed under 64 x magnification, partial overlap between neuroserpin and ER-marker immunoreactivity was demonstrated. This suggested that at least a portion of neuroserpin protein present in subplate neurons was made in the protein synthesising apparatus of these cells, as opposed to being entirely taken up from the extracellular environment. However, other intracellular areas of neuroserpin immunoreactivity were also visible outside the ER. These may correspond to secretory vesicles. Figure 3.10 and Table 3.8 summarise the results, all analysis presented is qualitative.

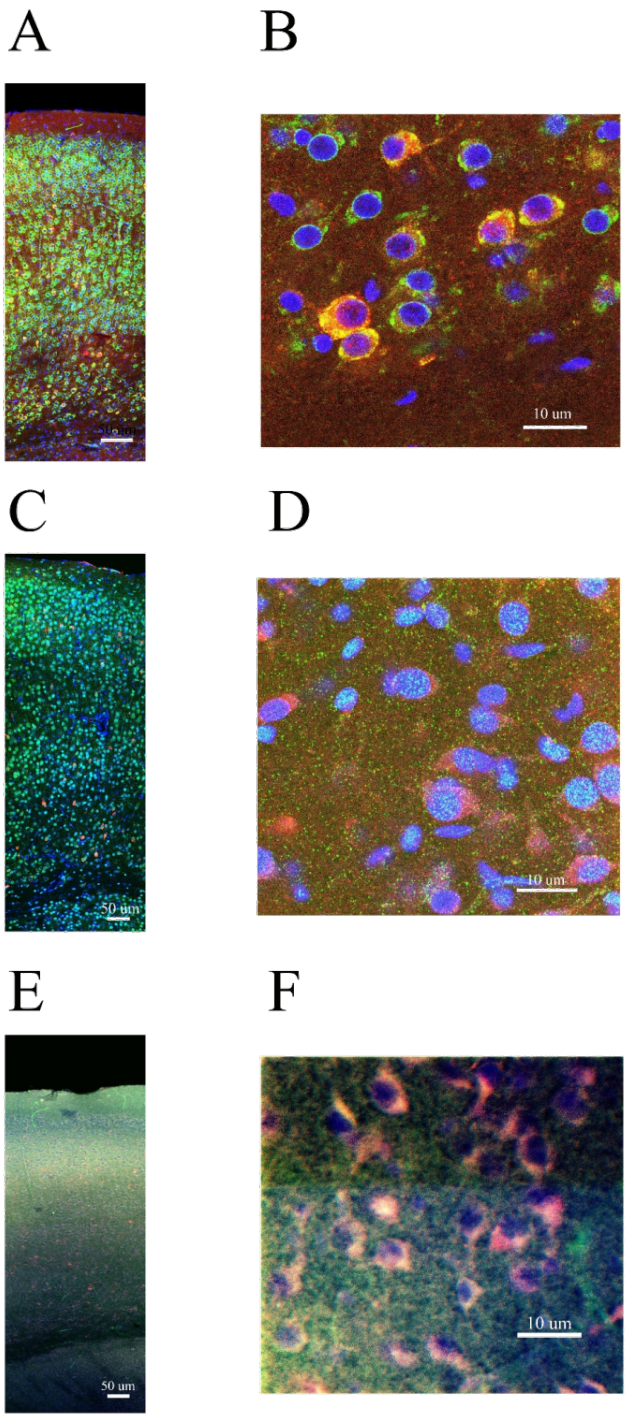


Figure 3.10 – Co-Localisation of Neuroserpin Protein with Endoplasmic Reticulum (ER) and Endoplasmic Reticulum Stress (ER-stress) markers in P8 Mouse. (A) Co-localisation of ER-stress marker KDEL (green) with neuroserpin (red) using the 20 x magnification objective. Counterstained with DAPI (blue). Scale bar indicates 50µm width area. (B) Co-localisation of KDEL (green) with neuroserpin (red) using the 64 x magnification objective. Scale bar indicates 10µm interval. (C) Co-localisation of ER structural marker Calreticulin (green) with neuroserpin (red) using the 20 x magnification objective. (D) Co-localisation of Calreticulin (green) with neuroserpin (red) using the 64 x magnification objective. (E) Co-localisation of ER-stress marker CHOP (green) with neuroserpin (red) using the 20x magnification objective. (F) Co-localisation of CHOP (green) with neuroserpin (red) using the 64x magnification objective.

The utility of this preliminary investigation is limited. One caveat is the non-specific expression of calreticulin in other intracellular membrane structures, such as the nuclear envelope, (reviewed in Michalak et al., 1999; Johnson et al., 2001). This manifests as a grainy immunoreactivity visible throughout the nucleus and cytoplasm on the images acquired at 64 x magnification, as shown in Panel D of Figure 3.10. The antibody used to detect CHOP immunoreactivity was also not ideal, requiring overexposure to observe immunoreactivity, as documented in previous publications which used this antibody for tissue staining (Shrivastava et al., 2016; Zhang et al., 2016). Alternative methods for perfusion and antigen retrieval may alleviate this poor CHOP staining (Hong et al., 2018), yet were not pursued here as detailed analysis of neuroserpin-CHOP co-immunoreactivity was not a primary aim of this thesis.

ER Molecular Marker	Strain	Age	N	20 x Magnification	64 x Magnification
KDEL	C57BL/6J	P3	3	+	
	C57BL/6J	P8	3	+++	+++
	C57BL/6J	Adult	3	+++	
Calreticulin	C57BL/6J	P3	3	+	
	C57BL/6J	P8	3	++	+++
	C57BL/6J	Adult	3	++	
CHOP	C57BL/6J	P3	3	-	
	C57BL/6J	P8	3	+	+
	C57BL/6J	Adult	3	+	

Table 3.8 – Summary of Co-Localisation of Immunoreactivity between ER-structural and ER-stress Markers with Neuroserpin by Immunohistochemistry. KDEL, Calreticulin, and CHOP, markers which indicate substantial ER-activity, were detected by immunoreactivity in cortical neurons immuno-reactive for neuroserpin. Overlap was detected at maximal confocal microscope magnification using the 64 x objective. Some intracellular neuroserpin protein is likely to be present in the ER.
- = no immunoreactivity detected, + = immunoreactivity detected but faint and localised to a small number of cells per cortical stack, ++ = immunoreactivity detected in a large number of cells within the cortical stack, +++ = substantial immunoreactivity detected in a high qualitative proportion of cells.

These results are interesting preliminaries which suggest that subplate neuronal neuroserpin may be synthesised within the neurons themselves. However, much work remains before the relationship between neuroserpin and ER-stress can be understood.

Molecular markers for other subcellular structures, such as synaptophysin for presynaptic vesicles (reviewed in Südhof, 2004), will be needed to localise the remaining pockets of neuroserpin immunoreactivity visible outside the ER at magnification with the 64 x objective. Electron microscopy studies will be needed to conclusively pinpoint the subcellular organelles expressing neuroserpin protein in subplate and other neurons.

3.3.2.2 Developmental Expression of Metabolic Stress Markers Heat Shock Proteins (HSPs) HSP60 and HSP90 and Co-Localisation with Neuroserpin in Mouse

As high secretory load has previously been associated with increased metabolic stress on cells (reviewed in Schroder and Kaufman, 2005; Wu and Kaufman, 2006; Kondo et al., 2011), expression of generalised molecular markers of cellular stress was investigated in neuroserpin-immunoreactive subplate neurons. The family of stress markers selected were the heat shock proteins (HSPs). HSPs are a large family of proteins, many with chaperone roles, which often demonstrate an increased rate in synthesis in response to cellular stress (Whitely et al., 1999; reviewed in Benjamin and McMillan, 1998; Feder and Hofmann, 1999; Kregel, 2002). Specific HSPs are up-regulated in response to a range of metabolic stressors, including: exposure to exogenous material in the digestive and urinary tracts (Tanguay et al., 1993; Barton et al., 2003); oxidative stress within the mitochondria (Salo et al., 1991; Polla et al., 1996; Calabrese et al., 2003); starvation and caloric restriction (Ehrenfried et al., 1996); hypoxia (Mestril et al., 1994; Plumier et al., 1995; Li et al., 2007), including neonatal hypoxia ischaemia (Dwyer et al., 1989; Ferriero et al., 1990). In addition, a

number of HSPs, particularly HSP90, have been shown to interact with hypoxia-inducible factor 1 α (HIF1α) (Katschinski et al., 2002; Zhou et al., 2004; reviewed in Chi and Karliner et al., 2004).

The two HSP family proteins selected for further investigation here were HSP60 and HSP90. HSP60 is known to have a role in neurodegeneration in the brain stem (Chan et al., 2007; Lehnardt et al., 2008), where it is expressed within the mitochondria (Izaki et al., 2001; Veereshwarayya et al., 2006) and is upregulated in response to preterm brain injury (Lai et al., 2006). HSP90 is known to be expressed in the brain (Lai et al., 1984; Garnier et al., 2001; reviewed in Picard, 2002; Neckers, 2007), where it reduces permanent denaturation of proteins (Loones et al., 2000) and has a role in reorganisation of the cystoskeletal architecture (Loones et al., 2000; Benites et al., 2014) and in protein folding (Picard, 2002).

These two markers underwent quantitative analysis across development and qualitative co-localisation with neuroserpin immunoreactivity. Results indicated that neuroserpin and HSP immunoreactivity patterns, although partially overlapping, did not display a clear relationship. Preliminary qualitative analysis of P8 sections stained for neuroserpin and HSP90 did detect co-immunoreactive cells in subplate. However, when the HSP developmental expression profile was studied in more detail, strongest immunoreactivity was detected early in development before neuroserpin immunoreactivity reached its peak. HSP90 immunoreactivity in NeuN-co-immunoreactive subplate neurons was highest at E18 (4.2 ± 0.9), remaining stable at P3 (2.1 ± 1.2) and P8 (3.1 ± 1.1), before vanishing at P21 (0 ± 0). HSP60 showed an even greater fluctuation, with immunoreactivity dropping from E18 (2.4 ± 0.9) and P3 (1.2 ± 1.0) to undetectable levels at P8 (0 ± 0) and P21 (0 ± 0). Results are shown in

Figure 3.11 and Table 3.9.

The pattern of HSP60 immunoreactivity observed was not in complete agreement with previously published mRNA expression patterns from *in situ* hybridisation experiments (Calabrese et al., 2002). These differences could be accounted for by non-specific primary antibody binding. It is possible that HSP60 immunoreactivity was under-reported due to its short half-life of only 3.2 (Chun et al., 2010), compared to the longer 42 hour half-life of HSP90 (Wu et al., 2012), as some HSP60 protein may have degraded during perfusion or fixation. Non-neuronal labelling for both HSP60 and HSP90 occurred in vascular endothelial cells (Pfister et al., 2005; Presley et al., 2010), and HSP60 has been described in pericyte cells (Mohammad et al., 2011), which could also have skewed estimates of neuronal expression. As characterising HSP expression was not the primary aim of this investigation, these methodological concerns have not been addressed here.

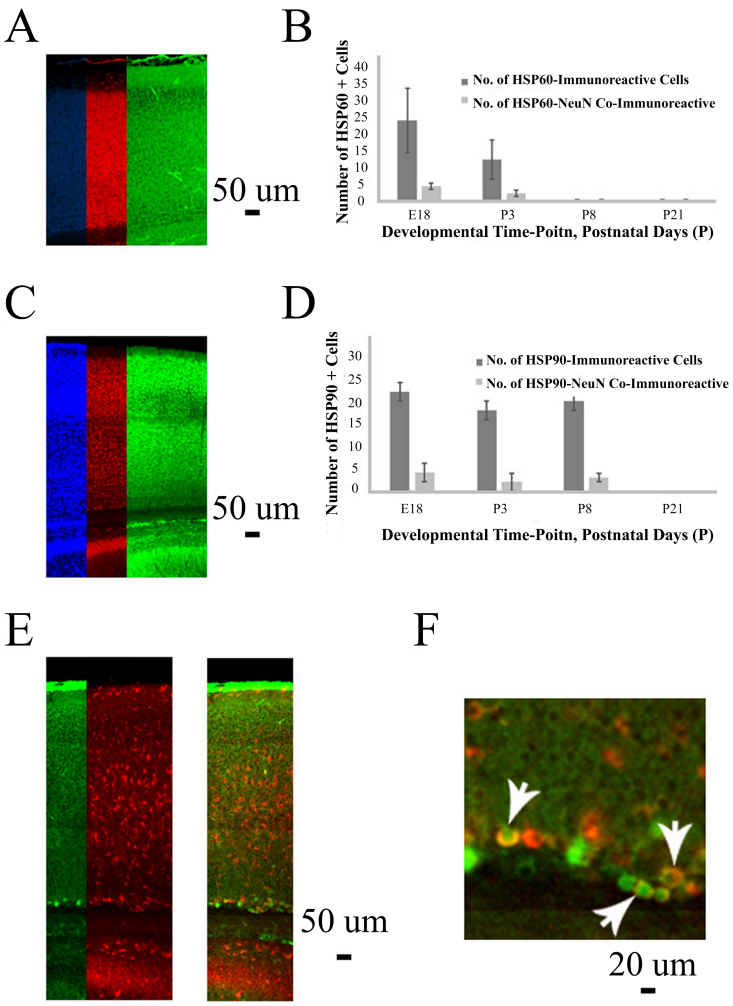


Figure 3.11 – Quantification of Metabolic Stress Markers Heat Shock Proteins (HSPs) HSP60 and HSP90 in Developing Mouse Cerebral Cortex and Qualitative Co-Localisation of HSP90 with Neuroserpin Protein by Fluorescent Immunohistochemistry. (A) Representative confocal image of cortical stacks stained for DAPI in blue, NeuN in red, and HSP60 in green. Scale bars indicate 50µm width area. (B) Quantitative analysis of the number and proportion of HSP60- and NeuN-immunoreactive cells in subplate across developmental time-points (mean ± SD). (C) Representative confocal image of cortical stacks stained for DAPI in blue, NeuN in red, and HSP90 in green. Scale bars indicate 50µm width area. (B) Quantitative analysis of the number and proportion of HSP90-immunoreactive and NeuN-immunoreactive cells in subplate across developmental time-points (mean ± SD). (E) Representative confocal image of cortical stacks stained for DAPI in blue, neuroserpin in red, and HSP90 in green. Scale bars indicate 50µm width area. (F) Enlarged area of representative confocal image of cortical stacks stained for DAPI in blue, NeuN in red, and HSP60 in green taken using the 20 x magnification objective. Scale bars indicate 20µm width area. Confocal image and quantification analysis carried out in collaboration with visiting student Christiana Trandafir, unpublished.

Strain	Genotype	Age	N	Raw Number of HSP60-Immunoreactive Cells Counted	Raw Number of HSP90-Immunoreactice Cells Counted
NIHS	WT	E18	6	443	404
NIHS	WT	P3	6	216	325
NIHS	WT	P8	4	0	249
NIHS	WT	P21	3	0	0

				Qualitative Assessment of HSP60-Immunoreactivity	Qualitative Assessment of HSP90-Immunpreactivity	Qualitative Assessment of Neuroserpin-Immunoreactivity
C57BL/6J	WT	P9	4	-	++	+++
C57BL/6J	Het	P9	2	-	++	+++
C57BL/6J	KO	P9	2	-	++	-
C57BL/6J	WT	Adult	3	-	-	+
C57BL/6J	KO	Adult	3	-	-	-

Table 3.9 - Summary of Quantitative and Qualitative Immunohistochemistry Experiments Investigating Expression Pattern of Heat Shock Proteins (HSPs) HSP60 and HSP90 in Developing Mouse Cerebral Cortex. Immunoreactivity was quantified over several developmental time-points for HSP60 and HSP90. Co-localisation was also determined using immunohistochemistry for HSPs and neuroserpin immunoreactivity in the developing and adult *Serpini1* knock-out mouse. Neuroserpin immunoreactivity partially overlapped with HSP90 immunoreactivity, but was not complete of exclusive for either marker. Neuroserpin and HSP60 immunoreactivity appeared to follow distinct non-overlapping patterns.
WT = C57BL/6J homozygote wild-type, Het = C57BL/6J x B6.129-Serpini1tm1Dpw/J heterozygote, KO = B6.129-Serpini1tm1Dpw/J homozygote Serpini1 knock-out, - = no immunoreactivity detected, + = immunoreactivity detected but faint and localised to a small number of cells per cortical stack, ++ = immunoreactivity detected in a large number of cells within the cortical stack, +++ = substantial immunoreactivity detected in a high qualitative proportion of cells.

The results presented here do not suggest a strong relationship between developmental patterns of neuroserpin immunoreactivity and either heat shock protein HSP60 or HSP90. Expression of metabolic stress markers is not mutually exclusive with expression of neuroserpin, yet there is little overall relation between the expression profiles of these proteins over time. More work is needed to refine the HSP expression profile to specific cell types of more time-points, yet this would have little clear connection to neuroserpin based on this evidence.

3.3.3 Quantification of Cortical Neuroserpin Protein in a Model of Neonatal Neuronal Plasticity, Monocular Enucleation at P1

One significant barrier to potential therapeutic adaptation of neuroserpin for neonatal hypoxia ischaemia is the proposed role of neuroserpin in neuronal plasticity (reviewed in Millar et al., 2017). Tissue plasminogen activator (tPA), the primary molecular target of neuroserpin enzymatic cleavage (Osterwalder et al., 1998; Barker-Carlson et al., 2002), enhanced NMDA-receptor mediated classical neuronal plasticity (Nicole et al., 2001; Matys and Strickland, 2003; reviewed in Bronstein and Tsirka, 2017). The first direct evidence that neuroserpin may have a role in plasticity involved delivering exogenous neuroserpin to endocrine cell lines, which subsequently extended neurite-like processes (Hill et al., 2001; Jacovina et al., 2001; Borges et al., 2010). Only one direct investigation has been carried out into the role of neuroserpin in plasticity *in vivo*, in which monocular enucleation in P11 mouse led to a semi-quantitative decrease *Serpini1* mRNA expression in contralateral primary visual cortex (V1) demonstrated by *in situ* hybridisation (Wannier-Morino et al., 2003). No quantitative information exists to confirm a change in neuroserpin enzyme function during neuronal plasticity in living animals.

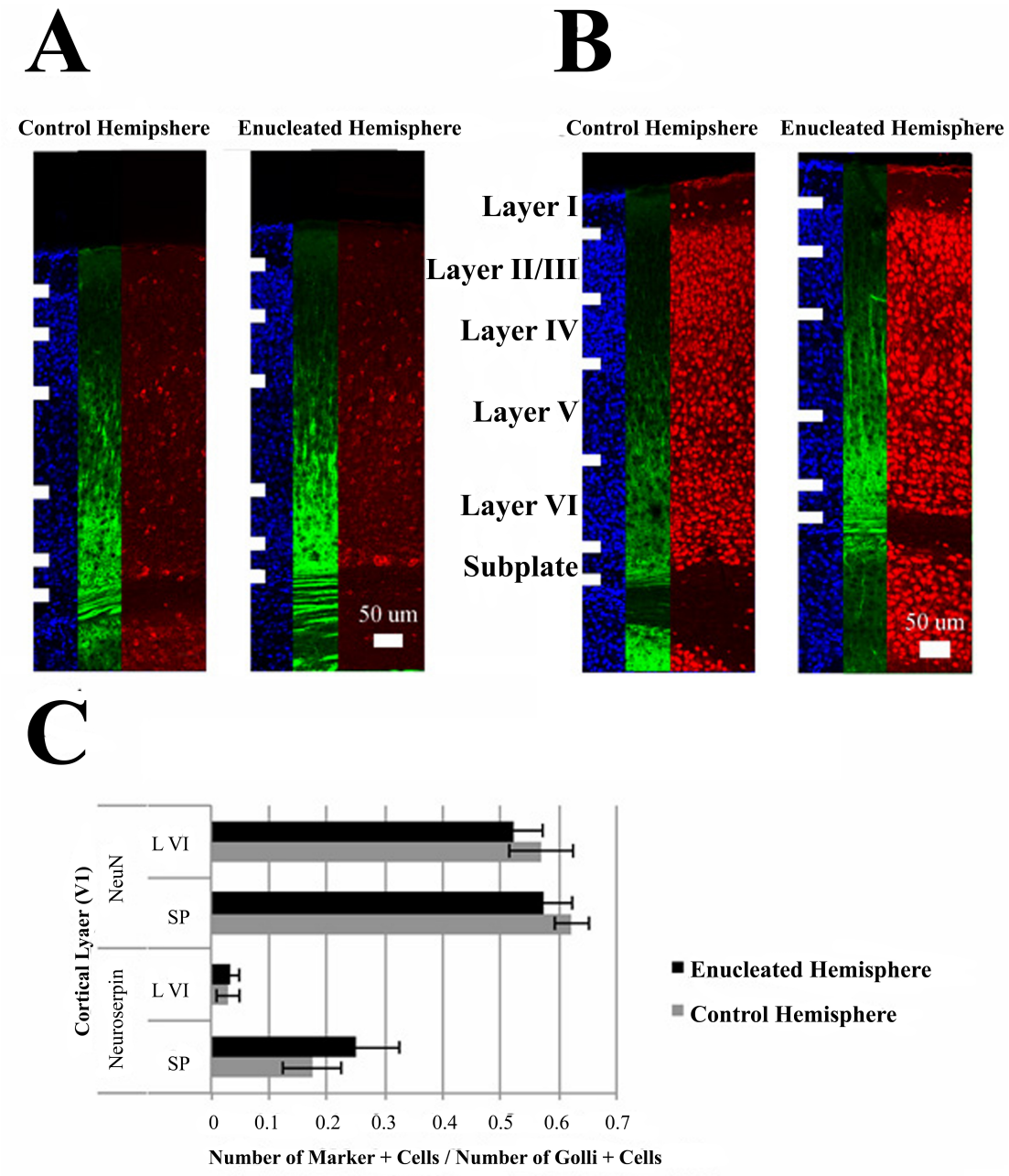


Figure 3.12 – Quantitative Analysis of Neuroserpin Immunoreactivity in P6 Golli-τ-GFP Mouse Primary Visual Cortex (V1) following Unilateral Monocular Enucleation at P1. There is a trend towards increased proportion of Golli-τ-eGFP subplate cells immunoreactive for neuroserpin, but this was not statistically significant at N = 3. (A) Representative confocal image of cortical stacks stained for neuroserpin in red, and DAPI in blue. Golli-τ-eGFP cells are shown in green. Scale bars indicate 50µm width areas. (B) Representative cortical stacks stained for NeuN in red, and DAPI in blue. Golli-τ-eGFP cells are shown in green. (C) Quantitative analysis of the proportion of neuroserpin-immunoreactive and NeuN-immunoreactive cells expressing Golli-τ-eGFP in Layer VI and subplate (SP) (mean ± SD). Two-way ANOVA demonstrated a statistically significant difference between groups based on layer but not hemisphere (condition) for proportion of both neuroserpin- and NeuN-immunoreactive neurons relative to the number of Golli-τ-eGFP immunoreactive neurons. Unpaired T-tests were not conducted to compare neuroserpin immunoreactivity between hemispheres. * denotes a P-value > 0.01, ** denotes a P-value > 0.005, *** denotes a P-value > 0.001

An adaptation of Wannier-Morino et al.'s 2003 experiment was conducted using tissue collected from P6 Golli-τ-eGFP mice following monocular enucleation at P1. Brains were generated by Dr. Eleanor Grant according to methods described in Grant et al., 2016. A trend was observed towards an increased number of neuroserpin-immunoreactive cells in subplate within V1 of the cortical hemisphere contralateral to the enucleated eye: 25% (± 6%) in the input-deprived contralateral hemisphere compared to 17% (± 6%) in the negative control ipsilateral hemisphere. There was no difference in total neuronal number of subplate neurons between hemispheres as assessed by NeuN-immunoreactivity (57% ± 10% in the input-deprived hemisphere, 62% ± 6% in the control hemisphere). However, at N = 3 animals, this trend was not statistically significant and no change in the distribution of neuroserpin-immuno-reactive neurons was observed. Results are shown in Figure 3.12 and Table 3.10.

Strain (Condition)	**Age**	**N**	**Raw Number Neuroserpin-Immunoreactive Cells Counted**	**Proportion Neuroserpin-Golli-τ-Co-Immunoreactive Cells (± SD)**
Golli-τ-eGFP (Deprived Hemisphere)	P6	3	LVI: 60 SP: 274	LVI: 0.03 (± 0.03) SP: 0.25 (± 0.15)
Golli-τ-eGFP (Control Hemisphere)	P6	3	LVI: 42 SP: 154	LVI: 0.02 (± 0.04) SP: 0.17 (± 0.10)
			Raw Number NeuN-Immunoreactive Cells Counted	**Proportion NeuN-Golli-τ-Co-Immunoreactive Cells (± SD)**
Golli-τ-eGFP (Deprived Hemisphere)	P6	3	LVI: 1530 SP: 573	LVI: 0.58 (± 0.10) SP: 0.51 (± 0.16)
Golli-τ-eGFP (Control Hemisphere)	P6	3	LVI: 1737 SP: 683	LVI: 0.61 (± 0.11) SP: 0.57 (± 0.10)
			Raw Number Golli-τ-Positive Cells Counted	
Golli-τ-eGFP (Deprived Hemisphere)	P6	3	LVI: 1978 SP: 1144	
Golli-τ-eGFP (Control Hemisphere)	P6	3	LVI: 2037 SP: 933	

Table 3.10 – Raw numbers of neuroserpin- and NeuN- immunoreactive cells counted relative to the raw number of Golli-τ-eGFP-positive cells counted in primary visual cortex (V1) of P6 mouse following unilateral monocular enucleation at P1. Columns 5 shows the proportion of neuroserpin-immunoreactive cells relative to the number of Golli-τ-eGFP-expressing cells. Although there was a trend towards increased numbers of neuroserpin-immunoreactive cells in the enucleated hemisphere, this was not significant at N = 3. Two-way ANOVA demonstrated a statistically significant difference between groups based on layer but not hemisphere (condition) for proportion of both neuroserpin- and NeuN-immunoreactive neurons relative to the number of Golli-τ-eGFP immunoreactive neurons. Unpaired T-tests were not conducted to compare neuroserpin immunoreactivity between hemispheres. * denotes a P-value > 0.01, ** denotes a P-value > 0.005, *** denotes a P-value > 0.001

The relatively low proportions of Golli-τ-eGFP-expressing neurons co-immunoreactive for NeuN may be explained by the reduced proportion of neurons expressing NeuN in the developing mouse brain at P6 (Sarnat et al., 1998). Alternatively, the discrepancy may be due to the relatively greater brightness of the eGFP fluorophore in comparison to the Alx568 used to label NeuN, making assignment of eGFP neurons to the correct Z-plane difficult.

It is apparent that the methods used here vary from those reported by Wannier-Morino et al., 2003. Animals analysed here underwent enucleation at P1 and brains were collected at P6, whereas those in the previous study underwent enucleation at P11 and brains were collected at P17. Additionally, Wannier-Morino et al. documented *Serpini1* mRNA levels, whereas this result quantified neuroserpin protein expression. The role of neuroserpin in plasticity must be investigated in much greater detail before therapeutics aimed at neonates can be developed. Extensive experiments comprising multiple *in vivo* models of developmental synaptic plasticity will be needed to detect any essential stabilising role that neuroserpin may play in normal developmental plasticity.

3.3.4 Neuroserpin Protein Expression in Preterm and Neonatal Human Brain Tissue

The expression pattern of *Serpini1* mRNA and protein has been systematically described in developing mouse (Krueger et al., 1997; reviewed in Millar et al., 2017), yet far less is currently known concerning the human *Serpini1* orthologue gene. A neuroserpin homologue protein with 80% amino acid sequence similarity to chicken neuroserpin has been identified, and shown by Northern blot to be present in adult

human brain tissue (Schrimpf et al., 1997). Additionally, inclusion bodies formed from misfolded neuroserpin protein have been found in the brains of human patients with a rare familial early-onset dementia with or without epilepsy (Davis et al., 1999; 2002; Davies et al., 2009; Davis and Collins, 2011; Takao et al., 2000; Miranda et al., 2008). However, only one publication to date has assessed neuroserpin protein distribution in the healthy human brain. Immunohistochemistry and *in situ* hybridisation in post-mortem tissue from adult individuals aged 44-78 years demonstrated neuroserpin-immunoreactive neurons in the hippocampus and *Serpini1* mRNA expression throughout the brain (Teesalu et al., 2004).

Due to the dearth of neuroserpin profiling published in human tissue, it was undertaken to stain preterm and neonatal human brain tissue available from The Human Developmental Biology Resource, Institute of Child Health, London, (Lindsay et al., 2016) to assess the translational relevance of the developmental expression pattern characterised in mouse. Immunohistochemistry revealed neuroserpin protein immunoreactivity in neurons within the human cortical plate at 15 and 40 post-conceptional weeks, as shown in Figure 3.13. Paraffin-embedded sections underwent antigen retrieval followed by immunohistochemistry as documented previously, for Panel A (Brøchner and Møllgård, 2016; Møllgård et al., 2017) and for Panel B (Adorján et al., 2019). This pattern of sparse deep-layer neuroserpin staining and neuronal cytoplasmic morphology complemented the pattern observed in P8 mouse tissue.

Primary and secondary antibody concentrations were first optimised in paraffin-embedded mouse brain tissue, negative controls included sections incubated with secondary antibody only. Negative controls for human foetal immunohistochemistry

depicted in Figure 3.13 Panel A (Lyngholm et al., 2008) and Panel B (Adorján et al., 2017) were carried out as described previously, respectively. For Panel A, sections were either incubated with secondary antibody only or incubated with matched isotype proteins instead of primary antibodies. For Panel B, each batch of sections stained included one section incubated with secondary antibody in the absence of primary antibody. At the time of writing, fresh-frozen foetal human brain tissue had been acquired for Western blot specificity analysis of antibodies.

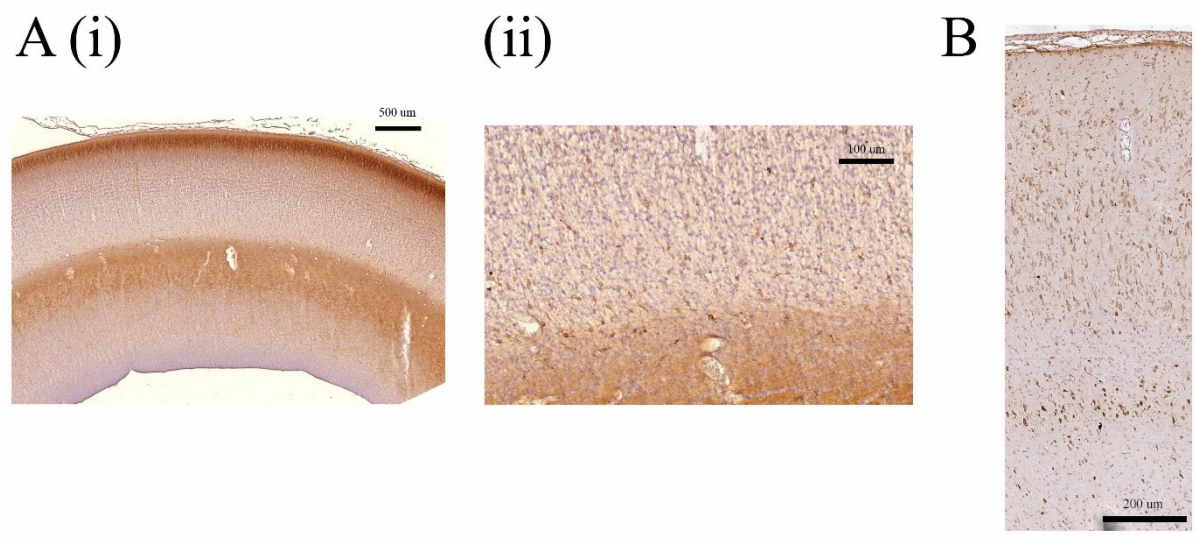


Figure 3.13 – Paraffin-Embedded Human Tissue Demonstrating Neuroserpin Protein Immunoreactivity in Deep Cortical Layers in Foetal Human. (A) Dorsolateral prefrontal cortex at 15 post-conceptual weeks stained with rabbit anti-neuroserpin primary antibody (Abcam, Cambridge, UK Ab33077) at 1:2,000 by Professor Kjeld Møllgård, University of Copenhagen, Denmark. (i) Light microscope image taken with the 5 x magnification objective. Scale bar indicates 500µm width area. (ii) Light microscope image taken with the 20 x magnification objective. Scale bar indicates 100µm width area. (B) Dorsal prefrontal cortex at 40 post-conceptional weeks from a minimally hypoxic individual stained with rabbit anti-neuroserpin primary antibody (Abcam, Cambridge, UK, Ab33077) at 1:2,000 from the Human Developmental Biology Resource Brain Bank, University of Newcastle, UK, and University College London, UK, (Lindsay et al., 2016) stained by Dr. István Adorján, University of Oxford, UK, and University of Budapest, Hungary. Light microscope image taking with the 20 x magnification objective. Scale bar indicates 200µm width area.

These results appeared to confirm that neuroserpin protein is expressed during development in the preterm and neonatal human brain, verifying the relevance of

results in mouse to human neuroserpin homologue expression. Antibodies will have to be verified for specificity in human tissue, and the number of human brains stained at each developmental time point will need to be expanded, before further conclusions can be drawn. It will also be important to complete quantitative analysis of neuroserpin expression in hypoxic ischaemic neonatal human brains relative to human controls which did not undergo neonatal hypoxia ischaemia.

3.4 Discussion

This chapter describes thorough characterisation of neuroserpin protein expression by fluorescent immunohistochemistry in murine cerebral cortex. An abundance of neurons in the subplate zone were documented as neuroserpin-immunoreactive during the developmental window around P8, equivalent to birth in humans.

3.4.1 Satisfaction of Chapter Aims

Experiments presented in this chapter were conducted in accordance with the aims stated in full in Section 3.1.1. This study achieved substantial success in quantifying the developmental pattern of neuroserpin expression in mouse. Other aims were partially satisfied, with further experiments needed.

The number and proportion of neuroserpin-immunoreactive expressing neurons in were quantified in primary somatosensory barrel cortex (S1) in two mouse strains. Low levels of co-immunoreactivity with glial markers and high co-immunoreactivity with pan-neuronal marker NeuN support the proposal that neuroserpin protein is

neuron-specific (Osterwalder et al., 1996; Hastings et al., 1997; Lee et al., 2015a). The results presented here complemented previously published non-quantitative *Serpini1* mRNA expression maps (Osterwalder et al., 1996; Krueger et al., 1997), and microarray data reporting relative enrichment in subplate compared to Layer VI of P8 mouse cortex (Hoerder-Suabedissen et al., 2009).

Immunohistochemistry identified neuroserpin protein to human neonatal brain development (Adorján et al., 2019), and potentially to neonatal hypoxia ischaemia. The presence of neuroserpin in deep layers of the human foetal cortex both at 15 postconceptional weeks (PCW) and at term shows that neuroserpin expression is endogenous in the developing human brain. A logical further experiment could use post-mortem tissue from human neonatal hypoxia ischaemia patients to assess the correlation between neuroserpin immunoreactivity and hypoxic damage (Woulfe et al., 2015; Lindsay et al., 2016).

Others aims of this chapter were satisfied with only partial success. Results presented here reveal that neuroserpin partially overlaps with three known subplate molecular markers (Heuer et al., 2003), complexin-3 (Xue et al., 2008), and nuclear receptor related 1 protein (Nurr1) (Arimatsu et al., 2003; Navarro et al., 2014). All three markers demonstrated enriched mRNA and protein expression throughout development in murine subplate (Hoerder-Suabedissen et al., 2009; 2013; Wang et al., 2011; Oeschger et al., 2012), yet the functional role of any one of these subpopulations remains unknown. Conversely, BrdU birth-dating (reviewed in Taupin, 2007; Kuhn and Cooper-Kuhn, 2007) of neuroserpin-immunoreactive subplate neurons suggested a unique identity for the neuroserpin-expressing subplate population as relatively early-born among subplate neurons (Hoerder-Suabedissen

and Molnár, 2013; Pedraza et al., 2014), suggesting neuroserpin-expressing subplate neurons may form a cohert subpopulate of subplate neurons.

Fluorescent microscopy revealed that neuroserpin overlapped with that of three endoplasmic reticulum (ER) markers (Han et al., 2013; Kondo et al., 2011), KDEL, calreticulin, and CHOP. This suggested that neuroserpin may be manufactured within subplate neurons themselves. However, electron microscopy co-localisation studies with ER and intracellular vesicle markers will be required before any strong conclusions can be drawn concerning subplate-secreted proteins (Kondo et al., 2015). Partial co-localisation observed between subplate neuroserpin-immunoreactivity and metabolic stress markers heat shock protein (HSP) HSP60 and HSP90 (reviewed in Feder and Hofmann, 1999; Kregel, 2002) is even more difficult to interpret, as detailed studies of this class of proteins in developing cortex are lacking.

Firm conclusions should not be drawn from data here concerning the role of neuroserpin in cortical plasticity, as the unchanged neuroserpin expression reported may be particular to the highly specific models investigated here. A range of experiments *in vivo* and *in vitro* will be needed to parse the role of neuroserpin in these highly complex physiological processes.

3.4.2 Developmental Neuroserpin Protein Expression Peak in Subplate Coincides with the End of Natural Neuronal Death in Mouse

The proportion of neuroserpin-immunoreactive neurons in subplate was higher than in any cortical layer throughout development. From P3 to P6, approximately 20% of subplate neurons expressed neuroserpin, compared to 10% of neurons in Layer V, and

less than 5% of neurons in Layers II/III, IV, and VI. During the neurodevelopmental time-period equivalent to birth in humans, P7 to P12 in mouse (Finlay and Darlington, 1995; Clancy et al., 2000; 2001; 2007), the proportion of neuroserpin-immunoreactive neurons in subplate increased to approximately 45%. There was no substantial change in the number or proportion of neuroserpin-immunoreactive neurons in any other cortical layer across early postnatal development. After P12, a sharp decline in neuroserpin immunoreactivity in subplate occurred, with less than 10% of Layer VIb neurons expressing neuroserpin in adulthood.

Neuronal identity of neuroserpin-immunoreactive subplate cells was confirmed by co-immunoreactivity for NeuN. This neuron-enrichment, short of complete specificity, complements finding from mouse RNAseq studies (Tasic et al., 2016; Zhong et al., 2018). These publications documented 10-fold higher *Serpini1* expression in adult Layer VIb neurons compared to other cortical layers. In addition, similar levels of *Serpini1* mRNA expression were detected in both glutamatergic Layer VIb neurons and GABA-ergic cortical neurons (Tasic et al., 2016). A fascinating future experiment could investigate neuroserpin co-expression with not only GABA, but markers of inhibitory cortical neuron subpopulations (reviewed in Markram et al., 2004; Kelsom and Lu, 2013; Tremblay et al., 2016). One RNAseq study in adult human Layer VIb neurons produced subtly different results from this investigation, reporting co-expression of *Serpini1* mRNA with *CPLX3*, the gene encoding complexin-3, but not *CTGF* or *NR4A2*, the gene encoding Nurr1 (Adorján et al., 2019). This study also detected no significant overlap between *Serpini1* and a rang of GABA-ergic interneuron markers, suggesting *Serpini1* mRNA may be expressed in a qualitatively different pattern in adult, and potentially over development, in human.

The peak in subplate neuroserpin expression coincides with the end of natural programmed cell death in the subplate (Valverde et al., 1995; Price et al., 1997; Hoerder-Suabedissen and Molnár, 2013; reviewed in Hoerder-Suabedissen and Molnár, 2015). Neuroserpin is the first documented subplate marker to have this pattern of expression documented.

It is possible that neuroserpin may be a marker of surviving cells. Microarray studies of mRNA expression in subplate neurons have shown different gene expression profiles in surviving adult Layer VIb neurons and subplate neurons in the early postnatal mouse brain (Hoerder-Suabedissen et al., 2009; 2013). Several genes reported as enriched in adult Layer VIb are part of apoptotic molecular cascades, although many regulators of apoptosis were relatively unchanged throughout murine subplate development. Due to its function inhibiting tPA-induced cell death, neuroserpin may represent a vulnerability marker. Neuroserpin was identified as Layer VIb-enriched in a recent study comparing gene expression in Layer VI subpopulations which project to different thalamic nuclei (Chevée et al., 2018). *Serpini1* expression was ten-fold higher in Layer VIb than Layer VIa. In this study, *Serpini1* mRNA expression was associated with functional projections to multiple thalamic nuclei. It is possible that during plasticity, neuroserpin selectively preserves these neurons that form active connections with the thalamus.

It is also possible that neuroserpin serves a neuroprotective role in surviving subplate neurons, whereas those which lack neuroserpin undergo programmed cell death. Ample *in vitro* evidence suggests neuroserpin is neuroprotective (reviewed in Millar et al., 2017). Currently, very little is known about the molecular pathways driving programmed cell death in the developing subplate (Valverde et al., 1995; Price and

Lotto, 1996; Price et al., 1997; reviewed in Kanold and Luhmann, 2010; Hoerder-Suabedissen and Molnár, 2015). The presence of neuroserpin immunoreactivity in surviving subplate neurons suggests the tPA cascade as a possible candidate for regulating cell death. tPA is synthesised and secreted by neurons (Krystosek and Seeds, 1981a; Lochner et al., 2006), and has been shown to interact with cell death pathways (reviewed in Benarroch, 2007; Yepes et al., 2009). As several neurodevelopmental conditions, including schizophrenia and autism, have been associated with reduced apoptosis in subplate (Hoerder-Suabedissen et al., 2013; reviewed in Kostović et al., 2011; Hutsler and Casanova, 2016), finding the molecular mechanisms behind this healthy cell death could illuminate pathogenesis.

There are limitations to the results presented here. Immunohistochemistry cannot be used to quantify the concentration of neuroserpin protein, it only provides insight into the distribution and number of cells that are immunoreactive. Interpreting the localisation of a secreted protein is additionally difficult, as any diffuse protein present in the extracellular matrix will be indistinguishable from a high background stain from the antibody. Only dense pockets of intracellular neuroserpin expression were quantified here. Different methodology will be needed to examine the extracellular profile of neuroserpin expression and beyond the cerebral cortex, such as semi-quantitative Western blot (Taylor et al., 2013; Taylor and Posch, 2014) as will be discussed in Chapter 4.

Further experiments could probe the neuroprotective properties of neuroserpin in developing cortex. Culturing cortical slices from transgenic lines which fluorescently label subplate neurons, such as the Lpar1-eGFP mouse (Grant et al., 2012; Marques-Smith et al., 2016) or the Drd1a-Cre mouse (Lemberger et al., 2007; Hoerder-

Suabedissen et al., 2018), could be used to refine previous *in vitro* demonstrations of neuroserpin-mediated neuroprotective function to the subplate. Cultured subplate neurons could be identified by fluorescent tags, which could allow neuroserpin neuroprotection to be assessed in subplate and deep cortical neurons separately. The relative toxicity of exogenous tPA to each of these populations could also be assessed. It would also be interesting to investigate subplate cell death in the *Serpini1* knock-out mouse (Cinelli et al., 2001; Madani et al., 2003; Gelderblom et al., 2013). Retrovirus (reviewed in Nadarajah et al., 2002) or bromodeoxyuridine (BrdU) (reviewed in Taupin, 2007) injection into cortical plate at E10, the developmental time-point at which the majority of neuroserpin-expressing subplate neurons are generated, could be used to track the number of subplate neurons surviving to P8 in the *Serpini1* knock-out or wild-type controls. However, before investing in this, it is essential to establish developmental neuroserpin expression in the human brain. It is possible murine subplate cell death pathways, as with some subplate molecular markers (Wang et al., 2011), are not conserved across all species.

In addition to confirming that cortical neuroserpin protein expression closely matches non-quantitative *Serpini1* mRNA expression patterns (Osterwalder et al., 1996; Krueger et al., 1998), the work presented here defines the developmental trajectory of a subplate marker present in mouse and human which may prove to be conserved across species. The known enzymatic interactions for neuroserpin (reviewed in Millar et al., 2017) suggest a possible molecular mechanism involving programmed subplate cell death during development, which may or may not involve the tPA cascade.

3.4.3 Conclusions

This chapter reports a thorough characterisation of neuroserpin protein expression in mouse and human cerebral cortex. Fluorescent immunohistochemistry was used to localise neuroserpin protein within mouse and human cerebral cortical neurons. Results demonstrated that neuroserpin immunoreactivity was almost entirely neuron-specific; enriched in early-generated subplate neurons; partially co-localised with known subplate molecular marker in neurons; co-localised to a modest extent with molecular stress markers; and was present within and out the endoplasmic reticulum of these neurons.

Quantitative fluorescent immunohistochemistry was used to analyse the proportion of cortical neurons immunoreactive for neuroserpin throughout postnatal development in mouse. Confirming previous non-quantitative *Serpini1* mRNA studies, neuroserpin was found to be selectively enriched in Layer V and subplate (Layer VIb) of primary somatosensory barrel cortex. An analogous pattern for deep layer neuroserpin immunoreactivity was documented in deep cortical plate neurons in human foetal tissue. A peak in subplate neuroserpin was observed at P8 in mouse, equivalent to birth in humans, the time-point at which natural programmed subplate cell death is complete. It is possible that neuroserpin serves a neuroprotective role or acts as a marker of cells vulnerable to apoptosis.

4 Characterisation of Neuroserpin Protein Expression in Rodent Models of Neonatal Hypoxia Ischaemia

4.1 Introduction

Any novel molecule proposed to play a role in a neurodevelopmental disorder must be rigorously studied in normal physiology and representative models of the condition of interest. In this chapter, the detailed anatomical information concerning cortical neuroserpin expression presented in the previous chapter is applied to rodent models of neonatal hypoxia ischaemia (HI).

The motivating evidence for studying neuroserpin in the context of neonatal HI largely derives from evidence of neuroprotection proposed in the literature in rodent models of adult hypoxic ischaemic stroke. Using models of ischaemic stroke involving artery ligation, highly analogous to the Rice-Vannucci model of neonatal HI (reviewed in Millar et al., 2017), several examples of neuroserpin neuroprotection have been described. Injection of purified neuroserpin protein prior to ischaemic stroke in adult rats decreases in infarct volume and expression of apoptosis markers (Yepes et al., 2000; Wu et al., 2010). Conversely, *Serpini1* knock-out mice show larger lesion volumes following adult HI than wild-type control animals (Cinelli et al., 2001; Gelderblom et al., 2013), whereas transgenic mice over-expressing neuroserpin are protected (Cinelli et al., 2001). From a therapeutic perspective, neuroserpin administration in rats increases the window for effective tPA treatment for stroke (Zhang et al., 2002). Evidence of neuroserpin neuroprotection has accumulated in the

adult rodent brain, particularly in models of hypoxic ischaemic damage.

In addition, a correlation has been described linking high concentrations of neuroserpin in blood samples from adult human stroke patients with better functional outcome (Rodríguez-González et al., 2011b; 2011c). However, attempts to associate *Serpini1* polymorphisms with occurrence of stroke have failed to detect strong evidence for protective genetic variants (Cole et al., 2007; Tjärnlund-Wolf et al., 2011). A number of in vitro experiments using cultured neurons also demonstrate neuroserpin neuroprotection under a range of conditions (Lebeurrier et al., 2005a; 2005b), including oxygen glucose deprivation (Wu et al., 2010; Rodríguez-González et al., 2011a; Ma et al., 2012b).

The literature does not currently contain any direct evidence of a neuroprotective role, if any, for neuroserpin protein in neonatal hypoxia ischaemia (reviewed in Millar et al., 2017). However, there are hints that this molecular cascade may contribute to neonatal HI injury. One known enzymatic target of neuroserpin, tissue plasminogen activator (tPA) has been observed to have a deleterious effect on the outcome of neonatal HI in rodents (Adhami et al., 2008; Omouendze et al., 2013; Henry et al., 2013). In addition, evidence is beginning to emerge that intracerebral injection of tPA inhibitors neuroserpin (Kuan et al., 2010), α2-antiplasmin (α2AP) (Adhami et al., 2008), and plasminogen-activator-inhibitor 1 (PAI1) (Yang and Kuan, 2015) in rodent models of neonatal HI can reduce brain damage. Tempering these hints towards potential significance for neuroserpin, several microarray studies fail to detect any change in *Serpini1* mRNA expression after rodent neonatal HI (Carmel et al., 2004; Maj et al., 2004a; 2004b; Juul et al., 2009; Nagel et al., 2012; Rognlien et al., 2014).

To understand the role of the neuroserpin/tPA cascade in preterm and neonatal

hypoxia ischaemia, detailed observation of endogenous regulation of these molecules following hypoxia ischaemic brain injury is a crucial preliminary. This chapter determines if substantial change can be detected in expression profile or quantity for neuroserpin following neonatal HI in related rodent models.

4.1.1 Aims of Chapter 4

The neuroprotective role of neuroserpin in adult rodent models of ischaemic stroke is a relatively recent discovery (reviewed in Millar et al., 2017), which has not yet been assessed for relevance to the developing brain. Quantitative immunohistochemistry and semi-quantitative Western blot studies of neuroserpin protein in cerebral cortex assess the pattern and quantity of protein expression in an experimental neonatal hypoxia ischaemia model generated by an adapted Rice-Vannucci method (Rice et al., 1981; Ferriero et al., 1996; reviewed in Vannucci et al., 1999; Vannucci and Hagberg, 2004; Vannucci and Vannucci, 2005). These experiments provide an indication of neuroserpin protein expression sensitivity to hypoxia, the characteristic distribution pattern of neuroserpin in response to hypoxia, and whether an inhibitory protein in the neuroserpin/tPA pathway is strongly regulated in unmedicated neonatal HI injury.

1) The expression of neuroserpin in cortex following neonatal HI injury was assessed in a rat model of preterm HI adapted from the Rice-Vannucci model via quantification of the number and proportion of neuroserpin-immunoreactive neurons per cortical layer against pan-neuronal marker neuronal nuclei (NeuN).

2) A complementary, strictly neonatal, mouse model of neonatal HI based on the Rice-Vannucci method was developed. The model was validated by immunohistochemistry for glial markers glial fibrillary acidic protein (GFAP), ionised calcium binding adaptor molecule 1 (Iba1), and cluster of differentiation 68 (CD68) associated with brain damage in the ischaemic hemisphere, the hypoxia-only hemisphere, and sham-operated controls.

3) Neonatal hypoxia ischaemia model parameters were optimised to investigate acute changes in neuroserpin expression by fluorescent immunohistochemistry over different durations of hypoxia and brain collection time-points, to determine the scope of neuroserpin involvement over different severities of neonatal HI injury.

4) Once the model was optimised, the number and proportion of neuroserpin-immunoreactive neurons was quantified per cortical layer against NeuN.

5) Expression of total neuroserpin protein, both intracellular and secreted, was assessed by semi-quantitative Western blot in cerebral cortex of P10 C57BL/6J mice which underwent the adapted Rice-Vannucci model of hypoxia ischaemia at P8.

(i) The continued cortical expression of neuroserpin protein following neonatal HI in mouse was confirmed.

(ii) Total neuroserpin protein expression in the hypoxic ischaemic hemisphere was compared with that of the hypoxia-only control hemisphere using semi-quantitative methods.

4.2 Methods

Animal husbandry and tissue collection are described in Chapter 2, Sections 2.1 and 2.3 respectively.

4.2.1 Neonatal Hypoxia Ischaemia in Mouse

In order to model the brain injury seen in human neonatal hypoxia ischaemia patients, a mouse model was adapted from the Rice-Vannucci method (Rice et al., 1981; reviewed in Vannucci et al., 1999; Volpe, 2012; Millar et al., 2017). The model involved left common carotid artery (LCC) ligation under anaesthesia in P8 mouse, followed by approximately 2 hours recovery with the dam, then exposure to hypoxia at 10% O_2. Figure 4.1 shows the sequence of procedures involved. Rice-Vannucci hypoxia ischaemia was carried out in C57BL/6J wild-type control mice. Details of the number and genotype of animals used are given in Table 4.1, specifics of mouse lines are described in Chapter 2, Section 2.1.

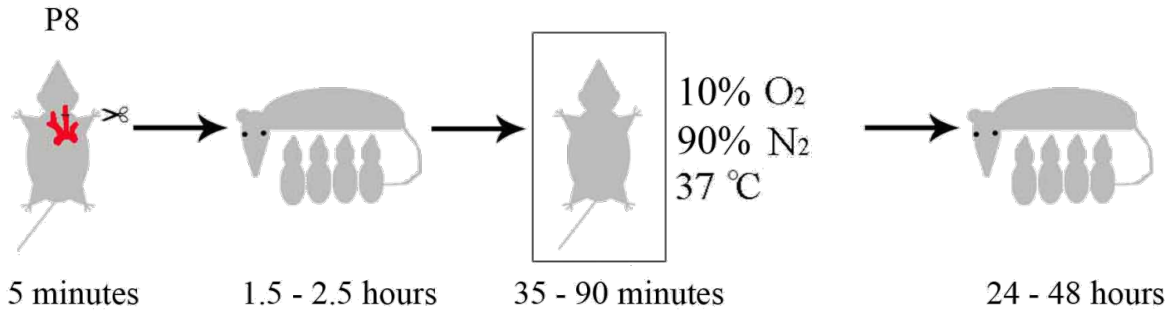


Figure 4.1 – Schematic Diagram of the Adapted Rice-Vannucci Hypoxia Ischaemia Mouse Model of Neonatal Hypoxia Ischaemia in C57BL/6J Mice. The left common carotid artery (LCC) was ligated under isofluorane anaesthesia in P8 mouse pups. Pups were returned to the dam for between 1.5 and 2.5 hours to recover from surgery. Pups were then placed into a sealed chamber and exposed to hypoxic conditions (10% O_2), exposure durations varied between experiments. Brains were collected 24 or 48 hours later.

Surgery was conducted on litters containing between 3 and 12 pups aged P8. Approximately half of the litter were removed from the dam and placed in a heated box set to 36°C. A single pup was removed and weighed with an electronic scale. Weights were recorded, pups weighing less than 3.5 g did not undergo surgery. Individual pups were placed in an anaesthesia induction box pre-filled with 4.0% isofluorane. The pup was observed in the induction box, when the righting reflex was lost, it was transferred to a heated mat and 3.0% isofluorane was delivered via a nosepiece. Forepaws were taped in place to expose the neck. Once full anaesthesia was confirmed using the tail-pinch and toe-pinch responses, surgery time did not exceed 5 minutes.

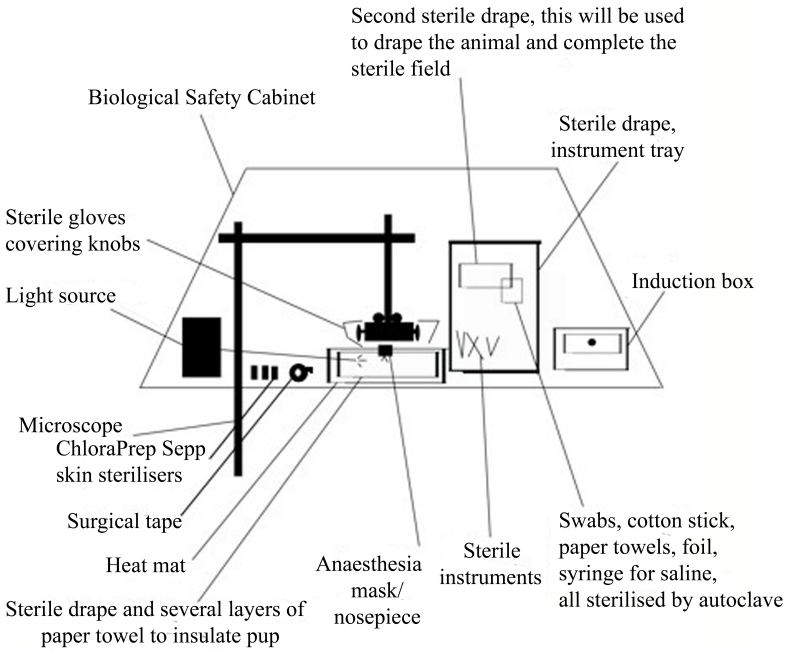


Figure 4.2 – Schematic Diagram of Surgical Set-Up for Rice-Vannucci Left Common Carotid Artery (LCC) Ligation and Sham Surgery. Anaesthesia was delivered as isofluorane gas via a custom nosepiece. Waste anaesthetic gas was collected by an active scavenging unit. Surgery was conducted on a heated mat padded with paper towels to maintain body temperature. Skin incision and LLC ligation were carried out with aid of a surgical microscope using the 9 x magnification objective. All surgical tools, drapes, and additional equipment such as foil and saline solution were sterilised prior to surgery using a steam autoclave. Surgical gloves, sutures, and skin disinfectant applicators were purchased in pre-sterilised packaging. Surgery was carried out inside a biological safety cabinet to maintain sterility.

All surgical tools, drapes, and additional equipment such as foil and saline solution were sterilised prior to surgery using a steam autoclave. Surgical gloves, sutures, and skin disinfectant applicators were purchased in pre-sterilised packaging. Figure 4.2 shows a schematic of the surgery area.

A small incision was made in the skin of the neck, slightly above the sternum, to the left of the midline. Microscopically blunted curved and straight forceps (Dumont Medical Forceps with Micro-Blunted Tip Straight Dumont No. 5, #11253-20, Fine Science Tools, Heidelberg, Germany; Dumont Medical Forceps with Micro-Blunted Tip Angled 90° Dumont No. 5, #11253-29, Fine Science Tools, Heidelberg, Germany) were used to locate the left common carotid artery (LCC). Forceps were used to separate the LCC from the Vagus nerve and jugular vein if necessary. A schematic of P8 mouse neck anatomy is shown in Figure 4.3. The LLC was ligated using a 6.0 biodegradable suture (6-0 Coated Vicryl Undyed 1X27" RB-1 Suture, #J212H, Ethicon Endo-Surgery, Johnson and Johnson Medical Supplies Ltd., Livingston, UK).

The skin was sutured using single interrupted sutures of the same material. Sham-operated animals were anaesthetised for 5 minutes and underwent skin incision, separation of the Vagus nerve from the LCC, and skin suturing, in the absence of LCC ligation. Post-suturing, pups were exposed to 100% O_2 for around 1 minute, then returned to the heated box to recover at 36°C.

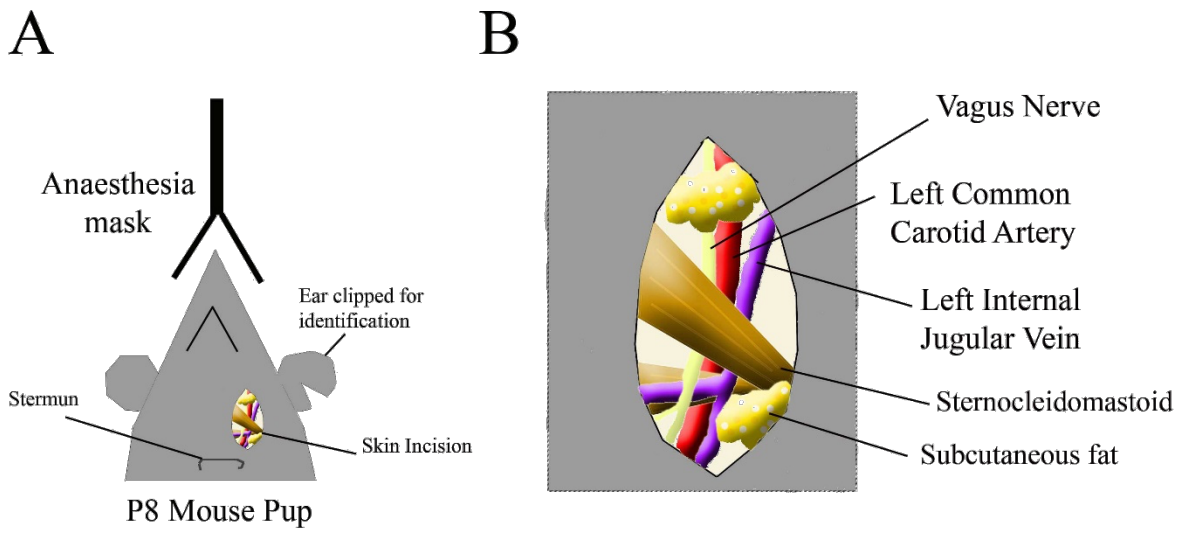


Figure 4.3 – Schematic Diagram of Mouse Neck Anatomy as encountered during Rice-Vannucci Common Carotid Artery Ligation Surgery. (A) Depiction of mouse in supine position undergoing left common carotid artery (LCC) ligation under isofluorane anaesthesia delivered via a mask. The skin incision is made above the sternum, which can be palpated through the skin, and to the left of the midline. (B) Magnification of mouse neck anatomy as encountered during surgery. The LLC is relatively deep, beneath subcutaneous fat and superficial veins (not shown). The neurovascular bundle including the LCC, the left internal jugular vein, and the Vagus nerve is located directly beneath the sternocleidomastoid neck muscle, approximately at the depth of the vocal cartilages. The LCC is the thickest structure within this bundle and can be identified by the presence of a pulse, and its vivid red colour, in contrast to the off-white Vagus nerve and dark red jugular vein.

Directly following surgery, animals were monitored in the heated box at 36°C until moving freely. Pups were returned to the dam for 1.5-2.5 hours to recover before undergoing hypoxia. An individually-ventilated cage was placed in a water-bath (28L General Purpose Water Bath, #TSGP28, Thermo Fisher, Hemel Hempstead, UK) set to 37.5°C. Air temperature inside the cage was monitored throughout using a secondary infra-red thermometer. After recovery with the dam, all surgery pups were placed into the individually-ventilated cage, which had been allowed to stabilise at 37.5°C for a minimum of 10 minutes. Pups were separated with a cardboard divider to avoid huddling, as huddling behaviour can create significant differences between the body temperatures of individual pups (Alberts, 1978; Pereira et al., 2006). The

individually-ventilated cage was pre-filled with custom gas consisting of 10% O_2 balanced by 90% N_2 (BOC, Linde Group, Guildford, UK). Constant 0.05 Pa 10% O_2 gas was supplied to the chamber to maintain hypoxia. Thermometer readings were observed throughout the experiment to ensure chamber temperature remained at 37.5℃ ± 0.5℃. Pups were visually monitored for normal respiratory rate and muscular convulsions which may have indicated seizure activity. Sham animals were removed from the dam and placed in a heated box set to 37.5℃ in room air. Once the specified duration of hypoxia required for that experiment was completed, all animals were returned to the dam.

Tissue was collected either 24 hours or 48 hours after hypoxia. Pups were injected with 0.1ml pentobarbital and transcardially perfused with 0.1M phosphate buffered saline (PBS) solution. Brains were dissected out and post-fixed for 48 hours in 4% paraformaldehyde (PFA) solution. All brains were then stored in PBS with 0.05% sodium azide (PBS-A). Composition of all solutions used here are detailed in Chapter 2, Section 2.6. Those used for immunohistochemistry were embedded in 4% agarose and cut coronally to 50µm using a vibrating microtome.

Duration of Hypoxia (minutes)	Genotype	Number of HI surgery animals	Number of sham animals	Total Number of Litters	Collection Post-HI (hours)
35	C57BL/6J	5	0	2	24
45	C57BL/6J	9	0	2	24
55	C57BL/6J	7	0	1	24
65	C57BL/6J	7	0	1	24
75	C57BL/6J	9	0	1	24
90	C57BL/6J	9	0	1	24
55	C57BL/6J	5	0	1	48
55	C57BL/6J	31	27	8	48

Table 4.1 – Number and Genotype of Brains Collected Across All Durations of Hypoxia Investigated via the Adapted Rice-Vannucci Mouse Model of Neonatal Hypoxia Ischaemia (HI). This table lists animals used to validate and optimise conditions for hypoxia, alongside those used to assess the distribution of neuroserpin protein throughout the cortex following neonatal hypoxia ischaemia by immunohistochemistry.

4.2.2 Immunohistochemistry

Fluorescent immunohistochemistry was used to stain for neuroserpin in addition to three glial molecular markers inflammatory damage markers: GFAP, Iba1, and CD68. The methods used for fluorescent immunohistochemistry are described in Chapter 3, Section 3.2.1. Details of all tissue used in immunohistochemistry experiments for this chapter are given in Table 4.2, and sources and concentrations of primary and secondary antibodies are detailed in Tables 4.3 and 4.4, respectively.

Experiment	Developmental Time Point (Postnatal Days)	Brains	Litters	Slices	Collection Method	Fixation (hours in 4% PFA)	Strain (Condition)
Neuroserpin Expression following Preterm Hypoxia Ischaemia in Rat							
	P8	5	6	3	PFA Perfused	24	Sprague-Dawley (Moderate HI)
	P8	5		3	PFA Perfused	24	Sprague-Dawley (Mild HI)
	P8	2		3	PFA Perfused	24	Sprague-Dawley (Sham Operated)
Neonatal Hypoxia Ischaemia by Adapted Rice-Vannucci Method in Mouse Brain Injury Validation							
	P10	5	2	3	PBS Perfused	48	C57BL/6J (HI, 55 mins hypoxia)
	P10	5		3	PBS Perfused	48	C57BL/6J (Sham Operated)
Optimising Neonatal Hypoxia Ischaemia by Adapted Rice-Vannucci Method in Mouse							
	P9	3	2	3	PBS Perfused	24	C57BL/6J (HI, 35 mins hypoxia)
	P9	9	2	3	PBS Perfused	24	C57BL/6J (HI, 45 mins hypoxia)
	P9	7	1	3	PBS Perfused	24	C57BL/6J (HI, 55 mins hypoxia)
	P10	5	1	3	PBS Perfused	48	C57BL/6J (HI, 55 mins hypoxia)
	P9	7	1	3	PBS Perfused	48	C57BL/6J (HI, 65 mins hypoxia)
	P9	9	1	3	PBS Perfused	48	C57BL/6J (HI, 75 mins hypoxia)
	P9	9	1	3	PBS Perfused	48	C57BL/6J (HI, 90 mins hypoxia)
Neuroserpin Expression following Neonatal Hypoxia Ischaemia in Mouse							
	P10	15	6	3	PBS Perfused	48	C57BL/6J (HI, 55 mins hypoxia)
	P10	15		3	PBS Perfused	48	C57BL/6J (Sham Operated)

Table 4.2 – Breakdown of the Number, Genotype, and Condition of Mouse Brains used across all Fluorescent Immunohistochemistry Experiments Described in This Chapter. Brains are categorised by developmental time-point (age of animals) and experimental aims. Results for each individual brain were generated from an average of cell counts across three pial to white matter cortical sections.

Experiment	Primary Antibody	Concentration	Supplier
Neuroserpin Expression following Preterm Hypoxia Ischaemia in Rat			
	Goat anti-neuroserpin	1:2,000	Abcam, Ab32901
	Mouse anti-NeuN	1:1,000	Chemicon, MAB377
Neonatal Hypoxia Ischaemia by Adapted Rice-Vannucci Method in Mouse Brain Injury Validation			
	Rabbit anti-GFAP	1:500	DAKO, Z0334
	Goat anti-Iba1	1:500	Abcam, Ab107159
	Mouse anti-CD68	1:50	Abcam, Ab955
Optimising Neonatal Hypoxia Ischaemia by Adapted Rice-Vannucci Method in Mouse			
	Goat anti-neuroserpin	1:2,000	Abcam, Ab32901
	Mouse anti-NeuN	1:1,000	Chemicon, MAB377
Neuroserpin Expression following Neonatal Hypoxia Ischaemia in Mouse			
	Goat anti-neuroserpin	1:1,000	Abcam, Ab32901
	Mouse anti-NeuN	1:1,000	Chemicon, MAB377

Table 4.3 – Primary Antibodies. These are listed by experimental aims, alongside relevant concentrations and sources. Relevant secondary antibodies listed in Table 4.4. Relevant combinations of primary and secondary antibodies are detailed in Section 4.3.

Experiment	Secondary Antibody	Concentration	Source
Neuroserpin Expression following Preterm Hypoxia Ischaemia in Rat			
	Donkey anti-goat Alx568	1:500	Invitrogen, A11057
	Donkey anti-mouse Alx488	1:500	Invitrogen, A21202
Neonatal Hypoxia Ischaemia by Adapted Rice-Vannucci Method in Mouse Brain Injury Validation			
	Donkey anti-rabbit Alx488	1:500	Invitrogen, A21206
	Donkey anti-goat Alx568	1:500	Invitrogen, A11057
	Donkey anti-mouse Alx488	1:500	Invitrogen, A21202
Optimising Neonatal Hypoxia Ischaemia by Adapted Rice-Vannucci Method in Mouse			
	Donkey anti-goat Alx568	1:500	Invitrogen, A11057
	Donkey anti-mouse Alx488	1:500	Invitrogen, A21202
Neuroserpin Expression following Neonatal Hypoxia Ischaemia in Mouse			
	Donkey anti-goat Alx568	1:500	Invitrogen, A11057
	Donkey anti-mouse Alx488	1:500	Invitrogen, A21202

Table 4.4 – Secondary Antibodies. These are listed by experimental aims, alongside relevant concentrations and sources. Relevant primary antibodies are listed in Table 4.3. Relevant combinations of primary and secondary antibodies are detailed in Section 4.3.

4.2.3 Semi-Quantitative Western Blot

Semi-quantitative Western blot analysis was undertaken (reviewed in Taylor et al., 2013; Taylor and Posch, 2014) (for non-quantitative Western blot, See Chapter 2, Section 2.7). Details of the number, genotype, and other relevant experimental conditions relating to tissue used in these experiments are given in Table 4.5. A schematic overview of the methodology is given in Figure 4.4.

Protein was extracted from fresh tissue dissected with autoclave-sterilised tools and

stored at -80°C (see Chapter 2, Section 2.3.3). Tissue was transferred to sterilised 2ml screw-cap tubes containing 0.5g of 1.4mm diameter ceramic beads (#03961-1-003, Stretton Scientific, Derbyshire, UK) for homogenisation. 300µl RIPA lysis buffer (#sc-364162, Santa Cruz Biotechnology, Heidelberg, Germany) was added to each tube. Tissue was mechanically homogenised in a Precellys® 24 tissue homogeniser (#432-3750, Peqlab Biotechnologie, Erlangen, Germany), at 5,000 rpm for 2 x 20 second intervals. The supernatant was then transferred to new sterilised 2ml Eppendorf tubes. 3µl of protein inhibitor cocktail (#sc-364162, Santa Cruz Biotechnology, Heidelberg, Germany) was added to each tube to prevent protein degradation. Total protein concentration was measured using a Micro BCA™ Protein Assay Kit (#23235, Thermo Fisher Scientific, Basingstoke, UK), then samples were stored at -80°C to prevent degradation.

Protein samples were then prepared for gel electrophoresis. A sample volume containing 3µg or 6µg total protein was added to a new sterile Eppendorf tube, followed by an equal volume of 2 x non-smelling Laemmli buffer (#38733, Sigma Aldrich, Gillingham, UK). Each tube was vortexed, and spun down in a microcentrifuge. Tubes were then placed on a heat-block set to 95°C for 5 minutes.

Samples were loaded onto a pre-cast 4–20% Mini-PROTEAN® TGX Stain-Free™ (#4568093, Bio-Rad Laboratories, Watford, UK) electrophoresis gel. A minimum of one lane per gel was reserved for a Spectra™ Multicolour Broad Spectrum Protein Ladder (#26634, Thermo Fisher, Basingstoke, UK). Electrophoresis was carried out in a BioRad Mini Trans-Blot Electrophoretic Transfer Cell blotting apparatus (#170-3930, Bio-Rad Laboratories, Watford, UK) filled with 1x Running Buffer. Gels were run at 60V for approximately 10 minutes at room temperature, or until samples were

clearly running into the stacking gel. At this point protein ladder separation was also visible. The gel was then run at 120V for approximately 1 hour at room temperature, or until the Laemmli buffer approached the bottom of the gel.

Proteins were transferred to a PVDF membrane (#1620174, Bio-Rad Laboratories, Watford, UK). Membranes, sponges (#1703933, Bio-Rad Laboratories, Watford, UK), and filter paper (#1703932, Bio-Rad Laboratories, Watford, UK) were soaked in 1x Transfer Buffer for 15 minutes prior to transfer. The gel contained trihalo-coupled tryptophan residues which were activated by exposure to UV light in a ChemiDoc™ XRS+ (#1708265, Bio-Rad Laboratories, Watford, UK) using the stain-free setting prior to transfer. Gel, membrane, sponges, and filter paper were assembled into a transfer stack and placed inside the blotting apparatus (#170-3930, Bio-Rad Laboratories, Watford, UK). The tank was filled with 1 x Transfer Buffer, and the custom ice-pack slotted in place. Transfer was run at 15V for a minimum of 12 hours overnight at approximately 4°C.

Membranes were then cut in half and blocked with 5% rabbit serum (#R9133, Sigma Aldrich, Gillingham, UK) in 10ml 1M tris buffered saline with Tween 20 (TBS-T) for 1 hours and 10 minutes at room temperature on a shaker plate. The membrane was then incubated with primary antibody in 5% rabbit serum in 10ml 1M TBS-T for 2 hours at room temperature on a shaker plate. Primary antibody was removed by three 10 minute washes in 10ml 1M TBS-T at room temperature on a shaker plate. Membranes were then incubated with secondary antibody in 5% rabbit serum in 10ml 1M TBS-T for 30 minutes at room temperature on a shaker plate. Secondary antibody was removed by three 5 minute washes in 20ml 1M TBS-T at room temperature on a shaker plate. Sources and concentrations of antibodies are given in Table 4.6.

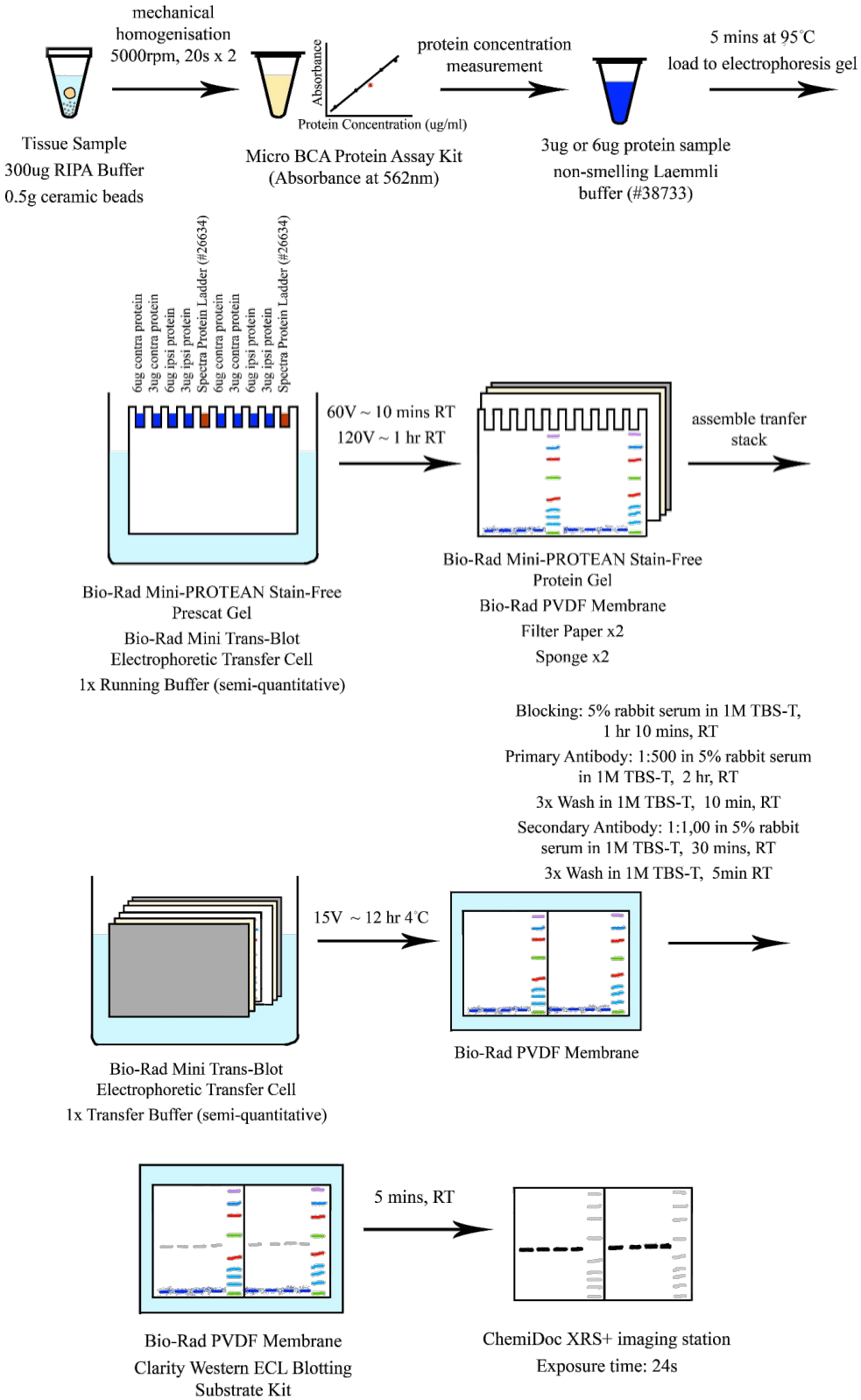


Figure 4.4 – Schematic Summary of Semi-Quantitative Western Blot Methodology. Important reagents, stages, and procedures and detailed in this figure. All unique features of the semi-quantitative Western blot protocol are marked on this figure. See Chapter 2, Section 2.6 for more information about frequently used solutions.

Protein-antibody binding on the membrane was detected using a ChemiDoc™ XRS+ with BioRad Image Lab™ software installed (#1708265, Bio-Rad Laboratories, Watford, UK). The first image taken used the stain-free setting to record the trihalo-coupled tryptophan amino acids present in the gel. To visualise antibody-specific binding, a Clarity™ Western ECL Blotting Substrate kit (#1705060, Bio-Rad Laboratories, Watford, UK) was applied to the membrane, and allowed to incubate for 5 minutes. Several images were then taken using the chemi-imaging setting. One image used the ChemiDoc™ automated exposure time setting, others were taken at 9, 12, 24 and 28 seconds with manual exposure. These images were saved as SCN files, for analysis using Bio-Rad Image Lab™ software. Some membrane were stripped and re-probed for β-actin staining, but will not be discussed here as the β-actin staining was not used in this thesis.

Experiment	Genotype	Developmental Time Point (Postnatal Days)	Brains	Litters	Duration of Hypoxia (mins)	Collection Post-HI (hours)	Tissue Collected
Semi-Quantitative Analysis of Neuroserpin Total Protein following Neonatal HI in Mouse							
	C57BL/6J	P10	11	3	55	48	cerebral cortex, subcortical brain regions, liver

Table 4.5 – Breakdown of the Number, Genotype, and Condition of Mouse Brains used across all Semi-Quantitative Western Blot Experiments. Brains are categorised by developmental time-point (age of animals) and experimental aims.

Experiment	Primary Antibody	Concentration	Supplier	Secondary Antibody
Semi-Quantitative Analysis of Neuroserpin Total Protein following Neonatal HI in Mouse				
	Goat anti-neuroserpin	1:250	Abcam, Ab32901	Rabbit Anti-Goat Horse Radish Peroxidase Conjugated 1:1,000 (Bethyl Laboratories, A50-100P)

Table 4.6 – Primary and Secondary Antibodies. These are listed by relevant experimental aims, along with concentrations, and sources. These details apply specifically to the semi-quantitative Western blot experiments in this chapter, primary and secondary antibodies used for immunohistochemistry are given in Tables 4.3 and 4.4, respectively.

4.2.4 Semi-Quantitative Western Blot Analysis

Western blot data was analysed using Bio-Rad Image Lab™ 6.0.1 software (SOFT-LIT-170-9690-ILSMAC6, Bio-Rad Laboratories, Watford, UK) ((http://www.bio-rad.com/en-uk/product/image-lab-software?ID=KRE6P5E8Z, last accessed: 02/05/2019).

Stain-free technology was used to provide total protein normalisation for each well. This was achieved in combination with the 4–20% Mini-PROTEAN® TGX Stain-Free™ Protein Gels (#4568093, Bio-Rad Laboratories, Watford, UK). These pre-cast gels contain a trihalo compound which conveys UV-induced fluorescence to tryptophan amino acid residues present within the protein sample (Gilda and Gomes, 2013; 2015; reviewed in Colella et al., 2012; http://www.bio-rad.com/en-uk/applications-technologies/stain-free-imaging-technology?ID=NZ0G1815, last accessed 10/08/2018). This method of protein normalisation was selected as it provides an average of signal intensity across several band lengths of protein detection, and removes the reliance on 'house-keeping genes' such as β-actin, β-tubulin, or glyceraldehyde 3-phosphate dehydrogenase (GAPDH), which do not reliably exhibit stable expression across disease conditions (Dittmer and Dittmer, 2006; Rocha-Martins et al., 2012; reviewed in Li and Shen, 2013).

Images of the trihalo-bound tryptophan stain-free signal were taken using ChemiDoc™ XRS+ automated stain-free settings. The membrane was then stained with a Clarity™ Western ECL Blotting Substrate kit (#1705060, Bio-Rad Laboratories, Watford, UK) and replaced in the ChemiDoc™ XRS+ to be imaged using chemi-imaging settings. Chemi-images with an exposure time of 24 seconds were used for analysis as bands were clearly visible on all membranes. Stain-free and

chemi- image files were saved as separate SCN files.

Image Lab™ software was used to generate semi-quantitative measures of Western blot staining. A multi-channel image was created from the stain-free and chemi- images corresponding to a single blot. Lanes were detected manually for the stain-free image. The number of lanes present in the blot was set to 5, and the boundaries of each lane were selected so that all protein content was assigned to the correct lane. Figure 4.5 depicts the lane and band detection process for a single representative blot.

Background staining was set for the stain-free image. The software automatically subtracted background uniformly across all lanes, which was manually adjusted as required. Identical background subtraction was applied to all lanes. The normalisation lane was selected as the protein sample from the contralateral control hemisphere. Normalisation was carried out separately for 3µg and 6µg protein samples from the same brain.

Bands were automatically detected in the chemi-image image using the low sensitivity threshold recommended for detection of prominent bands. Any visible bands not detected automatically were added manually. Band recognition was checked using the Band Profiler tool. This tool allowed quantitative measurements for the position and boundaries of the bands on the chemi-image to be reviewed. Band boundaries could be adjusted manually, but this was rarely necessary. Again, bands from lanes loaded with 3µg protein sample were analysed separately from bands with 6µg protein sample.

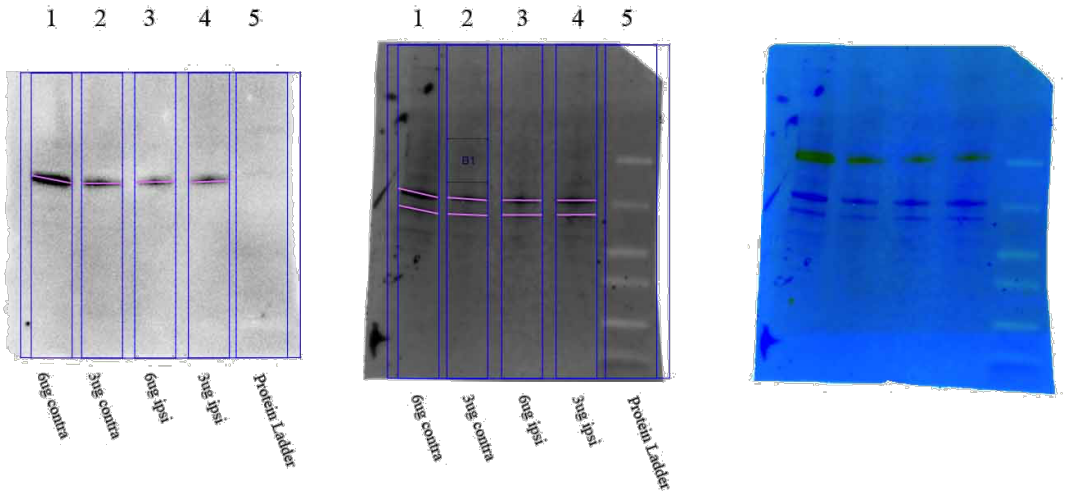


Figure 4.5 – Representative Images of Semi-Quantitative Western Blot SCN Files Analysed using Bio-Rad Image Lab™ Software (SOFT-LIT-170-9690-ILSMAC6, Bio-Rad Laboratories, Watford, UK). From left to right; ECL fluorescence image taken using the 'chemi-imaging' setting, stain-free total protein image taken using the 'stain-free' setting, composite image produced automatically by Image Lab™ software where ECL bands are shown in green and stain-free bands are shown in blue. Blue frames show the boundaries selected for each lane. B1 denotes the area selected as a representative of background staining on the stain-free image. Bands are marked by a pale purple line from edge to edge through the centre of the band. All bands were detected automatically by the Image Lab™ software, then any bands omitted were marked manually. A single band was present in each lane of the chemi-image, whereas two distinct bands were used as total protein controls in the strain-free image.

Once normalisation and band detection were complete, the software generated a measure of normalised band intensity for each lane in the chemi-image. This was recorded as the semi-quantitative measure of total protein concentration in the sample. Normalised intensity in the ipsilateral hypoxic-ischaemic hemisphere was compared to that in the contralateral hypoxia-only hemisphere using paired two-tailed t-tests in Microsoft Excel. A P-value of less than 0.05 was accepted as statistically significant.

4.3 Results

4.3.1 Quantification of Neuroserpin Protein Expression Following Neonatal Hypoxia Ischaemia in Rat by Cortical Layer

The extensive characterisation of neuroserpin expression profile in mouse brain outlined in Chapter 3 provided a wealth of information about the localisation of endogenous neuroserpin protein. These experiments demonstrated that neuroserpin in the developing neocortex peaks at P8, the rodent postnatal equivalent to birth in humans (Finlay and Darlington, 1995; Clancy et al., 2000; 2001; 2007; 2009; Finlay et al., 2001), this coincides with the natural apoptosis of subplate (Valverde et al., 1995; Price et al., 1997; Hoerder-Suabedissen and Molnár, 2013). In light of this increase at a developmental stage associated with programmed neuronal death around birth, it was undertaken to investigate neuroserpin expression through quantification of neuroserpin-immunoreactive cells in rodent models of hypoxia ischaemia (HI) in the developing brain.

Neuroserpin protein expression post-neonatal HI was initially investigated in a thoroughly validated rat model. Pups underwent unilateral ligation of the right common carotid artery (RCC) at P2, followed by exposure to 90-120 minutes of hypoxia at 6% O_2, brains were then collected at P8 (Okusa et al., 2014). All rat brain tissue was donated by Dr. Vanessa Ginet and Dr. Anita Truttmann of the University of Lausanne, Switzerland. The number and experimental condition of brains used are summarised in Table 4.7. Figure 4.6 shows a schematic of the model.

This model was employed in previous publications by Dr. Truttmann and colleagues which reported apoptosis, necrosis, and autophagy in the ipsilateral ischaemic

hemisphere following RCC ligation at the standard developmental time-point of P7 (Ginet et al., 2009a; 2009b; 2014a; 2014b; reviewed in Descloux et al., 2015), confirming neuronal cell death in this model. Tissue used here differed in that RCC ligation was carried out at P2, spanning intrauterine development. Okusa et al. 2014 extensively characterised this tissue for damage using quantitative cell density analysis of cresyl violet staining and cortical thickness measurements. Brains were divided into three injury categories based on these histological assessments: mild (no or mild atrophy, no decrease in cell density or cortical thickness); moderate (mild or moderate atrophy, decreased cell density, trend towards decreased cortical thickness) and severe (moderate or severe atrophy, presence of scar, statistically significant reduction in cortical thickness) (Okusa et al., 2014). This extensive characterisation allowed some of the natural variation in injury following neonatal HI (McQuillen et al., 2003; Failor et al., 2010) to be explicitly documented. Each severity classification was analysed separately for neuroserpin protein expression.

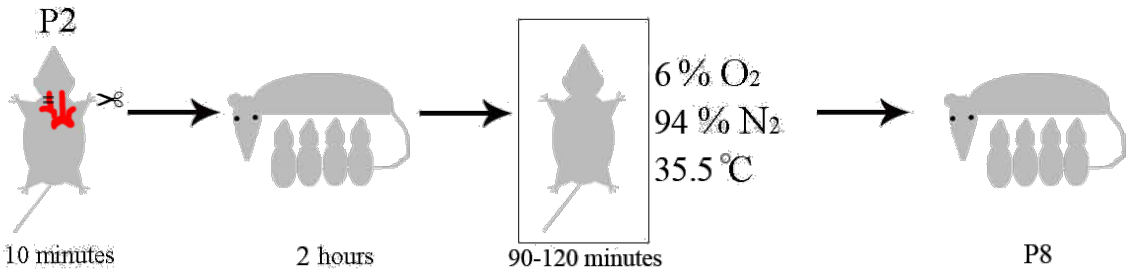


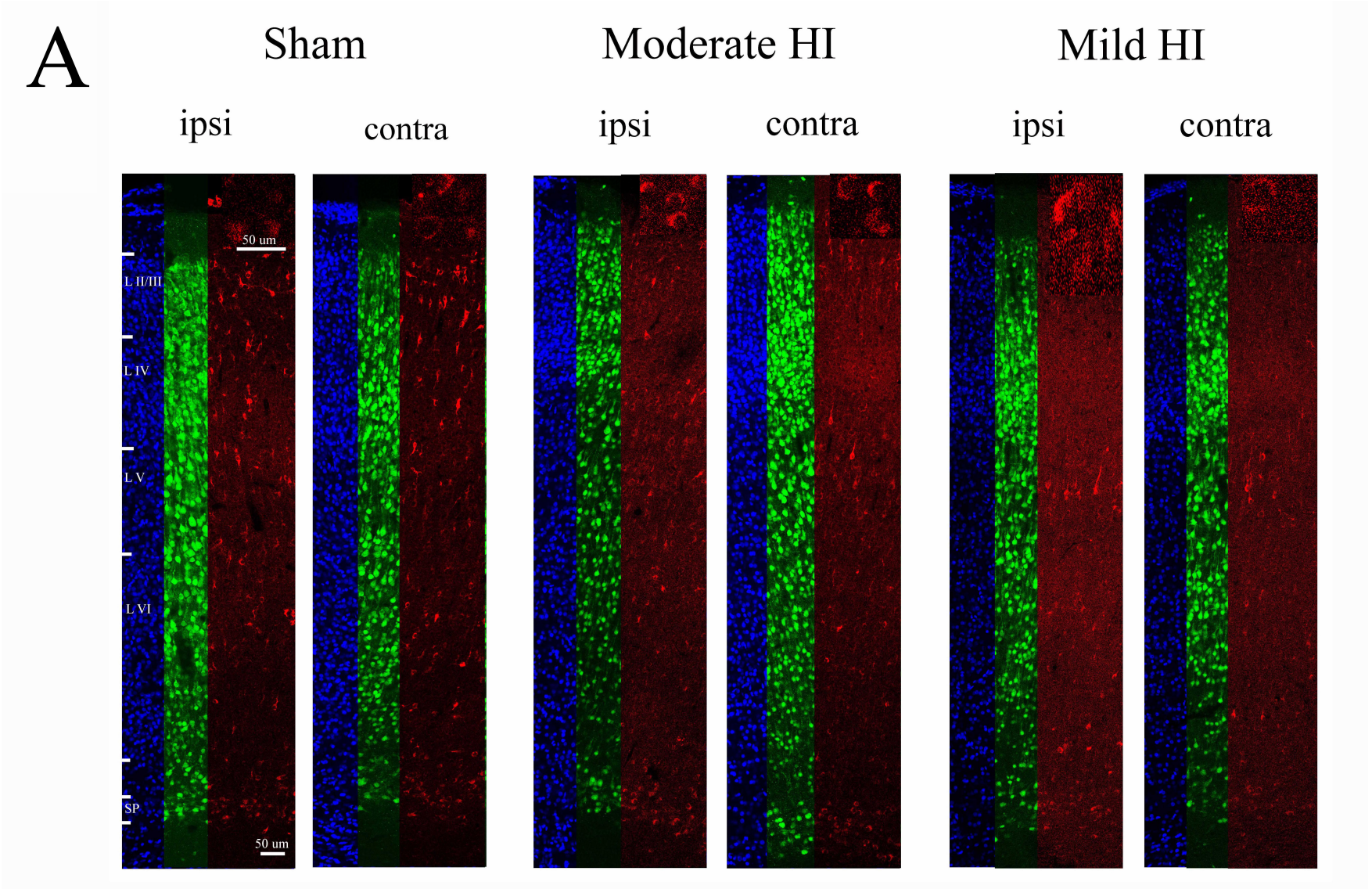
Figure 4.6 – Schematic Diagram of Sprague-Dawley Rat Pups undergoing a Modified Perinatal Variant of the Rice-Vannucci Model of Neonatal Hypoxia Ischaemia (Rice et al., 1981; Ginet et al., 2009a; Okusa et al., 2014). The right common carotid artery (RCC) was ligated under anaesthesia in P2 pups. Pups were returned to the dam for 2 hours to recover from surgery. Pups were then placed in a sealed chamber and exposed to hypoxic conditions (6% O_2) for 90-120 minutes. Pups were returned to the dam and brains collected at P8. Animal husbandry, surgery and tissue collection were carried out by Dr. Vanessa Ginet and Dr. Anita C. Truttmann at the University of Lausanne, Switzerland.

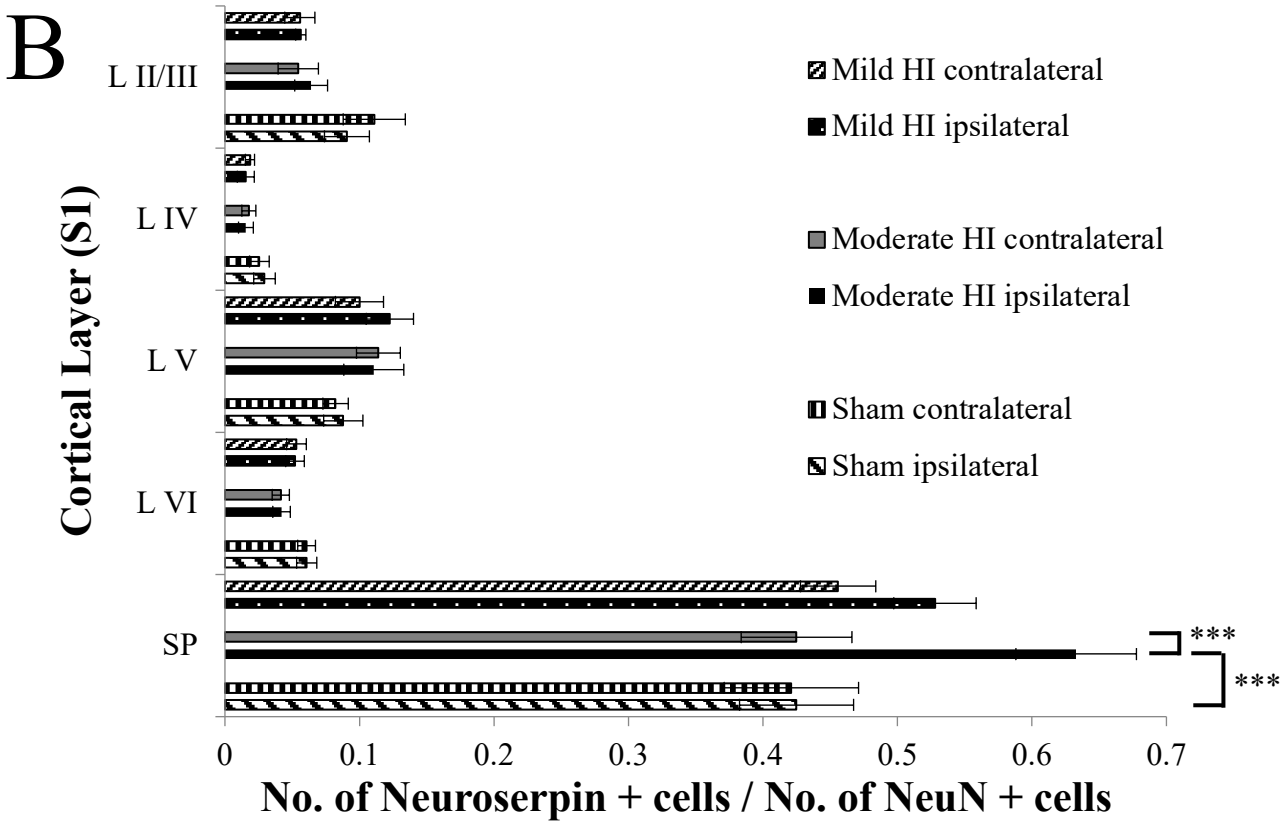
The number of neuroserpin-immunoreactive cells, and the proportion of neuroserpin-NeuN-co-immunoreactive neurons, were quantified for each layer of cerebral cortex in primary somatosensory barrel cortex (S1). Neuroserpin immunoreactivity was compared between the hemisphere ipsilateral to the ligated RCC (the hypoxic-ischaemic hemisphere) and the contralateral hemisphere (non-ischaemic hypoxia-only control), and to both hemispheres of animals that had undergone sham surgery (anaesthesia only with no ligation or hypoxia). In accordance with the developmental expression pattern of neuroserpin in mouse (see Chapter 3, Section 3.3.1), the subplate contained the greatest proportion of neuroserpin-immunoreactive neurons in the sham cortex: 43% (± 8%) of all NeuN-immunoreactive subplate neurons were co-immunoreactive for neuroserpin, whereas only 3-9% (± 2-3%) of neurons across other cortical layers were immunoreactive for neuroserpin.

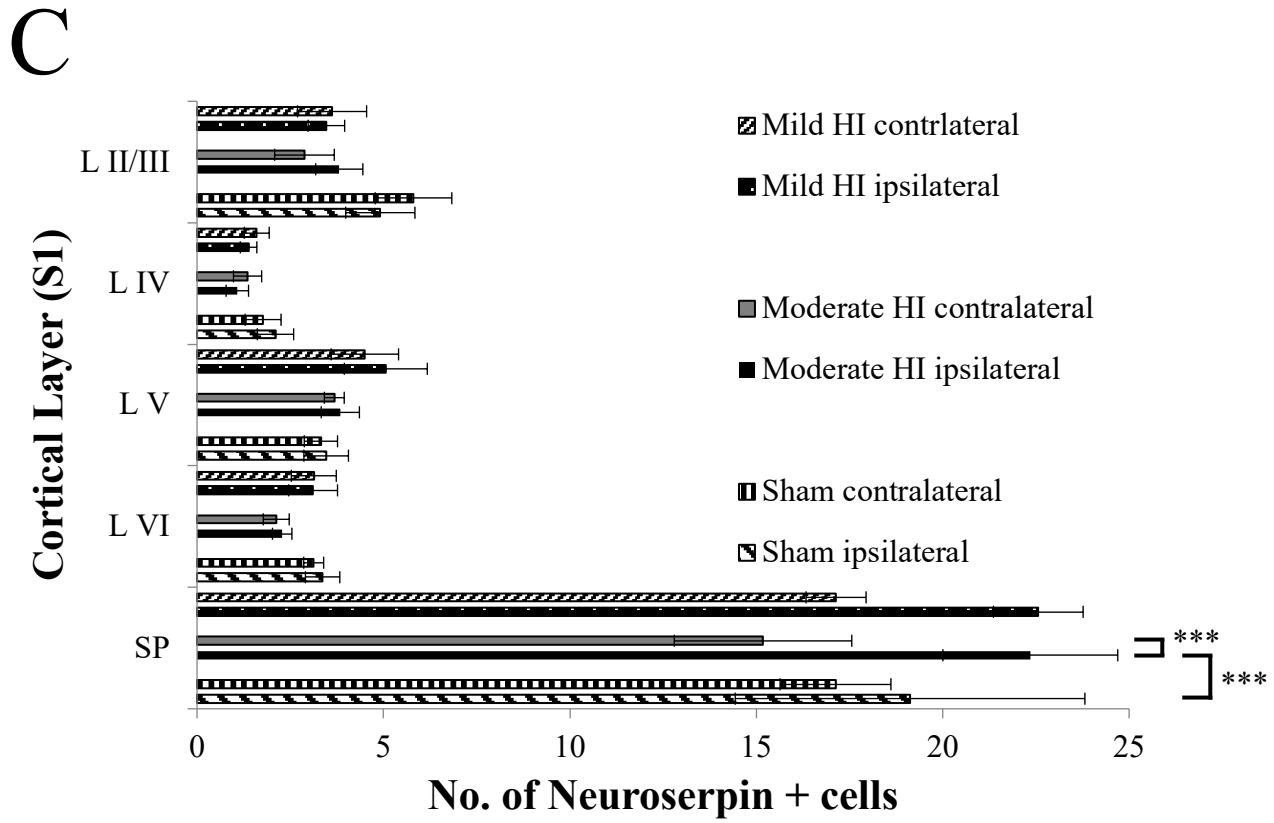
Raw numbers of neuroserpin-immunoreactive cells and proportions of total NeuN-immunoreactive subplate neurons expressing neuroserpin were significantly greater in the hypoxic-ischaemic hemisphere of brains which underwent moderate hypoxia-ischaemia (63% ± 9%) compared to the hypoxia-only contralateral control hemisphere (43% ± 8%), or either hemisphere of the sham-operated brains (43% ± 8% and 42% ± 9%). There was no statistically significant change in neuroserpin-NeuN co-immumoreactivity in any other cortical layer following HI. In brains classified as undergoing mild HI, there was a trend towards increased neuroserpin immunoreactivity in the hypoxic-ischaemic hemisphere (53% ± 6%), compared to the contralateral hemisphere of mild HI brains (47% ± 6%). However, this difference in the mild HI brains was not statistically significant, an neither was there a significant difference between the mild HI hemisphere and either hemisphere of the control brains. Total numbers of neuroserpin-immunoreactive cells per layer were analysed

separately, and complemented the conclusions of NeuN co-staining quantification. Results are summarised in Figure 4.7 and Table 4.7. The proportion of neuroserpin-NeuN-co-immunoreactive neurons in subplate, and their variance as assessed by standard deviation, was highly similar between the sham-operated controls and the hypoxia-only contralateral hemispheres of the experimental brains. There was no statistically significant difference between any of the control hemispheres. Further discussion of the merits of sham and intracerebral negative controls are given in Section 4.3.5 of this chapter. The original analysis by Okusa et al. also included data from brains with "severe" damage, characterised by cresyl violet staining as demonstrating extensive neocortical scarring (Okusa et al., 2014). This condition was not included here as only two severe HI brains were available, and cortical layers were no longer recognisable with DAPI staining.

This characterisation is a helpful preliminary to understanding the role of neuroserpin in neonatal hypoxia ischaemia. Sustained neuroserpin immunoreactivity in cortex six days following HI injury suggest production of neuroserpin is conserved under post-injury stress conditions. The increase in the proportion of subplate neurons immunoreactive for neuroserpin following HI could be interpreted as a role for neuroserpin in the endogenous response, perhaps neuroprotection, following intracerebral to injury. It is also possible that increased neuroserpin immunoreactivity is a result of decreased ability to maintain healthy proteolysis post-HI (reviewed in Kampfl et al., 1997; Blomgren et al., 1997), and does not reflect a functional protective role for neuroserpin.


A
Sham
Moderate HI
Mild HI
ipsi
contra
ipsi
contra
ipsi
contra
50 um
L II/III
L IV
L V
L VI
SP
50 um


B
L II/III
L IV
L V
L VI
SP
Cortical Layer (S1)
Mild HI contralateral
Mild HI ipsilateral
Moderate HI contralateral
Moderate HI ipsilateral
Sham contralateral
Sham ipsilateral
***
***
0
0.1
0.2
0.3
0.4
0.5
0.6
0.7
No. of Neuroserpin + cells / No. of NeuN + cells


C
L II/III
L IV
L V
L VI
SP
Cortical Layer (S1)
Mild HI contrlateral
Mild HI ipsilateral
Moderate HI contralateral
Moderate HI ipsilateral
Sham contralateral
Sham ipsilateral
***
***
0
5
10
15
20
25
No. of Neuroserpin + cells

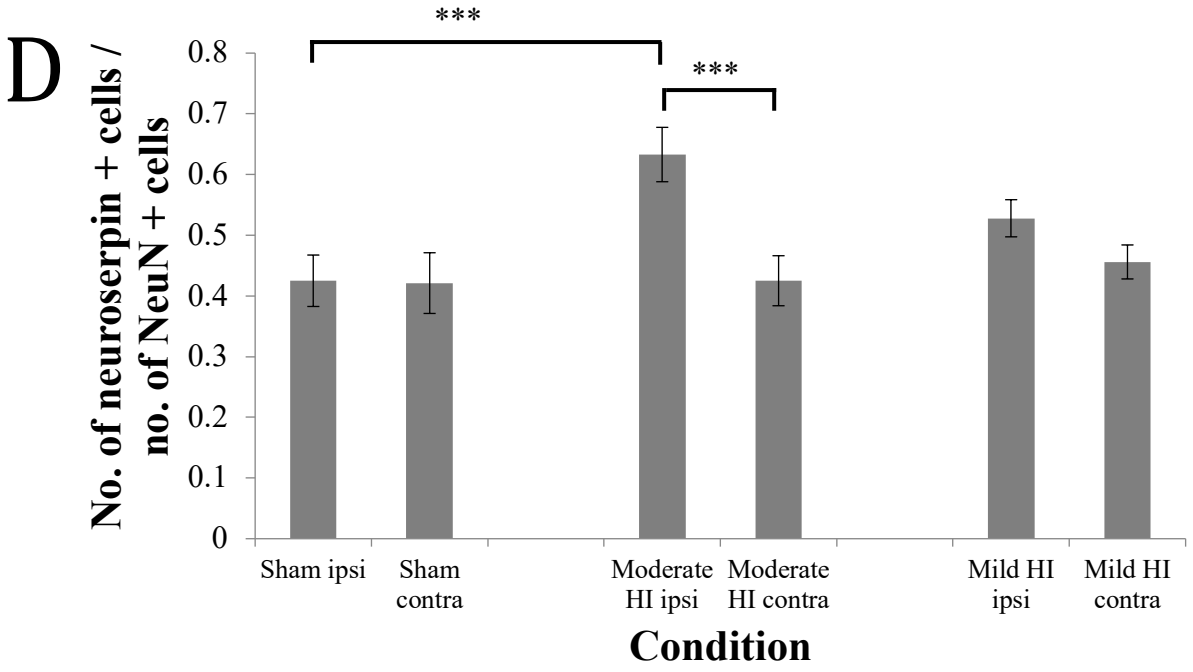


Figure 4.7 – Quantitative Analysis of Neuroserpin Expression in Primary Somatosensory Barrel Cortex (S1) of P8 Sprague-Dawley Rat following an Adapted Perinatal Variation of the Rice-Vannucci Model of Hypoxia Ischaemia (HI) at P2 (Rice et al., 1981; Ginet et al., 2009a). A significantly greater proportion of subplate neurons were co-immunoreactive for neuroserpin and NeuN in the hypoxic-ischaemic ipsilateral (ipsi) hemisphere of the moderate HI brains compared to the hypoxia-only contralateral (contra) control hemisphere of the same animals, or either hemisphere in sham-operated control brains. There was a trend towards an increased proportion of neuroserpin-NeuN co-immunoreactive neurons in subplate of mild HI brains, however this was not statistically significant at N = 6. (A) Representative confocal image of P6 cortical stacks stained for NeuN in green, neuroserpin in red, and DAPI in blue. Scale bars indicate 50 µm width areas. (B) Quantitative analysis of the proportion of neuroserpin-immunoreactive cells co-immunoreactive for NeuN per cortical layer (mean ± SD). (C) Quantitative analysis of the number of neuroserpin-immunoreactive cells per cortical layer (mean ± SD). (D) Quantitative analysis of the proportion of neuroserpin-immunoreactive cells co-immunoreactive for NeuN in subplate only across conditions (mean ± SD). Statistical significance was assessed using paired t-tests. Two-way ANOVA demonstrated a statistically significant difference between groups based on cortical layer and on condition for proportion of neuroserpin-immunoreactive neurons relative to the number of NeuN-immunoreactive neurons. Unpaired T-tests were conducted to compare neuroserpin immunoreactivity between HI animals and sham-operated controls, paired T-tests were used to compare neuroserpin immunoreactivity between hemispheres in HI animals undergoing either mild or moderate HI.
* denotes P-vale < 0.01, ** denotes P-value < 0.005, *** denotes P-value < 0.001

Strain	Condition	Age	N	Number of Neuroserpin-Immunoreactive Cells Counted	Number of NeuN-Immunoreactive Cells Counted	Neuroserpin-Immunoreactive Cells Co-Immunoreactive for NeuN
Sprague-Dawley	Moderate HI	P8	6	4,535	58,647	0.97
Sprague-Dawley	Mild HI	P8	6	4,959	59,911	0.98
Sprague-Dawley	Sham-Operated	P8	2	1,554	18,802	0.98

Table 4.7 – Raw Numbers of Neuroserpin-Immunoreactive Cells Counted Relative to the Number of NeuN-Immunoreactive Neurons Counted in Primary Somatosensory Cortex (S1) of P8 Sprague-Dawley Rat following an Adapted Rice-Vannucci Method of Hypoxia Ischaemia at P2 (Rice et al., 1981; Ginet et al., 2009a). Column 7 shows the proportion of neuroserpin-immunoreactive cells relative to the number of NeuN-immunoreactive cells. The number of neuroserpin-immunoreactive neurons in subplate showed a statistically significant increase following moderate HI, however no statistically significant difference in neuroserpin expression was recorded in any other cortical layer. Two-way ANOVA demonstrated a statistically significant difference between groups based on layer and condition (hemisphere). T-tests were conducted confirm statistical significance between groups.

The rat model used here is not an ideal basis for investigating neonatal HI, as surgery and hypoxia were carried out at P2, a time point commonly considered equivalent to preterm brain development in humans (Finlay and Darlington, 1995; Clancy et al., 2000; 2001; 2007; 2009; Finlay et al., 2001). Exposure to HI during the intrauterine or neonatal period has demonstrably distinct effects on the developing brain (reviewed in Volpe, 2001; Kaindl et al., 2009; Dean et al., 2015; Esakoff et al., 2015). Factors including the foetal immune response (Wolfberg et al., 2007; reviewed in Malaeb and Dammann, 2009; Hagberg and Gressens, 2012; Hagberg et al., 2015), GABA-ergic neuron depolarisation (Obata et al., 1978; Ben-Ari et al., 1989; reviewed in Ben-Ari, 2002; Ben-Ari, 2002; Spitzer, 2006), and the integrity of foetal blood vessels (Trommer et al., 1987; Ment et al., 1991; Jones et al., 2002; El-Khoury et al., 2006; reviewed in Volpe, 1989; Baburamani et al., 2012) differ greatly across these time periods, contributing to qualitatively different patterns of injury development.

This preterm model was a useful preliminary, as detailed anatomical evidence of brain

damage and severity classification had already been published (Okusa et al., 2014) at the time of experimental design, preventing the need for additional validation experiments during early investigation of a relatively understudied protein in the infant brain. It also offered the opportunity to probe the distribution of neuroserpin in a novel species, rat, revealing a highly analogous pattern of neocortical-enrichment and basal ganglia sparsity to that observed in mouse by immunohistochemistry (Kondo et al., 2015) and *in situ* hybridisation (Osterwalder et al., 1996; Krueger et al., 1997). Yet this model, as with any other, is highly specific to the preterm time-point it was generated at, so cannot inform on the distribution of exogenous neuroserpin protein following a hypoxic-ischaemic insult later in development.

Investigation of neuroserpin in a strictly neonatal model of HI injury was essential for evaluating the relevance of the neuroserpin/tPA protein cascade for the development of treatments administered after birth. Additionally, the relation of the rat *Serpini1* gene to that of humans has not received as much empirical study as that of the mouse (reviewed in Heit et al., 2013), making translational claims less robust. Despite the short-comings of this model, the knowledge that neuroserpin is present in the neonatal brain directly following HI confirmed neuroserpin as a potential molecular target for therapeutic treatment if replicated in appropriate future studies.

4.3.2 Development of Mouse Model of Neonatal Hypoxia Ischaemia

Due to the limitations of the rat model described in Section 4.3.1, a modified strictly neonatal variant of the Rice-Vannucci model of hypoxia ischaemia was developed in mouse and optimised to investigate the universality of the increase in subplate neuroserpin immunoreactivity documented in the preterm rat tissue.

Many animal models of neonatal hypoxia-ischaemia have been described in the literature, all with distinct advantages and disadvantages in recreating this human neurodevelopmental disease (reviewed in Hagberg et al., 2002; van der Worp et al., 2007; Yager and Ashwal, 2009; Dean et al., 2015; Millar et al., 2017). An overview of established animal models is given in Chapter 1, Section 1.3.3. The Rice-Vannucci method (Rice et al., 1981) was selected for its faithful reproduction of brain injury patterns observed in human neonates (Towfighi et al., 1991; 1995; reviewed in Vannucci et al., 1999; Millar et al., 2017); extensively documented behavioural impairments (reviewed in Arteni et al., 2003; Lubics et al., 2005; Millar et al., 2017); sensitivity to therapeutic hypothermia (Yager et al., 1993; Lee et al., 2010); and the presence of a non-ischaemic hypoxia-only control hemisphere within the experimental brain (Yager et al., 1991, 1992, 1996; Vannucci and Yager, 1992). The Rice-Vannucci technique has previously been successfully adapted from rat to mouse (Ditelberg et al., 1996; Ferriero et al., 1996; Sheldon et al., 1998; Kichev et al., 2014; Ek et al., 2015).

Additionally, a mouse model can be more readily informed by the extensive developmental characterisation of *Serpini1* mRNA expression in mouse and the detailed analysis of neuroserpin protein immunoreactivity documented in Chapter 3, Section 1.3.1. The mouse is also more amenable to genetic manipulation, as will be explored in Chapter 5 of this thesis, using the *Serpini1* knock-out mouse.

Extensive optimisation was carried out on the parameters used for the adapted Rice-Vannucci neonatal hypoxia ischaemia mouse model. The two parameters varied during optimisation were the duration of exposure to hypoxia and the developmental time-point (age of animal) at brain collection. Figure 4.8 and Table 4.8 summarise the

range of conditions investigated. Several durations of hypoxia were tested as wide variation in brain injury has been reported to be dependent on this variable, from minimal gross anatomical damage at around 30 minutes hypoxia at 8-10% O_2 partial pressure (Tsuji et al., 2004; Okusa et al., 2014), to extensive unilateral necrosis at greater than 60 minutes hypoxia at 8-10% O_2 (Xia et al., 2005; Lubics et al., 2005; Zhu et al., 2006). When the same experimenters have examined multiple durations of hypoxia, differences in brain lesion size of more than two-fold have been reported at 90 minutes compared to 30 minutes exposure (Ten et al., 2003; Hagberg et al., 2004). This study aimed to recreate "moderate" injury severity, reliably generating lesions in the cerebral cortex without the high incidences of animal death reported in some severe injury models (Ditelberg et al., 1996; Sheldon et al., 1998). This was the rationale for testing durations of hypoxia across the severity spectrum from 35 minutes (very mild) to 90 minutes (severe). Time point for brain collection was also optimised as neonatal hypoxic ischaemic injury evolves over time (reviewed in McLean and Ferriero, 2004). Injuries within the first hours after asphyxia are subtle (Takeoka et al., 2002), progressing over the following hours and days into a secondary acute post-injury phase characterised by emergence of substantial brain damage (reviewed in Inder and Volpe, 2000; Hamrick and Ferriero, 2003; Hagberg et al., 2009).

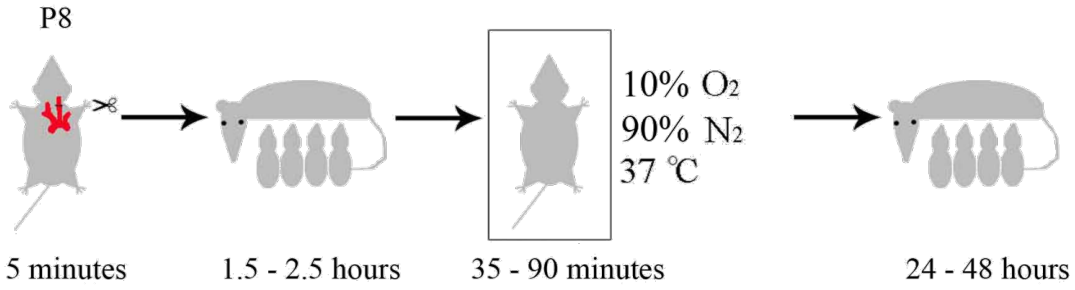


Figure 4.8 – Schematic Diagram of the Parameters Investigated during Optimisation of the Adapted Rice-Vannucci Hypoxia Ischaemia Mouse Model. The left common carotid artery (LCC) was ligated under anaesthesia in P8 pups. Pups were returned to the dam for between 1.5 and 2.5 hours to recover from surgery. Pups were then placed in a sealed chamber and exposed to hypoxic conditions (10% O_2). Exposure duration varied between experiments. Guided by the literature (reviewed in Millar et al., 2017), six different durations of hypoxia were investigated, spanning the interval 35 to 90 minutes. Pups were returned to the dam overnight, then brains were collected 24 or 48 hours later.

Duration of Hypoxia (minutes)	Genotype	Number of HI Brains	Number of Sham Brains	Total Number of Litters	Collection Post-HI (hours)
35	C57BL/6J	5	0	2	24
45	C57BL/6J	9	0	2	24
55	C57BL/6J	7	0	1	24
65	C57BL/6J	7	0	1	24
75	C57BL/6J	9	0	1	24
90	C57BL/6J	9	0	1	24
55	C57BL/6J	5	0	1	48
55	C57BL/6J	31	27	8	48

Table 4.8 – Number of Brains Collected across all Durations of Hypoxia Investigated at Validation and Optimisation by Modification of the Adapted Rice-Vannucci Mouse Model of Neonatal Hypoxia Ischaemia. Brains used in the validation stage are listed alongside those used to assess the distribution of neuroserpin protein throughout the cortex following neonatal hypoxia ischaemia by quantitative fluorescent immunohistochemistry (see Section 4.3.5).

All animal models have disadvantages, regardless of extensive optimisation. Flaws inherent to the Rice-Vannucci model include the high variability in size and severity of infarct between animals treated with identical methods (reviewed in Vannucci and Hagberg, 2004; Vannucci and Vannucci, 2005). Additionally, the highly invasive nature of severing the common carotid artery does not replicate mechanisms of injury in human patients (Ment et al., 1984; Hill, 1991). These limitations were

acknowledged during the experimental design process, however, the model's detailed injury characterisation and prevalence in the literature supported the use of this paradigm (reviewed in Millar et al., 2017).

4.3.3 Verification of Cortical Damage Following Neonatal Hypoxia Ischaemia by Adapted Rice-Vannucci Method in Mouse

Verification of brain injury was essential to validate the adapted Rice-Vannucci model as a model of neonatal hypoxia ischaemia. Two methods, one non-quantitative and one quantitative were used to confirm brain damage in experimental brains.

Gross anatomical brain injury was identified non-quantitatively in the first litter exposed to each duration of hypoxia as shown in Figure 4.9. Freshly dissected brains were either immersed directly in 2% 2,3,5-triphenyl tetrazolium chloride (TTC) in 0.1M PSB for 60 minutes at room temperature, or dissected into five coronal sections using a razor blade, and then immersed in 2% TTC for 60 minutes at 37°C (Bederson et al., 1986a; 1986b; Ten et al., 2003). Full details of a quantitative variant of the TTC method are given in Chapter 5, Section 5.2.4, using *Serpini1* knock-out mice. TTC stains metabolically active tissue red-pink on reduction by mitochondrial enzymes (reviewed in Berridge et al., 2005). Immersion of fresh tissue in TTC solution has been used extensively to characterise lesion volume in models of cerebral hypoxia ischaemia (Bederson et al., 1986a; 1986b; Park et al., 1988; Liszczak et al., 1984; Cole et al., 1990; Isayama et al., 1991; Murai et al., 1997; Ten et al., 2003). Both whole brains and coronal sections showed patches of white tissue where TTC was unreduced, indicating inefficient mitochondrial respiratory function in the hypoxic ischaemic hemisphere. These lesions varied widely in site and size, although this was

not unexpected from the rodent Rice-Vannucci model (reviewed in Vannucci and Hagberg, 2004; Vannucci and Vannucci, 2005). With this preliminary evidence indicating presence of brain lesions, quantitative evaluation was undertaken using fluorescent immunohistochemistry.

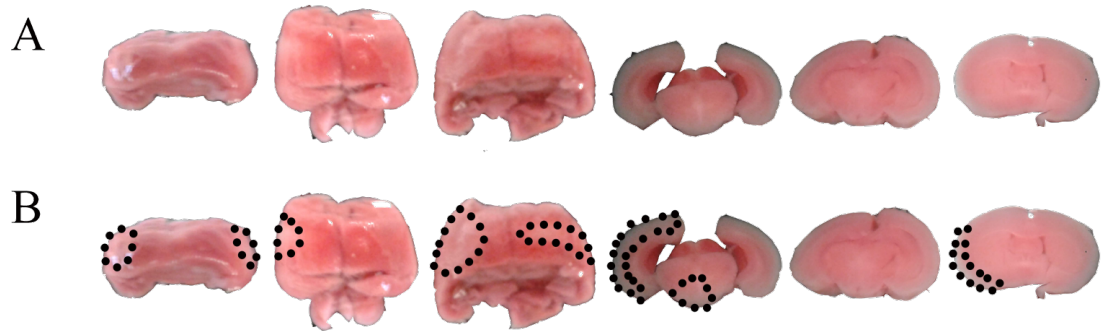


Figure 4.9 – Representative Light Microscope Images taken using the 1.6 x Objective of P9 C57BL/6J Mouse Brains Stained with 2% 2,3,5-triphenyl tetrazolium chloride (TTC) for 30 Minutes, 24 Hours After Neonatal Hypoxia Ischaemia by the Adapted Rice-Vannucci Method. Whole Brains dissected into 2-3 slices using a razor blade are shown on the end. Coronal Sections of brains dissected into 2-5 sections are shown on the right. (A) Light microscope images of representative brain slices. (B) Light microscope images indicating areas of focal brain damage indicated by reduced red-pink TTC staining. Potential lesion sites are indicated by a dotted line.

Quantitative brain injury was carried out by staining for three glial molecular markers extensively used to validate models of neonatal hypoxia ischaemia: astrocytic marker glial fibrillary acidic protein (GFAP); microglial marker ionised calcium binding adaptor molecule 1 (Iba1); and monocyte marker cluster of differentiation 68 (CD68) (Fathali et al., 2013; Pogledic et al., 2014; Savard et al., 2015; Zaghloul et al., 2017; Chip et al., 2017; McAdams et al., 2017).

Astrocytic GFAP is upregulated in the neonatal hypoxic ischaemic brain (Burtrum and Silverstein, 1994; reviewed in Nathaniel and Nathaniel, 1981; Pekny and Nilsson, 2005), and is present in the cerebrospinal fluid (CSF) of human infants who have

suffered hypoxia ischaemia (Blennow et al., 1995; 1996; 2001). GFAP is also upregulated in activated astrocytes in a range of diseases (Wilhelmsson et al., 2006; reviewed in Norenberg et al., 2005; 2007; Hol and Pekny, 2015).

Iba1, a marker of microglia (Ito et al., 1998; Ohsawa et al., 2000; 2004), was quantified using similar methods. Microglia are known to become activated in the acute post-HI period (Fujimoto et al., 1989; reviewed in Tahraoui et al., 2001; Kaur et al., 2007), and additional microglia migrate to damaged brain regions (reviewed in Leonardo and Pennypacker, 2009) throughout injury development. Although the role of microglia in the development of neonatal hypoxic ischaemic brain injury remains debated (reviewed in Mallard et al., 2013; Kaur et al., 2013), an increase numbers of microglia at HI injury sites is a generally accepted pathophysiological phenomenon (Ivacko et al., 1996; Rivera et al., 2002; Deng et al., 2008).

The third damage marker investigated was cluster of differentiation 68 (CD68). CD68 is expressed by macrophages (Holness and Simmons, 1993; Ramprasad et al., 1996) and activated, but not quiescent, microglia (Perego et al., 2011; reviewed in Kreutzberg, 1996; Billiards et al., 2006). Therefore, this marker also detects brain inflammation around an injury site.

All three markers were quantified for both the number of immunoreactive cells across S1 cortex, and for the total proportion of cortical area filled by fluorescent pixels. Cell counting techniques are detailed in Chapter 3, Sections 3.2.2 and 3.2.3, respectively. Some investigators have confined cortical area studies of glial marker expression in neonatal HI to a specific cortical layer (Sizonenko et al., 2005; Sullivan et al., 2010a; 2010b), or carried out morphological characterisation of individual glia to assess activation (Petito and Babiak, 1982; reviewed in Panickar and Norenberg, 2005). As

the aim of this experiment was to generate non-focal mild-to-moderate hypoxic ischaemic brain injury, only general glial marker quantification methods were investigated.

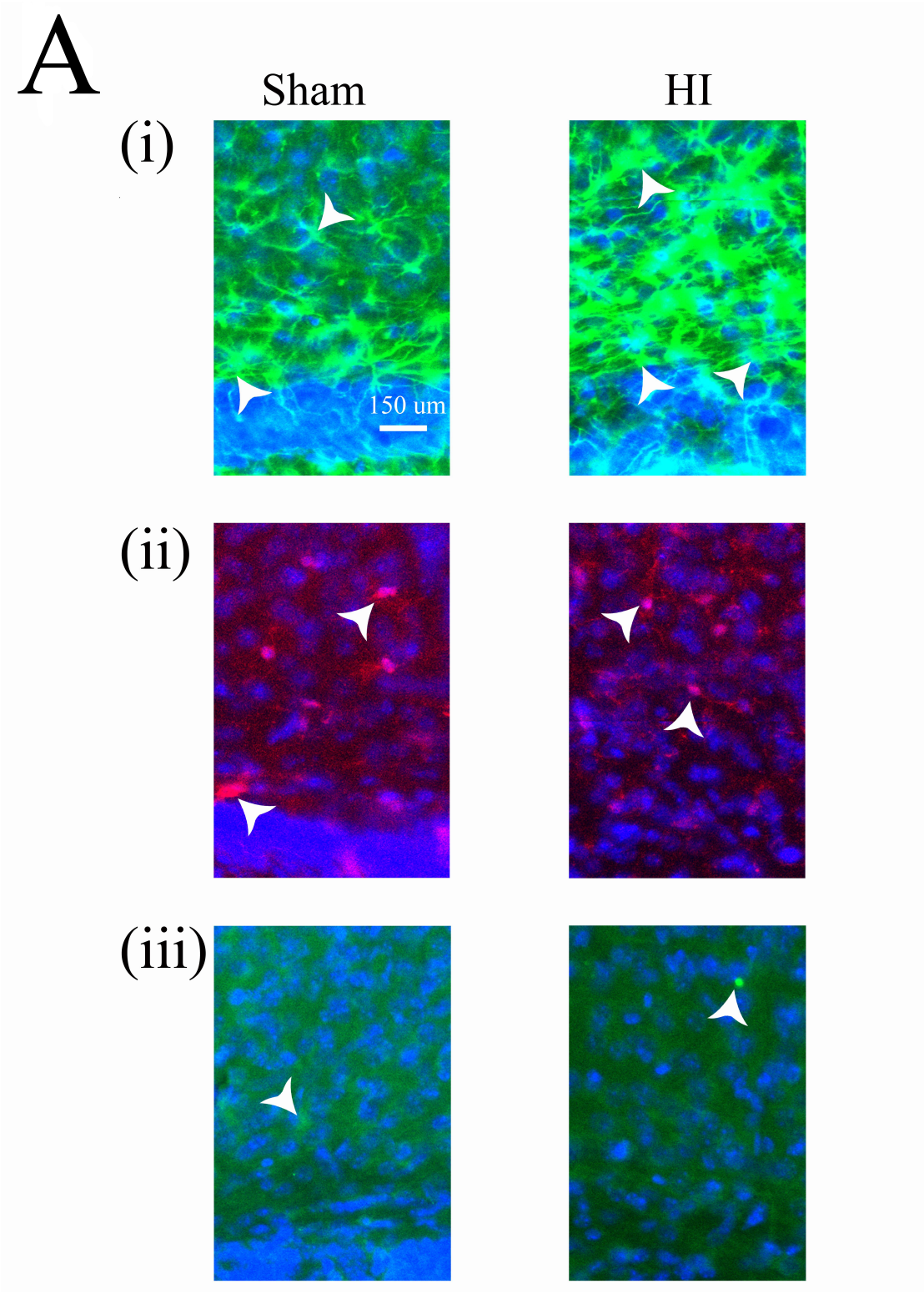
Individual cell counts demonstrated a statistically significant increase in the number of GFAP, Iba1, and CD68-immunoreactive cells in the hypoxic ischaemic hemisphere compared to the hypoxia-only control hemisphere of the same brains. There was a 28% increase in the number of GFAP-immunoreactive cells in the HI hemisphere, (263 ± 47 compared to 205 ± 46 in the control hemisphere). The HI hemisphere also demonstrated a significantly greater number of GFAP-immunoreactive positive cells compared to sham-operated control brains (199 ± 45). There was a 39% increase in the number of Iba1-immunoreactive cells in the HI hemisphere (317 ± 53 compared to 229 ± 77). However, the difference in the number of Iba1-immunoreactive cells between the HI brains and that of sham-operated controls (279 ± 104) was not statistically significant, although there was a trend towards greater numbers of Iba1-immunoreactive cells in the HI hemisphere. There was a 42% increase in the number of CD68-immunoreactive cells in the HI hemisphere (34 ± 13 compared to 24 ± 9). As the number of CD68-immunoreactive cells across the cortex was low in either hemisphere of the HI brains, CD68 staining was not carried out in the sham-operated controls. Overall, results are consistent with increases in glial marker expression previously described in the literature (reviewed in Millar et al., 2017). The modest proportional differences between conditions, alongside the lack of statistically significant difference in number of Iba1-immunoreactive microglia between the HI hemisphere of the experimental brains and that of sham-operated controls is suggestive of a mild inflammatory phenotype generated by the adapted Rice-Vannucci procedure used throughout this thesis. As glial markers were not quantified

outside of S1 neocortex, nor in individual cortical layers, it is possible that this overall mild cortical inflammation phenotype was comprised of locally more severe inflammation. One previous investigation has made a case for selective increases in activated glia in deep cortical layers (Sizonenko et al., 2005), although subplate was not discussed explicitly in this publication. Future studies of subplate specific glial infiltration and morphology could add to our current understand of subplate vulnerability to neonatal HI.

The results from the cortical area analysis did not show a clear increase in expression of inflammatory markers in the HI cortex. Although there were trends towards a greater area of cortex covered by glial marker-immunoreactive fluorescent pixels in the HI hemisphere compared to the hypoxia-only control hemisphere of experimental brains for all three markers, this was only statistically significant for GFAP at N = 5. The proportion of cortex covered by GFAP was greater in the HI hemisphere (17% ± 8% compared to 11% ± 5%). Although the proportion of cortex covered by Iba1 was greater in the HI hemisphere (9% ± 3% compared to 7% ± 3%), and the proportion covered by CD68 was greater in the HI hemisphere (3% ± 3% compared to 1% ± 2%), neither were statistically significant. There were no significant differences between the HI hemisphere of the experimental brains and the ipsilateral hemisphere of the sham-operated controls for any marker. Results are summarised in Figure 4.10 and Table 4.9.

A more precise method of investigating inflammatory glia focused on the morphology of these cells. Both astrocytes (reviewed in Panickar and Norenberg, 2005) and microglia (reviewed in McRae et al., 1995; Cho and Choi, 2017) are known to undergo marked changes in cytoplasmic shape and volume during intracerebral

inflammation. Qualitative cytoplasmic hypertrophy and increased branching have been documented in astrocytes following neonatal HI in rat (Sizonenko et al., 2008; Teo et al., 2015) and pig (Sullivan et al., 2010a; 2010b), with the latter study reporting increased subcortical white matter area covered by GFAP immunoreactivite pixels in HI brains using analogous methods to those employed here. The astrocytes observed in this study displayed a swollen shape in the HI hemisphere of the experimental brains, but not in other conditions, and shown in Figure 4.10 Panel A. This morphology was similar to that reported in pig (Sullivan et al., 2010b). Microglia are known to take on an amoeboid morphology in the brain following neonatal HI in rat (Gerhmann et al., 1992; Morioka et al., 1993; Ivacko et al., 1996; Teo et al., 2015). However, the microglia identified here did not display full amoeboid morphology, with a combination of ramified and hyper-ramified morphologies observed, as shown in Figure 4.10 Panel B. This study did not undertake blinded quantitative analysis of glial morphology, as other publications have previously used to support findings of increased astrocytic volume (Fu et al., 2007; Liu et al., 2014; Ruzafa et al., 2017). This detailed quantification could provide additional evidence as to whether the model used here was a valid reproduction of inflammatory brain damage. Yet glial activation is also known to exist on a spectrum, so mild increases in inflammatory activity may not be detected by morphological quantification (reviewed in Karperien et al., 2013; Fernandez-Arjona et al., 2017).


A
Sham
HI
(i)
150 um
(ii)
(iii)

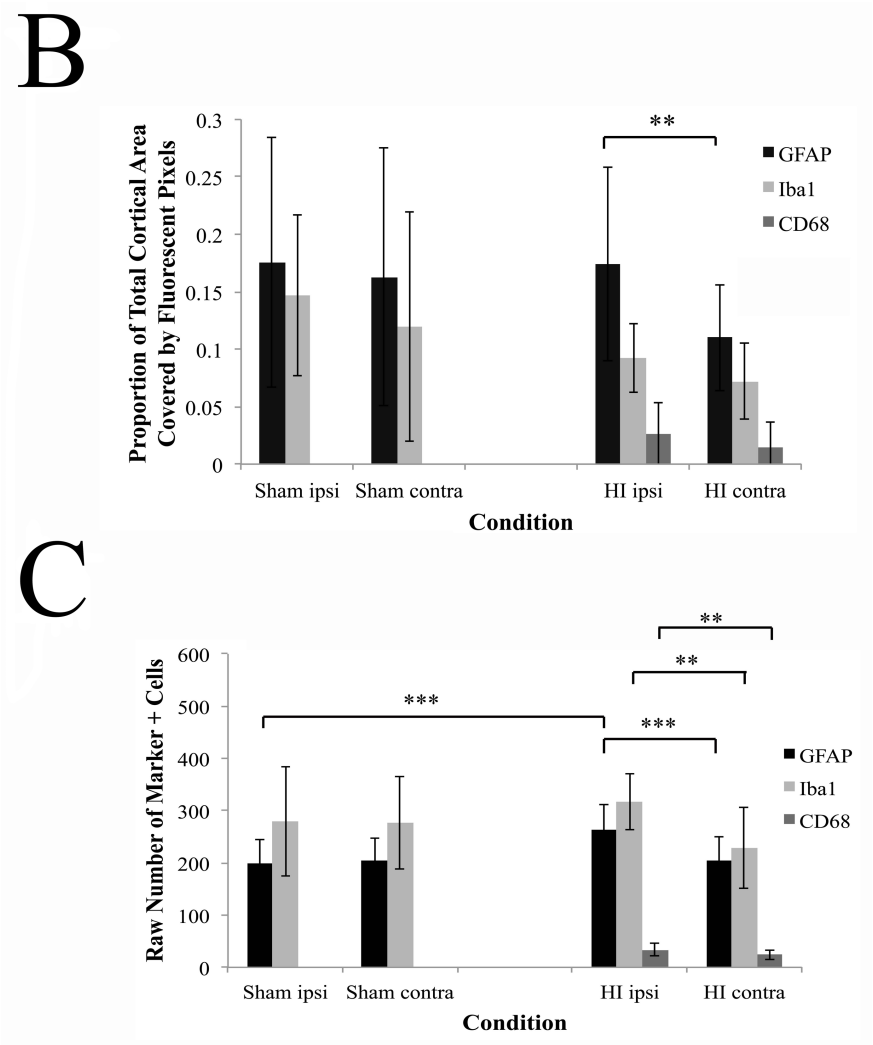


Figure 4.10 – Validation of the Adapted Rice-Vannucci Mouse Model of Neonatal Hypoxia Ischaemia (HI) in Mouse by Immunohistochemistry for Glial Markers Associated with Brain Injury and Inflammation. Quantitative Analysis in Primary Somatosensory Barrel Cortex (S1) of P10 C57BL/6J Mouse following Hypoxia Ischaemia at P8. A statistically significant increase in the raw number of glia present in the hypoxic-ischaemic ipsilateral (ipsi) hemisphere of experimental brains was detected, compared to either the hypoxia-only contralateral (contra) hemisphere of the same animals or either hemisphere in sham-operated negative controls. A statistically significant increase the cortical area covered by glial markers was detected in the ipsilateral hemisphere of the HI brains compared to the contralateral hemispheres of the same animals. However, there was no different between the ipsilateral hemisphere of the HI brains and that of sham-operated controls at N = 5. (A) Enlarged representative subplate zone from confocal images of P10 cortex from the ipsilateral hemispheres of experimental brains and sham-operated control brains. Arrowheads indicate glial marker-immunoreactive cells. (i) GFAP in green and DAPI in blue. (ii) Iba1 in red and DAPI in blue. (iii) CD68 in green and DAPI in blue. Scale bars indicate 10 µm width areas. (B) Quantitative analysis of the proportion of total cortical area covered by glia marker-immunoreactive pixels (mean ± SD). (C) Quantitative analysis of the raw number of neuroserpin-immunoreactive cells per cortical layer (mean ± SD). Two-way ANOVA demonstrated a statistically significant difference between groups based on experimental condition and glial marker. Unpaired T-tests were conducted to compare glial molecular marker immunoreactivity between HI animals and sham-operated controls, paired T-tests were used to compare glial marker immunoreactivity between hemispheres in HI animals undergoing HI.
* denotes P-vale < 0.01, ** denotes P-value < 0.005, *** denotes P-value < 0.001

Genotype	Age	Condition	N	Litters	Number of GFAP-Immunoreactive Cells Counted	Cortical Area GFAP-Immunoreactive (± SD)
C57BL/6J	P10	HI, 55 mins, ipsi	5	3	3,945	0.174 (± 0.084)
C57BL/6J	P10	HI, 55 mins, contra	5	3	3,070	0.110 (± 0.046)
C57BL/6J	P10	Sham, ipsi	5	3	2,978	0.176 (± 0.109)
C57BL/6J	P10	Sham, contra	5	3	3,050	0.163 (± 0.112)
					Number of Iba1-Immunoreactive Cells Counted	**Cortical Area Ibs1-Immunoreactive (± SD)**
C57BL/6J	P10	HI, 55 mins, ipsi	5	3	4,753	0.092 (± 0.030)
C57BL/6J	P10	HI, 55 mins, contra	5	3	4,270	0.072 (± 0.033)
C57BL/6J	P10	Sham, ipsi	5	3	4,185	0.147 (± 0.070)
C57BL/6J	P10	Sham, contra	5	3	4,151	0.120 (± 0.100)
					Number of CD68-Immunoreactive Cells Counted	**Cortical Area CD68-Immunoreactive (± SD)**
C57BL/6J	P10	HI, 55 mins, ipsi	5	3	506	0.026 (± 0.028)
C57BL/6J	P10	HI, 55 mins, contra	5	3	355	0.015 (± 0.021)
C57BL/6J	P10	Sham, ipsi	-	-	-	-
C57BL/6J	P10	Sham, contra	-	-	-	-

Table 4.9 – Validation of Brain Injury in the Adapted Rice-Vannucci Mouse Model of Neonatal Hypoxia Ischaemia (HI). All data was generated from fluorescent immunohistochemistry and confocal microscopy in primary somatosensory cortex (S1). Raw numbers of cells immunoreactive for brain injury molecular markers glial fibrillary acidic protein (GFAP), ionised calcium binding adaptor molecule 1 (Iba1), and cluster of differentiation 68 (CD68) are recorded alongside the proportion of total cortical area immunoreactive for these markers as analysed with ImageJ. The ipsilateral hemisphere of the hypoxic ischaemic experimental brains demonstrated a statistically significant greater number of glial cells, in addition to increased expression of molecular markers as a proportion of total cortical volume. This is consistent with previous data from mild-to-moderate rodent models of neonatal hypoxic ischaemic brain damage. Two-way ANOVA demonstrated a statistically significant difference between groups based on marker and condition (hemisphere). T-tests were conducted confirm statistical significance between groups.

This data is consistent with the presence of a mild brain inflammatory response as previously reported in studies of neonatal hypoxia ischaemia models (Ditelberg et al., 1996; Sheldon et al., 1998; Zhu et al., 2006; van der Kooij et al., 2010; Fan et al., 2011; Okusa et al., 2014).

It is possible that the lack of statistical significance when comparing glial marker immunoreactivity between the experimental and control brains could be accounted for by high variability in antibody penetration between brains which underwent different procedures. Supporting this, the standard deviation for cortical area measurements was greater than for raw cell numbers. Increasing the number of brains analysed may

allow statistical significance to be detected, yet it is also possible that the modest increase in glial activation initiated by this mild model of neonatal HI is fundamentally smaller than the inherent variation in staining efficacy or variation between individuals (reviewed in Hagberg and Vannucci, 2004; Vannucci and Vannucci, 2005). It is also possible that increasing the minimal particle size detected could reduce the effect of minute particles of artefact or background staining, although this would fail to include the genuine staining of truncated glial processes. Another potential explanation is the heterogeneity of lesion sites within the brain of rodents undergoing the Rice-Vannucci model of neonatal hypoxia ischaemia (reviewed in Volpe, 2012; Millar et al., 2017), which introduces the possibility that some mild HI brains display little to no damage within S1 neocortex.

Another limitation of the validation methods reported here is the lack of direct quantification of cell death markers. Cell death is a defining feature of many models of neonatal hypoxia ischaemia, and certainly occurs in human patients (see Chapter 1, Section 1.3.2.2.2, reviewed in Northington, 2011). The only measure of cell death here was indirect quantification of the density of NeuN-immunoreactive neurons. No significant difference was detected between the HI hemisphere of experimental animals and either the hypoxia-only hemisphere or sham-operated brains. Although severe models of neonatal HI have reported decreased numbers of NeuN-immunoreactive neurons following neonatal HI (Koike et al., 2008), in the absence of measures of total cortical volume it is impossible to know if the total number of cortical neurons changed. Validity of the model could have been enhanced by demonstrating increased occurrence of cell death following HI. Potential methods for investigating this include: indirectly studying the number and density of neurons through histological analysis, as was carried out for the perinatal rat model (Okusa et

al., 2014); quantification of dying cells by methods such as staining for DNA fragmentation using a terminal deoxynucleotidyl transferase dUTP nick-end labeling TUNEL assay (de Torres et al., 1997; Pulera et al., 1998; Koike et al., 2008; Cai et al., 2008; reviewed in Labat-Moleur et al., 1998); and direct measurement of immunoreactivity of apoptosis-mediating molecules such as cleaved caspase-3 (Zhu et al., 2000; Blomgren et al., 2001; Jantzie et al., 2005; reviewed in Porter and Jänicke, 1999; D'Amelio et al., 2010). Ideally, molecules involved in both apoptosis and necrosis would be investigated.

The adapted Rice-Vannucci model of neonatal hypoxia ischaemia was developed to study neuroserpin expression in a distinctly neonatal model of HI which could be validated using methods accepted in the literature. Increased immunoreactivity associated with glial markers GFAP, Iba1, and CD68 is extensively used as histological confirmation of injury in models of neonatal hypoxia ischaemia (Fathali et al., 2013; Pogledic et al., 2014; Savard et al., 2015; Zaghloul et al., 2017; Chip et al., 2017; McAdams et al., 2017). Although translational relevance of an animal model can only be confirmed with extensive behavioural testing (reviewed in Arteni et al., 2003; Lubics et al., 2005; Millar et al., 2017), which was not conducted for this adaptation of the comprehensively studied Rice-Vannucci model, the histological data presented are consistent with a valid model of mild brain injury.

4.3.4 Optimisation of Neonatal Hypoxia Ischaemia Protocol in Mouse

In order to capture the variation in injury severity generated by the rodent Rice-Vannucci model (reviewed in Vannucci and Hagberg, 2004; Vannucci and Vannucci, 2005), also observed in human neonatal hypoxia ischaemia patients (reviewed in

Millar et al., 2017). Quantitative fluorescent immunohistochemistry was used to assess the number and proportion of neuroserpin-NeuN-co-immunoreactive subplate neurons in primary somatosensory cortex (S1) following different durations of hypoxia. Details of hypoxic ischaemic conditions and numbers of brains investigated are given in Table 4.8 and Table 4.10.

Analysis of both the raw numbers of neuroserpin-immunoreactive neurons and the proportions of neuroserpin-NeuN-co-immunoreactive neurons revealed three distinct patterns of neuroserpin expression. In the mildest conditions, 35 and 45 minutes of hypoxia, there was a trend towards an increased proportion of neuroserpin-immunoreactive neurons in the subplate of the hypoxic-ischaemic hemisphere, but this was not statistically. Following 35 minutes of hypoxia, there was a trend towards difference in the proportion of neuroserpin-immunoreactive neurons (25% ± 4% in the hypoxic-ischaemic ipsilateral hemisphere compared to 20% ± 2% in the hypoxia-only contralateral hemisphere). Following 45 minutes hypoxia, a greater difference was detected (50% ± 23% in the hypoxic-ischaemic hemisphere compared to 33% ± 20% of neurons in the hypoxia-only hemisphere).

The second pattern was observed in animals subjected to 55 minutes of hypoxia, and comprised a statistically significant elevation in the proportion of neuroserpin-immunoreactive neurons in the hypoxic-ischaemic hemisphere. When brains were collected 24 hours after hypoxia, a statistically significant difference in the proportion of neuroserpin-immunoreactive neurons was documented (38% ± 10% in the hypoxic-ischaemic hemisphere compared to 21% ± 14% in the hypoxia-only hemisphere). At 48 hours post-surgery, a robust difference was detected, with less variation (37% ± 5% in the hypoxic-ischaemic hemisphere and 26% ± 10% of

neurons in the hypoxia-only hemisphere).

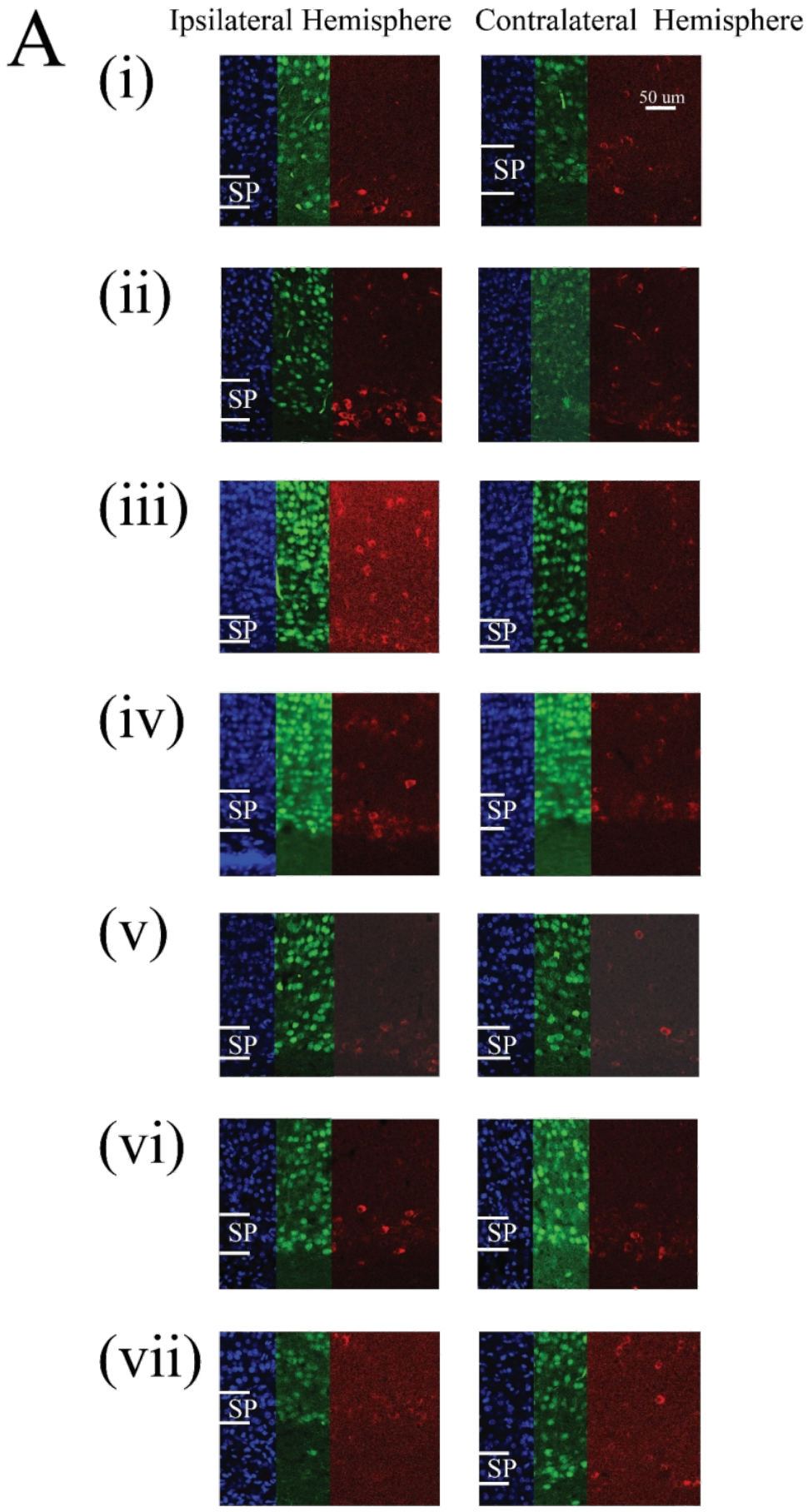
The third pattern was observed across brains from animals exposed to 65, 75, or 90 minutes hypoxia. At these longer exposure times, the proportion of subplate neurons immunoreactive for neuroserpin was indistinguishable between hemispheres. Following 65 minutes exposure to hypoxia, 49% ± 7% neurons in the hypoxic-ischaemic hemisphere were neuroserpin-immunoreactive compared to 44% ± 6% of neurons in the hypoxia-only hemisphere, both greater than the proportion of neuroserpin-immunoreactive neurons in the mild-insult brains. A similar pattern was detected in animals exposed to 75 minutes hypoxia (41% ± 6% compared to 39% ± 9%), and 90 minutes (44% ± 8% compared to 39% ± 5%).

These three patterns were also evident in the raw numbers of neuroserpin-immunoreactive neurons in subplate. The difference between 13 ± 2 neuroserpin-immunoreactive cells in the hypoxic-ischaemic subplate compared to 10 ± 2 neuroserpin-immunoreactive cells in the hypoxia-only subplate in animals exposed to 35 minutes hypoxia was not statistically significant. In contrast, the number of neuroserpin-immunoreactive neurons in animals exposed to 45 minutes hypoxia did demonstrate a statistically significant difference between 26 ± 15 in the hypoxic-ischaemic hemisphere and 14 ± 9 in the control hemisphere. Statistically significant differences were present in brains exposed to 55 minutes hypoxia. When collected 24 hours after surgery, the hypoxic-ischaemic hemisphere demonstrated a greater number of neuroserpin-immunoreactive neurons (19 ± 6 compared to 11 ± 5). This effect was conserved in brains collected 48 hours after surgery (18 ± 4 neurons in the hypoxic-ischaemic subplate compared to 12 ± 6 in the control hemisphere). No statistically significant difference was found in numbers of neuroserpin-

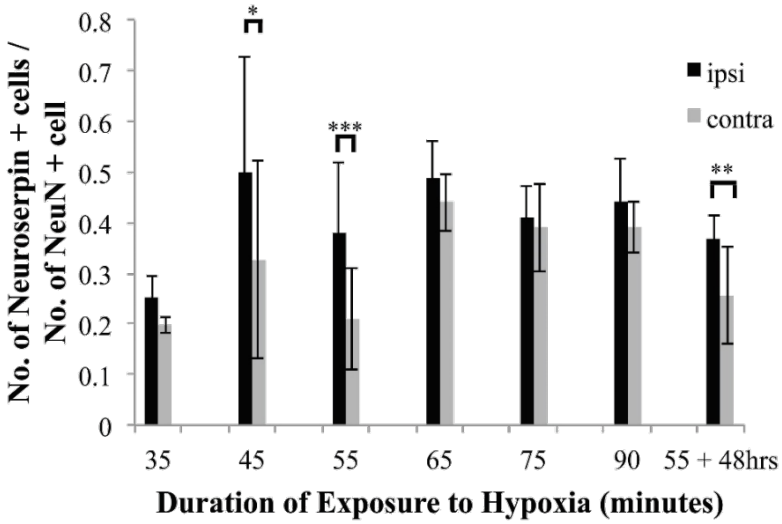
immunoreactive neurons between hemispheres of brains from animals exposed to 65, 75, or 90 minutes of hypoxia. Following exposure to 65 minutes of hypoxia, 23 ± 2 neuroserpin immunoreactive neurons were counted in the hypoxic-ischaemic hemisphere compared to 22 ± 4 neurons in the hypoxia-only hemisphere. Similarly, in animals exposed to 75 minutes hypoxia, there was no statistically significant difference between the 19 ± 4 neuroserpin-immunoreactive neurons in the hypoxic-ischaemic hemisphere compared to 20 ± 5 in the hypoxia-only hemisphere. The same was true of animals exposed to 90 minutes of hypoxia (17 ± 4 neuroserpin-immunoreactive neurons were documented in the HI hemisphere compared to 15 ± 6 in the hypoxia-only hemisphere. Results are shown in Table 4.10 and Figure 4.11.

Duration of Hypoxia (minutes)	Genotype	Age	N	Number of Neuroserpin-Immunoreactive Subplate Cells Counted	Number of NeuN-Immunoreactive Subplate Cells Counted	Proportion of NeuN-Immunoreactive Subplate Neurons Neuroserpin Co-Immunoreactive (± SD)
35	C57BL/6J	P9	2	136	588	0.96 (± 0.04)
45	C57BL/6J	P9	4	540	1,447	0.95 (± 0.07)
55	C57BL/6J	P9	8	540	2,226	0.99 (± 0.06)
65	C57BL/6J	P9	6	832	1,796	0.99 (± 0.05)
75	C57BL/6J	P9	8	801	1,733	0.97 (± 0.07)
90	C57BL/6J	P9	9	853	2,052	0.98 (± 0.07)
55	C57BL/6J	P10	8	712	2,008	0.99 (± 0.02)

Table 4.10 – Raw Numbers of Neuroserpin-Immunoreactive Cells Counted Relative NeuN-Immunoreactive Neurons Counted in Primary Somatosensory Barrel Cortex (S1) of P10 C57BL/6J Mouse following Neonatal Hypoxia Ischaemia by the Adapted Rice-Vannucci Model at P8. Neuroserpin immunoreactivity was quantified in subplate only over a range of hypoxia durations. Column 7 shows the proportion of neuroserpin-immunoreactive cells relative to the number of NeuN-immunoreactive cells. The majority of neuroserpin-immunoreactive cells were co-labelled with NeuN, suggesting these are neurons. The proportion of neuroserpin-immunoreactive subplate neurons increased in the hypoxic-ischaemic ipsilateral hemisphere at all durations of hypoxia from 35 to 90 minutes, with a shift towards an increased proportion of neuroserpin-immunoreactive neurons in both the hypoxic-ischaemic ipsilateral and hypoxia-only contralateral hemisphere when animals were exposed to hypoxia for 75 or 90 minutes. Two-way ANOVA demonstrated a statistically significant difference between groups based on duration of hypoxia and condition (hemisphere). T-tests were conducted confirm statistical significance between groups.


A
Ipsilateral Hemisphere
Contralateral Hemisphere
(i)
(ii)
(iii)
(iv)
(v)
(vi)
(vii)
SP
50 um

B


No. of Neuroserpin + cells / No. of NeuN + cell
0.8
0.7
0.6
0.5
0.4
0.3
0.2
0.1
0
*
***
**
ipsi
contra
35
45
55
65
75
90
55 + 48hrs
Duration of Exposure to Hypoxia (minutes)

C

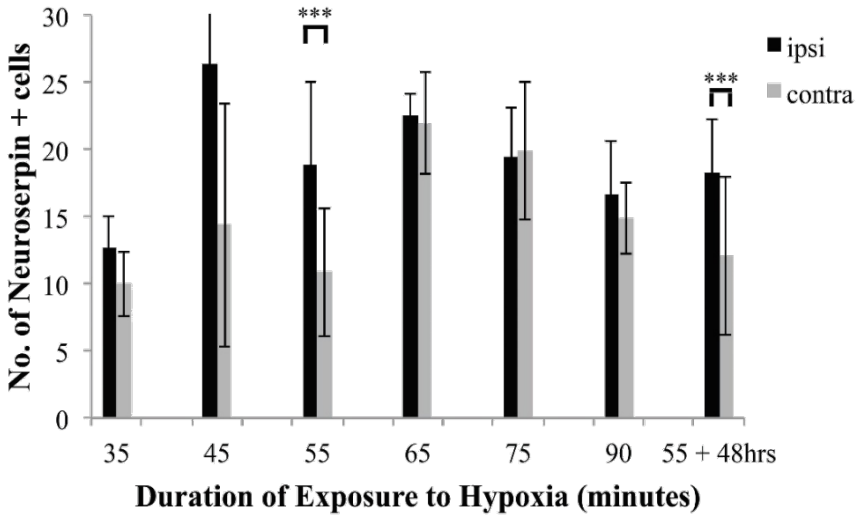

No. of Neuroserpin + cells
30
25
20
15
10
5
0
***
***
ipsi
contra
35
45
55
65
75
90
55 + 48hrs
Duration of Exposure to Hypoxia (minutes)

Figure 4.11 – Quantification of Subplate Neuroserpin Immunoreactivity in the Adapted Rice-Vannucci Mouse Model of Neonatal Hypoxia Ischaemia across Multiple Durations of Exposure to Hypoxia by Fluorescent Immunohistochemistry. Counting neuroserpin-immunoreactive neurons in subplate of primary somatosensory barrel cortex (S1) in P9 and P10 mouse following hypoxia ischaemia at P8 revealed three discreet patterns of neuroserpin expression in the hypoxic-ischaemic ipsilateral (ipsi) hemisphere compared to the hypoxia-only contralateral (contra) control hemispheres of the experimental brains. Following 35 minutes hypoxia, there was a trend towards an increase in the number and proportion of neuroserpin-immunoreactive neurons in ipsilateral subplate, but this was not statistically significant at N = 2. Following 45 or 55 minutes hypoxia, a statistically significant increase in number of and proportion of neuroserpin-immunoreactive neurons was detected in the subplate of the ipsilateral hemisphere compared to the contralateral hemisphere, demonstrating increased subplate neuroserpin immunoreactivity following a rodent model of neonatal hypoxia ischaemia. Following 65, 75, or 90 minutes hypoxia, the number and proportion of neuroserpin-immunoreactive neurons was increased in both hemispheres, with no statistically significant difference between the two hemispheres at N = 6, N = 8, and N = 9, respectively. (A) Representative confocal images of cortex stained for neuroserpin in red, NeuN in green and DAPI in blue. Images from both ipsilateral and contralateral subplate are shown corresponding to each duration of hypoxia. (i) 35 minutes hypoxia. (ii) 45 minutes hypoxia. (iii) 55 minutes hypoxia, brains collected 24 hours post-injury. (iv) 55 minutes hypoxia, brains collected 48 hours post-injury. (v) 65 minutes hypoxia. (vi) 75 minutes hypoxia. (vii) 90 minutes hypoxia. Scale bars indicate 50μm width areas. (B) Quantitative analysis of the proportion of neuroserpin-NeuN co-immunoreactive neurons in the subplate zone of S1 mouse cortex across durations of hypoxia (mean ± SD). (D) Quantitative analysis of the number of neuroserpin-immunoreactive cells per in the subplate zone across durations of hypoxia (mean ± SD). Two-way ANOVA demonstrated a statistically significant difference between groups based on duration of hypoxia and on condition for proportion of neuroserpin-immunoreactive subplate neurons relative to the number of NeuN-immunoreactive neurons. Paired T-tests were used to compare neuroserpin immunoreactivity between hemispheres in HI animals undergoing different durations of hypoxia.
* denotes P-vale < 0.01, ** denotes P-value < 0.005, *** denotes P-value < 0.001

This preliminary quantification of neuroserpin immunoreactivity in subplate neurons was informative for selecting the most appropriate conditions for a comprehensive investigation of neuroserpin in neonatal hypoxic ischaemic mouse. Prior analysis of the preterm rat model in Section 4.3.1 suggested that moderate HI brain injury is sufficient for detecting injury-induced changes in neuroserpin immunoreactivity in cortical neurons. The literature suggested an exposure duration of approximately 55 minutes hypoxia at 10% O_2 partial pressure as equivalent to mild-to-moderate injury in neonatal mouse (reviewed in Vannucci and Vannucci, 2005; Volpe, 2012; Millar et al., 2017). Therefore, this duration was selected as the mid-point of a small spectrum of hypoxia durations investigated. Presence of mild brain injury was confirmed by quantification of inflammatory glial markers, described in fill in Section 4.3.3.

Complementing the preterm rat model, an increase of 44% in the proportion of neuroserpin immunoreactive neurons was detected in the hypoxic-ischaemic subplate compared to the hypoxia-only hemisphere of P10 brains exposed to 55 minutes hypoxia at P8. This confirmed the relevance of neuroserpin in subplate to mild-to-moderate rodent neonatal hypoxia ischaemia and motivated further study.

This overview also expanded knowledge beyond selecting a mild-to-moderate neonatal HI condition. By including milder procedures, 35-45 minutes hypoxia, and more severe conditions, 65-90 minutes exposure to hypoxia, these experiments allowed insight into the role of neuroserpin within the wider spectrum of neonatal HI severities. The trend towards increased immunoreactivity in the mild conditions mirrors findings in the preterm rat model (see Section 4.3.1). In contrast, following a more severe protocol, the hypoxic-ischaemic and hypoxia-only control subplate became indistinguishable in terms of neuroserpin immunoreactivity, showing an elevated number and proportion of neuroserpin-immunoreactive neurons in both hemispheres. This suggests that the response of the neuroserpin-tPA cascade is closely dependent on the severity of HI injury, and perhaps the mechanisms of cell death which predominate (reviewed in Northington et al., 2001; 2011).

Neuroserpin is unlikely to enact uniform effects across this broad range of conditions, an important caveat to inform future investigations in single severity models of neonatal hypoxia ischaemia. Although this thesis will concentrate on the mild-to-moderate model of neonatal hypoxia ischaemia generated by exposure to 55 minutes of hypoxia, a wider range of models could better inform future studies, especially those which aim at treatment development.

4.3.5 Quantification of Neuroserpin Protein Expression Following Neonatal Hypoxia Ischaemia in Mouse by Cortical Layer

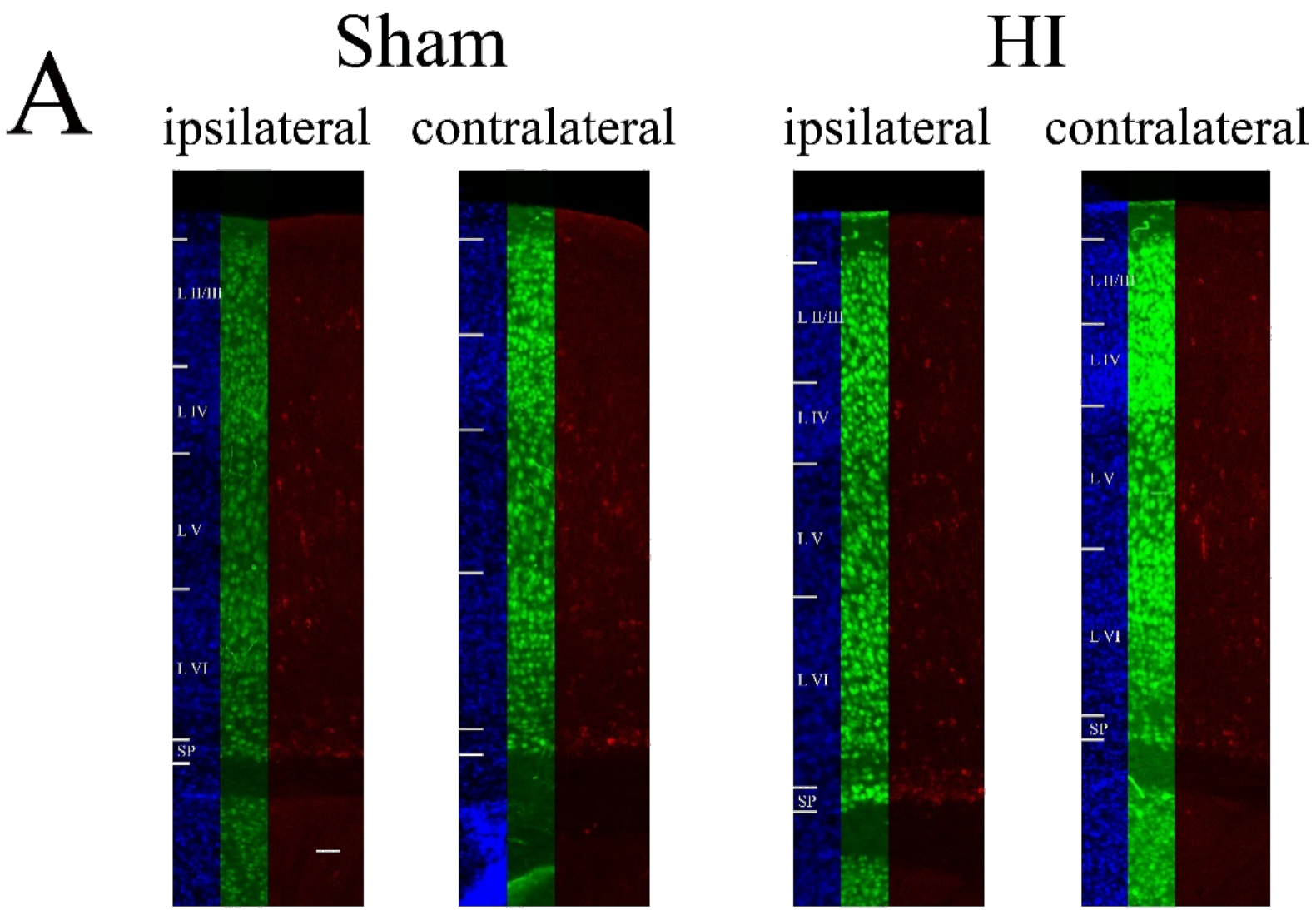
Once preliminary data on neuroserpin immunoreactivity in subplate had been collected from the adapted Rice-Vannucci model of neonatal hypoxia ischaemia, it was important to expand this quantification across all cortical layers in a greater total number of experimental animals. It was important to include brains from a relatively large number of experimental animals. To capture the full range of injury severities produced by this model, 15 hypoxic ischaemic brains across 5 litters and 5 sham-operated control animals were analysed, all following an identical procedure.

Data on the proportion of NeuN-immunoreactive neurons co-immunoreactive for neuroserpin across the cortex closely mirrored findings in the Lausanne rat model. The only cortical layer in which there was a statistically significant difference between the proportion neuroserpin-immunoreactive neuroserpin in the HI hemisphere and that of the hypoxia-only hemisphere or the sham-operated controls was subplate. 57% ± 11% of NeuN-immunoreactive subplate neurons expressed neuroserpin immunoreactivity in the HI hemisphere of experimental brains. This proportion was 37% greater than the percentage of neuroserpin-immunoreactive neurons in either the control hemisphere of the experimental brains, 41% ± 5%, or the sham-operated controls, 41% ± 10%. There was no significant difference in the proportion of neuroserpin-immunoreactive neurons between hemispheres in any other cortical layer at N = 15, although all other cortical layers exhibited similar number of neuroserpin-immunoreactive neurons to those quantified for the developmental time series (see Chapter 3, Section 3.3.1.1). All other layers contained substantially fewer neuroserpin-immunoreactive neurons than subplate, 3-10% ± 3-9% of neurons across

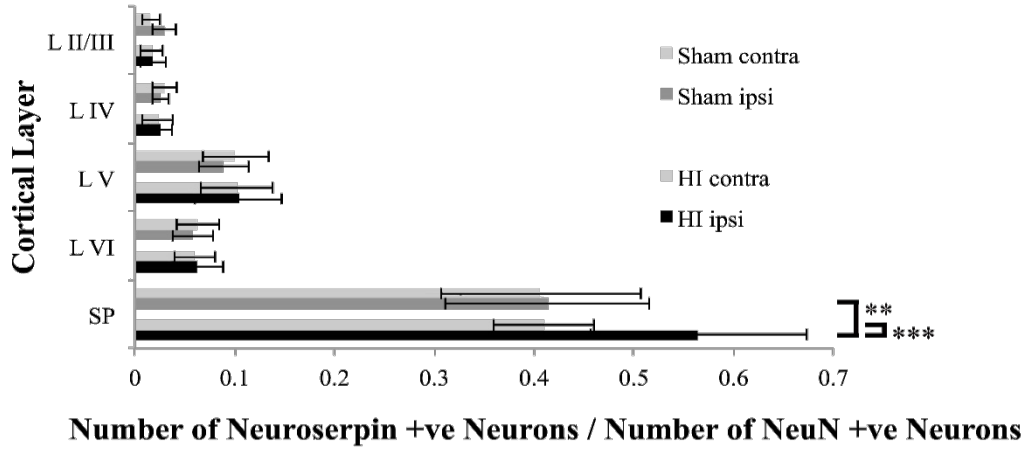
hemispheres and conditions.

This subplate-specific upregulation of neuroserpin immunoreactivity was also apparent when number of neuroserpin-immunoreactive neurons were analysed. In the HI hemisphere of experimental brains, an average of 30 ± 7 subplate neurons were immunoreactive for neuroserpin. This number was 24% greater than the 24 ± 5 neuroserpin-immunoreactive neurons expressed by the hypoxia-only control hemisphere of experimental brains, and 40% greater than the 21 ± 5 neurons expressed in sham-operated controls. No other cortical layers showed a significant difference in the number of neuroserpin-immunoreactive neurons between hemispheres. All demonstrated low numbers of neuroserpin-immunoreactive neurons, between 1-5 ± 1-2 neurons depending on the cortical layer. Results for the whole cortex are summarised in Figure 4.12 and Table 4.11. Figure 4.13 gives an overview of the results for subplate specifically.

As in the perinatal rat model described in Section 4.3.1, there was no significant difference in proportion or number of neuroserpin- or NeuN- immunoreactive neurons in the hypoxia-only hemisphere of the experimental brains and either hemisphere of the sham-operated animals. The variability, as assessed by standard deviation, was greater for the sham-operated controls, although this was likely due to the smaller number of sham-operated animals included in analysis. Variability was greater for the hypoxic-ischaemic hemisphere than for either the sham-operated or hypoxia-only controls. As the mean values and standard deviation for both intracerebral and sham controls were again highly similar, both were recorded as complementary controls.


A
Sham
HI
ipsilateral
contralateral
ipsilateral
contralateral
L II/III
L IV
L V
L VI
SP
L II/III
L IV
L V
L VI
SP
L II/III
L IV
L V
L VI
SP

B



C

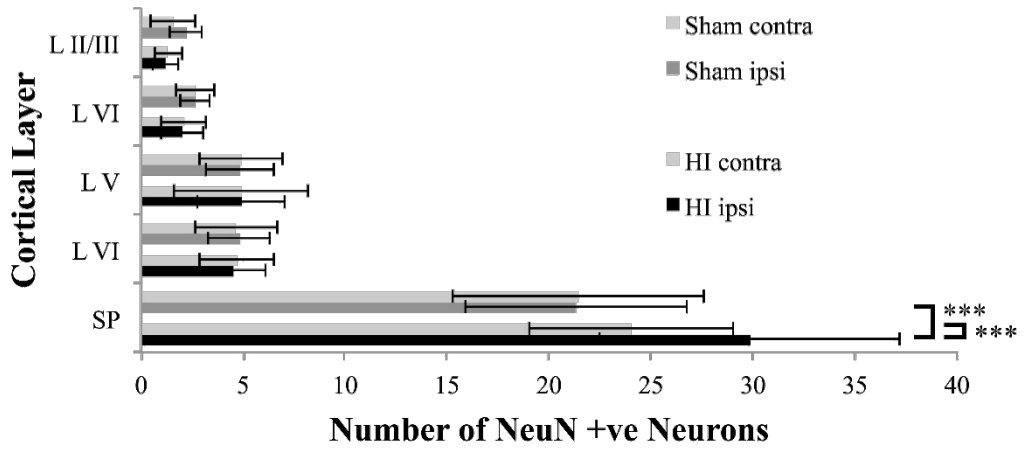


Figure 4.12 – Quantitative Analysis of Neuroserpin Immunoreactivity in Primary Somatosensory Cortex (S1) of P10 C57BL/6J Mouse following the Adapted Rice-Vannucci Model of Hypoxia Ischaemia at P8 under Optimised Conditions of 55 minutes Hypoxia at 10% O_2 Partial Pressure (see Section 4.3.3). A significantly greater proportion of subplate neurons were co-immunoreactive for neuroserpin and pan-neuronal marker neuronal nuclei (NeuN) in the hypoxic ischaemic (HI) ipsilateral (ipsi) hemisphere of the experimental brains compared to the hypoxia-only control contralateral (contra) hemisphere of the experimental brains, or either hemisphere in sham-operated control brains. No statistically significant difference was found in any other cortical layer between any conditions. (A) Representative confocal image of P10 cortical stacks stained for NeuN in green, neuroserpin in red, and DAPI in blue. Scale bars indicate 50µm width areas. (B) Quantitative analysis of the proportion of neuroserpin-immunoreactive cells co-immunoreactive for NeuN per cortical layer (mean ± SD). (C) Quantitative analysis of the number of neuroserpin-immunoreactive cells per cortical layer (mean ± SD). Two-way ANOVA demonstrated a statistically significant difference between groups based on cortical layer and condition for proportion of neuroserpin-immunoreactive neurons relative to the number of NeuN-immunoreactive neurons. Unpaired T-tests were conducted to compare neuroserpin immunoreactivity between HI animals and sham-operated controls, paired T-tests were used to compare neuroserpin immunoreactivity between hemispheres in HI animals undergoing either mild or moderate HI.
Statistical significance was assessed using paired T-test. * denotes P-vale < 0.01, ** denotes P-value < 0.005, *** denotes P-value < 0.001

Genotype	Condition	Age	N	Number of Neuroserpin-Immunoreactive Cells Counted	Number of NeuN-Immunoreactive Cells Counted	Proportion Neuroserpin-Immunoreactive Cells NeuN-Co-Immunoreactive (± SD)
C57BL/6J	HI, 55 Minutes Hypoxia	P10	15	6,943	58,369	0.98 (± 0.02)
C57BL/6J	Sham-Operated	P10	5	2,472	20,625	0.97 (± 0.03)

Table 3.11 – Raw Numbers of Neuroserpin-Immunoreactive Cells Counted relative to the Raw Number of NeuN-Immunoreactive Neurons Counted in Primary Somatosensory Barrel Cortex (S1) of P10 C57BL/6J Mouse following the Adapted Rice-Vannucci Model of Neonatal Hypoxia Ischaemia at P8. Column 7 shows the proportion of neuroserpin-immunoreactive cells relative to the number of NeuN-immunoreactive cells. The number of neuroserpin-immunoreactive neurons in subplate showed a statistically significant increase following mild-to-moderate neonatal HI, however no statistically significant difference in neuroserpin immunoreactivity was recorded in any other cortical layer, complementing the results from the preterm rat model detailed in Section 4.3.1. Two-way ANOVA demonstrated a statistically significant difference between groups based on layer and condition (hemisphere). T-tests were conducted confirm statistical significance between groups.

Detailed quantitative analysis was limited to S1 barrel cortex. However, more global neuroserpin immunoreactivity throughout the brain was observed for qualitative shifts in expression pattern in the sham-operated control and experimental animals. The pattern of neuroserpin expression observed closely mirrored that reported in developmental *in situ* hybridisation studies of *Serpini1* gene expression in mouse (Osterwalder et al., 1996; Krueger et al., 1997; http://mouse.brain-map.org/experiment/show?id=963, last accessed: 13/05/2019; Miller et al., 2014; reviewed in Galliciotti and Sonderegger, 2006) across cohorts. Neuroserpin immunoreactivity was detected throughout neocortex, from S1 through to V1. This cortical enrichment was also observed in allocortex, particularly in Layer 1 of piriform cortex and the olfactory tubercle. Neuroserpin immunoreactivity in the nuclei of the basal ganglia was extremely sparse in sham-operated brains, and demonstrated little qualitative difference in expression pattern in the HI hemispheres of experimental animals, corroborating results of *Serpini1* mRNA localisation studies. In both sham-operated controls and HI brains, neuroserpin immunoreactivity in the hippocampus, particularly within the pyramidal neurons of CA2/3, was strong. This would be an

interesting region to investigate in future studies, as the literature describes neuroprotection (Wu et al., 2010) and plasticity modulation effects (Yepes et al., 2002; Borges et al., 2010) properties for neuroserpin in cultured hippocampal neurons. Another interesting anatomical region which could have been investigated is the thalamus, where *in situ* hybridisation has reported nucleus-specific *Serpini1* mRNA expression patterns (Krueger et al., 1997), including enriched expression in the reuniens nucleus and lateral retuicular nucleus, among others, with little or no expression in the majority of thalamic nuclei. Although pockets of thalamic immunoreactivity were observed in this study, systematic identification of nuclei was not carried out in the hypoxic-ischaemic or control developing brain. *Serpini1* mRNA expression has also been documented in the cerebellum, hypothalamus, and olfactorty bulb (Krueger et al., 1997), where its function is currently unknown.

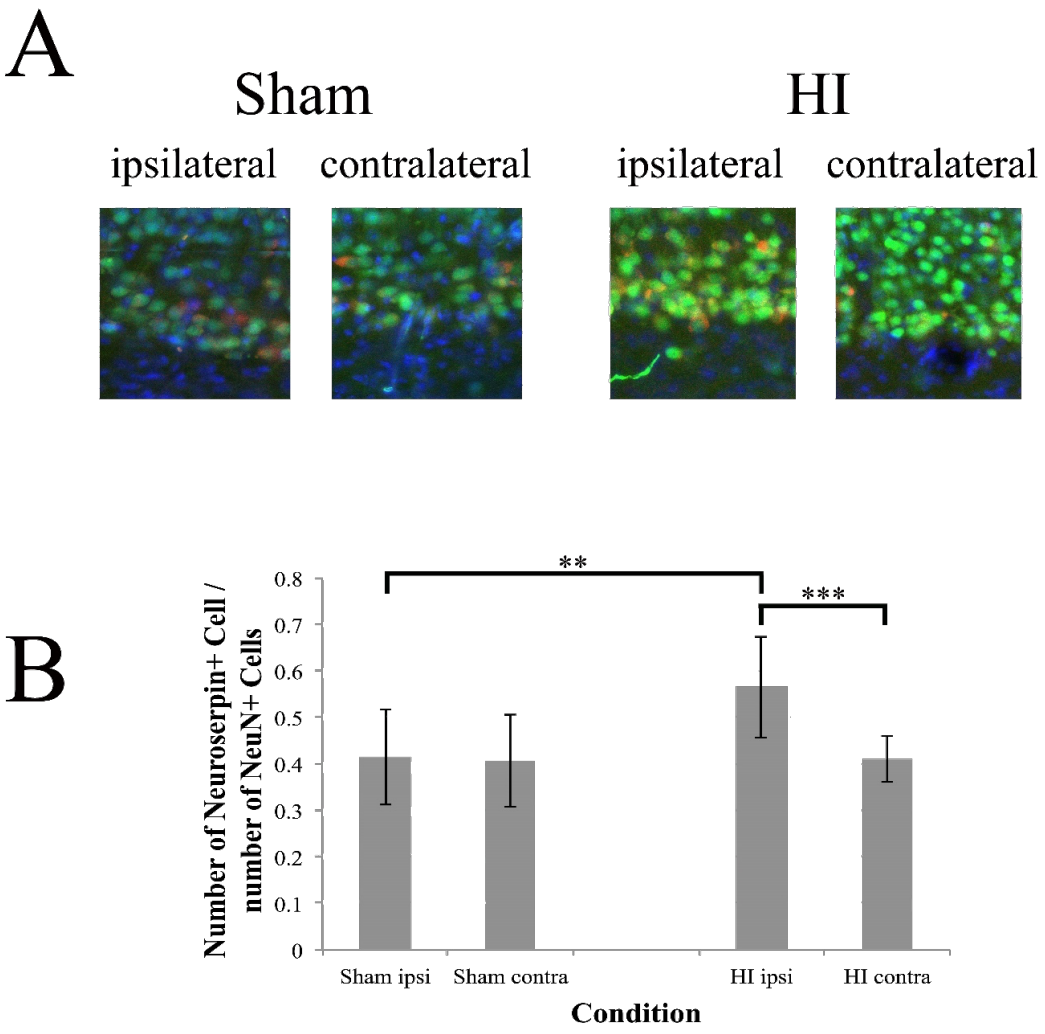


Figure 4.13 – Quantitative Analysis of Neuroserpin Immunoreactivity in Subplate of Primary Somatosensory Barrel Cortex (S1) of P10 C57BL/6J Mouse following the Adapted Rice-Vannucci Model of Neonatal Hypoxia Ischaemia at P8 under Optimised Conditions of 55 minutes Hypoxia at 10% O_2 Partial Pressure A significantly greater number and proportion of subplate neuroserpin-immunoreactive neurons were detected in the hypoxic ischaemic ipsilateral (ipsi) hemisphere of the experimental brains compared to the hypoxia-only control contralateral (contra) hemisphere of the experimental brains, or either hemisphere in sham-operated control brains. (A) Representative confocal image of P10 subplate, taken from cortical stacks, stained for NeuN in green, neuroserpin in red, and DAPI in blue. Scale bars indicate 50 μm width areas. (B) Quantitative analysis of the proportion of neuroserpin-immunoreactive cells co-immunoreactive for NeuN in subplate across conditions (mean ± SD). Two-way ANOVA demonstrated a statistically significant difference between groups based on cortical layer and condition for proportion of neuroserpin-immunoreactive neurons relative to the number of NeuN-immunoreactive neurons. Unpaired T-tests were conducted to compare neuroserpin immunoreactivity between HI animals and sham-operated controls, paired T-tests were used to compare neuroserpin immunoreactivity between hemispheres in HI animals undergoing either mild or moderate HI.
Statistical significance was assessed using paired T-test. * denotes P-vale < 0.01, ** denotes P-value < 0.005, *** denotes P-value < 0.001

From a methodological perspective, both intracerebral control hemispheres and sham-operated animals have limitations, motivating experimental design to include both. Intracerebral controls have the advantage that littermates do not need to be treated as clones, but injured tissue can be compared against healthy tissue from the same animal, eliminating differences in genetics (reviewed in Zurita et al., 2011), intrauterine environmment (Kinsley et al., 1986; reviewed in vom Saal et al., 1990), and parenting (Alleva et al., 1989; Moore and Power, 1992) that might exist between littermates. However, the hypoxia-only hemisphere has been exposed to reduced oxygen, and may contain abnormalities such as those documented in hypoxia-only animal models (see Chapter 1, Section 1.3.4.2, Appendix 8.1), making the hypoxia-only hemisphere not fully representative of healthy tissue.

Although these results present evidence for increased expression of neuronal neuroserpin in the HI hemisphere of the experimental mild-to-moderate HI neonatal mouse brain, there are several limitations to the method. Data on proportions of neuroserpin-NeuN-co-immunoreactive neurons is questioned by studies showing reduced NeuN immunoreactivity in metabolically active neurons following hypoxia (Ünal-Çevik et al., 2004), although this should not affect the validity of the cell number data on neuroserpin-immunoreactive neurons. Additionally, the Rice-Vannucci model has been criticised for initiating a severe vascular injury of little relevance to human neonatal HI pathology (Ment et al., 1989; Hill, 1991). Perhaps the most significant limitation is single duration of hypoxia ischaemia. Section 4.3.3 reveals that neuroserpin immunoreactivity patterns, and perhaps the role of the neuroserpin-tPA cascade, may be qualitatively different under specific severity conditions. The balance between different molecular pathways of cell death is known to shift from apoptosis to necrosis with increasing injury severity (reviewed in

Northington et al., 2001; 2007; 2011), and neuroserpin may interact with these diverse cell death cascades in different ways. One proposed experiment to address this issue could characterise injury severity using Nissl staining (Okusa et al., 2014), or dominant cell death cascade markers (Edwards and Mehmet, 1996; reviewed in Northington et al., 2011), in individual brains to generate an understanding of neuroserpin immunoreactivity post-HI more closely tied to the molecular profile of injury in the individual brains investigated.

This study suggests that neuroserpin protein is not only conserved by the neonatal hypoxic ischaemic rodent brain, but that it may undergo upregulated expression in subplate neurons. In light of extensive work documenting neuroserpin neuroprotection in oxygen glucose deprivation (OGD) *in vitro* (Wu et al., 2010; Rodriguez-Gonzalez et al., 2011a; Ma et al., 2012b) and adult hypoxia ischaemia *in vivo* (Yepes et al., 2000; Cinelli et al., 2001; Gelderblom et al., 2013), the serine-protease inhibitor may serve a similar protective function in the neonatal brain. Although far from a demonstration of a functional protective role, understanding the expression of this neonatally upregulated protein in a model of a potentially relevant neurodevelopmental condition could lead to a new set of candidate therapeutic molecules.

4.3.6 Semi-Quantitative Analysis of Total Cortical Neuroserpin Protein Following Neonatal Hypoxia Ischaemia in Mouse

In order to quantitatively determine whether the upregulation in subplate neuroserpin immunoreactivity described above is linked to a substantial increase in total neuroserpin protein following exposure to neonatal hypoxia ischaemia by the

optimised adapted Rice-Vannucci method in mouse, semi-quantitative Western blot was used to detect neuroserpin across the two hemispheres. Band intensity was analysed as described in Section 4.2.4.

There was no statistically significant difference in total neuroserpin protein content between the hypoxic ischaemic and hypoxia-only control cortical hemispheres after stain-free normalised band intensity values were averaged across 11 animals. When 3µg cortical protein was loaded from each hemisphere, the mean average normalised band intensity (in arbitrary intensity units generated by Image Lab™) was 4.9×10^7 ($\pm 4.6 \times 10^7$) in the HI hemisphere, compared to 4.5×10^7 ($\pm 3.9 \times 10^7$) in the hypoxia-only control hemisphere. A paired two-tailed T-test gave a P-value of 0.57, far from the lower bound of statistical significance. When 6µg cortical protein was loaded from each hemisphere, average normalised band intensity was measured as 6.4×10^7 ($\pm 6.4 \times 10^7$) in the HI hemisphere and 5.3×10^7 ($\pm 7.5 \times 10^7$) in the hypoxia-only hemisphere. Analysed separately, this higher loading volume produced a high P-value of 0.41 from a paired two-tailed T-test. Results are summarised in Figure 4.14. Lack of statistical significance was verified by independent analysis of the data by Dr. Kristina Parley (unpublished).

When averaged across all animals, it is clear that there is no systematic difference in neuroserpin total protein content between the hypoxic ischaemic and hypoxia-only control cortical hemispheres of mice exposed to mild-to-moderate neonatal HI using the adapted Rice-Vannucci model described in Section 4.2.1 and 4.3.2.

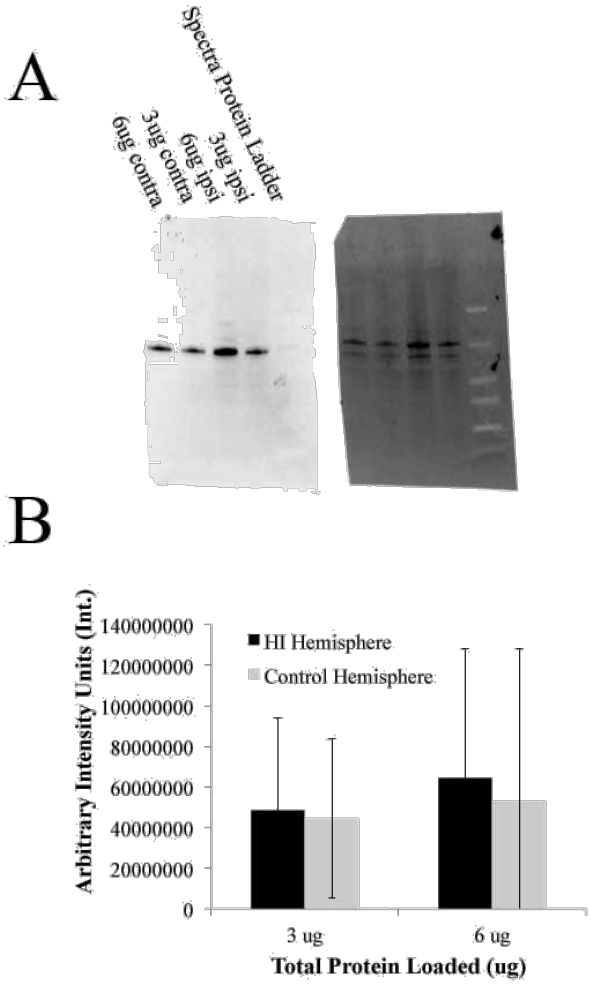


Figure 4.14 – Semi-Quantitative Western Blot Analysis of Total Neuroserpin Protein Content in the Hypoxic-Ischaemic Ipsilateral Hemisphere compared to Hypoxia-Only Intracerebral Control Contralateral Hemisphere of P10 Mice following Neonatal Hypoxia Ischaemia (HI) by the Optimised Adapted Rice-Vannucci Model at P8. There was no statistically significant difference in neuroserpin protein content between the two cortical hemispheres at N = 11. (A) Representative images of polyvinylidene fluoride or polyvinylidene difluoride (PVDF) membranes taken using a Bio-Rad ChemiDoc™ XRS+ imaging station. Left: ECL staining image taken using chemi-image settings. Right: stain-free image taken using stain-free settings. (B) Quantitative analysis of normalised band intensity in the HI hemisphere relative to the hypoxia-only hemisphere at two total protein loading conditions, 3µg and 6µg. The two loading conditions were analysed separately throughout. Mean average normalised band intensity as calculated by Bio-Rad Image Lab™ software for each hemisphere are shown. Error bars represent ± one standard deviation (±SD).

High variability in injury severity has been reported between brains undergoing Rice-Vannucci neonatal hypoxia ischaemia, even when carried out by the same experimenter (reviewed in Vannucci and Hagberg, 2004; Vannucci and Vannucci,

2005), which makes a large cohort of experimental animals essential. Differences in severity between different animals within the same cohort may also account for patterns within the data. For example, when 6μg protein was loaded, 4 of 11 animals demonstrated a band intensity of greater than 1.5 times the hypoxia-only control band in the hypoxic-ischaemic hemisphere. However, in the absence of detailed severity categorisation of individual brains, which could have removed damaged regions from Western blot analysis, it is impossible to meaningfully interpret the variation in results recorded here. Potentially, severity classification of brains could have been achieved by dissection of fresh tissue to remove small portions for histological analysis, or by conducting parallel Western blot for a molecular marker of injury, such as cleaved caspase-3 (reviewed in D'Amelio et al., 2010). It remains possible that there exist severity levels in which total cortical neuroserpin protein content exhibits robust and genuine change. This experiment was designed to complement conditions under which a subplate-specific increase in neuroserpin-immunoreactive neurons was detected using fluorescent immunohistochemistry (see Section 4.3.5), and therefore this experiment is sufficient to document that subplate-specific neuroserpin upregulation is not a product of greatly increased total cortical neuroserpin protein relative to control levels of total cortical protein. It would also have been interesting to convert this investigation to a truly quantitative measure using a purified recombinant protein standard. At the time of writing, only recombinant human neuroserpin protein was commercially available (#130-14, PeproTech EC Ltd., London, UK, see Chapter 5, Section 5.3.1.1). However, a recombinant mouse neuroserpin prtoein has recently become commercially available (#50926-M08H, Sino Biological., Pennsylvania, USA), which could be used to carry out this type of experiment in future.

Overall, the results support a conservation of cortical neuroserpin protein in the acute post-injury period in neonatal hypoxic ischaemic mouse. This complements previously conducted microarray studies which fail to find a change in cortical *Serpini1* mRNA expression following neonatal HI in rodents (Carmel et al., 2004; Maj et al., 2004a; 2004b; Juul et al., 2009; Nagel et al., 2012; Rognlien et al., 2014), [WEAK] ruling out the possibility of substantial change at the level of transcription. Although the semi-quantitative nature of Western blot does reduce its sensitivity to detection of small genuine changes in protein expression (Mollica et al., 2009; reviewed in Gassmann et al., 2009; Taylor and Posch, 2014), as will be discussed further below, it is reasonable to conclude from this experiment that no large-scale hemisphere-specific change in neuroserpin expression occurs in the neonatal HI cortex in the first 48 hours after injury. Industrial translation and redistribution of neuroserpin protein are unlikely to take place in the acute post-injury phase following mild neonatal hypoxia ischaemia in rodents.

4.4 Discussion

This chapter describes the expression profile of neuroserpin protein in the neocortex following models of neonatal hypoxia ischaemia in rodents. Although fluorescent immunohistochemistry detected a subplate-specific increase in neuroserpin-immunoreactive neurons in hypoxic-ischaemic rat and mouse, semi-quantitative Western blot analysis found no significant difference in neuroserpin protein levels between the two hemispheres of the hypoxic-ischaemic mouse brain.

4.4.1 Satisfaction of Chapter Aims

Experiments presented in this chapter were conducted in accordance with aims stated in full in Section 4.1.1. This study achieved success in quantifying the pattern of neuroserpin protein expression during the acute response to neonatal hypoxia ischaemia. However, these results also raised further questions that can only be addressed by different experimental techniques. Implications of the most significant results will be discussed in detail below.

Initial aims were also satisfied in the development of an adapted mouse model of mild-to-moderate neonatal hypoxia ischaemia, based on the Rice Vannucci method (Rice et al., 1981; reviewed in Millar et al., 2017), with immunohistochemistry for glial markers of brain inflammation confirming brain injury in accordance with models of mild neonatal HI previously reported in the literature (Gubits et al., 1993; Dreier et al., 2000; Dijkstra et al., 2000; reviewed in Girard et al., 2009). This systematic optimisation over different severity conditions accounting for qualitative shifts in molecular cell death cascades at different severities of HI (reviewed in Northington et al., 2001; 2007; 2011), and revealed multiple unique patterns of cortical neuroserpin immunoreactivity which would not have been accessible if only a single set of conditions had been investigated. Extensive quantification using optimised conditions, 55 minutes hypoxia and 48 hours collection post-injury, revealed a novel subplate-specific 37% increase in the proportion of neurons immunoreactive for neuroserpin, complementing results from a preterm rat model (Ginet et al., 2009a; 2009b; Okusa et al., 2014). Thus, neuroserpin expression is not only conserved in the acute injury period following neonatal hypoxia ischaemia, but may undergo active redistribution within the developing cortex.

The aim to investigate total neuroserpin protein content of the neocortex following neonatal hypoxia ischaemia in mouse was fulfilled using N equivalent to previous studies which have detected altered protein expression as a result of neonatal hypoxia ischaemia using Western blot experiments (Hagberg et al., 2004; Yata et al., 2007; Li et al., 2007; Carloni et al., 2008), yet produced a null result. It is possible that quantitative changes detected using immunohistochemistry are either too localised to be detected by semi-quantitative Western blot, or represent a redistribution as opposed to synthesis of neuroserpin protein within the developing cortex.

4.4.2 Neuroserpin Expression Following Neonatal Hypoxia Ischaemia

Intracellular neuroserpin protein expression was characterised by fluorescent immunohistochemistry in mouse pups which underwent a neonatal hypoxic ischaemic procedure based on the Rice-Vannucci method (Rice et al., 1981; reviewed in Millar et al., 2017) at P8. The left common carotid artery was ligated under anaesthesia followed by 55 minutes of hypoxia at 10% O2 partial pressure at 37°C. Acute brain injury was confirmed by increased glial molecular marker immunoreactivity in the hypoxic-ischaemic hemisphere of experimental brains. The model was optimised to generate mild-to-moderate injury, as quantified by these markers.

A statistically significant difference in the proportion of neuroserpin-immunoreactive subplate neurons was detected between the hypoxic-ischaemic hemisphere of experimental brains (57% ± 11%), the hypoxia-only hemispheres of the same brains (41% ± 5%) and sham-operated controls (41% ± 10%). No significant difference between the number or proportion of neuroserpin-immunoreactive neurons was documented for any other cortical layer. This analysis revealed that neuronal

neuroserpin is conserved, during the acute post-injury period in both mouse and rat, although semi-quantitative Western blot results argue against active upregulation throughout neocortex.

Neuroserpin may form part of the developing brain's innate response to neonatal hypoxic ischaemic injury. One known enzymatic target of neuroserpin, tissue plasminogen activator (tPA), is already known to contribute to the pathogenesis of neonatal hypoxia ischaemia in animal models. tPA was secreted by the cerebral microvasculature following neonatal HI in mouse (Henry et al., 2013), where it has a deleterious effect on neuronal metabolism. Administration of exogenous tPA in neonatal rodents exacerbated ischaemic brain injury (Adhami et al., 2008; Omouendze et al., 2013), whereas tPA inhibitors α2-antiplasmin (α2AP) (Adhami et al., 2008) or plasminogen activator inhibitor 1 (PAI1) (Yang et al., 2013; Yang and Kuan, 2015) were neuroprotective. Despite these publications, the tPA cascade is relatively understudied in neonatal hypoxia ischaemia. This may be explained by the absence of tPA and its inhibitors from microarray studies tracking changes in gene expression following rodent neonatal HI (Carmel et al., 2004; Maj et al., 2004a; 2004b; Nagel et al., 2012; Rognlien et al., 2014), which do not detect proteins regulated at the level of secretion or translation.

A novel finding reported is the subplate-specificity of changes following neonatal hypoxia ischaemia. This suggested that the relatively mature secretory system within subplate neurons may take on a functionally distinct role in cortical injury. Subplate neurons are known to be enriched in secreted proteins (Belgard et al., 2011; Hoerder-Suabedissen et al., 2013; Kostović et al., 2014), including neuroserpin (Kondo et al.,

2015), around P8. The role of subplate-secreted molecules for cortex globally remains largely unknown, but could be a focus for rapid distribution of anti-injury proteins.

Brains used in these investigations were not stratified by injury severity prior to neuroserpin immunoreactivity analysis. Previous publications have conducted severity classification based on histological (Okusa et al., 2014) or biochemical (Ikeda et al., 2002) markers of brain damage. This method can reduce variability, and may allow results to be detected with only occur within a narrow severity range. This can be particularly helpful when brain damage associated with a specific anatomical region is targeted, or when seeking to address only mild or severe injury. However, these categories are artificial in definition, with different papers using different histological features (Okusa et al., 2014; Mikhailova et al., 2017) and different lesion volumes (Ikeda et al., 2002; Ten et al., 2003) to define their "severe" category. Additionally, results which only apply to a single severity category are more likely to reflect a false-positive. This is especially true if outliers which do not fit any severity category, such as brains with no apparent lesions, are excluded although these animals may have gone on to develop behavioural phenotypes or a primarily tertiary late injury (Fleiss and Gressens, 2012).

This study did use the severity categories reported in Okusa et al., 2014 to inform the decision to design a mild-to-moderate mouse model of neonatal HI. If no difference in neuroserpin immunoreactivity across mild or moderate preterm rat brains had been detected, a more severe model would likely have been employed. Individual postnatal HI mouse brains were quantitatively assessed for brain injury, and spanned the spectrum from little to no discernible lesions to mild and moderate decrease in cortical thickness. No brains showed histological evidence of cortical scarring or

decreased NeuN-immunoreactive cells numbers, which might have indicated severe brain injury. However, as neuroserpin was being considered as a potential neuroprotective molecule, it was also important that results held across a range of severities as hypothermia does in human infants (reviewed in Tagin et al., 2012), reflecting the unknown outcome of neonatal HI in human patients at the time of therapeutic intervention.

Interpretation of these results is limited by the nature of immunohistochemistry. Only dense intracellular localisations of protein can be clearly recognised. Additionally, NeuN immunoreactivity, which was used here to classify neuroserpin-immunoreactive cells as neurons, may be decreased in surviving neurons following HI (Ünal-Çevik et al., 2004). This reduces the reliability of the proportion of neurons immunoreactive for neuroserpin following HI, but not all surviving neurons are necessarily labelled. Models based on the Rice-Vannucci technique generate large variation in lesion size and severity between animals (reviewed in Vannucci and Hagberg, 2004; Vannucci and Vannucci, 2005). Future experiments could resolve these concerns by employing a range of conditions *in vitro* and *in vivo*.

The role of the neuroserpin-tPA pathway in endogenous brain response to neonatal hypoxia ischaemia in humans could be assessed in future experiments. Tissue from hypoxic ischaemic neonates is currently available from some UK brain banks (Lindsay et al., 2016), and could be used to correlate expression of neuroserpin-tPA cascade proteins with severity of injury. This step will be essential before the therapeutic potential of these molecules as a human treatment can be evaluated.

It would also be interesting to interrogate the role of subplate in neuroserpin-mediated neuroprotection *in vitro*. Cortical slice cultures (Molnár and Blakemore, 1991; Götz

and Bolz, 1992; reviewed in Humpel, 2015) from animals with fluorescently-labelled subplate neurons, for example the Lpar1-eGFP mouse (Grant et al., 2012) or the Drd1a-Cre mouse (Hoerder-Suabedissen et al., 2018), could be grown *in vitro*. The effect of OGD could be investigated in intact slices, and those in which subplate has been removed.

4.4.3 Evaluation of Methodology

Total neuroserpin protein content of cerebral cortex was examined using semi-quantitative Western blot (Towbin et al., 1979; Taylor et al., 2013; reviewed in Taylor and Posch, 2014). This allowed an objective comparison, spanning both intracellular and extracellular pools, of secreted protein neuroserpin (Osterwalder et al., 1996) between the hemispheres of hypoxic-ischaemic mouse brains (Yager et al., 1991; 1992; 1996; Vannucci and Yager, 1992). There was no significant difference in neuroserpin content between hemispheres 48 hours after surgery.

This result reveals that neuroserpin is present in the hypoxic-ischaemic brain, but does not undergo substantial upregulation 48 hours post-injury. Any genuine change in intracerebral neuroserpin distribution may occur at a more local scale, allowing detection by immunohistochemistry but not semi-quantitative Western blot.

This null result at first appears incompatible with immunohistochemistry experiments discussed in Section 4.4.2. The Western blot data does appear to refute the possibility that certain neuroserpin immunoreactive subplate neurons in the brain are acting as a ‘secretory powerhouse’ (Kondo et al., 2015; reviewed in Millar et al., 2017), with several-fold increases in neuronal protein synthesis accounting for redistribution of

neuroserpin. Yet this conclusion also opens the possibility of more nuanced, localised, mechanisms of neuroserpin trafficking which could still support a neuroprotective role for this protein in an injured developing brain state where resources for protein synthesis are known to be limited (Mies et al., 1991; Hossmann, 1993; reviewed in Saugstad, 1996). Other mechanisms which could lead to functional enrichment of neuroserpin in subplate, independent of mass translational increase, include: selective uptake from the extracellular matrix (ECM); trafficking from the endoplasmic reticulum (ER) (Miranda et al., 2004; Davies et al., 2009; Ordónez and Marciniak, 2015) production of alternative splice variants (https://www.ncbi.nlm.nih.gov/refseq/, last accessed: 09/05/2019; O'Leary et al., 2016); or post-translational modification (Tapocik et al., 2016). Evidence from other members of the serpin superfamily of serine protease inhibitors show that any of these modifications may occur (Perlmutter et al., 1990; Nash et al., 2000), yet only alternative splicing has been confirmed as relevant to neuroserpin specifically (https://www.ncbi.nlm.nih.gov/refseq/, last accessed: 09/05/2019). Although promotor regulation of Serpini1 expression may play a role at later stages of injury development (Dutta et al., 2015; Bartoletti-Stella et al., 2018). It is also possible that enzyme dynamics are altered in the hypoxic state, with stability of neuroserpin-tPA complex, possible existence of a 'latent' form of neuroserpin, and cleavage of the enzyme itself all areas for potential functional modulation *in vivo* that have only been studied in purified protein to date (Osterwalder et al., 1998; Hill et al., 2001). All these potential mechanisms require thorough investigation *in vitro*. Generation of neuroserpin protein residues coupled to fluorescent FLAG™ moieties (Shi et al., unpublished; reviewed in Einhauer et al., 2001; Young et al., 2012) could be used to identify neuroserpin using high-resolution

confocal microscopy, allowing this protein to be tracked between intracellular compartments in neurons subjected to OGD.

It is also possible that this null result is due solely to the relatively small proportion of total cortical volume that is the subplate layer. This would be the simplest conclusion, and one that could be readily tested by experiment. Layer-specific cultures could be generated from the Lpar1-eGFP (Grant et al., 2012) or Drd1a-Cre (Lemberger et al., 2007; Hoerder-Suabedissen et al., 2018) mice which allow identification of subplate neurons by the presence of fluorescent molecules. This method would allow protein translation, trafficking, uptake, and secretion to be compared between different cortical layers.

There are several limitations to the interpretation of this work. Perhaps the most significant is the fundamental nature of the methodology itself, which is rarely described by researchers as more than 'semi-quantitative'. Although care was taken during experimental design to include the most robust available normalisation method, individual investigators are still susceptible to generate different intensity or volume value for the same Western blot band (Mollica et al., 2009; reviewed in Gassmann et al., 2009; reviewed in Taylor and Posch, 2014). One reviewer has claimed that densitometry techniques for analysing Western blot images have 'no sound scientific basis', with valid experiments into expression of a single protein by different experimenters producing P-values ranging between highly significant and not significant depending on analytical technique (Gassmann et al., 2009). Semi-quantitative Western blot is not a high precision tool. However, in the context of this experiment, it is likely that any genuine change in neuroserpin expression across

cortex is relatively minor, and that an upsurge in cortical neuroserpin does not occur 48 hours following mild neonatal hypoxia ischaemia in mouse.

Other limitations are independent of the semi-quantitative Western blot method. The first is the dissection of whole cortex for protein extraction. Although this crude approach gave helpful information concerning global neuroserpin protein in neonatal HI, a natural further investigation would be to employ anatomical microdissection techniques (Ladanyi et al., 2006; Wang et al., 2009; Molnár, 2011; Oeschger, 2011) to measure the neuroserpin content of subplate. Other potentially important variables which were not captured here are the progression of injury response with time, as unique and overlapping transcriptional profiles are known to be activated in the rodent brain 2, 8, 24, and 72 hours after exposure to hypoxia (Maj et al., 2004a; 2004b; Shankaran et al., 2005). The relative dearth of knowledge about *Serpini1* splice variants, cleaved neuroserpin (Osterwalder et al., 1998), and how these affect tertiary protein structure and antibody binding could all have affected the outcome of this experiment. These limitations mostly reflect the complexity of enzyme biology, and the great depth in which neuroserpin could be explored in future.

There are two directions for future research informed by these experiments. The first, and most crucial, is establishing neuronal tolerance of elevated concentrations of neuroserpin protein during development and neonatal hypoxia ischaemia. Relatively little is known about the effect of augmenting expression of other analogous protein inhibitors on the neonatal brain, broadening the relevance of toxicity testing to other candidate therapies such as PAI-1 (Yang et al., 2013; Yang and Kuan, 2015).

4.4.4 Conclusions

This chapter reports on neuroserpin throughout cerebral cortex during the acute post-injury response in rodent neonatal hypoxia ischaemia. Despite semi-quantitative Western blot documenting no significant difference in total neuroserpin protein between the hypoxic-ischaemic and hypoxia-only hemispheres in neonatal mouse brains, fluorescent immunohistochemistry detected an increased number and proportion of neuroserpin-immunoreactive neurons in the subplate layer, which may represent local redistribution in response to injury.

A mouse model based on the Rice-Vannucci model of neonatal hypoxia ischaemia (Rice et al., 1981) was developed and verified as causing mild-to-moderate brain injury. The model was associated with statistically significant increases in three inflammatory glial markers. A novel subplate-specific increase in the proportion of neurons immunoreactive for neuroserpin was detected, from 41% (+/- 10%) in sham-operated controls and 41% (+/- 5%) in the hypoxia-only hemisphere of the experimental brains, to 57% (+/- 11%) in the hypoxic ischaemic hemisphere.

In contrast, although substantial variation in total neuroserpin protein was found between brains of different animals, no overall difference was found in total neuroserpin protein content between the hypoxic ischaemic and hypoxia-only control hemispheres. The local subplate-enrichment of neuroserpin protein detected by immunohistochemistry may be caused by a redistribution or activation of neuroserpin already present within the cortex. Cortical layer-specific neuronal cultures *in vitro* are needed to establish which cells are secreting neuroserpin, and purified protein injection *in vivo* to determine whether macroscopic intracerebral elevations in total neuroserpin can be tolerated by the developing brain.

5 Preliminary Investigations into Vulnerability to Neonatal Hypoxia Ischaemia in the Absence of Neuroserpin Protein, using the *Serpini1* Knock-Out Mouse

5.1 Introduction

There exists considerable evidence that, in a laboratory setting, neuroserpin protein plays a role in injury severity in adult rodent models of ischaemic stroke (Yepes et al., 2000; Cinelli et al., 2001; Zhang et al., 2002; Gelderblom et al., 2013; reviewed in Yepes and Lawrence, 2004a; 2004b; 2004c; Millar et al., 2017).

Despite the pathophysiological and developmental differences between the infant and adult ischaemic brain (reviewed in Baburamani et al., 2012; Millar et al., 2017), methods used to simulate hypoxia-ischaemia are analogous across both time-points (Eklöf and Siesjö, 1973; Rice et al., 1981; Bederson et al., 1986). Evidence supporting a functional role for neuroserpin in adult ischaemic stroke has been documented in transgenic mice lacking neuroserpin expression. These animals develop larger brain lesions and more widespread inflammation than wild-type controls (Cinelli et al., 2001; Gelderblom et al., 2013). Conversely, elevated intracerebral neuroserpin protects against ischaemic stroke by decreasing lesion volume in adult rats injected with exogenous neuroserpin prior to surgery (Yepes et al., 2000; Zhang et al., 2002) and in adult transgenic mice over-expressing *Serpini1* mRNA (Cinelli et al., 2001). Protective effects of exogenous neuroserpin have also been described in plasminogen activator tissue type (*Plat*) knock-out mice (Wu et al., 2010; Gu et al., 2015).

The literature on neuroserpin is not restricted to *in vivo* surgical ligation studies. *In vitro*, the neuroprotective properties of neuroserpin have been investigated by subjecting dissociated neurons to oxygen glucose deprivation (OGD), a widely used model of hypoxia in culture (Goldberg and Choi, 1993; Strasser and Fischer, 1995; Copin et al., 1996; Taylor et al., 1999). A neuroprotective effect was discovered when exogenous neuroserpin was administered directly after OGD at doses between 0.125-1μM in rat mixed cortical neuron and astrocyte cultures (Rodríguez-Ganzález et al, 2011a). Other independent investigators found a similar effect when 900nM/L exogenous neuroserpin was added to rat cortical neurons 4 or 24 hours after OGD, neuronal viability was increased (Ma et al., 2012b). Exogenous neuroserpin was also protective against OGD-induced cell death in cortical neurons from *Plat* knock-out mice (Wu et al., 2010). However, the role of endogenous neuroserpin in the neuronal response to oxygen glucose deprivation is yet to be investigated, with no studies altering intracellular production of neuroserpin or including cells isolated from *Serpini1* transgenic mice.

The *Serpini1* knock-out mouse, B6.129-Serpini1^{tm1Dpw}/J, facilitated the first investigation of the role of neuroserpin in adult ischaemic stroke *in vivo*. Following stroke induced by surgical ligation of the left middle cerebral artery, *Serpini1* knock-out animals exhibit larger lesion volumes at seven days post-injury and greater tPA expression assessed by zymography compared to wild-type controls (Cinelli et al., 2001). *Serpini1* knock-out mice show lower survival rates, increased microglial numbers in the hippocampus, and higher microglial activation marker expression (Gelderblom et al., 2013). *Serpini1* over-expression mice, which generate three to six times the *Serpini1* mRNA produced by wild-type animals, display smaller lesions (Cinelli et al., 2001). In the absence of procedures, *Serpini1* knock-out mice exhibit

normal gross brain anatomy, fertility, breeding, spontaneous motor activity, and weight maintenance (Madani et al., 2003). An anxiety phenotype has been reported, as *Serpini1* knock-out animals display less exploratory behaviour in the novel object and open field tests compared to wild-type littermates, although this difference was not evident in all tests, including the elevated plus-maze (Madani et al., 2003).

This chapter undertakes the replication of previous experiments in the *Serpini1* knock-out mouse in an established neonatal model of hypoxia ischaemia, and in the oxygen glucose deprivation model *in vitro*. If neuroserpin contributes to neuroprotection in the neonatal brain, greater sensitivity to models of hypoxia ischaemia would be expected in the *Serpini1* knock-out both *in vitro* and *in vivo*.

5.1.1 Aims of Chapter 5

An adapted Rice-Vannucci method was carried out in mice, at the brain development time-point equivalent to birth in humans (Clancy et al., 2007), to investigate the possible generality of neuroserpin neuroprotection in adult ischaemic stroke to the developing infant brain. Dissociated neuronal culture experiments were also designed to probe the sensitivity of neurons from the *Serpini1* knock-mice to OGD.

1) The role of endogenous neuroserpin was investigated *in vitro* by culturing dissociated primary cortical neurons from E18 *Serpini1* knock-out and wild-type mice then exposing these to oxygen glucose deprivation (OGD).

i) Metabolic marker 3-(4,5-dimethylthiazol-2-yl)-2,5-diphenyltetrazolium bromide (MTT) was used to measure the approximate number of metabolically active viable neurons in culture 0, 2, 4, and 8 hours following OGD in B6.129-Serpini1^{tm1Dpw}/J *Serpini1* knock-out mice and C57BL/6J mice.

ii) Neuroprotective properties of exogenous neuroserpin were investigated by applying 1, 5, 10, 20, 40, or 60 ng/ml purified neuroserpin protein administered as pre-treatment 4 hours prior to OGD or as post-treatment directly following OGD.

2) The vulnerability of the *Serpini1* knock-out mouse to neonatal hypoxia ischaemia *in vivo*, generated by an adapted Rice-Vannucci method, was compared to wild-type littermate controls.

i) Animals were perfused with metabolic marker 2,3,5-triphenyl tetrazolium chloride (TTC) 48 hours after neonatal hypoxia ischaemia, intensity of TTC staining was quantified.

ii) Fluorescent immunohistochemistry for inflammatory markers glial fibrillary acidic protein (GFAP), ionized calcium binding adaptor molecule 1 (Iba1), and cluster of differentiation (CD68) was carried out as a secondary method to quantify brain damage.

5.2 Methods

Animal husbandry and tissue collection are described in Chapter 2, Sections 2.1 and

2.2, respectively. The full protocol for neonatal hypoxia ischaemia in wild-type mice is described in Chapter 4, Section 4.2.1. The modifications required for litters bred from B6.129-Serpini1^{tm1Dpw}/J heterozygotes are detailed in this chapter, Section 5.2.3.

5.2.1 Dissociated N2A Neuroblastoma Cell-Line and Cortical Neuronal Culture

All *in vitro* experiments were conducted in collaboration with Professor Lei Shi of Jinan University, China, who spent her sabbatical year at the Department of Physiology, Anatomy, and Genetics (DPAG), University of Oxford, UK, from September 2015 to April 2016. Neuro-2-A (N2A) neuroblastoma cell lines were used to optimise parameters for oxygen glucose deprivation (OGD). Methods used to culture and maintain N2A cells are detailed in Section 5.2.1.1 and Figure 5.1. Primary cortical neurons from E18 C57BL/6J wild-type and B6.129-Serpini1^{tm1Dpw}/J *Serpini1* knock-out mice were used to investigate the neuroprotective properties of exogenous purified neuroserpin protein in cortical neurons following OGD. Methods used to isolate, culture and maintain primary dissociated cortical neurons are detailed in Section 5.2.1.2 and Figure 5.2.

5.2.1.1 N2A Neuroblastoma Cell Culture

Mouse Neuro-2A (N2A) neuroblastoma cells were purchased frozen from the American Tissue Culture Collection (ATCC® #CCL-131™) at P179 (https://www.lgcstandards-atcc.org/products/all/CCL-131.aspx, last accessed: 01/10/2018). N2A cells were cultured in accordance with methods described in

Professor Shi's previous publications (Xiao et al., 2013; Tang et al., 2016; Xiang et al., 2016). Figure 5.1 summarises the method used to maintain these cells.

Frozen N2A cells were thawed in a Grant SUB Aqua 12 water bath (#SAP12, Grant Instruments, Royston, UK) set to 37°C for approximately 2 minutes, until the contents were fully liquid. The contents of the vial were transferred to a sterile 50ml Eppendorf tube containing 10ml N2A growth medium. The composition of growth medium, and other solutions used in storage and maintenance of N2A cells, are shown in Table 5.1. Tubes were spun at 800 rpm for 5 minutes in an Eppendorf Centrifuge 5702 (#5702000365, Eppendorf UK Ltd., Stevenage, UK) to remove cryoprotectant dimethyl sulphoxide (DMSO) present in the freezing medium. The supernatant was discarded and cells were resuspended in 10ml N2A growth medium in a $75cm^2$ tissue culture flask (Nunc™ EasYFlask™ Cell Culture Flasks, #159920, Thermo Fisher, Hemel Hempstead, UK).

N2A cells were maintained inside a SANYO™ MCO-17AIC CO_2 cell culture incubator (#5.519.188, VWR International, Leicestershire, UK) suffused with 5% CO_2 gas (BOC, Linde Group, Guildford, UK) at 37°C. Cells were cultured in N2A growth medium and sub-cultured at a ratio of 1:10 every three days.

To subculture, growth medium was removed and the cell monolayer washed with 5ml sterile 0.1M D-PBS (#14200-075, Thermo Fisher, Hemel Hempstead, UK) inside a Microflow Laminar Downflow Work-Station biological safety cabinet (#JALO76 AK19, VWR International, Leicestershire, UK). 1ml of 0.25% trypsin-EDTA (#25200-056, Thermo Fisher, Hemel Hempstead, UK) was added to the flask to dissociate N2A cells from the cell monolayer. N2A cells detached in less than 5 minutes, appearing spherical when viewed at 20x magnification under a light

microscope Nikon SMZ645 (#M219 E, Nikon Instruments Europe, Amsterdam, The Netherlands). Once cells became fully detached, 9ml growth medium was added to the flask to deactivate trypsin. 1ml of medium containing N2A cells was added to a new 75cm^2 tissue culture flask prefilled with 9ml warmed growth medium.

N2A cells required for oxygen glucose deprivation (OGD) optimisation were plated on autoclave-sterilised 24-well culture plates (Corning® Costar® TC-Treated Multiple Well Plates, #CLS3527, Sigma Aldrich, Gillingham, UK). Cells were allowed to recover from plating for 24 hours prior to experimental intervention.

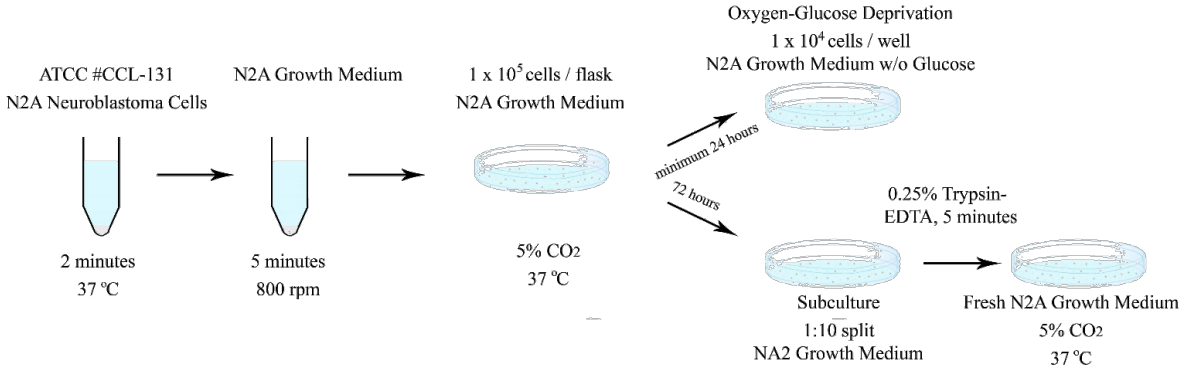


Figure 5.1 – Schematic Diagram Depicting Maintenance and Sub-Culture of N2A (Neuro-2A) Neuroblastoma Cells Used for Oxygen-Glucose Deprivation (OGD) Optimisation Experiments.

Solution	pH	Reagents	Quantity	Supplier
N2A Growth Medium	-	DMEM, high glucose, without L-glutamine	250ml	Thermo Fisher, 12491-015
		Foetal bovine serum, qualified, One Shot™ format, Australian origin	25ml	Invitrogen, 10099-141
		Opti-MEM 1 Reduced Serum Medium	250ml	Thermo Fisher, 31985-070
		Penicillin-Streptomycin	5ml	Invitrogen, 15140
Freezing Medium	-	DMEM, high glucose, with L-glutamine	44ml	Thermo Fisher, 11965-084
		Dimethyl sulphoxide (DMSO)	5ml	Sigma Aldrich, D2650
		Foetal bovine serum, qualified, One Shot™ format, Australian origin	25ml	Invitrogen, 10099-141
		Penicillin-Streptomycin	1ml	Invitrogen, 15140

Table 5.1 – Composition of Culture Mediums used in Maintenance of N2A (Neuro-2-A) Neuroblastoma Cells. Medium composition is broken down by reagents, quantity, and supplier. All solutions were filtered using a 0.2µm pore size Target2™ polytetrafluoroethylene (PTFE) syringe filter (#F2500-4, Thermo Fisher, Hemel Hempstead, UK).

5.2.1.2 Primary Cortical Neuron Culture

Dissociated cortical neurons were extracted from both C57BL/6J wild-type mice and B6.129-Serpini1^{tm1Dpw}/J *Serpini1* knock-out mice. Cells were extracted and cultured in accordance with Professor Shi's previously published methods (Shi et al., 2007; Tang et al., 2015). Figure 5.2 summarises the method used to extract, culture, and maintain dissociated primary cortical neurons from E18 mice.

Primary cortical neurons were plated on autoclave-sterilised 12mm diameter coverslips (#22293232, Thermo Fisher, Hemel Hempstead, UK) in autoclaved-sterilised 24-well culture plates (Corning® Costar® TC-Treated Multiple Well Plates, #CLS3527, Sigma Aldrich, Gillingham, UK). The day before primary neurons were isolated, wells were coated with 300µl Poly-D-Lysine Hydrobromide coating solution at room temperature inside a Microflow Laminar Downflow Work-Station biological safety cabinet (#JALO76 AK19, VWR International, Leicestershire, UK). The composition of coating solution, and all other solutions used in primary neuronal culture and maintenance, are given in Table 5.2. Wells were incubated in coating solution for 1 hour, then washed 5 times with 300µl sterile deionised water (#15230-162, Thermo Fisher, Hemel Hempstead, UK) and allowed to dry at room temperature.

Primary cortical neurons were extracted from E18 mouse embryos from timed-pregnant C57BL/6J and B6.129-Serpini1^{tm1Dpw}/J *Serpini1* knock-out dams. Females were culled by cervical dislocation. The uterus was opened and sprayed with 70% ethanol, then autoclave-sterilised surgical tools were used to dissect out the uterus. Embryos were transferred to Hank's Balanced Salt Solution (HBS) in a petri dish on ice. Embryos were decapitated, then fresh autoclave-sterilised surgical tools were used to dissect out the brain under a Leica FLUO™ light microscope (#MZFLIII,

Leica, London, UK). Cortical hemispheres were isolated and meninges surgically removed. Cortical tissue from all brains of the same genotype was transferred to a new Eppendorf tube containing 10ml HBS.

Medium was aspirated with a sterile 1ml pipette, tissue was taken up into pipette tip and added to 0.05% trypsin-EDTA solution. Tissue was incubated for 5 minutes at 37°C to break down the extracellular matrix. Tissue was then transferred to 0.5% trypsin inhibitor in HBS for 5 minutes to halt the protease reaction. This solution was removed and replaced with 1% DNA-se in HBS. The solution was titurated by drawing up liquid up into a sterile 1ml pipette-tip 5 times until no large pieces of tissue remained in suspension. Cells were then transferred to new HBS and centrifuged for 5 minutes at 1200 rpm in an Eppendorf Centrifuge 5702 (#5702000365, Eppendorf UK Ltd., Stevenage, UK).

Cell suspension was plated at 1 x 10^4 cells/well density in 500µl plating medium on 24-well plates. Cells were incubated in plating medium for a minimum of 12 hours in a SANYO™ MCO-17AIC CO_2 cell culture incubator (#5.519.188, VWR International, Leicestershire, UK) suffused with 5% CO_2 at 37°C. The following day, plating medium was removed and replaced with 1ml conditional neuronal growth medium. Neuronal cultures were maintained by removing 500µl medium and replacing with fresh warmed conditional growth medium once every three days.

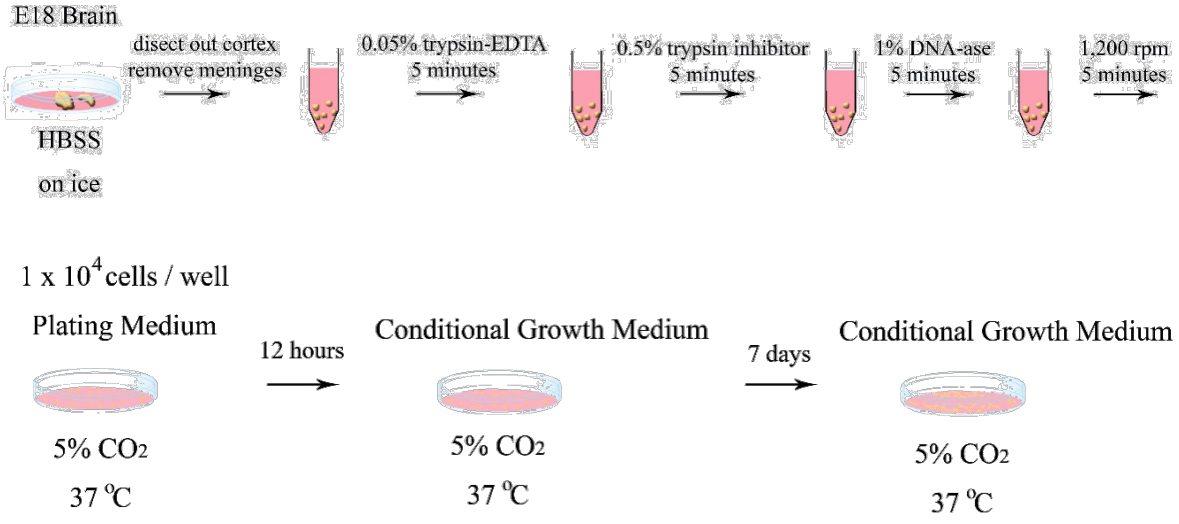


Figure 5.2 – Schematic Diagram Depicting the Extraction and Maintenance of Primary Mouse Cortical Neurons used for Oxygen-Glucose Deprivation (OGD) Optimisation Experiments.

Solution	pH	Reagents	Quantity	Supplier
Coating Solution	-	Poly-D-Lysine Hydrobromide	10mg	Sigma Aldrich, P0899
		Sterile Deionised H_2O	10ml	Thermo Fisher, 15230-162
70% Ethanol	-	Absolute Ethanol	700ml	Sigma Aldrich, 51976
		Sterile Deionised H_2O	300ml	-
Hank's Balanced Salt Solution (HBS)	7.4	HBSS, no calcium, no magnesium	242ml	Invitrogen, 14170
		1M HEPES Buffer	2.5ml	Invitrogen, 15630-080
		100mM Sodium Pyruvate	2.5ml	Invitrogen, 11360
		45% D-Glucose	0.33ml	Thermo Fisher, G8769
		Penicillin-Streptomycin	2.5ml	Invitrogen, 15140
		NaOH dropwise until pH = 7.4	-	Sigma Aldrich, S8045
0.05% Trypsin-EDTA	-	HBSS, no calcium, no magnesium	9ml	Invitrogen, 15630-080
		0.5% Trypsin-EDTA	1ml	Thermo Fisher, 25200-056
0.5% trypsin inhibitor	-	HBSS, no calcium, no magnesium	10ml	Invitrogen, 15630-080
		Soybean trypsin inhibitor, powder	0.05g	Thermo Fisher, 17075-029
1% DNA-se	-	HBSS, no calcium, no magnesium	10ml	Invitrogen, 15630-080
		DNase 1	0.1g	Roche, 10104159001
Plating medium	-	Minimum Essential Media (MEM)	232ml	Invitrogen, 61100-061
		200mM L-glutamine	2.5ml	Invitrogen, 25030-081
		45% D-glucose	0.33ml	Thermo Fisher, G8769
		100mM Sodium Pyruvate	2.5ml	Invitrogen, 11360
		100% Horse Serum	12.5ml	Invitrogen, 16050-130
Conditional Growth Medium	-	Neurobasal™ Medium	241ml	Invitrogen, 21103049
		Penicillin-Streptomycin	2.5ml	Invitrogen, 15140
		B-27™ Supplement, serum free	5ml	Invitrogen, 17504-044
		200mM L-glutamine	1.25ml	Invitrogen, 25030-081
		45% D-glucose	0.33ml	Thermo Fisher, G8769

Table 5.2 – Composition of Solutions used in Isolation and Maintenance of Primary Cortical Neurons from E18 Mouse. Solution composition is broken down by reagents, quantity, and supplier. All solutions were filtered using a 0.2µm pore size Target2™ polytetrafluoroethylene (PTFE) syringe filter (#F2500-4, Thermo Fisher, Hemel Hempstead, UK).

5.2.2 Oxygen Glucose Deprivation in Dissociated Neurons

Oxygen glucose deprivation (OGD) was carried out in accordance with previous publications which have used this method to demonstrate neuroprotective properties of neuroserpin in cultured mouse and rat dissociated neurons (Wu et al., 2010; Rodríguez-González et al., 2011a; Ma et al., 2012b). All OGD experiments were carried out in collaboration with Professor Lei Shi, Jinan University, China. Figure 5.3 summarises the OGD method in primary mouse cortical neurons.

N2A cells were used to optimise the conditions for OGD in cortical neurons. N2A growth medium was removed and replaced with N2A growth medium without glucose. The composition of glucose-free N2A medium, and all other solutions used in N2A cell and primary cortical neuron OGD experiments, are given in Table 5.3. One 24-well plate was placed inside a modular incubation chamber (#MIC-101, Billups-Rothenberg, California, USA). The chamber was suffused with 100% N_2 gas (BOC, Linde Group, Guildford, UK) at 200 kPa for 5 minutes. The sealed chamber was then returned to the SANYO™ MCO-17AIC CO_2 incubator (#5.519.188, VWR International, Leicestershire, UK) at 37°C for 0, 1, 2, 3, 4, or 8 hours. An identical plate was incubated in 5% CO_2 at 37°C as a negative control. After OGD, medium was removed and replaced with N2A medium with glucose. Both OGD and control plates were re-oxygenated in 5% CO_2 in glucose-rich media overnight at 37°C.

Cell viability was assayed using tetrazolium salt 3-(4,5-dimethylthylthiazol-2-yl)-2,5 diphenyl-tetrazolium bromide (MMT) (#M6494, Sigma Aldrich, Gillingham, UK). MMT undergoes a sharp colour change on mild reduction of its phenyl group from colourless to deep red-purple when in contact with respiring cells (Peckman and Runge, 1894a; 1894b; Matson et al., 1947; Marshall et al., 1995; reviewed in Berridge

et al., 2005), and has been used previously to quantify cell viability following OGD in cultured cells (Scopel et al., 2006; Kang et al., 2006; Zhao et al., 2009; Rodriguez-González et al., 2011a; Chen et al., 2013). The protocol used here was adapted from previously published methods (Chen et al., 2013; https://www.thermofisher.com/uk/en/home/references/protocols/cell-culture/mtt-assay-protocol/vybrant-mtt-cell-proliferation-assay-kit.html, last accessed: 01/10/2018).

10µl 12mM stock MTT solution was added to 200µl fresh glucose-rich growth medium in each well, including the negative controls. Plates were returned to the incubator for 2 hours at 5% CO_2 at 37°C. Then 150µl dimethyl sulphoxide (DMSO) (#D2650, Thermo Fisher, Hemel Hempstead, UK) was added to each well to dissolve red-purple formazan crystals into solution. Plates were incubated in 5% CO_2 at 37°C with DMSO for 10 minutes. Absorbance was measured at 540 nm using a Nanodrop ND-1000 Spectrophotometer (#ND-1000-GL, Thermo Fisher, Hemel Hempstead, UK). Absorbance readouts were averaged across a minimum of five wells per condition for N2A cell OGD optimisation.

Primary cortical neurons also underwent OGD. Dissociated neurons were maintained in glucose-rich medium (see Table 5.2) for nine days prior to initiation of OGD experiments. Medium was removed and replaced with conditional growth medium without glucose (see Table 5.3). One 24-well plate was placed inside the modular incubation chamber and suffused with 100% N_2 gas (BOC, Linde Group, Guildford, UK) at 200 kPa for 5 minutes. The sealed chamber was then returned to the incubator at 37°C for 4 hours. This time-point was selected from the N2A optimisation assays as producing a reliable decrease in cell viability (see Section 5.3.1.1). After OGD, medium was removed and replaced with glucose-rich conditional growth medium

(see Table 5.2). Both OGD and negative control plates were re-oxygenated overnight in 5% CO_2 at 37°C. The MTT assay was carried out as stated above for the N2A cells.

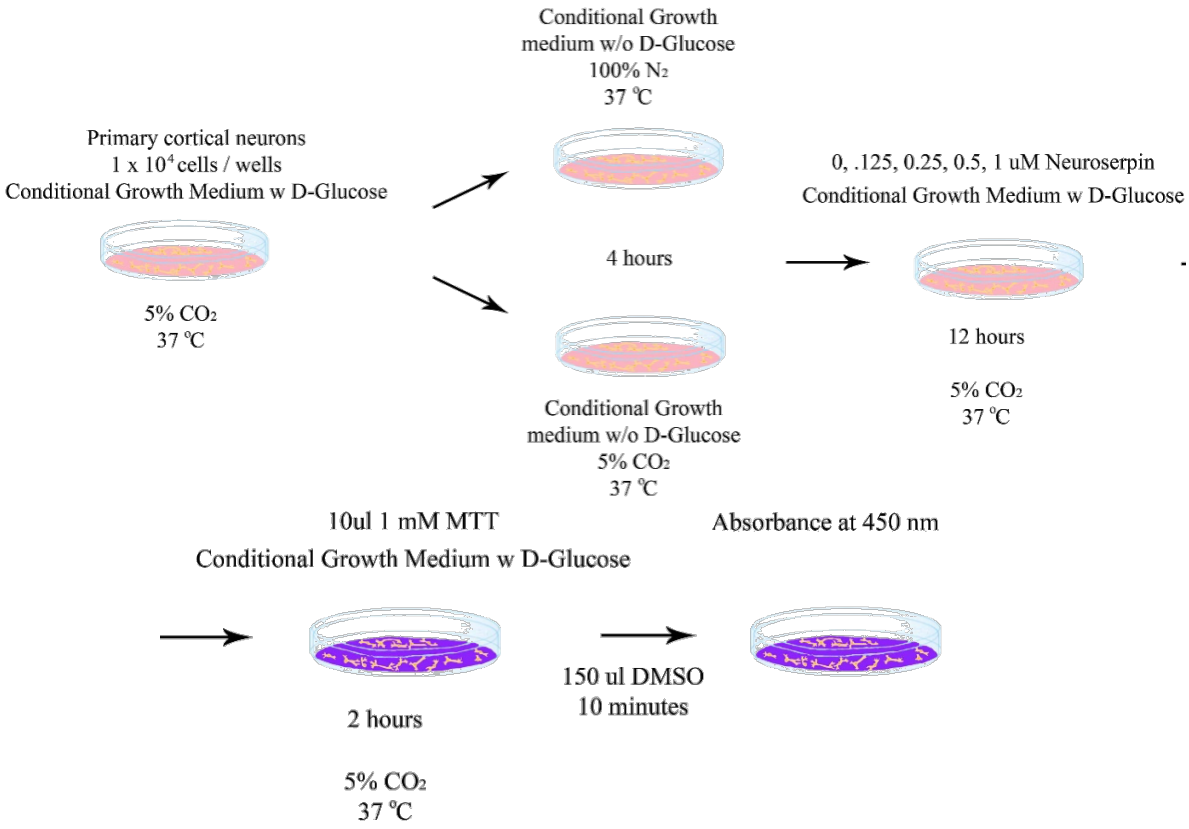


Figure 5.3 – Schematic Diagram Depicting the Adapted Oxygen Glucose Deprivation (OGD) Protocol used for Primary Mouse Cortical Neurons. Cultured neurons were maintained *in vitro* for nine days prior to OGD. Exogenous neuroserpin was added to culture medium directly following OGD at either 0, 0.125, 0.25, 0.5, or 1µM. Cell viability was quantified using the MTT assay.

In order to confirm the proposed neuroprotective properties of exogenous neuroserpin in culture (Wu et al., 2010; Rodriguez-González et al., 2011a; Ma et al., 2012b), purified recombinant human neuroserpin protein (#130-14, PeproTech EC Ltd., London, UK) was added to each well at 0, 0.125, 0.25, 0.5, or 1µM concentration directly following removal from the oxygen deprivation chamber. Exogenous

neuroserpin protein was added to a minimum of three wells per replicate, for a total of three experimental replicates.

Solution	pH	Reagents	Quantity	Supplier
N2A growth medium, without glucose	-	DMEM, without glucose, without L-glutamine	250ml	Thermo Fisher, 11966-025
		Foetal bovine serum, qualified, One Shot™ format, Australian origin	25ml	Invitrogen, 10099-141
		OptiMEM 1 Reduced Serum Medium	250ml	Thermo Fisher, 31985-070
		Penicillin-Streptomycin	5ml	Invitrogen, 15140
Conditional neuronal growth medium, without glucose	-	Neurobasal™-A Medium, no D-glucose, no sodium pyruvate	241ml	Thermo Fisher, A2477501
		Penicillin-Streptomycin	2.5ml	Invitrogen, 15140
		B-27™ Supplement, serum free	5ml	Invitrogen, 17504-044
		200mM L-glutamine	1.25ml	Invitrogen, 25030-081
		100mM Sodium Pyruvate	600µl	Invitrogen, 11360
12mM MMT Solution	-	3-(4,5-Dimethylthiazol-2-yl)-2,5-Diphenyltetrazolium Bromide (MTT)	5mg	Sigma Aldrich, M6494
		1M PBS, pH 7.4	1ml	Thermo Fisher, 10010023

Table 5.3 – Composition of Solutions used in Oxygen Glucose Deprivation (OGD) Optimisation with N2A Neuroblastoma Cells and Investigation with Dissociated Primary Cortical Neurons. Solution composition is broken down by reagents, quantity, and supplier. All solutions were filtered using a 0.2µm pore size Target2™ polytetrafluoroethylene (PTFE) syringe filter (#F2500-4, Thermo Fisher, Hemel Hempstead, UK). For any cell culture solutions not listed here, see Table 5.2.

OGD in cultured neurons has been demonstrated to replicate several characteristics of hypoxic ischaemic neuronal death (reviewed in Tasca et al., 2014; Ryou and Mallett, 2018). These similarities include selective vulnerability of certain populations of hippocampal neurons, equivalent to that observed in *in vivo* stroke models (Newell et al., 1990), and a time-dependent pattern of delayed cell death (Cho et al., 2004). Although *in vitro* models cannot replicate all of the factors which may influence the outcome of neonatal hypoxia ischaemia, such as hormone production (Gustafson et al., 1999; Simonides et al., 2008; reviewed in Weinstock, 2007; Manson, 2008), or the long distance axonal projection patterns present between neocortex and thalamus (reviewed in Sherman and Guillery, 2009; 2013), it does offer a highly controlled environment in which to quantify neuronal death in response to hypoxic conditions.

5.2.3 Rice-Vannucci Neonatal Hypoxia Ischaemia in *Serpini1* Knock-Out Mouse

In order to replicate the mild-to-moderate brain injury observed in C57BL/6J mice (Chapter 4, Section 4.3.3) in *Serpini1* knock-out mice and wild-type litter mates, the adapted Rice-Vannucci model was carried out in P8 litters from *Serpini1* heterozygote x heterozygote crosses. The procedure had to be modified from that described previously in Chapter 4, Section 4.2.1 to reduce the number of animals culled due to poor condition in the hypoxia chamber. The total number and genotype of animals which underwent neonatal hypoxia ischaemia are detailed in Table 5.4, and the number brains available for lesion analysis by 2,3,5-triphenyl tetrazolium chloride (TTC) staining in Table 5.5. Figure 5.4 summarises the modified procedure.

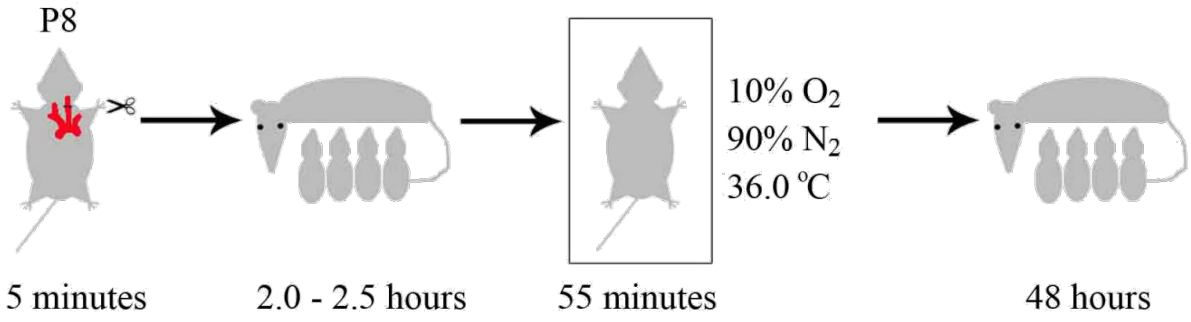


Figure 5.4 – Schematic Diagram Depicting the Modified Rice-Vannucci Hypoxia Ischaemia Mouse Model used to generate Results for Chapter 5, Section 5.3.2. The left common carotid artery (LCC) was ligated under anaesthesia in P8 pups. Pups were then returned to the dam for between 2.0 and 2.5 hours to recover from surgery. Pups were then placed into a sealed chamber and exposed to hypoxic conditions (10% O_2) for 55 minutes. Brains were collected 48 hours post-surgery.

Surgery was conducted on litters containing between 3 and 12 pups. Approximately half of the litter were placed in a heated box set to 36°C. Each individual pup was

weighed with an electronic scale accurate to ± 0.05g. Weights were recorded, and pups weighing less than 3.5g did not undergo surgery. Pups were placed in an anaesthesia induction box prefilled with 4.0% isofluorane. When the righting reflex was lost, pups were transferred to a heated mat and 3.0% isofluorane was delivered via a nosepiece. Full anaesthesia was confirmed by the tail-pinch and toe-pinch responses.

Surgery time did not exceed 5 minutes. A small incision was made in the neck, slightly above the sternum to the left of the midline. Microscopically blunted curved and straight forceps were used to locate the left common carotid artery (LCC). Forceps were used to separate the LCC from the Vagus nerve and jugular vein if necessary. The LLC was ligated using a 6.0 biodegradable suture (6-0 Coated Vicryl Undyed 1X27" RB-1 Suture, #J212H, Ethicon Endo-Surgery, Johnson and Johnson Medical Supplies Ltd., Livingston, UK). The skin was closed using single interrupted sutures of the same material. A tissue sample was cut from the ear and transferred to a clean Eppendorf tube for genotyping. Pups were exposed to 100% O_2 for approximately 1 minute, then returned to the heated box to recover at 36℃ ± 0.5℃.

Following surgery, animals were monitored until moving freely. Pups were returned to the dam for 2.0-2.5 hours to recover before undergoing hypoxia. An individually-ventilated cage was placed in a water-bath (28L General Purpose Water Bath, #TSGP28, Thermo Fisher, Hemel Hempstead, UK) set to 37.5℃ or 36.0℃. Air temperature inside the cage was monitored using a secondary infra-red thermometer. The cage was pre-filled with custom gas consisting of 10% O_2 balanced by 90% N_2 (BOC, Linde Group, Guildford, UK). After recovery with the dam, all surgery pups were placed in the individually-ventilate cage. Constant 0.05 Pa 10% O_2 gas was

supplied to the chamber to maintain hypoxia. Thermometer readings were observed throughout the experiment, and hypoxia was stopped and surgical pups removed from the chamber if the set temperature deviated by ± 0.5°C. Animals were then returned to the dam. Tissue was collected 48 hours after hypoxia. Pups were injected with 0.1ml pentobarbital and transcardially perfused with 5% 2,3,5-triphenyl tetrazolium chloride (TTC) in 0.1M PBS (see Section 5.2.4).

Litters underwent exposure to hypoxia at one of two set temperatures: 36.0°C or 37.5°C. Originally, 37.5°C was chosen as the set temperature to complement experiments carried out in C57BL/6J wild-type animals with minimal complications (See Chapter 4, Section 4.3.2). However, greater than 20% of pups across all genotypes had to be culled when hypoxia was carried out at 37.5°C in animals from B6.129-Serpini1^{tm1Dpw}/J heterozygote x heterozygote crosses (see Table 5.4). Many animals showed pale extremities, no response to handling, and shallow breathing when placed in the hypoxia chamber. These experiments were stopped immediately, and the affected animals culled for welfare reasons. As the proportion of animals culled during the experiment was deemed excessive, milder conditions were implemented. When the temperature during hypoxia was decreased to 36.0°C ± 0.5°C for four further litters, no animals exhibited signs of poor welfare.

There are multiple possible explanations for the difference in outcome between experimental populations. It is possible that the genetic background of the C57BL/6 animals was more robust than that of the B6.129-Serpini1^{tm1Dpw}/J heterozygote x heterozygote cross animals. The former were purchased from Charles River (http://www.criver.com/products-services/ basic-research/find-a-model/c57bl-6n-mouse, last accessed: 10/08/2018), whereas the latter were bred on a Jackson

Laboratories background (https://www.jax.org/strain/019121, last accessed: 10/08/2018). It is possible that these background strains exhibit different vulnerabilities to neonatal hypoxia ischaemia (Sheldon et al., 1998). In addition, substantial variation in injury severity has been reported by different experimenters using similar conditions to those investigated here (reviewed in Vannucci and Hagberg, 2004; Vannucci and Vannucci, 2005). Some experimenters reported >20% mortality rate at 45-65 minutes hypoxia (McQuillen et al., 2003; Ten et al., 2003; McAuliffe et al., 2009; Lin et al., 2014; Ogawa et al., 2018), whereas others reported <10% pup mortality under analogous conditions (Hagberg et al., 2004; Tsuji et al., 2004; McAuliffe et al., 2006; Lafemina et al., 2006; Carlsson et al., 2012; Kichev et al., 2018). Across the literature, exposure of pups to 90-120 minutes hypoxia has been reported to cause between 5% and 60% mortality, depending on the experimenter and potentially other hidden variables (Ditelberg et al., 1996; Ferriero et al., 1996; Demers et al., 2005; Chen et al., 2014). There is no single precedent in the literature which could explain the death rates observed at 37.5°C. Increased mortality was likely caused by interaction of different factors. However, it is evident that temperature of the hypoxia chamber exhibits a substantial effect on the outcome of neonatal hypoxia-ischaemia in rodents (Rogalska et al., 2004, 2009; Caputa et al., 2005; Robertson and Iwata, 2007; reviewed in Rogalska et al., 2006).

Cross	Genotype	N	Missing	Culled	Survived 24 hr	Survived 48 hr	Litters	Litters in which pups died	Temperature (°C)
C57BL/6J x C57BL/6J (wild-type x wild-type) (see Chapter 4, Section 4.3.4)									
	WT	187	11	2	174	174	27	4	37.5
(C57BL/6J x B6.129-Serpini1^{tm1Dpw}/J) x (C57BL/6J x B6.129-Serpini1^{tm1Dpw}/J) (heterozygote x heterozygote)									
	WT	15	2	7	6	6	8	3	37.5
	Het	27	3	12	16	16			
	KO	16	2	6	8	8			
(C57BL/6J x B6.129-Serpini1^{tm1Dpw}/J) x (C57BL/6J x B6.129-Serpini1^{tm1Dpw}/J) (heterozygote x heterozygote)									
	WT	3	0	0	3	3	4	0	36.0
	Het	12	0	0	12	12			
	KO	12	0	0	12	12			

Table 5.4 – Breakdown of Number, Genotype, and Condition of Animals which underwent Neonatal Hypoxia Ischaemia (HI) by the Adapted Rice-Vannucci method. Mice are categorised by genotype, outcome post-HI, and temperature at which pups were exposed to hypoxia (10% O_2 partial pressure). Death rates were considerably higher across all genotypes in litters from the Het x Het crosses at 37.5°C, but reduced when the temperature was decreased to 36.0°C. Experiments were stopped if hypoxia chamber temperature deviated the chosen temperature by ± 0.5°C or more.
WT = C57BL/6J homozygote wild-type (+/+), Het = C57BL/6J x B6.129-Serpini1^{tm1Dpw}/J heterozygote (+/-), KO = B6.129-Serpini1^{tm1Dpw}/J homozygote *Serpini1* knock-out (-/-)

Genotype	Duration of hypoxia (minutes)	N	Litters	Collection Post-HI (hours)	Temperature throughout hypoxia (°C)
WT	55	6	6	48	37.5
Het	55	16			
KO	55	8			
WT	55	3	4		36.0
Het	55	12			
KO	55	12			

Table 5.5 – Number of Brains Collected following Neonatal Hypoxia Ischaemia (HI) in Litters from *Serpini1* Heterozygote x Heterozygote crosses. Brains are categorised by genotype, duration of hypoxia, and temperature during hypoxia. Brains across temperature conditions were pooled for 2,3,5-triphenyl tetrazolium chloride (TTC) lesion analysis.
WT = C57BL/6J homozygote wild-type (+/+), Het = C57BL/6J x B6.129-Serpini1^{tm1Dpw}/J heterozygote (+/-), KO = B6.129-Serpini1^{tm1Dpw}/J homozygote *Serpini1* knock-out (-/-)

5.2.4 2,3,5-Triphenyltetrazolium chloride (TTC) Perfusion

Quantitative assessment of lesion volume in P10 B6.129-Serpini1^{tm1Dpw}/J *Serpini1* knock-out (KO) and C57BL/6J wild-type (WT) mouse following the adapted Rice-Vannucci neonatal hypoxia ischaemia was achieved by perfusing animals with a marker of metabolic activity. Tetrazolium salt 2,3,5-triphenyl tetrazolium chloride (TTC) undergoes a sharp colour change on reduction of its phenyl group from

colourless to deep red-purple, which occurs if TTC is taken up into respiring cells (Peckman, 1894; Matson, 1947; Marshall et al., 1995; reviewed in Berridge et al., 2005). In contrast, TTC remains colourless when in contact with non-respiring dead or damaged tissue. TTC has been used to quantitatively delineate lesion boundaries in adult and infant models of hypoxia ischaemia (Hatfield et al., 1991; Sun et al., 2012). This protocol was adapted from a previously published method (Sun et al., 2012).

5% TTC solution and 0.1M PBS were preheated to 37°C in a water-bath (Precision™ General Purpose 28L Water Bath, #TSGP28, Thermo Fisher Scientific, Hemel Hempstead, UK) for a minimum of 30 minutes prior to the beginning of the procedure. Composition of 5% TTC solution is given in Table 5.6 below, composition of 0.1M PBS is given in Chapter 2, Section 2.6, Table 2.7.

P10 mice were given an intraperitoneal injection of 0.1ml 1.4M mannitol in 0.1M PBS. Animals were monitored for 30 minutes whilst inside a heated box set to 36°C. This allowed the mannitol to partially breakdown the blood brain barrier (BBB) (Cosolo et al., 1989; Brown et al., 2004; Bellavance et al., 2007; Joshi et al., 2011; Sun et al., 2012; reviewed in Bellavance et al., 2008), increasing TTC penetration into the brain during perfusion. Animals showing stress or poor condition were determined to be culled immediately, although this precaution was not required for this experimental cohort.

Pups were terminally anaesthetised with a 0.1ml intra-peritoneal injection of pentobarbitone (#XVD 135, Pentoject, Animal Care Ltd, York, UK). Animals were then transcardially perfused with approximately 10ml pre-warmed 5% TTC in 0.1M PBS. Perfusion was stopped when the extremities darkened to a deep red-purple

colour that was not enhanced by further perfusion. A face mask was worn during perfusion for personal protection.

Brains were dissected out immediately with autoclave-sterilised fixative-free surgical tools. Whole brains were transferred to heated 0.1M PBS inside a water-bath set to 37℃ for approximately 1 hour to allow TTC permeation to continue and staining to mature. Brains were then transferred to 4% PFA in 0.1M PBS (see Table 2.7) for 48 hours at 4℃ for thorough fixation. Brains were stored in 0.1M PBS with 0.05% sodium azide at 4℃.

Solution	pH	Components	Quantity	Supplier
1.4 M Mannitol in 0.1M PBS	-	D-Mannitol	12g	Sigma Aldrich, M4125
		0.1M PBS	Up to 50ml	See Table 2.7
5% TTC in 0.1M PBS	-	2,3,5-Triphenyltetrazolium chloride	2.5g	Sigma Aldrich, T8877
		0.1M PBS	Up to 50ml	See Table 2.7
4% paraformaldehyde in 0.1M PBS	7.4	Deionised H_2O	50ml	-
		Paraformaldehyde (PFA) powder	4g	Sigma Aldrich, F8775
		0.1M PBS	50ml	See Table 2.7

Table 5.6 – Solutions used in 2,3,5-triphenyltetrazolium chloride (TTC) Perfusion, Listed by Reagents, Quantity, and Supplier.

5.2.5 Analysis of TTC staining in whole brains

TTC staining intensity was quantified from light microscopy images taken with the 2.5x magnification objective using a Leica DMR microscope (#933789, Leica Microsystems, Milton Keynes, UK). All images were taken using identical conditions. Brains were placed on a transparent petri-dish during imaging and returned to 0.1M PBS with 0.05% sodium azide (see Chapter 2, Section 2.6, Table 2.7) immediately to prevent drying out. All brains used for TTC quantification are listed by age, genotype, and experimental procedure in Table 5.7. Figure 5.5

summarises the methods used for image analysis. Imaging and TTC analysis were performed blind to the genotype by Dr. Anna Hoerder-Suabedissen.

Analysis of images was carried out using ImageJ 1.50i (http://imagej.nih.gov/ij, last accessed: 10/08/2018), using techniques previously described for particle detection (Jensen, 2013; Syvertsson et al., 2016; https://imagej.nih.gov/ij/docs/menus/analyze.html, last accessed: 10/08/2018). A region of interest (ROI) encompassing both cortical hemispheres was defined using the ROI Manager tool. Region of interest boundaries for each individual brain were drawn freehand, guided by gross anatomy, as shown in Figure 5.5.

Original RGB images were converted to greyscale images to average intensity information across colour channels into a single value. A cumulative pixel intensity histogram was generated for each brain showing the proportion of the total pixels contained within the ROI corresponding to each intensity value between 1 and 255. Cumulative pixel intensity curves were averaged across brains of the same genotype and normalised to the darkest group of images (here labelled the discarded brains), which were set to 1.0. Figure 5.5 shows a summary of TTC stain intensity quantification method.

From Figure 5.5, it is evident that shine marks and shadows have been captured during whole brain imaging. Retrospective quantification of the area of the shine marks on each hemisphere of each brain revealed no significant difference in area covered by reflections between hemisphere or genotype. Therefore, this is unlikely to have biased analysis. However, the inclusion of these artefacts is not ideal, as these markers could have obscured or exacerbated genuine differences in TTC staining intensity. Further experiments could employ a light microscope capable of taking

images in precisely-specified Z-planes and reconciling these to reduce these effects (reviewed in Sibarita, 2005; Brecko et al., 2014).

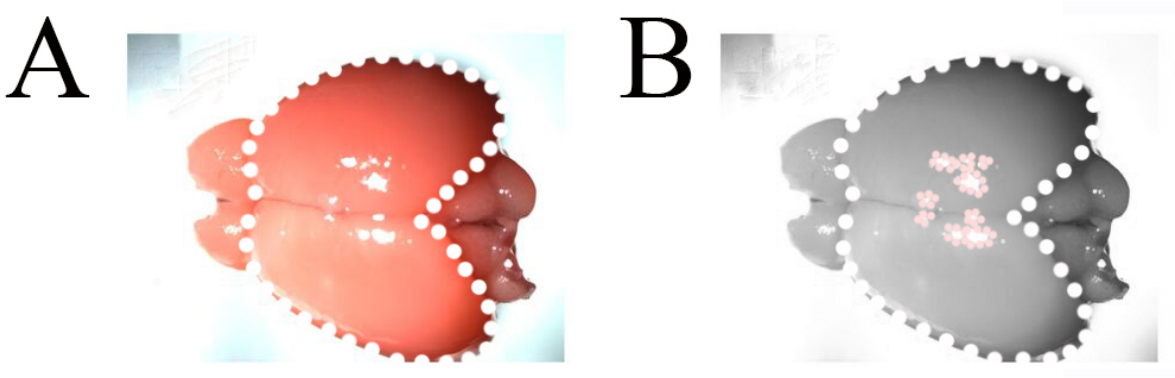


Figure 5.5 – Example Images of TTC Staining Quantification Using ImageJ. (A) Region of interest (ROI) was defined manually for each brain to include both cortical hemispheres. Example image of a wild-type (WT) (+/+) brain, the ROI has been marked by a white dotted line. (B) Greyscale image of example brain. RGB images were processed automatically to retain only a single value for pixel intensity. Pale pink dotted lines indicate where retrospective analysis to remove shine marks was carried out. The top-left area of the background has been smoothed with a healing tool in Photoshop CS3 to remove text, no adjustment was made to images for analysis. The brain itself is unaltered. Images were acquired blind to the genotype by Dr. Anna Hoerder-Suabedissen.

Experiment	Genotype	Developmental Time-Point (Postnatal Days)	Condition (Experimental Procedures)	N	Litters
Quantification of TTC Staining in Whole Brain					
	WT	P10	nHI at P8 + 48 hr	4	4
	Het	P10	nHI at P8 + 48 hr	11	5
	KO	P10	nHI at P8 + 48 hr	8	5
	Mixed (Discarded)	P10	nHI at P8 + 48 hr	6	5

Table 5.7 – Breakdown of the Number of Brains used across TTC staining quantification experiments. Brains are categorised by genotype, developmental time point (age), and experimental procedures (condition). The Mixed (Discarded) category refers to a group of brains with an intense staining pattern substantially different from all other brains analysed. The discarded group contained brains of all three genotypes, those included in the discarded category were not analysed alongside other brains of the same genotype.
WT = C57BL/6J homozygote wild-type, Het = C57BL/6J x B6.129-Serpini1^{tm1Dpw}/J heterozygote, KO = B6.129-Serpini1^{tm1Dpw}/J homozygote *Serpini1* knock-out, nHI = neonatal hypoxia ischaemia by the Rice-Vannucci method described in Chapter 4, Section 4.2.1 and Chapter 5, Section 5.2.4

5.2.6 Immunohistochemistry

In order to confirm brain damage following the adapted Rice-Vannucci method in the

C57BL/6 wild-type (WT) and B6.129-Serpini1^{tm1Dpw}/J *Serpini1* knock-out mice (KO), fluorescent immunohistochemistry was used to stain for three inflammatory damage markers: GFAP, Iba1, and CD68. The methods used for immunohistochemistry in 50µm thickness coronal sections from P10 mouse brains are described in Chapter 3, Section 3.2.1. Details of all tissue used in immunohistochemistry experiments for this chapter are given in Table 5.8, and sources and concentrations of antibodies are detailed in Table 5.9.

Experiment	Genotype	Developmental Time Point (Postnatal Days)	Collection time post-HI (hours)	N	Litters
Quantification of Brain Damage Markers					
	WT homozygote (+/+)	P10	48	5	4
	Het heterozygote (+/-)	P10	48	5	4
	KO homozygote (-/-)	P10	48	5	4

Table 5.8 – Breakdown of the Number of Brains used across all Fluorescent Immunohistochemistry experiments detailed in this chapter. Brains are categorised by genotype, developmental time-point (age), and experimental condition (neonatal HI, collection time-point in hours post-procedure). WT = C57BL/6J homozygote wild-type, Het = C57BL/6J x B6.129-Serpini1^{tm1Dpw}/J heterozygote, KO = B6.129-Serpini1^{tm1Dpw}/J homozygote *Serpini1* knock-out

Experiment	Primary Antibody	Concentration	Source	Secondary Antibody
Quantification of Brain Damage Markers				
	Rabbit anti-GFAP	1:500	DAKO, Z0334	Donkey anti-rabbit Alx488 1:500 (Invitrogen, A21206)
	Goat anti-Iba1	1:500	Abcam, 107159	Donkey anti-goat Alx568 1:500 (Invitrogen, A11057)
	Mouse anti-CD68	1:50	Abcam, Ab955	Donkey anti-mouse Alx488 1:500 (Invitrogen, A21202)

Table 5.9 – Primary and Secondary Antibodies used in Immunohistochemistry Experiments detailed in this chapter. Antibodies are listed by relevant experimental aims, concentration, and supplier.

5.3 Results

5.3.1 Neuroprotective Properties of Exogenous Neuroserpin Protein *in vitro*

In order to investigate the hypothesised neuroprotective properties of neuroserpin in hypoxia ischaemia (reviewed in Yepes and Lawrence, 2004a; 2004c; Miranda and Lomas, 2006; Millar et al., 2017), *in vitro* models were developed. The first aim of these experiments was to confirm previously reported neuroprotective effects of exogenous neuroserpin protein following oxygen glucose deprivation (OGD) in cultured neurons (Wu et al., 2010; Rodríguez-González et al., 2011a; Ma et al., 2012b). The second aim was to investigate the sensitivity of dissociated neurons from *Serpini1* knock-out mice to OGD compared to wild-type controls.

5.3.1.1 Optimisation of Oxygen Glucose Deprivation (OGD) Protocol in vitro using N2A (Neuro-2-A) Neuroblastoma cells

In order to optimise the OGD protocol, N2A neuroblastoma cells (see Section 5.2.1.1) were exposed to multiple durations of OGD and recovery periods. These experiments established a protocol which reliably decreased cell viability by approximately 50%, measured by MTT assay, when compared with negative controls. The investigation also aimed to test whether this decreased viability could be partially reversed by administering exogenous neuroserpin protein.

Several durations of OGD were tested with N2A cells during optimisation, as assessed by MTT staining. The literature describing neuroserpin neuroprotection *in vitro* all employed different experimental conditions for OGD. Durations of exposure

varied between 55 minutes (Ma et al., 2012b), 2 hours (Wu et al., 2010) and 150 minutes (Rodríguez-González et al., 2011a); using either 100% N_2 gas (Ma et al., 2012b), or 95% N_2 balanced with 5% CO_2 (Wu et al., 2010; Rodríguez-González et al., 2011a); and a variety of commercial and custom media (Wu et al., 2010; Rodríguez-González et al., 2011a). N2A have previously been demonstrated to show vulnerability to OGD under similar conditions to those investigated in neurons (Mazzio et al., 2003; Shen et al., 2006; Yin et al., 2010; Mahesh et al., 2011; Ghorbani et al., 2015; Yang et al., 2015).

N2A cells were exposed to 100% N_2 for 0, 1, 2, 3, 4, or 8 hour intervals. When MTT cell viability staining was conducted directly following exposure to OGD, there were no significant different in MTT absorbance between any of the experimental conditions and the negative control wells at N = 3 replicates. When cells were allowed to recover in the cell culture incubator in 5% CO_2 at 37°C, statistically significant differences were detected in MTT absorbance between the negative control exposed to 0 hours OGD (0.682 ± 0.311) and cells exposed to OGD for 2 hours (0.339 ± 0.049), 4 hours (0.323 ± 0.199), and 8 hours (0.268 ± 0.022) at N = 4 replicates. Both 2 hours and 4 hours OGD were investigated further. Figure 5.6 Panel A and Table 5.10 summarise results of the OGD optimisation with N2A cells.

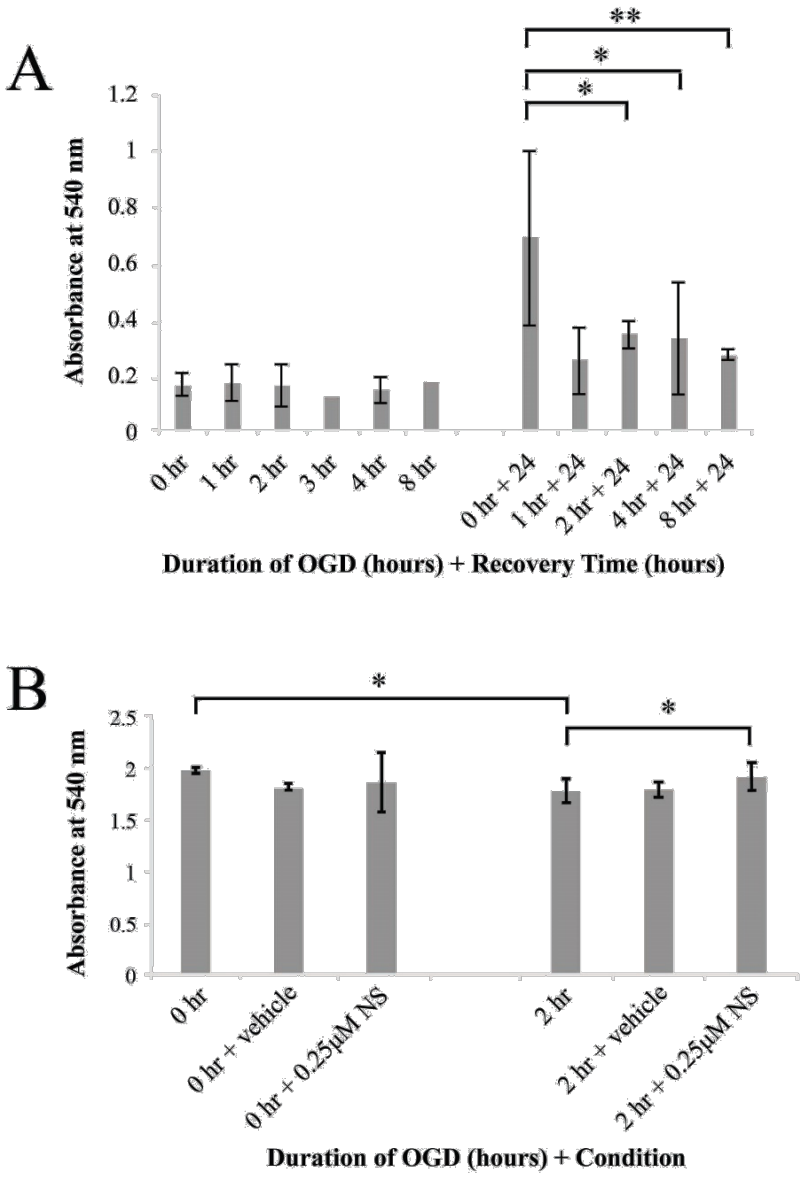


Figure 5.6 – Optimisation of Oxygen Glucose Deprivation (OGD) Protocol in N2A (Neuro-2-A) Neuroblastoma Cells. Exposure to oxygen glucose deprivation at 100% N_2 in glucose-free medium for 2, 4, and 8 hours followed by 24 hours recovery produced a statistically significant decrease in MTT staining. This decrease in cell viability marker staining was partially reversed by administration of 0.25 μM exogenous neuroserpin protein directly following OGD. (A) Quantification of MTT absorbance at 450 nm to cultured N2A cells following 0, 1, 2, 3, 4, and 8 hours, both with and without a recovery period of 24 hours (mean ± SD). Statistically significant decreases in MTT staining were detected following 2, 4, and 8 hours OGD followed by 24 hours recovery. (B) Quantification of MTT absorbance in cultured N2A cells following administration of 0.25 μM exogenous neuroserpin or a vehicle directly following 2 hours OGD. Cultured cells were allowed to recover for 24 hours prior to analysis. Neuroserpin administration led to a statistically significant increase in MTT staining, which may be explained by an increase in cell viability following OGD in the presence of neuroserpin. One-way ANOVA demonstrated a statistically significant difference between groups based on duration of OGD. Unpaired T-tests were conducted to compare MTT absorbance between specific groups.
* denotes a P-value > 0.01, ** denotes a P-value > 0.005, *** denotes a P-value > 0.001
OGD + 24 hr = oxygen glucose deprivation followed by 24 hr reoxygenation (recovery), NS = exogenous neuroserpin #130-14, Peprotech EC Ltd., London, UK

Cells	Duration of OGD (hours)	Duration of Recovery (hours)	Vehicle (µM / well)	Exogenous Neuroserpin (µM / well)	Number of Replicates	Wells / Replicate	Average Absorbance at 540nm (± SD)
N2A Cells	0	0	-	-	2	3	0.161 (± 0.039)
N2A Cells	1	0	-	-	2	3	0.167 (± 0.067)
N2A Cells	2	0	-	-	2	3	0.157 (± 0.073)
N2A Cells	3	0	-	-	1	3	0.122
N2A Cells	4	0	-	-	2	3	0.142 (± 0.047)
N2A Cells	8	0	-	-	1	3	0.174
N2A Cells	0	24	-	-	3	4	0.682 (± 0.311)
N2A Cells	1	24	-	-	2	4	0.246 (± 0.118)
N2A Cells	2	24	-	-	3	4	0.339 (± 0.049)
N2A Cells	4	24	-	-	3	4	0.323 (± 0.199)
N2A Cells	8	24	-	-	2	4	0.268 (± 0.022)
N2A Cells	0	24	-	-	2	4	1.982 (± 0.008)
N2A Cells	0	24	0.25	-	2	4	1.812 (± 0.029)
N2A Cells	0	24	-	0.25	2	4	1.855 (± 0.286)
N2A Cells	2	24	-	-	2	4	1.774 (± 0.118)
N2A Cells	2	24	0.25	-	2	4	1.789 (± 0.078)
N2A Cells	2	24	-	0.25	2	4	1.912 (± 0.135)

Table 5.10 – Breakdown of NA2 Neuroblastoma cell Oxygen-Glucose Deprivation (OGD) Optimisation Conditions. Experiments are listed by duration of OGD in hours, duration of reoxygenation recovery in glucose-rich medium in hours, concentration of exogenous neuroserpin protein or vehicle, and number of replicates carried out. For statistical analysis, the absorbance measurement was taken three times for each well and averaged across all wells in each condition. Column 8 shows that a decrease in MTT staining, measured by absorbance at 540 nm, was observed after OGD, and partially reversed on administration of 0.25 µM exogenous neuroserpin (#130-14 Peprotech ECL Ltd., London, UK). One-way ANOVA demonstrated a statistically significant difference between groups based on duration of OGD.

The neuroprotective properties of exogenous neuroserpin on N2A cells was initially investigated after 2 hours OGD, within the range previously reported in primary cortical neurons (Wu et al., 2010; Rodríguez-González et al., 2011a; Ma et al., 2012b). In negative controls not subjected to OGD, there was no statistically significant difference in MTT staining absorbance in negative controls (1.98 ± 0.01) and those administered with vehicle (1.81 ± 0.03), or 0.25µM exogenous neuroserpin (1.86 ± 0.29). However, administration of 0.25µM exogenous neuroserpin after 2 hours of OGD resulted in a statistically significant difference in MTT staining following 24 hours recovery. Cells dosed with exogenous neuroserpin demonstrated greater absorbance (1.91 ± 0.13) compared to negative controls administered nothing (1.77 ± 0.12) or vehicle alone (1.79 ± 0.08). Despite achieving statistical significance,

this difference was extremely modest. Figure 5.6 Panel B and Table 5.10 summarise the results of neuroserpin administration following OGD with N2A cells.

Overall, the results of preliminary optimisation OGD experiments using the N2A cell line demonstrated that an exposure duration of 2 hours or more produced a reliable decrease in cell viability as measured by MTT assay. An extremely modest, yet statistically significant, restorative effect was detected when 0.25 μM exogenous neuroserpin was administered directly following 2 hours OGD. This dose has previously been shown to produce neuroprotective effects in cultured neurons *in vitro* (Wu et al., 2010; Rodríguez-González et al., 2011a; Ma et al., 2012b). The magnitude of the observed changes was small, both comparing OGD cultures with negative controls and comparing OGD cultures with and without exogenous neuroserpin, yet the effect was statistically significant in highly homogenous cultures of N2A cells. For the primary cortical neuron cultures, 4 hours OGD was selected test the neuroprotective properties of neuroserpin further.

N2A cells were used for this preliminary experiment as these stem cells share neural-crest lineage with fully differentiated neurons (reviewed in Shastry et al., 2001), and proliferate in culture, making these cells ideal for optimising experimental conditions for neurons. However, these cells are not neurons. Transcriptomic analysis (Yin et al., 2016; Gil-Ibánez et al., 2017), and response to neurotoxic chemicals (Yamada et al., 2015; Popova et al., 2017) differs substantially between neuroblastoma-derived cells and true rodent neurons. Thus, confirmation of all effects in primary cultured neurons was essential.

5.3.1.2 Neuroprotective properties of Exogenous Neuroserpin Protein in Cultured Primary Cortical Neurons from Wild-Type and *Serpini1* Knock-Out Mouse

Optimised OGD experiments were carried out in dissociated primary cortical neurons from E18 wild-type C57BL/6J and *Serpini1* knock-out mouse brains. The aim was to compare the sensitivity of neurons of the two genotypes to OGD.

Experiments carried out to investigate the sensitivity of cortical neurons from the *Serpini1* knock-out mouse to OGD were not successful, due to the presence of bacterial contamination in cultured neurons. A single uncontaminated replicate suggested a small difference in cell viability between genotypes as measured by MTT absorbance after 4 hours OGD followed by 24 recovery. In this experiment, a mean absorbance of 0.188 was measured across all wells containing wild-type neurons following OGD, compared to an absorbance of 0.125 for the *Serpini1* knock-out neurons. Both showed modest partial restoration of MTT staining at 540 nm when administered 0.25 μM exogenous neuroserpin protein directly following OGD, with absorbance rising to 0.215 in the wild-type cultures and 0.175 in knock-out cultures. No standard deviation (SD) is given, as these results are reported from a single experiment. Only one replicate maintained sufficiently healthy neurons by day 9 post-plating to subject to OGD. Potential reasons for this are discussed below. Although a greater number of replicates are required before meaningful conclusions can be drawn, results are summarised in Figure 5.7 and Table 5.11.

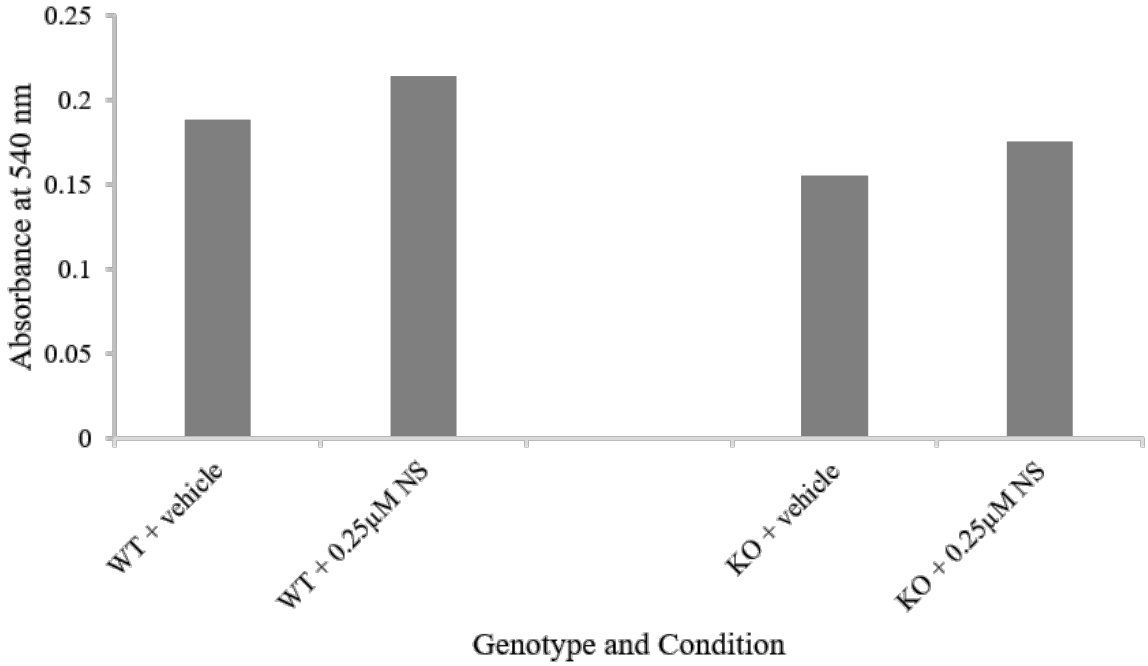


Figure 5.7 – Preliminary Experiment Characterising Sensitivity of Dissociated Primary Cortical Neurons from Wild-type and *Serpini1* Knock-out Mice to Oxygen Glucose Deprivation (OGD) followed by Treatment with 0.25µM Exogenous Neuroserpin. Exposure to oxygen glucose deprivation at 100% N_2 in glucose-free medium for 4 hours followed by 24 hours recovery produced a slightly lower value for MTT staining intensity in the KO neurons compared to the WT neurons. Both appeared to be modestly restored by administration of exogenous neuroserpin directly following OGD However, a single replicate is not sufficient for any conclusions to be drawn. Hence error bars are not shown on this graph. Due to the single replicate available, statistical analysis was not carried out.
WT = C57BL/6J, KO = B6.129-Serpini1^{tm1Dpw}/J *Serpini1* knock-out, NS = exogenous neuroserpin #130-14, Peprotech EC Ltd., London, UK

Replicate	Genotype	Number of Dams	Number of Embryos Pooled
1	C57BL/6J	2	6
	B6.129-Serpini1^{tm1Dpw}/J	2	6
2	C57BL/6J	2	9
	B6.129-Serpini1^{tm1Dpw}/J	2	9
3	C57BL/6J	2	5
	B6.129-Serpini1^{tm1Dpw}/J	2	7
4	C57BL/6J	2	4
	B6.129-Serpini1^{tm1Dpw}/J	2	6
5	C57BL/6J	1	9
	B6.129-Serpini1^{tm1Dpw}/J	1	8

Table 5.11 – Number of E18 Mouse Brain available for Primary Neuronal Culture. Experimental replicates are categorised by genotype, number of dams, and number of embryos pooled for neuronal culture. For each replicate, cortical hemispheres from all embryos of the same genotype were pooled for dissociation and culture. All cultures were plated onto lipofectamine-coated coverslips in 12-well and 24-well cell culture plates. Statistical analysis was not carried out.

A number of limitations contributed to the inadequacy of these results. Primarily, evidence of bacterial contamination was discovered in the cultured neurons from the fifth replicate. It is possible that low-level bacterial or fungal contamination was present in all five replicates of this experiment, as neuronal densities were decreased from projected values based on Professor Lei Shi's previous experience using a similar protocol at Jinan University, China (Shi et al., 2007; Tang et al., 2015). In addition, the number of replicates was not sufficient. A greater number of replicates would be preferable for the design of future experiments to test the sensitivity of *Serpini1* knock-out dissociated neurons to OGD, in line with the existing literature reporting neuroserpin neuroprotection *in vitro* which reported between 6 (Rodríguez-González et al., 2011a) and 15 replicates (Wu et al., 2010).

Using the experimental design and OGD protocol optimised at the University of Oxford and outlined above, Professor Lei Shi then carried out successful validation of exogenous neuroserpin as a neuroprotective agent in cultured primary cortical neurons *in vitro* at Jinan University, China. These results are shown, with the permission of Professor Shi, in Figure 5.8. Following 4 hours oxygen glucose deprivation (OGD) at 100% N_2 at 37°C, absorbance of MTT was significantly reduced compared to negative control neurons which were maintained in glucose-rich media in the incubator at 5% CO_2 at 37°C. This OGD-induced decrease in neuronal viability was confirmed using the LIVE/DEAD® Viability/ Cytotoxicity Kit (#L3224, Thermo Fisher, Hemel Hempstead, UK) to confirm a statistically significantly greater proportion of 'dead' cells, defined by the assay as those expressing cytotoxic markers, in the OGD cultures relative to negative controls. This supports a robust model of OGD-induced toxicity in cultured neurons.

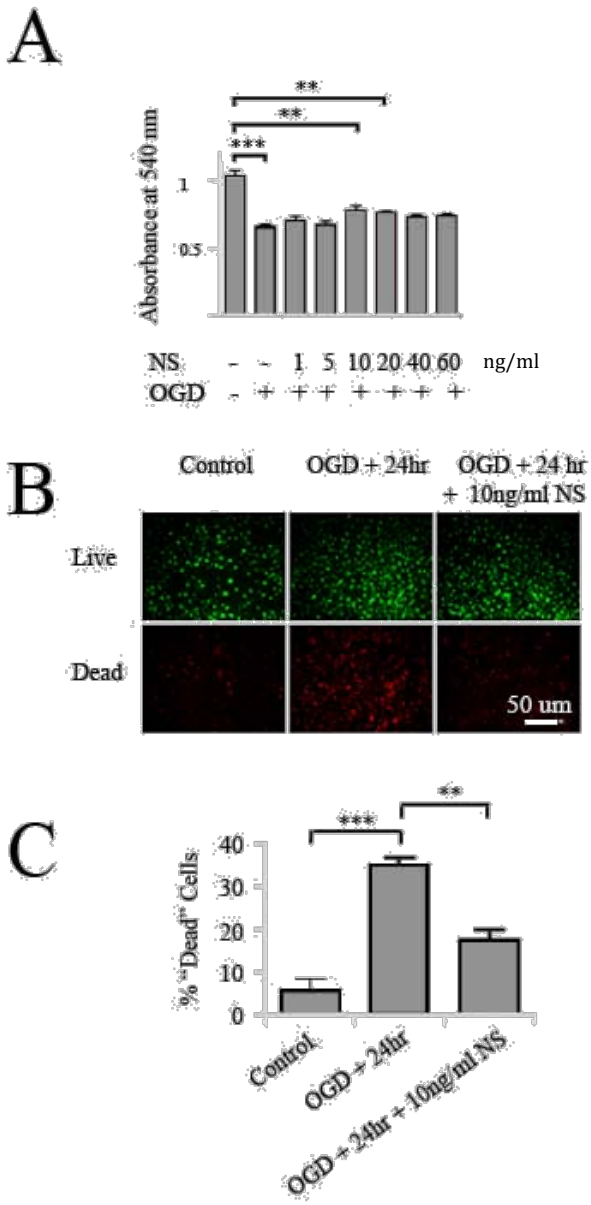


Figure 5.8 – Putative Evidence for Neuroprotective Effects of Exogenous Neuroserpin Administration as 4 hour Pre-Treatment in Dissociated Mouse Primary Cortical Neurons Prior to 4 hours Oxygen Glucose Deprivation (OGD). Experiments carried out and data provided by collaborators Dr. Qinghua Zhang, Dr. Qiaoyun Shi and Professor Lei Shi of Jinan University, China. (A) Quantification of MTT absorbance in cultured primary cortical neurons following administration of 0, 1, 5, 10, 20, 40, 60 ng/ml exogenous neuroserpin or vehicle during 4 hour pre-treatment phase prior to 4 hours OGD. Cultured neurons were allowed to recover for 24 hours prior to analysis. Neuroserpin administration led to a statistically significant increase in MTT staining, supporting previous reports of neuroserpin neuroprotection following OGD in cultured neurons. (B) Representative fluorescent immunohistochemistry images of primary neuronal cultures stained with LIVE/DEAD® Viability/ Cytotoxicity Kit (#L3224, Thermo Fisher, Hemel Hempstead, UK) Scale bar indicates area of 50µm width. These images have been altered to increase brightness for clarity. All images are modified uniformly. (C) Quantification of the proportion of the total number of cells labelled with the LIVE/DEAD® Viability/Cytotoxicity Kit recorded as "dead", detected with red fluorescence but not detected with green fluorescence. Statistical significant was assessed by unpaired T-tests.
* denotes a P-value > 0.01, ** denotes a P-value > 0.005, *** denotes a P-value > 0.001
NS = exogenous neuroserpin #130-14, Peprotech EC Ltd. UK

However, the restorative effect of exogenous neuroserpin in these cultures was again modest. There was a statistically significant increase in MTT absorbance in cultures pre-treated with 10 or 20 ng/ml exogenous neuroserpin for 4 hours prior to OGD, compared to cultures which were pre-treated with vehicle prior to exposure to OGD. However, cultures exposed to 1, 5, 40, or 60 ng/ml exogenous neuroserpin did not demonstrate statistically significant differences in MMT absorbance compared to vehicle treated cultures. At the two doses which did result in a significant increase in MTT absorbance, 10 ng/ml and 20 ng/ml, pre-treatment with neuroserpin did not fully restore MTT staining to the levels measured in negative control cultures that did not undergo OGD. Recombinant neuroserpin was purchased as a powder (#130-14, Peprotech EC Ltd., London, UK), and dissolved in culture medium prior to administration. The negative control vehicle constituted the same volume of medium without dissolved neuroserpin.

The relatively harsh OGD protocol described here, compared to durations of 55 to 150 minutes reported in the literature (Wu et al., 2010; Rodríguez-González et al., 2011a; Ma et al., 2012b), may be too severe to be fully alleviated by exogenous neuroserpin protein. It is possible that neuroserpin only creates a substantial neuroprotective effect in mild OGD conditions. Several other methodological differences, including strain of mouse, plating density, medium composition, and duration of reoxygenation, could account for differences between these results and those previously reported. It is not possible to draw any strong conclusions from these experiments in the context of the literature, as there is currently no consensus on standard methodology for producing OGD-induced damage in cultured primary cortical neurons, which would allow independent validation of any one result.

The results reported in collaboration with Professor Lei Shi's group at Jinan University in China define a replicable protocol for inducing cell death in primary cortical neurons by OGD. However, the potency of a neuroserpin neuroprotective effect remain inconclusive. Now that a robust paradigm has been identified, further experiments are needed to quantify the effect of exogenous neuroserpin following different durations of OGD and in neurons from the *Serpini1* knock-out mouse.

5.3.2 Brain Damage in *Serpini1* Knock-Out and Wild-type Brains following Neonatal Hypoxia Ischaemia in Mouse

In order to investigate the role of neuroserpin in sensitivity to neonatal hypoxia ischaemia *in vivo*, two established methods of quantifying brain injury were carried out in P10 *Serpini1* knock-out mice and wild-type littermates following neonatal HI at P8. Methods were informed by previous studies documenting a greater lesion volume (Cinelli et al., 2001; Gelderblom et al., 2013) and increased intracerebral infiltration of inflammatory cells (Gelderblom et al., 2013) in adult *Serpini1* knock-out animals following ischaemic stroke, relative to wild-type animals.

The first method assessed lesion volume by staining brains with respiratory activity marker 2,3,5-triphenyltetrazolium chloride (TTC) (Ten et al., 2003; Sun et al., 2012). The second method quantified the number of inflammatory marker immunoreactive cells present in primary somatosensory cortex (S1), and total cortical area covered by immunoreactive pixels, across the two cortical hemispheres of *Serpini1* knock-out, heterozygote, and wild-type animals 48 hours after exposure to hypoxia (Nathaniel and Nathaniel, 1981; Kreutzberg, 1996; Ito et al., 1998).

5.3.2.1 Metabolic Activity in *Serpini1* Knock-Out and Wild-type Brains following Neonatal Hypoxia Ischaemia in Mouse

In order to test the vulnerability of *Serpini1* knock-out to neonatal hypoxic ischaemic brain injury, lesion volume was investigated by TTC staining in P10 mice following a modified Rice-Vannucci method.

The tetrazolium salt, 2,3,5-triphenyl tetrazolium chloride (TTC), which undergoes a sharp colour change from colourless to red-purple on mild reduction, has been used extensively to characterise lesion volume in animal models of neonatal hypoxia ischaemia (Hatfield et al., 1991; Ashwal et al., 1995; Ten et al., 2003; Jatana et al., 2006; Wei et al., 2006; Williams et al., 2013). TTC staining was also selected as one of the methods employed to detect lesions in adult *Serpini1* knock-out mice following ischaemic stroke (Gelderblom et al., 2013). TTC staining is reduced in non-respiring tissue, allowing the differentiation of dead tissue at the lesion site which appears white, from healthy respiring tissue which appears dark red (reviewed in Berridge et al., 2005).

Following TTC perfusion, brains were dissected out and photographed using the 1.6 x objective magnification lens under a light microscope (Leica DMR microscope, #933789, Leica Microsystems, Milton Keynes, UK). All brains were imaged using identical microscope magnification, illumination, and camera settings. Details of all brains included in TTC staining analysis are given in Table 5.7. Brains were divided into groups by genotype. A number of brains across all genotypes were analysed separately due to a pattern of atypical dark purple-black staining across the whole exterior surface, which was not consistent with the literature or the other tissue generated for this study. These brains were analysed together under a separate

‘discarded’ category. None of the brains across any genotype showed large distinctly bounded lesions as reported following more severe HI injury paradigms (Ten et al., 2003; Sun et al., 2012). Figure 5.9 shows representative images of TTC-perfused brains in each category.

Intensity of TTC staining was analysed blind to the genotype. Pixel intensity values from each brain were compared via a frequency histogram by Dr. Anna Hoerder-Suabedissen. Mean pixel intensities across the red channel were lower in *Serpini1* knock-out whole brains compared to wild-type and heterozygote littermates. It is possible that *Serpini1* knock-out brains exhibited greater damage as a result of neonatal HI injury compared to wild-type littermates, and therefore less cellular respiration was detected by TTC staining. However, it is more likely that high variability generated by manual TTC perfusion is responsible for the modest fluctuations between TTC staining patterns observed here. A more severe surgical procedure which produces clearly defined lesions across all genotypes is needed for such comparisons to be made reliably. Results are summarised in Figure 5.9.

This method will require substantial optimisation before it can reliably be used as a method of lesion volume quantification following neonatal hypoxia ischaemia. The penetration of TTC staining to deep brain structures was unpredictable compared to that previously reported in the literature (Ten et al., 2003; Sun et al., 2012). Some brains demonstrated the presence of localised red-purple crystals of solid TTC in deep brains structures, where others showed little or no staining deeper than the pial surface. Figure 5.10 displays representative images capturing the variability in TTC staining patterns between individual *Serpini1* knock-out brains.

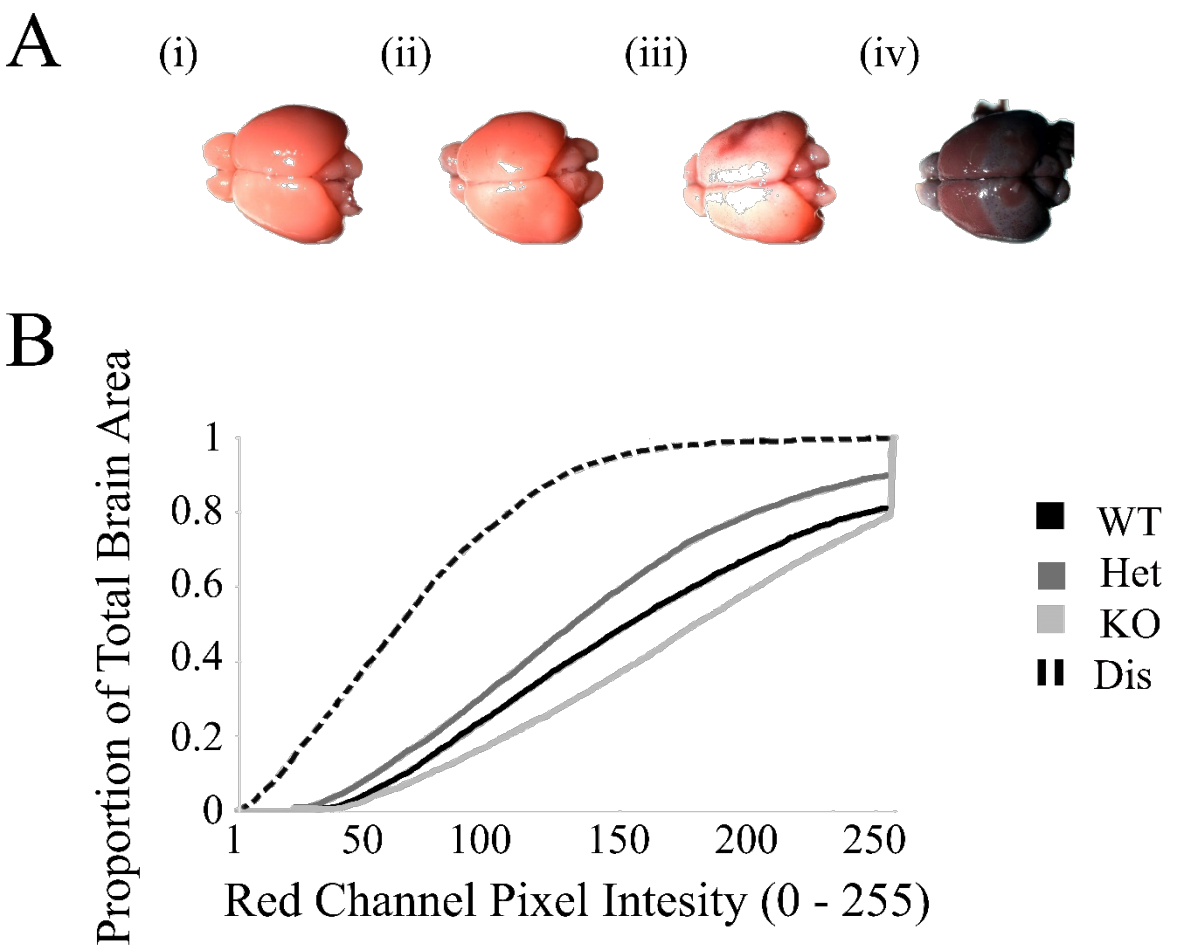


Figure 5.9 – Quantitative Analysis of 2,3,5-Triphenyltetrazolium chloride (TTC) Staining Intensity in TTC-Perfused Whole Brains of P10 Mice Following Neonatal Hypoxia-Ischaemia by the Adapted Rice-Vannucci model at P8. Microscope images were acquired and TTC-staining intensity analysis was carried out blind to the genotype by Dr. Anna Hoerder-Suabedissen. Results are reproduced here with her permission. Clearly defined lesion sites were not visible in any genotype. TTC staining across red channel frequencies was slightly lower across whole brains of *Serpini1* KO animals compared to WT and Het animals, however, high variability of staining intensity and low TTC penetration (see Figure 5.10) prevented meaningful analysis of statistical significance of TTC staining analysis in whole brains. (A) Representative light microscopy images taken using the 1.6 x magnification objective of TTC-perfused whole brains. (i) Wild-type (WT). (ii) Heterozygote (Het). (iii) *Serpini1* knock-out (KO). (iv) Representative image of brain discarded from analysis, discarded brains included examples from all genotypes. (B) Frequency histogram generated with Image J. Values generated from hand-drawn regions of interest (ROI) including the whole brain, both cortical hemispheres and the olfactory bulbs, excluding the cerebellum when present. Adapted from a figure created by Dr. Anna Hoerder-Suabedissen (unpublished). No statistical significance analysis was undertaken on these results.
WT = C57BL/6J homozygote wild-type, Het = C57BL/6J x B6.129-Serpini1^{tm1Dpw}/J heterozygote, KO = B6.129-Serpini1^{tm1Dpw}/J homozygote *Serpini1* knock-out, Dis. = discarded, mixed genotypes



Figure 5.10 – Representative 50µm Thickness Coronal Sections from Five Individual *Serpini1* Knock-Out Brains demonstrating the High Variability in 2,3,5-triphenyl tetrazolium chloride (TTC) Staining Penetration into Deep Brain Structures. All brains were taken from animals of identical genotype which underwent the adapted Rice-Vannucci method of hypoxia ischaemia 48 hours prior to perfusion with TTC. Images were acquired by Dr. Anna Hoerder-Suabedissen. All five brains demonstrated different patterns of TTC signal absorbance. The left-most brain exhibited large red/purple TTC crystals in the cerebral cortex, with no evidence of staining beneath the subcortical white matter. The second and third brains from the left show evidence of sparse TTC crystals in the cerebral cortex, with isolated crystals present in the hippocampus. The fourth and fifth brains from the left do not contain any macroscopic TTC crystals, although these brains appear to possess a red/purple tint in the vasculature. All five brains appeared visibly red externally prior to vibratome sectioning. Scale bar indicates area of 250µm and 100µm width.

There are several potential explanations for this low penetration of TTC into the brain. The first concern the perfusion process itself. Previous publications in adult rodents have perfused intracerebrally through the middle cerebral artery (Sun et al., 2012). Although this method delivers TTC molecules directly to the brain, it raises methodological challenges of its own, in that lesion volumes could be exaggerated in animals which have received some damage to the middle cerebral artery and its capillaries selectively, and it provides no direct perfusion to other cerebral vasculature. One possible method to improve the penetration of TTC staining could employ fresh-tissue sectioning apparatus to produce brain slices of approximately

2mm in thickness, which could then be incubated in TTC at 37°C for between 30 minutes and 1 hour to allow staining to mature (Ten et al., 2003). It is also possible that the vibratome frequency used to generate the 50µm sections shown in Figure 5.10 disrupted the TTC crystal structure, resulting in substantial leakage of dye into the incubating 0.1M PBS solution during sectioning.

The difference in TTC staining intensity did not suggest a substantial global difference in respiration as measured from images of whole brains. Coronal brain sections revealed that the TTC perfusion penetration was low, which can be resolved by experimental optimisation. None of the brains analysed demonstrated evidence of well-defined lesion sites. Future experiments will be needed to determine whether this is the result of low TTC penetration or low severity of injury resulting from the relatively mild exposure to 10% O_2 partial pressure for 55 minutes at 36.5°C.

5.3.2.2 Inflammatory Markers in *Serpini1* Knock-Out and Wild-type Brains following Neonatal Hypoxia Ischaemia in Mouse

A second method for quantifying brain damage was employed to complement TTC staining and relate these results to the neuroserpin-immunoreactivity quantification in wild-type mice subjected to 55 minutes hypoxia described in Chapter 3, Section 3.3.3. Following TTC analysis, brains were sectioned and underwent immunohistochemistry with antibodies against glial inflammatory markers GFAP, Iba1, and CD68.

Glial fibrillary acidic protein (GFAP), ionised calcium-binding adapter molecule 1 (Iba1), and cluster of differentiation 68 (CD68), have all been used extensively to demonstrate cerebral inflammation in rodent models of neonatal hypoxia ischaemia

(Fathali et al., 2013; Pogledic et al., 2014; Savard et al., 2015; Zaghloul et al., 2017; Chip et al., 2017; McAdams et al., 2017). In addition, one investigation into adult ischaemic stroke in mice described in increase in the number of CD11b-positive CD45-high microglia in the brains of *Serpini1* knock-out mice post-stroke compared to wild-type controls (Gelderblom et al., 2013). This study also reported a greater number of 'activated' microglia, here defined as CD11b-positive CD45-high cells co-expressing tumour necrosis factor α (TNFα), in the *Serpini1* knock-outs. However, this investigation reported that numbers of brain macrophages, neutrophils, lymphocytes and dendritic cells were not significantly different from that of wild-type controls. The authors suggested that in the absence of neuroserpin, the brain may produce a hyper-inflammatory response to ischaemic stroke (Gelderblom et al., 2013). It is unknown whether this hyper-inflammatory response extends to other resident cells such as astrocytes, or if it is present at all in the infant brain.

The occurrence of modest yet statistically significant increases in inflammatory marker immunoreactivity was confirmed for all genotypes for one or more marker. Numbers of immunoreactive cells and the proportion of total cortical area covered by fluorescent pixels was quantified from P10 mouse primary somatosensory cortex imaged with the 20 x objective lens of a confocal microscope (Zeiss LSM 710, Carl Zeiss Microimaging, Oberkochen, Germany). For full details of the immunoreactivity quantification see Chapter 3, Sections 3.2.2 and 3.2.3.

The number of GFAP-immunoreactive cells was significantly higher in the hypoxic-ischaemic ipsilateral hemisphere compared to the hypoxia-only contralateral hemisphere across all layers of cortex in wild-type (227 ± 38 compared with 208 ± 48), heterozygote (218 ± 54 compared with 182 ± 57) and *Serpini1* knock-out (220 ±

40 compared with 201 ± 24) brains. However, there was no statistically significant difference between genotypes in the number of GFAP-immunoreactive cells. Only heterozygote animals demonstrated a statistically significant different number of Iba1-immunoreactive cells between ipsilateral and contralateral hemispheres (245 ± 64 compared with 189 ± 54), with wild-type (185 ± 25 compared with 183 ± 55) and *Serpini1* knock-out (236 ± 50 compared with 210 ± 41), only demonstrating trends towards increased Iba1-immunoreactive microglial cell numbers in the hypoxic ischaemic hemisphere. The only significant different between genotypes was observed in the number of cortical cells quantified as CD68-immunoreactive. All genotypes demonstrated a statistically significant difference in the number of CD68-immunoreactive cells between hemispheres, with both wild-types (4 ± 3 compared with 3 ± 2) and heterozygotes (3 ± 1 compared with 2 ±1) exhibiting significantly smaller numbers of CD68-immunoreactive cells in the hypoxic-ischaemic hemisphere compared to *Serpini1* knock-outs (15 ± 16 compared with 6 ± 8). It is possible that the increase in the number of CD68-immunoreactive cells indicates increased recruitment of specific populations of inflammatory cells in the *Serpini1* knock-out brain in the absence of neuroserpin. However, the lack of a statistically significant difference in GFAP and Iba1 immunoreactivity between genotypes argues against a global increase in brain inflammation in this model. Results are shown in Figure 5.11 and Table 5.12.

Analysis of immunoreactive cortical area values corresponded strongly to that of cell number quantification described above. The GFAP-immunoreactive proportion of total cortical area was significantly higher in the ipsilateral hemisphere in heterozygote (0.098 ± 0.037 compared with 0.070 ± 0.026) and *Serpini1* knock-out (0.116 ± 0.066 compared with 0.076 ± 0.042) brains, although there was no significant difference between hemispheres in wild-type animals (0.103 ± 0.036

compared with 0.094 ± 0.035). There was no significant difference between genotypes. In all three genotypes, a greater proportion of cortex was covered by Iba1-immunoreactive pixels in the ipsilateral hemisphere, yet there was no significant difference between the proportion of cortical area in the hypoxic-ischaemic hemisphere covered by Iba1-immunoreactive pixels in wild-type (0.022 ± 0.007 compared with 0.017 ± 0.006), heterozygote (0.042 ± 0.032 compared with 0.029 ± 0.013) and knock-out (0.027 ± 0.010 compared with 0.021 ± 0.008) genotypes. Again, the only significant difference between genotypes occurred with CD68-immunoreactivity. Both wild-types (0.003 ± 0.004 compared with 0.001 ± 0.001) and heterozygotes (0.002 ± 0.004 compared with 0.002 ± 0.002) exhibited a significantly smaller proportion of total cortical area covered by CD68-immunoreactity compared to the *Serpini1* knock-outs (0.025 ± 0.029 compared with 0.012 ± 0.017). These results support the conclusions from the cell counts described above, that a small yet statistically significant increase in intracerebral inflammation in the hypoxia-ischaemic hemisphere occurs, with uniform inflammatory response across genotypes.

Glial morphology, in addition to number, also serves as an indicator of inflammation (reviewed in Panickar and Norenberg, 2005; Liu et al., 2014; Ruzafa et al., 2017). All three genotypes demonstrated astrocytes with activated morphology, although this was not quantified. Hypertrophic astrocytes were observed in the injured hemispheres of all brains, with a potential enrichment within the subplate and subcortical white matter in the injured hemisphere of knock-out brains. All brains contained astrocytes across the spectrum of morphology. However, there was little qualitative difference in morphology of microglia in the injured hemisphere between genotypes. All three genotypes showed evidence of weak microglial activation, with no distinctly amoeboid cells. Overall, a similar pattern of mild hypertrophy described in Chapter 4,

Section 4.3.3. Another measure which could have been compared directly between brains of different genotypes is that of cell death. Again, there was no significant difference between genotypes in number or density of NeuN-immunoreactive cells, however, this is at best an indirect measure of cell death which may fail to detect genuine loss of neurons (see Chapter 4, Section 4.3.3). No cell death cascade molecules were directly investigated.

Genotype	Age	Hemisphere	N	Litters	Number of GFAP-Immunoreactive Cells Counted	Cortical Area GFAP-Immunoreactive (± SD)
WT (+/+)	P10	Ipsilateral	5	4	2,724	0.103 (± 0.036)
WT (+/+)	P10	Contralateral	5	4	2,499	0.094 (± 0.035)
Het (+/-)	P10	Ipsilateral	5	4	2,610	0.098 (± 0.036)
Het (+/-)	P10	Contralateral	5	4	2,644	0.070 (± 0.027)
KO (-/-)	P10	Ipsilateral	5	4	2,644	0.116 (± 0.066)
KO (-/-)	P10	Contralateral	5	4	2,413	0.076 (± 0.042)
					Number of Iba1-Immunoreactive Cells Counted	**Cortical Area Iba1-Immunoreactive (± SD)**
WT (+/+)	P10	Ipsilateral	5	4	2,222	0.022 (± 0.007)
WT (+/+)	P10	Contralateral	5	4	2,194	0.016 (± 0.007)
Het (+/-)	P10	Ipsilateral	5	4	2,937	0.043 (± 0.032)
Het (+/-)	P10	Contralateral	5	4	2,271	0.029 (± 0.013)
KO (-/-)	P10	Ipsilateral	5	4	2,833	0.027 (± 0.010)
KO (-/-)	P10	Contralateral	5	4	2,525	0.021 (± 0.008)
					Number of CD68-Immunoreactive Cells Counted	**Cortical Area CD68-Immunoreactive (± SD)**
WT (+/+)	P10	Ipsilateral	5	4	52	0.003 (± 0.004)
WT (+/+)	P10	Contralateral	5	4	37	0.001 (± 0.001)
Het (+/-)	P10	Ipsilateral	5	4	40	0.002 (± 0.004)
Het (+/-)	P10	Contralateral	5	4	36	0.002 (± 0.002)
KO (-/-)	P10	Ipsilateral	5	4	217	0.025 (± 0.029)
KO (-/-)	P10	Contralateral	5	4	85	0.012 (± 0.017)

Table 5.12 – Comparison of Inflammatory Brain Damage Markers between Wild-Type, *Serpini1* Knock-Out Heterozygote, and *Serpini1* Knock-Out Homozygote Brains Following Neonatal Hypoxia Ischaemia by Fluorescent Immunohistochemistry. All images were taken in primary somatosensory barrel cortex (S1). The raw number of GFAP-immunoreactive astrocytes, Iba1-immunoreactive microglia, and CD68-immunoreactive phagocytes are shown alongside the total proportion of cortical area covered by fluorescent pixels. Brains of all three genotypes showed modest evidence of increased inflammation in the hypoxic-ischaemic ipsilateral hemisphere compared to the hypoxia-only contralateral hemisphere, suggesting mild brain injury. However, the only difference between genotypes was increased CD68 immunoreactivity in the KO brains. Two-way ANOVA demonstrated a statistically significant difference between groups based on glial molecular marker and condition (hemisphere). T-tests were conducted to confirm statistical significance between groups.
WT = C57BL/6J homozygote wild-type, Het = C57BL/6J x B6.129-Serpini1^{tm1Dpw}/J heterozygote, KO = B6.129-Serpini1^{tm1Dpw}/J homozygote *Serpini1* knock-out

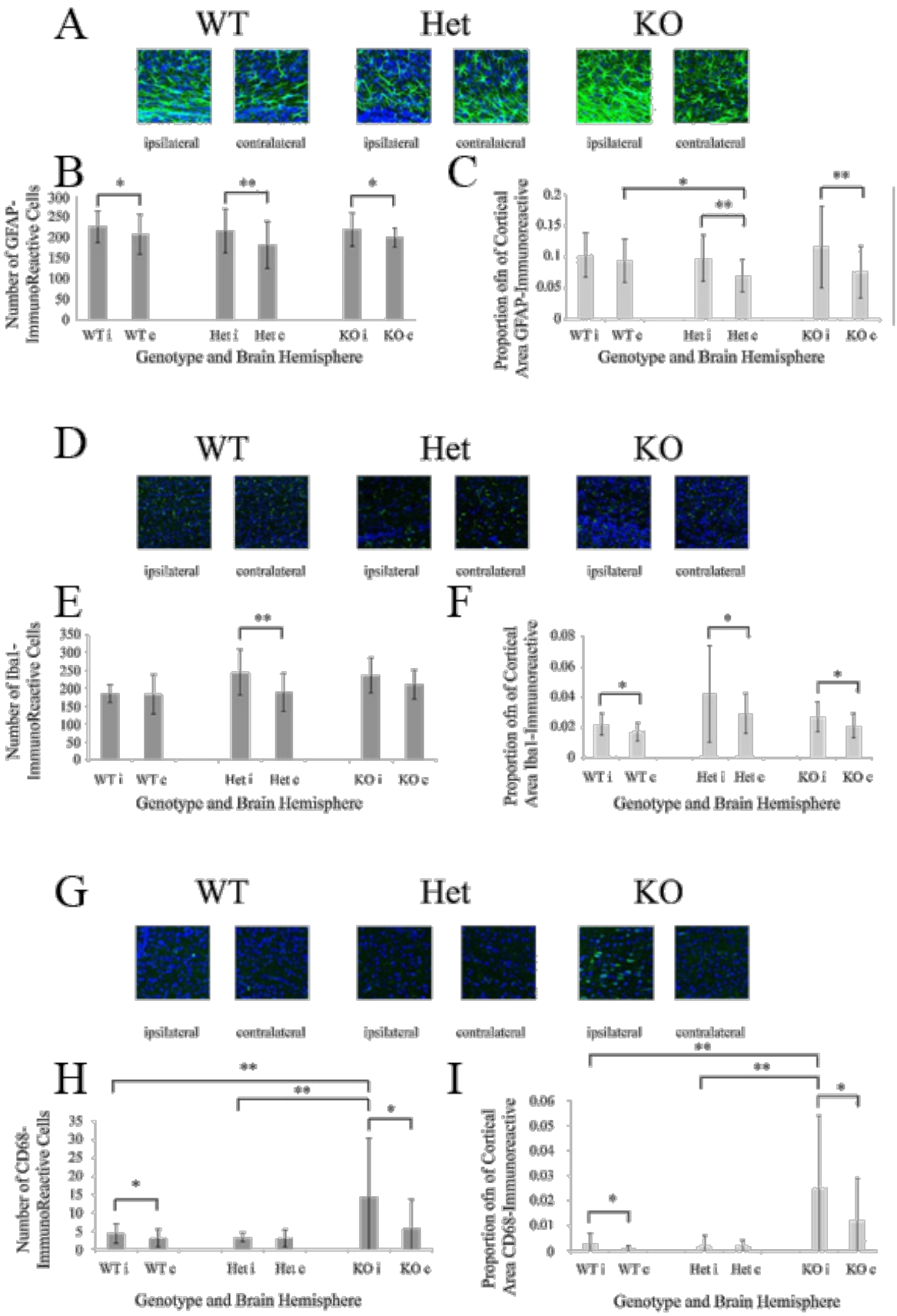

A
WT
Het
KO
ipsilateral
contralateral
B
Number of GFAP-ImmunoReactive Cells
WT i
WT c
Het i
Het c
KO i
KO c
Genotype and Brain Hemisphere
C
Proportion ofn of Cortical Area GFAP-Immunoreactive
Genotype and Brain Hemisphere
D
E
Number of Iba1-ImmunoReactive Cells
F
Proportion ofn of Cortical Area Iba1-Immunoreactive
G
H
Number of CD68-ImmunoReactive Cells
I
Proportion ofn of Cortical Area CD68-Immunoreactive

Figure 5.11 – Quantification of Inflammatory Glial Markers in the adapted Rice-Vannucci Mouse Model of Neonatal Hypoxia Ischaemia (HI) by Immunohistochemistry in Primary Somatosensory Cortex (S1) of P10 Mouse following Hypoxia Ischaemia at P8. The hypoxic-ischaemic ipsilateral (ipsi) hemisphere and hypoxic-only contralateral (contra) hemispheres were analysed separated for littermates of WT, Het, and KO genotypes. In this pilot experiment, there was little evidence of increased brain inflammation in the *Serpini1* KO mouse. All three genotypes showed increased immunoreactivity in ipsilateral hemisphere compared to the contralateral hemisphere across one or more of the inflammatory markers investigated. However, the only statistically significant difference in inflammatory marker immunoreactivity between genotypes was for CD68. Although mild statistically significant differences in inflammatory marker immunoreactive cells and the proportion of the total cortical area immunoreactive were observed between hemispheres, confirming increase inflammation as a results of neonatal hypoxia ischaemia in all genotypes, there was little different in marker immunoreactivity between genotypes at N = 5. (A) Expanded representative confocal images of P10 subplate stained for GFAP in green and DAPI in blue. Scale bar indicates area of 10 μm width. (B) Quantitative analysis of the raw number of GFAP-immunoreactive cells across all cortical layers (mean ± SD). (C) Quantitative analysis of the proportion of total cortical area covered by GFAP immunoreactivity (mean ± SD). (D) Expanded representative confocal images of P10 subplate stained for Iba1 in green and DAPI in blue. (E) Quantitative analysis of the raw number of Iba1-immunoreactive cells across all cortical layers (mean ± SD). (F) Quantitative analysis of the proportion of total cortical area covered by Iba1 immunoreactivity (mean ± SD). (G) Expanded representative confocal images of P10 subplate stained for CD68 in green and DAPI in blue. (H) Quantitative analysis of the raw number of CD68-immunoreactive cells across all cortical layers (mean ± SD). (I) Quantitative analysis of the proportion of total cortical area covered by CD68 immunoreactivity (mean ± SD). Two-way ANOVA demonstrated a statistically significant difference between groups based on glial molecular marker and on condition for marker immunoreactivity. Unpaired T-tests were conducted to compare immunoreactivity between HI animals and sham-operated controls, paired T-tests were used to compare immunoreactivity between hemispheres in HI animals undergoing either mild or moderate HI.
* denotes P-value < 0.01, ** denotes P-value < 0.005, *** denotes P-value < 0.001
WT = C57BL/6J homozygote wild-type, Het = C57BL/6J x B6.129-Serpini1^{tm1Dpw}/J heterozygote, KO = B6.129-Serpini1^{tm1Dpw}/J homozygote *Serpini1* knock-out

Overall, the results of these experiments provide more information about the usefulness of the model than about the inherent role of neuroserpin in rodent models of neonatal hypoxia ischaemia. The small yet statistically significant differences in the number of glial marker-immunoreactive cells in the hypoxic-ischaemic hemisphere compared to the hypoxia-only control hemisphere support the presence of mild inflammatory brain injury in animals of all genotypes. However, constraints placed on the model to reduce mortality, and the high variability in injury severity between littermates (Vannucci and Hagberg, 2004; Vannucci and Vannucci, 2005), prevented systematic evaluation of moderate-to-severe injury without causing an unduly high mortality rate for a pilot study.

Although experiments found a statistically significant increase in CD68-immunoreactivity in *Serpini1* knock-out mice compared to wild-type and heterozygous animals, there was no difference in GFAP- and Iba1-immunoreactivity between genotypes. This may suggest an increase in phagocyte infiltration in knock-out animals, yet there is no evidence of a global hyper-inflammatory response following neonatal hypoxia ischaemia in the absence of neuroserpin.

There are several methodological limitations to these experiments. The first is the presence of TTC staining in brains processed for immunohistochemistry. Although the blue and green channels were used to minimise interference from the red-purple TTC stain, it is possible that interference from the red channel artificially increased variability in immunohistochemistry quantification. The high variability in Rice-Vannucci neonatal hypoxia ischaemia brain damage outcome between littermates (reviewed in Vannucci and Vannucci, 2005) requires a large number of individual animals to support a positive result. At N = 5, any strong effects detected would require validation with a new cohort including a larger number of animals in future. These pilot results provide some rationale for pursuit of the number of CD68-immunoreactive phagocytes in a larger number of animals, but do not support an expanded study of numbers of astrocytes of microglia across genotypes following neonatal hypoxia ischaemia.

Explorative experiments provided little evidence for increased sensitivity to neonatal hypoxia ischaemia in *Serpini1* knock-out mice, although this mostly negative result is highly qualified by the specifics of the experimental paradigms selected for inducing neonatal hypoxia ischaemia in animals.

5.4 Discussion

This chapter describes the inconclusive results generated in experiments designed to probe the sensitivity of *Serpini1* knock-out animals to oxygen glucose deprivation (OGD) *in vitro* and neonatal hypoxia ischaemia *in vivo*. These experiments did not find strong evidence for difference in injury sensitivity between *Serpini1* knock-out and wild-type animals, although the wide variability in standard methodologies used to pose these questions do not preclude the possibility of demonstrating *Serpini1* hyper-sensitivity to hypoxic ischaemic damage by other experimental protocols.

5.4.1 Satisfaction of Chapter Aims

The aims of this chapter, stated in full in Section 5.1.1, were investigated with partial success, consistent with a modest neuroserpin-mediated effect in both *in vitro* and *in vivo* models of neonatal hypoxia ischaemia. This chapter establishes experimental designs which could be used to test if the hyper-sensitivity to ischaemic stroke reported in adult *Serpini1* knock-out animals (Cinelli et al., 2001; Madani et al., 2003; Gelderblom et al., 2013) extends to neonatal hypoxia ischaemia.

Neuro-2-A (N2A) neuroblastoma cells lines and primary cortical neurons were used to establish a reproducible oxygen glucose deprivation (OGD) protocol which generated partial reduction in cell viability as assessed by MTT assay. However, these experiments did not clearly replicate previously reported evidence of exogenous neuroserpin neuroprotection (Wu et al., 2010; Rodríguez-González et al., 2011a; Ma et al., 2012b). This may be due to lack of consensus within the literature regarding standard conditions optimal for OGD, leading to wide variation in methodologies

across multiple parameters between researchers. Assessment of OGD sensitivity of *Serpini1* knock-out mouse neurons could not be satisfied due to the small number of replicates and the high probability of bacterial contamination in cultures. In future, these experiments could be re-established with the protocol outlined in this chapter.

The vulnerability of the *Serpini1* knock-out mouse to neonatal hypoxia ischaemia (HI) was also investigated *in vivo*. Shallow penetration of TTC into the brains of many experimental animals suggests methodological optimisation will be required before lesion volume analysis can be compared between *Serpini1* knock-out and wild-type littermates. Injury confirmation by immunohistochemistry also revealed only modest differences in inflammatory marker immunoreactivity between genotypes. The only statistically significant difference was elevated numbers of CD68-immunoreactive phagocytes in knock-out animals. It is possible that *Serpini1* knock-out mice do experience an increase in specific sub-types of inflammatory cells following neonatal hypoxia ischaemia. However, this can only be resolved using a greater number of animals, potentially divided across multiple severities of HI.

5.4.2 Evaluation of Vulnerability to Neonatal Hypoxia Ischaemia in the *Serpini1* Knock-Out Mouse *In Vivo*

The results of these initial experiments provide little more than a hint of increased injury sensitivity in the absence of neuroserpin. In the absence of behavioural testing, which is required for meaningful validation of any rodent model of a human neurodevelopmental disease (reviewed in Arteni et al., 2003; Lubics et al., 2005; Millar et al., 2017), these anatomical results can be taken as evidence of mild brain injury, similar to that previously reported in animal models of neonatal hypoxia

ischaemia (Rice et al., 1981; Towfighi et al., 1991; 1995; Ditelberg et al., 1996; Ferriero et al., 1998; Okusa et al., 2014).

Mean TTC staining intensity was slightly reduced in *Serpini1* knock-out brains compared to wild-type and heterozygote brains. Intensity patterns overlapped across the three genotypes, which does not support a categorical different in injury between genotypes. Well-defined lesion sites on the cortical surface could not be discerned on the surface of any brains, contrary to previous publications which have used this method (Ten et al., 2003; Sun et al., 2012), questioning the utility of these results. It is possible that 55 minute exposure to 10% O_2 balanced with 90% N_2 at 36.5℃ was too mild to produce macroscopic lesions. Body temperature during hypoxia is known to substantially affect injury severity (Rogalska et al., 2004; 2006; 2009; Caputa et al., 2005; Robertson and Iwata, 2007), and the inherent variability in outcomes between animals (reviewed in Vannucci and Hagberg, 2004; Vannucci and Vannucci, 2005) could account for brains with no macroscopic evidence of necrosis or scarring within cohorts subjected to relatively severe models of neonatal HI (Huang et al., 2009; Ligam et al., 2009; Srivastava et al., 2012; Okusa et al., 2014). It is also possible that failure to detect lesions resulted not from the procedure used to produce hypoxia ischaemia, but from the TTC perfusion paradigm. Future experiments could improve penetration by combining the pericardial perfusion technique (Sun et al., 2012) with fresh tissue slicing and incubation in warmed TTC (Ten et al., 2003), to maximise the area of brain tissue exposed to TTC. In the perfusion method, TTC must enter the brain through the cerebral vasculature which may have undergone necrosis and neovascularisation that could affect blood flow (reviewed in Alvarez-Diaz et al., 2007) irrespective of the health of the neuronal tissue itself. The fresh slice method is also limited, as dissected tissue cannot fully represent the condition of a live animal.

The only conclusion is that gross brain anatomy did not differ substantially following mild neonatal HI, which is in itself meaningful.

The result of the quantitative immunohistochemistry is more readily interpretable. The was no difference in either the number of immunoreactive cells or proportion of total cortical area covered by GFAP or Iba1. This latter finding contrasts with a publication which claimed a greater number of activated microglia by flow cytometry in the brains of adult *Serpini1* knock-out mice following induction of adult ischaemic stroke (Gelderblom et al., 2013). However, the phagocyte marker CD68 was expressed at significantly higher levels in the *Serpini1* knock-out cortex following neonatal hypoxia ischaemia compared to either the wild-type or heterozygote. This difference may be the first evidence of an altered cerebral inflammatory response in the absence of neuroserpin in the neonatal brain. Even if this does prove robust and replicable, it is still a relatively modest marker-specific finding.

The elevated expression of CD68-immunoreactive cells in the *Serpini1* knock-out observed merits further investigation. There is some evidence that tissue plasminogen activator (tPA), one enzymatic target of neuroserpin (Osterwalder et al., 1996), and other proteins tPA interacts with, have a role in the differentiation of monocytes to phagocytotic macrophages (Stoppelli et al., 1985; Crutchley et al., 1989; Devaraj et al., 2003; 2009). It is possible that, in the absence of neuroserpin in the *Serpini1* knock-out mouse, monocyte differentiation occurs at an enhanced rate. Although the monoclonal antibody Ab955 (Abcam, London, UK) used to stain for CD68 has been validated in previous publications (Gordon et al., 2017; Liu et al., 2017; Yang et al., 2017), verification of the specificity of the batch used here would heighten the validity of this claim.

If this effect is genuine it could shed light on an interesting area of division in the field. There is currently debate surrounding whether phagocytosis and autophagy observed in neonatal hypoxia ischaemia is beneficial or deleterious (Lockshin and Zakeri, 1994; Carloni et al., 2008; Ginet et al., 2009; reviewed in Millar et al., 2017). One study found that the drug rapamycin, which increases autophagy, decreased overall cell death in the HI hemisphere of P7 rat brains, whereas drugs which inhibited autophagy merely triggered an increase in necrotic cell death (Carloni et al., 2007). However, the same autophagy inhibitor, 3-methyladenine, administered prior to HI at P12 was found to decrease lesion volume (Puyal et al., 2009). Transgenic animals lacking expression of the gene Autophagy related 7 (*Atg7*) also demonstrated smaller lesion volumes (Koike et al., 2008). This is an interesting question which deserves further investigation.

Another interpretation of these modest results is as a confirmation of the distinct biological differences between the adult and neonatal brain. Many complex cascades in the adult brain interact differently in the infant, from NMDA-receptor mediated excitotoxicity to free radical generating enzymes to the structural integrity of the blood brain barrier (reviewed in Baburamani et al., 2012; Millar et al., 2017). It is possible that the neuroserpin/tPA cascade is another significant point of difference between these two developmental stages. Despite the widespread use of recombinant tPA as an acute treatment for adult stroke patients (Hacke et al., 1995; reviewed in Graham, 2003; Hacke et al., 2004; 2008; Lansberg et al., 2009; Whiteley et al., 2012; Wardlaw et al., 2012; IST-3 Collaborative Group, 2012), it is possible that this molecular cascade plays a completely different role in neonatal brain injury. Several microarray studies in rodents failed to detect significant changes in *PLAT*, the gene which encodes tPA in mouse, or *Serpini1* expression in the brain following neonatal

HI (Carmel et al., 2004; Maj et al., 2004a; 2004b; Juul et al., 2009; Nagel et al., 2012; Rognlien et al., 2014). However, there is evidence that tPA inhibitor enzymes α2-antiplasmin (α2AP) (Adhami et al., 2008) and plasminogen-activator-inhibitor 1 (PAI1) (Yang et al., 2013; Yang and Kuan, 2015) can alleviate the behavioural deficits caused by neonatal HI in rats. It is unclear from the relatively sparse literature how important this cascade's function is in neonatal HI, and whether these molecules could one day come to play any role in treatment as recombinant tPA does in adult ischaemic stroke.

It is clear that further investigation of vulnerability in the *Serpini1* knock-out mouse is required, which would ideally account for the methodological limitations of the work reported here. One significant limitation of the current immunohistochemistry protocol is that it focuses on a small number of inflammatory markers and excludes many cellular and molecular cascades known to undergo regulation during neonatal hypoxic ischaemic injury (reviewed in Millar et al., 2017). In future investigations, transcriptomic analysis at multiple phases of injury (Maj et al., 2004a; 2004b; Juul et al., 2009), proteome analysis (Hu et al., 2006; Magagnin et al., 2007) or novel "secretome" methods (Brown et al., 2012; reviewed in Hathout, 2007) could be used to capture a greater range of pathways potentially undergoing disease-related regulation in the injured brain. These methods could confirm upregulation of damage markers, and identify specific cellular injury processes, such as phagocytosis, which may be reliant on the presence of functional neuroserpin.

Ideal experiments would also include a range of injury severities (Okusa et al., 2014). To account for the substantial differences in mortality rate reported in the literature (see Section 5.2.3) across similar experimental procedures (McQuillen et al., 2003;

Ten et al., 2003; Hagberg et al., 2004; Tsuji et al., 2004; McAucliffe et al., 2006; 2007; Lafemina et al., 2008; Carlsson et al., 2012; Lin et al., 2014; Ogawa et al., 2018; Kichev et al., 2018), it would be informative to classify brains into injury severity groups. This could allow different severities of injury to be assessed for potentially different mechanisms of neuropathology, and allow more objective comparison within the literature. Ideally, a range of durations of hypoxia would also be carried out and a range of collection times would be used to capture the greatest portion of this gradually evolving complex injury (reviewed in Fleiss and Gressens, 2012; Millar et al., 2017). It is known that the balance of cell death cascades shifts from predominantly apoptotic in mild cases to predominantly necrotic in severe cases of neonatal HI (Daval and Vert, 2004; Nakajima et al., 2000; reviewed in Northington et al., 2007, 2011). This shift gives rise to a completely different molecular pathology landscape at different injury severities, with certain putative therapies likely to be most effective across a specific injury severity range.

The *Serpini1* knock-out mouse investigated here is only one potential model of loss of function. At the time of writing, this was the only commercially available mouse model of altered *Serpini1* gene function. The universality of this knock-out, which does not produce neuroserpin in any tissue type at any developmental time-point (Cinnelli et al., 2001; Madani et al., 2003) made this a useful initial model. The utility of tissue-specific conditional knock-out models (reviewed in Rossant and McMahon, 1999; Kos, 2004; Guan et al., 2010) for investigating neuroserpin is currently unknown, as neuroserpin protein is known to be secreted (Osterwalder et al., 1996) and to be transported in the bloodstream (Rodriguez-Gonzalez et al., 2011b; 2011c). Currently, the primary sites of neuroserpin synthesis and its trafficking routes are not well understood, and further work with fluorescent-tagged protein (reviewed in

Einhauar et al., 2001; Young et al., 2012) could gather useful preliminary information before an expensive tissue-specific knock-out animal is developed. Time-point specific inducible knock-out mice could have been developed, to target the E10.5 window in which the majority of neuroserpin-immunoreactive neurons undergo neurogenesis (see Chapter 3, Section 3.3.1.4), or to remove neuroserpin production at the peak of expression around P8 (see Chapter 3, Section 3.1.1.1). This model could potentially provide interesting information concerning the role of neuroserpin expression in developmental apoptosis of subplate, determining whether equal numbers of subplate neurons undergo programmed cell death when none expression neuroserpin in early postnatal development. Equally, *Serpini1* knock-down by siRNA (reviewed in Achenbach et al., 2003; Dorsett and Tuschl, 2004), shRNA (reviewed in Yu and McMahon, 2006), or CRISPR (reviewed in Peters et al., 2015; Shalem et al., 2015) could mediate time-point specific *Serpini1* expression loss which could potentially eliminate the developmental anxiety phenotype observed in these animals (Madani et al., 2003) by reducing gene expression in post-natal development only. Despite clear utility in many research projects, the modest and unvalidated injury phenotype produced in the Serpini1 knock-out mouse in response to neonatal HI does not readily suggest a need for additional mouse models.

5.4.3 Evaluation of Methodology

This chapter has been unsuccessful in demonstrating neuroserpin neuroprotection in the neonatal mouse brain. It is possible that these results reflect a small or non-existent contribution of endogenous neuroserpin to rodent neonatal HI. Another explanation is that the low statistical power of these pilot investigations masked any

genuine protective effects. The third possibility is that the methods employed here were not best suited to interrogate the hypothesis proposed in this chapter. A high degree of variation is manifest across oxygen glucose deprivation in primary neurons, rodent models of neonatal hypoxia ischaemia, and TTC perfusion. None of these techniques have validated standardised protocols. Instead, these methods represent a range of related models united by a common theory but combining multiple values for different parameters, producing qualitatively different results when carried out by different experimenters.

Variation in methodology between the three publications investigating neuroserpin neuroprotection in oxygen glucose deprivation (OGD) *in vitro* demonstrates the span of protocols under the definition of a single model. Durations of exposure to OGD reported included 55 minutes (Ma et al., 2012b), 2 hours (Wu et al., 2010), and 150 minutes (Rodríguez-González et al., 2011a), using either 100% N_2 gas (Ma et al., 2012b) or 95% N_2 balanced with CO_2 (Wu et al., 2010; Rodríguez-González et al., 2011a), and a variety of commercial and custom glucose-free growth media (Wu et al., 2010; Rodríguez-González et al., 2011a). Experimental designs also varied in that the cultured neurons originated from either cerebral cortex (Ma et al., 2012b) or hippocampus (Rodríguez-González et al., 2011a) or both cortical and hippocampal neuron co-culture (Wu et al., 2010), and the period neurons were cultured prior to OGD from 7 days (Ma et al., 2012b) to 10 days (Rodríguez-González et al., 2011a), and cell viability tests were unique to each study (Wu et al., 2010; Rodríguez-González et al., 2011a; Ma et al., 2012b).

In vivo experiments are characterised by an even greater number of relevant parameters. The Rice-Vannucci method, which comprises surgery, exposure to

hypoxia, and recovery period, is the most thoroughly standardised rodent model of neonatal hypoxia ischaemia. Restricting analysis to publications in which the Rice-Vannucci model has been verified with anatomical and behavioural experiments, there are substantial methodological inconsistencies between researchers. Age of mice or rats at procedure varies from P2/3 (Zhu et al., 2006; Kida et al., 2013; Okusa et al., 2014), to P7/8 (Yager et al., 1993; Balduini et al., 2000; Ikeda et al., 2001; Lee et al., 2010), to P12 (Wang et al., 2007a; Tsuji et al., 2012; Lin et al., 2014). Duration of exposure to hypoxia varies between 30 minutes (Yager et al., 1993; Ten et al., 2003; Kida et al., 2013; Ogawa et al., 2018), 45 minutes (McQuillen et al., 2004; McAucliffe et al., 2006; Ogawa et al., 2018), 60 minutes (Ten et al., 2003; McAucliffe et al., 2006; Lin et al., 2013; Kichev et al., 2018), 120 minutes (Ferriero et al., 1996; Ikeda et al., 2001; Wang et al., 2007a), and 210 minutes (Balduini et al., 2000; Lee et al., 2010). Hypoxic gas composition varies between 6% O_2 (Kida et al., 2013), 8% O_2 (Yager et al., 1993; Balduini et al., 2000; Ikeda et al., 2001; Lee et al., 2010), and 10% O_2 (Wang et al., 2007a; Lin et al., 2013), and the temperature of the hypoxia chamber between 33°C (Ikeda et al., 2001), 36°C (Ginet et al., 2009; Lee et al., 2010; Kichev et al., 2018), and 37°C (Yager et al., 1993; Balduini et al., 2000; Kida et al., 2013). Some experimenters measure pup body temperature with a rectal probe (Carlsson et al., 2012), whereas others record only the chamber temperature (Kida et al., 2013), with many failing to specify how temperature was measured. Recovery time with the dam post-hypoxia ranged between 6 hours (Yager et al., 1993; Koike et al., 2008), 24 hours (Wang et al., 2007a; Kida et al., 2013; Wang et al., 2007a), 48 hours (Balduini et al., 2000), and 72 hours (Koike et al., 2008). There are many other finer details of methodology, such as precise duration of anaesthesia, litter size, and pup weight, amongst others, that are not discussed here which could have an

impact on procedure severity and neuropathology. The Rice-Vannucci method appears to capture multiple related procedures.

This heterogeneity in experimental design suggests that publications which define their experiments under a single paradigm may not be measuring the same effect. The contribution of variables such as body temperature during hypoxia (Rogalska et al., 2004; 2006; 2009; Caputa et al., 2005; Robertson and Iwata, 2007) are substantial, and differences in injury severity reported as caused by administration of putative therapies may depend more on the precise properties of the experimental model than the efficacy or translational value of the therapy itself (reviewed in Lai and Yang, 2011; Millar et al., 2017). These barriers to the development of effective translational therapies are not insurmountable. Reliability of treatment development in animal models of neonatal hypoxia ischaemia may be enhanced by a collaborative approach which pools data from different investigators using related variants of a certain neonatal hypoxia ischaemia model, or using animal models which include more conditions to account for relevant variables such as temperature.

Important questions to address during the design of future studies will be the "lurking variables" (Joiner, 1981) which account for the wide variability in injury severity between researchers reported using analogous models (reviewed in Vannucci and Hagberg, 2004; Vannucci and Vannucci, 2005). Identifying and addressing these hidden inconsistencies could facilitate rapid replication of putative therapeutic molecules by independent investigators. Only through better understanding of the salient factors contributing to injury can science hope to improve the translational relevance and replicability of animal models, and work more effectively towards development of clinical treatments.

5.4.4 Conclusions

This chapter reports experiments designed to assess the sensitivity of the *Serpini1* knock-out mouse, which does not express endogenous neuroserpin protein (Cinelli et al., 2001; Madani et al., 2003), to neonatal hypoxia ischaemia using *in vitro* and *in vivo* models. Results were consistent with a modest increase in brain injury in *Serpini1* knock-out animals. However, substantial methodological design and execution limitations preclude formation of conclusions.

In vitro experiments in dissociated primary cortical neurons provided confirmation of previously reported neuroserpin neuroprotection following oxygen glucose deprivation (OGD) (Wu et al., 2010; Rodríguez-González et al., 2011a; Ma et al., 2012b). A robust OGD protocol was developed using Neuro-2-A neuroblastoma cells, then applied cortical neurons from E18 mice. 3-(4,5-dimethylthiazol-2-yl)-2,5-diphenyl-tetrazolium bromide (MMT) staining was used to detect respiring cells. Pre-treatment with 10 ng/ml or 20 ng/ml exogenous neuroserpin protein for 4 hours prior to 4 hours OGD at 100% N_2 at 37°C produced a significant increase in MTT staining intensity compared to cultures pre-treated with an inert vehicle. However, this effect was modest, and there was no effect with higher doses 40 ng/ml and 60 ng/ml neuroserpin. These experiments employed a relatively severe oxygen glucose deprivation protocol by the standards of the literature (Wu et al., 2010; Rodríguez-González et al., 2011a; Ma et al., 2012b), which may account for the limited effectiveness of exogenous neuroserpin treatment.

Additionally, *Serpini1* knock-out mouse pups and wild-type littermates underwent an adapted Rice-Vannucci method to induce neonatal hypoxia ischaemia at P8. Brains were collected and analysed for injury severity 48 hours post-injury. Lesion volume,

assessed by 2,3,5-triphenyltetrazolium chloride (TTC) perfusion (Sun et al., 2012), failed to show a difference in staining intensity across whole brains between genotypes. Relatively superficial TTC penetration will require improvement before meaningful comparison can be made. The second method used to analyse brain damage, immunohistochemistry for glial inflammatory markers glial fibrillary acidic protein (GFAP), ionised calcium binding adaptor molecule 1 (Iba1), and cluster of differentiation 68 (CD68), produced only modest evidence of increased vulnerability in the *Serpini1* knock-outs. There was no significant difference in GFAP or Iba1 immunoreactivity between wild-type and knock-out brains. However, the number of CD68 immunoreactive cells and the proportion of cortical area covered by CD68 immunoreactive pixels was elevated in the hypoxic-ischaemic hemisphere of the knock-out brains compared to wild-type and heterozygote littermates, suggesting a potential increase intracerebral phagocyte invasion.

These experiments provide no conclusive evidence for hyper-sensitivity to neonatal hypoxia ischaemia in *Serpini1* knock-out animals, in contrast to the more robust evidence in adult ischaemic stroke (Cinelli et al., 2001; Gelderblom et al., 2013). It is possible that the unique neuropathology of neonatal hypoxia ischaemia in the infant brain does not accommodate the molecular pathways behind the neuroprotective effect of neuroserpin in adult animals. It is also possible that the specific experimental paradigms investigated here did not include the optimal severity, developmental time-point, or injury phase required to observe any genuine contribution of neuroserpin to this complex neurodevelopmental condition.

6 Discussion

The primary aim of thesis was to investigate the expression profile of subplate-enriched protein neuroserpin in the neocortex, both in the developing brain and under conditions of neonatal hypoxia ischaemia.

Three major research questions were addressed:

1) What is the pattern of neuroserpin protein expression throughout the neocortex across neonatal development in mouse and human?

2) Is there a change in neuroserpin protein expression in cortex following neonatal hypoxia ischaemia in rodent?

3) Is neuroserpin protective against neonatal hypoxic ischaemic in mice?

This general discussion contains three subsections. Section 6.1 summarises findings described in results Chapters 3, 4, and 5, in accordance with the major research questions. Section 6.2 proposes potential implications for the work presented here. This is divided into two subsections. Section 6.2.1 addresses current hypotheses for the function of neuroserpin in the developing brain in the light of these novel results. Section 6.2.2 evaluates the suitability of neuroserpin as a potential therapeutic target in the development of new treatments for neonatal hypoxia ischaemia in humans. Finally, Section 6.3 will state the author's conclusions from the thesis as a whole.

6.1 Summary of major findings

6.1.1 Cortical Neuroserpin Protein Expression Peaks in Subplate during Neonatal Development in Mouse and Human

A peak in neuroserpin expression was documented in subplate neurons at the mouse developmental time-point equivalent to birth in humans using fluorescent immunohistochemistry.

Neuroserpin-immunoreactive neurons were found across all cortical layers throughout development. A greater number and proportion of neurons in subplate (Layer VIb) were immunoreactive for neuroserpin than in any other cortical layer in mouse. From postnatal day P3 to P6, approximately 20% subplate neurons were immunoreactive for neuroserpin, 10% of neurons in Layer V, and less than 5% of neurons in Layers II/III, IV, and VIa. At the mouse brain developmental age equivalent to birth in humans (Finlay and Darlington, 1995; Clancy et al., 2000; 2001; 2007), P8 to P12, immunoreactivity peaked at approximately 45% of subplate neurons, 15% of neurons in Layer V, and less than 5% of neurons in other cortical layers. From P13 onward, the proportion of subplate neuroserpin-immunoreactive neurons declined to 8%, with the proportion of in other cortical layers unchanged.

Permanent immunohistochemistry in human foetal tissue at 15 and 40 post-conceptional weeks (PCW) confirmed the presence of neuroserpin immunoreactivity in human cortical cells. Neuroserpin-immunoreactive cells demonstrated neuronal morphology and appeared more densely localised in the deep cortical layers, mirroring the expression pattern in mouse.

These results complement previous non-quantitative in situ hybridisation data showing diffuse cortical expression of *Serpini1* mRNA with increased cell density in subplate of developing mouse brains (Osterwalder et al., 1996; Krueger et al., 1997). *Serpini1* mRNA, which encodes neuroserpin protein, is relatively enriched in subplate (Hoerder-Suabedissen et al., 2009), now it is known that translated neuroserpin protein remains enriched in subplate. This developmental pattern of expression informed these studies of endogenous neuroserpin function.

6.1.2 Neuroserpin Protein Expression May be Regulated in Subplate Following Neonatal Hypoxia Ischaemia in Rodents

Semi-quantitative measures of total cortical neuroserpin protein was found to be conserved following neonatal hypoxia ischaemia in mouse, alongside a potentially significant redistribution of neuroserpin immunoreactivity in subplate specifically.

A statistically significant increase in the number and proportion of neuroserpin-immunoreactivity neurons in subplate was initially detected in a preterm rat hypoxia ischaemia model generated at the University of Lausanne, Switzerland (Ginet et al., 2009a; 2009b; Okusa et al., 2014). In the hypoxic ischaemic hemisphere of moderately injured experimental brains 63% of subplate neurons were immunoreactive for neuroserpin, compared to 43% in sham-operated controls.

This result was investigated further in an optimised mouse mild-to-moderate severity neonatal hypoxia ischaemia model adapted from the Rice-Vannucci method (Rice et al., 1981). Animals exposed to hypoxia at 10% O_2 partial pressure at 37°C for 55 minutes showed an increase in the number and proportion of neuroserpin-

immunoreactive neurons in subplate of the ischaemic hemisphere in experimental brains. There was a statistically significant difference between the number and proportion of neuroserpin-immunoreactive neurons in the hypoxic ischaemic hemisphere, in which 57% of subplate neurons expressed neuroserpin, and the sham-operated control animals, in which 41% of neurons were immunoreactive for neuroserpin. No significant difference in neuroserpin expression was detected in any other cortical layer.

Neuroserpin total protein content of brain tissue was further probed using validated antibodies in semi-quantitative Western blot analysis. There was no statistically significant difference in neuroserpin protein content between the hypoxic ischaemic and hypoxia-only hemispheres across whole cortex of P10 brains which underwent the adapted Rice-Vannucci model of hypoxia ischaemia at P8. It is possible that layer-specific changes in neuroserpin did occur, but were obscured or diluted by the analysis of whole cortex as a single tissue sample.

Neuroserpin upregulation in the subplate sub-compartment of cortex may form part of the innate response to neonatal hypoxia ischaemia. The best understood enzymatic target of neuroserpin, tissue plasminogen activator (tPA) (Osterwalder et al., 1998; Barker-Carlson et al., 2002; Ricagno et al., 2009; 2010), is known to have a deleterious effect in neonatal hypoxia ischaemia (Adhami et al., 2008; Omouendze et al., 2013; reviewed in Millar et al., 2017). It is possible that neuroserpin synthesised in the subplate has some function in regulating the tPA molecular cascade during brain injury.

6.1.3 Inconclusive Evidence Consistent with Modest Neuroprotective Properties of Neuroserpin Protein in Models of Neonatal Hypoxia Ischaemia

The *Serpini1* knock-out mouse, which lacks functional neuroserpin protein (Cinelli et al., 2001; Madani et al., 2003), was used to investigate the proposed neuroprotective role of neuroserpin in neonatal hypoxia ischaemia. It was hypothesised that neuroserpin is protective in mouse models of hypoxic brain injury. However, results presented in here will require further methodological refinement before strong conclusions can be drawn concerning the neuroprotective properties of neuroserpin in the developing brain. A trend was detected towards decreased intensity of TTC staining in *Serpini1* knock-out animals subjected to neonatal hypoxia ischaemic compared to wild-type littermates. However, deep brain tissue was minimally stained in all brains and methodological alterations will be needed to increase the depth of TTC stain and increase the reliability of these results.

In addition, quantitative fluorescent immunohistochemistry for glial markers was also conducted. Although a statistically significant difference was detected in markers of astrocytes, microglia, and macrophages between the hypoxic-ischaemic and hypoxia-only control hemispheres across all genotypes, only one of the three markers investigated showed any differential expression when brains of different genotypes were compared. Overall, this was suggestive a highly specific difference in molecular injury response between *Serpini1* knock-out and wild-type littermate brains as opposed to a global shifts in injury severity. The important of putative results presented here will not be known until the therapeutic effect of neuroserpin injection has been investigated and evaluated, however this preliminary evidence does not suggest a substantial neuroprotective effect for neuroserpin in the developing brain.

6.2 General Discussion

This section will give an overview of potential implications for the results presented in this thesis. The work will be evaluated with respect to two open research questions. Section 6.2.1 will address the developmental function of neuroserpin. Section 6.2.2 will evaluate development of new treatments for neonatal hypoxia ischaemia in humans.

The work presented in this thesis is the first to address the expression and function of neuroserpin in idiosyncratic neurodevelopmental disease. This developmental application of previous work exclusively in adults may offer new understating of neonatal brain injury.

6.2.1 Role for neuroserpin in brain development and neonatal hypoxia ischaemia

Neuroserpin, a serine protease inhibitor, is known to be expressed in the developing rodent brain (Osterwalder et al., 1996; Krueger et al., 1997). However, its function remains obscure. In this section, proposed functions for neuroserpin have been reviewed.

6.2.1.1 Establishing the Profile of Neuroserpin Protein Expression in Developing Brain

Aside from cataloguing *Serpini1* mRNA expression (Krueger et al., 1997), neuroserpin has received little consideration in the developing brain, qualitative

evidence that *Serpini1* mRNA is expressed at early postnatal time-points (Hoerder-Suabedissen et al., 2009; 2013). Anatomical expression profiles can give valuable insights into potential functions of biological molecules, and highlight known roles or vulnerabilities exhibited by anatomical regions of interest for further study.

Neuroserpin protein peak immunoreactivity in subplate coincided with the end of natural programmed subplate cell death (Valverde et al., 1995; Price et al., 1997; Hoerder-Suabedissen and Molnár, 2013), a period of increased sensitivity in the cortex to hypoxic ischaemic brain injury (Bunney et al., 1997; Back et al., 2001; reviewed in McQuillen and Ferriero, 2005). The first subplate molecular marker to show this property, neuroserpin may indicate a structural protective role within the developing cerebral cortex.

A potential neuroprotective role facilitated by developing subplate neurons could describe a novel role for the subplate beyond its recognised function in establishing thalamocortical (Allendoerfer and Shatz, 1994; reviewed in Kanold and Luhmann, 2010; Hoerder-Suabedissen and Molnár, 2015) and corticothalamic (Grant et al., 2016; Hoerder-Suabedissen et al., 2018) synaptic connections. Although synaptic connections from subplate to cortical Layer IV are removed following development of direct synaptic connections from the primary thalamic nuclei onto layer IV (Friauf et al., 1990; Kanold, 2003), many subplate neurons remain in the interstitial white matter zone after birth in several mammalian species, including humans (Kostović and Rakić, 1990; Price et al., 1997; Connor et al., 2009; Hoerder-Suabedissen and Molnár, 2013). The function of these persisting subplate neurons is currently unknown (reviewed in Kanold and Luhmann, 2010; Hoerder-Suabedissen and Molnár, 2015). Failure of natural subplate apoptosis has been linked to

neurodevelopmental disorders (Akbarian et al., 1993; reviewed in Kostović, 2011) by post-mortem and brain imaging studies, suggesting that these interstitial white matter cells are not entirely quiescent.

It is possible that neuroserpin, among other molecules secreted by subplate neurons (Kondo et al., 2015), has a structural protective role across cortex. Analysis of the mouse subplate transcriptome at P8 highlighted the maturity of this layer (Hoerder-Suabedissen et al., 2009; 2013; Miller et al., 2014). Genes associated with synaptic maturation, myelination, regulation of cell division, and secretion (Hoerder-Suabedissen et al., 2013) were all enriched in P8 subplate compared to Layer VIa. Fluorescent immunohistochemistry conducted for this thesis detected partial overlap between neuroserpin immunoreactivity and known endoplasmic reticulum (ER) markers. The full catalogue of proteins secreted by subplate throughout development are not known (Hoerder-Suabedissen et al., 2013; Kondo et al., 2015), but subplate has the genetic and anatomical potential to act as a secretory powerhouse regulating the extracellular environment of other cortical neurons.

Strong evidence exists linking subplate neurons to protein secretion, yet interpretations of these results will remain modest until these secretions have been systematically catalogued. Generating a comprehensive ‘secretome’ will invariably fail to detect proteins expressed at low concentrations and is highly sensitive to the presence of contamination by non-subplate cells in culture, but several studies have made advances towards a technique for non-selective analysis of cellular secretions (Tjalsma et al., 2004; Chevallet et al., 2007; Agrawal et al., 2010). Rich subplate transcriptome data (Hoerder-Suabedissen et al., 2009; 2013) could also be used to pre-select subplate transcribed candidates for secretion analysis, leading to more

reliable directed confirmation of protein secretion. Once the catalogue of secreted molecules has been identified, it will be important to determine the function of these secretions. Culturing cortical slices (Götz and Bolz, 1992; reviewed in Humpel, 2015) from transgenic lines which fluorescently label subplate, such as the Lpar1-eGFP mouse (Grant et al., 2012; 2016; Hoerder-Suabedissen et al., 2018) or the Drd1a-Cre mouse (Lemberger et al., 2007; Hoerder-Suabedissen et al., 2018), could be grown with and without the subplate layer intact. Expression of cell death markers and sensitivity to toxic molecules such as NMDA and tPA could be assessed to interrogate the effect of these subplate secreted molecules on the viability of cortex.

Neuroserpin is a molecule long associated with neuroprotection (reviewed in Yepes and Lawrence, 2004a; Galliciotti and Sonderegger, 2006; Millar et al., 2017). It is likely that neuroserpin is among the cohort of proteins secreted by subplate neurons (Hoerder-Suabedissen et al., 2013; Kondo et al., 2015) to serve an unknown purpose across the layers of developing cortex.

6.2.1.2 Role of Neuroserpin in the Acute Post-Injury Period following Neonatal Hypoxia Ischaemia

Informed by the neuroserpin expression peak around P8, and ample literature describing neuroprotective properties for neuroserpin *in vitro* and *in vivo* (reviewed in Yepes and Lawrence, 2004a; Galliciotti and Sonderegger, 2006; Ma et al., 2012a; Millar et al., 2017), neuroserpin protein function was investigated in neonatal hypoxia ischaemia.

Serpini1 knock-out animals and their wild-type littermates survived exposure to hypoxia at 10% O_2 partial pressure for 55 minutes at 36°C, and were perfused with metabolic activity marker TTC (Sun et al., 2012). *Serpini1* knock-out whole brains did display a trend towards lower intensity of TTC-staining, however, penetrance of TTC by intracardial perfusion was low across all brains. This may reflect the high variability in injury severity between individuals subjected to the Rice-Vannucci method (reviewed in Hagberg and Vannucci, 2004; Vannucci and Vannucci, 2005), or may simply indicate a lack of functional neuroserpin protein has minimal impact on the outcome of neonatal hypoxic ischaemic brain injury. Quantification of glial inflammatory markers indicated a modest, marker-specific, increase in cluster of differentiation 68 (CD68) immunoreactive cells, suggestive of minor differences between genotypes in macrophage response (Holness and Simmons, 1993). However, there was no difference between genotypes in the expression of other reliable glial markers of inflammatory brain damage.

Studies of the innate response to neonatal hypoxic ischaemic injury could inform new approaches to the development of neuroprotective therapies (reviewed in Ferriero, 2004; Fan et al., 2010; Millar et al., 2017). However, there are clear limitations to the interpretation of work presented here. The model investigated only relatively mild hypoxic brain injury, and it is possible that neuroserpin expression is not conserved in more severe cases of neonatal hypoxia ischaemia. Additionally, this study focused exclusively on neocortex. The lower expression profile of neuroserpin outside of cerebral cortex may reduce its neuroprotective effect in patients displaying a basal-ganglia-thalamic injury pattern (Himmelmann et al., 2007; Steinman et al., 2009; Martinez-Biarge et al., 2011). Additionally, behavioural testing will be required to assess the functional consequences of injury (reviewed in Lubics et al., 2005; Millar

et al., 2017). However, the reported anxiety phenotype in both the *Serpini1* knockout and *Serpini1* over-expressing mouse lines (Madani et al., 2003) introduces a developmental abnormality independent of hypoxia ischaemia.

The therapeutic potential of neuroserpin, or any potential treatment for neonatal hypoxia ischaemia, can only be assessed by determining the effect of replacement and augmentation on neonatal hypoxic ischaemic brain damage. Neuroserpin protein replacement therapy could be studied in animal models of varying severities of neonatal hypoxic ischaemic brain injury. Retroviral injection of a *Serpini1*-expressing viral construct at E10 (reviewed in Nadarajah et al., 2002) could be used to replace neuroserpin protein in mouse subplate, and potentially protect against neonatal hypoxia ischaemia later in development.

Viral injection treatments are impractical and expensive in a clinical setting, therefore exogenous protein injection could be investigated. Injection of neuroserpin directly into the brain of adult rodents proved neuroprotective following induced excitotoxicity (Yepes et al., 2000; Lebeurrier et al., 2005a). Intracerebral injections of other tPA inhibitors α2-antiplasmin (Adhami et al., 2008) and plasminogen-activator-inhibitor 1 (PAI1) (Yang et al., 2013; Yang and Kuan, 2015) have already been demonstrated to reduce behavioural deficits following neonatal hypoxia ischaemia. These proteins are not brain-specific (Hastings et al., 1997), therefore could potentially have more side-effects than neuroserpin if carried forwards to clinical trial. However, finding the treatment with greatest demonstrable efficacy remains the primary concern for science. Although suitable for validation of neuroserpin neuroprotective in animal models, intracerebral injection is still too invasive to be used as a routine treatment method in human neonates. A potential non-invasive

peptide delivery method is the nasal spray (reviewed in Sayani and Chien, 1996; Antosova et al., 2009), which could effectively deliver neuroserpin protein into the brain. Currently, no pharmacological small molecules are available to target neuroserpin. Drugs targeting serine proteases and their inhibitors have already been developed (reviewed in Drag and Salvesen, 2010), and could be screened for neuroserpin binding properties. Any of these future experiments could more comprehensively determine whether neuroserpin has the required efficacy to be further investigated in a clinical setting.

Although work determining the effect of loss of neuroserpin in the *Serpini1* knock-out mouse on severity of brain damage remain in the preliminary stages, expression data support some function for neuroserpin in hypoxic ischaemic brain injury in the neonatal brain.

6.2.1.3 Proposing Functions for Neuroserpin in the Developing Brain: Neuroprotection

The main findings in this thesis support a modest role for neuroserpin in neuroprotection. The literature is rich in evidence for neuroprotective functions of neuroserpin. In cultured neurons, (Lebeurrier et al., 2005a; 2005b; Mohsenifar et al., 2007; Lee et al., 2008; Wu et al., 2010; Rodríguez-González et al., 2011a; Ma et al., 2012b) and *in vivo* in rodent models of brain damage (Yepes et al., 2000; Cinelli et al., 2001; Yepes et al., 2002; Gelderblom et al., 2013; Gu et al., 2015). Aberrant neuroserpin expression in prostate cancer cells has even been associated with resistance against chemotherapy-induced cell death (Chang et al., 2000; Hasumi et al., 2005; Valiente et al., 2014). Results presented in this thesis complement this

extensive catalogue by supplementing a novel condition where enriched neuroserpin expression may serve a protective role. In the *Serpini1* knock-out mouse, there is tentative preliminary evidence of slightly greater brain damage in the animals which lack neuroserpin protein.

The robust endogenous increase in subplate neuroserpin immunoreactivity in rodent neonatal hypoxia ischaemia support the hypothesis that neuroserpin protein is produced for secretion in the acute post-injury period. However, whole cortical protein analysis by Western blot failed to detect a difference in neuroserpin expression between the ischaemic and control hemispheres, tempering any theories of large scale neuroserpin production. It is still possible that small local quantities of neuroserpin protein released into the extracellular matrix have a demonstrable effect on tPA cleavage. The greatest contribution of this work to the literature is perhaps the suggestion of putative physiological conditions during development in which the neuroserpin/tPA molecular cascade has thus far received little attention (reviewed in Millar et al., 2017).

Neuroprotection remains a rich area for investigation. Do surviving subplate neurons survive because of their neuroserpin expression, or is this protein produced later when survival is already assured? This could be assessed by co-injection of bromodeoxyuridine (BrdU) and *Serpini1*-expressing retrovirus in E10-13 subplate neurons. Another interesting question could fuse the developing subplate and neonatal hypoxia ischaemic narratives reported in this thesis. For example, the rate and extent of natural subplate cell death could be tracked in the *Serpini1* over-expressing mouse compared to wild-type littermates, perhaps using BrdU injection to track the prevalence of early-born cortical neurons.

The unknown enzymatic targets of neuroserpin continue to vex those pursuing a comprehensive molecular understating of neuroserpin neuroprotection. Neuroserpin is known to weakly bind plasmin and urokinase plasminogen activator (uPA) (Osterwalder et al., 1998). Other reported effects (Wu et al., 2010; Gu et al., 2015) may be independent of all known targets, preventing sound hypotheses about the mechanisms behind neuroserpin neuroprotection. Although neuroserpin binding to N-cadherin has been reported (Lee et al., 2007), and structural analysis has identified reactive domains which likely participate in molecular interactions due to similarities to other serine protease inhibitors (Ishigami et al., 2007; Ricagno et al., 2009), the mechanism of this interaction remains unexplored. This issue will remain even after the methodology establishing injury and behaviour in the neonatal hypoxic ischaemic mouse has been resolved. The sheer number of molecular cascades which can trigger cell death allows prolific *in vitro* experimentation on any novel neuroprotective candidate molecule. Fascinating questions that could potentially be asked include defining the specific pathway for cell death neuroserpin is most effective at moderating (reviewed in Northington et al., 2001; 2011). The dependence of neuroserpin neuroprotection on active secretion *in vitro* could also be assessed using toxin administration (reviewed in Humeau et al., 2000) to prevent the successful secretion of dense-core vesicles. The potential for further molecular investigation is truly staggering.

Much remains to be done to extend the observed neuroserpin neuroprotection in the adult brain to the developing brain. The known damage caused by tPA in neonatal brain injury (Adhami et al., 2008; Omouendze et al., 2013; Henry et al., 2013) supports a greater understanding of its sole neuron-specific inhibitor (Osterwalder et

al., 1996; Hastings et al., 1997) in the unique molecular landscape of the developing brain.

6.2.1.4 Proposing Functions for Neuroserpin in the Developing Brain: Neuronal Plasticity

A second major function proposed for neuroserpin is in neuronal plasticity (reviewed in Galliciotti and Sonderegger, 2006; Millar et al, 2017). A function for neuroserpin in plasticity could be problematic for development of therapeutics, as human neuronal circuitry undergoes substantial modification during the neonatal period (reviewed in Aoki and Siekevitz, 1988; Partanen et al., 2013; Simpson et al., 2014).

The earliest evidence supporting plasticity-enhancing properties for neuroserpin was described in endocrine cell lines (Hill et al., 2001; Jacovina et al., 2001; Borges et al., 2010) and in neuronal cultures (Berger et al., 1999; Ishigami et al., 2007). One enzymatic target of neuroserpin, tissue plasminogen activator (tPA), is known to activate NMDA-receptors (Qian et al., 1993; Nicole et al., 2001), promote vesicular exocytosis (Wu et al., 2015; Yepes et al., 2016; Jeanneret et al., 2016), and is induced following learning (Müller and Griesinger, 1998; Seeds et al., 1995; 2003). One *in vivo* study has proposed a direct role for neuroserpin in fine-tuning neuronal circuitry. Monocular enucleation in P11 mouse led to decreased *Serpini1* mRNA expression in primary visual cortex compared to the control hemisphere at P17 (Wannier-Morino et al., 2003).

As the only *in vivo* study currently describing a specific model of neuronal plasticity was non-quantitative (Wannier-Morino et al., 2003), a neonatal adaptation of this

experiment was conducted using Golli-τ-eGFP mice enucleated at P1 (Grant et al., 2016). Although there was a trend towards increased neuroserpin immunoreactivity in subplate at P6 in the input-deprived hemisphere, this was not statistically significant. Fluorescent immunohistochemistry may have failed to detect small differences in neuroserpin concentration, yet other plasticity-associated molecules such as tPA undergo changes visible using this technique (Seeds et al., 1995). *Serpini1* transgenic mice also offer ambivalent evidence of a plasticity function for neuroserpin, as both strains exhibit normal motor, breeding, and visual behaviour (Madani et al., 2003). Taken together, these observations suggest neuroserpin plays a lesser role in plasticity than its target tPA. The investigation reported in this thesis only assessed one post-enucleation time-point. It is possible that the change in neuroserpin expression accompanying neuronal plasticity simply occurs earlier or later.

To successfully resolve these unanswered questions, classical neuronal plasticity could be assessed *in vivo* by subjected *Serpini1* knock-out mice to the Morris water maze (Morris, 1984; reviewed in McNamara and Skelton, 1993; D'Hooge and De Deyn, 2001), and other related behavioural tasks (O'Keefe and Dostoyevsky, 1971; Burgess et al., 2002). This could be complemented by *in vitro* work investigating the molecular basis for the neuroserpin-mediated inhibition of effect on NMDA-mediated excitotoxicity (Lebeurrier et al., 2005a; Ma et al., 2012b), perhaps employing inhibition of NMDA receptors by MK-801 or another pharmacological antagonist (Wong et al., 1986; reviewed in Ogden and Traynelis, 2011) to determine whether neuroserpin promotes plasticity through this classical pathway.

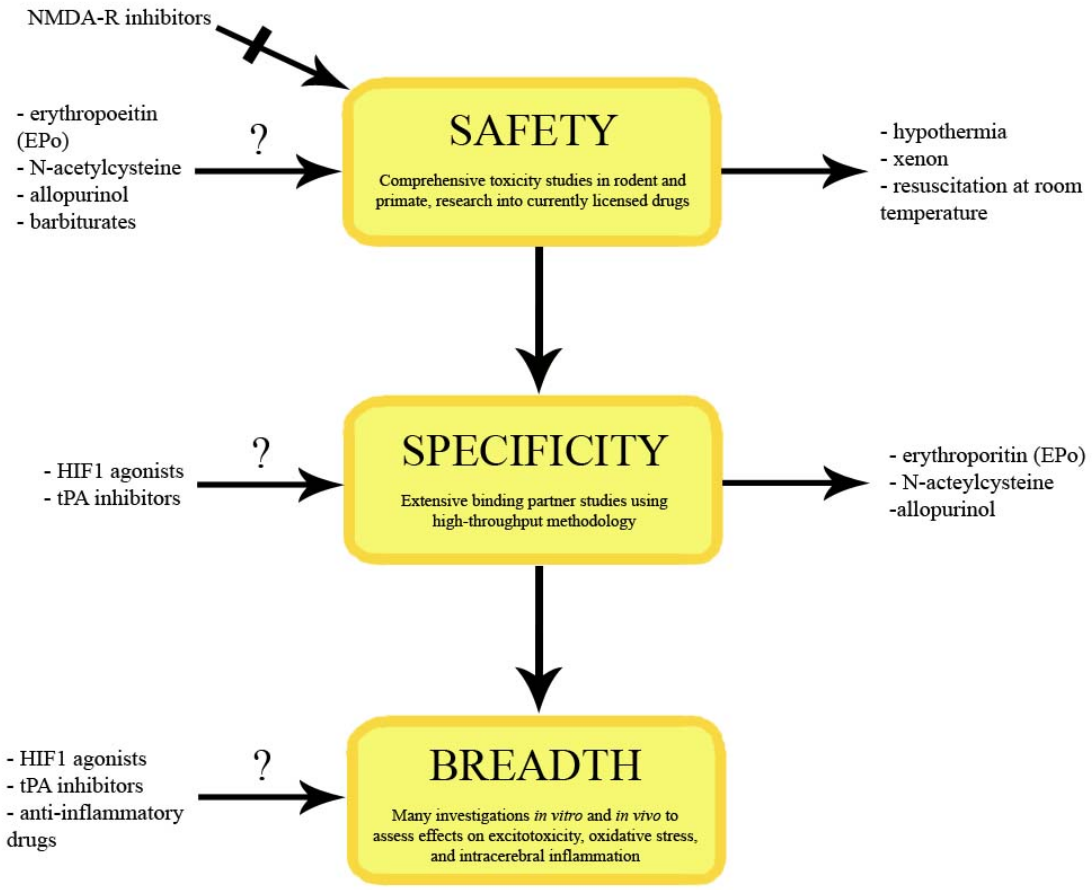


Figure 6.1 – Schematic Depiction of Proposed Filters for Putative Therapies for Infant Hypoxia Ischaemia. All putative treatments should satisfy safety prior to investigation in human infants. Specificity may also decrease off-target effects, and breadth may increase treatment efficacy. Several current treatments under development are listed by which criteria these satisfy.
HIF1 = hypoxia inducible factor 1, tPA = tissue plasminogen activator, NMDA-R = N-methyl-D-aspartate receptor, EPo = erythropoietin

6.2.2 Challenges for the Development of new therapeutics for neonatal hypoxia ischaemia

Drawing on the detailed yet incomplete knowledge of the physiology of neonatal hypoxia ischaemia represented in the literature, several factors must be satisfied in a new potential therapy. All potential treatments should be safe for vulnerable neonates and not interfere with essential developmental milestones. Treatments should also be

specific, with minimal off-target effects on normal brain development to avoid extreme adverse effects in these vulnerable infants. The ideal treatment would target molecules common to the excitotoxicity, oxidative stress and inflammation pathways (reviewed in Robertson J.D. et al., 2002; Starkov et al., 2004; Fischer and Maier, 2015; Chamorro et al., 2016; Burd et al., 2016). Targeting these common mediators would allow a single therapy to be efficacious against multiple brain damage and cell death cascades, instead of merely eliciting a reshuffle of pathways to favour a different method of cell death (reviewed in Northington et al., 2007; 2011). These concepts for potential treatment design are summarised in Figure 6.1.

6.2.2.1 Review of current neonatal hypoxia ischaemia treatments under research and development

Despite the high prevalence of long-term disability in human survivors of neonatal hypoxia ischaemic (reviewed in Volpe, 2012; Lee et al., 2013; Millar et al., 2017), only one licensed treatment is currently available in the UK: hypothermia (Gunn et al., 1997; 2005; Gunn and Gunn, 1998; reviewed in Choi et al., 2012; Tagin et al., 2012). However, hypothermia alone is not sufficient to prevent all brain injury or neurological symptoms. The development of novel treatments to supplement hypothermia is imperative. In this section, the work in this thesis will be discussed with respect to its utility in informing future therapeutic development.

Since the discovery of the neuroprotective effect of hypothermia, relatively little progress has been made in identifying additive pharmacological therapies. Few potential treatments have reached clinical trials. Two interventions have been deemed safe in neonates. Resuscitation at room temperature (Vento et al., 2001; Rabi et al.,

2007) and xenon gas administration (Hobbs et al., 2008; Thoresen et al., 2009) have been investigated in a humans alongside hypothermia, yet the limited success reported in these studies is now under speculation (Azzopardi et al., 2013, 2015; Dingley et al., 2014; Sabir et al., 2016).

Pharmacological agents have also been investigated in neonatal patients with limited success. Barbiturate anticonvulsants had no effect on neurological development (Goldberg et al., 1986; Hall et al., 1998; Singh et al., 2004; Vargas-Origel et al., 2004; Evans et al., 2007). Recent clinical studies suggested that high-dose erythropoietin (EPo) treatment in term neonates reduces disability (Strunk et al., 2008; Zhu et al., 2009; McPherson and Juul, 2010). High-dose EPo is currently under investigation in phase II clinical trials (Wu et al., 2016; Frymoyer et al., 2017). There is hope for erythropoietin (EPo) as a future additive treatment. Several more small molecules are being investigated in human neonatal HI patients including free radical scavengers N-acetylcysteine (Jatana et al., 2006; Moss et al., 2018) and allopurinol (Palmer et al., 1990; Martinello et al., 2017). The field still awaits a candidate neuroprotective molecule which is both safe and effective in human neonates (reviewed in Lai and Yang, 2011; Pazos et al., 2012).

One example of the difficulty involved in selecting targets for new therapies is the lack of clinical translation of the extensive work on NMDA receptor-mediated excitotoxicity in the neonatal hypoxic ischaemic brain. Drugs that block NMDA receptors are protective in rodent models (McDonald et al., 1989; 1990). Despite the efficacy of NMDA antagonists at reducing infarct volumes in rats, this has not been pursued in humans as NMDA-mediated classical neuronal plasticity is essential for normal brain development (Ikonomidou et al., 1999; Lim et al., 2012; Inta et al., 2016). Effective NMDA antagonists could cause more damage to the circuitry of the

neonatal brain than is justified by their anti-excitotoxicity function, undermining the medical philosophy enshrined in the Hippocratic oath: to do no harm.

6.2.2.2 Evaluation of Criteria for Treatment Development for Human Neonatal Hypoxia Ischaemia

The suitability of neuroserpin, and any future small molecules targeting the neuroserpin-tPA cascade, for use in human neonates will depend greatly on the efficacy of these treatments in experimental models of neonatal HI. It is clear that safety is an essential criteria for any treatment developed for use in human patients, but there is no consensus in the field over what other qualities scientists should use to efficiently screen candidate therapies.

Specificity could come to rank among those desired characteristics of any potential pharmacological therapy for neonates, as faithfulness of a single molecular target minimises the likelihood of off-target side-effects. The cardiovascular and respiratory systems of neonates are vulnerable in premature birth and following hypoxic ischaemia injury (Finer et al., 1981; Richardson et al., 1996), so brain-specific neuroprotective treatments are desirable. Molecular specificity is essential in addition to organ specificity. Extensive characterisation of the binding partners of not only the pharmacological molecule, but also its targets, is time-consuming but essential work if a therapy is to be estimated as safe enough for clinical trials. Extensive characterisation of the binding partners of not only the pharmacological molecule, but also its targets, is time-consuming but essential work if a therapy is to be estimated as safe enough for clinical trials. As high-throughput screening methods are increasingly refined for use throughout the pharmaceutical industry (reviewed in Pereira and

Williams, 2007; Macarron et al., 2011), capturing specificity is becoming a realistic research goal.

Breadth of action is essential for the efficacy of a therapy designed for neonatal hypoxia ischaemic, in which a wide range of neuronal death pathways are active simultaneously in the injured brain (reviewed in McLean and Ferriero, 2004; Northington et al., 2011; Millar et al., 2017). These cascades are not entirely independent of one another. It may be possible to identify a molecule which has some properties of a "master regulator". This hypothetical single molecule would dampen multiple brain damage pathways, inhibiting a key activator (or activators) of each respective process, and perhaps trigger other neuroprotective cascades, to protect vulnerable developing neurons. But how probable is it that a "master regulator" will be discovered? Is it possible that one has already been documented and simply remains to be exploited?

The concept of a "master regulator" for any complex disease appears enticing, but is its promise only linguistic trickery? Identification of candidate proteins will not be a simple process, likely requiring many experiments spanning multiple methods. One possible starting point is microarray data collected following neonatal hypoxia ischaemia in rodents (Carmel et al., 2004; Maj et al., 2004a; 2004b; Juul et al., 2009; Nagel et al., 2012; Rognlien et al., 2014). A wealth of data is available from this method, however, microarrays are highly sensitive to the time of tissue collection post-injury, and do not detect changes in protein content mediated by translational modification or secretion. For example, none of these studies detected changes in tPA transcription, although tPA is increased in the brain by neuronal secretion (Krystosek and Seeds, 1981; Gualandris et al., 1996) and influx through the blood brain barrier

(Henry et al., 2013). Another proposed "master regulator", hypoxia inducible factor 1 (HIF1) (Sheldon et al., 2009; reviewed in Semenza, 2000; 2002; 2012), also fails to be detected by several microarray studies. Other potential candidates include secreted inflammatory molecules such as interleukin 1β (reviewed in Basu et al., 2004). Generating a neonatal hypoxia ischaemia 'secretome' (Tjalsma et al., 2004; Chevallat et al., 2007; Agrawal et al., 2010) could help identify the earliest changes in protein activity directly following neonatal brain injury. However, detailed study of any candidate molecules' efficacy at inhibiting excitotoxicity, oxidative stress, and brain inflammation will need to be meticulously assessed *in vitro* to confirm the biochemistry behind this breadth.

Much remains unknown about the regulation of neuroserpin, its role in signalling cascades, and post-transcriptional modification. Recent studies are beginning to identify mechanisms, including trafficking from the endoplasmic reticulum to the Golgi apparatus (Miranda et al., 2004; Davies et al., 2009), post-translational modification by micro-RNAs (Tapocik et al., 2016), and sites for proposed carbohydrate attachment (Takao et al., 2000). Sequence analysis in both human (Schrimpf et al., 1997; Yazaki et al., 2001) and chicken (Osterwalder et al., 1996) have detected two likely signal sequence cleavage sites at the N-terminus of the protein based on probabilistic methods, yet these have not been directly demonstrated to bind regulatory molecules. Many of these studies hint towards interesting and complex molecular regulation pathways, yet the current evidence cannot determine which of these is the dominant form of neuroserpin regulation, or to what extent these processes affect secretion or enzymatic function.

Some proteins are already known to span multiple cell death cascades. These are clearly the most accessible candidates for "master regulator" properties. NMDA receptors, major mediators of neuronal death by excitotoxicity (reviewed in Hagberg et al., 1987), can be directly or indirectly activated by free radicals (Schanne et al., 1979; Robertson J.D. et al., 2002; Starkov et al., 2004), combining two lethal molecular cascades often treated as separate in the literature. Inflammatory pathways also mediate excitotoxicity and oxidative stress. In rodents, pre-treatment with IL-1ß, IL-6, IL-9, or TNF-α enhances brain damage caused by NMDA agonists (Marret et al., 1995; Dommergues et al., 2000). In addition, activated microglia produce inflammatory cytokines, glutamate, nitric oxide, and free radicals (Wood, 1995; reviewed in Kaur and Ling, 2009), influencing all three cascades simultaneously. It is these overlaps between cascades at which a "master regulator" could act. The transcription factor HIF1 is known to regulate a minimum of 60 genes (reviewed in Semenza 2002; 2003), including the putative therapeutic molecule erythropoietin (EPo), several growth factors, and mitochondrial proteins. Another possible candidate, tPA has established roles crossing boundaries between excitotoxicity, oxidative stress, brain inflammation reviewed in Yepes and Lawrence, 2004b; Yepes et al., 2009, and is secreted by microglia (Flavin et al., 2000). The relative dearth of candidates proposed here perhaps reflects our incomplete knowledge of the molecular mechanisms underpinning neonatal hypoxic ischaemic brain damage.

There is no clear single "master regulator" protein documented in the literature of this complex neurodevelopmental disorder (reviewed in Millar et al., 2017), and it is unlikely that any one molecule can completely prevent hypoxic ischaemic cell death. However, this does not restrain future experimenters from seizing on those few currently supported candidates, for further development. This discussion has posed

one important question concerning the efficacy of the neuroserpin-tPA cascade to regulate multiple cell death cascades. Can any one molecular target down-regulate excitotoxicity, oxidative stress, and brain inflammation simultaneously? If so, does the neuroserpin-tPA cascade could represent an untapped hoard of neuroprotective molecules?

6.2.2.3 The Future for Neuroserpin and its Derivatives as a Potential Treatment for Neonatal Hypoxia Ischaemia

Neuroserpin was initially selected for study in models of neonatal hypoxia ischaemia, as it theoretically possesses all the characteristics discussed in Section 6.2.2.2. Neuroserpin thus far promises limited and unverified partial fulfilment of the criteria for a future neonatal hypoxia ischaemia therapy. Extensive repetition with larger cohorts of animals across a range of severity conditions are required to substantiate even the modest findings presented here. Yet this thesis has added to knowledge of the neuroserpin-tPA cascade in neonatal hypoxia ischaemia.

Neuroserpin is expressed endogenously by human cortical neurons (Teesalu et al., 2004; Adorján et al., 2019) and is found in the bloodstream (Rodriguez-Gonzalez et al., 2011b; 2011c). In this thesis evidence is presented that neuroserpin protein is expressed by deep cortical neurons in the term neonatal brain. This suggests that neuroserpin is tolerated by the developing brain. Neuroserpin injection experiments *in vivo* (Yepes et al., 2000; Zhang et al., 2002; Lebeurrier et al., 2005a) do not report toxicity caused by doses of up to 30 pM in the adult rodent brain. It is clear that more studies are needed in the unique environment of the developing brain to establish the safety of neuroserpin.

Extensive characterisation of *Serpini1* mRNA expression in rodents suggests it is brain-specific (Osterwalder et al., 1996; Hastings et al., 1997; Lee et al., 2015), minimising the risk of side-effects in the vulnerable cardiovascular or pulmonary systems. Western blots conducted here confirmed absence of neuroserpin protein from liver and skeletal muscle in mice, yet it remains a possibility that neuroserpin is trafficked to other organs outside the central nervous system. Molecular specificity is essential in addition to organ specificity. The literature often asserts that the primary enzymatic target of neuroserpin is tissue plasminogen activator (tPA) (Osterwalder et al., 1998; Barker-Carlson et al., 2002; Ricagno et al., 2009, 2010), although tPA-independent actions have been described (reviewed in Ma et al., 2012; Millar et al., 2017). The alternative targets behind these tPA-independent effects are not known, preventing analysis of neuroserpin specificity. Accurate identification of all neuroserpin molecular interactions will be needed to build up a comprehensive understanding of the therapeutic properties of this protein.

Although evaluating the full neuroprotective force of neuroserpin is beyond the scope of this thesis, several basic questions have been addressed. The vital question of the efficacy of neuroserpin as a neuroprotective molecule has produced a modest hint towards neuroprotection in mice, with no evidence for a global intracerebral effect on lesion size or inflammation. This thesis also presents the first putative evidence that neuroserpin undergoes localised re-distribution within the cerebral cortex in the acute post-injury period following neonatal hypoxia ischaemia. Although far from conclusive, neonatal hypoxia ischaemia conducted in the *Serpini1* knock-out mouse is consistent with an extremely modest increase in sensitivity to brain damage in animals lacking functional neuroserpin.

Experiments in human post-mortem tissue could be carried out alongside animal work to better understand neuroserpin function in the human neonatal brain. Antibodies targeting rodent neuroserpin also stain neurons with a similar distribution in human foetal tissue (Adorján et al., 2019). It would greatly enhance the argument for translating this work to the clinic if human foetal tissue from brain banks (Lindsey et al., 2016) could be assessed for neuroserpin expression by immunohistochemistry. Expression patterns in severely hypoxic ischaemic brains could be compared to those of patients who experienced little hypoxia. In addition, the concentration of serum neuroserpin in blood samples from surviving neonates could be correlated with structural MRI damage or long-term behavioural outcome, inspired by a similar non-invasive experiment in adult ischaemic stroke patients (Rodriguez-Gonzalez et al., 2011b; 2011c).

6.3 Conclusions

This thesis set out to expand current knowledge of neuroserpin protein expression patterns and proposed neuroprotective functions to the developing brain, and in the acute post-injury period following neonatal hypoxia ischaemia. Specifically, the work presented here set out to: describe the pattern of neuroserpin protein expression throughout the neocortex across neonatal development in mouse and human; quantify cortical neuroserpin following neonatal hypoxia ischaemia in rodent models; and investigate the proposed neuroprotective properties of neuroserpin in the developing brain, specifically in neonatal hypoxia ischaemia.

Neuroserpin protein was detected in neurons across all cortical layers throughout development in mouse, with a peak in subplate which peaked at the mouse cortical developmental stage equivalent to birth in humans (Finlay and Darlington, 1995; Clancy et al., 2000; 2001; 2007). Fluorescent immunohistochemistry was used to quantify the number and proportion of neuroserpin-NeuN-co-immunoreactive neurons in the mouse brain from postnatal day 3 (P3) to adulthood. Neuroserpin enrichment in transitory cortical layer VIb, the subplate, demonstrated translation of subplate-enriched *Serpini1* mRNA previously reported in this layer (Krueger et al., 1997; Hoerder-Suabedissen et al., 2009; 2013). This upregulation of neuroserpin around P8 coincided with the end of natural programmed cell death in subplate (Kostović and Rakić, 1990; Price et al., 1997; Connor et al., 2009; Hoerder-Suabedissen and Molnár, 2013), suggesting the neuroserpin-tPA cascade as a potential mediator of developmental apoptosis. Non-quantitative immunohistochemistry in foetal human brain tissue at 15 and 40 post-conceptional weeks revealed an analogous pattern of neuroserpin-immunoreactive neurons in the deep cortex. Neuroserpin expression is now known to be enhanced in the developing brain, where it could play a unique role.

Due to the reported neuroprotective properties of neuroserpin in the adult ischaemic rodent brain (reviewed in Yepes and Lawrence, 2004a; Galliciotti and Sonderegger, 2006; Millar et al., 2017), the expression profile of this protein was investigated in the neonatal hypoxic ischaemic brain. In both a preterm rat and neonatal mouse model of hypoxia ischaemia adapted from the Rice-Vannucci method (Rice et al., 1981), an increase in the proportion of neuroserpin immunoreactive neurons in subplate was detected in the hypoxic ischaemic hemisphere of moderately injured brains. This increase was a subplate-specific property. No other cortical layer displayed changes in neuronal neuroserpin, and semi-quantitative Western blot failed to detect a significant

difference in total cortical neuroserpin between the hypoxic ischaemic and hypoxia-only hemispheres of P10 mice which had undergone hypoxia ischaemia at P8. This result is consistent with the proposed secretory function of subplate neurons (Hoerder-Suabedissen et al., 2013; Kondo et al., 2015), which may produce a number of proteins, including neuroserpin, in the injured neonatal brain.

Motivated by the broad number of cell death cascades influenced by the primary molecular target of neuroserpin, tissue plasminogen activator (tPA) (reviewed in Millar et al., 2017), results presented here are tentatively consistent with a modestly increased vulnerability to neonatal hypoxia ischaemia in transgenic *Serpini1* knock-out mice. Analysis of metabolic activity 48 hours after hypoxic-ischaemic injury by TTC staining (Sun et al., 2012) demonstrated a slight reduction in staining intensity in the *Serpini1* knock-out brains compared to those of wild-type littermates. Quantitative immunohistochemistry for inflammatory glial markers also produced evidence of a modest, marker-specific, difference between genotypes. Methodological refinement will be needed to strengthen these results, in addition to neuroserpin injection (Yepes et al., 2000; Lebeurrier et al., 2005a), or transgenic neuroserpin over-expression (Cinelli et al., 2001), following neonatal hypoxia ischaemia. Extensive work is required to form firm conclusions on the efficacy of neuroserpin as a potential candidate treatment for neonatal hypoxia ischaemia.

This thesis demonstrates a novel developmental enrichment of neuroserpin protein in the cerebral cortex, and reorganisation in subplate following neonatal hypoxia ischaemic. The molecular pathway centred around tissue plasminogen activator promises desirable qualities in moderating neonatal neuronal death and could constitute a potential mine for future treatments.

7 References

ABCAM, P., 2018-last update, **Anti-Neuroserpin antibody (ab32901)**. Available: https://www.abcam.com/neuroserpin-antibody-ab32901.html [08/10, 2018].

ABCAM, P., 2018-last update, **Anti-Neuroserpin antibody (ab33077)**. Available: http://www.abcam.com/neuroserpin-antibody-ab33077.html [08/10, 2018].

ABCAM, P., 2018-last update, **Sorry, Anti-Neuroserpin antibody (ab55587) is not available**. Available: http://www.abcam.com/neuroserpin-antibody-ab55587.html [08/10, 2018].

ACHENBACH, T.V., BRUNNER, B., HEERMEIER, K., 2003. Oligonucleotide-based knockdown technologies: antisense versus RNA interference. *Chembiochem.*, **4**(10), 928-35.

ADAMSONS, K. and MYERS, R.E., 1973. Perinatal asphyxia, causes, detection and neurologic sequelae. *Pediatric clinics of North America,* **20**(2), pp. 465-480.

ADEN, U., HALLDNER, L., LAGERCRANTZ, H., DALMAU, I., LEDENT, C. and FREDHOLM, B.B., 2003. Aggravated brain damage after hypoxic ischemia in immature adenosine A2A knockout mice. *Stroke; a journal of cerebral circulation,* **34**(3), pp. 739-744.

ADHAMI, F., YU, D., YIN, W., SCHLOEMER, A., BURNS, K.A., LIAO, G., DEGEN, J.L., CHEN, J. and KUAN, C., 2008. Deleterious effects of plasminogen activators in neonatal cerebral hypoxia-ischemia. *The American journal of pathology,* **172**(6), pp. 1704-1716.

ADOBE SYSTEMS, I., 2007-last update, Adobe® Photoshop® CS3 Users Guide. Available: https://help.adobe.com/archive/en_US/photoshop/cs3/photoshop_cs3_help.pdf [08/10, 2018].

ADORJAN, I., AHMED, B., FEHER, V., KRUG, K., ESIRI, M., CHANCE, S.A. and SZELE, F.G., 2017. Calretinin interneuron density in the caudate nucleus is lower in autism spectrum disorder. *Brain,* **140**(7), pp. 2028-2040.

ADORJAN, I., AHMED, B., FEHER, V., TORSO, M., KRUG, K., ESIRI, M., CHANCE, S.A., SZELE, F.G., 2017. Calretinin interneuron density in the caudate nucleus is lower in autism spectrum disorder. *Brain.,* **140**(7), 2028-40.

ADORJAN, I., TYLER, T., BHADURI, A., DEMHARTER, S., FINSZTER, C.K., BAKO, M., SEBOK, O.M., NOWAKOWSKI, T.J., KHODOSEVICH, K., MOLLGARD, K., KRIEGSTEIN, A.R., SHI, L., HOERDER-SUABEDISSEN, A., ANSORGE, O., MOLNAR, Z., 2019. Neuroserpin expression during human brain development and in adult brain revealed by immunohistochemistry and single cell RNA sequencing. *Journal of anatomy.*

AGMON, A., YANG, L.T., O'DOWD, D.K. and JONES, E.G., 1993. Organized growth of thalamocortical axons from the deep tier of terminations into layer IV of developing mouse barrel cortex. *The Journal of neuroscience : the official journal of the Society for Neuroscience,* **13**(12), pp. 5365-5382.

AGRAWAL, G.K., JWA, N., LEBRUN, M., JOB, D. and RAKWAL, R., 2010. Plant secretome: unlocking secrets of the secreted proteins. *Proteomics,* **10**(4), pp. 799-827.

AGRAWAL, V. and HIRSCH, E., 2012. Intrauterine infection and preterm labor. *Seminars in fetal & neonatal medicine,* **17**(1), pp. 12-19.

AKBARIAN, S., BUNNEY, W.E.,JR, POTKIN, S.G., WIGAL, S.B., HAGMAN, J.O., SANDMAN, C.A. and JONES, E.G., 1993. Altered distribution of nicotinamide-adenine dinucleotide phosphate-diaphorase cells in frontal lobe of schizophrenics implies disturbances of cortical development. *Archives of General Psychiatry,* **50**(3), pp. 169-177.

AKBARIAN, S., KIM, J.J., POTKIN, S.G., HETRICK, W.P., BUNNEY, W.E.,JR and JONES, E.G., 1996. Maldistribution of interstitial neurons in prefrontal white matter of the brains of schizophrenic patients. *Archives of General Psychiatry,* **53**(5), pp. 425-436.

AKBARIAN, S., VINUELA, A., KIM, J.J., POTKIN, S.G., BUNNEY, W.E.,JR and JONES, E.G., 1993. Distorted distribution of nicotinamide-adenine dinucleotide phosphate-diaphorase neurons in temporal lobe of schizophrenics implies anomalous cortical development. *Archives of General Psychiatry,* **50**(3), pp. 178-187.

ALBERTS, J.R., 1978. Huddling by rat pups: group behavioral mechanisms of temperature regulation and energy conservation. *Journal of comparative and physiological psychology,* **92**(2), pp. 231.

ALBRECHT, J., HANGANU, I.L., HECK, N. and LUHMANN, H.J., 2005. Oxygen and glucose deprivation induces major dysfunction in the somatosensory cortex of the newborn rat. *The European journal of neuroscience,* **22**(9), pp. 2295-2305.

ALEXANDER, M., GARBUS, H., SMITH, A., ROSENKRANTZ, T. and FITCH, R., 2014. Behavioral and histological outcomes following neonatal HI injury in a preterm (P3) and term (P7) rodent model. *Behavioural brain research,* **259**, pp. 85-96.

AL-GHOUL, W.M. and MILLER, M.W., 1989. Transient expression of Alz-50 immunoreactivity in developing rat neocortex: a marker for naturally occurring neuronal death? *Brain research,* **481**(2), pp. 361-367.

ALLEN INSTITUTE FOR BRAIN SCIENCE, ORG., 2018-last update, Allen Brain Developing Mouse Brain Atlas P4 Nissl Stain Coronal . Available: http://developingmouse.brain-map.org/experiment/ivt?id=100034998&popup=true, [08/10, 2018].

ALLEN INSTITUTE FOR BRAIN SCIENCE, ORG., 2018-last update, Allen Brain Developing Mouse Brain Atlas P4 Nissl Stain Coronal . Available: http://mouse.brain-map.org/experiment/show?id=963 [09/05, 2019].

ALLENDOERFER, K.L. and SHATZ, C.J., 1994. The subplate, a transient neocortical structure: its role in the development of connections between thalamus and cortex. *Annual Review of Neuroscience,* **17**, pp. 185-218.

ALLEVA, E., CAPRIOLI, A., LAVIOLA, G., 1989. Litter gender composition affects maternal behavior of the primiparous mouse dam (Mus musculus). *Journal of comparative Psychology.*, **103**(1), 83.

ALSHARNOUBI, J.M., ODLAND, H.H. and SAUGSTAD, O.D., 2012. Nicotine does not influence NF-kappaB activity in neonatal mice reoxygenated with room-air or 100% oxygen. *The journal of maternal-fetal & neonatal medicine : the official journal of the European Association of Perinatal Medicine, the Federation of Asia and Oceania Perinatal Societies, the International Society of Perinatal Obstetricians,* **25**(10), pp. 2102-2105.

ALVAREZ-DIAZ, A., HILARIO, E., DE CERIO, F.G., VALLS-I-SOLER, A. and ALVAREZ-DIAZ, F.J., 2007. Hypoxic-ischemic injury in the immature brain--key vascular and cellular players. *Neonatology,* **92**(4), pp. 227-235.

AMERICAN PSYCHIATRIC ASSOCIATION, 2013. *Diagnostic and statistical manual of mental disorders (DSM-5®).* American Psychiatric Pub.

AMERICAN PSYCHIATRIC ASSOCIATION and AMERICAN PSYCHIATRIC ASSOCIATION, 1994. Diagnostic and statistical manual of mental disorders (DSM). *Washington, DC: American psychiatric association,* , pp. 143-147.

AMERICAN TISSUE CULTURE COLLECTION, ORG., 2016-last update, **Neuro-2a (ATCC® CCL-131™)**. Available: https://www.lgcstandards-atcc.org/products/all/CCL-131.aspx [10/01, 2018].

ANASTASIADES, P.G., MARQUES-SMITH, A., LYNGHOLM, D., LICKISS, T., RAFFIQ, S., KATZEL, D., MIESENBOCK, G. and BUTT, S.J., 2016. GABAergic interneurons form transient layer-specific circuits in early postnatal neocortex. *Nature communications,* **7**, pp. 10584.

ANDERSEN, S.L., 2003. Trajectories of brain development: point of vulnerability or window of opportunity? *Neuroscience & Biobehavioral Reviews,* **27**(1), pp. 3-18.

ANDINE, P., THORDSTEIN, M., KJELLMER, I., NORDBORG, C., THIRINGER, K., WENNBERG, E. and HAGBERG, H., 1990. Evaluation of brain damage in a rat

model of neonatal hypoxic-ischemia. *Journal of neuroscience methods,* **35**(3), pp. 253-260.

ANGEVINE, J.B.,JR and SIDMAN, R.L., 1961. Autoradiographic study of cell migration during histogenesis of cerebral cortex in the mouse. *Nature,* **192**, pp. 766-768.

ANJU, T., SMIJIN, S., CHINTHU, R. and PAULOSE, C., 2012. Dexmedetomidine and clonidine are alpha-2 adrenoceptor agonists increasingly used in the critical care unit as sedative agents for their benzodiazepine-sparing effects and their limited depressing effect on breathing. However adverse effects on breathing have been also reported with alpha-2 adrenoceptor agonists and their central effects on the respiratory rhythm generator are poorly known. We therefore... *Respiratory Physiology & Neurobiology,* **180**(1), pp. 132-140.

ANJU, T.R., ABRAHAM, P.M., ANTONY, S. and PAULOSE, C.S., 2010. Alterations in cortical GABAB receptors in neonatal rats exposed to hypoxic stress: role of glucose, oxygen, and epinephrine resuscitation. *Molecular and cellular biochemistry,* **343**(1-2), pp. 1-11.

ANJU, T.R., AJAYAN, M.S. and PAULOSE, C.S., 2013. Disruption of cerebellar cholinergic system in hypoxic neonatal rats and its regulation with glucose, oxygen and epinephrine resuscitations. *Neuroscience,* **236**, pp. 253-261.

ANJU, T.R., ANITHA, M., CHINTHU, R. and PAULOSE, C.S., 2012. Cerebellar GABA(A) receptor alterations in hypoxic neonatal rats: Role of glucose, oxygen and epinephrine supplementation. *Neurochemistry international,* **61**(3), pp. 302-309.

ANJU, T.R., BINOY, J., ANITHA, M. and PAULOSE, C.S., 2012. Striatal GABA receptor alterations in hypoxic neonatal rats: role of glucose, oxygen and epinephrine treatment. *Neurochemical research,* **37**(3), pp. 629-638.

ANJU, T.R., JAYANARAYANAN, S. and PAULOSE, C.S., 2011. Decreased GABAB receptor function in the cerebellum and brain stem of hypoxic neonatal rats: role of glucose, oxygen and epinephrine resuscitation. *Journal of Biomedical Science,* **18**, pp. 31-0127-18-31.

ANJU, T.R., KORAH, P.K., JAYANARAYANAN, S. and PAULOSE, C.S., 2011. Enhanced brain stem 5HT(2)A receptor function under neonatal hypoxic insult: role of glucose, oxygen, and epinephrine resuscitation. *Molecular and cellular biochemistry,* **354**(1-2), pp. 151-160.

ANJU, T.R., MATHEW, J., JAYANARAYANAN, S. and PAULOSE, C.S., 2010. Cerebellar 5HT2A receptor function under hypoxia in neonatal rats: role of glucose, oxygen, and epinephrine resuscitation. *Respiratory physiology & neurobiology,* **172**(3), pp. 147-153.

ANJU, T.R., NAIJIL, G., SHILPA, J., ROSHNI, T. and PAULOSE, C.S., 2013. Neonatal hypoxic insult-mediated cholinergic disturbances in the brain stem: effect of glucose, oxygen and epinephrine resuscitation. *Neurological sciences : official*

journal of the Italian Neurological Society and of the Italian Society of Clinical Neurophysiology, **34**(3), pp. 287-296.

ANJU, T.R., NANDHU, M.S., JES, P. and PAULOSE, C.S., 2011. Endocrine regulation of neonatal hypoxia: role of glucose, oxygen, and epinephrine supplementation. *Fetal and pediatric pathology,* **30**(5), pp. 338-349.

ANJU, T.R. and PAULOSE, C.S., 2013. Striatal cholinergic functional alterations in hypoxic neonatal rats: role of glucose, oxygen, and epinephrine resuscitation. *Biochemistry and cell biology = Biochimie et biologie cellulaire,* **91**(5), pp. 350-356.

ANJU, T.R. and PAULOSE, C.S., 2011. Amelioration of hypoxia-induced striatal 5-HT(2A) receptor, 5-HT transporter and HIF1 alterations by glucose, oxygen and epinephrine in neonatal rats. *Neuroscience letters,* **502**(3), pp. 129-132.

ANJU, T.R., PEEYUSH KUMAR, T. and PAULOSE, C.S., 2010. Decreased GABAA receptors functional regulation in the cerebral cortex and brainstem of hypoxic neonatal rats: effect of glucose and oxygen supplementation. *Cellular and molecular neurobiology,* **30**(4), pp. 599-606.

ANJU, T.R., SMIJIN, S., CHINTHU, R. and PAULOSE, C.S., 2012. Decreased cholinergic function in the cerebral cortex of hypoxic neonatal rats: role of glucose, oxygen and epinephrine resuscitation. *Respiratory physiology & neurobiology,* **180**(1), pp. 8-13.

ANJU, T.R., SMIJIN, S., KORAH, P.K. and PAULOSE, C.S., 2011. Cortical 5HT 2A receptor function under hypoxia in neonatal rats: role of glucose, oxygen, and epinephrine resuscitation. *Journal of molecular neuroscience : MN,* **43**(3), pp. 350-357.

ANTHONY, T.E., KLEIN, C., FISHELL, G. and HEINTZ, N., 2004. Radial glia serve as neuronal progenitors in all regions of the central nervous system. *Neuron,* **41**(6), pp. 881-890.

ANTONINI, A., SHATZ, C.J., 1990. Relation between putative transmitter phenotypes and connectivity of subplate neurons during cerebral cortical development. *European Journal of Neuroscience*. **2**(9), 744-61.

ANTOSOVA, Z., MACKOVA, M., KRAL, V. and MACEK, T., 2009. Therapeutic application of peptides and proteins: parenteral forever? *Trends in biotechnology,* **27**(11), pp. 628-635.

AOKI, C. and SIEKEVITZ, P., 1988. Plasticity in brain development. *Scientific American,* **259**(6), pp. 56-64.

APPLEGATE, C.D., JENSEN, F., BURCHFIEL, J.L. and LOMBROSO, C., 1996. The effects of neonatal hypoxia on kindled seizure development and electroconvulsive shock profiles. *Epilepsia,* **37**(8), pp. 723-727.

ARIMATSU, Y., ISHIDA, M., KANEKO, T., ICHINOSE, S. and OMORI, A., 2003. Organization and development of corticocortical associative neurons expressing the orphan nuclear receptor Nurr1. *The Journal of comparative neurology,* **466**(2), pp. 180-196.

ARTENI, N.S., SALGUEIRO, J., TORRES, I., ACHAVAL, M. and NETTO, C.A., 2003. Neonatal cerebral hypoxia–ischemia causes lateralized memory impairments in the adult rat. *Brain research,* **973**(2), pp. 171-178.

ASAHI, M., ASAHI, K., WANG, X. and LO, E.H., 2000. Reduction of tissue plasminogen activator-induced hemorrhage and brain injury by free radical spin trapping after embolic focal cerebral ischemia in rats. *Journal of Cerebral Blood Flow & Metabolism,* **20**(3), pp. 452-457.

ASHWAL, S., COLE, D.J., OSBORNE, S., OSBORNE, T.N. and PEARCE, W.J., 1995. A new model of neonatal stroke: reversible middle cerebral artery occlusion in the rat pup. *Pediatric neurology,* **12**(3), pp. 191-196.

ASO, K., SCHER, M.S. and BARMADA, M.A., 1989. Neonatal electroencephalography and neuropathology. *Journal of clinical neurophysiology : official publication of the American Electroencephalographic Society,* **6**(2), pp. 103-123.

ATKINSON, J. and BRADDICK, O., 2011. From genes to brain development to phenotypic behavior: "dorsal-stream vulnerability" in relation to spatial cognition, attention, and planning of actions in Williams syndrome (WS) and other developmental disorders. *Progress in brain research,* **189**, pp. 261-283.

AUJLA, P.K., FETELL, M.R. and JENSEN, F.E., 2009. Talampanel suppresses the acute and chronic effects of seizures in a rodent neonatal seizure model. *Epilepsia,* **50**(4), pp. 694-701.

AUTHEMAN, D., SHELDON, R.A., CHAUDHURI, N., VON ARX, S., SIEGENTHALER, C., FERRIERO, D.M. and CHRISTEN, S., 2012. Glutathione peroxidase overexpression causes aberrant ERK activation in neonatal mouse cortex after hypoxic preconditioning. *Pediatric research,* **72**(6), pp. 568-575.

AVINO, T.A. and HUTSLER, J.J., 2010. Abnormal cell patterning at the cortical gray-white matter boundary in autism spectrum disorders. *Brain research,* **1360**, pp. 138-146.

AZZOPARDI, D.V., STROHM, B., EDWARDS, A.D., DYET, L., HALLIDAY, H.L., JUSZCZAK, E., KAPELLOU, O., LEVENE, M., MARLOW, N. and PORTER, E., 2009. Moderate hypothermia to treat perinatal asphyxial encephalopathy. *New England Journal of Medicine,* **361**(14), pp. 1349-1358.

AZZOPARDI, D., ROBERTSON, N.J., BAINBRIDGE, A., CADY, E., CHARLES-EDWARDS, G., DEIERL, A., FAGIOLO, G., FRANKS, N.P., GRIFFITHS, J., HAJNAL, J., JUSZCZAK, E., KAPETANAKIS, B., LINSELL, L., MAZE, M., OMAR, O., STROHM, B., TUSOR, N. and EDWARDS, A.D., 2015. Moderate

hypothermia within 6 h of birth plus inhaled xenon versus moderate hypothermia alone after birth asphyxia (TOBY-Xe): a proof-of-concept, open-label, randomised controlled trial. *The Lancet.Neurology,* .

AZZOPARDI, D., ROBERTSON, N.J., KAPETANAKIS, A., GRIFFITHS, J., RENNIE, J.M., MATHIESON, S.R. and EDWARDS, A.D., 2013. Anticonvulsant effect of xenon on neonatal asphyxial seizures. *Archives of disease in childhood.Fetal and neonatal edition,* **98**(5), pp. F437-9.

BABURAMANI, A.A., EK, C.J., WALKER, D.W. and CASTILLO-MELENDEZ, M., 2012. Vulnerability of the developing brain to hypoxic-ischemic damage: contribution of the cerebral vasculature to injury and repair? *Frontiers in physiology,* **3**, pp. 424.

BACK, S.A., GAN, X., LI, Y., ROSENBERG, P.A. and VOLPE, J.J., 1998. Maturation-dependent vulnerability of oligodendrocytes to oxidative stress-induced death caused by glutathione depletion. *The Journal of neuroscience : the official journal of the Society for Neuroscience,* **18**(16), pp. 6241-6253.

BACK, S.A., LUO, N.L., BORENSTEIN, N.S., LEVINE, J.M., VOLPE, J.J., KINNEY, H.C., 2001. Late oligodendrocyte progenitors coincide with the developmental window of vulnerability for human perinatal white matter injury. *Journal of Neuroscience.,* **21**(4), 1302-12.

BALARAM, P., YOUNG, N.A. and KAAS, J.H., 2014. Histological features of layers and sublayers in cortical visual areas V1 and V2 of chimpanzees, macaque monkeys, and humans. *Eye and brain,* **2014**(6 Suppl 1), pp. 5-18.

BALDUINI, W., DE ANGELIS, V., MAZZONI, E. and CIMINO, M., 2000. Long-lasting behavioral alterations following a hypoxic/ischemic brain injury in neonatal rats. *Brain research,* **859**(2), pp. 318-325.

BALDUINI, W., CARLONI, S. and BUONOCORE, G., 2012. Autophagy in hypoxia-ischemia induced brain injury. *The journal of maternal-fetal & neonatal medicine : the official journal of the European Association of Perinatal Medicine, the Federation of Asia and Oceania Perinatal Societies, the International Society of Perinatal Obstetricians,* **25 Suppl 1**, pp. 30-34.

BALDUINI, W., DE ANGELIS, V., MAZZONI, E. and CIMINO, M., 2001. Simvastatin protects against long-lasting behavioral and morphological consequences of neonatal hypoxic/ischemic brain injury. *Stroke; a journal of cerebral circulation,* **32**(9), pp. 2185-2191.

BALE, T.L., BARAM, T.Z., BROWN, A.S., GOLDSTEIN, J.M., INSEL, T.R., MCCARTHY, M.M., NEMEROFF, C.B., REYES, T.M., SIMERLY, R.B. and SUSSER, E.S., 2010. Early life programming and neurodevelopmental disorders. *Biological psychiatry,* **68**(4), pp. 314-319.

BARDEHLE, S., KRUGER, M., BUGGENTHIN, F., SCHWAUSCH, J., NINKOVIC, J., CLEVERS, H., SNIPPERT, H.J., THEIS, F.J., MEYER-

LUEHMANN, M., BECHMANN, I., DIMOU, L., 2013. Live imaging of astrocyte responses to acute injury reveals selective juxtavascular proliferation. *Nature neuroscience.,* **16**(5), 580.

BARKER, A., 2018. Fractal-dimensional properties of subordinators. *Journal of Theoretical Probability,* , pp. 1-18.

BARKER, A., 2018. Transience and Recurrence of Markov Processes with Constrained Local Time. *arXiv preprint arXiv:1806.05965,* .

BARKER, R., KEHOE, P.G. and LOVE, S., 2012. Activators and inhibitors of the plasminogen system in Alzheimer's disease. *Journal of Cellular and Molecular Medicine,* **16**(4), pp. 865-876.

BARKER-CARLSON, K., LAWRENCE, D.A. and SCHWARTZ, B.S., 2002. Acyl-enzyme complexes between tissue-type plasminogen activator and neuroserpin are short-lived in vitro. *The Journal of biological chemistry,* **277**(49), pp. 46852-46857.

BARKOVICH, A.J., MILLER, S.P., BARTHA, A., NEWTON, N., HAMRICK, S.E., MUKHERJEE, P., GLENN, O.A., XU, D., PARTRIDGE, J.C., FERRIERO, D.M. and VIGNERON, D.B., 2006. MR imaging, MR spectroscopy, and diffusion tensor imaging of sequential studies in neonates with encephalopathy. *AJNR.American journal of neuroradiology,* **27**(3), pp. 533-547.

BARKOVICH, A.J., WESTMARK, K., PARTRIDGE, C., SOLA, A. and FERRIERO, D.M., 1995. Perinatal asphyxia: MR findings in the first 10 days. *AJNR.American journal of neuroradiology,* **16**(3), pp. 427-438.

BARTH, T.M. and STANFIELD, B.B., 1990. The recovery of forelimb-placing behavior in rats with neonatal unilateral cortical damage involves the remaining hemisphere. *The Journal of neuroscience : the official journal of the Society for Neuroscience,* **10**(10), pp. 3449-3459.

BARTOLETTI-STELLA, A., BAIARDI, S., STANZANI-MASERATI, M., PIRAS, S., CAFFARRA, P., RAGGI, A., PANTIERI, R., BALDASSARI, S., CAPORALI, L. and ABU-RUMEILEH, S., 2018. Identification of rare genetic variants in Italian patients with dementia by targeted gene sequencing. *Neurobiology of aging,* **66**, pp. 180. e23-180. e31.

BARTON, S.G.R., RAMPTON, D., WINROW, V., DOMIZIO, P. and FEAKINS, R., 2003. Expression of heat shock protein 32 (hemoxygenase-1) in the normal and inflamed human stomach and colon: an immunohistochemical study. *Cell stress & chaperones,* **8**(4), pp. 329-334.

BASU, A., KRADY, J.K. and LEVISON, S.W., 2004. Interleukin-1: a master regulator of neuroinflammation. *Journal of neuroscience research,* **78**(2), pp. 151-156.

BAUD, O., DAIRE, J.L., DALMAZ, Y., FONTAINE, R.H., KRUEGER, R.C., SEBAG, G., EVRARD, P., GRESSENS, P. and VERNEY, C., 2004. Gestational

hypoxia induces white matter damage in neonatal rats: a new model of periventricular leukomalacia. *Brain pathology (Zurich, Switzerland),* **14**(1), pp. 1-10.

BAUER, H.C., BAUER, H., LAMETSCHWANDTNER, A., AMBERGER, A., RUIZ, P. and STEINER, M., 1993. Neovascularization and the appearance of morphological characteristics of the blood-brain barrier in the embryonic mouse central nervous system. *Brain research.Developmental brain research,* **75**(2), pp. 269-278.

BAYATTI, N., MOSS, J.A., SUN, L., AMBROSE, P., WARD, J.F., LINDSAY, S. and CLOWRY, G.J., 2008. A molecular neuroanatomical study of the developing human neocortex from 8 to 17 postconceptional weeks revealing the early differentiation of the subplate and subventricular zone. *Cerebral cortex (New York, N.Y.: 1991),* **18**(7), pp. 1536-1548.

BEAR, M.F., CONNORS, B.W. and PARADISO, M.A., 2007. *Neuroscience.* Lippincott Williams & Wilkins.

BEASLEY, C.L., COTTER, D.R. and EVERALL, I.P., 2002. Density and distribution of white matter neurons in schizophrenia, bipolar disorder and major depressive disorder: no evidence for abnormalities of neuronal migration. *Molecular psychiatry,* **7**(6), pp. 564-570.

BEDERSON, J.B., PITTS, L.H., TSUJI, M., NISHIMURA, M.C., DAVIS, R.L. and BARTKOWSKI, H., 1986. Rat middle cerebral artery occlusion: evaluation of the model and development of a neurologic examination. *Stroke; a journal of cerebral circulation,* **17**(3), pp. 472-476.

BEDERSON, J.B., PITTS, L.H., GERMANO, S.M., NISHIMURA, M.C., DAVIS, R.L., BARTKOWSKI, H.M., 1986. Evaluation of 2, 3, 5-triphenyltetrazolium chloride as a stain for detection and quantification of experimental cerebral infarction in rats. *Stroke.*, **17**(6), 1304-8.

BELGARD, T.G., MARQUES, A.C., OLIVER, P.L., ABAAN, H.O., SIREY, T.M., HOERDER-SUABEDISSEN, A., GARCIA-MORENO, F., MOLNAR, Z., MARGULIES, E.H. and PONTING, C.P., 2011. A transcriptomic atlas of mouse neocortical layers. *Neuron,* **71**(4), pp. 605-616.

BELL, M.J. and HALLENBECK, J.M., 2002. Effects of intrauterine inflammation on developing rat brain. *Journal of neuroscience research,* **70**(4), pp. 570-579.

BELLAVANCE, M., BLANCHETTE, M. and FORTIN, D., 2008. Recent advances in blood–brain barrier disruption as a CNS delivery strategy. *The AAPS journal,* **10**(1), pp. 166-177.

BELORGEY, D., SHARP, L.K., CROWTHER, D.C., ONDA, M., JOHANSSON, J. and LOMAS, D.A., 2004. Neuroserpin Portland (Ser52Arg) is trapped as an inactive intermediate that rapidly forms polymers: implications for the epilepsy seen in the dementia FENIB. *European journal of biochemistry,* **271**(16), pp. 3360-3367.

BEN-ARI, Y.E., CHERUBINI, E.N., CORRADETTI, R.E., GAIARSA, J.L., 1989. Giant synaptic potentials in immature rat CA3 hippocampal neurones. *The Journal of physiology.,* **416**(1), 303-25.

BEN-ARI, Y., 2002. Excitatory actions of gaba during development: the nature of the nurture. *Nature Reviews Neuroscience,* **3**(9), pp. 728.

BEN-ARI, Y., CHERUBINI, E., CORRADETTI, R. and GAIARSA, J., 1989. Giant synaptic potentials in immature rat CA3 hippocampal neurones. *The Journal of physiology,* **416**(1), pp. 303-325.

BENARROCH, E.E., 2007. Tissue plasminogen activator: beyond thrombolysis. *Neurology,* **69**(8), pp. 799-802.

BENCHENANE, K., LÓPEZ-ATALAYA, J.P., FERNÁNDEZ-MONREAL, M., TOUZANI, O. and VIVIEN, D., 2004. Equivocal roles of tissue-type plasminogen activator in stroke-induced injury. *Trends in neurosciences,* **27**(3), pp. 155-160.

BENCHENANE, K., LÓPEZ-ATALAYA, J.P., FERNÁNDEZ-MONREAL, M., TOUZANI, O. and VIVIEN, D., 2004. Equivocal roles of tissue-type plasminogen activator in stroke-induced injury. *Trends in neurosciences,* **27**(3), pp. 155-160.

BENITEZ, M., SÁNCHEZ-PONCE, D., GARRIDO, J. and WANDOSELL, F., 2014. Hsp90 activity is necessary to acquire a proper neuronal polarization. *Biochimica et Biophysica Acta (BBA)-Molecular Cell Research,* **1843**(2), pp. 245-252.

BENNET, L., PEEBLES, D.M., EDWARDS, A.D., RIOS, A. and HANSON, M.A., 1998. The cerebral hemodynamic response to asphyxia and hypoxia in the near-term fetal sheep as measured by near infrared spectroscopy. *Pediatric research,* **44**(6), pp. 951-957.

BERGER, P., KOZLOV, S.V., CINELLI, P., KRÜGER, S.R., VOGT, L. and SONDEREGGER, P., 1999. Neuronal depolarization enhances the transcription of the neuronal serine protease inhibitor neuroserpin. *Molecular and Cellular Neuroscience,* **14**(6), pp. 455-467.

BERGERON, J.D., DESLAURIERS, J., GRIGNON, S., FORTIER, L.C., LEPAGE, M., STROH, T., POYART, C. and SEBIRE, G., 2013. White matter injury and autistic-like behavior predominantly affecting male rat offspring exposed to group B streptococcal maternal inflammation. *Developmental neuroscience,* **35**(6), pp. 504-515.

BERNARD, S.A., GRAY, T.W., BUIST, M.D., JONES, B.M., SILVESTER, W., GUTTERIDGE, G. and SMITH, K., 2002. Treatment of comatose survivors of out-of-hospital cardiac arrest with induced hypothermia. *New England Journal of Medicine,* **346**(8), pp. 557-563.

BERRIDGE, M.V., HERST, P.M. and TAN, A.S., 2005. Tetrazolium dyes as tools in cell biology: new insights into their cellular reduction. *Biotechnology annual review,* **11**, pp. 127-152.

BERRY, M. and ROGERS, A.W., 1965. The migration of neuroblasts in the developing cerebral cortex. *Journal of anatomy,* **99**(Pt 4), pp. 691-709.

BILLIARDS, S.S., HAYNES, R.L., FOLKERTH, R.D., TRACHTENBERG, F.L., LIU, L.G., VOLPE, J.J. and KINNEY, H.C., 2006. Development of microglia in the cerebral white matter of the human fetus and infant. *Journal of Comparative Neurology,* **497**(2), pp. 199-208.

BIO-RAD LABORATORIES, I., 2018-last update, **Stain-Free Imaging Technology**. Available: http://www.bio-rad.com/en-uk/applications-technologies/stain-free-imaging-technology?ID=NZ0G1815 [08/10, 2018].

BLAISE, S.A., NEDELEC, E., ALBERTO, J.M., SCHROEDER, H., AUDONNET, S., BOSSENMEYER-POURIE, C., GUEANT, J.L. and DAVAL, J.L., 2009. Short hypoxia could attenuate the adverse effects of hyperhomocysteinemia on the developing rat brain by inducing neurogenesis. *Experimental neurology,* **216**(1), pp. 231-238.

BLENNOW, M., SÄVMAN, K., ILVES, P., THORESEN, M. and ROSENGREN, L., 2001. Brain-specific proteins in the cerebrospinal fluid of severely asphyxiated newborn infants. *Acta paediatrica,* **90**(10), pp. 1171-1175.

BLENNOW, M., HAGBERG, H. and ROSENGREN, L., 1995. Glial fibrillary acidic protein in the cerebrospinal fluid: a possible indicator of prognosis in full-term asphyxiated newborn infants? *Pediatric research,* **37**(3), pp. 260.

BLENNOW, M., ROSENGREN, L., JONSSON, S., FORSSBERG, H., KATZ-SALAMON, M., HAGBERG, H., HESSER, U. and LAGERCRANTZ, H., 1996. Glial fibrillary acidic protein is increased in the cerebrospinal fluid of preterm infants with abnormal neurological findings. *Acta Paediatrica (Oslo, Norway : 1992),* **85**(4), pp. 485-489.

BLOMGREN, K., MCRAE, A., ELMERED, A., BONA, E., KAWASHIMA, S., SAIDO, T.C., ONO, T. and HAGBERG, H., 1997. The calpain proteolytic system in neonatal hypoxic-ischemia. *Annals of the New York Academy of Sciences,* **825**(1), pp. 104-119.

BLOMGREN, K. and HAGBERG, H., 2006. Free radicals, mitochondria, and hypoxia-ischemia in the developing brain. *Free radical biology & medicine,* **40**(3), pp. 388-397.

BLOMGREN, K., ZHU, C., WANG, X., KARLSSON, J.O., LEVERIN, A.L., BAHR, B.A., MALLARD, C., HAGBERG, H., 2001. Synergistic activation of caspase-3 by m-calpain after neonatal hypoxia-ischemia a mechanism of "pathological apoptosis"?. *Journal of Biological Chemistry.*, **276**(13), 10191-8.

BLOOM, W., 1968. DW Fawcett A textbook of histology. *Saunders, Amsterdam,* , pp. 582.

BOKSA, P., ZHANG, Y. and NOUEL, D., 2015. Maternal Oxytocin Administration Before Birth Influences the Effects of Birth Anoxia on the Neonatal Rat Brain. *Neurochemical research,* **40**(8), pp. 1631-1643.

BONA, E., HAGBERG, H., LØBERG, E.M., BÅGENHOLM, R. and THORESEN, M., 1998. Protective effects of moderate hypothermia after neonatal hypoxia-ischemia: short-and long-term outcome. *Pediatric research,* **43**(6), pp. 738-745.

BONIFACIO, S.L., GLASS, H.C., PELOQUIN, S. and FERRIERO, D.M., 2011. A new neurological focus in neonatal intensive care. *Nature Reviews Neurology,* **7**(9), pp. 485-494.

BORGES, V.M., LEE, T.W., CHRISTIE, D.L. and BIRCH, N.P., 2010. Neuroserpin regulates the density of dendritic protrusions and dendritic spine shape in cultured hippocampal neurons. *Journal of neuroscience research,* **88**(12), pp. 2610-2617.

BOSS, V., SOLA, A., WEN, T.C. and DECKER, M.J., 2005. Mild intermittent hypoxia does not induce stress responses in the neonatal rat brain. *Biology of the neonate,* **88**(4), pp. 313-320.

BOYLAN, G.B., YOUNG, K., PANERAI, R.B., RENNIE, J.M. and EVANS, D.H., 2000. Dynamic cerebral autoregulation in sick newborn infants. *Pediatric research,* **48**(1), pp. 12-17.

BRACKMANN, F.A., LINK, A.S., JUNG, S., RICHTER, M., ZOGLAUER, D., WALKINSHAW, G., ALZHEIMER, C. and TROLLMANN, R., 2013. Activin A regulation under global hypoxia in developing mouse brain. *Brain research,* **1531**, pp. 65-74.

BRANDON, N.J. and SAWA, A., 2011. Linking neurodevelopmental and synaptic theories of mental illness through DISC1. *Nature Reviews Neuroscience,* **12**(12), pp. 707-722.

BRECKO, J., MATHYS, A., DEKONINCK, W., LEPONCE, M., VANDEN-SPIEGEL, D., SEMAL, P., 2014. Focus stacking: Comparing commercial top-end set-ups with a semi-automatic low budget approach. A possible solution for mass digitization of type specimens. *ZooKeys.*, **464**, 1.

BREHMER, F., BENDIX, I., PRAGER, S., VAN DE LOOIJ, Y., REINBOTH, B.S., ZIMMERMANNS, J., SCHLAGER, G.W., BRAIT, D., SIFRINGER, M., ENDESFELDER, S., SIZONENKO, S., MALLARD, C., BUHRER, C., FELDERHOFF-MUESER, U. and GERSTNER, B., 2012. Interaction of inflammation and hyperoxia in a rat model of neonatal white matter damage. *PloS one,* **7**(11), pp. e49023.

BRIGSTOCK, D.R., 1999. The Connective Tissue Growth Factor/Cysteine-Rich 61/Nephroblastoma Overexpressed (CCN) Family 1. *Endocrine reviews,* **20**(2), pp. 189-206.

BROCHNER, C.B. and MOLLGARD, K., 2016. SSEA-4 and YKL-40 positive progenitor subtypes in the subventricular zone of developing human neocortex. *Glia,* **64**(1), pp. 90-104.

BROCHU, M.E., GIRARD, S., LAVOIE, K. and SEBIRE, G., 2011. Developmental regulation of the neuroinflammatory responses to LPS and/or hypoxia-ischemia between preterm and term neonates: An experimental study. *Journal of neuroinflammation,* **8**, pp. 55-2094-8-55.

BRODMANN, K., 1909. Vergleichende Lokalisationslehre der Großhirnrinde in ihren Prinzipien dargestellt auf Grund des Zellbaues. Leipzig: Johann Ambrosius Barth.

BRONSTEIN, R. and TSIRKA, S., 2017. Tissue Plasminogen Activator Signaling in the Normal and Diseased Brain. *Primer on Cerebrovascular Diseases (Second Edition).* Elsevier, pp. 288-291.

BROOKS, K.J., CLARK, J.B. and BATES, T.E., 1996. Assessment of energy metabolism in the developing brain following aglycemic hypoxia by1H and31P NMR. *Neurochemical research,* **21**(9), pp. 1089-1095.

BROWN, N.A., ANTONIW, J. and HAMMOND-KOSACK, K.E., 2012. The predicted secretome of the plant pathogenic fungus Fusarium graminearum: a refined comparative analysis. *PloS one,* **7**(4), pp. e33731.

BROWN, R.C., EGLETON, R.D. and DAVIS, T.P., 2004. Mannitol opening of the blood-brain barrier: regional variation in the permeability of sucrose, but not 86Rb+ or albumin. *Brain research,* **1014**(1-2), pp. 221-227.

BRUNING, M., LUMMER, M., BENTELE, C., SMOLENAARS, M.M., RODENBURG, K.W. and RAGG, H., 2007. The Spn4 gene from Drosophila melanogaster is a multipurpose defence tool directed against proteases from three different peptidase families. *The Biochemical journal,* **401**(1), pp. 325-331.

BRUNJES, P.C., 1990. The precocial mouse, Acomys cahirinus. *Psychobiology,* **18**(3), pp. 339-350.

BRUNJES, P.C., 1989. A comparative study of prenatal development in the olfactory bulb, neocortex and hippocampal region of the precocial mouse Acomys cahirinus and rat. *Brain research.Developmental brain research,* **49**(1), pp. 7-25.

BRUNJES, P.C., 1985. A stereological study of neocortical maturation in the precocial mouse, Acomys cahirinus. *Brain research,* **351**(2), pp. 279-287.

BRUNJES, P.C., KOROL, D.L. and STERN, K.G., 1989. Prenatal neurogenesis in the telencephalon of the precocial mouse Acomys cahirinus. *Neuroscience letters,* **107**(1-3), pp. 114-119.

BUDDAY, S., RAYBAUD, C. and KUHL, E., 2014. A mechanical model predicts morphological abnormalities in the developing human brain. *Scientific reports,* **4**.

BUESCHER, A.V., CIDAV, Z., KNAPP, M. and MANDELL, D.S., 2014. Costs of autism spectrum disorders in the United Kingdom and the United States. *JAMA pediatrics,* **168**(8), pp. 721-728.

BULLMORE, E. and SPORNS, O., 2012. The economy of brain network organization. *Nature Reviews Neuroscience,* **13**(5), pp. 336-349.

BULLMORE, E. and SPORNS, O., 2009. Complex brain networks: graph theoretical analysis of structural and functional systems. *Nature Reviews Neuroscience,* **10**(3), pp. 186-198.

BUNNEY, W.E. and BUNNEY, B.G., 2000. Molecular clock genes in man and lower animals: possible implications for circadian abnormalities in depression. *Neuropsychopharmacology,* **22**(4), pp. 335.

BUNNEY, B.G., POTKIN, S.G. and BUNNEY, W.E., 1997. Neuropathological studies of brain tissue in schizophrenia. *Journal of psychiatric research,* **31**(2), pp. 159-173.

BURD, I., WELLING, J., KANNAN, G. and JOHNSTON, M.V., 2016. Chapter Five-Excitotoxicity as a Common Mechanism for Fetal Neuronal Injury with Hypoxia and Intrauterine Inflammation. *Advances in pharmacology,* **76**, pp. 85-101.

BURGESS, N., MAGUIRE, E.A. and O'KEEFE, J., 2002. The human hippocampus and spatial and episodic memory. *Neuron,* **35**(4), pp. 625-641.

BURTRUM, D. and SILVERSTEIN, F.S., 1994. Hypoxic-ischemic brain injury stimulates glial fibrillary acidic protein mRNA and protein expression in neonatal rats.

BUSTAMANTE, D., MORALES, P., PEREYRA, J.T., GOINY, M. and HERRERA-MARSCHITZ, M., 2007. Nicotinamide prevents the effect of perinatal asphyxia on dopamine release evaluated with in vivo microdialysis 3 months after birth. *Experimental brain research,* **177**(3), pp. 358-369.

BUWALDA, B., NYAKAS, C., VOSSELMAN, H.J. and LUITEN, P.G., 1995. Effects of early postnatal anoxia on adult learning and emotion in rats. *Behavioural brain research,* **67**(1), pp. 85-90.

BYSTRON, I., BLAKEMORE, C. and RAKIC, P., 2008. Development of the human cerebral cortex: Boulder Committee revisited. *Nature Reviews Neuroscience,* **9**(2), pp. 110.

CACCIA, S., RICAGNO, S. and BOLOGNESI, M., 2010. Molecular bases of neuroserpin function and pathology. *Biomolecular concepts,* **1**(2), pp. 117-130.

CAI, J., KANG, Z., LIU, K., LIU, W., LI, R., ZHANG, J.H., LUO, X. and SUN, X., 2009. Neuroprotective effects of hydrogen saline in neonatal hypoxia–ischemia rat model. *Brain research,* **1256**, pp. 129-137.

CAI, J., KANG, Z., LIU, W.W., LUO, X., QIANG, S., ZHANG, J.H., OHTA, S., SUN, X., XU, W., TAO, H., LI, R., 2008. Hydrogen therapy reduces apoptosis in neonatal hypoxia–ischemia rat model. *Neuroscience letters.*, **441**(2), 167-72.

CAI, Z., PANG, Y., XIAO, F. and RHODES, P.G., 2001. Chronic ischemia preferentially causes white matter injury in the neonatal rat brain. *Brain research,* **898**(1), pp. 126-135.

CALABRESE, V., SCAPAGNINI, G., COLOMBRITA, C., RAVAGNA, A., PENNISI, G., STELLA, A.G., GALLI, F. and BUTTERFIELD, D., 2003. Redox regulation of heat shock protein expression in aging and neurodegenerative disorders associated with oxidative stress: a nutritional approach. *Amino acids,* **25**(3-4), pp. 437-444.

CAPUTA, M., ROGALSKA, J., WENTOWSKA, K. and NOWAKOWSKA, A., 2005. Perinatal asphyxia, hyperthermia and hyperferremia as factors inducing behavioural disturbances in adulthood: a rat model. *Behavioural brain research,* **163**(2), pp. 246-256.

CARLONI, S., BUONOCORE, G. and BALDUINI, W., 2008. Protective role of autophagy in neonatal hypoxia-ischemia induced brain injury. *Neurobiology of disease,* **32**(3), pp. 329-339.

CARLONI, S., CARNEVALI, A., CIMINO, M. and BALDUINI, W., 2007. Extended role of necrotic cell death after hypoxia-ischemia-induced neurodegeneration in the neonatal rat. *Neurobiology of disease,* **27**(3), pp. 354-361.

CARLOS, R., SEIDLER, F.J., LAPPI, S. and SLOTKIN, T.A., 1991. Fetal dexamethasone exposure affects basal ornithine decarboxylase activity in developing rat brain regions and alters acute responses to hypoxia and maternal separation. *Neonatology,* **59**(2), pp. 69-77.

CARLSSON, Y., WANG, X., SCHWENDIMANN, L., ROUSSET, C.I., JACOTOT, E., GRESSENS, P., THORESEN, M., MALLARD, C. and HAGBERG, H., 2012. Combined effect of hypothermia and caspase-2 gene deficiency on neonatal hypoxic-ischemic brain injury. *Pediatric research,* **71**(5), pp. 566-572.

CARMEL, J.B., KAKINOHANA, O., MESTRIL, R., YOUNG, W., MARSALA, M. and HART, R.P., 2004. Mediators of ischemic preconditioning identified by microarray analysis of rat spinal cord. *Experimental neurology,* **185**(1), pp. 81-96.

CARMELIET, P. and STORKEBAUM, E., 2002. Vascular and neuronal effects of VEGF in the nervous system: implications for neurological disorders. *Seminars in cell & developmental biology,* **13**(1), pp. 39-53.

CASOLINI, P., ZUENA, A.R., CINQUE, C., MATTEUCCI, P., ALEMA, G.S., ADRIANI, W., CARPINELLI, G., SANTORO, F., ALLEVA, E., BOSCO, P., NICOLETTI, F., LAVIOLA, G. and CATALANI, A., 2005. Sub-neurotoxic neonatal anoxia induces subtle behavioural changes and specific abnormalities in brain group-I

metabotropic glutamate receptors in rats. *Journal of neurochemistry,* **95**(1), pp. 137-145.

CAVINESS, V. and SIDMAN, R., 1973. Time of origin of corresponding cell classes in the cerebral cortex of normal and reeler mutant mice: an autoradiographic analysis. *Journal of Comparative Neurology,* **148**(2), pp. 141-151.

CAVINESS, V.S.,JR and FROST, D.O., 1980. Tangential organization of thalamic projections to the neocortex in the mouse. *The Journal of comparative neurology,* **194**(2), pp. 335-367.

CEPEDA, C., ANDRE, V.M., WU, N., YAMAZAKI, I., UZGIL, B., VINTERS, H.V., LEVINE, M.S. and MATHERN, G.W., 2007. Immature neurons and GABA networks may contribute to epileptogenesis in pediatric cortical dysplasia. *Epilepsia,* **48 Suppl 5**, pp. 79-85.

CHAMORRO, A., DIRNAGL, U., URRA, X. and PLANAS, A.M., 2016. Neuroprotection in acute stroke: targeting excitotoxicity, oxidative and nitrosative stress, and inflammation. *The Lancet.Neurology,* **15**(8), pp. 869-881.

CHAN, J.Y., CHENG, H.L., CHOU, J.L., LI, F.C., DAI, K.Y., CHAN, S.H. and CHANG, A.Y., 2007. Heat shock protein 60 or 70 activates nitric-oxide synthase (NOS) I- and inhibits NOS II-associated signaling and depresses the mitochondrial apoptotic cascade during brain stem death. *The Journal of biological chemistry,* **282**(7), pp. 4585-4600.

CHANG, W.W., CHANG, N., LIN, S., WU, C. and WU, F.Y., 2000. Tissue-specific cancer-related serpin gene cluster at human chromosome band 3q26. *Genes, Chromosomes and Cancer,* **29**(3), pp. 240-255.

CHAN-PALAY, V. and PALAY, S.L., 1977. Immunocytochemical identification of substance P cells and their processes in rat sensory ganglia and their terminals in the spinal cord: light microscopic studies. *Proceedings of the National Academy of Sciences of the United States of America,* **74**(8), pp. 3597-3601.

CHARLES RIVER LABORATORIES, I., 2018-last update, C57BL/6-Elite (SOPF) Mouse. Available: http://www.criver.com/products-services/basic-research/find-a-model/c57bl-6n-mouse [08/10, \2018].

CHAU, V., CLÉMENT, J., ROBITAILLE, Y., D'ANJOU, G. and VANASSE, M., 2008. Congenital axonal neuropathy and encephalopathy. *Pediatric neurology,* **38**(4), pp. 261-266.

CHAU, V., POSKITT, K.J. and MILLER, S.P., 2012. Magnetic resonance imaging in hypoxic-ischemic encephalopathy: still a cool test. *Archives of Pediatrics & Adolescent Medicine,* **166**(7), pp. 669-671.

CHAU, V., POSKITT, K.J., SARGENT, M.A., LUPTON, B.A., HILL, A., ROLAND, E. and MILLER, S.P., 2009. Comparison of computer tomography and

magnetic resonance imaging scans on the third day of life in term newborns with neonatal encephalopathy. *Pediatrics,* **123**(1), pp. 319-326.

CHAU, V., SYNNES, A., GRUNAU, R.E., POSKITT, K.J., BRANT, R. and MILLER, S.P., 2013. Abnormal brain maturation in preterm neonates associated with adverse developmental outcomes. *Neurology,* **81**(24), pp. 2082-2089.

CHAUDHARI, P., YE, Z. and JANG, Y.Y., 2014. Roles of reactive oxygen species in the fate of stem cells. *Antioxidants & redox signaling,* **20**(12), pp. 1881-1890.

CHAVEZ-VALDEZ, R., MARTIN, L.J., RAZDAN, S., GAUDA, E.B. and NORTHINGTON, F.J., 2014. Sexual dimorphism in BDNF signaling after neonatal hypoxia-ischemia and treatment with necrostatin-1. *Neuroscience,* **260**, pp. 106-119.

CHEN, J., YANG, C., WANG, Y., LEE, J., CHENG, C. and CHOU, C., 2013. Acrylamide-induced mitochondria collapse and apoptosis in human astrocytoma cells. *Food and chemical toxicology,* **51**, pp. 446-452.

CHEN, Y., MAGNANI, D., THEIL, T., PRATT, T. and PRICE, D.J., 2012. Evidence that descending cortical axons are essential for thalamocortical axons to cross the pallial-subpallial boundary in the embryonic forebrain. *PloS one,* **7**(3), pp. e33105.

CHEN, C., CUI, X., MATSUNAGA, F., MA, J., MA, N., ABEL, T. and LIU, R., 2014. Salvinorin A decreases mortality and improves neurological outcome in a neonatal mouse hypoxia model. *Translational perioperative and pain medicine,* **1**(2), pp. 9-13.

CHEN, H., SPAGNOLI, F., BURRIS, M., ROLLAND, W.B., FAJILAN, A., DOU, H., TANG, J. and ZHANG, J.H., 2012. Nanoerythropoietin is 10-times more effective than regular erythropoietin in neuroprotection in a neonatal rat model of hypoxia and ischemia. *Stroke; a journal of cerebral circulation,* **43**(3), pp. 884-887.

CHENG, A., HAYDAR, T.F., YAROWSKY, P.J. and KRUEGER, B.K., 2004. Concurrent generation of subplate and cortical plate neurons in developing trisomy 16 mouse cortex. *Developmental neuroscience,* **26**(2-4), pp. 255-265.

CHENG, Y., DESHMUKH, M., D'COSTA, A., DEMARO, J.A., GIDDAY, J.M., SHAH, A., SUN, Y., JACQUIN, M.F., JOHNSON, E.M. and HOLTZMAN, D.M., 1998. Caspase inhibitor affords neuroprotection with delayed administration in a rat model of neonatal hypoxic-ischemic brain injury. *The Journal of clinical investigation,* **101**(9), pp. 1992-1999.

CHESSEL, D., DUFOUR, A.B. and THIOULOUSE, J., 2004. The ade4 package-I-One-table methods. *R news,* **4**(1), pp. 5-10.

CHEVALLET, M., DIEMER, H., VAN DORSSEALER, A., VILLIERS, C. and RABILLOUD, T., 2007. Toward a better analysis of secreted proteins: the example of the myeloid cells secretome. *Proteomics,* **7**(11), pp. 1757-1770.

CHEVÉE, M., ROBERTSON, J.D.J., CANNON, G.H., BROWN, S.P. and GOFF, L.A., 2018. Variation in activity state, axonal projection, and position define the transcriptional identity of individual neocortical projection neurons. *Cell reports,* **22**(2), pp. 441-455.

CHI, N.C. and KARLINER, J.S., 2004. Molecular determinants of responses to myocardial ischemia/reperfusion injury: focus on hypoxia-inducible and heat shock factors. *Cardiovascular research,* **61**(3), pp. 437-447.

CHIA, R., ACHILLI, F., FESTING, M.F. and FISHER, E.M., 2005. The origins and uses of mouse outbred stocks. *Nature genetics,* **37**(11), pp. 1181.

CHIAPPE-GUTIERREZ, M., KITZMUELLER, E., LABUDOVA, O., FUERST, G., HOEGER, H., HARDMEIER, R., NOHL, H., GILLE, L. and LUBEC, B., 1998. mRNA levels of the hypoxia inducible factor (HIF-1) and DNA repair genes in perinatal asphyxia of the rat. *Life Sciences,* **63**(13), pp. 1157-1167.

CHIP, S., FERNÁNDEZ-LÓPEZ, D., LI, F., FAUSTINO, J., DERUGIN, N. and VEXLER, Z.S., 2017. Genetic deletion of galectin-3 enhances neuroinflammation, affects microglial activation and contributes to sub-chronic injury in experimental neonatal focal stroke. *Brain, behavior, and immunity,* **60**, pp. 270-281.

CHOI, H.A., BADJATIA, N. and MAYER, S.A., 2012. Hypothermia for acute brain injury—mechanisms and practical aspects. *Nature Reviews Neurology,* **8**(4), pp. 214-222.

CHO, K., and CHOI, G.E., 2017. Microglia: physiological functions revealed through morphological profiles. *Folia biologica.*, **63**(3), 85.

CHO, S., LIU, D., FAIRMAN, D., LI, P., JENKINS, L., MCGONIGLE, P., WOOD, A., 2004. Spatiotemporal evidence of apoptosis-mediated ischemic injury in organotypic hippocampal slice cultures. *Neurochemistry international.*, **45**(1), 117-27.

CHOI, D.W., 1992. Excitotoxic cell death. *Journal of neurobiology,* **23**(9), pp. 1261-1276.

CHOI, D.W., 1988. Calcium-mediated neurotoxicity: relationship to specific channel types and role in ischemic damage. *Trends in neurosciences,* **11**(10), pp. 465-469.

CHRISTAKI, E. and GIAMARELLOS-BOURBOULIS, E.J., 2014. The beginning of personalized medicine in sepsis: small steps to a bright future. *Clinical genetics,* **86**(1), pp. 56-61.

CHUN, J.N., CHOI, B., LEE, K.W., LEE, D.J., KANG, D.H., LEE, J.Y., SONG, I.S., KIM, H.I., LEE, S. and KIM, H.S., 2010. Cytosolic Hsp60 is involved in the NF-κB-dependent survival of cancer cells via IKK regulation. *PLoS One,* **5**(3), pp. e9422.

CHUN, J.J., NAKAMURA, M.J. and SHATZ, C.J., 1987. Transient cells of the developing mammalian telencephalon are peptide-immunoreactive neurons. *Nature,* **325**(6105), pp. 617-620.

CHUN, J.J. and SHATZ, C.J., 1989. The earliest-generated neurons of the cat cerebral cortex: characterization by MAP2 and neurotransmitter immunohistochemistry during fetal life. *The Journal of neuroscience : the official journal of the Society for Neuroscience,* **9**(5), pp. 1648-1667.

CINELLI, P., MADANI, R., TSUZUKI, N., VALLET, P., ARRAS, M., ZHAO, C.N., OSTERWALDER, T., RÜLICKE, T. and SONDEREGGER, P., 2001. Neuroserpin, a neuroprotective factor in focal ischemic stroke. *Molecular and Cellular Neuroscience,* **18**(5), pp. 443-457.

CLANCY, B., DARLINGTON, R. and FINLAY, B., 2001. Translating developmental time across mammalian species. *Neuroscience,* **105**(1), pp. 7-17.

CLANCY, B., DARLINGTON, R.B. and FINLAY, B.L., 2000. The course of human events: Predicting the timing of primate neural development. *Developmental Science,* **3**(1), pp. 57-66.

CLANCY, B. and CAULLER, L.J., 1999. Widespread projections from subgriseal neurons (layer VII) to layer I in adult rat cortex. *The Journal of comparative neurology,* **407**(2), pp. 275-286.

CLANCY, B., FINLAY, B.L., DARLINGTON, R.B. and ANAND, K.J., 2007. Extrapolating brain development from experimental species to humans. *Neurotoxicology,* **28**(5), pp. 931-937.

CLANCY, B., TEAGUE-ROSS, T.J. and NAGARAJAN, R., 2009. Cross-species analyses of the cortical GABAergic and subplate neural populations. *Frontiers in neuroanatomy,* **3**, pp. 20.

CLEARY, R.T., SUN, H., HUYNH, T., MANNING, S.M., LI, Y., ROTENBERG, A., TALOS, D.M., KAHLE, K.T., JACKSON, M., RAKHADE, S.N., BERRY, G. and JENSEN, F.E., 2013. Bumetanide enhances phenobarbital efficacy in a rat model of hypoxic neonatal seizures. *PloS one,* **8**(3), pp. e57148.

COLE, D., DRUMMOND, J., GHAZAL, E. and SHAPIRO, H., 1990. A reversible component of cerebral injury as identified by the histochemical stain 2, 3, 5-triphenyltetrazolium chloride (TTC). *Acta Neuropathologica,* **80**(2), pp. 152-155.

COLE, J.W., NAJ, A.C., O'CONNELL, J.R., STINE, O.C., SORKIN, J.D., WOZNIAK, M.A., STERN, B.J., YEPES, M., LAWRENCE, D.A. and REINHART, L.J., 2007. Neuroserpin polymorphisms and stroke risk in a biracial population: the stroke prevention in young women study. *BMC neurology,* **7**(1), pp. 1.

COLELLA, A.D., CHEGENII, N., TEA, M.N., GIBBINS, I.L., WILLIAMS, K.A. and CHATAWAY, T.K., 2012. Comparison of Stain-Free gels with traditional immunoblot loading control methodology. *Analytical Biochemistry,* **430**(2), pp. 108-110.

CONNOR, C.M., GUO, Y. and AKBARIAN, S., 2009. Cingulate white matter neurons in schizophrenia and bipolar disorder. *Biological psychiatry,* **66**(5), pp. 486-493.

COPIN, J.C., REOLA, L.F., CHAN, T.Y., LI, Y., EPSTEIN, C.J. and CHAN, P.H., 1996. Oxygen deprivation but not a combination of oxygen, glucose, and serum deprivation induces DNA degradation in mouse cortical neurons in vitro: attenuation by transgenic overexpression of CuZn-superoxide dismutase. *Journal of neurotrauma,* **13**(5), pp. 233-244.

COQ, J.O., STRATA, F., RUSSIER, M., SAFADI, F.F., MERZENICH, M.M., BYL, N.N. and BARBE, M.F., 2008. Impact of neonatal asphyxia and hind limb immobilization on musculoskeletal tissues and S1 map organization: implications for cerebral palsy. *Experimental neurology,* **210**(1), pp. 95-108.

CORBETT-DETIG, J., HABAS, P.A., SCOTT, J.A., KIM, K., RAJAGOPALAN, V., MCQUILLEN, P.S., BARKOVICH, A.J., GLENN, O.A. and STUDHOLME, C., 2011. 3D global and regional patterns of human fetal subplate growth determined in utero. *Brain structure & function,* **215**(3-4), pp. 255-263.

COSOLO, W.C., MARTINELLO, P., LOUIS, W.J. and CHRISTOPHIDIS, N., 1989. Blood-brain barrier disruption using mannitol: time course and electron microscopy studies. *The American Journal of Physiology,* **256**(2 Pt 2), pp. R443-7.

COUTELIER, M., ANDRIES, S., GHARIANI, S., DAN, B., DUYCKAERTS, C., VAN RIJCKEVORSEL, K., RAFTOPOULOS, C., DECONINCK, N., SONDEREGGER, P., SCARAVILLI, F., VIKKULA, M. and GODFRAIND, C., 2008. Neuroserpin mutation causes electrical status epilepticus of slow-wave sleep. *Neurology,* **71**(1), pp. 64-66.

COWAN, F., RUTHERFORD, M., GROENENDAAL, F., EKEN, P., MERCURI, E., BYDDER, G.M., MEINERS, L.C., DUBOWITZ, L.M. and DE VRIES, L.S., 2003. Origin and timing of brain lesions in term infants with neonatal encephalopathy. *The Lancet,* **361**(9359), pp. 736-742.

CRAIG, A., LING LUO, N., BEARDSLEY, D.J., WINGATE-PEARSE, N., WALKER, D.W., HOHIMER, A.R. and BACK, S.A., 2003. Quantitative analysis of perinatal rodent oligodendrocyte lineage progression and its correlation with human. *Experimental neurology,* **181**(2), pp. 231-240.

CRAWFORD, M.A. and SINCLAIR, A.J., 1971. Nutritional influences in the evolution of mammalian brain. In: lipids, malnutrition & the developing brain. *Ciba Foundation symposium,* , pp. 267-292.

CRAWLEY, J.N., BELKNAP, J.K., COLLINS, A., CRABBE, J.C., FRANKEL, W., HENDERSON, N., HITZEMANN, R.J., MAXSON, S.C., MINER, L.L. and SILVA, A.J., 1997. Behavioral phenotypes of inbred mouse strains: implications and recommendations for molecular studies. *Psychopharmacology,* **132**(2), pp. 107-124.

CRUTCHLEY, D.J., MCPHEE, G.V., TERRIS, M.F. and CANOSSA-TERRIS, M.A., 1989. Levels of three hemostatic factors in relation to serum lipids. Monocyte procoagulant activity, tissue plasminogen activator, and type-1 plasminogen activator inhibitor. *Arteriosclerosis (Dallas, Tex.),* **9**(6), pp. 934-939.

D'HOOGE, R. and DE DEYN, P.P., 2001. Applications of the Morris water maze in the study of learning and memory. *Brain Research Reviews,* **36**(1), pp. 60-90.

DAADI, M.M., LEE, S.H., ARAC, A., GRUETER, B.A., BHATNAGAR, R., MAAG, A.L., SCHAAR, B., MALENKA, R.C., PALMER, T.D. and STEINBERG, G.K., 2009. Functional engraftment of the medial ganglionic eminence cells in experimental stroke model. *Cell transplantation,* **18**(7), pp. 815-826.

DAADI, M.M., LI, Z., ARAC, A., GRUETER, B.A., SOFILOS, M., MALENKA, R.C., WU, J.C. and STEINBERG, G.K., 2009. Molecular and magnetic resonance imaging of human embryonic stem cell-derived neural stem cell grafts in ischemic rat brain. *Molecular therapy : the journal of the American Society of Gene Therapy,* **17**(7), pp. 1282-1291.

DALITZ, P., HARDING, R., REES, S.M. and COCK, M.L., 2003. Prolonged reductions in placental blood flow and cerebral oxygen delivery in preterm fetal sheep exposed to endotoxin: possible factors in white matter injury after acute infection. *Journal of the Society for Gynecologic Investigation,* **10**(5), pp. 283-290.

D'AMELIO, M., CAVALLUCCI, V., CECCONI, F., 2010. Neuronal caspase-3 signaling: not only cell death. *Cell death and differentiation.*, **17**(7), 1104.

DAMMANN, O. and LEVITON, A., 2014. Intermittent or sustained systemic inflammation and the preterm brain. *Pediatric research,* **75**(3), pp. 376-380.

DAMMANN, O. and O'SHEA, T.M., 2008. Cytokines and perinatal brain damage. *Clinics in perinatology,* **35**(4), pp. 643-63, v.

DANEMAN, A., EPELMAN, M., BLASER, S. and JARRIN, J.R., 2006. Imaging of the brain in full-term neonates: does sonography still play a role? *Pediatric radiology,* **36**(7), pp. 636-646.

DANYSZ, W. and PARSONS, C.G., 1998. Glycine and N-methyl-D-aspartate receptors: physiological significance and possible therapeutic applications. *Pharmacological reviews,* **50**(4), pp. 597-664.

DAVAL, J.L., POURIE, G., GROJEAN, S., LIEVRE, V., STRAZIELLE, C., BLAISE, S. and VERT, P., 2004. Neonatal hypoxia triggers transient apoptosis followed by neurogenesis in the rat CA1 hippocampus. *Pediatric research,* **55**(4), pp. 561-567.

DAVAL, J.L. and VERT, P., 2004. Apoptosis and neurogenesis after transient hypoxia in the developing rat brain. *Seminars in perinatology,* **28**(4), pp. 257-263.

DAVIES, M.J., MIRANDA, E., ROUSSEL, B.D., KAUFMAN, R.J., MARCINIAK, S.J. and LOMAS, D.A., 2009. Neuroserpin polymers activate NF-kappaB by a calcium signaling pathway that is independent of the unfolded protein response. *The Journal of biological chemistry,* **284**(27), pp. 18202-18209.

DAVIS, R.L. and COLLINS, G.H., 2011. 48 Familial Encephalopathy with Neuroserpin Inclusion Bodies. *Neurodegeneration: The Molecular Pathology of Dementia and Movement Disorders,* , pp. 456.

DAVIS, R.L., HOLOHAN, P.D., SHRIMPTON, A.E., TATUM, A.H., DAUCHER, J., COLLINS, G.H., TODD, R., BRADSHAW, C., KENT, P. and FEIGLIN, D., 1999. Familial encephalopathy with neuroserpin inclusion bodies. *The American journal of pathology,* **155**(6), pp. 1901-1913.

DAVIS, R.L., SHRIMPTON, A.E., CARRELL, R.W., LOMAS, D.A., GERHARD, L., BAUMANN, B., LAWRENCE, D.A., YEPES, M., KIM, T.S. and GHETTI, B., 2002. Association between conformational mutations in neuroserpin and onset and severity of dementia. *The Lancet,* **359**(9325), pp. 2242-2247.

DAWSON, V.L., DAWSON, T.M., LONDON, E.D., BREDT, D.S., SNYDER, S.H., 1991. Nitric oxide mediates glutamate neurotoxicity in primary cortical cultures. *Proceedings of the National Academy of Sciences.,* **88**(14), 6368-71.

DE CARLOS, J.A. and O'LEARY, D.D., 1992. Growth and targeting of subplate axons and establishment of major cortical pathways. *The Journal of neuroscience : the official journal of the Society for Neuroscience,* **12**(4), pp. 1194-1211.

DE CARLOS, J.A., LOPEZ-MASCARAQUE, L., VALVERDE, F.,1996. Dynamics of cell migration from the lateral ganglionic eminence in the rat. *Journal of Neuroscience.,* **16**(19), 6146-56.

DE HAAN, H.H., GUNN, A.J. and GLUCKMAN, P.D., 1997. Fetal heart rate changes do not reflect cardiovascular deterioration during brief repeated umbilical cord occlusions in near-term fetal lambs. *American Journal of Obstetrics and Gynecology,* **176**(1 Pt 1), pp. 8-17.

DE HAAN, H.H., GUNN, A.J., WILLIAMS, C.E. and GLUCKMAN, P.D., 1997. Brief repeated umbilical cord occlusions cause sustained cytotoxic cerebral edema and focal infarcts in near-term fetal lambs. *Pediatric research,* **41**(1), pp. 96-104.

DE HAAN, H.H., GUNN, A.J., WILLIAMS, C.E., HEYMANN, M.A. and GLUCKMAN, P.D., 1997. Magnesium sulfate therapy during asphyxia in near-term fetal lambs does not compromise the fetus but does not reduce cerebral injury. *American Journal of Obstetrics and Gynecology,* **176**(1 Pt 1), pp. 18-27.

DE SOUZA, S.W. and RICHARDS, B., 1978. Neurological sequelae in newborn babies after perinatal asphyxia. *Archives of Disease in Childhood,* **53**(7), pp. 564-569.

DE TORRES, C., MUNELL, F., FERRER, I., REVENTÓS, J. and MACAYA, A., 1997. Identification of necrotic cell death by the TUNEL assay in the hypoxic-ischemic neonatal rat brain. *Neuroscience letters,* **230**(1), pp. 1-4.

DE VRIES, L.S. and GROENENDAAL, F., 2010. Patterns of neonatal hypoxic-ischaemic brain injury. *Neuroradiology,* **52**(6), pp. 555-566.

DEAN, J.M., SHI, Z., FLEISS, B., GUNN, K.C., GROENENDAAL, F., VAN BEL, F., DERRICK, M., JUUL, S.E., TAN, S., GRESSENS, P., MALLARD, C., BENNET, L. and GUNN, A.J., 2015. A Critical Review of Models of Perinatal Infection. *Developmental neuroscience,* **37**(4-5), pp. 289-304.

DEAN, J.M., VAN DE LOOIJ, Y., SIZONENKO, S.V., LODYGENSKY, G.A., LAZEYRAS, F., BOLOURI, H., KJELLMER, I., HUPPI, P.S., HAGBERG, H. and MALLARD, C., 2011. Delayed cortical impairment following lipopolysaccharide exposure in preterm fetal sheep. *Annals of Neurology,* **70**(5), pp. 846-856.

DEAN, N. and PELHAM, H.R., 1990. Recycling of proteins from the Golgi compartment to the ER in yeast. *The Journal of cell biology,* **111**(2), pp. 369-377.

DEBILLON, T., GRAS-LEGUEN, C., LEROY, S., CAILLON, J., ROZE, J.C. and GRESSENS, P., 2003. Patterns of cerebral inflammatory response in a rabbit model of intrauterine infection-mediated brain lesion. *Brain research.Developmental brain research,* **145**(1), pp. 39-48.

DECKER, M., HUE, G., CAUDLE, W., MILLER, G., KEATING, G. and RYE, D., 2003. Episodic neonatal hypoxia evokes executive dysfunction and regionally specific alterations in markers of dopamine signaling. *Neuroscience,* **117**(2), pp. 417-425.

DECKER, M.J., JONES, K.A., SOLOMON, I.G., KEATING, G.L. and RYE, D.B., 2005. Reduced extracellular dopamine and increased responsiveness to novelty: neurochemical and behavioral sequelae of intermittent hypoxia. *Sleep,* **28**(2), pp. 169-176.

DEL RIO, J.A., MARTINEZ, A., AULADELL, C. and SORIANO, E., 2000. Developmental history of the subplate and developing white matter in the murine neocortex. Neuronal organization and relationship with the main afferent systems at embryonic and perinatal stages. *Cerebral cortex (New York, N.Y.: 1991),* **10**(8), pp. 784-801.

DEL RIO, J.A., SORIANO, E. and FERRER, I., 1992. Development of GABA-immunoreactivity in the neocortex of the mouse. *The Journal of comparative neurology,* **326**(4), pp. 501-526.

DELL'ANNA, E., GELOSO, M.C., MAGARELLI, M. and MOLINARI, M., 1996. Development of GABA and calcium binding proteins immunoreactivity in the rat hippocampus following neonatal anoxia. *Neuroscience letters,* **211**(2), pp. 93-96.

DELL'ANNA, M.E., GELOSO, M.C., DRAISCI, G. and LUTHMAN, J., 1995. Transient changes in Fos and GFAP immunoreactivity precede neuronal loss in the rat

hippocampus following neonatal anoxia. *Experimental neurology,* **131**(1), pp. 144-156.

DELL'ANNA, M.E., LUTHMAN, J., LINDQVIST, E. and OLSON, L., 1993. Development of monoamine systems after neonatal anoxia in rats. *Brain research bulletin,* **32**(2), pp. 159-170.

DELL'ANNA, M., CALZOLARI, S., MOLINARI, M., IUVONE, L. and CALIMICI, R., 1991. Neonatal anoxia induces transitory hyperactivity, permanent spatial memory deficits and CA1 cell density reduction in developing rats. *Behavioural brain research,* **45**(2), pp. 125-134.

DEMAREST, T.G., SCHUH, R.A., WAITE, E.L., WADDELL, J., MCKENNA, M.C. and FISKUM, G., 2016. Sex dependent alterations in mitochondrial electron transport chain proteins following neonatal rat cerebral hypoxic-ischemia. *Journal of Bioenergetics and Biomembranes,* .

DEMAREST, T.G., WAITE, E.L., KRISTIAN, T., PUCHE, A.C., WADDELL, J., MCKENNA, M.C. and FISKUM, G., 2016. Sex-dependent mitophagy and neuronal death following rat neonatal hypoxia-ischemia. *Neuroscience,* **335**, pp. 103-113.

DEMERS, E.J., MCPHERSON, R.J. and JUUL, S.E., 2005. Erythropoietin protects dopaminergic neurons and improves neurobehavioral outcomes in juvenile rats after neonatal hypoxia-ischemia. *Pediatric research,* **58**(2), pp. 297-301.

DENG, W., ROSENBERG, P.A., VOLPE, J.J. and JENSEN, F.E., 2003. Calcium-permeable AMPA/kainate receptors mediate toxicity and preconditioning by oxygen-glucose deprivation in oligodendrocyte precursors. *Proceedings of the National Academy of Sciences of the United States of America,* **100**(11), pp. 6801-6806.

DENG, Y.Y., LU, J., LING, E.A. and KAUR, C., 2009. Monocyte chemoattractant protein-1 (MCP-1) produced via NF-kappaB signaling pathway mediates migration of amoeboid microglia in the periventricular white matter in hypoxic neonatal rats. *Glia,* **57**(6), pp. 604-621.

DEPARTMENT OF WORK AND PENSIONS, 2013-last update, Fulfilling Potential: Building a deeper understanding of disability in the UK today. Available: https://www.gov.uk/government/uploads/system/uploads/attachment_data/file/320509/building-understanding-main-report.pdf [29/07, 2016].

DEPARTMENT OF WORK AND PENSIONS, 2012-last update, Family Resources Survey 2010/2011. Available: https://www.gov.uk/government/uploads/system/uploads/attachment_data/file/222839/frs_2010_11_report.pdf [29/07, 2016].

DERRICK, M., DROBYSHEVSKY, A., JI, X. and TAN, S., 2007. A model of cerebral palsy from fetal hypoxia-ischemia. *Stroke; a journal of cerebral circulation,* **38**(2 Suppl), pp. 731-735.

DERRICK, M., LUO, N.L., BREGMAN, J.C., JILLING, T., JI, X., FISHER, K., GLADSON, C.L., BEARDSLEY, D.J., MURDOCH, G., BACK, S.A. and TAN, S., 2004. Preterm fetal hypoxia-ischemia causes hypertonia and motor deficits in the neonatal rabbit: a model for human cerebral palsy? *The Journal of neuroscience : the official journal of the Society for Neuroscience,* **24**(1), pp. 24-34.

DESCLOUX, C., GINET, V., CLARKE, P.G., PUYAL, J. and TRUTTMANN, A.C., 2015. Neuronal death after perinatal cerebral hypoxia-ischemia: Focus on autophagy-mediated cell death. *International journal of developmental neuroscience : the official journal of the International Society for Developmental Neuroscience,* **45**, pp. 75-85.

DEVARAJ, S., SINGH, U. and JIALAL, I., 2009. The evolving role of C-reactive protein in atherothrombosis. *Clinical chemistry,* **55**(2), pp. 229-238.

DEVARAJ, S., XU, D.Y. and JIALAL, I., 2003. C-reactive protein increases plasminogen activator inhibitor-1 expression and activity in human aortic endothelial cells: implications for the metabolic syndrome and atherothrombosis. *Circulation,* **107**(3), pp. 398-404.

DIJKSTRA, S., GEISERT JR, E.E., GISPEN, W.H., BÄR, P.R. and JOOSTEN, E.A., 2000. Up-regulation of CD81 (target of the antiproliferative antibody; TAPA) by reactive microglia and astrocytes after spinal cord injury in the rat. *Journal of Comparative Neurology,* **428**(2), pp. 266-277.

DILENGE, M.E., MAJNEMER, A. and SHEVELL, M.I., 2001. Long-term developmental outcome of asphyxiated term neonates. *Journal of child neurology,* **16**(11), pp. 781-792.

DINGLEY, J., TOOLEY, J., LIU, X., SCULL-BROWN, E., ELSTAD, M., CHAKKARAPANI, E., SABIR, H. and THORESEN, M., 2014. Xenon ventilation during therapeutic hypothermia in neonatal encephalopathy: a feasibility study. *Pediatrics,* **133**(5), pp. 809-818.

DITELBERG, J.S., SHELDON, R.A., EPSTEIN, C.J. and FERRIERO, D.M., 1996. Brain injury after perinatal hypoxia-ischemia is exacerbated in copper/zinc superoxide dismutase transgenic mice. *Pediatric research,* **39**(2), pp. 204-208.

DITTMER, A. and DITTMER, J., 2006. Beta-actin is not a reliable loading control in Western blot analysis. *Electrophoresis,* **27**(14), pp. 2844-2845.

DOBBING, J., 1974. Human brain development and its vulnerability, *Mead Johnson Symposium on perinatal and developmental medicine* 1974, pp. 3-12.

DOCAGNE, F., NICOLE, O., MARTI, H.H., MACKENZIE, E.T., BUISSON, A. and VIVIEN, D., 1999. Transforming growth factor-beta1 as a regulator of the serpins/t-PA axis in cerebral ischemia. *FASEB journal : official publication of the Federation of American Societies for Experimental Biology,* **13**(11), pp. 1315-1324.

DOMMERGUES, M., PLAISANT, F., VERNEY, C. and GRESSENS, P., 2003. Early microglial activation following neonatal excitotoxic brain damage in mice: a potential target for neuroprotection. *Neuroscience,* **121**(3), pp. 619-628.

DOMMERGUES, M.A., PATKAI, J., RENAULD, J.C., EVRARD, P. and GRESSENS, P., 2000. Proinflammatory cytokines and interleukin-9 exacerbate excitotoxic lesions of the newborn murine neopallium. *Annals of Neurology,* **47**(1), pp. 54-63.

DORSETT, Y., and TUSCHL, T., 2004. siRNAs: applications in functional genomics and potential as therapeutics. *Nature reviews Drug discovery.*, **3**(4), 318.

DOUGLAS, R.J. and MARTIN, K.A., 2004. Neuronal circuits of the neocortex. *Annu.Rev.Neurosci.,* **27**, pp. 419-451.

DOUGLAS-ESCOBAR, M. and WEISS, M.D., 2015. Hypoxic-ischemic encephalopathy: a review for the clinician. *JAMA pediatrics,* **169**(4), pp. 397-403.

DRAG, M. and SALVESEN, G.S., 2010. Emerging principles in protease-based drug discovery. *Nature reviews Drug discovery,* **9**(9), pp. 690.

DREIER, J.P., EBERT, N., PRILLER, J., MEGOW, D., LINDAUER, U., KLEE, R., REUTER, U., IMAI, Y., EINHÄUPL, K.M. and VICTOROV, I., 2000. Products of hemolysis in the subarachnoid space inducing spreading ischemia in the cortex and focal necrosis in rats: a model for delayed ischemic neurological deficits after subarachnoid hemorrhage? *Journal of neurosurgery,* **93**(4), pp. 658-666.

DROBYSHEVSKY, A., DERRICK, M., WYRWICZ, A.M., JI, X., ENGLOF, I., ULLMAN, L.M., ZELAYA, M.E., NORTHINGTON, F.J. and TAN, S., 2007. White matter injury correlates with hypertonia in an animal model of cerebral palsy. *Journal of Cerebral Blood Flow & Metabolism,* **27**(2), pp. 270-281.

DROBYSHEVSKY, A., DERRICK, M., PRASAD, P.V., JI, X., ENGLOF, I. and TAN, S., 2007. Fetal brain magnetic resonance imaging response acutely to hypoxia-ischemia predicts postnatal outcome. *Annals of Neurology,* **61**(4), pp. 307-314.

DROBYSHEVSKY, A., SONG, S.K., GAMKRELIDZE, G., WYRWICZ, A.M., DERRICK, M., MENG, F., LI, L., JI, X., TROMMER, B., BEARDSLEY, D.J., LUO, N.L., BACK, S.A. and TAN, S., 2005. Developmental changes in diffusion anisotropy coincide with immature oligodendrocyte progression and maturation of compound action potential. *The Journal of neuroscience : the official journal of the Society for Neuroscience,* **25**(25), pp. 5988-5997.

DU, L., HICKEY, R.W., BAYIR, H., WATKINS, S.C., TYURIN, V.A., GUO, F., KOCHANEK, P.M., JENKINS, L.W., REN, J., GIBSON, G., CHU, C.T., KAGAN, V.E. and CLARK, R.S., 2009. Starving neurons show sex difference in autophagy. *The Journal of biological chemistry,* **284**(4), pp. 2383-2396.

D'UDINE, B. and ALLEVA, E., 1988. The Acomys cahirinus (spiny mouse) as a new model for biological and neurobehavioural studies. *Polish journal of pharmacology and pharmacy,* **40**(5), pp. 525-534.

DUNCAN, J.R., COCK, M.L., SCHEERLINCK, J.P., WESTCOTT, K.T., MCLEAN, C., HARDING, R. and REES, S.M., 2002. White matter injury after repeated endotoxin exposure in the preterm ovine fetus. *Pediatric research,* **52**(6), pp. 941-949.

DUPONT, E., HANGANU, I.L., KILB, W., HIRSCH, S. and LUHMANN, H.J., 2006. Rapid developmental switch in the mechanisms driving early cortical columnar networks. *Nature,* **439**(7072), pp. 79-83.

DUTTA, U.R., HANSMANN, I. and SCHLOTE, D., 2015. Molecular cytogenetic characterization of a familial pericentric inversion 3 associated with short stature. *European journal of medical genetics,* **58**(3), pp. 154-159.

DWYER, B.E., NISHIMURA, R.N. and BROWN, I.R., 1989. Synthesis of the major inducible heat shock protein in rat hippocampus after neonatal hypoxia-ischemia. *Experimental neurology,* **104**(1), pp. 28-31.

DZHALA, V.I., STALEY, K.J., 2003. Transition from interictal to ictal activity in limbic networks in vitro. *Journal of Neuroscience.,* **23**(21), 7873-80.

DZIEGIELEWSKA, K.M., DAIKUHARA, Y., OHNISHI, T., WAITE, M.P.E., EK, J., HABGOOD, M.D., LANE, M.A., POTTER, A. and SAUNDERS, N.R., 2000. Fetuin in the developing neocortex of the rat: distribution and origin. *Journal of Comparative Neurology,* **423**(3), pp. 373-388.

EAST, C.E., DUNSTER, K.R. and COLDITZ, P.B., 1998. Fetal oxygen saturation and uterine contractions during labor. *American Journal of Perinatology,* **15**(6), pp. 345-349.

EASTWOOD, S.L. and HARRISON, P.J., 2005. Interstitial white matter neuron density in the dorsolateral prefrontal cortex and parahippocampal gyrus in schizophrenia. *Schizophrenia research,* **79**(2-3), pp. 181-188.

EASTWOOD, S.L. and HARRISON, P.J., 2003. Interstitial white matter neurons express less reelin and are abnormally distributed in schizophrenia: towards an integration of molecular and morphologic aspects of the neurodevelopmental hypothesis. *Molecular psychiatry,* **8**(9), pp. 769, 821-31.

EDWARDS, A. and MEHMET, H., 1996. Apoptosis in perinatal hypoxic-ischaemic cerebral damage. *Neuropathology and applied neurobiology,* **22**(6), pp. 494-498.

EDWARDS, A., YUE, X., COX, P., HOPE, P., AZZOPARDI, D., SQUIER, M. and MEHMET, H., 1997. Apoptosis in the brains of infants suffering intrauterine cerebral injury. *Pediatric research,* **42**(5), pp. 684-689.

EHRENFRIED, J.A., EVERS, B.M., CHU, K.U., TOWNSEND, C.M.,JR and THOMPSON, J.C., 1996. Caloric restriction increases the expression of heat shock protein in the gut. *Annals of Surgery,* **223**(5), pp. 592-7; discussion 597-9.

EICHER, D.J., WAGNER, C.L., KATIKANENI, L.P., HULSEY, T.C., BASS, W.T., KAUFMAN, D.A., HORGAN, M.J., LANGUANI, S., BHATIA, J.J. and GIVELICHIAN, L.M., 2005. Moderate hypothermia in neonatal encephalopathy: efficacy outcomes. *Pediatric neurology,* **32**(1), pp. 11-17.

EINHAUER, A. and JUNGBAUER, A., 2001. The FLAG™ peptide, a versatile fusion tag for the purification of recombinant proteins. *Journal of Biochemical and Biophysical Methods,* **49**(1-3), pp. 455-465.

EK, C.J., D'ANGELO, B., BABURAMANI, A.A., LEHNER, C., LEVERIN, A., SMITH, P.L., NILSSON, H., SVEDIN, P., HAGBERG, H. and MALLARD, C., 2015. Brain barrier properties and cerebral blood flow in neonatal mice exposed to cerebral hypoxia-ischemia. *Journal of Cerebral Blood Flow & Metabolism,* **35**(5), pp. 818-827.

EK, C.J., DZIEGIELEWSKA, K.M., STOLP, H. and SAUNDERS, N.R., 2006. Functional effectiveness of the blood-brain barrier to small water-soluble molecules in developing and adult opossum (Monodelphis domestica). *Journal of Comparative Neurology,* **496**(1), pp. 13-26.

EK, C.J., HABGOOD, M.D., DZIEGIELEWSKA, K.M. and SAUNDERS, N.R., 2003. Structural characteristics and barrier properties of the choroid plexuses in developing brain of the opossum (Monodelphis domestica). *Journal of Comparative Neurology,* **460**(4), pp. 451-464.

EKEN, P., JANSEN, G.H., GROENENDAAL, F., RADEMAKER, K.J. and DE VRIES, L.S., 1994. Intracranial lesions in the fullterm infant with hypoxic ischaemic encephalopathy: ultrasound and autopsy correlation. *Neuropediatrics,* **25**(6), pp. 301-307.

EKLIND, S., MALLARD, C., ARVIDSSON, P. and HAGBERG, H., 2005. Lipopolysaccharide induces both a primary and a secondary phase of sensitization in the developing rat brain. *Pediatric research,* **58**(1), pp. 112-116.

EKLIND, S., MALLARD, C., LEVERIN, A.L., GILLAND, E., BLOMGREN, K., MATTSBY-BALTZER, I. and HAGBERG, H., 2001. Bacterial endotoxin sensitizes the immature brain to hypoxic--ischaemic injury. *The European journal of neuroscience,* **13**(6), pp. 1101-1106.

EKLÖF, B. and SIESJÖ, B.K., 1973. Cerebral blood flow in ischemia caused by carotid artery ligation in the rat. *Acta Physiologica Scandinavica,* **87**(1), pp. 69-77.

EL-KHOURY, N., BRAUN, A., HU, F., PANDEY, M., NEDERGAARD, M., LAGAMMA, E.F. and BALLABH, P., 2006. Astrocyte end-feet in germinal matrix, cerebral cortex, and white matter in developing infants. *Pediatric research,* **59**(5), pp. 673-679.

ELLGAARD, L. and HELENIUS, A., 2003. Quality control in the endoplasmic reticulum. *Nature reviews Molecular cell biology,* **4**(3), pp. 181.

ELLISDON, A.M., ZHANG, Q., HENSTRIDGE, M.A., JOHNSON, T.K., WARR, C.G., LAW, R.H. and WHISSTOCK, J.C., 2014. High resolution structure of cleaved Serpin 42 Da from Drosophila melanogaster. *BMC structural biology,* **14**(1), pp. 1.

ELSTON, G.N., 2003. Cortex, cognition and the cell: new insights into the pyramidal neuron and prefrontal function. *Cerebral cortex (New York, N.Y.: 1991),* **13**(11), pp. 1124-1138.

EMERY, J.A., ROPER, S.N., ROJIANI, A.M., 1997. White matter neuronal heterotopia in temporal lobe epilepsy: a morphometric and immunohistochemical study. *Journal of Neuropathology & Experimental Neurology.,* **56**(12), 1276-82.

ENG, L., VANDERHAEGHEN, J., BIGNAMI, A. and GERSTL, B., 1971. An acidic protein isolated from fibrous astrocytes. *Brain research,* **28**(2), pp. 351-354.

ENG, L.F., 1985. Glial fibrillary acidic protein (GFAP): the major protein of glial intermediate filaments in differentiated astrocytes. *Journal of neuroimmunology,* **8**, pp. 203-214.

ENG, L.F., GHIRNIKAR, R.S. and LEE, Y.L., 2000. Glial fibrillary acidic protein: GFAP-thirty-one years (1969–2000). *Neurochemical research,* **25**(9-10), pp. 1439-1451.

ENG, L., GERSTL, B. and VANDERHAEGHEN, J., 1970. A study of proteins in old multiple sclerosis plaques. *Trans Am Soc Neurochem,* **1**(42),.

ENNEN, C.S., HUISMAN, T.A., SAVAGE, W.J., NORTHINGTON, F.J., JENNINGS, J.M., EVERETT, A.D., GRAHAN, E.M., 2001. Glial fibrillary acidic protein as a biomarker for neonatal hypoxic-ischemic encephalopathy treated with whole-body cooling. *American journal of obstetrics and gynecology.,* **205**(3), 251-e1.

ENVIGO INTERNATIONAL, L., 2018-last update, NIH Swiss outbred mice. Available: https://www.envigo.com/products-services/research-models-services/models/research-models/mice/outbred/nih-swiss-outbred-mice/ [08/10, 2018].

ENZO LIFE SCIENCES, I., 2018-last update, Oxidative Stress: Comprehensive Tools for Qualifying Cellular Responses to Oxidative Damage**Comprehensive Tools for Quantifying Cellular Responses to Oxidative Damage Comprehensive Tools for Quantifying Cellular Responses to Oxidative Damage**. Available: http://www.enzolifesciences.com/platforms/cellular-analysis/oxidative-stress/ [08/07, 2018].

EPSTEIN, H.T., 1986. Stages in human brain development. *Developmental Brain Research,* **30**(1), pp. 114-119.

ESAKOFF, T.F., KILPATRICK, S.J. and PALANISAMY, A., 2015. Fetal and neonatal neurologic injury. In: D.H. CHESTNUT, C.A. WONG, L.C. TSEN, W.D.N. KEE, Y. BEILIN and J. MHYRE, eds, *Chestnut's Obstetric Anesthesia: Principles and Practice E-Book.* Fifth edn. Philadelphia, United States of America: Elsevier Health Sciences., pp. 192-192-296.

ESKIOCAK, S., TUTUNCULER, F., BASARAN, U.N., TASKIRAN, A. and CAKIR, E., 2007. The effect of melatonin on protein oxidation and nitric oxide in the brain tissue of hypoxic neonatal rats. *Brain & development,* **29**(1), pp. 19-24.

ESTRADA, C. and DEFELIPE, J., 1998. Nitric oxide-producing neurons in the neocortex: morphological and functional relationship with intraparenchymal microvasculature. *Cerebral cortex (New York, N.Y.: 1991),* **8**(3), pp. 193-203.

EVANS, D.J., LEVENE, M.I. and TSAKMAKIS, M., 2007. Anticonvulsants for preventing mortality and morbidity in full term newborns with perinatal asphyxia. *The Cochrane database of systematic reviews,* **(3)**(3), pp. CD001240.

EZQUER, M.E., VALDEZ, S.R. and SELTZER, A.M., 2006. Inflammatory responses of the substantia nigra after acute hypoxia in neonatal rats. *Experimental neurology,* **197**(2), pp. 391-398.

EZQUER, M.E., VALDEZ, S.R., SELTZER, A.M. and JAHN, G.A., 2008. Advancement of reproductive senescence and changes in the early expression of estrogen, progesterone and micro-opioid receptors induced by neonatal hypoxia in the female rat. *Brain research,* **1214**, pp. 73-83.

FAGERBERG, L., HALLSTROM, B.M., OKSVOLD, P., KAMPF, C., DJUREINOVIC, D., ODEBERG, J., HABUKA, M., TAHMASEBPOOR, S., DANIELSSON, A., EDLUND, K., ASPLUND, A., SJOSTEDT, E., LUNDBERG, E., SZIGYARTO, C.A., SKOGS, M., TAKANEN, J.O., BERLING, H., TEGEL, H., MULDER, J., NILSSON, P., SCHWENK, J.M., LINDSKOG, C., DANIELSSON, F., MARDINOGLU, A., SIVERTSSON, A., VON FEILITZEN, K., FORSBERG, M., ZWAHLEN, M., OLSSON, I., NAVANI, S., HUSS, M., NIELSEN, J., PONTEN, F. and UHLEN, M., 2014. Analysis of the human tissue-specific expression by genome-wide integration of transcriptomics and antibody-based proteomics. *Molecular & cellular proteomics : MCP,* **13**(2), pp. 397-406.

FAHN, S., DAVIS, J.N. and ROWLAND, L.P., 1979. *Cerebral hypoxia and its consequences.* Raven Press.

FAILOR, S., NGUYEN, V., DARCY, D.P., CANG, J., WENDLAND, M.F., STRYKER, M.P. and MCQUILLEN, P.S., 2010. Neonatal cerebral hypoxia-ischemia impairs plasticity in rat visual cortex. *The Journal of neuroscience : the official journal of the Society for Neuroscience,* **30**(1), pp. 81-92.

FAN, X., HEIJNEN, C.J., VAN DER KOOIJ, MICHAEL A, GROENENDAAL, F. and VAN BEL, F., 2011. Beneficial effect of erythropoietin on sensorimotor function and white matter after hypoxia-ischemia in neonatal mice. *Pediatric research,* **69**(1), pp. 56.

FAN, X., KAVELAARS, A., HEIJNEN, C.J., GROENENDAAL, F. and VAN BEL, F., 2010. Pharmacological neuroprotection after perinatal hypoxic-ischemic brain injury. *Current neuropharmacology,* **8**(4), pp. 324-334.

FATEMI, A., WILSON, M.A. and JOHNSTON, M.V., 2009. Hypoxic-ischemic encephalopathy in the term infant. *Clinics in perinatology,* **36**(4), pp. 835-58, vii.

FATHALI, N., KHATIBI, N.H., OSTROWSKI, R.P. and ZHANG, J.H., 2011. The evolving landscape of neuroinflammation after neonatal hypoxia-ischemia. *Intracerebral Hemorrhage Research.* Springer, pp. 93-100.

FATHALI, N., LEKIC, T., ZHANG, J.H. and TANG, J., 2010. Long-term evaluation of granulocyte-colony stimulating factor on hypoxic-ischemic brain damage in infant rats. *Intensive care medicine,* **36**(9), pp. 1602-1608.

FATHALI, N., OSTROWSKI, R.P., HASEGAWA, Y., LEKIC, T., TANG, J. and ZHANG, J.H., 2013. Splenic immune cells in experimental neonatal hypoxia–ischemia. *Translational stroke research,* **4**(2), pp. 208-219.

FAVRAIS, G., VAN DE LOOIJ, Y., FLEISS, B., RAMANANTSOA, N., BONNIN, P., STOLTENBURG-DIDINGER, G., LACAUD, A., SALIBA, E., DAMMANN, O., GALLEGO, J., SIZONENKO, S., HAGBERG, H., LELIEVRE, V. and GRESSENS, P., 2011. Systemic inflammation disrupts the developmental program of white matter. *Annals of Neurology,* **70**(4), pp. 550-565.

FEDER, M.E. and HOFMANN, G.E., 1999. Heat-shock proteins, molecular chaperones, and the stress response: evolutionary and ecological physiology. *Annual Review of Physiology,* **61**(1), pp. 243-282.

FELDERHOFF-MUESER, U., SIFRINGER, M., PESDITSCHEK, S., KUCKUCK, H., MOYSICH, A., BITTIGAU, P. and IKONOMIDOU, C., 2002. Pathways leading to apoptotic neurodegeneration following trauma to the developing rat brain. *Neurobiology of disease,* **11**(2), pp. 231-245.

FELLMAN, V., HELLSTRÖM-WESTAS, L., NORMAN, M., WESTGREN, M., KÄLLÉN, K., LAGERCRANTZ, H., MARSÁL, K., SERENIUS, F., WENNERGREN, M. and EXPRESS GROUP, 2010. One-year survival of extremely preterm infants after active perinatal care in Sweden. *Obstetric Anesthesia Digest,* **30**(1), pp. 22-23.

FERNANDEZ-ARJONA, M.D., GRONDONA, J.M., GRANADOS-DURAN, P., FERNANDEZ-LLEBREZ, P., LOPEZ-AVALOS, M.D., 2017. Microglia morphological categorization in a rat model of neuroinflammation by hierarchical cluster and principal components analysis. *Frontiers in cellular neuroscience.*, **11**, 235.

FERRARI, D.C., NESIC, O. and PEREZ-POLO, J.R., 2010. Perspectives on neonatal hypoxia/ischemia-induced edema formation. *Neurochemical research,* **35**(12), pp. 1957-1965.

FERRAZZANO, P., CHANANA, V., ULUC, K., FIDAN, E., AKTURE, E., KINTNER, D.B., CENGIZ, P., SUN, D., 2013. Age-dependent microglial activation in immature brains after hypoxia-ischemia. *CNS & Neurological Disorders-Drug Targets (Formerly Current Drug Targets-CNS & Neurological Disorders).,* **12**(3), 338-49.

FERRIERO, D.M., 2004. Neonatal brain injury. *New England Journal of Medicine,* **351**(19), pp. 1985-1995.

FERRIERO, D.M., HOLTZMAN, D.M., BLACK, S.M. and SHELDON, R.A., 1996. Neonatal mice lacking neuronal nitric oxide synthase are less vulnerable to hypoxic–ischemic injury. *Neurobiology of disease,* **3**(1), pp. 64-71.

FERRIERO, D.M., SOBERANO, H.Q., SIMON, R.P. and SHARP, F.R., 1990. Hypoxia—ischemia induces heat shock protein-like (HSP72) immunoreactivity in neonatal rat brain. *Developmental Brain Research,* **53**(1), pp. 145-150.

FERRIERO, D.M., 2001. Oxidant mechanisms in neonatal hypoxia-ischemia. *Developmental neuroscience,* **23**(3), pp. 198-202.

FINER, N., ROBERTSON, C., RICHARDS, R., PINNELL, L. and PETERS, K., 1981. Hypoxic-ischemic encephalopathy in term neonates: perinatal factors and outcome. *The Journal of pediatrics,* **98**(1), pp. 112-117.

FINER, N.N., ROBERTSON, C.M., PETERS, K.L. and COWARD, J.H., 1983. Factors affecting outcome in hypoxic-ischemic encephalopathy in term infants. *American Journal of Diseases of Children (1960),* **137**(1), pp. 21-25.

FINLAY, B.L., DARLINGTON, R.B. and NICASTRO, N., 2001. Developmental structure in brain evolution. *Behavioral and Brain Sciences,* **24**(2), pp. 263-278.

FINLAY, B.L. and DARLINGTON, R.B., 1995. Linked regularities in the development and evolution of mammalian brains. *Science (New York, N.Y.),* **268**(5217), pp. 1578-1584.

FINNEY, E.M., STONE, J.R. and SHATZ, C.J., 1998. Major glutamatergic projection from subplate into visual cortex during development. *The Journal of comparative neurology,* **398**(1), pp. 105-118.

FISCHER, R. and MAIER, O., 2015. Interrelation of oxidative stress and inflammation in neurodegenerative disease: role of TNF. *Oxidative medicine and cellular longevity,* **2015**, pp. 610813.

FLAVIN, M., ZHAO, G. and HO, L., 2000. Microglial tissue plasminogen activator (tPA) triggers neuronal apoptosis in vitro. *Glia,* **29**(4), pp. 347-354.

FLEISS, B. and GRESSENS, P., 2012. Tertiary mechanisms of brain damage: a new hope for treatment of cerebral palsy? *The Lancet.Neurology,* **11**(6), pp. 556-566.

FOLKERTH, R.D., 2005. Neuropathologic substrate of cerebral palsy. *Journal of child neurology,* **20**(12), pp. 940-949.

FONTAINE, D.A. and DAVIS, D.B., 2016. Attention to Background Strain Is Essential for Metabolic Research: C57BL/6 and the International Knockout Mouse Consortium. *Diabetes,* **65**(1), pp. 25-33.

FORDER, J.P. and TYMIANSKI, M., 2009. Postsynaptic mechanisms of excitotoxicity: Involvement of postsynaptic density proteins, radicals, and oxidant molecules. *Neuroscience,* **158**(1), pp. 293-300.

FOX, K., SCHLAGGAR, B.L., GLAZEWSKI, S. and O'LEARY, D.D., 1996. Glutamate receptor blockade at cortical synapses disrupts development of thalamocortical and columnar organization in somatosensory cortex. *Proceedings of the National Academy of Sciences of the United States of America,* **93**(11), pp. 5584-5589.

FRACKOWIAK, R.S., FRISTON, K.J., FRITH, C.D., DOLAN, R.J., PRICE, C.J., ZEKI, S., ASHBURNER, J.T. and PENNY, W.D., 2004. *Human brain function.* Academic press.

FRIAUF, E., MCCONNELL, S.K. and SHATZ, C.J., 1990. Functional synaptic circuits in the subplate during fetal and early postnatal development of cat visual cortex. *The Journal of neuroscience : the official journal of the Society for Neuroscience,* **10**(8), pp. 2601-2613.

FRIAUF, E. and SHATZ, C.J., 1991. Changing patterns of synaptic input to subplate and cortical plate during development of visual cortex. *Journal of neurophysiology,* **66**(6), pp. 2059-2071.

FRIEDLANDER, M.J. and TORRES-REVERON, J., 2009. The changing roles of neurons in the cortical subplate. *Frontiers in neuroanatomy,* **3**, pp. 15.

FRYMOYER, A., JUUL, S.E., MASSARO, A.N., BAMMLER, T.K., WU, Y.W., 2017. High-dose erythropoietin population pharmacokinetics in neonates with hypoxic–ischemic encephalopathy receiving hypothermia. *Pediatric research.*, **81**(6), 865.

FU, X., LI, Q., FENG, Z., MU, D., 2007. The roles of aquaporin-4 in brain edema following neonatal hypoxia ischemia and reoxygenation in a cultured rat astrocyte model. *Glia.*, **55**(9), 935-41.

FUJIHARA, M., MUROI, M., TANAMOTO, K., SUZUKI, T., AZUMA, H. and IKEDA, H., 2003. Molecular mechanisms of macrophage activation and deactivation by lipopolysaccharide: roles of the receptor complex. *Pharmacology & therapeutics,* **100**(2), pp. 171-194.

FUJIMORI, A., ITOH, K., GOTO, S., HIRAKAWA, H., WANG, B., KOKUBO, T., KITO, S., TSUKAMOTO, S. and FUSHIKI, S., 2014. Disruption of Aspm causes

microcephaly with abnormal neuronal differentiation. *Brain & development,* **36**(8), pp. 661-669.

FUJIMOTO, E., MIKI, A. and MIZOGUTI, H., 1989. Histochemical study of the differentiation of microglial cells in the developing human cerebral hemispheres. *Journal of anatomy,* **166**, pp. 253-264.

FUSTER, J.M., 2003. *Cortex and mind: Unifying cognition.* Oxford university press.

GALLICIOTTI, G. and SONDEREGGER, P., 2006. Neuroserpin. *Front Biosci,* **11**, pp. 33-45.

GAO, P., SULTAN, K.T., ZHANG, X.J. and SHI, S.H., 2013. Lineage-dependent circuit assembly in the neocortex. *Development (Cambridge, England),* **140**(13), pp. 2645-2655.

GARCIA-MARIN, V., BLAZQUEZ-LLORCA, L., RODRIGUEZ, J.R., GONZALEZ-SORIANO, J. and DEFELIPE, J., 2010. Differential distribution of neurons in the gyral white matter of the human cerebral cortex. *The Journal of comparative neurology,* **518**(23), pp. 4740-4759.

GARNIER, C., LAFITTE, D., JORGENSEN, T.J., JENSEN, O.N., BRIAND, C. and PEYROT, V., 2001. Phosphorylation and oligomerization states of native pig brain HSP90 studied by mass spectrometry. *European journal of biochemistry,* **268**(8), pp. 2402-2407.

GARNIER, Y., BERGER, R., ALM, S., VON DUERING, M.U., COUMANS, A.B., MICHETTI, F., BRUSCHETTINI, M., LITUANIA, M., HASAART, T.H. and GAZZOLO, D., 2006. Systemic endotoxin administration results in increased S100B protein blood levels and periventricular brain white matter injury in the preterm fetal sheep. *European journal of obstetrics, gynecology, and reproductive biology,* **124**(1), pp. 15-22.

GARNIER, Y., COUMANS, A., BERGER, R., JENSEN, A. and HASAART, T.H., 2001. Endotoxemia severely affects circulation during normoxia and asphyxia in immature fetal sheep. *Journal of the Society for Gynecologic Investigation,* **8**(3), pp. 134-142.

GASSMANN, M., GRENACHER, B., ROHDE, B. and VOGEL, J., 2009. Quantifying Western blots: pitfalls of densitometry. *Electrophoresis,* **30**(11), pp. 1845-1855.

GEHRMANN, J., BONNEKOH, P., MIYAZAWA, T., HOSSMANN, K.A., KREITZBERG, G.W., 1992. Immunocytochemical study of an early microglial activation in ischemia. *Journal of Cerebral Blood Flow & Metabolism.*, **12**(2), 257-69.

GELDERBLOM, M., NEUMANN, M., LUDEWIG, P., BERNREUTHER, C., KRASEMANN, S., ARUNACHALAM, P., GERLOFF, C., GLATZEL, M. and MAGNUS, T., 2013. Deficiency in serine protease inhibitor neuroserpin exacerbates

ischemic brain injury by increased postischemic inflammation. *PloS one,* **8**(5), pp. e63118.

GENSAT, O., 2018-last update. Available: http://www.gensat.org/imagenavigator.jsp?imageID=32798 [08/10, 2018].

GHORBANI, A., SADEGHNIA, H.R. and ASADPOUR, E., 2015. Mechanism of protective effect of lettuce against glucose/serum deprivation-induced neurotoxicity. *Nutritional Neuroscience,* **18**(3), pp. 103-109.

GHOSH, A., ANTONINI, A., MCCONNELL, S.K. and SHATZ, C.J., 1990. Requirement for subplate neurons in the formation of thalamocortical connections. *Nature,* **347**(6289), pp. 179-181.

GHOSH, A. and SHATZ, C.J., 1992. Involvement of subplate neurons in the formation of ocular dominance columns. *Science (New York, N.Y.),* **255**(5050), pp. 1441-1443.

GHOSH, A., SHATZ, C.J., 1992. Pathfinding and target selection by developing geniculocortical axons. *Journal of Neuroscience.,* **12**(1), 39-55.

GIAMPIETRO, C., LIONETTI, M.C., COSTANTINI, G., MUTTI, F., ZAPPERI, S. and LA PORTA, C.A., 2017. Cholesterol impairment contributes to neuroserpin aggregation. *Scientific reports,* **7**, pp. 43669.

GIL-IBANEZ, P., BELINCHON, M.M., MORTE, B., OBREGON, M.J., BERNAL, J., 2017. Is the intrinsic genomic activity of thyroxine relevant in vivo? Effects on gene expression in primary cerebrocortical and neuroblastoma cells. *Thyroid.*, **27**(8), 1092-8.

GILBERT, C. and KELLY, J., 1975. The projections of cells in different layers of the cat's visual cortex. *Journal of Comparative Neurology,* **163**(1), pp. 81-105.

GILBERT, C.D., 1983. Microcircuitry of the visual cortex. *Annual Review of Neuroscience,* **6**(1), pp. 217-247.

GILDA, J.E. and GOMES, A.V., 2015. Western blotting using in-gel protein labeling as a normalization control: stain-free technology. *Methods in molecular biology (Clifton, N.J.),* **1295**, pp. 381-391.

GILDA, J.E. and GOMES, A.V., 2013. Stain-Free total protein staining is a superior loading control to beta-actin for Western blots. *Analytical Biochemistry,* **440**(2), pp. 186-188.

GILLANI, Q.A., AKBAR, A., ALI, M. and IQBAL, F., 2015. Gender-specific effects of CGP 55845, GABAB receptor antagonist, on neuromuscular coordination, learning and memory formation in albino mouse following neonatal hypoxia–ischemia insult. *Neurological Sciences,* **36**(6), pp. 961-969.

GINET, V., PUYAL, J., MAGNIN, G., CLARKE, P.G. and TRUTTMANN, A.C., 2009. Limited role of the c-Jun N-terminal kinase pathway in a neonatal rat model of cerebral hypoxia–ischemia. *Journal of neurochemistry,* **108**(3), pp. 552-562.

GINET, V., PITTET, M.P., RUMMEL, C., OSTERHELD, M.C., MEULI, R., CLARKE, P.G., PUYAL, J. and TRUTTMANN, A.C., 2014. Dying neurons in thalamus of asphyxiated term newborns and rats are autophagic. *Annals of Neurology,* **76**(5), pp. 695-711.

GINET, V., PUYAL, J., CLARKE, P.G. and TRUTTMANN, A.C., 2009. Enhancement of autophagic flux after neonatal cerebral hypoxia-ischemia and its region-specific relationship to apoptotic mechanisms. *The American journal of pathology,* **175**(5), pp. 1962-1974.

GINET, V., PUYAL, J., RUMMEL, C., AUBRY, D., BRETON, C., CLOUX, A.J., MAJJIGAPU, S.R., SORDAT, B., VOGEL, P., BRUZZONE, S., NENCIONI, A., DUCHOSAL, M.A. and NAHIMANA, A., 2014. A critical role of autophagy in antileukemia/lymphoma effects of APO866, an inhibitor of NAD biosynthesis. *Autophagy,* **10**(4), pp. 603-617.

GIRARD, S., KADHIM, H., ROY, M., LAVOIE, K., BROCHU, M., LAROUCHE, A. and SÉBIRE, G., 2009. Role of perinatal inflammation in cerebral palsy. *Pediatric neurology,* **40**(3), pp. 168-174.

GIRARD, S., KADHIM, H., BEAUDET, N., SARRET, P. and SEBIRE, G., 2009. Developmental motor deficits induced by combined fetal exposure to lipopolysaccharide and early neonatal hypoxia/ischemia: a novel animal model for cerebral palsy in very premature infants. *Neuroscience,* **158**(2), pp. 673-682.

GIRARD, S., KADHIM, H., LAROUCHE, A., ROY, M., GOBEIL, F. and SEBIRE, G., 2008. Pro-inflammatory disequilibrium of the IL-1 beta/IL-1ra ratio in an experimental model of perinatal brain damages induced by lipopolysaccharide and hypoxia-ischemia. *Cytokine,* **43**(1), pp. 54-62.

GIRARD, S., SEBIRE, H., BROCHU, M.E., BRIOTA, S., SARRET, P. and SEBIRE, G., 2012. Postnatal administration of IL-1Ra exerts neuroprotective effects following perinatal inflammation and/or hypoxic-ischemic injuries. *Brain, behavior, and immunity,* **26**(8), pp. 1331-1339.

GITTINS, R. and HARRISON, P.J., 2004. Neuronal density, size and shape in the human anterior cingulate cortex: a comparison of Nissl and NeuN staining. *Brain research bulletin,* **63**(2), pp. 155-160.

GLASSMAN, R.B., 1987. An hypothesis about redundancy and reliability in the brains of higher species: analogies with genes, internal organs, and engineering systems. *Neuroscience and biobehavioral reviews,* **11**(3), pp. 275-285.

GLEES, P., 1955. *Neuroglia: morphology and function.* Thomas.

GLENN, O.A., LUDEMAN, N.A., BERMAN, J.I., WU, Y.W., LU, Y., BARTHA, A.I., VIGNERON, D.B., CHUNG, S.W., FERRIERO, D.M., BARKOVICH, A.J. and HENRY, R.G., 2007. Diffusion tensor MR imaging tractography of the pyramidal tracts correlates with clinical motor function in children with congenital hemiparesis. *AJNR.American journal of neuroradiology,* **28**(9), pp. 1796-1802.

GLUCKMAN, P.D., WYATT, J.S., AZZOPARDI, D., BALLARD, R., EDWARDS, A.D., FERRIERO, D.M., POLIN, R.A., ROBERTSON, C.M., THORESEN, M. and WHITELAW, A., 2005. Selective head cooling with mild systemic hypothermia after neonatal encephalopathy: multicentre randomised trial. *The Lancet,* **365**(9460), pp. 663-670.

GOLDBERG, M.P. and CHOI, D.W., 1993. Combined oxygen and glucose deprivation in cortical cell culture: calcium-dependent and calcium-independent mechanisms of neuronal injury. *The Journal of neuroscience : the official journal of the Society for Neuroscience,* **13**(8), pp. 3510-3524.

GOLDBERG, R.N., MOSCOSO, P., BAUER, C.R., BLOOM, F.L., CURLESS, R.G., BURKE, B. and BANCALARI, E., 1986. Use of barbiturate therapy in severe perinatal asphyxia: a randomized controlled trial. *The Journal of pediatrics,* **109**(5), pp. 851-856.

GONZALEZ, D.L., FUCHS, J.L., DROGE, M.H., 1993. Distribution of NMDA receptor binding in developing mouse spinal cord. *Neuroscience letters.,* **151**(2), 134-137.

GONZALEZ, F.F. and MILLER, S.P., 2006. Does perinatal asphyxia impair cognitive function without cerebral palsy? *Archives of disease in childhood.Fetal and neonatal edition,* **91**(6), pp. F454-9.

GORDON, S.R., MAUTE, R.L., DULKEN, B.W., HUTTER, G., GEORGE, B.M., MCCRACKEN, M.N., GUPTA, R., TSAI, J.M., SINHA, R., COREY, D., RING, A.M., CONNOLLY, A.J. and WEISSMAN, I.L., 2017. PD-1 expression by tumour-associated macrophages inhibits phagocytosis and tumour immunity. *Nature,* **545**(7655), pp. 495-499.

GORMLEY, M., ONA, K., KAPIDZIC, M., GARRIDO-GOMEZ, T., ZDRAVKOVIC, T. and FISHER, S.J., 2017. Preeclampsia: novel insights from global RNA profiling of trophoblast subpopulations. *American Journal of Obstetrics and Gynecology,* **217**(2), pp. 200. e1-200. e17.

GOTZ, M. and BOLZ, J., 1992. Formation and preservation of cortical layers in slice cultures. *Journal of neurobiology,* **23**(7), pp. 783-802.

GOZZO, S., DIMITRIEVA, N., IACOPINO, C. and D'UDINE, B., 1985. A comparative study of mossy fiber distribution in the brain of the precocial Acomys cahirinus and of the altricial Rattus norvegicus: neuroanatomical bases and behavioral correlates. *The International journal of neuroscience,* **28**(3-4), pp. 163-172.

GRAHAM, E.M., RUIS, K.A., HARTMAN, A.L., NORTHINGTON, F.J. and FOX, H.E., 2008. A systematic review of the role of intrapartum hypoxia-ischemia in the causation of neonatal encephalopathy. *American Journal of Obstetrics and Gynecology,* **199**(6), pp. 587-595.

GRAHAM, G.D., 2003. Tissue plasminogen activator for acute ischemic stroke in clinical practice: a meta-analysis of safety data. *Stroke,* **34**(12), pp. 2847-2850.

GRANT, E., HOERDER-SUABEDISSEN, A. and MOLNAR, Z., 2016. The Regulation of Corticofugal Fiber Targeting by Retinal Inputs. *Cerebral cortex (New York, N.Y.: 1991),* **26**(3), pp. 1336-1348.

GRANT, E., HOERDER-SUABEDISSEN, A. and MOLNAR, Z., 2012. Development of the corticothalamic projections. *Frontiers in neuroscience,* **6**, pp. 53.

GREGGIO, S., DE PAULA, S., DE OLIVEIRA, I.M., TRINDADE, C., ROSA, R.M., HENRIQUES, J.A. and DACOSTA, J.C., 2011. NAP prevents acute cerebral oxidative stress and protects against long-term brain injury and cognitive impairment in a model of neonatal hypoxia–ischemia. *Neurobiology of disease,* **44**(1), pp. 152-159.

GREGGIO, S., ROSA, R.M., DOLGANOV, A., DE OLIVEIRA, I.M., MENEGAT, F.D., HENRIQUES, J.A. and DACOSTA, J.C., 2009. NAP prevents hippocampal oxidative damage in neonatal rats subjected to hypoxia-induced seizures. *Neurobiology of disease,* **36**(3), pp. 435-444.

GREIG, L.C., WOODWORTH, M.B., GALAZO, M.J., PADMANABHAN, H. and MACKLIS, J.D., 2013. Molecular logic of neocortical projection neuron specification, development and diversity. *Nature reviews.Neuroscience,* **14**(11), pp. 755-769.

GRESSENS, P., 2005. Neuronal migration disorders. *Journal of child neurology,* **20**(12), pp. 969-971.

GROENENDAAL, F., DE VRIES, L.S. and VAN BEL, F., 2006. Favourable results with surgical treatment in 43 children with hypoplastic left-heart syndrome or similar disorders, 1999-2005. *Nederlands tijdschrift voor geneeskunde,* **150**(49), pp. 2731-2; author reply 2732.

GROENENDAAL, F., MEINERS, L.C., GOOSKENS, R. and DE VRIES, L.S., 1994. Cerebral proton magnetic resonance spectroscopic imaging in a neonate with tuberous sclerosis. *Neuropediatrics,* **25**(3), pp. 154-157.

GROW, J. and BARKS, J.D., 2002. Pathogenesis of hypoxic-ischemic cerebral injury in the term infant: current concepts. *Clinics in perinatology,* **29**(4), pp. 585-602.

GU, R., FU, L., JIANG, C., XU, Y., WANG, X. and YU, J., 2015. Retina Is Protected by Neuroserpin from Ischemic/Reperfusion-Induced Injury Independent of Tissue-Type Plasminogen Activator. *PloS one,* **10**(7), pp. e0130440.

GUALANDRIS, A., JONES, T.E., STRICKLAND, S. and TSIRKA, S.E., 1996. Membrane depolarization induces calcium-dependent secretion of tissue plasminogen activator. *The Journal of neuroscience : the official journal of the Society for Neuroscience,* **16**(7), pp. 2220-2225.

GUBITS, R.M., BURKE, R.E., CASEY-MCINTOSH, G., BANDELE, A. and MUNELL, F., 1993. Immediate early gene induction after neonatal hypoxia-ischemia. *Molecular Brain Research,* **18**(3), pp. 228-238.

GYNASEKAR, P.G., KANTHASAMY, A.G., BOROWITZ, J.L., ISOM, G.E., 1995. NMDA receptor activation produces concurrent generation of nitric oxide and reactive oxygen species: implications for cell death. *Journal of neurochemistry.,* **65**(5), 2016-21.

GUAN, C., YE, C., YANG, X., GAO, J., 2010. A review of current large-scale mouse knockout efforts. *Genesis.*, **48**(2), 73-85.

GUNN, A.J. and GUNN, T.R., 1998. Thepharmacology'of neuronal rescue with cerebral hypothermia. *Early human development,* **53**(1), pp. 19-35.

GUNN, A.J., BATTIN, M., GLUCKMAN, P.D., GUNN, T.R. and BENNET, L., 2005. Therapeutic hypothermia: from lab to NICU. *Journal of perinatal medicine,* **33**(4), pp. 340-346.

GUNN, A.J., GUNN, T.R., DE HAAN, H.H., WILLIAMS, C.E. and GLUCKMAN, P.D., 1997. Dramatic neuronal rescue with prolonged selective head cooling after ischemia in fetal lambs. *The Journal of clinical investigation,* **99**(2), pp. 248-256.

GUNN, A.J., PARER, J.T., MALLARD, E.C., WILLIAMS, C.E. and GLUCKMAN, P.D., 1992. Cerebral histologic and electrocorticographic changes after asphyxia in fetal sheep. *Pediatric research,* **31**(5), pp. 486-491.

GUNTURKUN, O. and BUGNYAR, T., 2016. Cognition without Cortex. *Trends in cognitive sciences,* **20**(4), pp. 291-303.

GÜRTLER, A., KUNZ, N., GOMOLKA, M., HORNHARDT, S., FRIEDL, A.A., MCDONALD, K., KOHN, J.E. and POSCH, A., 2013. Stain-Free technology as a normalization tool in Western blot analysis. *Analytical Biochemistry,* **433**(2), pp. 105-111.

GUSEL'NIKOVA, V.V. and KORZHEVSKIY, D.E., 2015. NeuN As a Neuronal Nuclear Antigen and Neuron Differentiation Marker. *Acta naturae,* **7**(2), pp. 42-47.

GUSTAFSON, K., HAGBERG, H., BENGTSSON, B.A., BRANTSING, C., ISGAARD, J., 1999. Possible protective role of growth hormone in hypoxia-ischemia in neonatal rats. *Pediatric research.*, **45**(3), 318.

HACK, M., BRESLAU, N., ARAM, D., WEISSMAN, B., KLEIN, N. and BORAWSKI-CLARK, E., 1992. The effect of very low birth weight and social risk

on neurocognitive abilities at school age. *Journal of Developmental & Behavioral Pediatrics,* **13**(6), pp. 412-420.

HACKE, W., DONNAN, G., FIESCHI, C., KASTE, M., VON KUMMER, R., BRODERICK, J.P., BROTT, T., FRANKEL, M., GROTTA, J.C., HALEY, E.C.,JR, KWIATKOWSKI, T., LEVINE, S.R., LEWANDOWSKI, C., LU, M., LYDEN, P., MARLER, J.R., PATEL, S., TILLEY, B.C., ALBERS, G., BLUHMKI, E., WILHELM, M., HAMILTON, S., ATLANTIS TRIALS INVESTIGATORS, ECASS TRIALS INVESTIGATORS and NINDS RT-PA STUDY GROUP INVESTIGATORS, 2004. Association of outcome with early stroke treatment: pooled analysis of ATLANTIS, ECASS, and NINDS rt-PA stroke trials. *Lancet (London, England),* **363**(9411), pp. 768-774.

HACKE, W., KASTE, M., BLUHMKI, E., BROZMAN, M., DAVALOS, A., GUIDETTI, D., LARRUE, V., LEES, K.R., MEDEGHRI, Z., MACHNIG, T., SCHNEIDER, D., VON KUMMER, R., WAHLGREN, N., TONI, D. and ECASS INVESTIGATORS, 2008. Thrombolysis with alteplase 3 to 4.5 hours after acute ischemic stroke. *The New England journal of medicine,* **359**(13), pp. 1317-1329.

HACKE, W., KASTE, M., FIESCHI, C., TONI, D., LESAFFRE, E., VON KUMMER, R., BOYSEN, G., BLUHMKI, E., HOXTER, G. and MAHAGNE, M.H., 1995. Intravenous thrombolysis with recombinant tissue plasminogen activator for acute hemispheric stroke. The European Cooperative Acute Stroke Study (ECASS). *Jama,* **274**(13), pp. 1017-1025.

HADJICONSTANTINOU, M., YATES, A.J. and NEFF, N.H., 1990. Hypoxia-induced neurotransmitter deficits in neonatal rats are partially corrected by exogenous GM1 ganglioside. *Journal of neurochemistry,* **55**(3), pp. 864-869.

HAGBERG, H., 2004. Mitochondrial impairment in the developing brain after hypoxia–ischemia. *Journal of Bioenergetics and Biomembranes,* **36**(4), pp. 369-373.

HAGBERG, H., GRESSENS, P. and MALLARD, C., 2012. Inflammation during fetal and neonatal life: implications for neurologic and neuropsychiatric disease in children and adults. *Annals of Neurology,* **71**(4), pp. 444-457.

HAGBERG, H., MALLARD, C., FERRIERO, D.M., VANNUCCI, S.J., LEVISON, S.W., VEXLER, Z.S. and GRESSENS, P., 2015. The role of inflammation in perinatal brain injury. *Nature Reviews Neurology,* **11**(4), pp. 192-208.

HAGBERG, H., PEEBLES, D. and MALLARD, C., 2002. Models of white matter injury: Comparison of infectious, hypoxic-ischemic, and excitotoxic insults. *Mental retardation and developmental disabilities research reviews,* **8**(1), pp. 30-38.

HAGBERG, H., ANDERSSON, P., KJELLMER, I., THIRINGER, K. and THORDSTEIN, M., 1987. Extracellular overflow of glutamate, aspartate, GABA and taurine in the cortex and basal ganglia of fetal lambs during hypoxia-ischemia. *Neuroscience letters,* **78**(3), pp. 311-317.

HAGBERG, H., MALLARD, C., ROUSSET, C.I. and XIAOYANG, W., 2009. Apoptotic mechanisms in the immature brain: involvement of mitochondria. *Journal of child neurology,* **24**(9), pp. 1141-1146.

HAGBERG, H., THORNBERG, E., BLENNOW, M., KJELLMER, I., LAGERCRANTZ, H., THIRINGER, K., HAMBERGER, A. and SANDBERG, M., 1993. Excitatory amino acids in the cerebrospinal fluid of asphyxiated infants: relationship to hypoxic-ischemic encephalopathy. *Acta Paediatrica (Oslo, Norway : 1992),* **82**(11), pp. 925-929.

HAGBERG, H., WILSON, M.A., MATSUSHITA, H., ZHU, C., LANGE, M., GUSTAVSSON, M., POITRAS, M.F., DAWSON, T.M., DAWSON, V.L., NORTHINGTON, F. and JOHNSTON, M.V., 2004. PARP-1 gene disruption in mice preferentially protects males from perinatal brain injury. *Journal of neurochemistry,* **90**(5), pp. 1068-1075.

HALL, R.T., HALL, F.K. and DAILY, D.K., 1998. High-dose phenobarbital therapy in term newborn infants with severe perinatal asphyxia: a randomized, prospective study with three-year follow-up. *The Journal of pediatrics,* **132**(2), pp. 345-348.

HAMRE, K.M., CASSELL, M.D. and WEST, J.R., 1989. The development of laminar staining for neuron-specific enolase in the rat somatosensory cortex. *Brain research.Developmental brain research,* **46**(2), pp. 213-220.

HAMRE, K.M., HYMAN, B.T., GOODLETT, C.R., WEST, J.R. and VAN HOESEN, G.W., 1989. Alz-50 immunoreactivity in the neonatal rat: changes in development and co-distribution with MAP-2 immunoreactivity. *Neuroscience letters,* **98**(3), pp. 264-271.

HAMRICK, S.E. and FERRIERO, D.M., 2003. The injury response in the term newborn brain: can we neuroprotect? *Current opinion in neurology,* **16**(2), pp. 147-154.

HAN, J., BACK, S.H., HUR, J., LIN, Y., GILDERSLEEVE, R., SHAN, J., YUAN, C.L., KROKOWSKI, D., WANG, S. and HATZOGLOU, M., 2013. ER-stress-induced transcriptional regulation increases protein synthesis leading to cell death. *Nature cell biology,* **15**(5), pp. 481.

HANGANU, I.L., KILB, W. and LUHMANN, H.J., 2002. Functional synaptic projections onto subplate neurons in neonatal rat somatosensory cortex. *The Journal of neuroscience : the official journal of the Society for Neuroscience,* **22**(16), pp. 7165-7176.

HANGANU, I.L., KILB, W. and LUHMANN, H.J., 2001. Spontaneous synaptic activity of subplate neurons in neonatal rat somatosensory cortex. *Cerebral cortex (New York, N.Y.: 1991),* **11**(5), pp. 400-410.

HANSEN, R.L. and ROGERS, S.J., 2012. *Autism and other neurodevelopmental disorders.* American Psychiatric Pub.

HARDY, P., NUYT, A.M., DUMONT, I., PERI, K.G., HOU, X., VARMA, D.R. and CHEMTOB, S., 1999. Developmentally increased cerebrovascular NO in newborn pigs curtails cerebral blood flow autoregulation. *Pediatric research,* **46**(4), pp. 375-382.

HASEGAWA, K., YOSHIOKA, H., SAWADA, T. and NISHIKAWA, H., 1991. Lipid peroxidation in neonatal mouse brain subjected to two different types of hypoxia. *Brain and Development,* **13**(2), pp. 101-103.

HASEGAWA, J., WATANABE, M., KANEDA, T., OSAKI, S., HISATOME, I., KOTAKE, H. and MASHIBA, H., 1993. Effects of hypoxia on the use-dependent inhibition of conduction velocity induced by cibenzoline in guinea pig ventricular myocardium. *Journal of clinical pharmacology,* **33**(5), pp. 444-449.

HASEGAWA, K., YOSHIOKA, H., SAWADA, T. and NISHIKAWA, H., 1993. Direct measurement of free radicals in the neonatal mouse brain subjected to hypoxia: an electron spin resonance spectroscopic study. *Brain research,* **607**(1-2), pp. 161-166.

HASTINGS, G.A., COLEMAN, T.A., HAUDENSCHILD, C.C., STEFANSSON, S., SMITH, E.P., BARTHLOW, R., CHERRY, S., SANDKVIST, M. and LAWRENCE, D.A., 1997. Neuroserpin, a brain-associated inhibitor of tissue plasminogen activator is localized primarily in neurons Implications for the regulation of motor learning and neuronal survival. *Journal of Biological Chemistry,* **272**(52), pp. 33062-33067.

HASUMI, H., ISHIGURO, H., NAKAMURA, M., SUGIURA, S., OSADA, Y., MIYOSHI, Y., FUJINAMI, K., YAO, M., HAMADA, K. and YAMADA-OKABE, H., 2005. Neuroserpin (PI-12) is upregulated in high-grade prostate cancer and is associated with survival. *International journal of cancer,* **115**(6), pp. 911-916.

HAYASHI, T., IWAI, M., IKEDA, T., JIN, G., DEGUCHI, K., NAGOTANI, S., ZHANG, H., SEHARA, Y., NAGANO, I., SHOJI, M., IKENOUE, T., 2005. Neural precursor cells division and migration in neonatal rat brain after ischemic/hypoxic injury. *Brain research.,* **1038**(1), 41-9.

HATANAKA, Y. and MURAKAMI, F., 2002. In vitro analysis of the origin, migratory behavior, and maturation of cortical pyramidal cells. *The Journal of comparative neurology,* **454**(1), pp. 1-14.

HATFIELD, R., MENDELOW, A., PERRY, R., ALVAREZS, L. and MODHA, P., 1991. Triphenyltetrazolium chloride (TTC) as a marker for ischaemic changes in rat brain following permanent middle cerebral artery occlusion. *Neuropathology and applied neurobiology,* **17**(1), pp. 61-67.

HATHOUT, Y., 2007. Approaches to the study of the cell secretome. *Expert review of proteomics,* **4**(2), pp. 239-248.

HATTORI, H. and WASTERLAIN, C.G., 1990. Excitatory amino acids in the developing brain: ontogeny, plasticity, and excitotoxicity. *Pediatric neurology,* **6**(4), pp. 219-228.

HAUBENSAK, W., ATTARDO, A., DENK, W., HUTTNER, W.B., 2004. Neurons arise in the basal neuroepithelium of the early mammalian telencephalon: a major site of neurogenesis. *Proceedings of the National Academy of Sciences.,* **101**(9), 3196-201.

HEDNER, T., BERGMAN, B. and HOLMGREN, M., 1980. Adrenal catecholamines during and following hypoxia in neonatal rats. *Medical biology,* **58**(4), pp. 228-231.

HEDNER, T. and LUNDBORG, P., 1980. 5-HIAA Levels in brain and cerebrospinal fluid of the neonatal rat during oxygen deprivation. *Neuroscience letters,* **19**(3), pp. 315-318.

HEDNER, T. and LUNDBORG, P., 1980. Catecholamine metabolism in neonatal rat brain during asphyxia and recovery. *Acta Physiologica Scandinavica,* **109**(2), pp. 169-175.

HEDNER, T. and LUNDBORG, P., 1980. Serotonin metabolism in neonatal rat brain during asphyxia and recovery. *Acta Physiologica Scandinavica,* **109**(2), pp. 163-168.

HEIT, C., JACKSON, B.C., MCANDREWS, M., WRIGHT, M.W., THOMPSON, D.C., SILVERMAN, G.A., NEBERT, D.W. and VASILIOU, V., 2013. Update of the human and mouse SERPIN gene superfamily. *Human genomics,* **7**(1), pp. 22.

HELMY, M.M., TOLNER, E.A., VANHATALO, S., VOIPIO, J. and KAILA, K., 2011. Brain alkalosis causes birth asphyxia seizures, suggesting therapeutic strategy. *Annals of Neurology,* **69**(3), pp. 493-500.

HENRY, V.J., LECOINTRE, M., LAUDENBACH, V., ALI, C., MACREZ, R., JULLIENNE, A., BEREZOWSKI, V., CARMELIET, P., VIVIEN, D. and MARRET, S., 2013. High t-PA release by neonate brain microvascular endothelial cells under glutamate exposure affects neuronal fate. *Neurobiology of disease,* **50**, pp. 201-208.

HERRMANN, K., ANTONINI, A. and SHATZ, C.J., 1994. Ultrastructural evidence for synaptic interactions between thalamocortical axons and subplate neurons. *The European journal of neuroscience,* **6**(11), pp. 1729-1742.

HEUER, H., CHRIST, S., FRIEDRICHSEN, S., BRAUER, D., WINCKLER, M., BAUER, K. and RAIVICH, G., 2003. Connective tissue growth factor: a novel marker of layer VII neurons in the rat cerebral cortex. *Neuroscience,* **119**(1), pp. 43-52.

HIDA, K., SUZUKI, N., KWEE, I.L. and NAKADA, T., 1991. pH-lactate dissociation in neonatal anoxia: Proton and 31P NMR spectroscopic studies in rat pups. *Magnetic resonance in medicine,* **22**(1), pp. 128-132.

HIGASHI, S., MOLNAR, Z., KUROTANI, T. and TOYAMA, K., 2002. Prenatal development of neural excitation in rat thalamocortical projections studied by optical recording. *Neuroscience,* **115**(4), pp. 1231-1246.

HILL, A., 1991. Current concepts of hypoxic-ischemic cerebral injury in the term newborn. *Pediatric neurology,* **7**(5), pp. 317-325.

HILL., R.M., PARMAR PK, COATES LC, MEZEY E, PEARSON JF, BIRCH NP. 2000. Neuroserpin is expressed in the pituitary and adrenal glands and induces the extension of neurite-like processes in AtT-20 cells. *Biochemical Journal.,* 345(3), 595-601.

HILL, C.A. and FITCH, R.H., 2012. Sex differences in mechanisms and outcome of neonatal hypoxia-ischemia in rodent models: implications for sex-specific neuroprotection in clinical neonatal practice. *Neurology research international,* **2012**.

HILL, I.E., MACMANUS, J.P., RASQUINHA, I. and TUOR, U.I., 1995. DNA fragmentation indicative of apoptosis following unilateral cerebral hypoxia-ischemia in the neonatal rat. *Brain research,* **676**(2), pp. 398-403.

HILL, R.M., BRENNAN, S.O. and BIRCH, N.P., 2001. Expression, purification, and functional characterization of the serine protease inhibitor neuroserpin expressed in Drosophila S2 cells. *Protein expression and purification,* **22**(3), pp. 406-413.

HILL, C.A., ALEXANDER, M.L., MCCULLOUGH, L.D. and FITCH, R.H., 2011. Inhibition of X-linked inhibitor of apoptosis with embelin differentially affects male versus female behavioral outcome following neonatal hypoxia-ischemia in rats. *Developmental neuroscience,* **33**(6), pp. 494-504.

HIMMELMANN, K., HAGBERG, G., BECKUNG, E., HAGBERG, B. and UVEBRANT, P., 2005. The changing panorama of cerebral palsy in Sweden. IX. Prevalence and origin in the birth-year period 1995–1998. *Acta Paediatrica,* **94**(3), pp. 287-294.

HIMMELMANN, K., HAGBERG, G., WIKLUND, L.M., EEK, M.N. and UVEBRANT, P., 2007. Dyskinetic cerebral palsy: a population-based study of children born between 1991 and 1998. *Developmental medicine and child neurology,* **49**(4), pp. 246-251.

HIRSCH, S. and LUHMANN, H.J., 2008. Pathway-specificity in N-methyl-D-aspartate receptor-mediated synaptic inputs onto subplate neurons. *Neuroscience,* **153**(4), pp. 1092-1102.

HISANAGA, K., ONODERA, H. and KOGURE, K., 1986. Changes in levels of purine and pyrimidine nucleotides during acute hypoxia and recovery in neonatal rat brain. *Journal of neurochemistry,* **47**(5), pp. 1344-1350.

HOBBS, C., THORESEN, M., TUCKER, A., AQUILINA, K., CHAKKARAPANI, E. and DINGLEY, J., 2008. Xenon and hypothermia combine additively, offering long-term functional and histopathologic neuroprotection after neonatal hypoxia/ischemia. *Stroke; a journal of cerebral circulation,* **39**(4), pp. 1307-1313.

HOERDER-SUABEDISSEN, A., WANG, W.Z., LEE, S., DAVIES, K.E., GOFFINET, A.M., RAKIĆ, S., PARNAVELAS, J., REIM, K., NICOLIĆ, M. and

PAULSEN, O., 2008. Novel markers reveal subpopulations of subplate neurons in the murine cerebral cortex. *Cerebral Cortex,* **19**(8), pp. 1738-1750.

HOERDER-SUABEDISSEN, A., HAYASHI, S., UPTON, L., NOLAN, Z., CASAS-TORREMOCHA, D., GRANT, E., VISWANATHAN, S., KANOLD, P.O., CLASCA, F., KIM, Y., MOLNÁR, Z., 2018. Subset of cortical layer 6b neurons selectively innervates higher order thalamic nuclei in mice. *Cerebral Cortex.,* **28**(5), 1882-97.

HOERDER-SUABEDISSEN, A. and MOLNAR, Z., 2015. Development, evolution and pathology of neocortical subplate neurons. *Nature reviews.Neuroscience,* **16**(3), pp. 133-146.

HOERDER-SUABEDISSEN, A. and MOLNAR, Z., 2013. Molecular diversity of early-born subplate neurons. *Cerebral cortex (New York, N.Y.: 1991),* **23**(6), pp. 1473-1483.

HOERDER-SUABEDISSEN, A., OESCHGER, F.M., KRISHNAN, M.L., BELGARD, T.G., WANG, W.Z., LEE, S., WEBBER, C., PETRETTO, E., EDWARDS, A.D. and MOLNAR, Z., 2013. Expression profiling of mouse subplate reveals a dynamic gene network and disease association with autism and schizophrenia. *Proceedings of the National Academy of Sciences of the United States of America,* **110**(9), pp. 3555-3560.

HOERDER-SUABEDISSEN, A., WANG, W.Z., LEE, S., DAVIES, K.E., GOFFINET, A.M., RAKIC, S., PARNAVELAS, J., REIM, K., NICOLIC, M., PAULSEN, O. and MOLNAR, Z., 2009. Novel markers reveal subpopulations of subplate neurons in the murine cerebral cortex. *Cerebral cortex (New York, N.Y.: 1991),* **19**(8), pp. 1738-1750.

HOL, E.M. and PEKNY, M., 2015. Glial fibrillary acidic protein (GFAP) and the astrocyte intermediate filament system in diseases of the central nervous system. *Current opinion in cell biology,* **32**, pp. 121-130.

HOLLANDS, C., 1986. The Animals (scientific procedures) Act 1986. *Lancet (London, England),* **2**(8497), pp. 32-33.

HOLMES, G.L., 1991. The long-term effects of seizures on the developing brain: clinical and laboratory issues. *Brain & development,* **13**(6), pp. 393-409.

HOLMES, G.L. and BEN-ARI, Y., 2001. The neurobiology and consequences of epilepsy in the developing brain. *Pediatric research,* **49**(3), pp. 320-325.

HOLNESS, C.L. and SIMMONS, D.L., 1993. Molecular cloning of CD68, a human macrophage marker related to lysosomal glycoproteins. *Blood,* **81**(6), pp. 1607-1613.

HONG, J., KIM, K., PARK, E., LEE, J., MARKOFSKI, M.M., MARRELLI, S.P. and PARK, Y., 2018. Exercise ameliorates endoplasmic reticulum stress-mediated vascular dysfunction in mesenteric arteries in atherosclerosis. *Scientific reports,* **8**(1), pp. 7938.

HORI, Y., and KANDA, K., 1994. Developmental alterations in NMDA receptor-mediated [Ca2+] i elevation in substantia gelatinosa neurons of neonatal rat spinal cord. *Developmental brain research.,* **80**(1-2), 141-8.

HORN, E.P., BEIN, B., BROCH, O., IDEN, T., BOHM, R., LATZ, S.K. and HOCKER, J., 2016. Warming before and after epidural block before general anaesthesia for major abdominal surgery prevents perioperative hypothermia: A randomised controlled trial. *European journal of anaesthesiology,* **33**(5), pp. 334-340.

HOSSMANN, K., 1993. Disturbances of cerebral protein synthesis and ischemic cell death. *Progress in brain research.* Elsevier, pp. 161-177.

HOU, X., DING, H., TENG, Y., ZHOU, C., TANG, X., LI, S. and DING, H., 2007. Research on the relationship between brain anoxia at different regional oxygen saturations and brain damage using near-infrared spectroscopy. *Physiological Measurement,* **28**(10), pp. 1251-1265.

HU, S., LOO, J.A. and WONG, D.T., 2006. Human body fluid proteome analysis. *Proteomics,* **6**(23), pp. 6326-6353.

HU, B.R., LIU, C.L., OUYANG, Y., BLOMGREN, K. and SIESJO, B.K., 2000. Involvement of caspase-3 in cell death after hypoxia-ischemia declines during brain maturation. *Journal of cerebral blood flow and metabolism : official journal of the International Society of Cerebral Blood Flow and Metabolism,* **20**(9), pp. 1294-1300.

HU, X., QIU, J., GRAFE, M.R., REA, H.C., RASSIN, D.K. and PEREZ-POLO, J.R., 2003. Bcl-2 family members make different contributions to cell death in hypoxia and/or hyperoxia in rat cerebral cortex. *International journal of developmental neuroscience : the official journal of the International Society for Developmental Neuroscience,* **21**(7), pp. 371-377.

HUANG, Z., LIU, J., CHEUNG, P. and CHEN, C., 2009. Long-term cognitive impairment and myelination deficiency in a rat model of perinatal hypoxic-ischemic brain injury. *Brain research,* **1301**, pp. 100-109.

HUANG, D., DESBOIS, A. and HOU, S.T., 2005. A novel adenoviral vector which mediates hypoxia-inducible gene expression selectively in neurons. *Gene therapy,* **12**(18), pp. 1369-1376.

HUDSPETH, W.J. and PRIBRAM, K.H., 1990. Stages of brain and cognitive maturation. .

HUMEAU, Y., DOUSSAU, F., GRANT, N.J. and POULAIN, B., 2000. How botulinum and tetanus neurotoxins block neurotransmitter release. *Biochimie,* **82**(5), pp. 427-446.

HUMPEL, C., 2015. Organotypic brain slice cultures: A review. *Neuroscience,* **305**, pp. 86-98.

HUNT, R.W., NEIL, J.J., COLEMAN, L.T., KEAN, M.J. and INDER, T.E., 2004. Apparent diffusion coefficient in the posterior limb of the internal capsule predicts outcome after perinatal asphyxia. *Pediatrics,* **114**(4), pp. 999-1003.

HURTLEY, S.M. and HELENIUS, A., 1989. Protein oligomerization in the endoplasmic reticulum. *Annual Review of Cell Biology,* **5**, pp. 277-307.

HUTSLER, J.J. and CASANOVA, M.F., 2016. Cortical construction in autism spectrum disorder: columns, connectivity and the subplate. *Neuropathology and applied neurobiology,* **42**(2), pp. 115-134.

HUTSLER, J.J., LOVE, T. and ZHANG, H., 2007. Histological and magnetic resonance imaging assessment of cortical layering and thickness in autism spectrum disorders. *Biological psychiatry,* **61**(4), pp. 449-457.

HUTTON, L.C., ABBASS, M., DICKINSON, H., IRELAND, Z. and WALKER, D.W., 2009. Neuroprotective properties of melatonin in a model of birth asphyxia in the spiny mouse (Acomys cahirinus). *Developmental neuroscience,* **31**(5), pp. 437-451.

IADECOLA, C., ZHANG, F., CASEY, R., NAGAYAMA, M., ROSS, M.E., 1997. Delayed reduction of ischemic brain injury and neurological deficits in mice lacking the inducible nitric oxide synthase gene. *Journal of Neuroscience.,* **17**(23), 9157-64.

IKEDA, K., TANIHARA, H., HONDA, Y., TATSUNO, T., NOGUCHI, H. and NAKAYAMA, C., 1999. BDNF attenuates retinal cell death caused by chemically induced hypoxia in rats. *Investigative ophthalmology & visual science,* **40**(9), pp. 2130-2140.

IKEDA, T., MISHIMA, K., YOSHIKAWA, T., IWASAKI, K., FUJIWARA, M., XIA, Y.X. and IKENOUE, T., 2001. Selective and long-term learning impairment following neonatal hypoxic-ischemic brain insult in rats. *Behavioural brain research,* **118**(1), pp. 17-25.

IKEDA, T., XIA, Y.X., KANEKO, M., SAMESHIMA, H., IKENOUE, T., 2002. Effect of the free radical scavenger, 3-methyl-1-phenyl-2-pyrazolin-5-one (MCI-186), on hypoxia-ischemia-induced brain injury in neonatal rats. *Neuroscience letters.*, **329**(1), 33-6.

IKONOMIDOU, C., BOSCH, F., MIKSA, M., BITTIGAU, P., VOCKLER, J., DIKRANIAN, K., TENKOVA, T.I., STEFOVSKA, V., TURSKI, L. and OLNEY, J.W., 1999. Blockade of NMDA receptors and apoptotic neurodegeneration in the developing brain. *Science (New York, N.Y.),* **283**(5398), pp. 70-74.

IKONOMIDOU, C. and KAINDL, A.M., 2011. Neuronal death and oxidative stress in the developing brain. *Antioxidants & redox signaling,* **14**(8), pp. 1535-1550.

IM, S., YU, J., PARK, E., LEE, J., KIM, H., PARK, K., KIM, G., PARK, C. and CHO, S., 2010. Induction of striatal neurogenesis enhances functional recovery in an

adult animal model of neonatal hypoxic-ischemic brain injury. *Neuroscience,* **169**(1), pp. 259-268.

INAN, M. and CRAIR, M.C., 2007. Development of cortical maps: perspectives from the barrel cortex. *The Neuroscientist : a review journal bringing neurobiology, neurology and psychiatry,* **13**(1), pp. 49-61.

INDER, T.E., HUPPI, P.S., WARFIELD, S., KIKINIS, R., ZIENTARA, G.P., BARNES, P.D., JOLESZ, F. and VOLPE, J.J., 1999. Periventricular white matter injury in the premature infant is followed by reduced cerebral cortical gray matter volume at term. *Annals of Neurology,* **46**(5), pp. 755-760.

INDER, T., NEIL, J., KROENKE, C., DIENI, S., YODER, B. and REES, S., 2005. Investigation of cerebral development and injury in the prematurely born primate by magnetic resonance imaging and histopathology. *Developmental neuroscience,* **27**(2-4), pp. 100-111.

INDER, T., NEIL, J., YODER, B. and REES, S., 2005. Patterns of cerebral injury in a primate model of preterm birth and neonatal intensive care. *Journal of child neurology,* **20**(12), pp. 965-967.

INDER, T.E., HUNT, R.W., MORLEY, C.J., COLEMAN, L., STEWART, M., DOYLE, L.W. and JACOBS, S.E., 2004. Randomized trial of systemic hypothermia selectively protects the cortex on MRI in term hypoxic-ischemic encephalopathy. *The Journal of pediatrics,* **145**(6), pp. 835-837.

INDER, T.E. and VOLPE, J.J., 2000. Mechanisms of perinatal brain injury. *Seminars in neonatology : SN,* **5**(1), pp. 3-16.

INTA, I., VOGT, M.A., VOGEL, A.S., BETTENDORF, M., GASS, P., INTA, D., 2016. Minocycline exacerbates apoptotic neurodegeneration induced by the NMDA receptor antagonist MK-801 in the early postnatal mouse brain. *European archives of psychiatry and clinical neuroscience.*, **266**(7), 673-7.

IRELAND, Z., DICKINSON, H., FLEISS, B., HUTTON, L.C. and WALKER, D.W., 2010. Behavioural effects of near-term acute fetal hypoxia in a small precocial animal, the spiny mouse (Acomys cahirinus). *Neonatology,* **97**(1), pp. 45-51.

IRELAND, Z., DICKINSON, H., SNOW, R. and WALKER, D.W., 2008. Maternal creatine: does it reach the fetus and improve survival after an acute hypoxic episode in the spiny mouse (Acomys cahirinus)? *American Journal of Obstetrics and Gynecology,* **198**(4), pp. 431.e1-431.e6.

IRELAND, Z., RUSSELL, A.P., WALLIMANN, T., WALKER, D.W. and SNOW, R., 2009. Developmental changes in the expression of creatine synthesizing enzymes and creatine transporter in a precocial rodent, the spiny mouse. *BMC developmental biology,* **9**, pp. 39-213X-9-39.

ISAYAMA, K., PITTS, L.H. and NISHIMURA, M.C., 1991. Evaluation of 2,3,5-triphenyltetrazolium chloride staining to delineate rat brain infarcts. *Stroke,* **22**(11), pp. 1394-1398.

ISHIGAMI, S., SANDKVIST, M., TSUI, F., MOORE, E., COLEMAN, T.A. and LAWRENCE, D.A., 2007. Identification of a novel targeting sequence for regulated secretion in the serine protease inhibitor neuroserpin. *The Biochemical journal,* **402**(1), pp. 25-34.

IST-3 COLLABORATIVE GROUP, 2012. The benefits and harms of intravenous thrombolysis with recombinant tissue plasminogen activator within 6 h of acute ischaemic stroke (the third international stroke trial [IST-3]): a randomised controlled trial. *The Lancet,* **379**(9834), pp. 2352-2363.

ITO, D., IMAI, Y., OHSAWA, K., NAKAJIMA, K., FUKUUCHI, Y. and KOHSAKA, S., 1998. Microglia-specific localisation of a novel calcium binding protein, Iba1. *Brain research.Molecular brain research,* **57**(1), pp. 1-9.

IUVONE, L., GELOSO, M.C. and DELL'ANNA, E., 1996. Changes in open field behavior, spatial memory, and hippocampal parvalbumin immunoreactivity following enrichment in rats exposed to neonatal anoxia. *Experimental neurology,* **139**(1), pp. 25-33.

IYER, N.V., LEUNG, S.W. and SEMENZA, G.L., 1998. The human hypoxia-inducible factor 1alpha gene: HIF1A structure and evolutionary conservation. *Genomics,* **52**(2), pp. 159-165.

IVACKO, J.A., SUN, R., SILVERSTEIN, F.S., 1996. Hypoxic-ischemic brain injury induces an acute microglial reaction in perinatal rats1. *Pediatric research.,* **39**(1), 39.

IZAKI, K., KINOUCHI, H., WATANABE, K., OWADA, Y., OKUBO, A., ITOH, H., KONDO, H., TASHIMA, Y., TAMURA, S. and YOSHIMOTO, T., 2001. Induction of mitochondrial heat shock protein 60 and 10 mRNAs following transient focal cerebral ischemia in the rat. *Molecular Brain Research,* **88**(1-2), pp. 14-25.

JABAUDON, D., SCANZIANI, M., GAHWILER, B.H. and GERBER, U., 2000. Acute decrease in net glutamate uptake during energy deprivation. *Proceedings of the National Academy of Sciences of the United States of America,* **97**(10), pp. 5610-5615.

JACKSON, M.R., NILSSON, T. and PETERSON, P.A., 1990. Identification of a consensus motif for retention of transmembrane proteins in the endoplasmic reticulum. *The EMBO journal,* **9**(10), pp. 3153-3162.

JACOBS, E.C., CAMPAGNONI, C., KAMPF, K., REYES, S.D., KALRA, V., HANDLEY, V., XIE, Y., HONG-HU, Y., SPREUR, V. and FISHER, R.S., 2007. Visualization of corticofugal projections during early cortical development in a τ-GFP-transgenic mouse. *European Journal of Neuroscience,* **25**(1), pp. 17-30.

JACOBS, S., HUNT, R., TARNOW-MORDI, W., INDER, T. and DAVIS, P., 2005. 181 Cooling for Newborns with Hypoxic Ischaemic Encephalopathy. *Pediatric research,* **58**(2), pp. 385-385.

JACOBS, S., BERG, M., HUNT, R., TARNOW-MORDI, W., INDER, T. and DAVIS, P., 2013. Cooling for newborns with hypoxic ischaemic en-cephalopathy. *status and date: Edited (no change to conclusions), published in,* (3),.

JACOVINA, A.T., ZHONG, F., KHAZANOVA, E., LEV, E., DEORA, A.B. and HAJJAR, K.A., 2001. Neuritogenesis and the nerve growth factor-induced differentiation of PC-12 cells requires annexin II-mediated plasmin generation. *The Journal of biological chemistry,* **276**(52), pp. 49350-49358.

JAHNEN-DECHENT, W., HEISS, A., SCHAFER, C. and KETTELER, M., 2011. Fetuin-A regulation of calcified matrix metabolism. *Circulation research,* **108**(12), pp. 1494-1509.

JANSEN, E.M. and LOW, W.C., 1996. Long-term effects of neonatal ischemic-hypoxic brain injury on sensorimotor and locomotor tasks in rats. *Behavioural brain research,* **78**(2), pp. 189-194.

JANSEN, E.M. and LOW, W.C., 1996. Quantitative analysis of contralateral hemisphere hypertrophy and sensorimotor performance in adult rats following unilateral neonatal ischemic-hypoxic brain injury. *Brain research,* **708**(1), pp. 93-99.

JANSEN, E.M., SOLBERG, L., UNDERHILL, S., WILSON, S., COZZARI, C., HARTMAN, B.K., FARIS, P.L. and LOW, W.C., 1997. Transplantation of fetal neocortex ameliorates sensorimotor and locomotor deficits following neonatal ischemic–hypoxic brain injury in rats. *Experimental neurology,* **147**(2), pp. 487-497.

JANTZIE, L.L., CORBETT, C.J., BERGLASS, J., FIRL, D.J., FLORES, J., MANNIX, R. and ROBINSON, S., 2014. Complex pattern of interaction between in utero hypoxia-ischemia and intra-amniotic inflammation disrupts brain development and motor function. *Journal of neuroinflammation,* **11**, pp. 131-2094-11-131.

JANTZIE, L.L., CORBETT, C.J., FIRL, D.J. and ROBINSON, S., 2015. Postnatal Erythropoietin Mitigates Impaired Cerebral Cortical Development Following Subplate Loss from Prenatal Hypoxia-Ischemia. *Cerebral cortex (New York, N.Y.: 1991),* **25**(9), pp. 2683-2695.

JANTZIE, L.L., HU, M.Y., PARK, H.K., JACKSON, M.C., YU, J., MAXWELL, J.R. and JENSEN, F.E., 2015. Chloride cotransporter NKCC1 inhibitor bumetanide protects against white matter injury in a rodent model of periventricular leukomalacia. *Pediatric research,* **77**(4), pp. 554-562.

JANTZIE, L.L., WINER, J.L., MAXWELL, J.R., CHAN, L.A. and ROBINSON, S., 2015. Modeling Encephalopathy of Prematurity Using Prenatal Hypoxia-ischemia with Intra-amniotic Lipopolysaccharide in Rats. *Journal of visualized experiments : JoVE,* **(105). doi**(105), pp. 10.3791/53196.

JANTZIE, L.L., CHEUNG, P.Y., TODD, K.G., 2005. Doxycycline reduces cleaved caspase-3 and microglial activation in an animal model of neonatal hypoxia-ischemia. *Journal of Cerebral Blood Flow & Metabolism.*, **25**(3), 314-24.

JARVIS, S., GLINIANAIA, S.V., ARNAUD, C., FAUCONNIER, J., JOHNSON, A., MCMANUS, V., TOPP, M., UVEBRANT, P., CANS, C., KRAGELOH-MANN, I. and SCPE COLLABORATION OF EUROPEAN CEREBRAL PALSY REGISTERS, 2005. Case gender and severity in cerebral palsy varies with intrauterine growth. *Archives of Disease in Childhood,* **90**(5), pp. 474-479.

JATANA, M., SINGH, I., SINGH, A.K. and JENKINS, D., 2006. Combination of systemic hypothermia and N-acetylcysteine attenuates hypoxic-ischemic brain injury in neonatal rats. *Pediatric research,* **59**(5), pp. 684-689.

JATANA, M., SINGH, I., SINGH, A.K. and JENKINS, D., 2006. Combination of systemic hypothermia and N-acetylcysteine attenuates hypoxic-ischemic brain injury in neonatal rats. *Pediatric research,* **59**(5), pp. 684-689.

JEANNERET, V., WU, F., MERINO, P., TORRE, E., DIAZ, A., CHENG, L. and YEPES, M., 2016. Tissue-type plasminogen activator (tPA) modulates the postsynaptic response of cerebral cortical neurons to the presynaptic release of glutamate. *Frontiers in molecular neuroscience,* **9**, pp. 121.

JELINSKI, S.E., YAGER, J.Y. and JUURLINK, B.H., 1999. Preferential injury of oligodendroblasts by a short hypoxic–ischemic insult. *Brain research,* **815**(1), pp. 150-153.

JENDELOVÁ, P., HERYNEK, V., URDZIKOVA, L., GLOGAROVÁ, K., KROUPOVÁ, J., ANDERSSON, B., BRYJA, V., BURIAN, M., HÁJEK, M. and SYKOVÁ, E., 2004. Magnetic resonance tracking of transplanted bone marrow and embryonic stem cells labeled by iron oxide nanoparticles in rat brain and spinal cord. *Journal of neuroscience research,* **76**(2), pp. 232-243.

JENSEN, F., 1995. An animal model of hypoxia-induced perinatal seizures. *The Italian Journal of Neurological Sciences,* **16**(1-2), pp. 59-68.

JENSEN, F., BLUME, H., ALVARADO, S., FIRKUSNY, I. and GEARY, C., 1995. NBQX blocks acute and late epileptogenic effects of perinatal hypoxia. *Epilepsia,* **36**(10), pp. 966-972.

JENSEN, A., GARNIER, Y. and BERGER, R., 1999. Dynamics of fetal circulatory responses to hypoxia and asphyxia. *European journal of obstetrics, gynecology, and reproductive biology,* **84**(2), pp. 155-172.

JENSEN, E.C., 2013. Quantitative analysis of histological staining and fluorescence using ImageJ. *Anatomical record (Hoboken, N.J.: 2007),* **296**(3), pp. 378-381.

JESTADT, R. and SANDRITTER, W., 1959. Erfahrungen mit der TTC (Triphenyltetrazoliumchlorid) Reaktion für die pathologisch-anatomische Diagnose des frischen Herzinfarktes. *Kreislaufforsch,* **48**, pp. 802-809.

JIN, Y., SILVERMAN, A.J., VANNUCCI, S.J., 2007. Mast cell stabilization limits hypoxic-ischemic brain damage in the immature rat. *Developmental neuroscience.,* **29**(4-5), 373-84.

JIN, Y., SILVERMAN, A.J., VANNUCCI, S.J., 2009. Mast cells are early responders after hypoxia-ischemia in immature rat brain. *Stroke.,* **40**(9), 3107-12.

JOHNSON, S., MICHALAK, M., OPAS, M. and EGGLETON, P., 2001. The ins and outs of calreticulin: from the ER lumen to the extracellular space. *Trends in cell biology,* **11**(3), pp. 122-129.

JOHNSON, M.B., KAWASAWA, Y.I., MASON, C.E., KRSNIK, Z., COPPOLA, G., BOGDANOVIC, D., GESCHWIND, D.H., MANE, S.M., STATE, M.W. and SESTAN, N., 2009. Functional and evolutionary insights into human brain development through global transcriptome analysis. *Neuron,* **62**(4), pp. 494-509.

JOHNSTON, M.V., 2009. Plasticity in the developing brain: implications for rehabilitation. *Developmental disabilities research reviews.,* **15**(2), 94-101.

JOHNSTON, M.V., 2005. Excitotoxicity in perinatal brain injury. *Brain pathology (Zurich, Switzerland),* **15**(3), pp. 234-240.

JOHNSTON, M.V., 2001. Excitotoxicity in neonatal hypoxia. *Mental retardation and developmental disabilities research reviews,* **7**(4), pp. 229-234.

JOHNSTON, M.V. and HAGBERG, H., 2007. Sex and the pathogenesis of cerebral palsy. *Developmental medicine and child neurology,* **49**(1), pp. 74-78.

JOINER, B.L., 1981. Lurking variables: Some examples. *The American Statistician,* **35**(4), pp. 227-233.

JONES, A.R., OVERLY, C.C. and SUNKIN, S.M., 2009. The Allen brain atlas: 5 years and beyond. *Nature Reviews Neuroscience,* **10**(11), pp. 821.

JONES, L., BELLIS, M.A., WOOD, S., HUGHES, K., MCCOY, E., ECKLEY, L., BATES, G., MIKTON, C., SHAKESPEARE, T. and OFFICER, A., 2012. Prevalence and risk of violence against children with disabilities: a systematic review and meta-analysis of observational studies. *The Lancet,* **380**(9845), pp. 899-907.

JONES, E.G. and WISE, S.P., 1977. Size, laminar and columnar distribution of efferent cells in the sensory-motor cortex of monkeys. *The Journal of comparative neurology,* **175**(4), pp. 391-438.

JONES, M.K., SZABO, I.L., KAWANAKA, H., HUSAIN, S.S. and TARNAWSKI, A.S., 2002. von Hippel Lindau tumor suppressor and HIF-1alpha: new targets of NSAIDs inhibition of hypoxia-induced angiogenesis. *FASEB journal : official publication of the Federation of American Societies for Experimental Biology,* **16**(2), pp. 264-266.

JONES, N.M. and BERGERON, M., 2001. Hypoxic preconditioning induces changes in HIF-1 target genes in neonatal rat brain. *Journal of cerebral blood flow and metabolism : official journal of the International Society of Cerebral Blood Flow and Metabolism,* **21**(9), pp. 1105-1114.

JOSE, A. and SORIANO, E., 1989. Immunocytochemical detection of 5′-bromodeoxyuridine incorporation in the central nervous system of the mouse. *Developmental Brain Research,* **49**(2), pp. 311-317.

JOSEPH, B., NANDHU, M.S. and PAULOSE, C.S., 2010. Dopamine D1 and D2 receptor functional down regulation in the cerebellum of hypoxic neonatal rats: neuroprotective role of glucose and oxygen, epinephrine resuscitation. *Pharmacological research,* **61**(2), pp. 136-141.

JOSHI, S., ERGIN, A., WANG, M., REIF, R., ZHANG, J., BRUCE, J.N. and BIGIO, I.J., 2011. Inconsistent blood brain barrier disruption by intraarterial mannitol in rabbits: implications for chemotherapy. *Journal of neuro-oncology,* **104**(1), pp. 11-19.

JUDAS, M., RADOS, M., JOVANOV-MILOSEVIC, N., HRABAC, P., STERN-PADOVAN, R. and KOSTOVIC, I., 2005. Structural, immunocytochemical, and mr imaging properties of periventricular crossroads of growing cortical pathways in preterm infants. *AJNR.American journal of neuroradiology,* **26**(10), pp. 2671-2684.

JUDAS, M., SEDMAK, G. and KOSTOVIC, I., 2013. The significance of the subplate for evolution and developmental plasticity of the human brain. *Frontiers in human neuroscience,* **7**, pp. 423.

JUDAS, M., SEDMAK, G. and PLETIKOS, M., 2010. Early history of subplate and interstitial neurons: from Theodor Meynert (1867) to the discovery of the subplate zone (1974). *Journal of anatomy,* **217**(4), pp. 344-367.

JUUL, S.E., BEYER, R.P., BAMMLER, T.K., MCPHERSON, R.J., WILKERSON, J. and FARIN, F.M., 2009. Microarray analysis of high-dose recombinant erythropoietin treatment of unilateral brain injury in neonatal mouse hippocampus. *Pediatric research,* **65**, pp. 485-492.

KAGEYAMA, G.H., ROBERTSON, R.T., 1993. Development of gemculocortical projections to visual cortex in rat: Evidence for early lngrowth and synaptogenesis. *Journal of Comparative Neurology.,* **335**(1), 123-48.

KAINDL, A.M., FAVRAIS, G. and GRESSENS, P., 2009. Molecular mechanisms involved in injury to the preterm brain. *Journal of child neurology,* **24**(9), pp. 1112-1118.

KAMPFL, A., POSMANTUR, R., ZHAO, X., SCHMUTZHARD, E., CLIFTON, G. and HAYES, R., 1997. Mechanisms of calpain proteolysis following traumatic brain injury: implications for pathology and therapy: a review and update. *Journal of neurotrauma,* **14**(3), pp. 121-134.

KANDEL, E., 2013. The new science of mind and the future of knowledge. *Neuron,* **80**(3), pp. 546-560.

KANEKO, K., 1985. The effect of perinatal anoxia on amino acid metabolism in the developing brain. Part II: The effect of perinatal anoxia on the free amino acid patterns in CSF of infants and children. *Brain & development,* **7**(4), pp. 400-407.

KANEKO, T., SAWADA, T., KINUGAWA, H., KURIYAMA, Y. and NARITOMI, H., 1985. A case of inverse ocular bobbing associated with cluster respiration in hypoxic encephalopathy. *Rinsho shinkeigaku = Clinical neurology,* **25**(10), pp. 1192-1195.

KANG, T.H., HUR, J.Y., KIM, H.B., RYU, J.H. and KIM, S.Y., 2006. Neuroprotective effects of the cyanidin-3-O-β-d-glucopyranoside isolated from mulberry fruit against cerebral ischemia. *Neuroscience letters,* **391**(3), pp. 122-126.

KANG, H.J., KAWASAWA, Y.I., CHENG, F., ZHU, Y., XU, X., LI, M., SOUSA, A.M., PLETIKOS, M., MEYER, K.A., SEDMAK, G., GUENNEL, T., SHIN, Y., JOHNSON, M.B., KRSNIK, Z., MAYER, S., FERTUZINHOS, S., UMLAUF, S., LISGO, S.N., VORTMEYER, A., WEINBERGER, D.R., MANE, S., HYDE, T.M., HUTTNER, A., REIMERS, M., KLEINMAN, J.E. and SESTAN, N., 2011. Spatio-temporal transcriptome of the human brain. *Nature,* **478**(7370), pp. 483-489.

KANOLD, P.O., 2009. Subplate neurons: crucial regulators of cortical development and plasticity. *Frontiers in neuroanatomy,* **3**, pp. 16.

KANOLD, P.O., 2004. Transient microcircuits formed by subplate neurons and their role in functional development of thalamocortical connections. *Neuroreport,* **15**(14), pp. 2149-2153.

KANOLD, P.O., KARA, P., REID, R.C. and SHATZ, C.J., 2003. Role of subplate neurons in functional maturation of visual cortical columns. *Science (New York, N.Y.),* **301**(5632), pp. 521-525.

KANOLD, P.O. and LUHMANN, H.J., 2010. The subplate and early cortical circuits. *Annual Review of Neuroscience,* **33**, pp. 23-48.

KANOLD, P.O. and SHATZ, C.J., 2006. Subplate neurons regulate maturation of cortical inhibition and outcome of ocular dominance plasticity. *Neuron,* **51**(5), pp. 627-638.

KARALIS, F., SOUBASI, V., GEORGIOU, T., NAKAS, C.T., SIMEONIDOU, C., GUIBA-TZIAMPIRI, O. and SPANDOU, E., 2011. Resveratrol ameliorates hypoxia/ischemia-induced behavioral deficits and brain injury in the neonatal rat brain. *Brain research,* **1425**, pp. 98-110.

KARLSSON, M., TOOLEY, J.R., SATAS, S., HOBBS, C.E., CHAKKARAPANI, E., STONE, J., PORTER, H., THORESEN, M., 2008. Delayed hypothermia as selective head cooling or whole body cooling does not protect brain or body in newborn pig subjected to hypoxia-ischemia. *Pediatric research.,* **64**(1), 74.

KARPERIEN, A., AHAMMER, H., JELINEK, H., 2013. Quantitating the subtleties of microglial morphology with fractal analysis. *Frontiers in cellular neuroscience.*, **7**, 3.

KATSCHINSKI, D.M., LE, L., HEINRICH, D., WAGNER, K.F., HOFER, T., SCHINDLER, S.G. and WENGER, R.H., 2002. Heat induction of the unphosphorylated form of hypoxia-inducible factor-1alpha is dependent on heat shock protein-90 activity. *The Journal of biological chemistry,* **277**(11), pp. 9262-9267.

KATTWINKEL, J., PERLMAN, J.M., AZIZ, K., COLBY, C., FAIRCHILD, K., GALLAGHER, J., HAZINSKI, M.F., HALAMEK, L.P., KUMAR, P., LITTLE, G., MCGOWAN, J.E., NIGHTENGALE, B., RAMIREZ, M.M., RINGER, S., SIMON, W.M., WEINER, G.M., WYCKOFF, M. and ZAICHKIN, J., 2010. Part 15: neonatal resuscitation: 2010 American Heart Association Guidelines for Cardiopulmonary Resuscitation and Emergency Cardiovascular Care. *Circulation,* **122**(18 Suppl 3), pp. S909-19.

KAUFMAN, S.A., MILLER, S.P., FERRIERO, D.M., GLIDDEN, D.H., BARKOVICH, A.J. and PARTRIDGE, J.C., 2003. Encephalopathy as a predictor of magnetic resonance imaging abnormalities in asphyxiated newborns. *Pediatric neurology,* **28**(5), pp. 342-346.

KAUR, C. and LING, E., 2009. Periventricular white matter damage in the hypoxic neonatal brain: role of microglial cells. *Progress in neurobiology,* **87**(4), pp. 264-280.

KAUR, C., DHEEN, S.T. and LING, E., 2007. From blood to brain: amoeboid microglial cell, a nascent macrophage and its functions in developing brain 1. *Acta Pharmacologica Sinica,* **28**(8), pp. 1087-1096.

KAUR, C., RATHNASAMY, G. and LING, E., 2013. Roles of activated microglia in hypoxia induced neuroinflammation in the developing brain and the retina. *Journal of Neuroimmune Pharmacology,* **8**(1), pp. 66-78.

KELSOM, C., and LU, W., 2013. Development and specification of GABAergic cortical interneurons. *Cell & bioscience.,* **3**(1), 19.

KEMP, G.J. and RADDA, G.K., 1994. Quantitative interpretation of bioenergetic data from 31P and 1H magnetic resonance spectroscopic studies of skeletal muscle: an analytical review. *Magnetic resonance quarterly,* **10**(1), pp. 43-63.

KHAZIPOV, R., VALEEVA, G., KHALILOV, I., 2015. Depolarizing GABA and developmental epilepsies. *CNS neuroscience & therapeutics.,* **21**(2), 83-91.

KHOZHAI, L.I. and OTELLIN, V.A., 2013. Reactive microglial changes in rat neocortex and hippocampus after exposure to acute perinatal hypoxia. *Morfologiia (Saint Petersburg, Russia),* **143**(1), pp. 23-27.

KICHEV, A., BABURAMANI, A.A., VONTELL, R., GRESSENS, P., BURKLY, L., THORNTON, C. and HAGBERG, H., 2018. TWEAK Receptor Deficiency Has

Opposite Effects on Female and Male Mice Subjected to Neonatal Hypoxia-Ischemia. *Frontiers in neurology,* **9**, pp. 230.

KICHEV, A., ROUSSET, C.I., BABURAMANI, A.A., LEVISON, S.W., WOOD, T.L., GRESSENS, P., THORNTON, C. and HAGBERG, H., 2014. Tumor necrosis factor-related apoptosis-inducing ligand (TRAIL) signaling and cell death in the immature central nervous system after hypoxia-ischemia and inflammation. *The Journal of biological chemistry,* **289**(13), pp. 9430-9439.

KIDA, H., NOMURA, S., SHINOYAMA, M., IDEGUCHI, M., OWADA, Y. and SUZUKI, M., 2013. The effect of hypothermia therapy on cortical laminar disruption following ischemic injury in neonatal mice. *PloS one,* **8**(7), pp. e68877.

KIM, G.S., CHO, S., NELSON, J.W., ZIPFEL, G.J. and HAN, B.H., 2014. TrkB agonist antibody pretreatment enhances neuronal survival and long-term sensory motor function following hypoxic ischemic injury in neonatal rats. *PloS one,* **9**(2), pp. e88962.

KIM, B.J., KIM, M.J., PARK, J.M., LEE, S.H., KIM, Y.J., RYU, S., KIM, Y.H. and YOON, B.W., 2009. Reduced neurogenesis after suppressed inflammation by minocycline in transient cerebral ischemia in rat. *Journal of the neurological sciences,* **279**(1-2), pp. 70-75.

KIM, G.J., SHATZ, C.J. and MCCONNELL, S.K., 1991. Morphology of pioneer and follower growth cones in the developing cerebral cortex. *Journal of neurobiology,* **22**(6), pp. 629-642.

KIM, K.K., ADELSTEIN, R.S. and KAWAMOTO, S., 2009. Identification of neuronal nuclei (NeuN) as Fox-3, a new member of the Fox-1 gene family of splicing factors. *The Journal of biological chemistry,* **284**(45), pp. 31052-31061.

KIM, Y.H., PARK, J.H., HONG, S.H. and KOH, J.Y., 1999. Nonproteolytic neuroprotection by human recombinant tissue plasminogen activator. *Science (New York, N.Y.),* **284**(5414), pp. 647-650.

KINNEY, H.C., HAYNES, R.L., XU, G., ANDIMAN, S.E., FOLKERTH, R.D., SLEEPER, L.A. and VOLPE, J.J., 2012. Neuron deficit in the white matter and subplate in periventricular leukomalacia. *Annals of Neurology,* **71**(3), pp. 397-406.

KINSLEY, C.H., KONEN, C.M., MIELE, J.L., GHIRALDI, L., SVARE, B, 1986.. Intrauterine position modulates maternal behaviors in female mice. *Physiology & behavior.*, **36**(5), 793-9.

KLETKIEWICZ, H., NOWAKOWSKA, A., SIEJKA, A., MILA-KIERZENKOWSKA, C., WOZNIAK, A., CAPUTA, M. and ROGALSKA, J., 2016. Deferoxamine prevents cerebral glutathione and vitamin E depletions in asphyxiated neonatal rats: role of body temperature. *International journal of hyperthermia : the official journal of European Society for Hyperthermic Oncology, North American Hyperthermia Group,* , pp. 1-10.

KLIONSKY, D.J. and EMR, S.D., 2000. Autophagy as a regulated pathway of cellular degradation. *Science (New York, N.Y.),* **290**(5497), pp. 1717-1721.

KNAPP, M., ROMEO, R. and BEECHAM, J., 2007. The economic consequences of autism in the UK.

KNAPP, M., ROMEO, R. and BEECHAM, J., 2009. Economic cost of autism in the UK. *Autism : the international journal of research and practice,* **13**(3), pp. 317-336.

KNIESEL, U., RISAU, W. and WOLBURG, H., 1996. Development of blood-brain barrier tight junctions in the rat cortex. *Brain research.Developmental brain research,* **96**(1-2), pp. 229-240.

KOH, S. and JENSEN, F.E., 2001. Topiramate blocks perinatal hypoxia-induced seizures in rat pups. *Annals of Neurology,* **50**(3), pp. 366-372.

KOIKE, M., SHIBATA, M., TADAKOSHI, M., GOTOH, K., KOMATSU, M., WAGURI, S., KAWAHARA, N., KUIDA, K., NAGATA, S. and KOMINAMI, E., 2008. Inhibition of autophagy prevents hippocampal pyramidal neuron death after hypoxic-ischemic injury. *The American journal of pathology,* **172**(2), pp. 454-469.

KONDO, S., AL-HASANI, H., HOERDER-SUABEDISSEN, A., WANG, W.Z. and MOLNÁR, Z., 2015. Secretory function in subplate neurons during cortical development. *Frontiers in neuroscience,* **9**.

KONDO, S., HINO, S.I., SAITO, A., KANEMOTO, S., KAWASAKI, N., ASADA, R., IZUMI, S., IWAMOTO, H., OKI, M., MIYAGI, H., KANEKO, M., NOMURA, Y., URANO, F. and IMAIZUMI, K., 2012. Activation of OASIS family, ER stress transducers, is dependent on its stabilization. *Cell death and differentiation,* **19**(12), pp. 1939-1949.

KONDO, S., MURAKAMI, T., TATSUMI, K., OGATA, M., KANEMOTO, S., OTORI, K., ISEKI, K., WANAKA, A. and IMAIZUMI, K., 2005. OASIS, a CREB/ATF-family member, modulates UPR signalling in astrocytes. *Nature cell biology,* **7**(2), pp. 186-194.

KONDO, S., SAITO, A., ASADA, R., KANEMOTO, S. and IMAIZUMI, K., 2011. Physiological unfolded protein response regulated by OASIS family members, transmembrane bZIP transcription factors. *IUBMB life,* **63**(4), pp. 233-239.

KORZHEVSKII, D. and KIRIK, O., 2016. Brain microglia and microglial markers. *Neuroscience and behavioral physiology,* **46**(3), pp. 284-290.

KOSTOVIC, I., Molliver, M.E., 1974. New interpretation of laminar development of cerebral-cortex-synaptogenesis in different layers of neopallium in human fetus. *Anatomical Record,* **178**(2), pp. 395-395.

KOSTOVIC, I., 1986. Prenatal development of nucleus basalis complex and related fiber systems in man: a histochemical study. *Neuroscience,* **17**(4), pp. 1047-1077.

KOSTOVIC, I. and GOLDMAN-RAKIC, P.S., 1983. Transient cholinesterase staining in the mediodorsal nucleus of the thalamus and its connections in the developing human and monkey brain. *The Journal of comparative neurology,* **219**(4), pp. 431-447.

KOSTOVIC, I. and JOVANOV-MILOSEVIC, N., 2006. The development of cerebral connections during the first 20-45 weeks' gestation. *Seminars in fetal & neonatal medicine,* **11**(6), pp. 415-422.

KOSTOVIC, I., JOVANOV-MILOSEVIC, N., RADOS, M., SEDMAK, G., BENJAK, V., KOSTOVIC-SRZENTIC, M., VASUNG, L., CULJAT, M., RADOS, M., HUPPI, P. and JUDAS, M., 2014. Perinatal and early postnatal reorganization of the subplate and related cellular compartments in the human cerebral wall as revealed by histological and MRI approaches. *Brain structure & function,* **219**(1), pp. 231-253.

KOS, M., O'BRIEN, S., FLOURIOT, G., GANNON, F., 2000. Tissue-specific expression of multiple mRNA variants of the mouse estrogen receptor α gene. *FEBS letters.*, **477**(1-2), 15-20.

KOSTOVIC, I. and JUDAS, M., 2010. The development of the subplate and thalamocortical connections in the human foetal brain. *Acta Paediatrica (Oslo, Norway : 1992),* **99**(8), pp. 1119-1127.

KOSTOVIC, I. and JUDAS, M., 2007. Transient patterns of cortical lamination during prenatal life: do they have implications for treatment? *Neuroscience and biobehavioral reviews,* **31**(8), pp. 1157-1168.

KOSTOVIC, I. and JUDAS, M., 2006. Prolonged coexistence of transient and permanent circuitry elements in the developing cerebral cortex of fetuses and preterm infants. *Developmental medicine and child neurology,* **48**(5), pp. 388-393.

KOSTOVIC, I., JUDAS, M., RADOS, M. and HRABAC, P., 2002. Laminar organization of the human fetal cerebrum revealed by histochemical markers and magnetic resonance imaging. *Cerebral cortex (New York, N.Y.: 1991),* **12**(5), pp. 536-544.

KOSTOVIC, I., JUDAS, M. and SEDMAK, G., 2011. Developmental history of the subplate zone, subplate neurons and interstitial white matter neurons: relevance for schizophrenia. *International journal of developmental neuroscience : the official journal of the International Society for Developmental Neuroscience,* **29**(3), pp. 193-205.

KOSTOVIC, I. and KRMPOTIC, J., 1976. Early prenatal ontogenesis of the neuronal connections in the interhemispheric cortex of the human gyrus cinguli. *Verhandlungen der Anatomischen Gesellschaft,* **(70 Pt 1)**(70 Pt 1), pp. 305-316.

KOSTOVIC, I. and RAKIC, P., 1990. Developmental history of the transient subplate zone in the visual and somatosensory cortex of the macaque monkey and human brain. *The Journal of comparative neurology,* **297**(3), pp. 441-470.

KOSTOVIC, I. and RAKIC, P., 1984. Development of prestriate visual projections in the monkey and human fetal cerebrum revealed by transient cholinesterase staining. *The Journal of neuroscience : the official journal of the Society for Neuroscience,* **4**(1), pp. 25-42.

KOSTOVIC, I. and RAKIC, P., 1980. Cytology and time of origin of interstitial neurons in the white matter in infant and adult human and monkey telencephalon. *Journal of neurocytology,* **9**(2), pp. 219-242.

KOSTOVIC, I., SEDMAK, G., VUKSIC, M., JUDAS, M., 2015. The relevance of human fetal subplate zone for developmental neuropathology of neuronal migration disorders and cortical dysplasia. *CNS neuroscience & therapeutics.,* **21**(2), 74-82.

KRAJNC, D., NORTON, H.N. and HADJICONSTANTINOU, M., 1996. Glutamate, glutamine and glutamine synthetase in the neonatal rat brain following hypoxia. *Brain research,* **707**(1), pp. 134-137.

KRAJNC, D., WEMLINGER, T.A., NEFF, N.H. and HADJICONSTANTINOU, M., 1994. Neonatal hypoxia: early neurotransmitter responses and the consequences of treatment with GM1 ganglioside. *The Journal of pharmacology and experimental therapeutics,* **271**(3), pp. 1299-1305.

KREGEL, K.C., 2002. Invited review: heat shock proteins: modifying factors in physiological stress responses and acquired thermotolerance. *Journal of applied physiology,* **92**(5), pp. 2177-2186.

KREUTZBERG, G.W., 1996. Microglia: a sensor for pathological events in the CNS. *Trends in neurosciences,* **19**(8), pp. 312-318.

KRIEGSTEIN, A.R. and NOCTOR, S.C., 2004. Patterns of neuronal migration in the embryonic cortex. *Trends in neurosciences,* **27**(7), pp. 392-399.

KRMPOTIC-NEMANIC, J., KOSTOVIC, I., KELOVIC, Z., NEMANIC, D. and MRZLJAK, L., 1983. Development of the human fetal auditory cortex: growth of afferent fibres. *Acta Anatomica,* **116**(1), pp. 69-73.

KRUEGER, S.R., GHISU, G.P., CINELLI, P., GSCHWEND, T.P., OSTERWALDER, T., WOLFER, D.P. and SONDEREGGER, P., 1997. Expression of neuroserpin, an inhibitor of tissue plasminogen activator, in the developing and adult nervous system of the mouse. *The Journal of neuroscience : the official journal of the Society for Neuroscience,* **17**(23), pp. 8984-8996.

KRUGER, O., LADEWIG, J., KOSTER, K. and RAGG, H., 2002. Widespread occurrence of serpin genes with multiple reactive centre-containing exon cassettes in insects and nematodes. *Gene,* **293**(1-2), pp. 97-105.

KRYSTOSEK, A. and SEEDS, N.W., 1981. Plasminogen activator release at the neuronal growth cone. *Science (New York, N.Y.),* **213**(4515), pp. 1532-1534.

KRYSTOSEK, A. and SEEDS, N.W., 1981. Plasminogen activator secretion by granule neurons in cultures of developing cerebellum. *Proceedings of the National Academy of Sciences of the United States of America,* **78**(12), pp. 7810-7814.

KUAN, C., LAWRENCE, D.A., YANG, D.E. and ADHAMI, F., 2010. *Plasminogen activator inhibitor amelioration of newborn hypoxic ischemic brain injury, .*

KUBICKI, M., MCCARLEY, R., WESTIN, C.F., PARK, H.J., MAIER, S., KIKINIS, R., JOLESZ, F.A. and SHENTON, M.E., 2007. A review of diffusion tensor imaging studies in schizophrenia. *Journal of psychiatric research,* **41**(1-2), pp. 15-30.

KUHN, H.G. and COOPER-KUHN, C.M., 2007. Bromodeoxyuridine and the detection of neurogenesis. *Current Pharmaceutical Biotechnology,* **8**(3), pp. 127-131.

KWON, Y.T. and TSAI, L., 1998. A novel disruption of cortical development in p35−/− mice distinct from reeler. *Journal of Comparative Neurology,* **395**(4), pp. 510-522.

KYRIAKOPOULOS, M., BARGIOTAS, T., BARKER, G.J. and FRANGOU, S., 2008. Diffusion tensor imaging in schizophrenia. *European psychiatry : the journal of the Association of European Psychiatrists,* **23**(4), pp. 255-273.

LABAT-MOLEUR, F., GUILLERMET, C., LORIMIER, P., ROBERT, C., LANTUEJOUL, S., BRAMBILLA, E., NEGOESCU, A., 1998. TUNEL apoptotic cell detection in tissue sections: critical evaluation and improvement. *Journal of Histochemistry & Cytochemistry.*, **46**(3), 327-34.

L'ABEE, C., DE VRIES, L.S., VAN DER GROND, J. and GROENENDAAL, F., 2005. Early diffusion-weighted MRI and 1H-Magnetic Resonance Spectroscopy in asphyxiated full-term neonates. *Biology of the neonate,* **88**(4), pp. 306-312.

LADANYI, A., SIPOS, F., SZOKE, D., GALAMB, O., MOLNAR, B. and TULASSAY, Z., 2006. Laser microdissection in translational and clinical research. *Cytometry Part A: The Journal of the International Society for Analytical Cytology,* **69**(9), pp. 947-960.

LAFEMINA, M.J., SHELDON, R.A. and FERRIERO, D.M., 2006. Acute hypoxia-ischemia results in hydrogen peroxide accumulation in neonatal but not adult mouse brain. *Pediatric research,* **59**(5), pp. 680-683.

LAFUENTE, H., ALVAREZ, F.J., PAZOS, M.R., ALVAREZ, A., REY-SANTANO, M.C., MIELGO, V., MURGIA-ESTEVE, X., HILARIO, E., MARTINEZ-ORGADO, J., 2011. Cannabidiol reduces brain damage and improves functional recovery after acute hypoxia-ischemia in newborn pigs. *Pediatric research.,* **70**(3), 272.

LAI, T., JABAUDON, D., MOLYNEAUX, B.J., AZIM, E., ARLOTTA, P., MENEZES, J.R. and MACKLIS, J.D., 2008. SOX5 controls the sequential generation of distinct corticofugal neuron subtypes. *Neuron,* **57**(2), pp. 232-247.

LAI, B.T., CHIN, N.W., STANEK, A.E., KEH, W. and LANKS, K.W., 1984. Quantitation and intracellular localization of the 85K heat shock protein by using monoclonal and polyclonal antibodies. *Molecular and cellular biology,* **4**(12), pp. 2802-2810.

LAI, M.C. and YANG, S.N., 2011. Perinatal hypoxic-ischemic encephalopathy. *Journal of biomedicine & biotechnology,* **2011**, pp. 609813.

LAI, Y., STANGE, C., WISNIEWSKI, S.R., ADELSON, P.D., JANESKO-FELDMAN, K.L., BROWN, D.S., KOCHANEK, P.M. and CLARK, R.S., 2006. Mitochondrial heat shock protein 60 is increased in cerebrospinal fluid following pediatric traumatic brain injury. *Developmental neuroscience,* **28**(4-5), pp. 336-341.

LAKE, B.B., AI R., KAESER, G.E., SALATHIA, N.S., YUNG, Y.C., LIU, R., WILDBERG, A., GAO, D., FUNG, H.L., CHEN, S., VIJAYARAGHAVAN, R., 2016. Neuronal subtypes and diversity revealed by single-nucleus RNA sequencing of the human brain. *Science.,* **352**(6293), 1586-90.

LAM, J.S., ANDERSON, E.M. and HAO, Y., 2014. LPS quantitation procedures. *Methods in molecular biology (Clifton, N.J.),* **1149**, pp. 375-402.

LANSBERG, M.G., BLUHMKI, E. and THIJS, V.N., 2009. Efficacy and safety of tissue plasminogen activator 3 to 4.5 hours after acute ischemic stroke: a metaanalysis. *Stroke,* **40**(7), pp. 2438-2441.

LAPTOOK, A.R., SHANKARAN, S., AMBALAVANAN, N., CARLO, W.A., MCDONALD, S.A., HIGGINS, R.D., DAS, A. and HYPOTHERMIA SUBCOMMITTEE OF THE NICHD NEONATAL RESEARCH NETWORK, 2009. Outcome of term infants using apgar scores at 10 minutes following hypoxic-ischemic encephalopathy. *Pediatrics,* **124**(6), pp. 1619-1626.

LAROIA, N., MCBRIDE, L., BAGGS, R. and GUILLET, R., 1997. Dextromethorphan ameliorates effects of neonatal hypoxia on brain morphology and seizure threshold in rats. *Developmental Brain Research,* **100**(1), pp. 29-34.

LARROCHE, J.C., 1977. *Developmental pathology of the neonate.* Excerpta Medica.

LARROQUE, B., BREART, G., KAMINSKI, M., DEHAN, M., ANDRE, M., BURGUET, A., GRANDJEAN, H., LEDESERT, B., LEVEQUE, C., MAILLARD, F., MATIS, J., ROZE, J.C., TRUFFERT, P. and EPIPAGE STUSY GROUP, 2004. Survival of very preterm infants: Epipage, a population based cohort study. *Archives of disease in childhood.Fetal and neonatal edition,* **89**(2), pp. F139-44.

LAVDAS, A.A., GRIGORIOU, M., PACHNIS, V., PARNAVELAS, J.G., 1999. The medial ganglionic eminence gives rise to a population of early neurons in the developing cerebral cortex. *Journal of Neuroscience.,* **19**(18), 7881-8.

LAWN, J.E., COUSENS, S., ZUPAN, J. and LANCET NEONATAL SURVIVAL STEERING TEAM, 2005. 4 million neonatal deaths: when? Where? Why? *The lancet,* **365**(9462), pp. 891-900.

LAWTON, C., ACOSTA, S., WATSON, N., GONZALES-PORTILLO, C., DIAMANDIS, T., TAJIRI, N., KANEKO, Y., SANBERG, P.R., BORLONGAN, C.V., 2015. Enhancing endogenous stem cells in the newborn via delayed umbilical cord clamping. *Neural regeneration research.,* **10**(9), 1359.

LEBEURRIER, N., LIOT, G., LOPEZ-ATALAYA, J.P., ORSET, C., FERNANDEZ-MONREAL, M., SONDEREGGER, P., ALI, C. and VIVIEN, D., 2005. The brain-specific tissue-type plasminogen activator inhibitor, neuroserpin, protects neurons against excitotoxicity both in vitro and in vivo. *Molecular and Cellular Neuroscience,* **30**(4), pp. 552-558.

LEBEURRIER, N., LIOT, G., LOPEZ-ATALAYA, J., FERNANDEZ-MONREAL, M., SONDEREGGER, P., VIVIEN, D. and ALI, C., 2005. Neuroprotective activity of neuroserpin against NMDA receptor-mediated excitotoxicity. *Journal of Cerebral Blood Flow & Metabolism,* **25**, pp. S455-S455.

LEE, A.S., 1987. Coordinated regulation of a set of genes by glucose and calcium ionophores in mammalian cells. *Trends in biochemical sciences,* **12**, pp. 20-23.

LEE, B.S., WOO, C., KIM, S. and KIM, K., 2010. Long-term neuroprotective effect of postischemic hypothermia in a neonatal rat model of severe hypoxic ischemic encephalopathy: a comparative study on the duration and depth of hypothermia. *Pediatric research,* **68**(4), pp. 303-308.

LEE, T.W., COATES, L.C. and BIRCH, N.P., 2008. Neuroserpin regulates N-cadherin-mediated cell adhesion independently of its activity as an inhibitor of tissue plasminogen activator. *Journal of neuroscience research,* **86**(6), pp. 1243-1253.

LEE, T.W., TSANG, V.W. and BIRCH, N.P., 2015. Physiological and pathological roles of tissue plasminogen activator and its inhibitor neuroserpin in the nervous system. *Frontiers in cellular neuroscience,* **9**.

LEE, A.C., KOZUKI, N., BLENCOWE, H., VOS, T., BAHALIM, A., DARMSTADT, G.L., NIERMEYER, S., ELLIS, M., ROBERTSON, N.J., COUSENS, S. and LAWN, J.E., 2013. Intrapartum-related neonatal encephalopathy incidence and impairment at regional and global levels for 2010 with trends from 1990. *Pediatric research,* **74 Suppl 1**, pp. 50-72.

LEE, A.S., 2005. The ER chaperone and signaling regulator GRP78/BiP as a monitor of endoplasmic reticulum stress. *Methods (San Diego, Calif.),* **35**(4), pp. 373-381.

LEE, A.S., 2001. The glucose-regulated proteins: stress induction and clinical applications. *Trends in biochemical sciences,* **26**(8), pp. 504-510.

LEE, T.W., MONTGOMERY, J.M. and BIRCH, N.P., 2012. The serine protease inhibitor neuroserpin regulates the growth and maturation of hippocampal neurons through a non-inhibitory mechanism. *Journal of neurochemistry,* **121**(4), pp. 561-574.

LEGIDO, A., CLANCY, R.R. and BERMAN, P.H., 1991. Neurologic outcome after electroencephalographically proven neonatal seizures. *Pediatrics,* **88**(3), pp. 583-596.

LEHNARDT, S., MASSILLON, L., FOLLETT, P., JENSEN, F.E., RATAN, R., ROSENBERG, P.A., VOLPE, J.J. and VARTANIAN, T., 2003. Activation of innate immunity in the CNS triggers neurodegeneration through a Toll-like receptor 4-dependent pathway. *Proceedings of the National Academy of Sciences of the United States of America,* **100**(14), pp. 8514-8519.

LEHNARDT, S., SCHOTT, E., TRIMBUCH, T., LAUBISCH, D., KRUEGER, C., WULCZYN, G., NITSCH, R. and WEBER, J.R., 2008. A vicious cycle involving release of heat shock protein 60 from injured cells and activation of toll-like receptor 4 mediates neurodegeneration in the CNS. *The Journal of neuroscience : the official journal of the Society for Neuroscience,* **28**(10), pp. 2320-2331.

LEICA MICROSYSTEMS CAMBRIDGE, L., 2007-last update, Leica FireCam Users Manual. Available: https://meyerinst.com/digital-cameras/leica/ec3/DFC_FireCam.pdf [08/10, 2018].

LEIN, E.S., FINNEY, E.M., MCQUILLEN, P.S. and SHATZ, C.J., 1999. Subplate neuron ablation alters neurotrophin expression and ocular dominance column formation. *Proceedings of the National Academy of Sciences of the United States of America,* **96**(23), pp. 13491-13495.

LEMBERGER, T., PARLATO, R., DASSESSE, D., WESTPHAL, M., CASANOVA, E., TURIAULT, M., TRONCHE, F., SCHIFFMANN, S.N. and SCHÜTZ, G., 2007. Expression of Cre recombinase in dopaminoceptive neurons. *BMC neuroscience,* **8**(1), pp. 4.

LEONARDO, C.C. and PENNYPACKER, K.R., 2009. Neuroinflammation and MMPs: potential therapeutic targets in neonatal hypoxic-ischemic injury. *Journal of neuroinflammation,* **6**, pp. 13-2094-6-13.

LETINIC, K., ZONCU, R., RAKIC, P., 2002. Origin of GABAergic neurons in the human neocortex. *Nature.,* **417**, 645.

LEVENE, M., GRINDULIS, H., SANDS, C. and MOORE, J., 1986. Comparison of two methods of predicting outcome in perinatal asphyxia. *The Lancet,* **327**(8472), pp. 67-69.

LEVITON, A. and GRESSENS, P., 2007. Neuronal damage accompanies perinatal white-matter damage. *Trends in neurosciences,* **30**(9), pp. 473-478.

LEVITON, A., PANETH, N., REUSS, M.L., SUSSER, M., ALLRED, E.N., DAMMANN, O., KUBAN, K., VAN MARTER, L.J., PAGANO, M., HEGYI, T., HIATT, M., SANOCKA, U., SHAHRIVAR, F., ABIRI, M., DISALVO, D., DOUBILET, P., KAIRAM, R., KAZAM, E., KIRPEKAR, M., ROSENFELD, D., SCHONFELD, S., SHARE, J., COLLINS, M., GENEST, D. and SHEN-SCHWARZ, S., 1999. Maternal infection, fetal inflammatory response, and brain damage in very low birth weight infants. Developmental Epidemiology Network Investigators. *Pediatric research,* **46**(5), pp. 566-575.

LEWIS, M.J. and PELHAM, H.R., 1992. Ligand-induced redistribution of a human KDEL receptor from the Golgi complex to the endoplasmic reticulum. *Cell,* **68**(2), pp. 353-364.

LEWIS, M.J. and PELHAM, H.R., 1990. A human homologue of the yeast HDEL receptor. *Nature,* **348**(6297), pp. 162-163.

LI, A.M., CHAU, V., POSKITT, K.J., SARGENT, M.A., LUPTON, B.A., HILL, A., ROLAND, E. and MILLER, S.P., 2009. White matter injury in term newborns with neonatal encephalopathy.
. *Pediatric research,* **61**(1), pp. 85-89.

LI, L., QU, Y., LI, J., XIONG, Y., MAO, M. and MU, D., 2007. Relationship between HIF-1α expression and neuronal apoptosis in neonatal rats with hypoxia–ischemia brain injury. *Brain research,* **1180**, pp. 133-139.

LI, M., YU, A., ZHANG, F., DAI, G., CHENG, H., WANG, X. and AN, Y., 2012. Treatment of one case of cerebral palsy combined with posterior visual pathway injury using autologous bone marrow mesenchymal stem cells. *Journal of translational medicine,* **10**(1), pp. 100.

LI, R. and SHEN, Y., 2013. An old method facing a new challenge: re-visiting housekeeping proteins as internal reference control for neuroscience research. *Life Sciences,* **92**(13), pp. 747-751.

LI, W., ASAKAWA, T., HAN, S., XIAO, B., NAMBA, H., LU, C., DONG, Q. and WANG, L., 2017. Neuroprotective effect of neuroserpin in non-tPA-induced intracerebral hemorrhage mouse models. *BMC neurology,* **17**(1), pp. 196.

LI, C. and JACKSON, R.M., 2002. Reactive species mechanisms of cellular hypoxia-reoxygenation injury. *American journal of physiology.Cell physiology,* **282**(2), pp. C227-41.

LI, W., LI, Y., GUAN, S., FAN, J., CHENG, C.F., BRIGHT, A.M., CHINN, C., CHEN, M. and WOODLEY, D.T., 2007. Extracellular heat shock protein-90alpha: linking hypoxia to skin cell motility and wound healing. *The EMBO journal,* **26**(5), pp. 1221-1233.

LIAO, Y., COTTEN, M., TAN, S., KURTZBERG, J. and CAIRO, M.S., 2013. Rescuing the neonatal brain from hypoxic injury with autologous cord blood. *Bone marrow transplantation,* **48**(7), pp. 890-900.

LIAW, A. and WIENER, M., 2002. Classification and regression by randomForest. *R news,* **2**(3), pp. 18-22.

LICHTMAN, J.W. and CONCHELLO, J.A., 2005. Fluorescence microscopy. *Nature methods,* **2**(12), pp. 910-919.

LIEBLEIN-BOFF, J.C., MCKIM, D.B., SHEA, D.T., WEI, P., DENG, Z., SAWICKI, C., QUAN, N., BILBO, S.D., BAILEY, M.T., MCTIGUE, D.M. and GODBOUT,

J.P., 2013. Neonatal E. coli infection causes neuro-behavioral deficits associated with hypomyelination and neuronal sequestration of iron. *The Journal of neuroscience : the official journal of the Society for Neuroscience,* **33**(41), pp. 16334-16345.

LIGAM, P., HAYNES, R.L., FOLKERTH, R.D., LIU, L., YANG, M., VOLPE, J.J. and KINNEY, H.C., 2009. Thalamic damage in periventricular leukomalacia: novel pathologic observations relevant to cognitive deficits in survivors of prematurity. *Pediatric research,* **65**(5), pp. 524.

LIM, A.L., TAYLOR, D.A., MALONE, D.T., 2012. Consequences of early life MK-801 administration: long-term behavioural effects and relevance to schizophrenia research. *Behavioural brain research.*, **227**(1), 276-86.

LIN, E.P., MILES, L., HUGHES, E.A., MCCANN, J.C., VORHEES, C.V., MCAULIFFE, J.J. and LOEPKE, A.W., 2014. A combination of mild hypothermia and sevoflurane affords long-term protection in a modified neonatal mouse model of cerebral hypoxia-ischemia. *Anesthesia & Analgesia,* **119**(5), pp. 1158-1173.

LIN, W., CHANG, Y., HO, C. and HUANG, C., 2013. Ischemic preconditioning reduces neurovascular damage after hypoxia-ischemia via the cellular inhibitor of apoptosis 1 in neonatal brain. *Stroke,* **44**(1), pp. 162-169.

LINDSAY, S.J., XU, Y., LISGO, S.N., HARKIN, L.F., COPP, A.J., GERRELLI, D., CLOWRY, G.J., TALBOT, A., KEOGH, M.J. and COXHEAD, J., 2016. HDBR expression: a unique resource for global and individual gene expression studies during early human brain development. *Frontiers in neuroanatomy,* **10**, pp. 86.

LISZCZAK, T., HEDLEY-WHYTE, E., ADAMS, J., HAN, D., KOLLURI, V., VACANTI, F., HEROS, R. and ZERVAS, N., 1984. Limitations of tetrazolium salts in delineating infarcted brain. *Acta Neuropathologica,* **65**(2), pp. 150-157.

LIU, Q., ZHANG, H., LIN, J., ZHANG, R., CHEN, S., LIU, W., SUN, M., DU, W., HOU, J. and YU, B., 2017. C1q/TNF-related protein 9 inhibits the cholesterol-induced Vascular smooth muscle cell phenotype switch and cell dysfunction by activating AMP-dependent kinase. *Journal of Cellular and Molecular Medicine,* **21**(11), pp. 2823-2836.

LIU, Y., SILVERSTEIN, F.S., SKOFF, R. and BARKS, J.D., 2002. Hypoxic-ischemic oligodendroglial injury in neonatal rat brain. *Pediatric research,* **51**(1), pp. 25-33.

LIU, S., ZHU, S., ZOU, Y., WANG, T., FU, X., 2015. Knockdown of IL-1β Improves Hypoxia–ischemia Brain Associated with IL-6 Up-regulation in Cell and Animal Models. *Molecular neurobiology.*, **51**(2), 743-52.

LOCHNER, J.E., HONIGMAN, L.S., GRANT, W.F., GESSFORD, S.K., HANSEN, A.B., SILVERMAN, M.A. and SCALETTAR, B.A., 2006. Activity-dependent release of tissue plasminogen activator from the dendritic spines of hippocampal neurons revealed by live-cell imaging. *Journal of neurobiology,* **66**(6), pp. 564-577.

LOCKSHIN, R.A. and ZAKERI, Z., 1994. Programmed cell death: early changes in metamorphosing cells. *Biochemistry and cell biology = Biochimie et biologie cellulaire,* **72**(11-12), pp. 589-596.

LOCKSHIN, R.A., and ZAKERI, Z., 2004. Apoptosis, autophagy, and more. *The international journal of biochemistry & cell biology.,* **36**(12), 2405-19.

LODISH, H.F., 1988. Transport of secretory and membrane glycoproteins from the rough endoplasmic reticulum to the Golgi. A rate-limiting step in protein maturation and secretion. *The Journal of biological chemistry,* **263**(5), pp. 2107-2110.

LOONES, M.T., CHANG, Y. and MORANGE, M., 2000. The distribution of heat shock proteins in the nervous system of the unstressed mouse embryo suggests a role in neuronal and non-neuronal differentiation. *Cell stress & chaperones,* **5**(4), pp. 291-305.

LOPEZ-BENDITO, G. and MOLNAR, Z., 2003. Thalamocortical development: how are we going to get there? *Nature reviews.Neuroscience,* **4**(4), pp. 276-289.

LOREK, A., TAKEI, Y., CADY, E.B., WYATT, J.S., PENRICE, J., EDWARDS, A.D., PEEBLES, D., WYLEZINSKA, M., OWEN-REECE, H. and KIRKBRIDE, V., 1994. Delayed ("secondary") cerebral energy failure after acute hypoxia-ischemia in the newborn piglet: continuous 48-hour studies by phosphorus magnetic resonance spectroscopy. *Pediatric research,* **36**(6), pp. 699-706.

LORENZ, N., LOEF, E.J., VERDON, D.J., CHEN, C.J., MANSELL, C.J., ANGEL, C.E., BROOKS, A.E., DUNBAR, P. and BIRCH, N.P., 2015. Human T cell activation induces synaptic translocation and alters expression of the serine protease inhibitor neuroserpin and its target protease. *Journal of leukocyte biology,* **97**(4), pp. 699-710.

LORON, G., OLIVIER, P., SEE, H., LE SACHE, N., ANGULO, L., BIRAN, V., BRUNELLE, N., BESSON-LESCURE, B., KITZIS, M.D., PANSIOT, J., BINGEN, E., GRESSENS, P., BONACORSI, S. and BAUD, O., 2011. Ciprofloxacin prevents myelination delay in neonatal rats subjected to E. coli sepsis. *Annals of Neurology,* **69**(2), pp. 341-351.

LU, Q.R., PARK, J.K., NOLL, E., CHAN, J.A., ALBERTA, J., YUK, D., ALZAMORA, M.G., LOUIS, D.N., STILES, C.D., ROWITCH, D.H. and BLACK, P.M., 2001. Oligodendrocyte lineage genes (OLIG) as molecular markers for human glial brain tumors. *Proceedings of the National Academy of Sciences of the United States of America,* **98**(19), pp. 10851-10856.

LU, Q.R., YUK, D., ALBERTA, J.A., ZHU, Z., PAWLITZKY, I., CHAN, J., MCMAHON, A.P., STILES, C.D. and ROWITCH, D.H., 2000. Sonic hedgehog--regulated oligodendrocyte lineage genes encoding bHLH proteins in the mammalian central nervous system. *Neuron,* **25**(2), pp. 317-329.

LUBICS, A., REGLŐDI, D., TAMÁS, A., KISS, P., SZALAI, M., SZALONTAY, L. and LENGVÁRI, I., 2005. Neurological reflexes and early motor behavior in rats

subjected to neonatal hypoxic–ischemic injury. *Behavioural brain research,* **157**(1), pp. 157-165.

LUBKE, J. and FELDMEYER, D., 2007. Excitatory signal flow and connectivity in a cortical column: focus on barrel cortex. *Brain structure & function,* **212**(1), pp. 3-17.

LUHMANN, H.J., REIPRICH, R.A., HANGANU, I. and KILB, W., 2000. Cellular physiology of the neonatal rat cerebral cortex: intrinsic membrane properties, sodium and calcium currents. *Journal of neuroscience research,* **62**(4), pp. 574-584.

LUHMANN, H.J., KILB, W., HANGANU-OPATZ, I., 2009. Subplate cells: amplifiers of neuronal activity in the developing cerebral cortex. *Frontiers in neuroanatomy.,* **3**, 19.

LUKIC-PANIN, V., DEGUCHI, K., YAMASHITA, T., SHANG, J., ZHANG, X., TIAN, F., LIU, N., KAWAI, H., MATSUURA, T. and ABE, K., 2010. Free radical scavenger edaravone administration protects against tissue plasminogen activator induced oxidative stress and blood brain barrier damage. *Current neurovascular research,* **7**(4), pp. 319-329.

LUSKIN, M.B. and SHATZ, C.J., 1985. Studies of the earliest generated cells of the cat's visual cortex: cogeneration of subplate and marginal zones. *The Journal of neuroscience : the official journal of the Society for Neuroscience,* **5**(4), pp. 1062-1075.

LUTH, H.J., HEDLICH, A., HILBIG, H., WINKELMANN, E. and MAYER, B., 1994. Morphological analyses of NADPH-diaphorase/nitric oxide synthase positive structures in human visual cortex. *Journal of neurocytology,* **23**(12), pp. 770-782.

LYNGHOLM, M., HOYER, P.E., VORUM, H., NIELSEN, K., EHLERS, N., MOLLGARD, K., 2008. Immunohistochemical markers for corneal stem cells in the early developing human eye. *Experimental eye research.,* **87**(2), 115-21.

MA, J., TONG, Y., YU, D. and MAO, M., 2012. Tissue plasminogen activator-independent roles of neuroserpin in the central nervous system. *Neural regeneration research,* **7**(2), pp. 146.

MA, J., YU, D., TONG, Y. and MAO, M., 2012. Effect of neuroserpin in a neonatal hypoxic-ischemic injury model ex vivo. *Biological research,* **45**(4), pp. 357-362.

MACARRON, R., BANKS, M.N., BOJANIC, D., BURNS, D.J., CIROVIC, D.A., GARYANTES, T., GREEN, D.V., HERTZBERG, R.P., JANZEN, W.P., PASLAY, J.W., SCHOPFER, U., 2011. Impact of high-throughput screening in biomedical research. *Nature reviews Drug discovery.*, **10**(3), 188.

MACARRON, R., and HERTZBERG, R.P., 2011. Design and implementation of high throughput screening assays. *Molecular biotechnology.*, **47**(3), 270-85.

MADANI, R., KOZLOV, S., AKHMEDOV, A., CINELLI, P., KINTER, J., LIPP, H., SONDEREGGER, P. and WOLFER, D.P., 2003. Impaired explorative behavior and

neophobia in genetically modified mice lacking or overexpressing the extracellular serine protease inhibitor neuroserpin. *Molecular and Cellular Neuroscience,* **23**(3), pp. 473-494.

MAGAGNIN, M.G., SERGEANT, K., VAN DEN BEUCKEN, T., ROUSCHOP, K.M., JUTTEN, B., SEIGNEURIC, R., LAMBIN, P., DEVREESE, B., KORITZINSKY, M. and WOUTERS, B.G., 2007. Proteomic analysis of gene expression following hypoxia and reoxygenation reveals proteins involved in the recovery from endoplasmic reticulum and oxidative stress. *Radiotherapy and oncology,* **83**(3), pp. 340-345.

MAGNANI, D., HASENPUSCH-THEIL, K. and THEIL, T., 2013. Gli3 controls subplate formation and growth of cortical axons. *Cerebral cortex (New York, N.Y.: 1991),* **23**(11), pp. 2542-2551.

MAHESH, R., JUNG, H.W., HAN, C., CHO, C. and PARK, Y., 2011. Joongpoongtang 05 (JP05) confers neuroprotection via anti-apoptotic activities in Neuro-2a cells during oxygen–glucose deprivation and reperfusion. *Toxicology in vitro,* **25**(1), pp. 177-184.

MAJ, H., MALLARD, C., EKLIND, S., GUSTAFSON-BRYWE, K. and HAGBERG, H., 2004. Global gene expression in the immature brain after hypoxia-ischemia. *Journal of Cerebral Blood Flow & Metabolism,* **24**(12), pp. 1317-1332.

MAJ, H., MALLARD, C. and HAGBERG, H., 2004. Inflammatory gene profiling in the developing mouse brain after hypoxia-ischemia. *Journal of Cerebral Blood Flow & Metabolism,* **24**(12), pp. 1333-1351.

MALAEB, S. and DAMMANN, O., 2009. Fetal inflammatory response and brain injury in the preterm newborn. *Journal of child neurology,* **24**(9), pp. 1119-1126.

MALAEB, S.N., DAVIS, J.M., PINZ, I.M., NEWMAN, J.L., DAMMANN, O. and RIOS, M., 2014. Effect of sustained postnatal systemic inflammation on hippocampal volume and function in mice. *Pediatric research,* **76**(4), pp. 363-369.

MALATESTA, P., HACK, M.A., HARTFUSS, E., KETTENMANN, H., KLINKERT, W., KIRCHHOFF, F. and GOTZ, M., 2003. Neuronal or glial progeny: regional differences in radial glia fate. *Neuron,* **37**(5), pp. 751-764.

MALLARD, C., DAVIDSON, J.O., TAN, S., GREEN, C.R., BENNET, L., ROBERTSON, N.J. and GUNN, A.J., 2013. Astrocytes and microglia in acute cerebral injury underlying cerebral palsy associated with preterm birth. *Pediatric research,* **75**(1-2), pp. 234-240.

MALLARD, E., WALDVOGEL, H., WILLIAMS, C., FAULL, R. and GLUCKMAN, P., 1995. Repeated asphyxia causes loss of striatal projection neurons in the fetal sheep brain. *Neuroscience,* **65**(3), pp. 827-836.

MALLARD, E., WILLIAMS, C., JOHNSTON, B., GUNNING, M., DAVIS, S. and GLUCKMAN, P., 1995. Repeated episodes of umbilical cord occlusion in fetal sheep

lead to preferential damage to the striatum and sensitize the heart to further insults. *Pediatric research,* **37**(6), pp. 707.

MALLARD, C., WELIN, A.K., PEEBLES, D., HAGBERG, H. and KJELLMER, I., 2003. White matter injury following systemic endotoxemia or asphyxia in the fetal sheep. *Neurochemical research,* **28**(2), pp. 215-223.

MALLARD, E.C., WILLIAMS, C.E., GUNN, A.J., GUNNING, M.I. and GLUCKMAN, P.D., 1993. Frequent episodes of brief ischemia sensitize the fetal sheep brain to neuronal loss and induce striatal injury. *Pediatric research,* **33**(1), pp. 61-65.

MAN, H. and MA, X., 2012. A role for neuroserpin in neuron morphological development. *Journal of neurochemistry,* **121**(4), pp. 495-496.

MANCARCI, B.O., TOKER, L., TRIPATHY, S., LI, B., ROCCO, B., SIBILLE, E., PAVLIDIS, P., 2016. NeuroExpresso: A cross-laboratory database of brain cell-type expression profiles with applications to marker gene identification and bulk brain tissue transcriptome interpretation. *bioRxiv.,* 089219.

MANSON, J.E., 2008. Prenatal exposure to sex steroid hormones and behavioral/cognitive outcomes. *Metabolism.,* **57**, S16-21.

MARIE, Y., SANSON, M., MOKHTARI, K., LEURAUD, P., KUJAS, M., DELATTRE, J.Y., POIRIER, J., ZALC, B. and HOANG-XUAN, K., 2001. OLIG2 as a specific marker of oligodendroglial tumour cells. *Lancet (London, England),* **358**(9278), pp. 298-300.

MARINI, A.M., JIANG, X., WU, X., PAN, H., GUO, Z., MATTSON, M.P., BLONDEAU, N., NOVELLI, A. and LIPSKY, R.H., 2007. Preconditioning and neurotrophins: a model for brain adaptation to seizures, ischemia and other stressful stimuli. *Amino acids,* **32**(3), pp. 299-304.

MARIN-PADILLA, M., 1999. Developmental neuropathology and impact of perinatal brain damage. III: gray matter lesions of the neocortex. *Journal of Neuropathology & Experimental Neurology,* **58**(5), pp. 407-429.

MARIN-PADILLA, M., 1997. Developmental neuropathology and impact of perinatal brain damage. II: white matter lesions of the neocortex. *Journal of neuropathology and experimental neurology,* **56**(3), pp. 219-235.

MARIN-PADILLA, M., 1996. Developmental neuropathology and impact of perinatal brain damage. I: Hemorrhagic lesions of neocortex. *Journal of neuropathology and experimental neurology,* **55**(7), pp. 758-773.

MARKRAM, H., TOLEDO-RODRIGUEZ, M., WANG, Y., GUPTA, A., SILBERBERG, G., WU, C., 2004. Interneurons of the neocortical inhibitory system. *Nature reviews neuroscience.,* **5**(10), 793.

MARLOW, N., WOLKW, D., BRACEWELL, M.A., SAMARA, M., 2005. Neurologic and developmental disability at six years of age after extremely preterm birth. *New England Journal of Medicine.,* **352**(1), 9-19.

MARQUES-SMITH, A., LYNGHOLM, D., KAUFMANN, A.K., STACEY, J.A., HOERDER-SUABEDISSEN, A., BECKER, E.B., WILSON, M.C., MOLNAR, Z. and BUTT, S.J., 2016. A Transient Translaminar GABAergic Interneuron Circuit Connects Thalamocortical Recipient Layers in Neonatal Somatosensory Cortex. *Neuron,* **89**(3), pp. 536-549.

MARRET, S., MUKENDI, R., GADISSEUX, J.F., GRESSENS, P. and EVRARD, P., 1995. Effect of ibotenate on brain development: an excitotoxic mouse model of microgyria and posthypoxic-like lesions. *Journal of neuropathology and experimental neurology,* **54**(3), pp. 358-370.

MARSHALL, N.J., GOODWIN, C.J. and HOLT, S.J., 1995. A critical assessment of the use of microculture tetrazolium assays to measure cell growth and function. *Growth regulation,* **5**(2), pp. 69-84.

MARTIN, L.J., BRAMBRINK, A., KOEHLER, R.C. and TRAYSTMAN, R.J., 1997. Primary sensory and forebrain motor systems in the newborn brain are preferentially damaged by hypoxia-ischemia. *Journal of Comparative Neurology,* **377**(2), pp. 262-285.

MARTIN, N., BOSSENMEYER-POURIE, C., KOZIEL, V., JAZI, R., AUDONNET, S., VERT, P., GUEANT, J.L., DAVAL, J.L. and POURIE, G., 2012. Non-injurious neonatal hypoxia confers resistance to brain senescence in aged male rats. *PloS one,* **7**(11), pp. e48828.

MARTIN, R., MOZET, C., MARTIN, H., WELT, K., ENGEL, C. and FITZL, G., 2011. The effect of Ginkgo biloba extract (EGb 761) on parameters of oxidative stress in different regions of aging rat brains after acute hypoxia. *Aging clinical and experimental research,* **23**(4), pp. 255-263.

MARTINELLO, K.A., SHEPHERD, E., MIDDLETON, P., CROWTHER, C.A., 2017. Allopurinol for women in pregnancy for neuroprotection of the fetus. *Cochrane Database of Systematic Reviews.*, **2017**(12).

MARTINELLO, K., HART, A.R., YAP, S., MITRA, S., ROBERTSON, N.J., 2017. Management and investigation of neonatal encephalopathy: 2017 update. *Archives of Disease in Childhood-Fetal and Neonatal Edition.,* **102**(4), F346-58.

MARTINEZ-BIARGE, M., DIEZ-SEBASTIAN, J., KAPELLOU, O., GINDNER, D., ALLSOP, J.M., RUTHERFORD, M.A. and COWAN, F.M., 2011. Predicting motor outcome and death in term hypoxic-ischemic encephalopathy. *Neurology,* **76**(24), pp. 2055-2061.

MATTSON, A.M., JENSEN, C.O. and DUTCHER, R.A., 1947. Triphenyltetrazolium Chloride as a Dye for Vital Tissues. *Science (New York, N.Y.),* **106**(2752), pp. 294-295.

MATYS, T. and STRICKLAND, S., 2003. Tissue plasminogen activator and NMDA receptor cleavage. *Nature medicine,* **9**(4), pp. 371-2; author reply 372-3.

MAZZIO, E., YOON, K.J. and SOLIMAN, K.F., 2003. Acetyl-L-carnitine cytoprotection against 1-methyl-4-phenylpyridinium toxicity in neuroblastoma cells. *Biochemical pharmacology,* **66**(2), pp. 297-306.

MCADAMS, R.M., FLEISS, B., TRAUDT, C., SCHWENDIMANN, L., SNYDER, J.M., HAYNES, R.L., NATARAJAN, N., GRESSENS, P. and JUUL, S.E., 2017. Long-Term Neuropathological Changes Associated with Cerebral Palsy in a Nonhuman Primate Model of Hypoxic-Ischemic Encephalopathy. *Developmental neuroscience,* **39**(1-4), pp. 124-140.

MCADAMS, R.M., MCPHERSON, R.J., KAPUR, R.P. and JUUL, S.E., 2017. Focal Brain Injury Associated with a Model of Severe Hypoxic-Ischemic Encephalopathy in Nonhuman Primates. *Developmental neuroscience,* **39**(1-4), pp. 107-123.

MCAULIFFE, J.J., LOEPKE, A.W., MILES, L., JOSEPH, B., HUGHES, E. and VORHEES, C.V., 2009. Desflurane, isoflurane, and sevoflurane provide limited neuroprotection against neonatal hypoxia-ischemia in a delayed preconditioning paradigm. *Anesthesiology: The Journal of the American Society of Anesthesiologists,* **111**(3), pp. 533-546.

MCAULIFFE, J.J., MILES, L. and VORHEES, C.V., 2006. Adult neurological function following neonatal hypoxia-ischemia in a mouse model of the term neonate: water maze performance is dependent on separable cognitive and motor components. *Brain research,* **1118**(1), pp. 208-221.

MCCONNELL, S.K., GHOSH, A. and SHATZ, C.J., 1994. Subplate pioneers and the formation of descending connections from cerebral cortex. *The Journal of neuroscience : the official journal of the Society for Neuroscience,* **14**(4), pp. 1892-1907.

MCCONNELL, S.K., GHOSH, A. and SHATZ, C.J., 1989. Subplate neurons pioneer the first axon pathway from the cerebral cortex. *Science (New York, N.Y.),* **245**(4921), pp. 978-982.

MCDONALD, F.B., DEMPSEY, E.M. and O'HALLORAN, K.D., 2016. Early Life Exposure to Chronic Intermittent Hypoxia Primes Increased Susceptibility to Hypoxia-Induced Weakness in Rat Sternohyoid Muscle during Adulthood. *Frontiers in physiology,* **7**, pp. 69.

MCDONALD, J.W., BEHRENS, M.I., CHUNG, C., BHATTACHARYYA, T. and CHOI, D.W., 1997. Susceptibility to apoptosis is enhanced in immature cortical neurons. *Brain research,* **759**(2), pp. 228-232.

MCDONALD, J.W., TRESCHER, W.H., JOHNSTON, M.V., 1990. The selective ionotropic-type quisqualate receptor agonist AMPA is a potent neurotoxin in immature rat brain. Brain research., **526**(1), 165-8.

MCDONALD, J.W., TRESCHER, W.H., JOHNSTON, M.V., 1992. Susceptibility of brain to AMPA induced excitotoxicity transiently peaks during early postnatal development. *Brain research.,* **583**(1-2), 54-70.

MCDONALD, J.W. and JOHNSTON, M.V., 1992. Neuroprotective synergism of 2-amino-3-phosphonoproprionate (D,L-AP3) and MK-801 against ibotenate induced brain injury. *Neuroscience letters,* **145**(2), pp. 213-216.

MCDONALD, J.W., ROESER, N.F., SILVERSTEIN, F.S. and JOHNSTON, M.V., 1989. Quantitative assessment of neuroprotection against NMDA-induced brain injury. *Experimental neurology,* **106**(3), pp. 289-296.

MCDONALD, J.W., SILVERSTEIN, F.S., CARDONA, D., HUDSON, C., CHEN, R. and JOHNSTON, M.V., 1990. Systemic administration of MK-801 protects against N-methyl-D-aspartate- and quisqualate-mediated neurotoxicity in perinatal rats. *Neuroscience,* **36**(3), pp. 589-599.

MCDONALD, J.W., SILVERSTEIN, F.S. and JOHNSTON, M.V., 1989. Neuroprotective effects of MK-801, TCP, PCP and CPP against N-methyl-D-aspartate induced neurotoxicity in an in vivo perinatal rat model. *Brain research,* **490**(1), pp. 33-40.

MCDONALD, J.W., SILVERSTEIN, F.S. and JOHNSTON, M.V., 1988. Neurotoxicity of N-methyl-D-aspartate is markedly enhanced in developing rat central nervous system. *Brain research,* **459**(1), pp. 200-203.

MCDONALD, J.W., UCKELE, J., SILVERSTEIN, F.S. and JOHNSTON, M.V., 1989. HA-966 (1-hydroxy-3-aminopyrrolidone-2) selectively reduces N-methyl-D-aspartate (NMDA)-mediated brain damage. *Neuroscience letters,* **104**(1-2), pp. 167-170.

MCLEAN, C. and FERRIERO, D., 2004. Mechanisms of hypoxic-ischemic injury in the term infant. *Seminars in perinatology,* **28**(6), pp. 425-432.

MCNAMARA, R.K. and SKELTON, R.W., 1993. The neuropharmacological and neurochemical basis of place learning in the Morris water maze. *Brain Research Reviews,* **18**(1), pp. 33-49.

MCPHERSON, R.J. and JUUL, S.E., 2010. Erythropoietin for infants with hypoxic-ischemic encephalopathy. *Current opinion in pediatrics,* **22**(2), pp. 139-145.

MCQUILLEN, P.S. and FERRIERO, D.M., 2005. Perinatal subplate neuron injury: implications for cortical development and plasticity. *Brain pathology (Zurich, Switzerland),* **15**(3), pp. 250-260.

MCQUILLEN, P.S. and FERRIERO, D.M., 2004. Selective vulnerability in the developing central nervous system. *Pediatric neurology,* **30**(4), pp. 227-235.

MCQUILLEN, P.S., SHELDON, R.A., SHATZ, C.J. and FERRIERO, D.M., 2003. Selective vulnerability of subplate neurons after early neonatal hypoxia-ischemia. *The*

Journal of neuroscience : the official journal of the Society for Neuroscience, **23**(8), pp. 3308-3315.

MCRAE, A., GILLAND, E., BONA, E. and HAGBERG, H., 1995. Microglia activation after neonatal hypoxic-ischemia. *Developmental Brain Research,* **84**(2), pp. 245-252.

MELDRUM, B., 1990. Protection against ischaemic neuronal damage by drugs acting on excitatory neurotransmission. *Cerebrovascular and brain metabolism reviews,* **2**(1), pp. 27-57.

MEINECKE, D.L., RAKIC, P., 1992. Expression of GABA and GABAA receptors by neurons of the subplate zone in developing primate occipital cortex: evidence for transient local circuits. *Journal of Comparative Neurology*. **317**(1), 91-101.

MENG, X., KAO, J.P. and KANOLD, P.O., 2014. Differential signaling to subplate neurons by spatially specific silent synapses in developing auditory cortex. *The Journal of neuroscience : the official journal of the Society for Neuroscience,* **34**(26), pp. 8855-8864.

MENT, L.R., DUNCAN, C.C. and EHRENKRANZ, R.A., 1984. Perinatal cerebral infarction. *Annals of Neurology,* **16**(5), pp. 559-568.

MENT, L.R., BADA, H.S., BARNES, P., GRANT, P.E., HIRTZ, D., PAPILE, L.A., PINTO-MARTIN, J., RIVKIN, M. and SLOVIS, T.L., 2002. Practice parameter: neuroimaging of the neonate: report of the Quality Standards Subcommittee of the American Academy of Neurology and the Practice Committee of the Child Neurology Society. *Neurology,* **58**(12), pp. 1726-1738.

MENT, L.R., STEWART, W.B., ARDITO, T.A. and MADRI, J.A., 1991. Beagle pup germinal matrix maturation studies. *Stroke; a journal of cerebral circulation,* **22**(3), pp. 390-395.

MERCURI, E., RICCI, D., COWAN, F.M., LESSING, D., FRISONE, M.F., HAATAJA, L., COUNSELL, S.J., DUBOWITZ, L.M. and RUTHERFORD, M.A., 2000. Head growth in infants with hypoxic-ischemic encephalopathy: correlation with neonatal magnetic resonance imaging. *Pediatrics,* **106**(2 Pt 1), pp. 235-243.

MESTRIL, R., CHI, S.H., SAYEN, M.R. and DILLMANN, W.H., 1994. Isolation of a novel inducible rat heat-shock protein (HSP70) gene and its expression during ischaemia/hypoxia and heat shock. *The Biochemical journal,* **298 Pt 3**, pp. 561-569.

MICHALAK, M., CORBETT, E.F., MESAELI, N., NAKAMURA, K. and OPAS, M., 1999. Calreticulin: one protein, one gene, many functions. *The Biochemical journal,* **344 Pt 2**, pp. 281-292.

MIES, G., ISHIMARU, S., XIE, Y., SEO, K. and HOSSMANN, K., 1991. Ischemic thresholds of cerebral protein synthesis and energy state following middle cerebral artery occlusion in rat. *Journal of Cerebral Blood Flow & Metabolism,* **11**(5), pp. 753-761.

MIGUEL, P.M., SCHUCH, C.P., ROJAS, J.J., CARLETTI, J.V., DECKMANN, I., MARTINATO, L.H.M., PIRES, A.V., BIZARRO, L. and PEREIRA, L.O., 2015. Neonatal hypoxia-ischemia induces attention-deficit hyperactivity disorder-like behavior in rats. *Behavioral neuroscience,* **129**(3), pp. 309.

MIKATI, M.A., ZEINIEH, M.P., KURDI, R.M., HARB, S.A., EL HOKAYEM, J.A., DADERIAN, R.H., SHAMSEDDINE, A., OBEID, M., BITAR, F.F. and EL SABBAN, M., 2005. Long-term effects of acute and of chronic hypoxia on behavior and on hippocampal histology in the developing brain. *Developmental Brain Research,* **157**(1), pp. 98-102.

MIKATI, M.A., EL HOKAYEM, J.A. and EL SABBAN, M.E., 2007. Effects of a single dose of erythropoietin on subsequent seizure susceptibility in rats exposed to acute hypoxia at P10. *Epilepsia,* **48**(1), pp. 175-181.

MIKHAILENKO, V.A., BUTKEVICH, I.P., BAGAEVA, T.R., MAKUKHINA, G.V. and OTELLIN, V.A., 2009. Short- and long-term influences of hypoxia during early postnatal period of development on behavioral and hormonal responses in rats. *Neuroscience letters,* **464**(3), pp. 214-217.

MIKHAILOVA, A., SUNKARA, N. and MCQUILLEN, P.S., 2017. Unbiased Quantification of Subplate Neuron Loss following Neonatal Hypoxia-Ischemia in a Rat Model. *Developmental neuroscience,* **39**(1-4), pp. 171-181.

MILLAR, L.J., 2018. Perinatal and Neonatal Hypoxia Ischaemia: The Unique Challenges of Treating the Infant Brain. In: K. DAS, ed, *Hypoxia and Anoxia.* 1 edn. London, UK: InTechOpen Publishers, .

MILLAR, L.J., SHI, L., HOERDER-SUABEDISSEN, A. and MOLNAR, Z., 2017. Neonatal Hypoxia Ischaemia: Mechanisms, Models, and Therapeutic Challenges. *Frontiers in cellular neuroscience,* **11**, pp. 78.

MILLER, S.P., RAMASWAMY, V., MICHELSON, D., BARKOVICH, A.J., HOLSHOUSER, B., WYCLIFFE, N., GLIDDEN, D.V., DEMING, D., PARTRIDGE, J.C. and WU, Y.W., 2005. Patterns of brain injury in term neonatal encephalopathy. *The Journal of pediatrics,* **146**(4), pp. 453-460.

MILLER, J.A., DING, S.L., SUNKIN, S.M., SMITH, K.A., NG, L., SZAFER, A., EBBERT, A., RILEY, Z.L., ROYALL, J.J., AIONA, K., ARNOLD, J.M., BENNET, C., BERTAGNOLLI, D., BROUNER, K., BUTLER, S., CALDEJON, S., CAREY, A., CUHACIYAN, C., DALLEY, R.A., DEE, N., DOLBEARE, T.A., FACER, B.A., FENG, D., FLISS, T.P., GEE, G., GOLDY, J., GOURLEY, L., GREGOR, B.W., GU, G., HOWARD, R.E., JOCHIM, J.M., KUAN, C.L., LAU, C., LEE, C.K., LEE, F., LEMON, T.A., LESNAR, P., MCMURRAY, B., MASTAN, N., MOSQUEDA, N., NALUAI-CECCHINI, T., NGO, N.K., NYHUS, J., OLDRE, A., OLSON, E., PARENTE, J., PARKER, P.D., PARRY, S.E., STEVENS, A., PLETIKOS, M., REDING, M., ROLL, K., SANDMAN, D., SARREAL, M., SHAPOURI, S., SHAPOVALOVA, N.V., SHEN, E.H., SJOQUIST, N., SLAUGHTERBECK, C.R., SMITH, M., SODT, A.J., WILLIAMS, D., ZOLLEI, L., FISCHL, B., GERSTEIN, M.B., GESCHWIND, D.H., GLASS, I.A., HAWRYLYCZ, M.J., HEVNER, R.F.,

HUANG, H., JONES, A.R., KNOWLES, J.A., LEVITT, P., PHILLIPS, J.W., SESTAN, N., WOHNOUTKA, P., DANG, C., BERNARD, A., HOHMANN, J.G. and LEIN, E.S., 2014. Transcriptional landscape of the prenatal human brain. *Nature,* **508**(7495), pp. 199-206.

MILLER, S.L., WALLACE, E.M. and WALKER, D.W., 2012. Antioxidant therapies: a potential role in perinatal medicine. *Neuroendocrinology,* **96**(1), pp. 13-23.

MILLER, S.P., VIGNERON, D.B., HENRY, R.G., BOHLAND, M.A., CEPPI-COZZIO, C., HOFFMAN, C., NEWTON, N., PARTRIDGE, J.C., FERRIERO, D.M. and BARKOVICH, A.J., 2002. Serial quantitative diffusion tensor MRI of the premature brain: development in newborns with and without injury. *Journal of magnetic resonance imaging : JMRI,* **16**(6), pp. 621-632.

MILLER, S.P., WEISS, J., BARNWELL, A., FERRIERO, D.M., LATAL-HAJNAL, B., FERRER-ROGERS, A., NEWTON, N., PARTRIDGE, J.C., GLIDDEN, D.V., VIGNERON, D.B. and BARKOVICH, A.J., 2002. Seizure-associated brain injury in term newborns with perinatal asphyxia. *Neurology,* **58**(4), pp. 542-548.

MIRANDA, E. and LOMAS, D., 2006. Neuroserpin: a serpin to think about. *Cellular and Molecular Life Sciences CMLS,* **63**(6), pp. 709-722.

MIRANDA, E., MACLEOD, I., DAVIES, M.J., PÉREZ, J., RÖMISCH, K., CROWTHER, D.C. and LOMAS, D.A., 2008. The intracellular accumulation of polymeric neuroserpin explains the severity of the dementia FENIB. *Human molecular genetics,* **17**(11), pp. 1527-1539.

MIRANDA, E., ROMISCH, K. and LOMAS, D.A., 2004. Mutants of neuroserpin that cause dementia accumulate as polymers within the endoplasmic reticulum. *The Journal of biological chemistry,* **279**(27), pp. 28283-28291.

MISHRA, O.P. and DELIVORIA-PAPADOPOULOS, M., 1989. Lipid peroxidation in developing fetal guinea pig brain during normoxia and hypoxia. *Brain research.Developmental brain research,* **45**(1), pp. 129-135.

MISSION, J.P., AUSTIN, C.P., TAKAHASHI, T., CEPKO, C.L. and CAVINESS, V.S.,JR, 1991. The alignment of migrating neural cells in relation to the murine neopallial radial glial fiber system. *Cerebral cortex (New York, N.Y.: 1991),* **1**(3), pp. 221-229.

MITHA, A., FOIX-L'HELIAS, L., ARNAUD, C., MARRET, S., VIEUX, R., AUJARD, Y., THIRIEZ, G., LARROQUE, B., CAMBONIE, G., BURGUET, A., BOILEAU, P., ROZE, J.C., KAMINSKI, M., TRUFFERT, P., ANCEL, P.Y. and EPIPAGE STUDY GROUP, 2013. Neonatal infection and 5-year neurodevelopmental outcome of very preterm infants. *Pediatrics,* **132**(2), pp. e372-80.

MIYATA, H., KAWAKAMI, H., HORI, T. and HIRANO, H., 2001. N-linked oligosaccharides predominantly distribute in rat cerebellar cortex. *Okajimas folia anatomica Japonica,* **78**(4), pp. 129-140.

MIYATA, T., KAWAGUCHI, A., SAITO, K., KAWANO, M., MUTO, T., OGAWA, M., 2004. Asymmetric production of surface-dividing and non-surface-dividing cortical progenitor cells. *Development.,* **131**(13), 3133-45.

MIZUKAWA, K., VINCENT, S.R., MCGEER, P.L. and MCGEER, E.G., 1989. Distribution of reduced-nicotinamide-adenine-dinucleotide-phosphate diaphorase-positive cells and fibers in the cat central nervous system. *The Journal of comparative neurology,* **279**(2), pp. 281-311.

MOHAMMAD, G. and KOWLURU, R.A., 2011. Novel role of mitochondrial matrix metalloproteinase-2 in the development of diabetic retinopathy. *Investigative ophthalmology & visual science,* **52**(6), pp. 3832-3841.

MOHSENIFAR, A., LOTFI, A.S., RANJBAR, B., ALLAMEH, A., ZAKER, F., HASANI, L., ETEMADI KIA, B. and HASANNIA, S., 2007. A study of the oxidation-induced conformational and functional changes in neuroserpin. *Iranian Biomedical Journal,* **11**(1), pp. 41-46.

MOLLGARD, K., DZIEGIELEWSKA, K.M., HOLST, C.B., HABGOOD, M.D. and SAUNDERS, N.R., 2017. Brain barriers and functional interfaces with sequential appearance of ABC efflux transporters during human development. *Scientific reports,* **7**(1), pp. 11603-017-11596-0.

MOLLICA, J.P., OAKHILL, J.S., LAMB, G.D. and MURPHY, R.M., 2009. Are genuine changes in protein expression being overlooked? Reassessing Western blotting. *Analytical Biochemistry,* **386**(2), pp. 270-275.

MOLLIVER, M.E., 1967. An ontogenetic study of evoked somesthetic cortical responses in the sheep. *Progress in brain research,* **26**, pp. 78-91.

MOLNÁR, Z., 2011. *Subplate populations in normal and pathological cortical development,* .

MOLNÁR, Z. and BLAKEMORE, C., 1991. Lack of regional specificity for connections formed between thalamus and cortex in coculture. *Nature,* **351**(6326), pp. 475.

MOLNAR, Z., ADAMS, R. and BLAKEMORE, C., 1998. Mechanisms underlying the early establishment of thalamocortical connections in the rat. *The Journal of neuroscience : the official journal of the Society for Neuroscience,* **18**(15), pp. 5723-5745.

MOLNAR, Z., ADAMS, R., GOFFINET, A.M. and BLAKEMORE, C., 1998. The role of the first postmitotic cortical cells in the development of thalamocortical innervation in the reeler mouse. *The Journal of neuroscience : the official journal of the Society for Neuroscience,* **18**(15), pp. 5746-5765.

MOLNAR, Z. and BLAKEMORE, C., 1995. How do thalamic axons find their way to the cortex? *Trends in neurosciences,* **18**(9), pp. 389-397.

MOLNAR, Z., HIGASHI, S. and LOPEZ-BENDITO, G., 2003. Choreography of early thalamocortical development. *Cerebral cortex (New York, N.Y.: 1991),* **13**(6), pp. 661-669.

MOLNAR, Z., KUROTANI, T., HIGASHI, S., YAMAMOTO, N. and TOYAMA, K., 2003. Development of functional thalamocortical synapses studied with current source-density analysis in whole forebrain slices in the rat. *Brain research bulletin,* **60**(4), pp. 355-371.

MOLYNEAUX, B.J., ARLOTTA, P., MENEZES, J.R. and MACKLIS, J.D., 2007. Neuronal subtype specification in the cerebral cortex. *Nature reviews.Neuroscience,* **8**(6), pp. 427-437.

MOORCRAFT, J., BOLAS, N.M., IVES, N.K., OUWERKERK, R., SMYTH, J., RAJAGOPALAN, B., HOPE, P.L. and RADDA, G.K., 1991. Global and depth resolved phosphorus magnetic resonance spectroscopy to predict outcome after birth asphyxia. *Archives of Disease in Childhood,* **66**(10 Spec No), pp. 1119-1123.

MOORE, A.R., FILIPOVIC, R., MO, Z., RASBAND, M.N., ZECEVIC, N. and ANTIC, S.D., 2009. Electrical excitability of early neurons in the human cerebral cortex during the second trimester of gestation. *Cerebral cortex (New York, N.Y.: 1991),* **19**(8), pp. 1795-1805.

MOORE, C.L., and POWER, K.L., 1992. Variation in maternal care and individual differences in play, exploration, and grooming of juvenile Norway rat offspring. Developmental Psychobiology: *The Journal of the International Society for Developmental Psychobiology.*, **25**(3), 165-82.

MOORE, A.R., ZHOU, W.L., JAKOVCEVSKI, I., ZECEVIC, N., ANTIC, S.D., 2011. Spontaneous electrical activity in the human fetal cortex in vitro. *Journal of Neuroscience.,* **31**(7), 2391-8.

MORIOKA, T., KALEHUA, A.N., STREIT, W.J., 1993. Characterization of microglial reaction after middle cerebral artery occlusion in rat brain. *Journal of Comparative Neurology.*, **327**(1), 123-32.

MORRIS, R., 1984. Developments of a water-maze procedure for studying spatial learning in the rat. *Journal of neuroscience methods,* **11**(1), pp. 47-60.

MORTOLA, J.P., 1999. How newborn mammals cope with hypoxia. *Respiration physiology,* **116**(2), pp. 95-103.

MORTOLA, J.P. and NASO, L., 1998. Thermogenesis in newborn rats after prenatal or postnatal hypoxia. *Journal of applied physiology (Bethesda, Md.: 1985),* **85**(1), pp. 84-90.

MOSS, H.G., BROWN, T.R., WIEST, D.B., JENKINS, D.D., 2018. N-Acetylcysteine rapidly replenishes central nervous system glutathione measured via magnetic resonance spectroscopy in human neonates with hypoxic-ischemic encephalopathy. *Journal of Cerebral Blood Flow & Metabolism.,* **38**(6), 950-8.

MOWRY, B.J. and GRATTEN, J., 2013. The emerging spectrum of allelic variation in schizophrenia: current evidence and strategies for the identification and functional characterization of common and rare variants. *Molecular psychiatry,* **18**(1), pp. 38-52.

MRZLJAK, L., UYLINGS, H.B., KOSTOVIC, I. and VAN EDEN, C.G., 1992. Prenatal development of neurons in the human prefrontal cortex. II. A quantitative Golgi study. *The Journal of comparative neurology,* **316**(4), pp. 485-496.

MRZLJAK, L., UYLINGS, H.B., KOSTOVIC, I. and VAN EDEN, C.G., 1988. Prenatal development of neurons in the human prefrontal cortex: I. A qualitative Golgi study. *The Journal of comparative neurology,* **271**(3), pp. 355-386.

MRZLJAK, L., UYLINGS, H.B., VAN EDEN, C.G. and JUDAS, M., 1990. Neuronal development in human prefrontal cortex in prenatal and postnatal stages. *Progress in brain research,* **85**, pp. 185-222.

MULLEN, R.J., BUCK, C.R. and SMITH, A.M., 1992. NeuN, a neuronal specific nuclear protein in vertebrates. *Development (Cambridge, England),* **116**(1), pp. 201-211.

MÜLLER, C.M. and GRIESINGER, C.B., 1998. Tissue plasminogen activator mediates reverse occlusion plasticity in visual cortex. *Nature neuroscience,* **1**(1), pp. 47.

MUNRO, S. and PELHAM, H.R., 1987. A C-terminal signal prevents secretion of luminal ER proteins. *Cell,* **48**(5), pp. 899-907.

MUNUSWAMY-RAMANUJAM, G., DAI, E., LIU, L., SHNABEL, M., SUN, Y.M., BARTEE, M., LOMAS, D.A. and LUCAS, A.R., 2010. Neuroserpin, a thrombolytic serine protease inhibitor (serpin), blocks transplant vasculopathy with associated modification of T-helper cell subsets. *Thrombosis & Haemostasis,* **103**(3), pp. 545.

MURABE, Y. and SANO, Y., 1982. Morphological studies on neuroglia. V. Microglial cells in the cerebral cortex of the rat, with special reference to their possible involvement in synaptic function. *Cell and tissue research,* **223**(3), pp. 493-506.

MURABE, Y. and SANO, Y., 1982. Morphological studies on neuroglia. VI. Postnatal development of microglial cells. *Cell and tissue research,* **225**(3), pp. 469-485.

MURAI, Y., ISHIBASHI, H., KOYAMA, S. and AKAIKE, N., 1997. Ca2 -activated K currents in rat locus coeruleus neurons induced by experimental ischemia, anoxia, and hypoglycemia. *Journal of neurophysiology,* **78**(5), pp. 2674-2681.

MURAMATSU, K., FUKUDA, A., TOGARI, H., WADA, Y. and NISHINO, H., 1997. Vulnerability to cerebral hypoxic-ischemic insult in neonatal but not in adult rats is in parallel with disruption of the blood-brain barrier. *Stroke; a journal of cerebral circulation,* **28**(11), pp. 2281-8; discussion 2288-9.

MURRAY, D.M., BALA, P., O'CONNOR, C.M., RYAN, C.A., CONNOLLY, S. and BOYLAN, G.B., 2010. The predictive value of early neurological examination in neonatal hypoxic-ischaemic encephalopathy and neurodevelopmental outcome at 24 months. *Developmental medicine and child neurology,* **52**(2), pp. e55-9.

MURRAY, D.M., BOYLAN, G.B., RYAN, C.A. and CONNOLLY, S., 2009. Early EEG findings in hypoxic-ischemic encephalopathy predict outcomes at 2 years. *Pediatrics,* **124**(3), pp. e459-67.

MYERS, M., 1975. Investigation of skin flap necrosis. *Skin flaps.* Little, Brown and Company Boston, pp. 3.

NADARAJAH, B. and PARNAVELAS, J.G., 2002. Modes of neuronal migration in the developing cerebral cortex. *Nature Reviews Neuroscience,* **3**(6), pp. 423.

NAGEL, S., PAPADAKIS, M., PFLEGER, K., GROND-GINSBACH, C., BUCHAN, A. and WAGNER, S., 2012. Microarray analysis of the global gene expression profile following hypothermia and transient focal cerebral ischemia. *Neuroscience,* **208**, pp. 109-122.

NAKAJIMA, W., ISHIDA, A. and TAKADA, G., 1997. Magnesium attenuates a striatal dopamine increase induced by anoxia in the neonatal rat brain: an in vivo microdialysis study. *Pediatric research,* **41**(6), pp. 809-814.

NAKAJIMA, W., ISHIDA, A., LANGE, M.S., GABRIELSON, K.L., WILSON, M.A., MARTIN, L.J., BLUE, M.E. and JOHNSTON, M.V., 2000. Apoptosis has a prolonged role in the neurodegeneration after hypoxic ischemia in the newborn rat. *The Journal of neuroscience : the official journal of the Society for Neuroscience,* **20**(21), pp. 7994-8004.

NALIVAEVA, N.N., FISK, L., AVILES, R.M.C., PLESNEVA, S.A., ZHURAVIN, I.A. and TURNER, A.J., 2003. Effects of prenatal hypoxia on expression of amyloid precursor protein and metallopeptidases in the rat brain. *Letters in Peptide Science,* **10**(5-6), pp. 455-462.

NASH, P., BARRY, M., SEET, B.T., VEUGELERS, K., HOTA, S., HEGER, J., HODGKINSON, C., GRAHAM, K., JACKSON, R.J. and MCFADDEN, G., 2000. Post-translational modification of the myxoma-virus anti-inflammatory serpin SERP-1 by a virally encoded sialyltransferase. *The Biochemical journal,* **347**(Pt 2), pp. 375-382.

NATHANIEL, E.J. and NATHANIEL, D.R., 1981. The reactive astrocyte. *Advances in cellular neurobiology.* Elsevier, pp. 249-301.

NATIONAL CENTRE FOR BIOTECHNOLOGY INFORMATION, US LIBRARY OF MEDICINE. Available: https://www.ncbi.nlm.nih.gov/refseq/ [09/05, 2019].

NATIONAL INSTITUTE OF HEALTH, GOV., 2018-last update, Analyze Menu. Available: https://imagej.nih.gov/ij/docs/menus/analyze.html [08/10, 2018].

NATIONAL INSTITUTE OF HEALTH, GOV., 2018-last update, ImageJ - Image Processing and Analysis in Java. Available: https://imagej.nih.gov/ij/ [08/10, 2018].

NAVAROVA, J., SCHMIDTOVA, M., UJHAZY, E., DUBOVICKY, M. and MACH, M., 2006. Selected biochemical variables in a model of neonatal anoxia in rats. *Neuro endocrinology letters,* **27 Suppl 2**, pp. 78-81.

NAVARRO, D., ALVARADO, M., MORTE, B., BERBEL, D., SESMA, J., PACHECO, P., MORREALE DE ESCOBAR, G., BERNAL, J. and BERBEL, P., 2014. Late maternal hypothyroidism alters the expression of Camk4 in neocortical subplate neurons: a comparison with Nurr1 labeling. *Cerebral cortex (New York, N.Y.: 1991),* **24**(10), pp. 2694-2706.

NECKERS, L., 2007. Heat shock protein 90: the cancer chaperone. *Heat Shock Proteins in Cancer.* Springer, pp. 231-252.

NEIL, J., MILLER, J., MUKHERJEE, P. and HUPPI, P.S., 2002. Diffusion tensor imaging of normal and injured developing human brain - a technical review. *NMR in biomedicine,* **15**(7-8), pp. 543-552.

NESS, J.K., ROMANKO, M.J., ROTHSTEIN, R.P., WOOD, T.L. and LEVISON, S.W., 2001. Perinatal hypoxia-ischemia induces apoptotic and excitotoxic death of periventricular white matter oligodendrocyte progenitors. *Developmental neuroscience,* **23**(3), pp. 203-208.

NEUFELD, M.D., FRIGON, C., GRAHAM, A.S. and MUELLER, B.A., 2005. Maternal infection and risk of cerebral palsy in term and preterm infants. *Journal of perinatology,* **25**(2), pp. 108-113.

NEWELL, D.W., MALOUF, A.T., FRANCK, J.E., 1990. Glutamate-mediated selective vulnerability to ischemia is present in organotypic cultures of hippocampus. *Neuroscience letters.*, **116**(3), 325-30.

NGUYEN, V. and MCQUILLEN, P.S., 2010. AMPA and metabotropic excitoxicity explain subplate neuron vulnerability. *Neurobiology of disease,* **37**(1), pp. 195-207.

NICOLE, O., DOCAGNE, F., ALI, C., MARGAILL, I., CARMELIET, P., MACKENZIE, E.T., VIVIEN, D. and BUISSON, A., 2001. The proteolytic activity of tissue-plasminogen activator enhances NMDA receptor-mediated signaling. *Nature medicine,* **7**(1), pp. 59-64.

NIJBOER, C.H., VAN DER KOOIJ, MICHAEL A, VAN BEL, F., OHL, F., HEIJNEN, C.J. and KAVELAARS, A., 2010. Inhibition of the JNK/AP-1 pathway reduces neuronal death and improves behavioral outcome after neonatal hypoxic–ischemic brain injury. *Brain, behavior, and immunity,* **24**(5), pp. 812-821.

NIJBOER, C.H., GROENENDAAL, F., KAVELAARS, A., HAGBERG, H.H., VAN BEL, F. and HEIJNEN, C.J., 2007. Gender-specific neuroprotection by 2-iminobiotin after hypoxia-ischemia in the neonatal rat via a nitric oxide independent pathway.

Journal of cerebral blood flow and metabolism : official journal of the International Society of Cerebral Blood Flow and Metabolism, **27**(2), pp. 282-292.

NIKOLETOPOULOU, V., MARKAKI, M., PALIKARAS, K., TAVERNARAKIS, N., 2013. Crosstalk between apoptosis, necrosis and autophagy. *Biochimica et Biophysica Acta (BBA)-Molecular Cell Research.,* **1833**(12), 3448-59.

NIKOLOV, N.M. and CUNNINGHAM, A.J., 2003. Mild therapeutic hypothermia to improve the neurologic outcome after cardiac arrest. *Survey of Anesthesiology,* **47**(4), pp. 219-220.

NILSSON, T., JACKSON, M. and PETERSON, P.A., 1989. Short cytoplasmic sequences serve as retention signals for transmembrane proteins in the endoplasmic reticulum. *Cell,* **58**(4), pp. 707-718.

NOBUTA, H., GHIANI, C.A., PAEZ, P.M., SPREUER, V., DONG, H., KORSAK, R.A., MANUKYAN, A., LI, J., VINTERS, H.V., HUANG, E.J., ROWITCH, D.H., SOFRONIEW, M.V., CAMPAGNONI, A.T., DE VELLIS, J. and WASCHEK, J.A., 2012. STAT3-mediated astrogliosis protects myelin development in neonatal brain injury. *Annals of Neurology,* **72**(5), pp. 750-765.

NOCTOR, S.C., FLINT, A.C., WEISSMAN, T.A., WONG, W.S., CLINTON, B.K. and KRIEGSTEIN, A.R., 2002. Dividing precursor cells of the embryonic cortical ventricular zone have morphological and molecular characteristics of radial glia. *The Journal of neuroscience : the official journal of the Society for Neuroscience,* **22**(8), pp. 3161-3173.

NOCTOR, S.C., MARTINEZ-CERDENO, V., IVIC, L. and KRIEGSTEIN, A.R., 2004. Cortical neurons arise in symmetric and asymmetric division zones and migrate through specific phases. *Nature neuroscience,* **7**(2), pp. 136-144.

NOCTOR, S.C., FLINT, A.C., WEISSMAN, T.A., DAMMERMAN, R.S., KRIEGSTEIN, A.R., 2001. Neurons derived from radial glial cells establish radial units in neocortex. *Nature.,* **409**(6821), 714.

NOH, M.R., KIM, S.K., SUN, W., PARK, S.K., CHOI, H.C., LIM, J.H., KIM, I.H., KIM, H.J., KIM, H. and EUN, B.L., 2006. Neuroprotective effect of topiramate on hypoxic ischemic brain injury in neonatal rats. *Experimental neurology,* **201**(2), pp. 470-478.

NOMURA SIAM, I., 2016-last update, Closed Colonies Mouse Jcl:ICR. Available: http://nomura-siam.com/en/animals/jclicr-en/ [09/05, 2018].

NORENBERG, M.D., JAYAKUMAR, A.R., RAMA RAO, K.V. and PANICKAR, K.S., 2007. New concepts in the mechanism of ammonia-induced astrocyte swelling. *Metabolic brain disease,* **22**(3-4), pp. 219-234.

NORENBERG, M.D., RAO, K.V. and JAYAKUMAR, A.R., 2005. Mechanisms of ammonia-induced astrocyte swelling. *Metabolic brain disease,* **20**(4), pp. 303-318.

NORTHINGTON, F.J., CHAVEZ-VALDEZ, R. and MARTIN, L.J., 2011. Neuronal cell death in neonatal hypoxia-ischemia. *Annals of Neurology,* **69**(5), pp. 743-758.

NORTHINGTON, F.J., FERRIERO, D.M., GRAHAM, E.M., TRAYSTMAN, R.J. and MARTIN, L.J., 2001. Early neurodegeneration after hypoxia-ischemia in neonatal rat is necrosis while delayed neuronal death is apoptosis. *Neurobiology of disease,* **8**(2), pp. 207-219.

NORTHINGTON, F.J., GRAHAM, E.M. and MARTIN, L.J., 2005. Apoptosis in perinatal hypoxic–ischemic brain injury: how important is it and should it be inhibited? *Brain Research Reviews,* **50**(2), pp. 244-257.

NORTHINGTON, F.J., ZELAYA, M.E., O'RIORDAN, D.P., BLOMGREN, K., FLOCK, D.L., HAGBERG, H., FERRIERO, D.M. and MARTIN, L.J., 2007. Failure to complete apoptosis following neonatal hypoxia-ischemia manifests as "continuum" phenotype of cell death and occurs with multiple manifestations of mitochondrial dysfunction in rodent forebrain. *Neuroscience,* **149**(4), pp. 822-833.

NOVIKOFF, A.B., 1976. The endoplasmic reticulum: a cytochemist's view (a review). *Proceedings of the National Academy of Sciences of the United States of America,* **73**(8), pp. 2781-2787.

OBATA, K., OIDE, M. and TANAKA, H., 1978. Excitatory and inhibitory actions of GABA and glycine on embryonic chick spinal neurons in culture. *Brain research,* **144**(1), pp. 179-184.

O'BRIEN, J.S. and SAMPSON, E.L., 1965. Myelin Membrane: a molecular abnormality. *Science (New York, N.Y.),* **150**(3703), pp. 1613-1614.

O'CONNELL, B., MORITZ, K., WALKER, D. and DICKINSON, H., 2013. Treatment of pregnant spiny mice at mid gestation with a synthetic glucocorticoid has sex-dependent effects on placental glycogen stores. *Placenta,* **34**(10), pp. 932-940.

OESCHGER, F., 2011. Subplate populations in normal and pathological cortical development. *(Doctoral dissertation, University of Oxford)*.

OESCHGER, F.M., WANG, W.Z., LEE, S., GARCIA-MORENO, F., GOFFINET, A.M., ARBONES, M.L., RAKIC, S. and MOLNAR, Z., 2012. Gene expression analysis of the embryonic subplate. *Cerebral cortex (New York, N.Y.: 1991),* **22**(6), pp. 1343-1359.

OGAWA, Y., TSUJI, M., TANAKA, E., MIYAZATO, M. and HINO, J., 2018. Bone Morphogenetic Protein (BMP)-3b Gene Depletion Causes High Mortality in a Mouse Model of Neonatal Hypoxic-Ischemic Encephalopathy. *Frontiers in neurology,* **9**, pp. 397.

OGDEN, K.K., and TRAYNELIS, S.F., 2011. New advances in NMDA receptor pharmacology. *Trends in pharmacological sciences.*, **32**(12), 726-33.

OGUNI, H., SUGAMA, M. and OSAWA, M., 2008. Symptomatic parieto-occipital epilepsy as sequela of perinatal asphyxia. *Pediatric neurology,* **38**(5), pp. 345-352.

OHSAWA, K., IMAI, Y., KANAZAWA, H., SASAKI, Y. and KOHSAKA, S., 2000. Involvement of Iba1 in membrane ruffling and phagocytosis of macrophages/microglia. *Journal of cell science,* **113 (Pt 17)**, pp. 3073-3084.

OHSAWA, K., IMAI, Y., SASAKI, Y. and KOHSAKA, S., 2004. Microglia/macrophage-specific protein Iba1 binds to fimbrin and enhances its actin-bundling activity. *Journal of neurochemistry,* **88**(4), pp. 844-856.

O'KEEFE, J. and DOSTROVSKY, J., 1971. The hippocampus as a spatial map: Preliminary evidence from unit activity in the freely-moving rat. *Brain research*.

OKIYONEDA, T., HARADA, K., TAKEYA, M., YAMAHIRA, K., WADA, I., SHUTO, T., SUICO, M.A., HASHIMOTO, Y. and KAI, H., 2004. Delta F508 CFTR pool in the endoplasmic reticulum is increased by calnexin overexpression. *Molecular biology of the cell,* **15**(2), pp. 563-574.

OKUSA, C., OESCHGER, F., GINET, V., WANG, W.Z., HOERDER-SUABEDISSEN, A., MATSUYAMA, T., TRUTTMANN, A.C. and MOLNAR, Z., 2014. Subplate in a rat model of preterm hypoxia-ischemia. *Annals of clinical and translational neurology,* **1**(9), pp. 679-691.

OLEY, M., LETZEL, M.C. and RAGG, H., 2004. Inhibition of furin by serpin Spn4A from Drosophila melanogaster. *FEBS letters,* **577**(1-2), pp. 165-169.

OLSON, E.C., 2014. Analysis of preplate splitting and early cortical development illuminates the biology of neurological disease. *Frontiers in pediatrics,* **2**, pp. 121.

OMOUENDZE, P.L., HENRY, V.J., PORTE, B., DUPRÉ, N., CARMELIET, P., GONZALEZ, B.J., MARRET, S. and LEROUX, P., 2013. Hypoxia-ischemia or excitotoxin-induced tissue plasminogen activator-dependent gelatinase activation in mice neonate brain microvessels. *PloS one,* **8**(8), pp. e71263.

O'RAHILLY, R.R. and MÜLLER, F., 2006. *The embryonic human brain: an atlas of developmental stages.* John Wiley & Sons.

ORDONEZ, A., and MARCINIAK, S.J., 2015 Endoplasmic Reticulum Stress and the Protein Overload Response in the Serpinopathies. *InThe Serpin Family,* (pp. 229-251). Springer, Cham.

OSHEROFF, H. and HATTEN, M.E., 2009. Gene expression profiling of preplate neurons destined for the subplate: genes involved in transcription, axon extension, neurotransmitter regulation, steroid hormone signaling, and neuronal survival. *Cerebral cortex (New York, N.Y.: 1991),* **19 Suppl 1**, pp. i126-34.

OSTERWALDER, T., CINELLI, P., BAICI, A., PENNELLA, A., KRUEGER, S.R., SCHRIMPF, S.P., MEINS, M. and SONDEREGGER, P., 1998. The axonally

secreted serine proteinase inhibitor, neuroserpin, inhibits plasminogen activators and plasmin but not thrombin. *Journal of Biological Chemistry,* **273**(4), pp. 2312-2321.

OSTERWALDER, T., CONTARTESE, J., STOECKLI, E.T., KUHN, T.B. and SONDEREGGER, P., 1996. Neuroserpin, an axonally secreted serine protease inhibitor. *The EMBO journal,* **15**(12), pp. 2944-2953.

OSTERWALDER, T., KUHNEN, A., LEISERSON, W.M., KIM, Y.S. and KESHISHIAN, H., 2004. Drosophila serpin 4 functions as a neuroserpin-like inhibitor of subtilisin-like proprotein convertases. *The Journal of neuroscience : the official journal of the Society for Neuroscience,* **24**(24), pp. 5482-5491.

OSTWALD, T.J. and MACLENNAN, D.H., 1974. Isolation of a high affinity calcium-binding protein from sarcoplasmic reticulum. *The Journal of biological chemistry,* **249**(3), pp. 974-979.

OTOYA, R.E., SELTZER, A.M. and DONOSO, A.O., 1997. Acute and long-lasting effects of neonatal hypoxia on ( )-3-[125 I] MK-801 binding to NMDA brain receptors. *Experimental neurology,* **148**(1), pp. 92-99.

OYADOMARI, S. and MORI, M., 2004. Roles of CHOP/GADD153 in endoplasmic reticulum stress. *Cell death and differentiation,* **11**(4), pp. 381.

OZER, E.A., YILMAZ, O., AKHISAROGLU, M., TUNA, B., BAKILER, A.R. and OZER, E., 2002. Heat shock protein 70 expression in neonatal rats after hypoxic stress. *The journal of maternal-fetal & neonatal medicine : the official journal of the European Association of Perinatal Medicine, the Federation of Asia and Oceania Perinatal Societies, the International Society of Perinatal Obstetricians,* **12**(2), pp. 112-117.

PALMER, C., VANNUCCI, R.C. and TOWFIGHI, J., 1990. Reduction of perinatal hypoxic-ischemic brain damage with allopurinol. *Pediatric research,* **27**(4 Pt 1), pp. 332-336.

PANG, Y., RODTS-PALENIK, S., CAI, Z., BENNETT, W.A. and RHODES, P.G., 2005. Suppression of glial activation is involved in the protection of IL-10 on maternal E. coli induced neonatal white matter injury. *Brain research.Developmental brain research,* **157**(2), pp. 141-149.

PANICKAR, K.S. and NORENBERG, M.D., 2005. Astrocytes in cerebral ischemic injury: morphological and general considerations. *Glia,* **50**(4), pp. 287-298.

PARK, C.K., MENDELOW, A.D., GRAHAM, D.I., MCCULLOCH, J., TEASDALE, G.M., 1988. Correlation of triphenyltetrazolium chloride perfusion staining with conventional neurohistology in the detection of early brain ischaemia. *Neuropathology and applied neurobiology.*, **14**(4), 289-98.

PARK, D., SHIN, K., CHOI, E., CHOI, Y., JANG, J., KIM, J., JEONG, H., LEE, W., LEE, Y. and KIM, S.U., 2015. Protective Effects of N-Acetyl-l-Cysteine in Human Oligodendrocyte Progenitor Cells and Restoration of Motor Function in Neonatal

Rats with Hypoxic-Ischemic Encephalopathy. *Evidence-Based Complementary and Alternative Medicine,* **2015**.

PARK, W.S., SUNG, S.I., AHN, S.Y., YOO, H.S., SUNG, D.K., IM, G.H., CHOI, S.J. and CHANG, Y.S., 2015. Hypothermia augments neuroprotective activity of mesenchymal stem cells for neonatal hypoxic-ischemic encephalopathy. *PloS one,* **10**(3), pp. e0120893.

PAROLINI, O., ALVIANO, F., BERGWERF, I., BORASCHI, D., DE BARI, C., DE WAELE, P., DOMINICI, M., EVANGELISTA, M., FALK, W., HENNERBICHLER, S., HESS, D.C., LANZONI, G., LIU, B., MARONGIU, F., MCGUCKIN, C., MOHR, S., NOLLI, M.L., OFIR, R., PONSAERTS, P., ROMAGNOLI, L., SOLOMON, A., SONCINI, M., STROM, S., SURBEK, D., VENKATACHALAM, S., WOLBANK, S., ZEISBERGER, S., ZEITLIN, A., ZISCH, A. and BORLONGAN, C.V., 2010. Toward cell therapy using placenta-derived cells: disease mechanisms, cell biology, preclinical studies, and regulatory aspects at the round table. *Stem cells and development,* **19**(2), pp. 143-154.

PARTANEN, E., KUJALA, T., NAATANEN, R., LIITOLA, A., SAMBETH, A. and HUOTILAINEN, M., 2013. Learning-induced neural plasticity of speech processing before birth. *Proceedings of the National Academy of Sciences of the United States of America,* **110**(37), pp. 15145-15150.

PAULOSE, C.S., CHATHU, F., KHAN, S.R. and KRISHNAKUMAR, A., 2008. Neuroprotective role of Bacopa monnieri extract in epilepsy and effect of glucose supplementation during hypoxia: glutamate receptor gene expression. *Neurochemical research,* **33**(9), pp. 1663-1671.

PAZAITI, A., SOUBASI, V., SPANDOU, E., KARKAVELAS, G., GEORGIOU, T., KARALIS, P. and GUIBA-TZIAMPIRI, O., 2009. Evaluation of long-lasting sensorimotor consequences following neonatal hypoxic-ischemic brain injury in rats: the neuroprotective role of MgSO4. *Neonatology,* **95**(1), pp. 33-40.

PAZOS, M., CINQUINA, V., GOMEZ, A., LAYUNTA, R., SANTOS, M., FERNÁNDEZ-RUIZ, J. and MARTÍNEZ-ORGADO, J., 2012. Cannabidiol administration after hypoxia–ischemia to newborn rats reduces long-term brain injury and restores neurobehavioral function. *Neuropharmacology,* **63**(5), pp. 776-783.

PECHMANN, H. and RUNGE, P., 1894. Oxydation der Formazylverbindungen. II. Mittheilung. *Berichte der deutschen chemischen Gesellschaft,* **27**(3), pp. 2920-2930.

PECHMANN, H. and RUNGE, P., 1894. Oxydation der Formazylverbindungen. *Berichte der deutschen chemischen Gesellschaft,* **27**(1), pp. 323-324.

PEDRAZA, M., HOERDER-SUABEDISSEN, A., ALBERT-MAESTRO, M.A., MOLNAR, Z. and DE CARLOS, J.A., 2014. Extracortical origin of some murine subplate cell populations. *Proceedings of the National Academy of Sciences of the United States of America,* **111**(23), pp. 8613-8618.

PEEBLES, D.M., MILLER, S., NEWMAN, J.P., SCOTT, R. and HANSON, M.A., 2003. The effect of systemic administration of lipopolysaccharide on cerebral haemodynamics and oxygenation in the 0.65 gestation ovine fetus in utero. *BJOG : an international journal of obstetrics and gynaecology,* **110**(8), pp. 735-743.

PEKNY, M. and NILSSON, M., 2005. Astrocyte activation and reactive gliosis. *Glia,* **50**(4), pp. 427-434.

PELHAM, H.R., 1990. The retention signal for soluble proteins of the endoplasmic reticulum. *Trends in biochemical sciences,* **15**(12), pp. 483-486.

PELHAM, H.R., 1989. Heat shock and the sorting of luminal ER proteins. *The EMBO journal,* **8**(11), pp. 3171-3176.

PELLITTERI, R., CATANIA, M.V., BONACCORSO, C.M., RANNO, E., DELL'ALBANI, P. and ZACCHEO, D., 2014. Viability of olfactory ensheathing cells after hypoxia and serum deprivation: Implication for therapeutic transplantation. *Journal of neuroscience research,* **92**(12), pp. 1757-1766.

PENG, Z., LI, J., LI, Y., YANG, X., FENG, S., HAN, S. and LI, J., 2013. Downregulation of miR-181b in mouse brain following ischemic stroke induces neuroprotection against ischemic injury through targeting heat shock protein A5 and ubiquitin carboxyl-terminal hydrolase isozyme L1. *Journal of neuroscience research,* **91**(10), pp. 1349-1362.

PENRICE, J., LOREK, A., CADY, E.B., AMESS, P.N., WYLEZINSKA, M., COOPER, C.E., D'SOUZA, P., BROWN, G.C., KIRKBRIDE, V., EDWARDS, A.D., WYATT, J.S. and REYNOLDS, E.O., 1997. Proton magnetic resonance spectroscopy of the brain during acute hypoxia-ischemia and delayed cerebral energy failure in the newborn piglet. *Pediatric research,* **41**(6), pp. 795-802.

PEREGO, C., FUMAGALLI, S., DE SIMONI, M.G., 2011. Temporal pattern of expression and colocalization of microglia/macrophage phenotype markers following brain ischemic injury in mice. *Journal of neuroinflammation.*, **8**(1), 174.

PEREIRA, D.A., and WILLIAMS, J.A., 2007. Origin and evolution of high throughput screening. *British journal of pharmacology.*, **152**(1), 53-61.

PEREIRA, D.H., BRANCO, L.G., CÁRNIO, E.C. and BARROS, R.C., 2006. nNOS is involved in behavioral thermoregulation of newborn rats during hypoxia. *Physiology & Behavior,* **89**(5), pp. 681-686.

PEREIRA, L.O., ARTENI, N.S., PETERSEN, R.C., DA ROCHA, A.P., ACHAVAL, M. and NETTO, C.A., 2007. Effects of daily environmental enrichment on memory deficits and brain injury following neonatal hypoxia-ischemia in the rat. *Neurobiology of learning and memory,* **87**(1), pp. 101-108.

PERERA, P.N.D., HU, Q., TANG, J., LI, L., BARNHART, M., DOYCHEVA, D.M., ZHANG, J.H. and TANG, J., 2014. Delayed remote ischemic postconditioning

improves long term sensory motor deficits in a neonatal hypoxic ischemic rat model. *PloS one,* **9**(2), pp. e90258.

PERKINS, L., HUGHES, E., SRINIVASAN, L., ALLSOP, J., GLOVER, A., KUMAR, S., FISK, N. and RUTHERFORD, M., 2008. Exploring cortical subplate evolution using magnetic resonance imaging of the fetal brain. *Developmental neuroscience,* **30**(1-3), pp. 211-220.

PERLMAN, J.M., 2006. Summary proceedings from the neurology group on hypoxic-ischemic encephalopathy. *Pediatrics,* **117**(Supplement 1), pp. S28-S33.

PERLMAN, J.M. and RISSER, R., 1993. Severe fetal acidemia: neonatal neurologic features and short-term outcome. *Pediatric neurology,* **9**(4), pp. 277-282.

PERLMAN, J.M., 1997. Intrapartum hypoxic-ischemic cerebral injury and subsequent cerebral palsy: medicolegal issues. *Pediatrics,* **99**(6), pp. 851-859.

PERLMUTTER, D.H., JOSLIN, G., NELSON, P., SCHASTEEN, C., ADAMS, S.P. and FALLON, R.J., 1990. Endocytosis and degradation of alpha 1-antitrypsin-protease complexes is mediated by the serpin-enzyme complex (SEC) receptor. *The Journal of biological chemistry,* **265**(28), pp. 16713-16716.

PETERS, J.M., SILVIS, M.R., ZHEO, D., HAWKINS, J.S., GROSS, C.A., QI, L.S., 2015. Bacterial CRISPR: accomplishments and prospects. *Current opinion in microbiology.*, **27**, 121-6.

PETERSEN, C.C., 2007. The functional organization of the barrel cortex. *Neuron,* **56**(2), pp. 339-355.

PETERSSON, K.H., PINAR, H., STOPA, E.G., FARIS, R.A., SADOWSKA, G.B., HANUMARA, R.C. and STONESTREET, B.S., 2002. White matter injury after cerebral ischemia in ovine fetuses. *Pediatric research,* **51**(6), pp. 768-776.

PETITO, C. and BABIAK, T., 1982. Early proliferative changes in astrocytes in postischemic noninfarcted rat brain. *Annals of Neurology: Official Journal of the American Neurological Association and the Child Neurology Society,* **11**(5), pp. 510-518.

PFEFFER, S.R. and ROTHMAN, J.E., 1987. Biosynthetic protein transport and sorting by the endoplasmic reticulum and Golgi. *Annual Review of Biochemistry,* **56**, pp. 829-852.

PFISTER, G., STROH, C.M., PERSCHINKA, H., KIND, M., KNOFLACH, M., HINTERDORFER, P. and WICK, G., 2005. Detection of HSP60 on the membrane surface of stressed human endothelial cells by atomic force and confocal microscopy. *Journal of cell science,* **118**(Pt 8), pp. 1587-1594.

PICARD, D., 2002. Heat-shock protein 90, a chaperone for folding and regulation. *Cellular and Molecular Life Sciences CMLS,* **59**(10), pp. 1640-1648.

PICHON, C., ARAR, K., STEWART, A.J., DODON, M.D., GAZZOLO, L., COURTOY, P.J., MAYER, R., MONSIGNY, M. and ROCHE, A.C., 1997. Intracellular routing and inhibitory activity of oligonucleopeptides containing a KDEL motif. *Molecular pharmacology,* **51**(3), pp. 431-438.

PINTO, D., PAGNAMENTA, A.T., KLEI, L., ANNEY, R., MERICO, D., REGAN, R., CONROY, J., MAGALHAES, T.R., CORREIA, C., ABRAHAMS, B.S., ALMEIDA, J., BACCHELLI, E., BADER, G.D., BAILEY, A.J., BAIRD, G., BATTAGLIA, A., BERNEY, T., BOLSHAKOVA, N., BOLTE, S., BOLTON, P.F., BOURGERON, T., BRENNAN, S., BRIAN, J., BRYSON, S.E., CARSON, A.R., CASALLO, G., CASEY, J., CHUNG, B.H., COCHRANE, L., CORSELLO, C., CRAWFORD, E.L., CROSSETT, A., CYTRYNBAUM, C., DAWSON, G., DE JONGE, M., DELORME, R., DRMIC, I., DUKETIS, E., DUQUE, F., ESTES, A., FARRAR, P., FERNANDEZ, B.A., FOLSTEIN, S.E., FOMBONNE, E., FREITAG, C.M., GILBERT, J., GILLBERG, C., GLESSNER, J.T., GOLDBERG, J., GREEN, A., GREEN, J., GUTER, S.J., HAKONARSON, H., HERON, E.A., HILL, M., HOLT, R., HOWE, J.L., HUGHES, G., HUS, V., IGLIOZZI, R., KIM, C., KLAUCK, S.M., KOLEVZON, A., KORVATSKA, O., KUSTANOVICH, V., LAJONCHERE, C.M., LAMB, J.A., LASKAWIEC, M., LEBOYER, M., LE COUTEUR, A., LEVENTHAL, B.L., LIONEL, A.C., LIU, X.Q., LORD, C., LOTSPEICH, L., LUND, S.C., MAESTRINI, E., MAHONEY, W., MANTOULAN, C., MARSHALL, C.R., MCCONACHIE, H., MCDOUGLE, C.J., MCGRATH, J., MCMAHON, W.M., MERIKANGAS, A., MIGITA, O., MINSHEW, N.J., MIRZA, G.K., MUNSON, J., NELSON, S.F., NOAKES, C., NOOR, A., NYGREN, G., OLIVEIRA, G., PAPANIKOLAOU, K., PARR, J.R., PARRINI, B., PATON, T., PICKLES, A., PILORGE, M., PIVEN, J., PONTING, C.P., POSEY, D.J., POUSTKA, A., POUSTKA, F., PRASAD, A., RAGOUSSIS, J., RENSHAW, K., RICKABY, J., ROBERTS, W., ROEDER, K., ROGE, B., RUTTER, M.L., BIERUT, L.J., RICE, J.P., SALT, J., SANSOM, K., SATO, D., SEGURADO, R., SEQUEIRA, A.F., SENMAN, L., SHAH, N., SHEFFIELD, V.C., SOORYA, L., SOUSA, I., STEIN, O., SYKES, N., STOPPIONI, V., STRAWBRIDGE, C., TANCREDI, R., TANSEY, K., THIRUVAHINDRAPDURAM, B., THOMPSON, A.P., THOMSON, S., TRYFON, A., TSIANTIS, J., VAN ENGELAND, H., VINCENT, J.B., VOLKMAR, F., WALLACE, S., WANG, K., WANG, Z., WASSINK, T.H., WEBBER, C., WEKSBERG, R., WING, K., WITTEMEYER, K., WOOD, S., WU, J., YASPAN, B.L., ZURAWIECKI, D., ZWAIGENBAUM, L., BUXBAUM, J.D., CANTOR, R.M., COOK, E.H., COON, H., CUCCARO, M.L., DEVLIN, B., ENNIS, S., GALLAGHER, L., GESCHWIND, D.H., GILL, M., HAINES, J.L., HALLMAYER, J., MILLER, J., MONACO, A.P., NURNBERGER, J.I.,JR, PATERSON, A.D., PERICAK-VANCE, M.A., SCHELLENBERG, G.D., SZATMARI, P., VICENTE, A.M., VIELAND, V.J., WIJSMAN, E.M., SCHERER, S.W., SUTCLIFFE, J.S. and BETANCUR, C., 2010. Functional impact of global rare copy number variation in autism spectrum disorders. *Nature,* **466**(7304), pp. 368-372.

PLACENCIA, F.X., KONG, L. and WEISMAN, L.E., 2009. Treatment of methicillin-resistant Staphylococcus aureus in neonatal mice: lysostaphin versus vancomycin. *Pediatric research,* **65**(4), pp. 420-424.

PLUMIER, J.C., ROSS, B.M., CURRIE, R.W., ANGELIDIS, C.E., KAZLARIS, H., KOLLIAS, G. and PAGOULATOS, G.N., 1995. Transgenic mice expressing the

human heat shock protein 70 have improved post-ischemic myocardial recovery. *The Journal of clinical investigation,* **95**(4), pp. 1854-1860.

POGGI, S.H., PARK, J., TOSO, L., ABEBE, D., ROBERSON, R., WOODARD, J.E. and SPONG, C.Y., 2005. No phenotype associated with established lipopolysaccharide model for cerebral palsy. *American Journal of Obstetrics and Gynecology,* **192**(3), pp. 727-733.

POGLEDIC, I., KOSTOVIC, I., FALLET-BIANCO, C., ADLE-BIASSETTE, H., GRESSENS, P. and VERNEY, C., 2014. Involvement of the subplate zone in preterm infants with periventricular white matter injury. *Brain pathology (Zurich, Switzerland),* **24**(2), pp. 128-141.

POLLA, B.S., KANTENGWA, S., FRANCOIS, D., SALVIOLI, S., FRANCESCHI, C., MARSAC, C. and COSSARIZZA, A., 1996. Mitochondria are selective targets for the protective effects of heat shock against oxidative injury. *Proceedings of the National Academy of Sciences of the United States of America,* **93**(13), pp. 6458-6463.

POPOVA, D., KARLSSON, J., JACOBSSON, S.O., 2017. Comparison of neurons derived from mouse P19, rat PC12 and human SH-SY5Y cells in the assessment of chemical-and toxin-induced neurotoxicity. *BMC Pharmacology and Toxicology.*, **18**(1), 42.

PORTER, A.G., and JANICKE, R.U., 1999. Emerging roles of caspase-3 in apoptosis. *Cell death and differentiation.*, **6**(2), 99.

PORTERA-CAILLIAU, C., PRICE, D.L. and MARTIN, L.J., 1997. Excitotoxic neuronal death in the immature brain is an apoptosis-necrosis morphological continuum. *The Journal of comparative neurology,* **378**(1), pp. 70-87.

PORTERA-CAILLIAU, C., PRICE, D.L. and MARTIN, L.J., 1997. Non-NMDA and NMDA receptor-mediated excitotoxic neuronal deaths in adult brain are morphologically distinct: further evidence for an apoptosis-necrosis continuum. *The Journal of comparative neurology,* **378**(1), pp. 88-104.

POURIE, G., BLAISE, S., TRABALON, M., NEDELEC, E., GUEANT, J.L. and DAVAL, J.L., 2006. Mild, non-lesioning transient hypoxia in the newborn rat induces delayed brain neurogenesis associated with improved memory scores. *Neuroscience,* **140**(4), pp. 1369-1379.

PRESLEY, T., VEDAM, K., DRUHAN, L.J. and ILANGOVAN, G., 2010. Hyperthermia-induced Hsp90.eNOS preserves mitochondrial respiration in hyperglycemic endothelial cells by down-regulating Glut-1 and up-regulating G6PD activity. *The Journal of biological chemistry,* **285**(49), pp. 38194-38203.

PRESSLER, R. and AUVIN, S., 2013. Comparison of Brain Maturation among Species: An Example in Translational Research Suggesting the Possible Use of Bumetanide in Newborn. *Frontiers in neurology,* **4**, pp. 36.

PRICE, D.J., JARMAN, A.P., MASON, J.O. and KIND, P.C., 2011. *Building brains: an introduction to neural development.* John Wiley & Sons.

PRICE, D.J., ASLAM, S., TASKER, L. and GILLIES, K., 1997. Fates of the earliest generated cells in the developing murine neocortex. *The Journal of comparative neurology,* **377**(3), pp. 414-422.

PRICE, D.J. and LOTTO, R.B., 1996. Influences of the thalamus on the survival of subplate and cortical plate cells in cultured embryonic mouse brain. *The Journal of neuroscience : the official journal of the Society for Neuroscience,* **16**(10), pp. 3247-3255.

PRYDS, O., GREISEN, G., LOU, H. and FRIIS-HANSEN, B., 1990. Vasoparalysis associated with brain damage in asphyxiated term infants. *The Journal of pediatrics,* **117**(1 Pt 1), pp. 119-125.

PU, Y., GARG, A., CORBY, R., GAO, J.H., ZENG, C.M., PU, Y. and LI, Q.F., 2008. A positive correlation between alpha-glutamate and glutamine on brain 1H-MR spectroscopy and neonatal seizures in moderate and severe hypoxic-ischemic encephalopathy. *AJNR.American journal of neuroradiology,* **29**(2), pp. 216.

PULERA, M.R., ADAMS, L.M., LIU, H., SANTOS, D.G., NISHIMURA, R.N., YANG, F., COLE, G.M. and WASTERLAIN, C.G., 1998. Apoptosis in a neonatal rat model of cerebral hypoxia-ischemia. *Stroke; a journal of cerebral circulation,* **29**(12), pp. 2622-2630.

PUYAL, J., VASLIN, A., MOTTIER, V. and CLARKE, P.G., 2009. Postischemic treatment of neonatal cerebral ischemia should target autophagy. *Annals of Neurology,* **66**(3), pp. 378-389.

QIAN, Z., GILBERT, M.E., COLICOS, M.A., KANDEL, E.R. and KUHL, D., 1993. Tissue-plasminogen activator is induced as an immediate–early gene during seizure, kindling and long-term potentiation.

R CORE TEAM, 2014. R: A language and environment for statistical computing. *R Foundation for Statistical Computing,* .

RABI, Y., RABI, D. and YEE, W., 2007. Room air resuscitation of the depressed newborn: a systematic review and meta-analysis. *Resuscitation,* **72**(3), pp. 353-363.

RAKHADE, S.N. and JENSEN, F.E., 2009. Epileptogenesis in the immature brain: emerging mechanisms. *Nature reviews.Neurology,* **5**(7), pp. 380-391.

RAKHADE, S.N., KLEIN, P.M., HUYNH, T., HILARIO-GOMEZ, C., KOSARAS, B., ROTENBERG, A. and JENSEN, F.E., 2011. Development of later life spontaneous seizures in a rodent model of hypoxia-induced neonatal seizures. *Epilepsia,* **52**(4), pp. 753-765.

RAKIC, P., 1990. Principles of neural cell migration. *Experientia,* **46**(9), pp. 882-891.

RAKIC, S., DAVIS, C., MOLNAR, Z., NIKOLIC, M. and PARNAVELAS, J.G., 2006. Role of p35/Cdk5 in preplate splitting in the developing cerebral cortex. *Cerebral cortex (New York, N.Y.: 1991),* **16 Suppl 1**, pp. i35-45.

RAMPRASAD, M.P., TERPSTRA, V., KONDRATENKO, N., QUEHENBERGER, O. and STEINBERG, D., 1996. Cell surface expression of mouse macrosialin and human CD68 and their role as macrophage receptors for oxidized low density lipoprotein. *Proceedings of the National Academy of Sciences of the United States of America,* **93**(25), pp. 14833-14838.

RASTOGI, R.N., PRICHARD, J.S. and LOWDEN, J.A., 1968. Elevation of phosphorus levels in serum and decreased rain content of gangliosides in rats following neonatal asphyxia. *Pediatric research,* **2**(2), pp. 125-130.

RAVEENDRAN, A.T. and SKARIA, P.C., 2013. Learning and cognitive deficits in hypoxic neonatal rats intensified by BAX mediated apoptosis: protective role of glucose, oxygen, and epinephrine. *The International journal of neuroscience,* **123**(2), pp. 80-88.

REDDY, K., MALLARD, C., GUAN, J., MARKS, K., BENNET, L., GUNNING, M., GUNN, A., GLUCKMAN, P. and WILLIAMS, C., 1998. Maturational change in the cortical response to hypoperfusion injury in the fetal sheep. *Pediatric research,* **43**(5), pp. 674-682.

REDLINE, R.W. and O'RIORDAN, M.A., 2000. Placental lesions associated with cerebral palsy and neurologic impairment following term birth. *Archives of Pathology & Laboratory Medicine,* **124**(12), pp. 1785-1791.

REISS, A.L., KESLER, S.R., VOHR, B., DUNCAN, C.C., KATZ, K.H., PAJOT, S., SCHNEIDER, K.C., MAKUCH, R.W., MENT, L.R., 2004. Sex differences in cerebral volumes of 8-year-olds born preterm. *The Journal of pediatrics.,* **145**(2), 242-249.

RENNIE, J.M., CHORLEY, G., BOYLAN, G.B., PRESSLER, R., NGUYEN, Y. and HOOPER, R., 2004. Non-expert use of the cerebral function monitor for neonatal seizure detection. *Archives of disease in childhood, Fetal and neonatal edition,* **89**(1), pp. F37-40.

REPRESA, A., TREMBLAY, E. and BEN-ARI, Y., 1989. Transient increase of NMDA-binding sites in human hippocampus during development. *Neuroscience letters,* **99**(1-2), pp. 61-66.

REYNOLDS, I.J., and HASTINGS, T.G., 1995. Glutamate induces the production of reactive oxygen species in cultured forebrain neurons following NMDA receptor activation. *Journal of Neuroscience.,* **15**(5), 3318-27.

RICAGNO, S., CACCIA, S., SORRENTINO, G., ANTONINI, G. and BOLOGNESI, M., 2009. Human neuroserpin: structure and time-dependent inhibition. *Journal of Molecular Biology,* **388**(1), pp. 109-121.

RICAGNO, S., PEZZULLO, M., BARBIROLI, A., MANNO, M., LEVANTINO, M., SANTANGELO, M.G., BONOMI, F. and BOLOGNESI, M., 2010. Two latent and two hyperstable polymeric forms of human neuroserpin. *Biophysical journal,* **99**(10), pp. 3402-3411.

RICE, J.E., VANNUCCI, R.C. and BRIERLEY, J.B., 1981. The influence of immaturity on hypoxic-ischemic brain damage in the rat. *Annals of Neurology,* **9**(2), pp. 131-141.

RICE, F.L. and VAN DER LOOS, H., 1977. Development of the barrels and barrel field in the somatosensory cortex of the mouse. *The Journal of comparative neurology,* **171**(4), pp. 545-560.

RICE, M.C. and O'BRIEN, S.J., 1980. Genetic variance of laboratory outbred Swiss mice. *Nature,* **283**(5743), pp. 157-161.

RICHARDSON, B., KORKOLA, S., ASANO, H., CHALLIS, J., POLK, D. and FRASER, M., 1996. Regional blood flow and the endocrine response to sustained hypoxemia in the preterm ovine fetus. *Pediatric research,* **40**(2), pp. 337-343.

RICHARDSON, B.S. and BOCKING, A.D., 1998. Metabolic and circulatory adaptations to chronic hypoxia in the fetus. *Comparative biochemistry and physiology.Part A, Molecular & integrative physiology,* **119**(3), pp. 717-723.

RICHARDSON, B.S., CARMICHAEL, L., HOMAN, J., JOHNSTON, L. and GAGNON, R., 1996. Fetal cerebral, circulatory, and metabolic responses during heart rate decelerations with umbilical cord compression. *American Journal of Obstetrics and Gynecology,* **175**(4 Pt 1), pp. 929-936.

RICHER, L.P., SHEVELL, M.I. and MILLER, S.P., 2001. Diagnostic profile of neonatal hypotonia: an 11-year study. *Pediatric neurology,* **25**(1), pp. 32-37.

RICHER, M.J., KEAYS, C.A., WATERHOUSE, J., MINHAS, J., HASHIMOTO, C. and JEAN, F., 2004. The Spn4 gene of Drosophila encodes a potent furin-directed secretory pathway serpin. *Proceedings of the National Academy of Sciences of the United States of America,* **101**(29), pp. 10560-10565.

RICHETTO, J., CALABRESE, F., MEYER, U. and RIVA, M.A., 2013. Prenatal versus postnatal maternal factors in the development of infection-induced working memory impairments in mice. *Brain, behavior, and immunity,* **33**, pp. 190-200.

RICHTER, K. and BUCHNER, J., 2001. Hsp90: chaperoning signal transduction. *Journal of cellular physiology,* **188**(3), pp. 281-290.

RIIKONEN, R.S., KERO, P.O. and SIMELL, O.G., 1992. Excitatory amino acids in cerebrospinal fluid in neonatal asphysia. *Pediatric neurology,* **8**(1), pp. 37-40.

RIJKEN, D., WIJNGAARDS, G. and WELBERGEN, J., 1980. Relationship between tissue plasminogen activator and the activators in blood and vascular wall. *Thrombosis research,* **18**(6), pp. 815-830.

RIJKEN, D., WIJNGAARDS, G., ZAAL-DE JONG, M. and WELBERGEN, J., 1979. Purification and partial characterization of plasminogen activator from human uterine tissue. *Biochimica et Biophysica Acta (BBA)-Protein Structure,* **580**(1), pp. 140-153.

RIVERA, S., OGIER, C., JOURQUIN, J., TIMSIT, S., SZKLARCZYK, A.W., MILLER, K., GEARING, A.J., KACZMAREK, L., KHRESTCHATISKY, M., 2002. Gelatinase B and TIMP-1 are regulated in a cell-and time-dependent manner in association with neuronal death and glial reactivity after global forebrain ischemia. *European Journal of Neuroscience.,* **15**(1), 19-32.

ROBERTSON, C., FINER, N. and GRACE, M., 1989. School performance of survivors of neonatal encephalopathy associated with birth asphyxia at term. *The Journal of pediatrics,* **114**(5), pp. 753-760.

ROBERTSON, N.J. and IWATA, O., 2007. Bench to bedside strategies for optimizing neuroprotection following perinatal hypoxia–ischaemia in high and low resource settings. *Early human development,* **83**(12), pp. 801-811.

ROBERTSON, C. and FINER, N., 1985. Term infants with hypoxic-ischemic encephalopathy: outcome at 3.5 years. *Developmental medicine and child neurology,* **27**(4), pp. 473-484.

ROBERTSON, J.D., ENOKSSON, M., SUOMELA, M., ZHIVOTOVSKY, B. and ORRENIUS, S., 2002. Caspase-2 acts upstream of mitochondria to promote cytochrome c release during etoposide-induced apoptosis. *The Journal of biological chemistry,* **277**(33), pp. 29803-29809.

ROBERTSON, N.J., COWAN, F.M., COX, I.J. and EDWARDS, A.D., 2002. Brain alkaline intracellular pH after neonatal encephalopathy. *Annals of Neurology,* **52**(6), pp. 732-742.

ROBERTSON, N.J., COX, I.J., COWAN, F.M., COUNSELL, S.J., AZZOPARDI, D. and EDWARDS, A.D., 1999. Cerebral intracellular lactic alkalosis persisting months after neonatal encephalopathy measured by magnetic resonance spectroscopy. *Pediatric research,* **46**(3), pp. 287-296.

ROBERTSON, R.T., ANNIS, C.M., BARATTA, J., HARALDSON, S., INGEMAN, J., KAGEYAMA, G.H., KIMM, E. and YU, J., 2000. Do subplate neurons comprise a transient population of cells in developing neocortex of rats? *The Journal of comparative neurology,* **426**(4), pp. 632-650.

ROBILLARD, K.N., LEE, K.M., CHIU, K.B. and MACLEAN, A.G., 2016. Glial cell morphological and density changes through the lifespan of rhesus macaques. *Brain, behavior, and immunity,* **55**, pp. 60-69.

ROBINSON, S., LI, Q., DECHANT, A. and COHEN, M.L., 2006. Neonatal loss of gamma-aminobutyric acid pathway expression after human perinatal brain injury. *Journal of neurosurgery,* **104**(6 Suppl), pp. 396-408.

ROCHA-FERREIRA, E. and HRISTOVA, M., 2015. Antimicrobial peptides and complement in neonatal hypoxia-ischemia induced brain damage. *Frontiers in immunology,* **6**, pp. 56.

ROCHA-MARTINS, M., NJAINE, B. and SILVEIRA, M.S., 2012. Avoiding pitfalls of internal controls: validation of reference genes for analysis by qRT-PCR and Western blot throughout rat retinal development. *PloS one,* **7**(8), pp. e43028.

ROCKEFELLER UNIVERSITY, U., 2018-last update, GENSAT Gene Expression Nervous System Atlas. Available: http://www.gensat.org/ [08/10, 2018].

ROCKLAND, K.S., DEFELIPE, J., 2018. Editorial: Why Have Cortical Layers? What Is the Function of Layering? Do Neurons in Cortex Integrate Information Across Different Layers? *Frontiers in Neuroanatomy.,* **12**, 78.

RODEWALD, A.K., ONDERDONK, A.B., WARREN, H.B. and KASPER, D.L., 1992. Neonatal mouse model of group B streptococcal infection. *The Journal of infectious diseases,* **166**(3), pp. 635-639.

RODRIGUEZ-ALVAREZ, N., JIMENEZ-MATEOS, E.M., DUNLEAVY, M., WADDINGTON, J.L., BOYLAN, G.B. and HENSHALL, D.C., 2015. Effects of hypoxia-induced neonatal seizures on acute hippocampal injury and later-life seizure susceptibility and anxiety-related behavior in mice. *Neurobiology of disease,* **83**, pp. 100-114.

RODRÍGUEZ-GONZÁLEZ, R., AGULLA, J., PÉREZ-MATO, M., SOBRINO, T. and CASTILLO, J., 2011. Neuroprotective effect of neuroserpin in rat primary cortical cultures after oxygen and glucose deprivation and tPA. *Neurochemistry international,* **58**(3), pp. 337-343.

RODRÍGUEZ-GONZÁLEZ, R., MILLÁN, M., SOBRINO, T., MIRANDA, E., BREA, D., PEREZ DE LA OSSA, NATALIA, BLANCO, M., PÉREZ, J., DORADO, L. and CASTELLANOS, M., 2011. The natural tissue plasminogen activator inhibitor neuroserpin and acute ischaemic stroke outcome. *Thrombosis and haemostasis,* **105**(3), pp. 421.

RODRÍGUEZ-GONZÁLEZ, R., SOBRINO, T., RODRÍGUEZ-YÁÑEZ, M., MILLÁN, M., BREA, D., MIRANDA, E., MOLDES, O., PÉREZ, J., LOMAS, D.A. and LEIRA, R., 2011. Association between neuroserpin and molecular markers of brain damage in patients with acute ischemic stroke. *J Transl Med,* **9**(1), pp. 58.

RODTS-PALENIK, S., WYATT-ASHMEAD, J., PANG, Y., THIGPEN, B., CAI, Z., RHODES, P., MARTIN, J.N., GRANGER, J. and BENNETT, W.A., 2004. Maternal infection-induced white matter injury is reduced by treatment with interleukin-10. *American Journal of Obstetrics and Gynecology,* **191**(4), pp. 1387-1392.

ROGALSKA, J. and CAPUTA, M., 2010. Neonatal asphyxia under hyperthermic conditions alters HPA axis function in juvenile rats. *Neuroscience letters,* **472**(1), pp. 68-72.

ROGALSKA, J., DANIELISOVA, V. and CAPUTA, M., 2006. Effect of neonatal body temperature on postanoxic, potentially neurotoxic iron accumulation in the rat brain. *Neuroscience letters,* **393**(2-3), pp. 249-254.

ROGALSKA, J., KANG, P., WOTHERSPOON, W., MACLEOD, M.R. and LAI, M., 2009. Effect of hyperthermia and anoxia on glucocorticoid and mineralocorticoid receptor expression in neonatal rat hippocampus. *Neuroscience letters,* **450**(2), pp. 196-200.

ROGNLIEN, A.G.W., WOLLEN, E.J., ATNEOSEN-ÅSEGG, M. and SAUGSTAD, O.D., 2014. Increased expression of inflammatory genes in the neonatal mouse brain after hyperoxic reoxygenation. *Pediatric research,* **77**(2), pp. 326-333.

ROGOVE, A.D., SIAO, C., KEYT, B., STRICKLAND, S. and TSIRKA, S.E., 1999. Activation of microglia reveals a non-proteolytic cytokine function for tissue plasminogen activator in the central nervous system. *Journal of cell science,* **112 (Pt 22)**(Pt 22), pp. 4007-4016.

RON, D. and HABENER, J.F., 1992. CHOP, a novel developmentally regulated nuclear protein that dimerizes with transcription factors C/EBP and LAP and functions as a dominant-negative inhibitor of gene transcription. *Genes & development,* **6**(3), pp. 439-453.

ROOHEY, T., RAJU, T.N. and MOUSTOGIANNIS, A.N., 1997. Animal models for the study of perinatal hypoxic-ischemic encephalopathy: a critical analysis. *Early human development,* **47**(2), pp. 115-146.

RORKE, L.B., 1992. Anatomical Features of the Developing Brain Implicated in Pathogenesis of Hypoxic-Ischemic Injury. *Brain Pathology,* **2**(3), pp. 211-221.

ROTH, S.C., EDWARDS, A.D., CADY, E.B., DELPY, D.T., WYATT, J.S., AZZOPARDI, D., BAUDIN, J., TOWNSEND, J., STEWART, A.L. and REYNOLDS, E.O., 1992. Relation between cerebral oxidative metabolism following birth asphyxia, and neurodevelopmental outcome and brain growth at one year. *Developmental medicine and child neurology,* **34**(4), pp. 285-295.

ROSSANT, J., and MCMAHON, A., 1999. “Cre”-ating mouse mutants—a meeting review on conditional mouse genetics. *Genes & development.*, **13**(2), 142-5.

ROTSTEIN, M., BASSAN, H., KARIV, N., SPEISER, Z., HAREL, S. and GOZES, I., 2006. NAP enhances neurodevelopment of newborn apolipoprotein E-deficient mice subjected to hypoxia. *The Journal of pharmacology and experimental therapeutics,* **319**(1), pp. 332-339.

ROUSSET, C.I., CHALON, S., CANTAGREL, S., BODARD, S., ANDRES, C., GRESSENS, P. and SALIBA, E., 2006. Maternal exposure to LPS induces hypomyelination in the internal capsule and programmed cell death in the deep gray matter in newborn rats. *Pediatric research,* **59**(3), pp. 428-433.

ROUSSET, C.I., KASSEM, J., AUBERT, A., PLANCHENAULT, D., GRESSENS, P., CHALON, S., BELZUNG, C. and SALIBA, E., 2013. Maternal exposure to lipopolysaccharide leads to transient motor dysfunction in neonatal rats. *Developmental neuroscience,* **35**(2-3), pp. 172-181.

RUGG, M.D., 2013. *Cognitive neuroscience.* Psychology Press.

RUIZ, C.C.U., ROSADO-DE-CASTRO, P.H., MENDEZ-OTERO, R. and PIMENTEL-COELHO, P.M., 2017. Mesenchymal Stromal Cell Therapy for Neonatal Hypoxic-Ischemic Encephalopathy. *Neurological Regeneration.* Springer, pp. 105-120.

RUIZ, S., DIEP, D., GORE, A., PANOPOULOS, A.D., MONTSERRAT, N., PLONGTHONGKUM, N., KUMAR, S., FUNG, H.L., GIORGETTI, A., BILIC, J., BATCHELDER, E.M., ZAEHRES, H., KAN, N.G., SCHOLER, H.R., MERCOLA, M., ZHANG, K. and IZPISUA BELMONTE, J.C., 2012. Identification of a specific reprogramming-associated epigenetic signature in human induced pluripotent stem cells. *Proceedings of the National Academy of Sciences of the United States of America,* **109**(40), pp. 16196-16201.

RUTH, V.J. and RAIVIO, K.O., 1988. Perinatal brain damage: predictive value of metabolic acidosis and the Apgar score. *BMJ (Clinical research ed.),* **297**(6640), pp. 24-27.

RUTHERFORD, M., COUNSELL, S., ALLSOP, J., BOARDMAN, J., KAPELLOU, O., LARKMAN, D., HAJNAL, J., EDWARDS, D. and COWAN, F., 2004. Diffusion-weighted magnetic resonance imaging in term perinatal brain injury: a comparison with site of lesion and time from birth. *Pediatrics,* **114**(4), pp. 1004-1014.

RUTHERFORD, M.A., PENNOCK, J.M., COUNSELL, S.J., MERCURI, E., COWAN, F.M., DUBOWITZ, L.M. and EDWARDS, A.D., 1998. Abnormal magnetic resonance signal in the internal capsule predicts poor neurodevelopmental outcome in infants with hypoxic-ischemic encephalopathy. *Pediatrics,* **102**(2 Pt 1), pp. 323-328.

RUZAFA, N., REY-SANTANO, C., MIELGO, V., PEREIRO, X., VECINO, E., 2017. Effect of hypoxia on the retina and superior colliculus of neonatal pigs. *PloS one.*, **12**(4), e0175301.

RYOU, M.G., and MALLET, R.T., 2018. An In Vitro Oxygen–Glucose Deprivation Model for Studying Ischemia–Reperfusion Injury of Neuronal Cells. In *Traumatic and Ischemic Injury*, (pp. 229-235). Humana Press, New York, NY.

SAADANI-MAKKI, F., KANNAN, S., LU, X., JANISSE, J., DAWE, E., EDWIN, S., ROMERO, R. and CHUGANI, D., 2008. Intrauterine administration of endotoxin leads to motor deficits in a rabbit model: a link between prenatal infection and cerebral palsy. *American Journal of Obstetrics and Gynecology,* **199**(6), pp. 651.e1-651.e7.

SABIR, H., OSREDKAR, D., MAES, E., WOOD, T. and THORESEN, M., 2016. Xenon Combined with Therapeutic Hypothermia Is Not Neuroprotective after Severe Hypoxia-Ischemia in Neonatal Rats. *PloS one,* **11**(6), pp. e0156759.

SADLER, T.W., 2011. *Langman's medical embryology.* Lippincott Williams & Wilkins.

SAKURADA, O., KENNEDY, C., JEHLE, J., BROWN, J.D., CARBIN, G.L. and SOKOLOFF, L., 1978. Measurement of local cerebral blood flow with iodo [14C] antipyrine. *The American Journal of Physiology,* **234**(1), pp. H59-66.

SALHAB, W.A., PERLMAN, J.M., SILVER, L. and BROYLES, R.S., 2004. Necrotizing enterocolitis and neurodevelopmental outcome in extremely low birth weight infants< 1000 g. *Journal of Perinatology,* **24**(9), pp. 534-540.

SALHAB, W.A., WYCKOFF, M.H., LAPTOOK, A.R. and PERLMAN, J.M., 2004. Initial hypoglycemia and neonatal brain injury in term infants with severe fetal acidemia. *Pediatrics,* **114**(2), pp. 361-366.

SALO, D.C., DONOVAN, C.M. and DAVIES, K.J., 1991. HSP70 and other possible heat shock or oxidative stress proteins are induced in skeletal muscle, heart, and liver during exercise. *Free Radical Biology and Medicine,* **11**(3), pp. 239-246.

SAMAIYA, P.K. and KRISHNAMURTHY, S., 2015. Characterization of mitochondrial bioenergetics in neonatal anoxic model of rats. *Journal of Bioenergetics and Biomembranes,* **47**(3), pp. 217-222.

SAMPATH, D., SHMUELI, D., WHITE, A.M. and RAOL, Y.H., 2015. Flupirtine effectively prevents development of acute neonatal seizures in an animal model of global hypoxia. *Neuroscience letters,* **607**, pp. 46-51.

SANCHES, E.F., ARTENI, N.S., SPINDLER, C., MOYSÉS, F., SIQUEIRA, I.R., PERRY, M.L. and NETTO, C.A., 2012. Effects of pre-and postnatal protein malnutrition in hypoxic–ischemic rats. *Brain research,* **1438**, pp. 85-92.

SANCHES, E., ARTENI, N., NICOLA, F., BOISSERAND, L., WILLBORN, S. and NETTO, C., 2013. Early hypoxia–ischemia causes hemisphere and sex-dependent cognitive impairment and histological damage. *Neuroscience,* **237**, pp. 208-215.

SANTIAGO, A.R., BAPTISTA, F.I., SANTOS, P.F., CRISTOVAO, G., AMBROSIO, A.F., CUNHA, R.A. and GOMES, C.A., 2014. Role of microglia adenosine A(2A) receptors in retinal and brain neurodegenerative diseases. *Mediators of inflammation,* **2014**, pp. 465694.

SARNAT, H.B., NOCHLIN, D. and BORN, D.E., 1998. Neuronal nuclear antigen (NeuN): a marker of neuronal maturation in early human fetal nervous system. *Brain & development,* **20**(2), pp. 88-94.

SATO, Y., HAYAKAWA, M., IWATA, O., OKUMURA, A., KATO, T., HAYAKAWA, F., KUBOTA, T., MARUYAMA, K., HASEGAWA, M., SATO, M.,

OSHIRO, M., KITO, O. and KOJIMA, S., 2008. Delayed neurological signs following isolated parasagittal injury in asphyxia at term. *European journal of paediatric neurology : EJPN : official journal of the European Paediatric Neurology Society,* **12**(5), pp. 359-365.

SAUGSTAD, O., 1996. Mechanisms of tissue injury by oxygen radicals: implications for neonatal disease. *Acta Paediatrica,* **85**(1), pp. 1-4.

SAUNDERS, N.R., DREIFUSS, J.J., DZIEGIELEWSKA, K.M., JOHANSSON, P.A., HABGOOD, M.D., MOLLGARD, K. and BAUER, H.C., 2014. The rights and wrongs of blood-brain barrier permeability studies: a walk through 100 years of history. *Frontiers in neuroscience,* **8**, pp. 404.

SAUNDERS, N.R., HABGOOD, M.D. and DZIEGIELEWSKA, K.M., 1999. Barrier mechanisms in the brain, II. Immature brain. *Clinical and experimental pharmacology & physiology,* **26**(2), pp. 85-91.

SAUNDERS, N.R., LIDDELOW, S.A. and DZIEGIELEWSKA, K.M., 2012. Barrier mechanisms in the developing brain. *Frontiers in pharmacology,* **3**, pp. 46.

SAVARD, A., BROCHU, M., CHEVIN, M., GUIRAUT, C., GRBIC, D. and SÉBIRE, G., 2015. Neuronal self-injury mediated by IL-1β and MMP-9 in a cerebral palsy model of severe neonatal encephalopathy induced by immune activation plus hypoxia-ischemia. *Journal of neuroinflammation,* **12**(1), pp. 111.

SAVMAN, K., BLENNOW, M., GUSTAFSON, K., TARKOWSKI, E. and HAGBERG, H., 1998. Cytokine response in cerebrospinal fluid after birth asphyxia. *Pediatric research,* **43**(6), pp. 746-751.

SAYANI, A.P. and CHIEN, Y.W., 1996. Systemic delivery of peptides and proteins across absorptive mucosae. *Critical reviews in therapeutic drug carrier systems,* **13**(1-2), pp. 85-184.

SCHANNE, F.A., KANE, A.B., YOUNG, E.E. and FARBER, J.L., 1979. Calcium dependence of toxic cell death: a final common pathway. *Science (New York, N.Y.),* **206**(4419), pp. 700-702.

SCHEEPENS, A., WASSINK, G., PIERSMA, M.J., VAN DE BERG, W.D. and BLANCO, C.E., 2003. A delayed increase in hippocampal proliferation following global asphyxia in the neonatal rat. *Brain research.Developmental brain research,* **142**(1), pp. 67-76.

SCHNEIDER, C.A., RASBAND, W.S. and ELICEIRI, K.W., 2012. NIH Image to ImageJ: 25 years of image analysis. *Nature methods,* **9**(7), pp. 671-675.

SCHOENWOLF, G.C., BLEYL, S.B., BRAUER, P.R. and FRANCIS-WEST, P.H., 2014. *Larsen's human embryology.* Elsevier Health Sciences.

SCHRIMPF, S.P., BLEIKER, A.J., BRECEVIC, L., KOZLOV, S.V., BERGER, P., OSTERWALDER, T., KRUEGER, S.R., SCHINZEL, A. and SONDEREGGER, P.,

1997. Human neuroserpin (PI12): cDNA cloning and chromosomal localization to 3q26. *Genomics,* **40**(1), pp. 55-62.

SCHRODER, M. and KAUFMAN, R.J., 2005. ER stress and the unfolded protein response. *Mutation research,* **569**(1-2), pp. 29-63.

SCHULZE, C. and FIRTH, J.A., 1992. Interendothelial junctions during blood-brain barrier development in the rat: morphological changes at the level of individual tight junctional contacts. *Brain research.Developmental brain research,* **69**(1), pp. 85-95.

SCHÜZ, A. and PALM, G., 1989. Density of neurons and synapses in the cerebral cortex of the mouse. *Journal of Comparative Neurology,* **286**(4), pp. 442-455.

SCOPEL, D., FOCHESATTO, C., CIMAROSTI, H., RABBO, M., BELLÓ-KLEIN, A., SALBEGO, C., NETTO, C.A. and SIQUEIRA, I.R., 2006. Exercise intensity influences cell injury in rat hippocampal slices exposed to oxygen and glucose deprivation. *Brain research bulletin,* **71**(1-3), pp. 155-159.

SEEDS, N.W., BASHAM, M.E. and FERGUSON, J.E., 2003. Absence of tissue plasminogen activator gene or activity impairs mouse cerebellar motor learning. *The Journal of neuroscience : the official journal of the Society for Neuroscience,* **23**(19), pp. 7368-7375.

SEEDS, N.W., WILLIAMS, B.L. and BICKFORD, P.C., 1995. Tissue plasminogen activator induction in Purkinje neurons after cerebellar motor learning. *Science (New York, N.Y.),* **270**(5244), pp. 1992-1994.

SEIDLER, F.J. and SLOTKIN, T.A., 1990. Effects of acute hypoxia on neonatal rat brain: regionally selective, long-term alterations in catecholamine levels and turnover. *Brain research bulletin,* **24**(2), pp. 157-161.

SEMENZA, G.L., 2012. Hypoxia-inducible factors in physiology and medicine. *Cell,* **148**(3), pp. 399-408.

SEMENZA, G.L., 2000. HIF-1: mediator of physiological and pathophysiological responses to hypoxia. *Journal of applied physiology,* **88**(4), pp. 1474-1480.

SEMENZA, G.L., AGANI, F., FELDSER, D., LYER, N., KOTCH, L., LAUGHNER, E. and YU, A., 2002. Hypoxia, HIF-1, and the pathophysiology of common human diseases. *Oxygen Sensing.* Springer, pp. 123-130.

SEMENZE, G.L., 2003. Targeting HIF-1 for cancer therapy. *Nature reviews cancer.*, **3**(10), 721.

SEMPLE, B.D., BLOMGREN, K., GIMLIN, K., FERRIERO, D.M. and NOBLE-HAEUSSLEIN, L.J., 2013. Brain development in rodents and humans: Identifying benchmarks of maturation and vulnerability to injury across species. *Progress in neurobiology,* **106**, pp. 1-16.

SEONG, E., SAUNDERS, T.L., STEWART, C.L. and BURMEISTER, M., 2004. To knockout in 129 or in C57BL/6: that is the question. *Trends in Genetics,* **20**(2), pp. 59-62.

SHAH, P.S., 2010. Hypothermia: a systematic review and meta-analysis of clinical trials, *Seminars in Fetal and Neonatal Medicine* 2010, Elsevier, pp. 238-246.

SHAH, P.S., BEYENE, J., TO, T., OHLSSON, A. and PERLMAN, M., 2006. Postasphyxial hypoxic-ischemic encephalopathy in neonates: outcome prediction rule within 4 hours of birth. *Archives of Pediatrics & Adolescent Medicine,* **160**(7), pp. 729-736.

SHAH, P.S., OHLSSON, A. and PERLMAN, M., 2007. Hypothermia to treat neonatal hypoxic ischemic encephalopathy: systematic review. *Archives of Pediatrics & Adolescent Medicine,* **161**(10), pp. 951-958.

SHALAK, L. and PERLMAN, J.M., 2004. Hypoxic-ischemic brain injury in the term infant-current concepts. *Early human development,* **80**(2), pp. 125-141.

SHALEM, O., SANJANA, N.E., ZHANG, F., 2015. High-throughput functional genomics using CRISPR–Cas9. *Nature Reviews Genetics.*, **16**(5), 299.

SHANKARAN, S., LAPTOOK, A.R., EHRENKRANZ, R.A., TYSON, J.E., MCDONALD, S.A., DONOVAN, E.F., FANAROFF, A.A., POOLE, W.K., WRIGHT, L.L. and HIGGINS, R.D., 2005. Whole-body hypothermia for neonates with hypoxic–ischemic encephalopathy. *New England Journal of Medicine,* **353**(15), pp. 1574-1584.

SHANKARAN, S., LAPTOOK, A.R., EHRENKRANZ, R.A., TYSON, J.E., MCDONALD, S.A., DONOVAN, E.F., FANAROFF, A.A., POOLE, W.K., WRIGHT, L.L. and HIGGINS, R.D., 2005. Whole-body hypothermia for neonates with hypoxic–ischemic encephalopathy. *New England Journal of Medicine,* **353**(15), pp. 1574-1584.

SHANKARAN, S., LAPTOOK, A., WRIGHT, L.L., EHRENKRANZ, R.A., DONOVAN, E.F., FANAROFF, A.A., STARK, A.R., TYSON, J.E., POOLE, K. and CARLO, W.A., 2002. Whole-body hypothermia for neonatal encephalopathy: animal observations as a basis for a randomized, controlled pilot study in term infants. *Pediatrics,* **110**(2), pp. 377-385.

SHANKARAN, S., PAPPAS, A., MCDONALD, S.A., VOHR, B.R., HINTZ, S.R., YOLTON, K., GUSTAFSON, K.E., LEACH, T.M., GREEN, C. and BARA, R., 2012. Childhood outcomes after hypothermia for neonatal encephalopathy. *New England Journal of Medicine,* **366**(22), pp. 2085-2092.

SHANKARAN, S., WOLDT, E., KOEPKE, T., BEDARD, M.P. and NANDYAL, R., 1991. Acute neonatal morbidity and long-term central nervous system sequelae of perinatal asphyxia in term infants. *Early human development,* **25**(2), pp. 135-148.

SHARMA, R., 2014. Prevention of Frey syndrome with superficial temporal fascia interpositioning: a retrospective study. *International journal of oral and maxillofacial surgery,* **43**(4), pp. 413-417.

SHASTRY, P., BASU, A., RAJADHYKSHA, M.S., 2001. Neuroblastoma Cell Lines-A Versatile in Vztro Model in Neurobiology. *International journal of neuroscience.*, **108**(1-2), 109-26.

SHELDON, R.A., SEDIK, C. and FERRIERO, D.M., 1998. Strain-related brain injury in neonatal mice subjected to hypoxia–ischemia. *Brain research,* **810**(1), pp. 114-122.

SHELDON, R.A., OSREDKAR, D., LEE, C.L., JIANG, X., MU, D. and FERRIERO, D.M., 2009. HIF-1 alpha-deficient mice have increased brain injury after neonatal hypoxia-ischemia. *Developmental neuroscience,* **31**(5), pp. 452-458.

SHELLHAAS, R.A., SOAITA, A.I. and CLANCY, R.R., 2007. Sensitivity of amplitude-integrated electroencephalography for neonatal seizure detection. *Pediatrics,* **120**(4), pp. 770-777.

SHEN, H., SIKORSKA, M., LEBLANC, J., WALKER, P. and LIU, Q., 2006. Oxidative stress regulated expression of ubiquitin Carboxyl-terminal Hydrolase-L1: role in cell survival. *Apoptosis,* **11**(6), pp. 1049-1059.

SHERMAN, S.M. and GUILLERY, R.W., 2013. *Functional connections of cortical areas: a new view from the thalamus.* MIT Press.

SHERMAN, S. and GUILLERY, R., 2009. Exploring the thalamus and its role in cortical function. MIT Press. *Cambridge, MA,* .

SHI, L., FU, W.Y., HUNG, K.W., PORCHETTA, C., HALL, C., FU, A.K. and IP, N.Y., 2007. Alpha2-chimaerin interacts with EphA4 and regulates EphA4-dependent growth cone collapse. *Proceedings of the National Academy of Sciences of the United States of America,* **104**(41), pp. 16347-16352.

SHI, L., SMITH, S.E., MALKOVA, N., TSE, D., SU, Y. and PATTERSON, P.H., 2009. Activation of the maternal immune system alters cerebellar development in the offspring. *Brain, behavior, and immunity,* **23**(1), pp. 116-123.

SHIMOMURA, C. and OHTA, H., 1988. Behavioral abnormalities and seizure susceptibility in rat after neonatal anoxia. *Brain & development,* **10**(3), pp. 160-163.

SHIPP, S., 2007. Structure and function of the cerebral cortex. *Current Biology.,* **17**(12), R443-9.

SHORE, R., 1997. Rethinking the brain: New insights into early development.

SIAO, C.J., and TSIRKA, S.E., 2002. Tissue plasminogen activator mediates microglial activation via its finger domain through annexin II. *Journal of Neuroscience.,* **22**(9), 3352-8.

SIAO, C.J., FERNANDEZ, S.R. and TSIRKA, S.E., 2003. Cell type-specific roles for tissue plasminogen activator released by neurons or microglia after excitotoxic injury. *The Journal of neuroscience : the official journal of the Society for Neuroscience,* **23**(8), pp. 3234-3242.

SIBARITA, J.B., 2005. Deconvolution microscopy. In *Microscopy Techniques*, (pp. 201-243). Springer, Berlin, Heidelberg.

SIDHU, R.S., TUOR, U.I. and DEL BIGIO, M.R., 1997. Nuclear condensation and fragmentation following cerebral hypoxia-ischemia occurs more frequently in immature than older rats. *Neuroscience letters,* **223**(2), pp. 129-132.

SIGMUND, C.D., 2000. are studies in genetically altered mice out of control? *Arteriosclerosis, Thrombosis, and Vascular Biology,* **20**(6), pp. 1425-1429.

SIMONIDES, W.S., MULCAHEY, M.A., REDOUT, E.M., MULLER, A., ZIUDWIJK, M.J., VISSER, T.J., WASSEN, F.W., CRESCENZI, A., DA-SILVA, W.S., HARNEY, J., ENGEL, F.B., 2008. Hypoxia-inducible factor induces local thyroid hormone inactivation during hypoxic-ischemic disease in rats. *The Journal of clinical investigation.*, **118**(3), 975-83.

SIMPSON, E.A., MURRAY, L., PAUKNER, A. and FERRARI, P.F., 2014. The mirror neuron system as revealed through neonatal imitation: presence from birth, predictive power and evidence of plasticity. *Philosophical transactions of the Royal Society of London.Series B, Biological sciences,* **369**(1644), pp. 20130289.

SINGH, D., KUMAR, P., MAJUMDAR, S. and NARANG, A., 2004. Effect of phenobarbital on free radicals in neonates with hypoxic ischemic encephalopathy--a randomized controlled trial. *Journal of perinatal medicine,* **32**(3), pp. 278-281.

SIZONENKO, S.V., KISS, J.Z., INDER, T., GLUCKMAN, P.D. and WILLIAMS, C.E., 2005. Distinctive neuropathologic alterations in the deep layers of the parietal cortex after moderate ischemic-hypoxic injury in the P3 immature rat brain. *Pediatric research,* **57**(6), pp. 865.

SIZONENKO, S.V., CAMM, E.J., DAYER, A., KISS, J.Z., 2008. Glial responses to neonatal hypoxic–ischemic injury in the rat cerebral cortex. *International journal of developmental neuroscience.,* **26**(1), 37-45.

SLOTKIN, T., LAPPI, S., MCCOOK, E., LORBER, B. and SEIDLER, F., 1995. Loss of neonatal hypoxia tolerance after prenatal nicotine exposure: implications for sudden infant death syndrome. *Brain research bulletin,* **38**(1), pp. 69-75.

SLOTKIN, T.A., COWDERY, T.S., ORBAND, L., PACHMAN, S. and WHITMORE, W.L., 1986. Effects of neonatal hypoxia on brain development in the rat: immediate and long-term biochemical alterations in discrete regions. *Brain research,* **374**(1), pp. 63-74.

SMART, I.H., DEHAY, C., GIROUD, P., BERLAND, M. and KENNEDY, H., 2002. Unique morphological features of the proliferative zones and postmitotic

compartments of the neural epithelium giving rise to striate and extrastriate cortex in the monkey. *Cerebral cortex,* **12**(1), pp. 37-53.

SMITH, P.L., HAGBERG, H., NAYLOR, A.S. and MALLARD, C., 2014. Neonatal peripheral immune challenge activates microglia and inhibits neurogenesis in the developing murine hippocampus. *Developmental neuroscience,* **36**(2), pp. 119-131.

SOARES, D.P. and LAW, M., 2009. Magnetic resonance spectroscopy of the brain: review of metabolites and clinical applications. *Clinical radiology,* **64**(1), pp. 12-21.

SOFRONIEW, M.V., 2009. Molecular dissection of reactive astrogliosis and glial scar formation. *Trends in neurosciences,* **32**(12), pp. 638-647.

SOFRONIEW, M.V. and VINTERS, H.V., 2010. Astrocytes: biology and pathology. *Acta Neuropathologica,* **119**(1), pp. 7-35.

SOKOLOFF, L., REIVICH, M., KENNEDY, C., DES ROSIERS, M., PATLAK, C.S., PETTIGREW, K.E.A., SAKURADA, O. and SHINOHARA, M., 1977. The [14C] deoxyglucose method for the measurement of local cerebral glucose utilization: theory, procedure, and normal values in the conscious and anesthetized albino rat1. *Journal of neurochemistry,* **28**(5), pp. 897-916.

SOUL, J.S., ROBERTSON, R.L., TZIKA, A.A., DU PLESSIS, A.J. and VOLPE, J.J., 2001. Time course of changes in diffusion-weighted magnetic resonance imaging in a case of neonatal encephalopathy with defined onset and duration of hypoxic-ischemic insult. *Pediatrics,* **108**(5), pp. 1211-1214.

SPEISER, Z., KATZIR, O., REHAVI, M., ZABARSKI, T. and COHEN, S., 1998. Sparing by rasagiline (TVP-1012) of cholinergic functions and behavior in the postnatal anoxia rat. *Pharmacology Biochemistry and Behavior,* **60**(2), pp. 387-393.

SPEISER, Z., UZIEL, J., DEFRIN-ASSA, R., GITTER, S. and URCA, G., 1991. Different behavioral deficits are induced by anoxia/hypoxia in neonatal and senescent rats: blockade by MK-801. *Behavioural brain research,* **42**(2), pp. 181-186.

SPITZER, N.C., 2006. Electrical activity in early neuronal development. *Nature,* **444**(7120), pp. 707.

SPORNS, O., 2002. Network analysis, complexity, and brain function. *Complexity,* **8**(1), pp. 56-60.

SPRAGGINS, Y., SEIDLER, F.J. and SLOTKIN, T.A., 1994. Cocaine Exacerbates Hypoxia-induced Cell Damage in the Developing Brain: Effects on Ornithine Decarboxylase Activity and Protein Synthesis. *Neonatology,* **66**(5), pp. 254-266.

SQUIRE, L., BERG, D., BLOOM, F.E., DU LAC, S., GHOSH, A. and SPITZER, N.C., 2012. *Fundamental neuroscience.* Academic Press.

SRIVASTAVA, I.N., SHPERDHEJA, J., BAYBIS, M., FERGUSON, T. and CRINO, P.B., 2016. mTOR pathway inhibition prevents neuroinflammation and neuronal death in a mouse model of cerebral palsy. *Neurobiology of disease,* **85**, pp. 144-154.

SRIVASTAVA, R.K., LI, C., AHMAD, A., ABRAMS, O., GORBATYUK, M.S., HARROD, K.S., WEK, R.C., AFAQ, F. and ATHAR, M., 2016. ATF4 regulates arsenic trioxide-mediated NADPH oxidase, ER-mitochondrial crosstalk and apoptosis. *Archives of Biochemistry and Biophysics,* **609**, pp. 39-50.

STALEY, K.J., SOLDO, B.L. and PROCTOR, W.R., 1995. Ionic mechanisms of neuronal excitation by inhibitory GABAA receptors. *Science (New York, N.Y.),* **269**(5226), pp. 977-981.

STARKOV, A.A., CHINOPOULOS, C. and FISKUM, G., 2004. Mitochondrial calcium and oxidative stress as mediators of ischemic brain injury. *Cell calcium,* **36**(3-4), pp. 257-264.

STEINMAN, K.J., GORNO-TEMPINI, M.L., GLIDDEN, D.V., KRAMER, J.H., MILLER, S.P., BARKOVICH, A.J. and FERRIERO, D.M., 2009. Neonatal watershed brain injury on magnetic resonance imaging correlates with verbal IQ at 4 years. *Pediatrics,* **123**(3), pp. 1025-1030.

STEWART, P.A. and HAYAKAWA, K., 1994. Early ultrastructural changes in blood-brain barrier vessels of the rat embryo. *Brain research.Developmental brain research,* **78**(1), pp. 25-34.

STILLER, R., VON MERING, R., KONIG, V., HUCH, A. and HUCH, R., 2002. How well does reflectance pulse oximetry reflect intrapartum fetal acidosis? *American Journal of Obstetrics and Gynecology,* **186**(6), pp. 1351-1357.

STOLL, B.J., HANSEN, N.I., ADAMS-CHAPMAN, I., FANAROFF, A.A., HINTZ, S.R., VOHR, B., HIGGINS, R.D. and NATIONAL INSTITUTE OF CHILD HEALTH AND HUMAN DEVELOPMENT NEONATAL RESEARCH NETWORK, 2004. Neurodevelopmental and growth impairment among extremely low-birth-weight infants with neonatal infection. *Jama,* **292**(19), pp. 2357-2365.

STOLP, H. and DZIEGIELEWSKA, K., 2009. Review: role of developmental inflammation and blood–brain barrier dysfunction in neurodevelopmental and neurodegenerative diseases. *Neuropathology and applied neurobiology,* **35**(2), pp. 132-146.

STOLP, H.B., LIDDELOW, S.A. and SAUNDERS, N.R., 2016. Editorial: Ontogeny and Phylogeny of Brain Barrier Mechanisms. *Frontiers in neuroscience,* **10**, pp. 41.

STONESTREET, B.S., BURGESS, G.H. and CSERR, H.F., 1992. Blood-brain barrier integrity and brain water and electrolytes during hypoxia/hypercapnia and hypotension in newborn piglets. *Brain research,* **590**(1-2), pp. 263-270.

STOPPELLI, M.P., CORTI, A., SOFFIENTINI, A., CASSANI, G., BLASI, F. and ASSOIAN, R.K., 1985. Differentiation-enhanced binding of the amino-terminal

fragment of human urokinase plasminogen activator to a specific receptor on U937 monocytes. *Proceedings of the National Academy of Sciences of the United States of America,* **82**(15), pp. 4939-4943.

STRASSER, U. and FISCHER, G., 1995. Quantitative measurement of neuronal degeneration in organotypic hippocampal cultures after combined oxygen/glucose deprivation. *Journal of neuroscience methods,* **57**(2), pp. 177-186.

STRIDH, L., MOTTAHEDIN, A., JOHANSSON, M.E., VALDEZ, R.C., NORTHINGTON, F., WANG, X. and MALLARD, C., 2013. Toll-like receptor-3 activation increases the vulnerability of the neonatal brain to hypoxia-ischemia. *The Journal of neuroscience : the official journal of the Society for Neuroscience,* **33**(29), pp. 12041-12051.

STRITT, C., STERN, S., HARTING, K., MANKE, T., SINSKE, D., SCHWARZ, H., VINGRON, M., NORDHEIM, A. and KNOLL, B., 2009. Paracrine control of oligodendrocyte differentiation by SRF-directed neuronal gene expression. *Nature neuroscience,* **12**(4), pp. 418-427.

STRUNK, T., HARTEL, C., TEMMING, P., MATZKE, N., ZIMMER, J. and SCHULTZ, C., 2008. Erythropoietin inhibits cytokine production of neonatal and adult leukocytes. *Acta Paediatrica (Oslo, Norway : 1992),* **97**(1), pp. 16-20.

STRUNK, T., INDER, T., WANG, X., BURGNER, D., MALLARD, C. and LEVY, O., 2014. Infection-induced inflammation and cerebral injury in preterm infants. *The Lancet.Infectious diseases,* **14**(8), pp. 751-762.

SUAREZ-SOLA, M.L., GONZALEZ-DELGADO, F.J., PUEYO-MORLANS, M., MEDINA-BOLIVAR, O.C., HERNANDEZ-ACOSTA, N.C., GONZALEZ-GOMEZ, M. and MEYER, G., 2009. Neurons in the white matter of the adult human neocortex. *Frontiers in neuroanatomy,* **3**, pp. 7.

SUDHOF, T.C., 2004. The synaptic vesicle cycle. *Annual Review of Neuroscience,* **27**, pp. 509.

SUKHORUKOVA, E.G., KORZHEVSKII, D.E., KIRIK, O.V. and KORZHEVSKAIA, V.F., 2010. Detection of brain astrocytes by the immunohistochemical method after craniocerebral injury. *Sudebno-meditsinskaia ekspertiza,* **53**(1), pp. 14-16.

SULLIVAN, S.M., BJÖRKMAN, S.T., MILLER, S.M., COLDITZ, P.B. and POW, D.V., 2010. Morphological changes in white matter astrocytes in response to hypoxia/ischemia in the neonatal pig. *Brain research,* **1319**, pp. 164-174.

SULLIVAN, S.M., BJÖRKMAN, S.T., MILLER, S.M., COLDITZ, P.B. and POW, D.V., 2010. Structural remodeling of gray matter astrocytes in the neonatal pig brain after hypoxia/ischemia. *Glia,* **58**(2), pp. 181-194.

SUN, J., JIA, P., FANOUS, A.H., WEBB, B.T., VAN DEN OORD, E.J., CHEN, X., BUKSZAR, J., KENDLER, K.S. and ZHAO, Z., 2009. A multi-dimensional

evidence-based candidate gene prioritization approach for complex diseases–schizophrenia as a case. *Bioinformatics,* **25**(19), pp. 2595-6602.

SUN, Y., YANG, D. and KUAN, C., 2012. Mannitol-facilitated perfusion staining with 2, 3, 5-triphenyltetrazolium chloride (TTC) for detection of experimental cerebral infarction and biochemical analysis. *Journal of neuroscience methods,* **203**(1), pp. 122-129.

SUN, J.J. and LUHMANN, H.J., 2007. Spatio-temporal dynamics of oscillatory network activity in the neonatal mouse cerebral cortex. *The European journal of neuroscience,* **26**(7), pp. 1995-2004.

SUNKIN, S.M., NG, L., LAU, C., DOLBEARE, T., GILBERT, T.L., THOMPSON, C.L., HAWRYLYCZ, M. and DANG, C., 2012. Allen Brain Atlas: an integrated spatio-temporal portal for exploring the central nervous system. *Nucleic acids research,* **41**(D1), pp. D996-D1008.

SVEDIN, P., HAGBERG, H., SAVMAN, K., ZHU, C. and MALLARD, C., 2007. Matrix metalloproteinase-9 gene knock-out protects the immature brain after cerebral hypoxia-ischemia. *The Journal of neuroscience : the official journal of the Society for Neuroscience,* **27**(7), pp. 1511-1518.

SVEDIN, P., KJELLMER, I., WELIN, A.K., BLAD, S. and MALLARD, C., 2005. Maturational effects of lipopolysaccharide on white-matter injury in fetal sheep. *Journal of child neurology,* **20**(12), pp. 960-964.

SYVERTSSON, S., VISCHER, N.O., GAO, Y. and HAMOEN, L.W., 2016. When Phase Contrast Fails: ChainTracer and NucTracer, Two ImageJ Methods for Semi-Automated Single Cell Analysis Using Membrane or DNA Staining. *PloS one,* **11**(3), pp. e0151267.

TAGER-FLUSBERG, H., 1999. *Neurodevelopmental disorders.* MIT press.

TAGIN, M.A., WOOLCOTT, C.G., VINCER, M.J., WHYTE, R.K. and STINSON, D.A., 2012. Hypothermia for neonatal hypoxic ischemic encephalopathy: an updated systematic review and meta-analysis. *Archives of Pediatrics & Adolescent Medicine,* **166**(6), pp. 558-566.

TAHRAOUI, S., MARRET, S., BODENANT, C., LEROUX, P., DOMMERGUES, M., EVRARD, P. and GRESSENS, P., 2001. Central role of microglia in neonatal excitotoxic lesions of the murine periventricular white matter. *Brain pathology,* **11**(1), pp. 56-71.

TAJIRI, N., KANEKO, Y., SHINOZUKA, K., ISHIKAWA, H., YANKEE, E., MCGROGAN, M., CASE, C. and BORLONGAN, C.V., 2013. Stem cell recruitment of newly formed host cells via a successful seduction? Filling the gap between neurogenic niche and injured brain site. *PloS one,* **8**(9), pp. e74857.

TAKADA, S., DOS SANTOS HAEMMERLE, C., MOTTA-TEIXEIRA, L., MACHADO-NILS, A., LEE, V., TAKASE, L., CRUZ-RIZZOLO, R., KIHARA, A.,

XAVIER, G. and WATANABE, I., 2015. Neonatal anoxia in rats: hippocampal cellular and subcellular changes related to cell death and spatial memory. *Neuroscience,* **284**, pp. 247-259.

TAKADA, S.H., MOTTA-TEIXEIRA, L.C., MACHADO-NILS, A.V., LEE, V.Y., SAMPAIO, C.A., POLLI, R.S., MALHEIROS, J.M., TAKASE, L.F., KIHARA, A.H., COVOLAN, L., XAVIER, G.F. and NOGUEIRA, M.I., 2016. Impact of neonatal anoxia on adult rat hippocampal volume, neurogenesis and behavior. *Behavioural brain research,* **296**, pp. 331-338.

TAKAHASHI, S., TANAKA, H. and OKI, J., 1999. Development of spinal motoneurons in rats after a neonatal hypoxic insult. *Pediatric neurology,* **21**(4), pp. 715-720.

TAKAO, M., BENSON, M.D., MURRELL, J.R., YAZAKI, M., PICCARDO, P., UNVERZAGT, F.W., DAVIS, R.L., HOLOHAN, P.D., LAWRENCE, D.A. and RICHARDSON, R., 2000. Neuroserpin mutation S52R causes neuroserpin accumulation in neurons and is associated with progressive myoclonus epilepsy. *Journal of Neuropathology & Experimental Neurology,* **59**(12), pp. 1070-1086.

TAKAO, K. and MIYAKAWA, T., 2015. Genomic responses in mouse models greatly mimic human inflammatory diseases. *Proceedings of the National Academy of Sciences of the United States of America,* **112**(4), pp. 1167-1172.

TAKEBAYASHI, H., YOSHIDA, S., SUGIMORI, M., KOSAKO, H., KOMINAMI, R., NAKAFUKU, M. and NABESHIMA, Y., 2000. Dynamic expression of basic helix-loop-helix Olig family members: implication of Olig2 in neuron and oligodendrocyte differentiation and identification of a new member, Olig3. *Mechanisms of development,* **99**(1-2), pp. 143-148.

TAKEOKA, M., SOMAN, T.B., YOSHII, A., CAVINESS, V.S.,JR, GONZALEZ, R.G., GRANT, P.E. and KRISHNAMOORTHY, K.S., 2002. Diffusion-weighted images in neonatal cerebral hypoxic-ischemic injury. *Pediatric neurology,* **26**(4), pp. 274-281.

TALOS, D.M., FISHMAN, R.E., PARK, H., FOLKERTH, R.D., FOLLETT, P.L., VOLPE, J.J. and JENSEN, F.E., 2006. Developmental regulation of alpha-amino-3-hydroxy-5-methyl-4-isoxazole-propionic acid receptor subunit expression in forebrain and relationship to regional susceptibility to hypoxic/ischemic injury. I. Rodent cerebral white matter and cortex. *The Journal of comparative neurology,* **497**(1), pp. 42-60.

TAN, X. and SHI, S., 2013. Neocortical neurogenesis and neuronal migration. *Wiley Interdisciplinary Reviews: Developmental Biology,* **2**(4), pp. 443-459.

TANAKA, H., TAKAHASHI, S., MIYAMOTO, A., OKI, J., CHO, K. and OKUNO, A., 1995. Effects of neonatal hypoxia on brainstem cholinergic neurons-pedunculopontine nucleus and laterodorsal tegmental nucleus. *Brain and Development,* **17**(4), pp. 264-270.

TANG, G., DONG, X., HUANG, X., HUANG, X., LIU, H., WANG, Y., YE, W. and SHI, L., 2015. A natural diarylheptanoid promotes neuronal differentiation via activating ERK and PI3K-Akt dependent pathways. *Neuroscience,* **303**, pp. 389-401.

TANG, G., LIU, X., MA, N., HUANG, X., WU, Z., ZHANG, W., WANG, Y., ZHAO, B., WANG, Z. and IP, F.C., 2016. Design and synthesis of dimeric securinine analogues with neuritogenic activities. *ACS chemical neuroscience,* **7**(10), pp. 1442-1451.

TANG, Y., PACARY, E., FRERET, T., DIVOUX, D., PETIT, E., SCHUMANN-BARD, P. and BERNAUDIN, M., 2006. Effect of hypoxic preconditioning on brain genomic response before and following ischemia in the adult mouse: identification of potential neuroprotective candidates for stroke. *Neurobiology of disease,* **21**(1), pp. 18-28.

TANGUAY, R.M., WU, Y. and KHANDJIAN, E., 1993. Tissue-specific expression of heat shock proteins of the mouse in the absence of stress. *Developmental genetics,* **14**(2), pp. 112-118.

TAO, F., LU, S.D., ZHANG, L.M., HUANG, Y.L. and SUN, F.Y., 2001. Role of excitatory amino acid transporter 1 in neonatal rat neuronal damage induced by hypoxia-ischemia. *Neuroscience,* **102**(3), pp. 503-513.

TAPOCIK, J.D., CENICCOLA, K., MAYO, C.L., SCHWANDT, M.L., SOLOMON, M., WANG, B.D., LUU, T.V., OLENDER, J., HARRIGAN, T., MAYNARD, T.M., ELMER, G.I., 2016. MicroRNAs are involved in the development of morphine-induced analgesic tolerance and regulate functionally relevant changes in Serpini1. *Frontiers in molecular neuroscience.*, **9**, 20.

TASCA, C.I., DAL-CIM, T., CIMAROSTI, H., 2015. In vitro oxygen-glucose deprivation to study ischemic cell death. InNeuronal Cell Death, (pp. 197-210). Humana Press, New York, NY.

ENCEPHALOPATHY, NEONATAL, AND NEUROLOGIC OUTCOME., 2014. "Report of the American College of Obstetricians and Gynecologists' Task Force on neonatal encephalopathy." *Pediatrics,* **133**(5), e1483-1488.

TAUPIN, P., 2007. BrdU immunohistochemistry for studying adult neurogenesis: paradigms, pitfalls, limitations, and validation. *Brain Research Reviews,* **53**(1), pp. 198-214.

TAYLOR, S.C., BERKELMAN, T., YADAV, G. and HAMMOND, M., 2013. A defined methodology for reliable quantification of Western blot data. *Molecular biotechnology,* **55**(3), pp. 217-226.

TAYLOR, C.P., WEBER, M.L., GAUGHAN, C.L., LEHNING, E.J. and LOPACHIN, R.M., 1999. Oxygen/glucose deprivation in hippocampal slices: altered intraneuronal elemental composition predicts structural and functional damage. *The Journal of neuroscience : the official journal of the Society for Neuroscience,* **19**(2), pp. 619-629.

TAYLOR, S.C. and POSCH, A., 2014. The design of a quantitative western blot experiment. *BioMed research international,* **2014**, pp. 361590.

TEASDALE, R.D. and JACKSON, M.R., 1996. Signal-mediated sorting of membrane proteins between the endoplasmic reticulum and the golgi apparatus. *Annual Review of Cell and Developmental Biology,* **12**, pp. 27-54.

TEESALU, T., KULLA, A., SIMISKER, A., SIRÉN, V., LAWRENCE, D.A., ASSER, T. and VAHERI, A., 2004. Tissue plasminogen activator and neuroserpin are widely expressed in the human central nervous system. *Thrombosis and haemostasis,* **92**(2), pp. 358-368.

TEMPLE, S., 2001. The development of neural stem cells. *Nature,* **414**(6859), pp. 112-117.

TEN, V.S., BRADLEY-MOORE, M., GINGRICH, J.A., STARK, R.I. and PINSKY, D.J., 2003. Brain injury and neurofunctional deficit in neonatal mice with hypoxic-ischemic encephalopathy. *Behavioural brain research,* **145**(1-2), pp. 209-219.

TEO, J.D., MORRIS, M.J., JONES, N.M., 2015. Hypoxic postconditioning reduces microglial activation, astrocyte and caspase activity, and inflammatory markers after hypoxia–ischemia in the neonatal rat brain. *Pediatric research.*, **77**(6), 757.

THE JACKSON LABORATORY, 2018-last update, **B6.129-Serpini1tm1Dpw/J - Mouse Strain Datasheet 019121**. Available: https://www.jax.org/strain/019121 [08/10, 2018].

THE JACKSON LABORATORY, (., 2018-last update, BALB/cJ Stock Number: 000651. Available: https://www.jax.org/strain/000651 [09/05, 2018].

THE R FOUNDATION, O., 2018-last update, **The R Project for Statistical Computing**. Available: https://www.r-project.org/ [08/10, 2018].

THERMO FISHER SCIENTIFIC, I., 2002-last update, **Vybrant® MTT Cell Proliferation Assay Kit**. Available: https://www.thermofisher.com/uk/en/home/references/protocols/cell-culture/mtt-assay-protocol/vybrant-mtt-cell-proliferation-assay-kit.html [10/01, 2018].

THOM, M., SISODIYA, S., HARKNESS, W., SCARAVILLI, F., 2001. Microdysgenesis in temporal lobe epilepsy: a quantitative and immunohistochemical study of white matter neurones. *Brain.,* **124**(11), 2299-309.

THOMPSON, C., PUTERMAN, A., LINLEY, L., HANN, F., VAN DER ELST, C., MOLTENO, C. and MALAN, A., 1997. The value of a scoring system for hypoxic ischaemic encephalopathy in predicting neurodevelopmental outcome. *Acta paediatrica,* **86**(7), pp. 757-761.

THOMPSON, D.K., WARFIELD, S.K., CARLIN, J.B., PAVLOVIC, M., WANG, H.X., BEAR, M., KEAN, M.J., DOYLE, L.W., EGAN, G.F. and INDER, T.E., 2007.

Perinatal risk factors altering regional brain structure in the preterm infant. *Brain : a journal of neurology,* **130**(Pt 3), pp. 667-677.

THOMSON, A.M. and BANNISTER, A.P., 2003. Interlaminar connections in the neocortex. *Cerebral cortex (New York, N.Y.: 1991),* **13**(1), pp. 5-14.

THOMSON, A.M. and LAMY, C., 2007. Functional maps of neocortical local circuitry. *Frontiers in neuroscience,* **1**(1), pp. 19-42.

THORESEN, M., SARAS, S., LOBERG, E.M., WHITELAW, A., ACOLET, D., LINDGREN, C., PENRICE, J., ROBERTSON, N., HAUG, E., STEEN, P.A., 2001. Twenty-four hours of mild hypothermia in unsedated newborn pigs starting after a severe global hypoxic-ischemic insult is not neuroprotective. *Pediatric research.,* **50**(3), 405.

THORESEN, M., HOBBS, C.E., WOOD, T., CHAKKARAPANI, E. and DINGLEY, J., 2009. Cooling combined with immediate or delayed xenon inhalation provides equivalent long-term neuroprotection after neonatal hypoxia-ischemia. *Journal of cerebral blood flow and metabolism : official journal of the International Society of Cerebral Blood Flow and Metabolism,* **29**(4), pp. 707-714.

TING, P., YAMAGUCHI, S., BACHER, J.D., KILLENS, R.H. and MYERS, R.E., 1983. Hypoxic-ischemic cerebral necrosis in midgestational sheep fetuses: physiopathologic correlations. *Experimental neurology,* **80**(1), pp. 227-245.

TISSIR, F. and GOFFINET, A.M., 2003. Reelin and brain development. *Nature Reviews Neuroscience,* **4**(6), pp. 496-505.

TJALSMA, H., ANTELMANN, H., JONGBLOED, J.D., BRAUN, P.G., DARMON, E., DORENBOS, R., DUBOIS, J.Y., WESTERS, H., ZANEN, G., QUAX, W.J., KUIPERS, O.P., BRON, S., HECKER, M. and VAN DIJL, J.M., 2004. Proteomics of protein secretion by Bacillus subtilis: separating the "secrets" of the secretome. *Microbiology and molecular biology reviews : MMBR,* **68**(2), pp. 207-233.

TJÄRNLUND-WOLF, A., OLSSON, S., JOOD, K., BLOMSTRAND, C. and JERN, C., 2011. No evidence for an association between genetic variation at the SERPINI1 locus and ischemic stroke. *Journal of neurology,* **258**(10), pp. 1885.

TOET, M.C., VAN DER MEIJ, W., DE VRIES, L.S., UITERWAAL, C.S. and VAN HUFFELEN, K.C., 2002. Comparison between simultaneously recorded amplitude integrated electroencephalogram (cerebral function monitor) and standard electroencephalogram in neonates. *Pediatrics,* **109**(5), pp. 772-779.

TOLNER, E.A., SHEIKH, A., YUKIN, A.Y., KAILA, K. and KANOLD, P.O., 2012. Subplate neurons promote spindle bursts and thalamocortical patterning in the neonatal rat somatosensory cortex. *The Journal of Neuroscience,* **32**(2), pp. 692-702.

TOLNER, E.A., HOCHMAN, D.W., HASSINEN, P., OTAHAL, J., GAILY, E., HAGLUND, M.M., KUBOVA, H., SCHUCHMANN, S., VANHATALO, S. and

KAILA, K., 2011. Five percent CO(2) is a potent, fast-acting inhalation anticonvulsant. *Epilepsia,* **52**(1), pp. 104-114.

TOMIMATSU, T., FUKUDA, H., ENDOH, M., MU, J., WATANABE, N., KOHZUKI, M., FUJII, E., KANZAKI, T., OSHIMA, K. and DOI, K., 2002. Effects of neonatal hypoxic–ischemic brain injury on skilled motor tasks and brainstem function in adult rats. *Brain research,* **926**(1), pp. 108-117.

TONONI, G., SPORNS, O. and EDELMAN, G.M., 1994. A measure for brain complexity: relating functional segregation and integration in the nervous system. *Proceedings of the National Academy of Sciences of the United States of America,* **91**(11), pp. 5033-5037.

TORRES-REVERON, J.E. and FRIEDLANDER, M.J., 2005. Quantal Analysis of Synaptic Connections Between Individual Subplate and Cortical Plate Neurons in Rat Visual Cortex. *Presented at Society for Neuroscience Annual Meeting, Washington, DC, USA, November 12–16., .*

TORRES-REVERON, J. and FRIEDLANDER, M.J., 2007. Properties of persistent postnatal cortical subplate neurons. *The Journal of neuroscience : the official journal of the Society for Neuroscience,* **27**(37), pp. 9962-9974.

TORO, S., WEGNER, J., MULLER, M., WESTERFIELD, M., VARGA, Z.M., 2009. Identification of differentially expressed genes in the zebrafish hypothalamic–pituitary axis. *Gene Expression Patterns.,* **9**(4), 200-8.

TOSO, L., POGGI, S., PARK, J., EINAT, H., ROBERSON, R., DUNLAP, V., WOODARD, J., ABEBE, D. and SPONG, C.Y., 2005. Inflammatory-mediated model of cerebral palsy with developmental sequelae. *American Journal of Obstetrics and Gynecology,* **193**(3 Pt 2), pp. 933-941.

TOWBIN, H., STAEHELIN, T. and GORDON, J., 1979. Electrophoretic transfer of proteins from polyacrylamide gels to nitrocellulose sheets: procedure and some applications. *Proceedings of the National Academy of Sciences of the United States of America,* **76**(9), pp. 4350-4354.

TOWFIGHI, J., YAGER, J., HOUSMAN, C. and VANNUCCI, R., 1991. Neuropathology of remote hypoxic-ischemic damage in the immature rat. *Acta Neuropathologica,* **81**(5), pp. 578-587.

TOWFIGHI, J., ZEC, N., YAGER, J., HOUSMAN, C. and VANNUCCI, R.C., 1995. Temporal evolution of neuropathologic changes in an immature rat model of cerebral hypoxia: a light microscopic study. *Acta Neuropathologica,* **90**(4), pp. 375-386.

TRAN, T.V. and WEISMAN, L.E., 2004. Dexamethasone effects on group B streptococcal infection in newborn rats. *The Pediatric infectious disease journal,* **23**(1), pp. 47-52.

TREMBLAY, E., ROISIN, M.P., REPRESA, A., CHARRIAUT-MARLANGUE, C. and BEN-ARI, Y., 1988. Transient increased density of NMDA binding sites in the developing rat hippocampus. *Brain research,* **461**(2), pp. 393-396.

TREMBLAY, R., LEE, S., RUDY, B., 2016. GABAergic interneurons in the neocortex: from cellular properties to circuits. *Neuron.,* **91**(2), 260-92.

TROMMER, B.L., GROOTHUIS, D.R. and PASTERNAK, J.F., 1987. Quantitative analysis of cerebral vessels in the newborn puppy: the structure of germinal matrix vessels may predispose to hemorrhage. *Pediatric research,* **22**(1), pp. 23-28.

TSAI, H.H., LI, H., FUENTEALBA, L.C., MOLOFSKY, A.V., TAVEIRA-MARQUES, R., ZHUANG, H., TENNEY, A., MURNEN, A.T., FANCY, S.P., MERKLE, F., KESSARIS, N., 2012. Regional astrocyte allocation regulates CNS synaptogenesis and repair. *Science.,* **337**(6092), 358-62.

TSIRKA, S.E., GUALANDRIS, A., AMARAL, D.G. and STRICKLAND, S., 1995. Excitotoxin-induced neuronal degeneration and seizure are mediated by tissue plasminogen activator. *Nature,* **377**(6547), pp. 340-344.

TSIRKA, S.E., ROGOVE, A.D. and STRICKLAND, S., 1996. Neuronal cell death and tPA. *Nature,* **384**(6605), pp. 123.

TSUJI, M., WILSON, M.A., LANGE, M.S. and JOHNSTON, M.V., 2004. Minocycline worsens hypoxic-ischemic brain injury in a neonatal mouse model. *Experimental neurology,* **189**(1), pp. 58-65.

TSUKANO, H., GOTOH, T., ENDO, M., MIYATA, K., TAZUME, H., KADOMATSU, T., YANO, M., IWAWAKI, T., KOHNO, K., ARAKI, K., MIZUTA, H. and OIKE, Y., 2010. The endoplasmic reticulum stress-C/EBP homologous protein pathway-mediated apoptosis in macrophages contributes to the instability of atherosclerotic plaques. *Arteriosclerosis, Thrombosis, and Vascular Biology,* **30**(10), pp. 1925-1932.

TU, Y.F., TSAI, Y.S., WANG, L.W., WU, H.C., HUANG, C.C. and HO, C.J., 2011. Overweight worsens apoptosis, neuroinflammation and blood-brain barrier damage after hypoxic ischemia in neonatal brain through JNK hyperactivation. *Journal of neuroinflammation,* **8**, pp. 40-2094-8-40.

TUOR, U., CHUMAS, P. and DEL BIGIO, M., 1995. Prevention of hypoxic-ischemic damage with dexamethasone is dependent on age and not influenced by fasting. *Experimental neurology,* **132**(1), pp. 116-122.

TUOR, U.I. and GREWAL, D., 1994. Autoregulation of cerebral blood flow: influence of local brain development and postnatal age. *The American Journal of Physiology,* **267**(6 Pt 2), pp. H2220-8.

TYZIO, R., HOLMES, G.L., BEN-ARI, Y., KHAZIPOV, R., 2007. Timing of the developmental switch in GABAA mediated signaling from excitation to inhibition in

CA3 rat hippocampus using gramicidin perforated patch and extracellular recordings. *Epilepsia.,* **48**, 96-105.

UEHARA, T., TABUCHI, M. and MORI, E., 1999. Risk factors for silent cerebral infarcts in subcortical white matter and basal ganglia. *Stroke; a journal of cerebral circulation,* **30**(2), pp. 378-382.

UJHAZY, E., SCHMIDTOVA, M., DUBOVICKY, M., NAVAROVA, J., BRUCKNEROVA, I. and MACH, M., 2006. Neurobehavioural changes in rats after neonatal anoxia: effect of antioxidant stobadine pretreatment. *Neuro endocrinology letters,* **27 Suppl 2**, pp. 82-85.

UNAL-CEVIK, I., KILINC, M., GURSOY-OZDEMIR, Y., GURER, G. and DALKARA, T., 2004. Loss of NeuN immunoreactivity after cerebral ischemia does not indicate neuronal cell loss: a cautionary note. *Brain research,* **1015**(1-2), pp. 169-174.

VALIENTE, M., OBENAUF, A.C., JIN, X., CHEN, Q., ZHANG, X.H., LEE, D.J., CHAFT, J.E., KRIS, M.G., HUSE, J.T. and BROGI, E., 2014. Serpins promote cancer cell survival and vascular co-option in brain metastasis. *Cell,* **156**(5), pp. 1002-1016.

VALVERDE, F., FACAL-VALVERDE, M.V., SANTACANA, M. and HEREDIA, M., 1989. Development and differentiation of early generated cells of sublayer VIb in the somatosensory cortex of the rat: a correlated Golgi and autoradiographic study. *The Journal of comparative neurology,* **290**(1), pp. 118-140.

VALVERDE, F., LOPEZ-MASCARAQUE, L., SANTACANA, M. and DE CARLOS, J.A., 1995. Persistence of early-generated neurons in the rodent subplate: assessment of cell death in neocortex during the early postnatal period. *The Journal of neuroscience : the official journal of the Society for Neuroscience,* **15**(7 Pt 1), pp. 5014-5024.

VAN EDEN, C.G., MRZLJAK, L., VOORN, P., UYLINGS, H.B., 1989. Prenatal development of GABA-ergic neurons in the neocortex of the rat. *Journal of Comparative Neurology*, **289**(2), 213-227.

VAN DER KOOIJ, MICHAEL A, OHL, F., ARNDT, S.S., KAVELAARS, A., VAN BEL, F. and HEIJNEN, C.J., 2010. Mild neonatal hypoxia–ischemia induces long-term motor-and cognitive impairments in mice. *Brain, behavior, and immunity,* **24**(5), pp. 850-856.

VAN DER LOOS, H. and WOOLSEY, T.A., 1973. Somatosensory cortex: structural alterations following early injury to sense organs. *Science (New York, N.Y.),* **179**(4071), pp. 395-398.

VAN DER WORP, H.B., SENA, E.S., DONNAN, G.A., HOWELLS, D.W. and MACLEOD, M.R., 2007. Hypothermia in animal models of acute ischaemic stroke: a systematic review and meta-analysis. *Brain : a journal of neurology,* **130**(Pt 12), pp. 3063-3074.

VAN LAERHOVEN, H., DE HAAN, T.R., OFFRINGA, M., POST, B. and VAN DER LEE, J.H., 2013. Prognostic tests in term neonates with hypoxic-ischemic encephalopathy: a systematic review. *Pediatrics,* **131**(1), pp. 88-98.

VANDENBERG, R.J. and RYAN, R.M., 2013. Mechanisms of glutamate transport. *Physiological Reviews,* **93**(4), pp. 1621-1657.

VANNUCCI, R., CONNOR, J., MAUGER, D., PALMER, C., SMITH, M., TOWFIGHI, J. and VANNUCCI, S., 1999. Rat model of perinatal hypoxic-ischemic brain damage. *Journal of neuroscience research,* **55**(2), pp. 158-163.

VANNUCCI, R.C., CHRISTENSEN, M.A. and STEIN, D.T., 1989. Regional cerebral glucose utilization in the immature rat: effect of hypoxia-ischemia. *Pediatric research,* **26**(3), pp. 208-214.

VANNUCCI, R.C., CHRISTENSEN, M.A. and YAGER, J.Y., 1993. Nature, time-course, and extent of cerebral edema in perinatal hypoxic-ischemic brain damage. *Pediatric neurology,* **9**(1), pp. 29-34.

VANNUCCI, R.C. and YAGER, J.Y., 1992. Glucose, lactic acid, and perinatal hypoxic-ischemic brain damage. *Pediatric neurology,* **8**(1), pp. 3-12.

VANNUCCI, R.C., BRUCKLACHER, R.M. and VANNUCCI, S.J., 2005. Glycolysis and perinatal hypoxic-ischemic brain damage. *Developmental neuroscience,* **27**(2-4), pp. 185-190.

VANNUCCI, R.C. and DUFFY, T.E., 1976. Carbohydrate metabolism in fetal and neonatal rat brain during anoxia and recovery. *The American Journal of Physiology,* **230**(5), pp. 1269-1275.

VANNUCCI, R.C., LYONS, D.T. and VASTA, F., 1988. Regional cerebral blood flow during hypoxia-ischemia in immature rats. *Stroke; a journal of cerebral circulation,* **19**(2), pp. 245-250.

VANNUCCI, R.C. and VANNUCCI, S.J., 2005. Perinatal hypoxic-ischemic brain damage: evolution of an animal model. *Developmental neuroscience,* **27**(2-4), pp. 81-86.

VANNUCCI, S.J. and HAGBERG, H., 2004. Hypoxia-ischemia in the immature brain. *The Journal of experimental biology,* **207**(Pt 18), pp. 3149-3154.

VANNUCCI, S.J. and VANNUCCI, R.C., 1980. Glycogen metabolism in neonatal rat brain during anoxia and recovery. *Journal of neurochemistry,* **34**(5), pp. 1100-1105.

VARGAS-ORIGEL, A., ESPINOSA-GARCIA, J.O., MUNIZ-QUEZADA, E., VARGAS-NIETO, M.A. and AGUILAR-GARCIA, G., 2004. Prevention of hypoxic-ischemic encephalopathy with high-dose, early phenobarbital therapy. *Gaceta medica de Mexico,* **140**(2), pp. 147-153.

VAUGHAN, D.W. and PETERS, A., 1974. Neuroglial cells in the cerebral cortex of rats from young adulthood to old age: an electron microscope study. *Journal of neurocytology,* **3**(4), pp. 405-429.

VEERESHWARAYYA, V., KUMAR, P., ROSEN, K.M., MESTRIL, R. and QUERFURTH, H.W., 2006. Differential effects of mitochondrial heat shock protein 60 and related molecular chaperones to prevent intracellular beta-amyloid-induced inhibition of complex IV and limit apoptosis. *The Journal of biological chemistry,* **281**(40), pp. 29468-29478.

VENEROSI, A., CUTULI, D., CHIAROTTI, F. and CALAMANDREI, G., 2006. C-section birth per se or followed by acute global asphyxia altered emotional behaviour in neonate and adult rats. *Behavioural brain research,* **168**(1), pp. 56-63.

VENTO, M., ASENSI, M., SASTRE, J., GARCIA-SALA, F., PALLARDO, F.V. and VINA, J., 2001. Resuscitation with room air instead of 100% oxygen prevents oxidative stress in moderately asphyxiated term neonates. *Pediatrics,* **107**(4), pp. 642-647.

VENTO, M., ASENSI, M., SASTRE, J., GARCIA-SALA, F. and VINA, J., 2001. Six years of experience with the use of room air for the resuscitation of asphyxiated newly born term infants. *Biology of the neonate,* **79**(3-4), pp. 261-267.

VERMA, P.K., PANERAI, R.B., RENNIE, J.M. and EVANS, D.H., 2000. Grading of cerebral autoregulation in preterm and term neonates. *Pediatric neurology,* **23**(3), pp. 236-242.

VERMEULEN, R.J., FETTER, W.P., HENDRIKX, L., VAN SCHIE, P.E., VAN DER KNAAP, M.S. and BARKHOF, F., 2003. Diffusion-weighted MRI in severe neonatal hypoxic ischaemia: the white cerebrum. *Neuropediatrics,* **34**(2), pp. 72-76.

VERNEY, C., POGLEDIC, I., BIRAN, V., ADLE-BIASSETTE, H., FALLET-BIANCO, C. and GRESSENS, P., 2012. Microglial reaction in axonal crossroads is a hallmark of noncystic periventricular white matter injury in very preterm infants. *Journal of neuropathology and experimental neurology,* **71**(3), pp. 251-264.

VINCER, M.J., ALLEN, A.C., JOSEPH, K.S., STINSON, D.A., SCOTT, H. and WOOD, E., 2006. Increasing prevalence of cerebral palsy among very preterm infants: a population-based study. *Pediatrics,* **118**(6), pp. e1621-6.

VISWANATHAN, S., BANDYOPADHYAY, S., KAO, J.P. and KANOLD, P.O., 2012. Changing microcircuits in the subplate of the developing cortex. *The Journal of neuroscience : the official journal of the Society for Neuroscience,* **32**(5), pp. 1589-1601.

VOHR, B.R., WRIGHT, L.L., DUSICK, A.M., MELE, L., VERTER, J., STEICHEN, J.J., SIMON, N.P., WILSON, D.C., BROYLES, S., BAUER, C.R., DELANEY-BLACK, V., YOLTON, K.A., FLEISHER, B.E., PAPILE, L.A. and KAPLAN, M.D., 2000. Neurodevelopmental and functional outcomes of extremely low birth weight

infants in the National Institute of Child Health and Human Development Neonatal Research Network, 1993-1994. *Pediatrics,* **105**(6), pp. 1216-1226.

VOIGT, T., OPITZ, T. and DE LIMA, A.D., 2001. Synchronous oscillatory activity in immature cortical network is driven by GABAergic preplate neurons. *The Journal of neuroscience : the official journal of the Society for Neuroscience,* **21**(22), pp. 8895-8905.

VOLPE, J., 2001. Hypoxic-ischemic encephalopathy in neurology of the newborn. *Philadelphia: WB Saunders,* .

VOLPE, J., 1995. Hypoxic-ischemic encephalopathy: neuropathology and pathogenesis. *Neurology of the Newborn,* , pp. 279-313.

VOLPE, J.J., 2012. Neonatal encephalopathy: an inadequate term for hypoxic–ischemic encephalopathy. *Annals of Neurology,* **72**(2), pp. 156-166.

VOLPE, J.J., 2008. *Neurology of the newborn.* Elsevier Health Sciences.

VOLPE, A.R., PETRONE, M.E., DE VIZIO, W., DAVIES, R.M. and PROSKIN, H.M., 1996. A review of plaque, gingivitis, calculus and caries clinical efficacy studies with a fluoride dentifrice containing triclosan and PVM/MA copolymer. *The Journal of clinical dentistry,* **7 Suppl**, pp. S1-S14.

VOLPE, J.J., 2009. The encephalopathy of prematurity--brain injury and impaired brain development inextricably intertwined. *Seminars in pediatric neurology,* **16**(4), pp. 167-178.

VOLPE, J.J., 1989. Intraventricular hemorrhage in the premature infant--current concepts. Part I. *Annals of Neurology,* **25**(1), pp. 3-11.

VOLPE, J.J., 1977. Neonatal seizures. *Clinics in perinatology,* **4**(1), pp. 43-63.

VOM SAAL, F.S., QUADAGNO, D.M., EVEN, M.D., KEISLER, L.W., KEISLER, D.H., KHAN, S., 1990. Paradoxical effects of maternal stress on fetal steroids and postnatal reproductive traits in female mice from different intrauterine positions. *Biology of Reproduction.*, **43**(5), 751-61.

VON ECONOMO, C. and KOSKINAS, G., 1925. The cytoarchitectonics of the adult human cortex. *Vienna and Berlin: Julius Springer Verlag,* .

WADDELL, J., HANSCOM, M., SHALON EDWARDS, N., MCKENNA, M.C. and MCCARTHY, M.M., 2016. Sex differences in cell genesis, hippocampal volume and behavioral outcomes in a rat model of neonatal HI. *Experimental neurology,* **275 Pt 2**, pp. 285-295.

WAHLE, P., LUBKE, J. and NAEGELE, J.R., 1994. Inverted pyramidal neurons and interneurons in cat cortical subplate zone are labelled by monoclonal antibody SP1. *The European journal of neuroscience,* **6**(7), pp. 1167-1178.

WALKER, T.L., OVERALL, R.W., VOGLER, S., SYKES, A.M., RUHWALD, S., LASSE, D., ICHWAN, M., FABEL, K. and KEMPERMANN, G., 2016. Lysophosphatidic acid receptor is a functional marker of adult hippocampal precursor cells. *Stem cell reports,* **6**(4), pp. 552-565.

WALSH, B.H., MURRAY, D.M. and BOYLAN, G.B., 2011. The use of conventional EEG for the assessment of hypoxic ischaemic encephalopathy in the newborn: a review. *Clinical neurophysiology : official journal of the International Federation of Clinical Neurophysiology,* **122**(7), pp. 1284-1294.

WANG, Y.F., TSIRKA, S.E., STRICKLAND, S., STIEG, P.E., SORIANO, S.G., LIPTON, S.A., 1998. Tissue plasminogen activator (tPA) increase neuronal damage after focal cerebral ischemia in wild-type and tPA-deficient mice. *Nature medicine.,* **4**(2), 228-31.

WANG, L.S., ZHOU, J., SHAO, X.M. and TANG, X.C., 2002. Huperzine A attenuates cognitive deficits and brain injury in neonatal rats after hypoxia–ischemia. *Brain research,* **949**(1), pp. 162-170.

WANG, W.Z., OESCHGER, F.M., MONTIEL, J.F., GARCÍA-MORENO, F., HOERDER-SUABEDISSEN, A., KRUBITZER, L., EK, C.J., SAUNDERS, N.R., REIM, K. and VILLALON, A., 2011. Comparative aspects of subplate zone studied with gene expression in sauropsids and mammals. *Cerebral cortex,* **21**(10), pp. 2187-2203.

WANG, W., OESCHGER, F.M., LEE, S. and MOLNÁR, Z., 2009. High quality RNA from multiple brain regions simultaneously acquired by laser capture microdissection. *BMC molecular biology,* **10**(1), pp. 69.

WANG, C.T., LIN, H.J., CHENG, B.C., LIN, M.T. and CHANG, C.P., 2015. Attenuating systemic inflammatory markers in simulated high-altitude exposure by heat shock protein 70-mediated hypobaric hypoxia preconditioning in rats. *Journal of the Formosan Medical Association = Taiwan yi zhi,* **114**(4), pp. 328-338.

WANG, J., STREJA, E., SOOHOO, M., CHEN, J.L., RHEE, C.M., KIM, T., MOLNAR, M.Z., KOVESDY, C.P., MEHROTRA, R. and KALANTAR-ZADEH, K., 2017. Concurrence of Serum Creatinine and Albumin With Lower Risk for Death in Twice-Weekly Hemodialysis Patients. *Journal of renal nutrition : the official journal of the Council on Renal Nutrition of the National Kidney Foundation,* **27**(1), pp. 26-36.

WANG, X., STRIDH, L., LI, W., DEAN, J., ELMGREN, A., GAN, L., ERIKSSON, K., HAGBERG, H., MALLARD, C., 2009. Lipopolysaccharide sensitizes neonatal hypoxic-ischemic brain injury in a MyD88-dependent manner. *The Journal of Immunology.,* **183**(11), 7471-7.

WANG, L., ZHANG, Y., ASAKAWA, T., LI, W., HAN, S., LI, Q., XIAO, B., NAMBA, H., LU, C. and DONG, Q., 2015. Neuroprotective effect of neuroserpin in oxygen-glucose deprivation- and reoxygenation-treated rat astrocytes in vitro. *PloS one,* **10**(4), pp. e0123932.

WANG, S., ZHANG, X.Q., SONG, C.G., XIAO, T., ZHAO, M., ZHU, G. and ZHAO, C.S., 2015. In vivo effects of bumetanide at brain concentrations incompatible with NKCC1 inhibition on newborn DGC structure and spontaneous EEG seizures following hypoxia-induced neonatal seizures. *Neuroscience,* **286**, pp. 203-215.

WANG, W.Z., HOERDER-SUABEDISSEN, A., OESCHGER, F.M., BAYATTI, N., IP, B.K., LINDSAY, S., SUPRAMANIAM, V., SRINIVASAN, L., RUTHERFORD, M., MOLLGARD, K., CLOWRY, G.J. and MOLNAR, Z., 2010. Subplate in the developing cortex of mouse and human. *Journal of anatomy,* **217**(4), pp. 368-380.

WANG, X., HAGBERG, H., NIE, C., ZHU, C., IKEDA, T. and MALLARD, C., 2007. Dual role of intrauterine immune challenge on neonatal and adult brain vulnerability to hypoxia-ischemia. *Journal of neuropathology and experimental neurology,* **66**(6), pp. 552-561.

WANG, X., HAGBERG, H., ZHU, C., JACOBSSON, B. and MALLARD, C., 2007. Effects of intrauterine inflammation on the developing mouse brain. *Brain research,* **1144**, pp. 180-185.

WANG, X., ROUSSET, C.I., HAGBERG, H. and MALLARD, C., 2006. Lipopolysaccharide-induced inflammation and perinatal brain injury. *Seminars in fetal & neonatal medicine,* **11**(5), pp. 343-353.

WANG, X., ZHU, C., QIU, L., HAGBERG, H., SANDBERG, M. and BLOMGREN, K., 2003. Activation of ERK1/2 after neonatal rat cerebral hypoxia-ischaemia. *Journal of neurochemistry,* **86**(2), pp. 351-362.

WANG, Z., LIU, D., ZHAN, J., XIE, K., WANG, X., XIAN, X., GU, J., CHEN, W. and HAO, A., 2013. Melatonin improves short and long-term neurobehavioral deficits and attenuates hippocampal impairments after hypoxia in neonatal mice. *Pharmacological research,* **76**, pp. 84-97.

WANNIER-MORINO, P., RAGER, G., SONDEREGGER, P. and GRABS, D., 2003. Expression of neuroserpin in the visual cortex of the mouse during the developmental critical period. *European Journal of Neuroscience,* **17**(9), pp. 1853-1860.

WARD, P., COUNSELL, S., ALLSOP, J., COWAN, F., SHEN, Y., EDWARDS, D. and RUTHERFORD, M., 2006. Reduced fractional anisotropy on diffusion tensor magnetic resonance imaging after hypoxic-ischemic encephalopathy. *Pediatrics,* **117**(4), pp. e619-30.

WARDLAW, J.M., MURRAY, V., BERGE, E., DEL ZOPPO, G., SANDERCOCK, P., LINDLEY, R.L. and COHEN, G., 2012. Recombinant tissue plasminogen activator for acute ischaemic stroke: an updated systematic review and meta-analysis. *The Lancet,* **379**(9834), pp. 2364-2372.

WASTERLAIN, S., CANDUSSO, D., HISSEL, D., HAREL, F., BERGMAN, P., MENARD, P. and ANWAR, M., 2010. Study of temperature, air dew point temperature and reactant flow effects on proton exchange membrane fuel cell

performances using electrochemical spectroscopy and voltammetry techniques. *Journal of Power Sources,* **195**(4), pp. 984-993.

WASTERLAIN, C.G., 1979. Does anoxemia play a role in the effects of neonatal seizures on brain growth? An experimental study in the rat. *European neurology,* **18**(4), pp. 222-229.

WATAKABE, A., ICHINOHE, N., OHSAWA, S., HASHIKAWA, T., KOMATSU, Y., ROCKLAND, K.S. and YAMAMORI, T., 2007. Comparative analysis of layer-specific genes in Mammalian neocortex. *Cerebral cortex (New York, N.Y.: 1991),* **17**(8), pp. 1918-1933.

WATANABE, S., FUKUDA, T. and UEKO, S., 1980. Changes in electroencephalogram of the rat following olfactory bulbectomy. *The Tohoku journal of experimental medicine,* **130**(1), pp. 41-48.

WEEKE, L.C., VILAN, A., TOET, M.C., VAN HAASTERT, I.C., DE VRIES, L.S., GROENENDAAL, F., 2017. A comparison of the Thompson encephalopathy score and amplitude-integrated electroencephalography in infants with perinatal asphyxia and therapeutic hypothermia. *Neonatology.,* **112**(1), 24-9.

WEGNER, M. and STOLT, C.C., 2005. From stem cells to neurons and glia: a Soxist's view of neural development. *Trends in neurosciences,* **28**(11), pp. 583-588.

WEI, L., HAN, B.H., LI, Y., KEOGH, C.L., HOLTZMAN, D.M. and YU, S.P., 2006. Cell death mechanism and protective effect of erythropoietin after focal ischemia in the whisker-barrel cortex of neonatal rats. *The Journal of pharmacology and experimental therapeutics,* **317**(1), pp. 109-116.

WEINBERGER, D.R., 1995. From neuropathology to neurodevelopment. *The Lancet,* **346**(8974), pp. 552-557.

WEEINSTOCK, M., 2007. Gender differences in the effects of prenatal stress on brain development and behaviour. *Neurochemical research.,* **32**(10), 1730-40.

WELSH, F.A., O'CONNOR, M.J., MARCY, V.R., SPATACCO, A.J. and JOHNS, R.L., 1982. Factors limiting regeneration of ATP following temporary ischemia in cat brain. *Stroke; a journal of cerebral circulation,* **13**(2), pp. 234-242.

WESTPHAL, O., 1965. Bacterial lipopolysaccharide-extraction with phenol water and further application of procedure. *Methods in carbohydrate chemistry,* **1**, pp. 83-91.

WEYER, A. and SCHILLING, K., 2003. Developmental and cell type-specific expression of the neuronal marker NeuN in the murine cerebellum. *Journal of neuroscience research,* **73**(3), pp. 400-409.

WHITELEY, W.N., SLOT, K.B., FERNANDES, P., SANDERCOCK, P. and WARDLAW, J., 2012. Risk factors for intracranial hemorrhage in acute ischemic

stroke patients treated with recombinant tissue plasminogen activator: a systematic review and meta-analysis of 55 studies. *Stroke,* **43**(11), pp. 2904-2909.

WHITLEY, D., GOLDBERG, S.P. and JORDAN, W.D., 1999. Heat shock proteins: a review of the molecular chaperones. *Journal of Vascular Surgery,* **29**(4), pp. 748-751.

WIGGLESWORTH, J.S. and PAPE, K.E., 1978. An integrated model for haemorrhagic and ischaemic lesions in the newborn brain. *Early human development,* **2**(2), pp. 179-199.

WIKIPEDIA FOUNDATION, I., 2018-last update, SERPINI1. Available: https://en.wikipedia.org/wiki/SERPINI1 [08/14, 2018].

WILHELMSSON, U., BUSHONG, E.A., PRICE, D.L., SMARR, B.L., PHUNG, V., TERADA, M., ELLISMAN, M.H. and PEKNY, M., 2006. Redefining the concept of reactive astrocytes as cells that remain within their unique domains upon reaction to injury. *Proceedings of the National Academy of Sciences of the United States of America,* **103**(46), pp. 17513-17518.

WILLIAMS, J.J., MAYURASAKORN, K., VANNUCCI, S.J., MASTROPIETRO, C., BAZAN, N.G., TEN, V.S. and DECKELBAUM, R.J., 2013. N-3 fatty acid rich triglyceride emulsions are neuroprotective after cerebral hypoxic-ischemic injury in neonatal mice. *PloS one,* **8**(2), pp. e56233.

WILLIAMS, C.E., GUNN, A.J., MALLARD, C. and GLUCKMAN, P.D., 1992. Outcome after ischemia in the developing sheep brain: an electroencephalographic and histological study. *Annals of Neurology,* **31**(1), pp. 14-21.

WILSON-COSTELLO, D., FRIEDMAN, H., MINICH, N., SINER, B., TAYLOR, G., SCHLUCHTER, M. and HACK, M., 2007. Improved neurodevelopmental outcomes for extremely low birth weight infants in 2000-2002. *Pediatrics,* **119**(1), pp. 37-45.

WOLF, H.K., BUSLEI, R., SCHMIDT-KASTNER, R., SCHMIDT-KASTNER, P.K., PIETSCH, T., WIESTLER, O.D. and BLUMCKE, I., 1996. NeuN: a useful neuronal marker for diagnostic histopathology. *The journal of histochemistry and cytochemistry : official journal of the Histochemistry Society,* **44**(10), pp. 1167-1171.

WOLFBERG, A.J., ROBINSON, J.N., MULKERN, R., RYBICKI, F. and DU PLESSIS, A.J., 2007. Identification of fetal cerebral lactate using magnetic resonance spectroscopy. *American Journal of Obstetrics and Gynecology,* **196**(1), pp. e9-e11.

WONG, E.H., KEMP, J.A., PRIESTLEY, T., KNIGHT, A.R., WOODRUFF, G.N., IVERSEN, L.L., 1986. The anticonvulsant MK-801 is a potent N-methyl-D-aspartate antagonist. *Proceedings of the National Academy of Sciences.*, **83**(18), 7104-8.

WOO, T.U., BEALE, J.M. and FINLAY, B.L., 1991. Dual fate of subplate neurons in a rodent. *Cerebral cortex (New York, N.Y.: 1991),* **1**(5), pp. 433-443.

WOOD, P.L., 1995. Microglia as a unique cellular target in the treatment of stroke: potential neurotoxic mediators produced by activated microglia. *Neurological research,* **17**(4), pp. 242-248.

WOOLSEY, T.A. and VAN DER LOOS, H., 2016. Erratum to "Re: Woolsey T.A., van der Loos H. 1970. The structural organization of layer IV in the somatosensory region (S I) of mouse cerebral cortex" [Brain Res. 17 (1970) 205-242. *Brain research,* **1651**, pp. 121.

WOOLSEY, T.A. and VAN DER LOOS, H., 1970. The structural organization of layer IV in the somatosensory region (SI) of mouse cerebral cortex. The description of a cortical field composed of discrete cytoarchitectonic units. *Brain research,* **17**(2), pp. 205-242.

WOULFE, J., GRAY, D.A. and MACKENZIE, I.R., 2010. FUS-immunoreactive intranuclear inclusions in neurodegenerative disease. *Brain Pathology,* **20**(3), pp. 589-597.

WU, F., TORRE, E., CUELLAR-GIRALDO, D., CHENG, L., BICHLER, E.K., GARCÍA, P.S. and YEPES, M., 2015. Tissue-type plasminogen activator triggers the synaptic vesicle cycle in cerebral cortical neurons. *Journal of Cerebral Blood Flow & Metabolism,* **35**(12), pp. 1966-1976.

WU, J., ECHEVERRY, R., GUZMAN, J. and YEPES, M., 2010. Neuroserpin protects neurons from ischemia-induced plasmin-mediated cell death independently of tissue-type plasminogen activator inhibition. *The American journal of pathology,* **177**(5), pp. 2576-2584.

WU, J. and KAUFMAN, R.J., 2006. From acute ER stress to physiological roles of the Unfolded Protein Response. *Cell death and differentiation,* **13**(3), pp. 374-384.

WU, P., TEOT, L., MURDOCH, G., MONAGHAN-NICHOLS, A.P. and MCFADDEN, K., 2014. Neuropathology of 22q11 deletion syndrome in an infant. *Pediatric and developmental pathology : the official journal of the Society for Pediatric Pathology and the Paediatric Pathology Society,* **17**(5), pp. 386-392.

WU, S.X., GOEBBLES, S., NAKAMURA, K., NAKAMURA, K., KOMETANI, K., MINATO, N., KANEKO, T., NAVE, K.A., TAMAMAKI, N., 2005. Pyramidal neurons of upper cortical layers generated by NEX-positive progenitor cells in the subventricular zone. *Proceedings of the National Academy of Sciences.,* **102**(47), 17172-7.

WU, Y.W., MATHUR, A.M., CHANG, T., MCKINSTRY, R.C., MILKEY, S.B., MAYOCK, D.E., VAN MEURS, K.P., ROGERS, E.E., GONZALEZ, F.F., COMSTOCK, B.A., JUUL, S.E., 2016. High-dose erythropoietin and hypothermia for hypoxic-ischemic encephalopathy: a phase II trial. *Pediatrics.*, **137**(6), e20160191.

WU, Z., GHOLAMI, A.M. and KUSTER, B., 2012. Systematic identification of the HSP90 candidate regulated proteome. *Molecular & cellular proteomics : MCP,* **11**(6), pp. M111.016675.

WYATT, J.S., EDWARDS, A.D., AZZOPARDI, D. and REYNOLDS, E.O., 1989. Magnetic resonance and near infrared spectroscopy for investigation of perinatal hypoxic-ischaemic brain injury. *Archives of Disease in Childhood,* **64**(7 Spec No), pp. 953-963.

XIA, W.J., YANG, M., FOK, T.F., LI, K., CHAN, W.Y., NG, P., NG, H.K., CHIK, K.W., WANG, C.C. and GU, G.J.S., 2005. Partial neuroprotective effect of pretreatment with tanshinone IIA on neonatal hypoxia-ischemia brain damage. *Pediatric research,* **58**(4), pp. 784.

XIANG, X., LI, S., ZHUANG, X. and SHI, L., 2016. Arhgef1 negatively regulates neurite outgrowth through activation of RhoA signaling pathways. *FEBS letters,* **590**(17), pp. 2940-2955.

XIAO, Y., PENG, Y., WAN, J., TANG, G., CHEN, Y., TANG, J., YE, W.C., IP, N.Y. and SHI, L., 2013. The atypical guanine nucleotide exchange factor Dock4 regulates neurite differentiation through modulation of Rac1 GTPase and actin dynamics. *The Journal of biological chemistry,* **288**(27), pp. 20034-20045.

XIN, H., LI, Y., SHEN, L.H., LIU, X., WANG, X., ZHANG, J., POURABDOLLAH-NEJAD, D.S., ZHANG, C., ZHANG, L., JIANG, H., ZHANG, Z.G. and CHOPP, M., 2010. Increasing tPA activity in astrocytes induced by multipotent mesenchymal stromal cells facilitate neurite outgrowth after stroke in the mouse. *PloS one,* **5**(2), pp. e9027.

XIONG, M., LI, J., MA, S., YANG, Y. and ZHOU, W., 2013. Effects of hypothermia on oligodendrocyte precursor cell proliferation, differentiation and maturation following hypoxia ischemia in vivo and in vitro. *Experimental neurology,* **247**, pp. 720-729.

XU, Q., DE LA CRUZ, E., ANDERSON, S.A., 2003. Cortical interneuron fate determination: diverse sources for distinct subtypes?. *Cerebral Cortex.,* **13**(6), 670-6.

XUE, M., STRADOMSKA, A., CHEN, H., BROSE, N., ZHANG, W., ROSENMUND, C. and REIM, K., 2008. Complexins facilitate neurotransmitter release at excitatory and inhibitory synapses in mammalian central nervous system. *Proceedings of the National Academy of Sciences of the United States of America,* **105**(22), pp. 7875-7880.

Y CAJAL, S.R., 1899. *Comparative study of the sensory areas of the human cortex.* Clark University.

YAGER, J., TOWFIGHI, J. and VANNUCCI, R., 1993. Influence of mild hypothermia on hypoxic-ischemic brain damage in the immature rat. *Pediatric research,* **34**(4), pp. 525-529.

YAGER, J.Y. and ASHWAL, S., 2009. Animal models of perinatal hypoxic-ischemic brain damage. *Pediatric neurology,* **40**(3), pp. 156-167.

YAGER, J.Y., BRUCKLACHER, R.M. and VANNUCCI, R.C., 1996. Paradoxical mitochondrial oxidation in perinatal hypoxic-ischemic brain damage. *Brain research,* **712**(2), pp. 230-238.

YAGER, J.Y., HEITJAN, D.F., TOWFIGHI, J. and VANNUCCI, R.C., 1992. Effect of insulin-induced and fasting hypoglycemia on perinatal hypoxic-ischemic brain damage. *Pediatric research,* **31**(2), pp. 138-142.

YAGER, J.Y., BRUCKLACHER, R.M. and VANNUCCI, R.C., 1991. Cerebral oxidative metabolism and redox state during hypoxia-ischemia and early recovery in immature rats. *The American Journal of Physiology,* **261**(4 Pt 2), pp. H1102-8.

YAMADA, Y., OHTANI, K., IMAJO, A., IZU, H., NALAMURA, H., SHIRAISHI, K., 2015. Comparison of the neurotoxicities between volatile organic compounds and fragrant organic compounds on human neuroblastoma SK-N-SH cells and primary cultured rat neurons. *Toxicology reports.*, **2**, 729-36.

YAMAMOTO, H., INABA, S., NISHIURA, Y., KISHI, F. and KAWAKAMI, Y., 1985. Acute inhalation of cigarette smoke augments hypoxic chemosensitivity in humans. *Journal of applied physiology (Bethesda, Md.: 1985),* **58**(3), pp. 717-723.

YAMAMOTO, H. and KATO, T., 1986. The effect of neonatal anoxia on brain cholecystokinin-8-like immunoreactivity and monoamine levels of mature rats. *Brain research,* **391**(2), pp. 285-288.

YAMAMOTO, K., YAMAMOTO, Y., FUJIMIYA, T. and OKAE, M., 1986. Effects of ethanol on the blood gas and acid-base state in hypoxic rats. *Nihon hoigaku zasshi = The Japanese journal of legal medicine,* **40**(4), pp. 357-360.

YAN, X.X., ZHENG, D.S., GAREY, L.J., 1992. Prenatal development of GABA-immunoreactive neurons in the human striate cortex. *Developmental brain research.,* **65**(2), 191-204.

YANG, B., ZHANG, H., MO, X., XIAO, H. and HU, Z., 2015. HspB8 is neuroprotective during oxygen glucose deprivation and reperfusion. *Current neurovascular research,* **12**(1), pp. 63-72.

YANG, D. and KUAN, C., 2015. Anti-tissue Plasminogen Activator (tPA) as an Effective Therapy of Neonatal Hypoxia–Ischemia with and without Inflammation. *CNS neuroscience & therapeutics,* **21**(4), pp. 367-373.

YANG, H., XU, W., ZHAO, W., GU, M. and WANG, W., 2018. 1, 3, 7-Trihydroxyxanthone, derived from Polygalae Radix, a herbal medicine, stimulates the expression of neurotrophic factors in rat astrocyte primary cultures via cAMP-and ERK-dependent pathways. *Biomedicine & Pharmacotherapy,* **98**, pp. 762-768.

YANG, L., SHEN, L., GAO, P., LI, G., HE, Y., WANG, M., ZHOU, H., YUAN, H., JIN, X. and WU, X., 2017. Effect of AMPK signal pathway on pathogenesis of abdominal aortic aneurysms. *Oncotarget,* **8**(54), pp. 92827.

YANG, D., LI, S.Y., YEUNG, C.M., CHANG, R.C., SO, K.F., WONG, D. and LO, A.C., 2012. Lycium barbarum extracts protect the brain from blood-brain barrier disruption and cerebral edema in experimental stroke. *PloS one,* **7**(3), pp. e33596.

YANG, D., SUN, Y.Y., LIN, X., BAUMANN, J.M., WARNOCK, M., LAWRENCE, D.A. and KUAN, C.Y., 2013. Taming neonatal hypoxic-ischemic brain injury by intranasal delivery of plasminogen activator inhibitor-1. *Stroke; a journal of cerebral circulation,* **44**(9), pp. 2623-2627.

YANG, D., SUN, Y.Y., NEMKUL, N., BAUMANN, J.M., SHEREEN, A., DUNN, R.S., WILLS-KARP, M., LAWRENCE, D.A., LINDQUIST, D.M. and KUAN, C.Y., 2013. Plasminogen activator inhibitor-1 mitigates brain injury in a rat model of infection-sensitized neonatal hypoxia-ischemia. *Cerebral cortex (New York, N.Y.: 1991),* **23**(5), pp. 1218-1229.

YANG, L., LIU, Z., RIOS, C., YUAN, H. and HE, B., 2009. Electrophysiological neuroimaging: cortical correlates of alpha rhythm modulation. *Conference proceedings : ...Annual International Conference of the IEEE Engineering in Medicine and Biology Society.IEEE Engineering in Medicine and Biology Society.Annual Conference,* **2009**, pp. 1934-1936.

YAO, L., KAN, E.M., KAUR, C., DHEEN, S.T., HAO, A., LU, J. and LING, E.A., 2013. Notch-1 signaling regulates microglia activation via NF-kappaB pathway after hypoxic exposure in vivo and in vitro. *PloS one,* **8**(11), pp. e78439.

YATA, K., MATCHETT, G.A., TSUBOKAWA, T., TANG, J., KANAMARU, K. and ZHANG, J.H., 2007. Granulocyte-colony stimulating factor inhibits apoptotic neuron loss after neonatal hypoxia–ischemia in rats. *Brain research,* **1145**, pp. 227-238.

YAZAKI, M., LIEPNIEKS, J.J., MURRELL, J.R., TAKAO, M., GUENTHER, B., PICCARDO, P., FARLOW, M.R., GHETTI, B. and BENSON, M.D., 2001. Biochemical characterization of a neuroserpin variant associated with hereditary dementia. *The American journal of pathology,* **158**(1), pp. 227-233.

YEPES, M., 2015. Tissue-type plasminogen activator is a neuroprotectant in the central nervous system. *Frontiers in cellular neuroscience,* **9**.

YEPES, M. and LAWRENCE, D.A., 2004. Neuroserpin: a selective inhibitor of tissue-type plasminogen activator in the central nervous system. *THROMBOSIS AND HAEMOSTASIS-STUTTGART-,* **91**(3), pp. 457-464.

YEPES, M. and LAWRENCE, D.A., 2004. Tissue-type plasminogen activator and neuroserpin: a well-balanced act in the nervous system? *Trends in cardiovascular medicine,* **14**(5), pp. 173-180.

YEPES, M., WU, F., TORRE, E., CUELLAR-GIRALDO, D., JIA, D. and CHENG, L., 2016. Tissue-type plasminogen activator induces synaptic vesicle endocytosis in cerebral cortical neurons. *Neuroscience,* **319**, pp. 69-78.

YEPES, M. and LAWRENCE, D.A., 2004. New functions for an old enzyme: nonhemostatic roles for tissue-type plasminogen activator in the central nervous system. *Experimental biology and medicine (Maywood, N.J.),* **229**(11), pp. 1097-1104.

YEPES, M., SANDKVIST, M., COLEMAN, T.A., MOORE, E., WU, J.Y., MITOLA, D., BUGGE, T.H. and LAWRENCE, D.A., 2002. Regulation of seizure spreading by neuroserpin and tissue-type plasminogen activator is plasminogen-independent. *The Journal of clinical investigation,* **109**(12), pp. 1571-1578.

YEPES, M., SANDKVIST, M., WONG, M.K., COLEMAN, T.A., SMITH, E., COHAN, S.L. and LAWRENCE, D.A., 2000. Neuroserpin reduces cerebral infarct volume and protects neurons from ischemia-induced apoptosis. *Blood,* **96**(2), pp. 569-576.

YEPES, M., ROUSSEL, B.D., ALI, C., VIVIEN, D., 2009. Tissue-type plasminogen activator in the ischemic brain: more than a thrombolytic. *Trends in neurosciences.*, **32**(1), 48-55.

YIN, K., BAILLIE, G.J., VETTER, I., 2016. Neuronal cell lines as model dorsal root ganglion neurons: A transcriptomic comparison. *Molecular pain.*, **12**, 1744806916646111.

YIN, K., CHEN, S., LEE, J., XU, J. and HSU, C.Y., 2002. ATM gene regulates oxygen-glucose deprivation–induced nuclear factor-κB DNA-binding activity and downstream apoptotic cascade in mouse cerebrovascular endothelial cells. *Stroke,* **33**(10), pp. 2471-2477.

YOON, B.H., KIM, C.J., ROMERO, R., JUN, J.K., PARK, K.H., CHOI, S.T. and CHI, J.G., 1997. Experimentally induced intrauterine infection causes fetal brain white matter lesions in rabbits. *American Journal of Obstetrics and Gynecology,* **177**(4), pp. 797-802.

YOU, Y. and KAUR, C., 2000. Expression of induced nitric oxide synthase in amoeboid microglia in postnatal rats following an exposure to hypoxia. *Neuroscience letters,* **279**(2), pp. 101-104.

YOUNG, C.L., BRITTON, Z.T. and ROBINSON, A.S., 2012. Recombinant protein expression and purification: a comprehensive review of affinity tags and microbial applications. *Biotechnology journal,* **7**(5), pp. 620-634.

YU, J., MCMAHON, A.P., 2006. Reproducible and inducible knockdown of gene expression in mice. *Genesis.*, **44**(5), 252-61.

YU, S.P., YEH, C.H., STRASSER, U., TIAN, M., CHOI, D.W., 1999. NMDA receptor-mediated K+ efflux and neuronal apoptosis. Science., **284**(5412), 336-9.

YUAN, T.M., YU, H.M., GU, W.Z. and LI, J.P., 2005. White matter damage and chemokine induction in developing rat brain after intrauterine infection. *Journal of perinatal medicine,* **33**(5), pp. 415-422.

ZAGHLOUL, N., PATEL, H. and AHMED, M.N., 2017. A model of Periventricular Leukomalacia (PVL) in neonate mice with histopathological and neurodevelopmental outcomes mimicking human PVL in neonates. *PloS one,* **12**(4), pp. e0175438.

ZANELLI, S., GOODKIN, H.P., KOWALSKI, S. and KAPUR, J., 2014. Impact of transient acute hypoxia on the developing mouse EEG. *Neurobiology of disease,* **68**, pp. 37-46.

ZECEVIC, N., and MILOSEVIC, A., 1997. Initial development of γ-aminobutyric acid immunoreactivity in the human cerebral cortex. Journal of Comparative *Neurology.,* **380**(4), 495-506.

ZEINIEH, M.P., TALHOUK, R.S., EL-SABBAN, M.E. and MIKATI, M.A., 2010. Differential expression of hippocampal connexins after acute hypoxia in the developing brain. *Brain & development,* **32**(10), pp. 810-817.

ZEINSTRA, E., FOCK, J.M., BEGEER, J.H., VAN WEERDEN, T.W., MAURITS, N.M. and ZWEENS, M.J., 2001. The prognostic value of serial EEG recordings following acute neonatal asphyxia in full-term infants. *European journal of paediatric neurology : EJPN : official journal of the European Paediatric Neurology Society,* **5**(4), pp. 155-160.

ZENG, H., SHEN, E.H., HOHMANN, J.G., OH, S.W., BERNARD, A., ROYALL, J.J., GLATTFELDER, K.J., SUNKIN, S.M., MORRIS, J.A., GUILLOZET-BONGAARTS, A.L., SMITH, K.A., EBBERT, A.J., SWANSON, B., KUAN, L., PAGE, D.T., OVERLY, C.C., LEIN, E.S., HAWRYLYCZ, M.J., HOF, P.R., HYDE, T.M., KLEINMAN, J.E., JONES, A.R., 2012. Large-scale cellular-resolution gene profiling in human neocortex reveals species-specific molecular signatures. *Cell.,* **149**(2), 483-96.

ZHANG, X., ZHANG, Q., LI, W., NIE, D., CHEN, W., XU, C., YI, X., SHI, J., TIAN, M. and QIN, J., 2014. Therapeutic effect of human umbilical cord mesenchymal stem cells on neonatal rat hypoxic–ischemic encephalopathy. *Journal of neuroscience research,* **92**(1), pp. 35-45.

ZHANG, C.P., ZHU, L.L., ZHAO, T., ZHAO, H., HUANG, X., MA, X., WANG, H. and FAN, M., 2006. Characteristics of neural stem cells expanded in lowered oxygen and the potential role of hypoxia-inducible factor-1Alpha. *Neuro-Signals,* **15**(5), pp. 259-265.

ZHANG, L., REN, F., ZHANG, X., WANG, X., SHI, H., ZHOU, L., ZHENG, S., CHEN, Y., CHEN, D., LI, L., ZHAO, C. and DUAN, Z., 2016. Peroxisome proliferator-activated receptor alpha acts as a mediator of endoplasmic reticulum stress-induced hepatocyte apoptosis in acute liver failure. *Disease models & mechanisms,* **9**(7), pp. 799-809.

ZHANG, Q., DING, Y., YAO, Y., YU, Y., YANG, L. and CUI, H., 2013. Creating rat model for hypoxic brain damage in neonates by oxygen deprivation. *PloS one,* **8**(12), pp. e83589.

ZHANG, Q., YUAN, L., LIU, D., WANG, J., WANG, S., ZHANG, Q., GONG, Y., LIU, H., HAO, A. and WANG, Z., 2014. Hydrogen sulfide attenuates hypoxia-induced neurotoxicity through inhibiting microglial activation. *Pharmacological research,* **84**, pp. 32-44.

ZHANG, Y., HE, K., WANG, F., LI, X. and LIU, D., 2015. Notch-1 signaling regulates astrocytic proliferation and activation after hypoxia exposure. *Neuroscience letters,* **603**, pp. 12-18.

ZHANG, Z., ZHANG, L., YEPES, M., JIANG, Q., LI, Q., ARNIEGO, P., COLEMAN, T.A., LAWRENCE, D.A. and CHOPP, M., 2002. Adjuvant treatment with neuroserpin increases the therapeutic window for tissue-type plasminogen activator administration in a rat model of embolic stroke. *Circulation,* **106**(6), pp. 740-745.

ZHAO, F., WANG, L. and LIU, K., 2009. In vitro anti-inflammatory effects of arctigenin, a lignan from Arctium lappa L., through inhibition on iNOS pathway. *Journal of ethnopharmacology,* **122**(3), pp. 457-462.

ZHAO, B.Q., TEJIMA, E. and LO, E.H., 2007. Neurovascular proteases in brain injury, hemorrhage and remodeling after stroke. *Stroke; a journal of cerebral circulation,* **38**(2 Suppl), pp. 748-752.

ZHAO, C., KAO, J.P. and KANOLD, P.O., 2009. Functional excitatory microcircuits in neonatal cortex connect thalamus and layer 4. *The Journal of neuroscience : the official journal of the Society for Neuroscience,* **29**(49), pp. 15479-15488.

ZHENG, T. and WEISS, M.D., 2013. Neonatal transplant in hypoxic injury. *Neural Progenitor Cells: Methods and Protocols,* , pp. 147-156.

ZHENG, X., ZHANG, S., YIN, F., TANG, J., YANG, Y., WANG, X. and ZHONG, L., 2012. Neuroprotection of VEGF-expression neural stem cells in neonatal cerebral palsy rats. *Behavioural brain research,* **230**(1), pp. 108-115.

ZHONG, S., ZHANG, S., FAN, X., WU, Q., YAN, L., DONG, J., ZHANG, H., LI, L., SUN, L. and PAN, N., 2018. A single-cell RNA-seq survey of the developmental landscape of the human prefrontal cortex. *Nature,* **555**(7697), pp. 524.

ZHOU, C., LIPPMAN, J.J., SUN, H. and JENSEN, F.E., 2011. Hypoxia-induced neonatal seizures diminish silent synapses and long-term potentiation in hippocampal CA1 neurons. *The Journal of neuroscience : the official journal of the Society for Neuroscience,* **31**(50), pp. 18211-18222.

ZHOU, J., SCHMID, T., FRANK, R. and BRUNE, B., 2004. PI3K/Akt is required for heat shock proteins to protect hypoxia-inducible factor 1alpha from pVHL-independent degradation. *The Journal of biological chemistry,* **279**(14), pp. 13506-13513.

ZHOU, Q., WANG, S. and ANDERSON, D.J., 2000. Identification of a novel family of oligodendrocyte lineage-specific basic helix-loop-helix transcription factors. *Neuron,* **25**(2), pp. 331-343.

ZHU, C., KANG, W., XU, F., CHENG, X., ZHANG, Z., JIA, L., JI, L., GUO, X., XIONG, H., SIMBRUNER, G., BLOMGREN, K. and WANG, X., 2009. Erythropoietin improved neurologic outcomes in newborns with hypoxic-ischemic encephalopathy. *Pediatrics,* **124**(2), pp. e218-26.

ZHU, C., XU, F., WANG, X., SHIBATA, M., UCHIYAMA, Y., BLOMGREN, K. and HAGBERG, H., 2006. Different apoptotic mechanisms are activated in male and female brains after neonatal hypoxia-ischaemia. *Journal of neurochemistry,* **96**(4), pp. 1016-1027.

ZHU, C., WANG, X., HAGBERG, H., BLOMGREN, K., 2000. Correlation between caspase-3 activation and three different markers of DNA damage in neonatal cerebral hypoxia-ischemia. *Journal of neurochemistry.*, **75**(2), 819-29.

ZURITA, E., CHAGOYEN, M., CANTERO, M., ALONSO, R., GONZALEZ-NEIRA, A., LOPEZ-JIMENEZ, A., LOPEZ-MORENO, J.A., LANDEL, C.P., BENITEZ, J., PAZOS, F. and MONTOLIU, L., 2011. Genetic polymorphisms among C57BL/6 mouse inbred strains. *Transgenic research,* **20**(3), pp. 481-489.

8 Appendices

Appendix 8.1 – Summary of Hypoxia-Only Literature

Reference	Species	Age	Temp. (°C)	O_2 Partial Pressure	CO_2 Partial Pressure	Duration of Hypoxia	Behavioural Phenotype	Molecular Phenotype
Rastogi et al., 1968	Rat	P0	-	0%	-	20 minutes	Increased anxiety in handling.	Slow growth, high levels of phosphorous expression, decreased glycolipid NANA.
Vannucci and Duffy, 1976	Rat	P7	37	0%	-	20 minutes	-	Glucose levels decreased throughout whole brain.
Wasterlain, 1979	Rat	P2, P11	-	0%	-	30 minutes (daily)	Neonatal seizures, slower development of reflexes such as swimming.	Decreased DNA, RNA, protein, and cholesterol throughout whole brain.
Vannucci and Vannucci, 1980	Rat	P0	37	0%	-	20 minutes	-	Glycogen levels decreased throughout whole brain.
Hedner et al., 1980	Rat	P1	-	6%	-	30 minutes	-	Dopamine levels decreased throughout whole brain.
Hedner and Lundborg, 1980a	Rat	P0	-	0%	-	30 minutes	-	5HT levels increased throughout whole brain for 6 hours.
Hedner and Lundborg, 1980b	Rat	P0	-	6%	-	30 minutes	-	No change in 5HT levels in whole brain or CFS.
Kaneko, 1985a	Rat	P1	-	0%	-	30 minutes	-	GABA, Tau, Asp, Thr, Glu, Gln and Ala, and total free amino acid level in whole brain decreased until P7. GABA and Gly levels decreased at P15.
Yamamoto et al., 1986	Rat	P0	RT	0%	-	25 minutes	-	Cholecystokinin-8 like immunoreactivity decreased in cortex and hippocampus.
Slotkin et al., 1986	Rat	P1, P8	-	7%	-	2 hours	-	Increased protein synthesis and suppressed ODC at P1. Short-term elevation of ODC and reduced protein synthesis, no increase

								in synaptic uptake at P8.
Hisanaga et al., 1986	Rat	P0	-	0%	-	20 minutes	-	ATP and GTP levels rapidly restored. CTP levels returned over 2-hours. UTP restoration slow and incomplete.
Shimomura and Ohta, 1988	Rat	P4	RT	0%	-	10 minutes	Hyperactivity in open field, poor motor coordination in screen test, hyperirritability in startle response, high susceptibility to PTZ.	-
Seidler and Slotkin, 1990	Rat	P0	37	7%	-	2 hours	-	Long-lasting increased turnover of dopamine and norepinephrine in midbrain and brain-stem, no effect in cerebral cortex or cerebellum.
Hadjiconstantinou et al, 1990	Rat	P7	37	7%	-	2 hours	-	Decreased cholinergic, serotonergic, and dopaminergic markers in frontal cortex, hippocampus and striatum.
Hida et al., 1991	Rat	P1	-	0%	-	22 minutes	-	NMR shows normal whole brain pH.
Dell'Anna et al., 1991	Rat	P1	35	0%	-	25 minutes	Transient hyperactivity in open field, lower performance in Morris water maze.	-
Hasegawa et al., 1991	Jcl-ICR Mouse	P1	25	0%	100%	20 minutes	-	Increased free radical production.
Carlos et al., 1991a	Rat	P1, P8	-	7%	-	2 hours	-	Brain damage shown by ODC.
Speiser et al., 1991	Rat	P0	-	0%	-	25 minutes	Hyperactivity in open field, lower performance in passive avoidance.	-
Dell-Anna et al., 1993	Rat	P2	35	0%	-	30 minutes	-	Noradrenaline increased in cerebellum, 5-HT and 5-HIAA decreased in cortex and cerebellum at P7. Noradrenaline and HVA increased in hippocampus. 5-HT decreased, 5-

								HIAA increased in striatum.
Hasegawa et al., 1993	Jcl-ICR Mouse	P1	25	0%	100%	20 minutes	-	Free radical density decreased throughout whole brain.
Spraggins et al., 1994	Rat	P1, P4, P8	37	7%	-	2 hours	-	Cocaine reduced ODC, decreased cell regeneration.
Krajnc et al., 1994	Rat	P0	37	8%	-	3 hours	-	Glutamate, dopamine and acetylcholine uptake decreased in striatum, hippocampus, and frontal cortex.
Tanaka et al., 1995	Rat	P7	37	8%	-	5 hours	-	Decreased choline acetyltransferase in brainstem, no difference in histology
Dell'Anna et al., 1995	Rat	P1	35	0%	-	25 minutes	-	Decreased fos-gene expression in hippocampus
Jensen, 1995	Rat	P5-P17	33	3%	-	-	Neonatal seizures.	Normal histology, increased immediate early gene activation.
Buwalda et al., 1995	Rat	P2	37	0%	-	20 minutes	Spatial memory impaired in hole board task, hyperactivity in open field, poor auditory attention, normal plus maze performance, normal shock probe test.	-
Slotkin et al., 1995	Rat	P1	37	5%	-	75 minutes	-	Decreased catecholamine production in whole brain and decreased respiratory response.
Dell'Anna et al., 1996	Rat	P2	35	0%	-	25 minutes	-	Decreased number of GABA-immuno-reactive neurons at P7 and P21, no CB-immunoreactive neurons detected.
Applegate et al., 1996	Rat	P10	-	3%	-	30 minutes	Kindled seizures not increased by hypoxia.	-
Brooks et al., 1996	Rat	P10	-	-	-	30 minutes	-	ATP and PCr levels decreased throughout whole brain, shown by NMR.
Iuvone et al., 1996	Rat	P0	35	0%	-	25 minutes	Transient hyperactivity in open field at P25-P40, lower performance on Morris water	Altered PV expression pattern.

							maze, partially improved by environmental enrichment.	
Krajnc et al., 1996	Rat	P0	37	8%	-	3 hours	-	Glutamine metabolism recovered within 6 hours of hypoxia.
Otoya et al., 1997	Rat	P7	36.5	6.50%	-	70 minutes	-	No effect on NMDA receptor binding with MK-801.
Nakajima et al., 1997	Rat	P5	35	0%	-	16 minutes	-	Increased dopamine throughout whole brain, eliminated by magnesium.
Laroia et al., 1997	Rat	P7	37	8%	-	20 minutes	Increased susceptibility to PTZ induced seizures in adulthood.	No necrosis or apoptosis in cortex, decreased cortical thickness.
Chiappe-Guiterrez et al., 1998	Rat	E19	37	10%	-	10 minutes	-	HIF-1 mRNA not detectable following hypoxia.
Speiser et al., 1998	Rat	P2	-	0%	-	30 minutes	Lower performance in passive avoidance test, decreased spatial memory in Morris water maze.	-
Mortola and Naso, 1998	Rat	P9	15, 33	10%	-	30 minutes	Impaired huddling in pups.	-
Takahashi et al., 1999	Rat	P0	37	5%	-	3 hours	-	Corticospinal neurons produced shorter dendrites, increased differences in cell body volume.
Ikeda et al., 1999	Rat	P7	33	8%	-	2-4 hours	-	HSP70 mRNA expression increased in brain and heart.
You and Kaur, 2000	Rat	P1	-	5%	-	2 hours	-	Microglia show immunohistochemical signs of competent phagocytosis.
Koh and Jensen, 2001	Rat	P10	33	7%	-	15 minutes	Increased sensitivity to AMPA-induced seizures.	-
Jones and Bergeron, 2001	Rat	P6	37	8%	-	3 hours	-	HIF-1 mRNA expression increased, protective against later seizure induction.
Ozer et al., 2002	Rat	P7	33	8%	-	2 hours	-	HSP70 expression increased in heart and hippocampus and, no effect in kidney.
Decker et al., 2003	Rat	P7	-	10%	5%	2 hours (intermittent)	Increased REM sleep, lower	-

							radial arm maze performance.	
Nalivaeva et al., 2003	Rat	E13	-	7%	-	3 hours	-	Increased expression of amyloid-β protein in adult.
Scheepen et al., 2003	Rat	E19	37	0%	-	19 minutes	-	Delay in hippocampal proliferation onset, no change in cerebellum proliferation.
Hu et al., 2003	Rat	P7	37	5%	-	40 minutes	-	Bcl-2 and Bcl-X(L) decreased 24 h after hypoxia. Increased cell death at 24h after hypoxia, hyperoxia or hypoxia + hyperoxia.
Daval et al., 2004	Rat	P1	36	0%	-	20 minutes	-	Transitory decrease in hippocampal cell density.
Rogalska et al., 2004	Rat	P0	33, 37, 39	0%	-	20 minutes	Circadian rhythms normal, spontaneous motor activity normal, stress-induced hyperactivity only in 39°C group.	-
Mikati et al., 2005	Rat	P10	RT	4%	-	1 minute (decreasing O_2 over 10 minutes)	Increased aggression in handling, lower performance in Morris water maze, no effect in open field.	-
Decker et al., 2005	Rat	P7	-	10%	-	6 hours (intermittent)	Hyperactivity in novel object task.	-
Caputa et al., 2005	Rat	P0	33, 37, 39	0%	-	25 minutes	Decreased open-field and stress-induced spontaneous motor activity, hyperactivity in plus-maze test, no effect at 33°C.	-
Casolini et al., 2005	Rat	P0-P7	30	0%	-	20 minutes	Attention deficit and increased anxiety in elevated plus-maze and sudden silence test, no impairment in Morris water maze.	No damage to brain detected by histology, reduced mGlut1 expression in cortex and hippocampus.
Tang et al., 2006	Rat	P1	31	0%	-	25 minutes	Emotional reactivity in open field evaluated.	-

Venerosi et al., 2006	Rat	E22	37	0%	-	20 minutes	Increased ultrasonic vocalisation, decreased exploration in open field, fear conditioning normal.	-
Ujhazy et al., 2006	Rat	P6	-	0%	-	10 minutes	Hyperactivity in open field, lower performance in rotarod test.	-
Ezquer et al., 2006	Rat	P7	37	7%	-	50 minutes	-	IGF-1, iNOS and eNOS in striatum not unchanged.
Pourie et al., 2006	Rat	P0, P1	36	0%	-	5 minutes	-	No histological markers of cell death, normal neurogenesis in hippocampus, slight delay in migration.
Rotstein et al., 2006	C57BL/6 Mouse	P0	RT	8%	-	35 minutes	Control and ApoE-deficient mice showed slower development of neonatal cliff avoidance reflex, hypoactivity in open field, lower Morris water maze performance, decreased body weight.	-
Zhang et al., 2006	Rat	P10	RT	6%	-	15 minutes	-	No effect on seizure induction in slice.
Rogalska et al., 2006	Rat	P0	33, 37, 39	0%	-	25 minutes	Behavioural disturbance in open-field, elevated plus-maze, and sudden silence tests, activity decreased in open field, hyperactivity in plus-maze.	-
Navarova et al., 2006	Rat	P2	36.5	0%	-	20 minutes	-	Increased levels of lactate throughout brain, CSF and liver.
Eskiocak et al., 2007	Rat	P7	37	8%	-	2 hours	-	Melatonin administration did not prevent protein oxidation.
Bustamante et al., 2007	Rat	E22	37	0%	-	18 minutes	-	Decreased levels of extracellular dopamine.

Mikati et al., 2007	Rat	P10	RT	4%	-	1 minute (decreasing O_2 over 10 minutes)	Epo reduced seizure susceptibility.	-
Hou et al., 2007	C57BL/6 Mouse	P6	-	3%	-	30 minutes	-	Ad/5HRE-3NRSE gene increased expression in neurons but not glial.
Paulose et al., 2008	Rat	P4	RT	2.60%	-	30 minutes	Lower Morris water maze performance in epileptic rats.	-
Coq et al., 2008	Rat	P0	37.5	0%	-	12 minutes	Hind limb immobilisation, muscle fibre atrophy, ECM changes in the muscle, ankle and knee joint degeneration.	-
Ezquer et al., 2008	Rat	P7	37	6.50%	-	50 minutes	Blunted preovulatory LH surges, early stage reproductive senescence.	-
Deng et al., 2009	Rat	P1	-	5%	-	-	-	No change in MCP-1 expression, monocyte proliferation throughout brain.
Rogalska et al., 2009	Rat	P2	33, 37, 39	0%	-	2 hours	-	Hyperthermia with or without anoxia caused induction of MR mRNA expression in hippocampus, no effect on GR mRNA.
Blaise et al., 2009	Rat	P0	36	0%	-	5 minutes	Decreased locomotor coordination at P19-21, decreased learning and memory in eight-arm maze at P80-84, partially improved by deficient diet.	Decreased morphological injury in hippocampal CA1 layer.
Aujla et al., 2009	Rat	P10	33	6%	-	15 minutes	Increased sensitivity to kainite- induced seizures.	-
Greggio et al., 2009	Rat	P10	RT	6%	-	12 minutes	Increased sensitivity to kainite- induced seizures.	-
Mikhailenko et al., 2009	Rat	P7	24	6%	-	3 hours	Increased performance in forced swim.	Decreased corticosterone production in forced swim.

Joseph et al., 2010	Rat	P4	-	2.60%	-	30 minutes	-	Transitory decreased D_1 and D_2 receptors in cerebellum.
Zeinieh et al., 2010	Rat	P10	RT	5%	-	10 minutes (decreasing O_2 levels)	-	Increased Cx30 protein 30min after reoxygenation, normalised at P11. Transiently decreased Cx36 protein at P11. Cx43 protein levels unchanged.
Anju et al., 2010a	Rat	P4	RT	2.60%	-	30 minutes	Respiratory inhibition.	Decrease in $GABA_A$ receptors.
Anju et al., 2010b	Rat	P4	RT	2.60%	-	30 minutes	Respiratory inhibition.	Decreased GABA and $GABA_B$ receptors, decreased $GABA_B$ and GAD gene expression in cortex. Increased HIF-1α.
Anju et al., 2010c	Rat	P0	RT	2.60%	-	30 minutes	Normal righting reflex, normal wire grasp, slightly lower radial arm maze performance.	Increased 5HT and $5HT_{2A}$ receptors, increased 5HTT and $5HT_{2A}$ receptor gene expression in cerebellum.
Rogalska and Caputa, 2010	Rat	P2	33, 37, 39	0%	-	2 hours	Hyperthermia decreased corticosterone response in open-field stress.	Hyperthermia decreased corticosterone response in open-field stress.
Wasterlain et al., 2010	Rat	P4	36	0%	-	3 minutes	Energy balance maintained in hyperglycaemic animals, compromised by concurrent hypoglycaemia, hyperthermia or hypoxia.	-
Martin et al., 2011	Rat	P0	36	0%	-	5 minutes	Increased memory retrieval in custom test. Sexual dimorphism observed.	-
Anju et al., 2011a	Rat	P0	RT	2.60%	-	30 minutes	-	Increased total 5HT and $5HT_{2A}$ receptor, increased $5HT_{2A}$ receptor and 5HTT gene expression in cortex.
Anju et al., 2011b	Rat	P0	RT	2.60%	-	30 minutes	-	Increased 5-HT, 5-HT_{2A} receptor, increased 5-HTT and 5-HT_{2A} receptor gene expression in brainstem.
Anju et al., 2011c	Rat	P0	RT	2.60%	-	30 minutes	-	Decreased GABA and $GABA_B$

								receptors, decreased $GABA_B$ receptor and GAD gene expression in cerebellum and brainstem.
Anju et al., 2011d	Rat	P0	RT	2.60%	-	30 minutes	-	Decreased 5HT, $5HT_{2A}$ receptor, $5HT_{2A}$ receptor and 5HT transporter gene expression in cortex.
Rakhade et al., 2011	Rat	P10	RT	6%	-	15 minutes	Spontaneous seizures in late adulthood, shown by EEG.	-
Zhou et al., 2011	Rat	P10	33	3%	-	-	-	Decreased silent synapses, increased synaptic AMPA receptors.
Anju et al., 2012a	Rat	P0	RT	2.60%	-	30 minutes	-	Decreased muscarinic receptors, decreased muscarinic M_1, M_2, and M_3 receptor gene expression in striatum.
Anju et al., 2012b	Rat	P0	RT	2.60%	-	30 minutes	-	Decreased GABA, $GABA_A$ and $GABA_B$ receptor and GAD expression in striatum.
Anju et al., 2012c	Rat	P0	RT	2.60%	-	30 minutes	Respiratory inhibition.	Decreased $GABA_A$, $GABA_{A(\alpha1)}$, $GABA_{A(\alpha5)}$, $GABA_{A(\delta)}$, and $GABA_{A(\gamma3)}$ receptor subunits in cerebellum.
Alsharnoubi et al., 2012	Rat	P7	32	4%	-	30 minutes	-	No differences in NF-κB activity in whole body or whole brain.
Sanchez et al., 2012	Rat	P10	33.5	6%	-	15 minutes	Some animals experience tonic-clonic seizures.	No gap junctions present in cortical slices.
Autheman et al., 2012	CD1 Mouse	P6	37	8%	-	45 minutes	-	GPx1 overexpression prevented global and nuclear increase in activated Erk1/2 at 30 minutes post-hypoxia.
Martin et al., 2012	Rat	P0	36	0%	-	5 minutes	-	Normal neurogenesis, reduced apoptosis in hippocampus, increased activation of Erk1/2 and decreased p38 and DAP kinase.
Raveendran and Skaria, 2013	Rat	P0	RT	2.60%	-	30 minutes	Lower Morris water mazer performance.	Increased cell death, assessed with TO-PRO3® and BAX mRNA.
Anju et al., 2013a	Rat	P0	RT	2.60%	-	30 minutes	-	Decreased muscarinic M_1, M_2, and M_3

								receptor gene expression in brainstem, decreased choline acetyl transferase.
Anju et al., 2013b	Rat	P0	RT	2.60%	-	30 minutes	-	Decreased M_1, M_2, and M_3 receptor gene expression in cerebellum.
Anju et al., 2013c	Rat	P0	RT	2.60%	-	30 minutes	-	Decreased M_1, M_2 and M_3 receptor gene expression in striatum.
Yao et al., 2013	Rat	P1	-	5%	-	2 hours	-	Increased TLR4 immunofluorescence and protein expression in corpus callosum and cerebellum in microglia.
Cleary et al., 2013	Rat	P10	RT	5%	-	15 minutes	-	Bumetanide increased phenobarbital efficacy in a rat model of hypoxic neonatal seizures.
Peng et al., 2013	Rat	P10	RT	5%	-	15 minutes	Neonatal seizures induced.	Decreased current amplitude in dentate granule cells.
Wang et al., 2013	Mouse	P1	-	5%	-	2 hours	Melatonin improved Morris water maze performance.	Melatonin decreased cell death in hippocampus.
Brackmann et al., 2013	C57BL/6 Mouse	P1	RT	8%	-	2 hours	-	No difference in activin A or Inhba expression.
Zhang et al., 2013	Rat	P7	37	8%	-	1.5 hours	-	Impaired neuronal functions, increased brain water weight, injuries in subcortex, hippocampus.
Zanelli et al., 2014	C57BL/6 Mouse	P3-P15	RT	0%	-	20 minutes	Electrographic seizures without behavioural manifestations.	-
Zhang et al., 2014	BALB.c Mouse	P1	-	5%	-	2 hours	-	NaHS attenuated neuronal death, suppressed microglial activation, cytokines and NO.
Pellitteri et al., 2014	Rat	P8	37	0%	-	2.5 minutes	-	Histological effects less severe than HI. Protective against HI.
Sampath et al., 2015	Rat	P7	36.5	4%	-	1 minute (decreasing O_2 levels over 15 minutes)	Neonatal seizures.	-
Rodriguez-Alvarez et al., 2015	C57BL/6 Mouse	P7	34	5%	-	15 minutes	Neonatal seizures, reduced curiosity in	-

							novel object test, weight loss.	
Takada et al., 2015	Rat	P1	36	0%	100%	25 minutes	Lower Morris water maze performance.	Increased TUNEL staining in hippocampus.
Wang et al., 2015	Rat	P10	33	3%	-	-	Neonatal seizures, normal Morris water maze performance.	Seizures increased the number of dentate gyrus cells, reduced apical dendritic complexity.
Samaiya and Krishnamurthy, 2015	Rat	P2	-	5%	-	10 minutes (twice)	Increased reflex latency observed after 24 hours.	Decrease in brain respiratory control ratio. Decreased NO in mitochondria.
Zhang et al., 2015	Rat	P1	-	5%	-	2 hours	-	Notch-1 upregulated in astrocytes. Blockade of Notch-1 signalling with DAPT suppressed astrocyte proliferation, decreased secretion of IL-1β, no significant change in TNF-α.
Boksa et al., 2015	Rat	E22	37	0%	-	5 or 16 minutes	-	Decreased brain ATP, injection of oxytocin to P2 rat pups followed by anoxia resulted in increased brain lactate and decreased ATP.
Takada et al., 2016	Rat	P1	37	0%	-	25 minutes	Lower Morris water maze performance.	MRI revealed hippocampal volume decrease in adult.
McDonald et al., 2016	Rat	P7	33, 38	10%	-	-	-	LPS increased TNFα, IL-1β, MCP-1, and IL-10.
Kletkiewicz et al, 2016	Rat	P2	33, 37, 39	0%	-	10 minutes	-	No change MDA, GSH and vitamin E at 33°C. Increased oxidative stress at 37°C or 39°C.

Table 8.1 – Summary of Hypoxia-Only Literature. Publications were identified using the Pubmed search: brain ((neonatal) AND hypoxia) NOT ischemia [Title]. Publications were included in this survey only if the studies contained experiments modelling neonatal hypoxia in the absence of ischaemia. The publications listed were unsuitable for statistical meta-analysis at this time due to high variation between methodologies.
RT = room temperature, E = embryonic day, P = postnatal day, Temp. = temperature of hypoxia chamber, - = information not available in publication.
Glycolipid NANA = glycolipid N-acetylneuraminic acid (ganglioside), 5 HT = 5-hydroxytryptamine (serotonin), 5HTT = 5-hydroxytryptamine transporter, Tau = taurine, Asp = aspartic acid, Thr = threonine, Glu = glutamic acid, Gln = glutamine, Ala = alanine, Gly = glycine, ODC = ornithine decarboxylase, ATP = adenosine triphosphate, GTP = guanosine triphosphate, CTP = cytidine triphosphate, UTP = uridine triphosphate, PTZ = pentylenetetrazol, 5HIAA = 5-Hydroxyindoleacetic acid, HVA = homovanillic acid, Jcl-ICR = albino mouse strain (http://nomura-siam.com/en/animals/jclicr-en/, last accessed 05/09/2018), CB = calbindin, PCr =

phosphocreatine, PV = parvalbumin, REM = rapid eye movement, Bcl-2 = B cell lymphoma 2 protein, BclX(L) = B cell lymphoma extra-large protein, mGlut1 = metabotropic glutamate transporter 1, ApoE = apolipoprotein E, NO = nitric oxide, IGF-1 = insulin-like growth factor 1, iNOS = inducible nitric oxide synthase, eNOS = endothelial nitric oxide synthase, Ad/5HRE-3NRSE = replication-defective adenovirus vector (Huang et al., 2005; Hou et al., 2007), LH = luteinising hormone, MCP-1 = monocyte chemoattractant protein 1, MR = mineralo-corticoid, GR = gluco-corticoid, CA1 = cornu ammon, layer of hippocampus, D_1 = dopamine metabotropic receptor 1, D_2 = dopamine metabotropic receptor 2, Cx30 = gap-junction β6 protein, Cx36 = gap-junction δ2 protein, Cx43 = gap-junction α1 protein, $GABA_A$ = γ-aminobutyric acid ionotropic receptor A, $GABA_B$ = γ-aminobutyric acid metabotropic receptor B, GAD = glutamate decarboxylase, $5HT_{2A}$ = 5-hydroxytryptamine transporter metabotropic receptor 2A, $GABA_{A(\alpha1)}$ = γ-aminobutyric acid ionotropic receptor A, subunit α1 $GABA_{A(\alpha5)}$ = γ-aminobutyric acid ionotropic receptor A, subunit α5, $GABA_{A(\delta)}$ = γ-aminobutyric acid ionotropic receptor A, subunit δ $GABA_{A(\gamma3)}$ = γ-aminobutyric acid ionotropic receptor A, subunit γ3, NF-κB = nuclear factor κ-light-chain-enhancer of activated B cells, GPx1 = glutathione peroxidase 1, Erk1 = extracellular signal-regulated kinase 2 (*Mapk3*), Erk2 = extracellular signal-regulated kinase 2 (*Mapk1*), TO-PRO3® = Iodide cell staining kit (#T3605, Sigma Aldrich, Hemel Hempstead, UK), BAX = Bcl2-associated X protein, p38 = p38 mitogen-associated protein kinase/cytokinin-specific binding protein, DAP kinase = death-associated protein kinase 1, M_1 = muscarinic metabotropic receptor 1, M_2 = muscarinic metabotropic receptor 2, M_3 = muscarinic metabotropic receptor 3, TLR4 = toll-like receptor 4, Inhba = inhibin subunit βA, BALB.c = inbred albino mouse strain (https://www.jax.org/strain /000651, last accessed 05/09/2018), NaHS = sodium hydrosulphide, DAPT = dual anti-platelet therapy. All other abbreviations given in the List of Abbreviations found on page viii.
Adapted from Supplementary Table 1 previously published in Millar et al., 2017.